AATSR Product Handbook

European Space Agency- EnviSat AATSR Product Handbook, Issue 2.2, 27 February 2007

Table of contents

Abstract

Chapter 1

The AATSR Products User Guide

The Advanced Along Track Scanning Radiometer (AATSR) is one of the Announcement of Opportunity (AO) instruments on board ENVISAT. It is the most recent in a series of instruments designed to measure Sea Surface Temperature (SST) to the high levels of accuracy and precision required for the monitoring and detection of climate change. In order to achieve this, the (A)ATSR instruments include several innovative features in their design:

- An along track scanning technique 1.1.3.1. ;
- Continuous on-board calibration of the thermal channels;
- An on-board calibration system for the visible and near infrared channels;
- Low-noise infrared detectors, cooled to near-optimum operating temperatures;
- A multi-channel approach to SST retrieval.

ATSR-1 was launched on the ESA satellite ERS-1 in July 1991 and operated until March 2000. ATSR-2 was launched on ERS-2 in April 1995 and is expected to continue to operate at least until the end of the ENVISAT commissioning phase. Together this family of instruments will establish a unique fifteen year data set supporting not only oceanographic and climate research, but also a wide range of land surface, cryosphere and atmospheric applications.

The purpose of this User Guide is to introduce users to the capabilities of the AATSR instrument and its data products. It provides a brief overview of the instrument, the geophysical measurements it retrieves and the measurement principles employed. It also provides information to help users select, read and understand AATSR data. Also included are a list of links and references for further reading, and a selection of example images in the form of an image gallery. The User Guide is intended to help users "get started" with AATSR data.

The AATSR User Guide has been produced in conjunction with an AATSR Reference Guide. The Reference Guide provides more detailed information on the heritage and evolution of the (A)ATSR series of instruments, the AATSR instrument itself and its products and data processing system. The Reference Guide is designed for use when more specific scientific or engineering information is required, and covers AATSR Products and Algorithms (Chapter 2.), The AATSR Instrument (Chapter 3.), Frequently Asked Questions (Chapter 4.), a Glossary (Chapter 5.) and detailed Data Format information (Chapter 6.).

1.1 Why Choose AATSR Data?

The AATSR instrument is capable of retrieving a variety of geophysical measurements. In order to exploit these effectively, it is necessary to understand exactly what AATSR measures, why the instrument has been designed to operate in this way and how these measurements are made.

AATSR data also offer a number of unique capabilities and advantages over data from similar imaging instruments. These are also covered in this User Guide.

The results of these features are data suitable for a wide range of potential applications. A summary of products and applications is provided to assist the user in identifying the most suitable product for his or her particular use.

Subsequent sections cover the following themes:

- Geophysical Measurements 1.1.1.
- Scientific Background 1.1.2.
- Principles of Measurement 1.1.3.
- Geophysical Coverage 1.1.4.
- Special Features of AATSR 1.1.5.
- Summary of Applications vs. Products 1.1.6.

The ENVISAT Data Policy

The conditions of data distribution for ENVISAT data are directly related to categories of use, as defined by the ENVISAT Data Policy (MMO-POL-0003-EOAD: ENVISAT Data

Policy, Issue 1 Revision 0, 23 August 2000).

- Category 1 use: Research and applications development use in support of the mission objectives, including research on long-term issues of Earth System science, research and development in preparation for future operational use, certification of receiving stations as part of the ESA functions, and ESA internal use;
- Category 2 use: All other uses that do not fall into Category 1, including operational and commercial use.

For Category 1 users, the Data Policy, applicable for both ERS and ENVISAT, provides the possibility to submit Category 1 use proposals at any time beyond the fixed dates imposed by specific Announcements of Opportunity.

How to Order AATSR Data

A number of interactive catalogues are available for browsing ESA earth observation data. These can be found at http://www.envisat.esa.int/services/.

For data distribution falling under Category 1 use, the data will be provided by ESA at reproduction cost or free of charge (to be waived by the Earth Observation Program Board). If you wish to submit a proposal for Category 1 use of data please follow the guidelines for proposal submittal at the dedicated Earth Observation Principal Investigator Portal at http://eopi.esa.int/esa/esa.

Category 1 users can receive ENVISAT data on media, via FTP or via the web, depending on the nature of the order. The ESA Earth Observation Help Desk Team (EOHelp@esa.int) can also advise on data access issues.

Should you wish to purchase ERS or ENVISAT data for commercial or operational use (Category 2), please contact either of the two distributing entities:

EMMA - represented by Eurimage

Customer Services

tel.: +39 06 406 94 1

fax: +39 06 406 94 232

e-mail: cust.services-staff@eurimage.com

http://www.eurimage.com

SARCOM - represented by Spot Image

Sales department

tel.: +33.562.194070

fax: +33.562.194055

e-mail: jean.bobo@spotimage.fr

http://www.spotimage.com

Under the terms of the ENVISAT Data Policy, in their capacity as AO Instrument Provider, DEFRA have the right to make and distribute copies of AATSR data for its own use, for use by other funding entities of AATSR and for research groups designated by DEFRA. Users with links to Defra or the other AATSR programme partners should consult their local contacts within these agencies.

1.1.1 Geophysical Measurements

1.1.1.1 Primary Geophysical Measurement

The primary mission objective of the AATSR instrument is to extend the long-term consistent set of global SST measurements started with ATSR-1 and continued with ATSR-2.

Sea Surface Temperature (SST)

AATSR has thermal infrared channels measuring upwelling radiance from the sea surface and the atmosphere at 3.7, 11 and 12 μm. From the calibrated top of the atmosphere Brightness Temperatures (BT) available from these bands, SST is calculated using the 11 and 12 μm channels during the day and the 11, 12 and 3.7 μm channels at night.

Very high levels of accuracy and precision are required to support global climate monitoring and change detection. Therefore, the AATSR instrument and ground processing system are required to produce SST retrievals routinely from the corresponding BTs with an absolute accuracy of better than 0.3K, globally, both for a single sample and when averaged over areas of 0.5° longitude by 0.5° latitude, under certain cloud free conditions (i.e. >20% cloud free samples within each area). The AATSR programme also aims to maintain an instrument stability of 0.1K during the mission lifetime.

It is important to note that the (A)ATSR instruments return SST measurements for the ocean's 'skin' and that the temperature of the sea skin surface is typically a few tenths of a degree cooler than the temperature a few centimetres below. Due to the limited penetration of thermal infrared radiation through the water column, the infrared radiometric temperature will be that of only the top few tens of micrometres, whereas the oceanographically understood SST is a measure of the temperature in the top 10 cm.

1.1.1.2 Additional Capabilities

Land Remote Sensing

AATSR also includes three visible/near infrared channels centred at 0.55, 0.67 and 0.87µm. These were first introduced on ATSR-2 and have extended the instrument's capabilities over land, particularly for the study of vegetation.

Much of the time, the basic calibrated top of the atmosphere reflectance measurements from the AATSR visible and near infrared channels are used for studies of vegetation quantity and quality. In order to cope with all possible normal variations in brightness over the Earth's surface without saturation whilst maximising the precision of the measurements, the gain and offset of the visible channels is selectable in flight. These channels have a signal to noise ratio of 20:1 at 0.5% spectral albedo and measure top of the atmosphere radiances to an absolute accuracy of 5% over its entire range.

Two specific geophysical parameters are also available in the AATSR products over land:

NDVI

The standard AATSR Level 2 product includes the Normalised Difference Vegetation Index (NDVI) using the 0.67 and 0.87 µm channels.

Land Surface Temperature

The AATSR thermal bands used for SST retrieval are also available over land and are used to retrieve Land Surface Temperature (LST) in the AATSR gridded (1 km) product. Algorithms for deriving LST using split-window radiances are sufficiently advanced that accuracies of 1-3 K are possible. Better accuracies (about 1 K) are obtained at night when differential surface heating is absent.

Measurements of radiance over exceptionally hot targets such as deserts, burning vegetation and volcanic eruptions are also possible using AATSR's 'low-gain' mode. This prevents saturation of the thermal channels and applies to targets with an upper limit of 500°C.

1.1.1.3 Cloud and Atmospheric Measurements

Currently AATSR does not retrieve cloud and atmospheric parameters on a routine basis. However, the different AATSR channels can be used directly to provide information on the basic location, extent and structure of clouds. Two fields in the Level 2 product have also been reserved for Cloud Top Temperature (CTT) and Cloud Top Height (CTH), should suitable retrieval algorithms become available in the future.

Work with ATSR-2 data has also demonstrated that the visible and thermal channels can be combined to estimate a number of specific properties within the cloud field. These include:

- Optical Depth, broadly related to the vertical dimension of the cloud;
- Phase, which determines whether the cloud contains ice or water;
- Particle Size, the effective radiative dimension of the cloud particles; and,
- Pressure, reflecting cloud top pressure or altitude.

The dual views provided by AATSR also offer a stereo viewing capability that can be used to discriminate between the different layers and structures within the cloud and also to estimate cloud top height.

1.1.1.4 Cryosphere

AATSR visible and thermal channel data can be used for studies of the cryosphere. Used on their own, or more often synergistically with other sensors, potential applications include snow cover monitoring, monitoring variations in annual sea ice growth and decay, location of boundaries and features of the Antarctic ice sheet, and feature mapping for radar altimetry over land and ice. The discriminatory power of the 1.6 μm channel for cloud and ice/snow is a topic of particular research interest.

1.1.2 Scientific Background

This section provides a summary of the scientific requirements upon which the AATSR mission is based. The primary driver has been the retrieval of high quality SST measurements, however, a secondary objective is to provide scientifically useful products over land. Although the AATSR mission is not specifically designed for applications in the atmosphere and cryosphere, consideration was also given to the high level requirements of such research, to ensure maximum flexibility in extending the applications of AATSR wherever possible.

1.1.2.1 SST

The scientific principles behind the design of the (A)ATSR instruments are dominated by the need for the high accuracy SSTs required for global climate monitoring and research. Accurate SST measurement is of great importance for climate research; for example, in modelling climatic phenomena such as the El Niño Southern Oscillation, in the monitoring of global warming due to the enhanced greenhouse effect, and in the investigation of ocean-atmosphere heat transfer. Consequently, the AATSR instrument and ground processing system are required to produce SST retrievals routinely with an absolute accuracy

of better than 0.3K, globally, both for a single sample and when averaged over areas of 0.5° longitude by 0.5° latitude, under certain cloud free conditions (i.e. >20% cloud free samples within each area).

The global coverage offered by AATSR is also very important. The response of weather and climate to SST is the subject of growing scientific interest, due to the large quantities of energy stored in the ocean, the energy exchanges possible with the atmosphere, and the effects of any carbon dioxide-induced climate change on the oceans. Predictions of the effects of anthropogenic doubling of atmospheric carbon dioxide show rises in the ocean mixed-layer temperature of up to a few degrees when globally averaged. Models also show that ocean warming is not spatially uniform, with variations in the magnitude of warming around the globe.

Surface observations of SST from ships of opportunity and buoys are too sparse to provide adequate analyses on this scale, except in the areas of heavily travelled shipping lanes. Ships of opportunity are also prone to measurement inconsistencies, due to the different ways in which SST data are collected (e.g. hull thermistors, cooling water intakes). In addition, measurements from buoys and from ships of opportunity are of bulk temperature, which can differ by several tenths of a degree from the true 'skin' temperature of the sea surface.

Data from AATSR will add to data received from predecessor instruments, ATSR-1 and ATSR-2, and lead to a 15+ year record of precise and accurate global sea surface temperature. Global historical SST fields are not only an important boundary condition on Atmospheric Global Circulation Models (GCM), but they can also be used for validation of model outputs (for example, SSTs are a predicted variable for ocean-atmosphere coupled General Circulation Models).

These high level objectives give rise to a number of more detailed requirements dictating instrument design.

Primary Sensing Wavelengths

The ocean surface is considered to be an emitter of radiation, with a peak in emission occurring at around 10 μm. Assessment of atmospheric absorption in this area shows that the region between 10 and 13 μm is a suitable window with both low atmospheric absorption and good radiance sensitivity to small changes in SST. The AATSR channels at 11 and 12 μm were selected on this basis. The 3.7 μm channel was selected to provide an additional channel at night, because although measurements in the 3-5 μm window are affected by reflected solar irradiance during the day, they show very high radiometric sensitivity at night.

Atmospheric Correction

Given the overall requirement for accurate SST measurements, it is important to precisely account for the contribution of atmospheric absorption and emission to the upwelling radiances observed by the instrument. Early work with Advanced Very High Resolution Radiometer (AVHRR) data demonstrated that differential measurements of upwelling radiances in two closely spaced thermal channels allow an accurate assessment of atmospheric effects, if the atmospheric effects differ between the two channels. Consequently, AATSR provides corrections for the effects of the atmosphere on the SST

retrievals through the use of multiple thermal channels in the retrieval.

However the strict demands placed on the accuracy of AATSR SST retrievals requires further improvements to atmospheric correction. This can be achieved by making two observations of the same ocean surface through different atmospheric path lengths. As a result, AATSR also employs a 'dual view' technique to achieve the best possible atmospheric correction.

Cloud Clearing

A key condition to meet the overall SST accuracy requirements is that of effective cloud clearing. AATSR employs a number of cloud tests using different combinations of thermal channel data. However, these techniques can be improved with reference to a visible channel during the daytime (when cloud will be bright compared to the sea surface), hence the inclusion of the additional channel at 1.6 μm, used primarily for cloud clearing.

Sampling Distance and Instantaneous Field of View (IFOV)

The overall SST accuracy requirement has been set on the basis that 20% of samples need to be cloud-free over a 0.5 degree by 0.5 degree cell. This means that for adequate noise reduction through averaging of individual sample values, a minimum of 500 cloud free samples are required. In the limiting scenario of 80% cloud cover, this requires a total of 2500 samples, which for a 50 by 50 km cell gives a sample size of 1 km. The AATSR sampling distance has therefore been set at 1 km. Research with previous sensors has also shown that 1 km is a reasonable compromise between data volume and spatial resolution for SST feature mapping.

In addition, for land applications a 1 km sampling distance is good for mapping and monitoring on large scales, whilst providing adequate discrimination of land surface types.

Co-alignment of the AATSR channel IFOVs is required to 0.1 of the sampling distance. This is to allow the cloud clearing algorithms to work successfully at the edge of cloud masses.

Calibration and Characterisation Requirements

To retrieve SST effectively from the AATSR detector signals, the spectral response and IFOV of the channels are measured prior to launch. In order to meet the strict accuracy requirements, a pre-launch end-to-end radiometric calibration of the instrument is also conducted.

In-orbit radiometric calibration will also play an important part in ensuring the long-term stability of AATSR SST measurements over the mission lifetime. To achieve this, the instrument carries two high precision black body targets. These are viewed during every scan to provide accurate in-orbit calibration of the thermal channels.

1.1.2.2 Remote Sensing Over Land

Visible and near infrared wavebands were added to ATSR-2 and AATSR specifically to enable land remote sensing studies. However, they have been added in such a way as to avoid

compromising the primary SST measurement requirements.

Work using Landsat and AVHRR data has shown that global monitoring of land, especially vegetation, at moderate resolution (i.e. ~1 to ~4 km) is of great value in studying a number of urgent global environmental problems. Parallel research has also demonstrated the benefit of using combinations of several visible bands for vegetation remote sensing. These are the principles behind the inclusion of AATSR visible bands, to combine the advantages of global coverage and improved spectral discrimination.

Band Selection

The reflectance spectrum of vegetation typically shows a low reflectance (~0.05) in the visible part of the spectrum coinciding with maximum solar irradiance, at which wavelengths light is absorbed by vegetation for photosynthesis. In the near infra-red (NIR), foliage has a high reflectance (~0.5), with a very rapid transition between the red and NIR regions at ~0.75 µm. Soil typically has a fairly flat spectrum (gradually rising at higher wavelengths) over the same region, though its absolute reflectance varies with soil-type and moisture (wet soil being darker than dry soil).

Either the ratio or difference between two spectral bands on either side of the ~0.75 µm transition will indicate the presence of photosynthetically active vegetation. Those bands usually chosen are centred in the red part of the spectrum at ~0.66 µm and in the NIR at ~0.87 µm. A number of 'vegetation indices' involving these two bands have been proposed. In order to provide assessment of vegetation quantity using these established vegetation indices, AATSR provides two reflection channels in the red and NIR spectral regions (at 0.67 and 0.87 µm).

Healthy growing vegetation has a reflectance peak in the green part of the spectrum, which is indicative of the amount of chlorophyll present. Thus, the reflectance in a green spectral band is reduced for senescent, diseased or damaged foliage. Studies using a green band in conjunction with the red and near-infrared bands show this effect, and important extra information is obtained on the growth stage (as well as indications of damage) by combining the three bands in this multi-spectral approach. AATSR includes a narrow band channel in the centred at 0.55 µm for this purpose.

Radiometric Requirements

The AATSR visible channels need to encompass all possible normal variations in brightness over the whole of the Earth's surface, except sunglint, without saturation. The maximum signal is derived by assuming the value at the top of the atmosphere with 100% spectral albedo of ideal Lambertian reflection. The 100% spectral albedo value should encompass most natural levels of reflected sunlight except sunglint. It is however possible that spectral radiance values greater than this can be obtained by the addition of an atmospheric signal due to aerosol scatter, or due to non-Lambertian reflection. For example, the highest cloud target reflectances are predicted to correspond to an effective albedo of 110-120%. Conversely, it may be found during flight that 100% albedo is unrealistically high for most situations of scientific interest. To maximise the precision of the measurements whilst retaining flexibility in the range of the instrument, the gain and offset of the AATSR visible channels are therefore selectable in flight.

In order for the instrument to successfully support land applications, it was considered desirable that AATSR should measure differences in vegetation reflectance of the order of ~1% for ~10% vegetation cover. Experience with the AVHRR (with 10-bit digitisation) and Landsat TM (with 8-bit digitisation) instruments has shown that in some circumstances they are inadequate, and that a signal-to-noise ratio of at least 20 to 1 at 0.5% albedo is necessary for the red and NIR bands. Also, ignoring atmospheric contributions, and with 10% ground cover by typical leaves (reflectances red: 5%, NIR: 50%) over a typical soil (reflectances red: 20%, NIR: 30%), this noise level would, in principle, enable ~2% differences in leaf area, for constant soil reflectances, to be measured. The signal to noise ratio for the AATSR visible channels has been set accordingly.
Calibration Requirements

To retrieve land parameters from AATSR detector signals by modelling, the spectral response and IFOV of the visible channels need to be measured prior to launch. Consequently, AATSR has undergone a rigorous pre-launch calibration campaign. In addition, for long term monitoring of land parameters, it is important to have confidence in the stability of the sensing system. Thus, an in-orbit calibration system for the visible channels is also included.

1.1.2.3 Cryosphere, Cloud and Atmospheric Measurements

Cloud and atmospheric measurements

The objective of research with (A)ATSR data in this field is to extend its usefulness as a research tool for cloud type identification and cloud top temperature measurement. The multi-channel and two-view features offered by the instruments are a powerful combination for cloud, aerosol and atmospheric investigations, in addition to the stereo viewing capability offered by the dual view.

Although the addition of the visible channels was primarily for land measurement, they also have a number of applications that will enhance cloud and atmospheric monitoring capabilities. In particular, the NIR band provides additional information, which is complementary to the 1.6 μm band, for ice/water cloud discrimination, and for sizing cloud droplets. Estimation of atmospheric aerosol loadings are of particular interest in quality assessing SST retrievals, which can be significantly affected during, for example, atmospheric contamination due to volcanic ash injections and schemes already exist to use the 1.6 μm channel to estimate aerosol optical depths over oceans.

Since a large part of the atmospheric attenuation/emission of thermal radiation in the atmospheric window regions used to remotely sense SST is caused by highly variable water vapour, it is possible to estimate the content of the atmospheric column from ATSR data. The accurate and precise measurement of atmospheric water vapour is potentially extremely important for climate research, as water vapour is the major greenhouse gas, and is also involved in atmospheric processes such as cloud formation, precipitation and evaporation.
Cryosphere

Variations in the annual sea ice growth and decay cycles in polar regions are a strong indicator of climatic change, particularly as modelling shows anthropogenic climate change to be pronounced in polar regions. In addition, the sea ice extent itself affects the climate (due to the difference in albedo of the sea ice in comparison with the ocean surface, and the thermal insulation), and so is an important parameter for climate modellers and for studies of ice-ocean-atmosphere exchanges.

Work with ATSR data, together with data from other ERS sensors (e.g. the Radar Altimeter (RA) and the Synthetic Aperture Radar (SAR)) has already proved effective in the study of Antarctic and Arctic sea ice boundaries, and the investigation of ice surface temperatures. The discriminatory power of the 1.6 μm channel for cloud and ice/snow is of particular interest, and the enhancements of cloud/ice discrimination with the reflection channels is a particular goal.

1.1.3 Principles of Measurement

The key measurement principles of the AATSR instrument are outlined below. Detailed information on the AATSR instrument can also be found in Section (Chapter 3.), The AATSR Instrument, of the Reference Guide.

1.1.3.1 The AATSR Instrument

The (A)ATSR instruments are unique in their use of along track scanning to provide two views of the surface and thus improve atmospheric correction. The surface is first viewed along the direction of the orbit track, at an angle of 55°, as the spacecraft flies towards the scene. Then, 150 seconds later, or when the satellite has moved approximately 1000 km forward along the ground track, a second observation is made of the same scene at the sub-satellite point, as shown in Figure 1.1 .

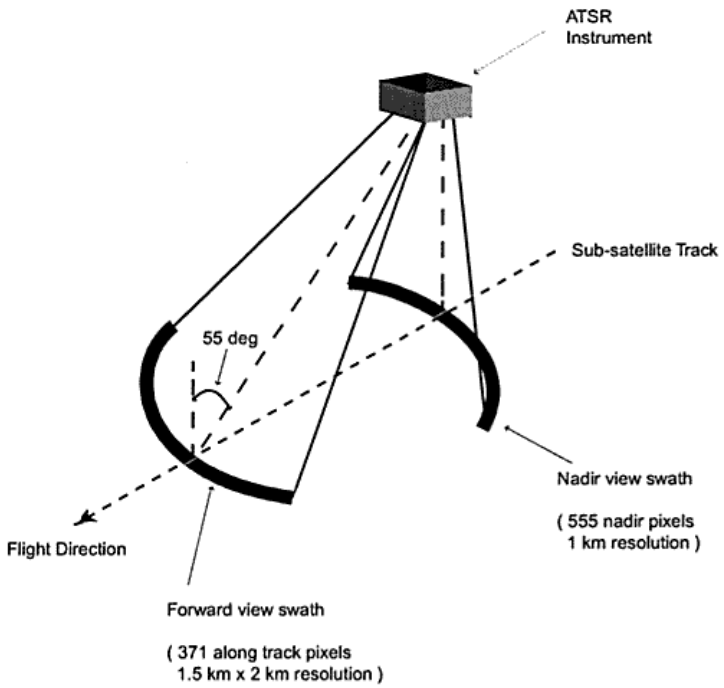

Figure 1.1 AATSR Viewing Geometry

The AATSR dual view is also described in more detail in Section 1.1.5. of this User Guide, on the Special Features of AATSR, with the geometry and pointing performance discussed in Section 3.2.1.3. of the Reference Guide.

The AATSR instrument itself is shown in Figure 1.2 .

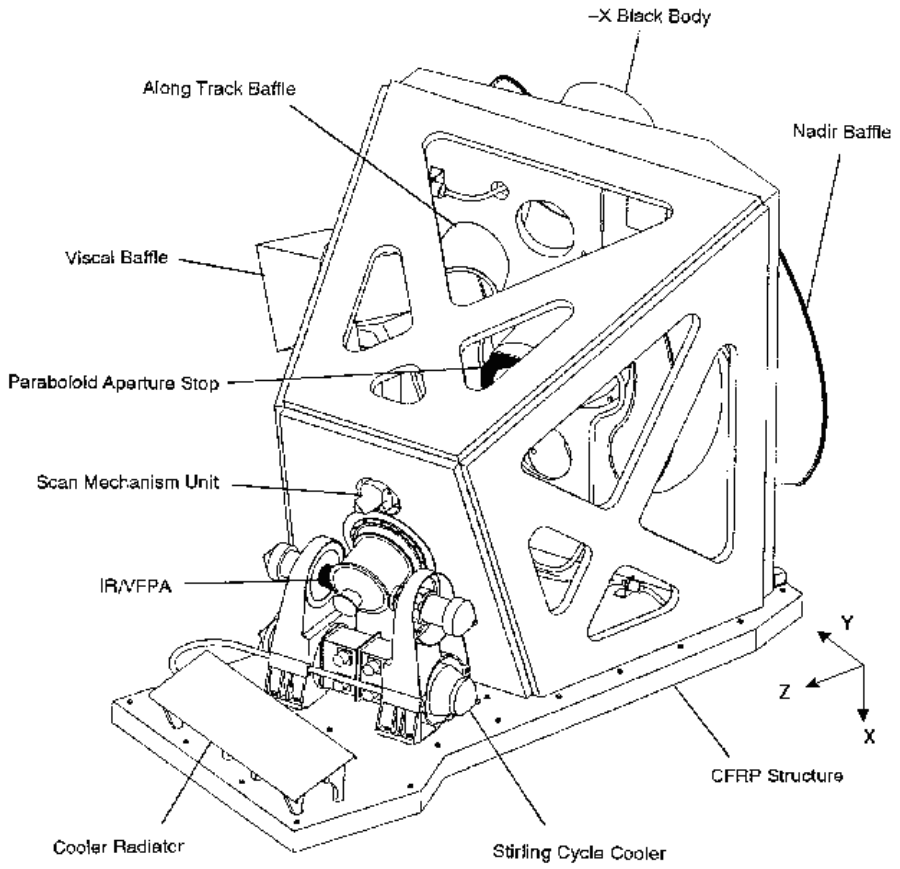

Figure 1.2 Main Features of the AATSR Instrument

In operation, infrared and visible energy is reflected off a Scan Mirror mounted on the Scan Mechanism onto a Paraboloid Mirror. From this mirror, the energy is then focused and reflected into the infrared and visible Focal Plane Assemblies (FPA) where detectors convert the radiant energy into electrical signals. The low level signals from the FPA are amplified, digitised formatted and passed onto other systems on the satellite to transmit them back to the Earth.

AATSR employs a pair of closed-cycle mechanical coolers
to maintain the thermal environment necessary for optimal operation of the infrared detectors. The FPA for the thermal infrared wavelength region is cooled to about 80 K whilst the FPA for the visible channels is maintained at ambient temperature.

In addition to the Earth view, the AATSR detectors also view calibration targets for the visible and thermal channels during each circular scan. Two stable high-accuracy blackbody targets provide calibration of the IR channels for every scan, whilst an on-board visible

calibration system (VISCAL) is viewed once per orbit.

Further information on the AATSR coolers and on-board calibration systems can also be found in Section 1.1.5. on the Special Features of AATSR.

1.1.3.2 AATSR Flight Operations

Information about the current and past status of the AATSR instrument and its performance is provided via the AATSR Operations website.

Modes

AATSR has a single operational mode, MEASUREMENT mode, for nominal routine operations. The only routine interruption to the data flow will occur when the cooled detectors are warmed up to ambient temperature to remove condensation that may have been deposited at low temperatures (a process known as outgassing).

Outgassing

Contaminants from the satellite continually condense onto the cold surfaces of the FPA and its detectors. This degrades instrument operation due to signal attenuation, and because the changed surface emissivities increase the radiative load on the cooler. Signal calibration is not affected by this phenomenon, as the view of the calibration targets is subject to the same modification as the Earth view. Nevertheless, occasionally the FPA is allowed to warm up to remove these contaminants.

Outgassing periods last about 2 days and occur at intervals of approximately 3 months. Information about such outgassing events is made available to users in advance on the AATSR Engineering Data System web site, accessible from the AATSR Operations website.

No useful thermal channel data are collected during these periods.

The operation of the visible detectors is unaffected by this warming, although care must be taken when using visible channel data acquired at this time. The 1.6um channel data is absent when the infrared FPA is warm, therefore the Flight Operations Support team are unable to generate daily ATS_VC1_AX files and there are no corresponding deliveries to the PDS.

Following an outgassing, for optimum calibration the supply of VC1 files once per orbit, rather than once per day, is recommended for approximately three weeks afterwards. The current FOS system is not designed to provide files at this frequency. Therefore, when the delivery of daily ATS_VC1_AX files resumes, the calibration of visible channel data acquired during this period is still considered to be sub-optimal.

A tool to provide VC1 files once per orbit for consolidated data processed off-line may be introduced in the future.

Low-Gain Configuration

It is possible to switch the 11 and 12 μm channels into a low-gain configuration, to facilitate the monitoring of 'hot' areas, however this can be done within MEASUREMENT mode, without the need to interrupt normal operations. The low-gain command applies for a number of scans in the range 1-1024, selectable by macrocommand. Data from the other 5 channels will be acquired as normal during this period. This function will only be used over large bodies of land, in order to preserve the primary mission objective of global SST retrieval. Use of this function will be restricted for the first few months of AATSR operation to allow for testing and improved configuration. Any operational use of this mode will be authorised by the AATSR Quality Working Group on a case by case basis.

Data Availability

Data from all of AATSR's channels will be available all of the time at full 12-bit digitisation. The improvements between ATSR-2 and AATSR in this respect are once again elaborated in section 1.1.5.4. , Special Features of AATSR.

Data from AATSR will be acquired globally, on a continuous basis, and stored on-board for subsequent transmission to the ground.

1.1.4 Geophysical Coverage

1.1.4.1 Instrument Swath

The AATSR field of view comprises two ~500 km-wide curved swaths, with 555 pixels across the nadir swath and 371 pixels across the forward swath, as shown in figure 1.3 . The nominal IFOV (pixel) size is 1 km^2 at the centre of the nadir swath and 1.5 km^2 at the centre of the forward swath. The scan cycle is repeated 6.6 times per second, and the sub-satellite point on the Earth's surface moves forward by 1 km (i.e. one pixel) during each scan cycle.

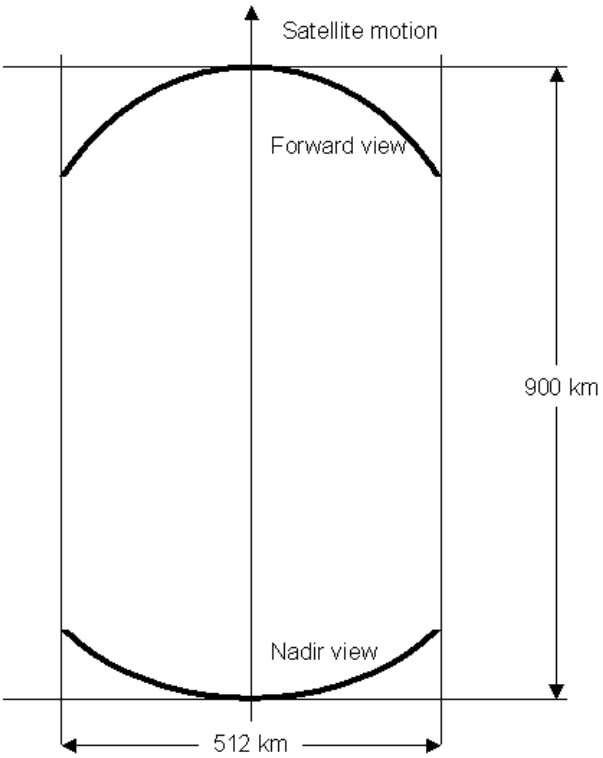

Figure 1.3 The AATSR Swath

1.1.4.2 Orbit and Repeat Cycle

ENVISAT is designed for a Sun-synchronous polar orbit. The planned operating altitude is 800 km, although a range of altitudes can be selected allowing variations in the repeat cycle of the ground track. In this way, ENVISAT can employ 3, 35 and 168-day repeat cycles. The 35 and 168-day cycles can provide complete global coverage by AATSR, but the 512 km swath width does not achieve complete coverage with the 3-day repeat cycle.

The local time at the equator for the descending node has been selected as 10:00 a.m., which optimises illumination conditions for the optical instruments. ENVISAT's orbit after launch will be adjusted to phase with ERS-2, such that the descending node crossing time of ENVISAT will be 30 minutes in advance of ERS-2.

The nominal orbit has a repeat cycle of 35 days and an orbital period of 100.6 minutes, with an inclination of 98.54 degrees. On-board systems allow the ground track to be maintained within 1 km and the local hour to within 5 minutes. In nominal operations, the satellite is pointed using star-trackers in a 'stellar yaw-steering mode'. In this mode, the satellite is

yawed to compensate for the apparent motion of the Earth across-track beneath the satellite.

1.1.5 Special Features of AATSR

AATSR has a number of special features including:

- On-board Calibration 1.1.5.1.
- Dual View 1.1.5.2.
- Coolers 1.1.5.3.
- Full 12 bit digitisation 1.1.5.4.

1.1.5.1 Onboard Calibration

The AATSR instrument has proven onboard calibration systems for the thermal and visible channels, to ensure that the science goals of AATSR are met.

Thermal Calibration System

Two black body reference targets are viewed on each scan, with one at roughly at 265K and the other at 305K, as this is expected to encompass the full global range of SSTs. They use the design concept which has been proven on ATSR-1 and ATSR-2.

The calibration sources are designed such that uncertainties in the radiance from them will not exceed an equivalent temperature error of more than 100mK throughout the mission (see section).

Visible Calibration

The visible calibration needs two sources for gain and offset measurements. By using one of the thermal calibration sources as a zero radiance calibration point, only one source of higher radiance is necessary. The calibration system for the reflection channels (VISCAL) provides a stable source for calibration once per orbit, using sunlight to illuminate a diffusing plate. The system has been proven on ATSR-2.

1.1.5.2 Dual View

As described already in section 1.1.3. , AATSR employs a dual view. This can improve the atmospheric correction and thus enable more precise sea surface temperature measurements. The (A)ATSR instruments have a viewing geometry where each terrestrial scene is viewed at two angles, at nadir and at a forward angle of 55°. From two views with different atmospheric path lengths, it is possible to obtain independent information about the atmospheric contributions to the signal, and perform an accurate atmospheric correction.

A dual view can also be used in land remote sensing to give information on the bi-directional reflectance distribution function of different surfaces.

1.1.5.3 Coolers

Another unique feature of the (A)ATSR design is the use of closed-cycle mechanical coolers to maintain the thermal environment necessary for optimal operation of the infrared detectors. The FPA for the thermal infrared wavelength region is cooled to about 80 K whilst the other is maintained at ambient temperature. ATSR-1 was the first environmental sensor to carry such a cooler into space.

1.1.5.4 Full 12 bit digitisation

AATSR offers the same combination of visible, near infrared and thermal channels as ATSR-2 but has the added advantage that the improved data rates available on ENVISAT will provide global coverage at the highest (12 bit) digital resolution over the whole swath throughout the orbit.

Details of the differences between the ATSR-2 and AATSR source packets are discussed in section 2.5.2. of the Reference Guide.

1.1.6 Summary of Applications vs Products

Table 1.1 lists the AATSR products and example applications for which they can be used. Further details of the AATSR products can be found in section (Chapter 2.), Products and Algorithms, and section (Chapter 6.), Data Formats, of the Reference Guide. Example images from ATSR-2 can also be found in the Image Gallery in section 1.4. of this User Guide.

Table 1.1 Summary of products vs. Applications

Product Name and ID	Contents	Applications
Level 0 6.4.1. ATS_NL_OP	Instrument Source Packets	Not generally available to users
Ungridded Counts (UCOUNTS)	Raw detector outputs in each channel, plus calibration data and auxiliary telemetry	A tool for AATSR instrument scientists and engineers Not an official ESA product, and not generally available to users
Ungridded Brightness Temperature/Reflectance Product (UBTR)	Calibrated measurement data in instrument scan geometry, plus target lat/long and ground track x/y coordinates for each pixel	A tool for AATSR instrument scientists and engineers. Also useful for scientific applications where it is important to retain pixel values in the original scan geometry and without

		cosmetic fill Not an official ESA product and not generally available to users.
Gridded Brightness Temperature/Reflectance Product 6.2.1. (GBTR) ATS_TOA_1P	Full (1 km) resolution TOA BT/reflectance for all channels and both views	L1B ocean, climate, land and cryosphere applications on local or regional scales: Ocean circulation Pollution monitoring Deforestation Land resource management Natural hazards urban growth/heat islands Land surface temperature Sea ice movement Cloud parameter retrieval
Gridded Surface Temperature Product 6.1.3. (GST) ATS_NR_2P	Full (1 km) resolution geophysical parameters over sea, land and cloud	L2 ocean, climate, land and cryosphere applications on local or regional scales: Surface/atmosphere heat transfer Climate modelling SST climatologies Oceanography Climate monitoring: greenhouse effect, El Niño Regional Land Surface Temperature Vegetation studies and resource management using NDVI Regional Cloud Top Temperature and Cloud Top Height*
Averaged Surface Temperature 6.1.1. (AST) ATS_AR_2P	Spatially averaged ocean, land and cloud parameters, plus spatially averaged BT/reflectance. Averaged over 10 and 30 arc minute and 17 and 50 km cells	Similar ocean, climate, land and cryosphere applications to GST above, but on a global scale.
Meteo Product 6.1.2. ATS_MET_2P	SST and averaged BT for all clear pixels in 10 arc min cells	NRT product for operational atmospheric and climate modelling
Browse Product 6.3.1. ATS_AST_BP	3 band colour composite browse image derived from L1b product, 4 x 4 km sampling	Low data volume NRT product for image previews and data selection

The 11µm BT is currently used in the GST product as a placeholder for Cloud Top Temperature retrievals. The Cloud Top Height field is currently set to zero.

1.2 How to use AATSR data

Documentation and Tools

An overview of the ENVISAT product formats is provided in the ENVISAT Products Specifications Document (PO-RS-MDA-GS-2009) Volume 5 - Product Structures Ref. [1.8].

Detailed product format information specific to the AATSR products can be found in Volume 7 of the ENVISAT Product Specifications Document Ref. [1.8] and in section (Chapter 6.) of the AATSR Reference Guide, on Data Formats (Chapter 6.)

There are a number of ways to approach the visualisation and analysis of AATSR data. The following subsections provide information on the software tools available:

- Software Tools 1.2.1. :
  - General tools 1.2.1.1.
  - EnviView 1.2.1.2.
  - Instrument Specific Software Tools 1.2.1.3.

Section 2.12. of the Reference Guide, Data Handling Cookbook, will also be used to detail miscellaneous tools and routines developed during the mission lifetime.

Disclaimers addressing issues affecting AATSR product quality are published at http://envisat.esa.int/dataproducts/availability/ .

Hints and Tips on Data Handling

There are a number of important concepts associated with the AATSR products that should be understood before trying to read and interpret the data. These include:

- The use of granules in the data processing.
- The use of tie points.
- The relationship between Measurement Data Sets and Annotation Data Sets.
- The AATSR GST product (ATS_NR__2P) as a 'switchable' product.
- The use of placeholder values, pending the development of more appropriate retrieval algorithms.
- How to visualise spatially averaged cells.
- The use of confidence words and exception values.
- Interpreting the AATSR topographic correction.

These are discussed in section 2.12.1. of the Reference Guide, in the Hints and Algorithms for Data Use section of the Data Handling Cookbook.

1.2.1 Software tools

The following categories of software tools can be used to explore AATSR products:

- General Tools 1.2.1.1.
- EnviView 1.2.1.2.
- Instrument Specific Software Tools 1.2.1.3.

1.2.1.1 General Tools

Users are free to write their own routines in C, IDL or other languages to read and process AATSR data. The detailed AATSR product specifications will assist with this task.

The EnviView 1.2.1.2. tool provided by ESA can also be used to convert ENVISAT data into hdf file format. This allows the data to be automatically read by any third-party software supporting this format. The use of this function within EnviView is strongly recommended for those who are unfamiliar with the ENVISAT product format.

A number of COTS image processing packages such as ERDAS, ENVI and Geomatica may

also extend their products to directly support the AATSR product format, in time.

The particular features of the AATSR products highlighted in section 1.2. under Data Handling Considerations should be taken into account when developing AATSR reading and data processing routines.

1.2.1.2 EnviView

EnviView is a tool specially developed to open and decode data in the ENVISAT format. It then provides the capability to display the contents of the products as simple text in HTML format, as graphs, or as images where these are appropriate. EnviView will also output products in hdf file format, allowing them to be read by other software packages supporting this format.

EnviView will be made freely available to all ENVISAT data users. Further information and copies of EnviView can also be obtained via EOHelp@esa.int.
The EnviView Charter

EnviView is a simple tool to provide a first look at ENVISAT data files in the PDS format. It is intended for the following purposes:

- To be able to open any Level 0, 1B, Level 2 or Auxiliary PDS data file;
- To determine the contents of a the file, and the value of any given fields in any data set (except raw source packets);
- To provide basic visualisation of data through simple 2D graphs;
- To visualise certain high level data sets in a meaningful manner where a 2D graph conveys little information:
  - image data sets from AATSR, ASAR and MERIS;
  - ASAR Wave spectra;
  - RA2 Waveform movie.
- To provide a representation of the geographic coverage;
- To export selected data to HDF, ASCII or binary data files, for analysis in other tools such as Mathematica, IDL, Excel, etc.;
- To save the contents of a record as HTML text for inclusion in reports;
- To print the contents of a record, or data view;
- To be highly portable, to reach as wide an audience as possible;
- It is guaranteed to run on Unix, Windows and MacOS and potentially other platforms too.

EnviView is not intended for the detailed analysis of ENVISAT data, there are many commercial and proprietary tools that provide better facilities.

The difference between such tools and EnviView is that they are more often than not aimed at certain classes of data, such as images or atmospheric data, or even data for a particular instrument. EnviView, however is a single solution for all PDS products.
Special Instructions

The following special instructions should be noted when using AATSR data in EnviView:
Gridded Surface Temperature (GST) Product: ATS_NR_2P

The GST product is switchable, meaning that the contents of the MDS depends on the settings of the land/cloud flags. The MDS also contains 2 image fields, the Nadir Field and the Combined Field. The mechanism for viewing these image fields within EnviView is currently as follows:

- Open the GST product.
- Select the New Image View menu item from the View menu.
- The Quantity drop-down box will display the available image fields in the MDS. Select the relevant field accordingly.
- Navigate around the image and adjust the colour settings as per the standard EnviView procedures.

Average Surface Temperature (AST) Product: ATS_AR_2P

The MDSs in the AST product represent images constructed from 10 and 30 arc minute and 17 and 50 km cells. These cells are referenced by cell latitude and longitude rather than being treated as pixels in a scan line. These images are therefore displayed on a world map using the EnviView 2-D Map View function, rather than using the Image Viewer. In this function, each cell is represented by a symbol (a solid box). The symbol size approximates the data sampling area and scales with the axis ranges of the map plot.

Taking the SST record 10 arc minute cell MDS as an example:

- Open the AST product.
- From the View menu, select the New 2-D Map View menu item.
- Select the data set of interest from the Data Set drop-down box, which in this case is SEA_ST_10_MIN_CELL_MDS
- Select the required field within the MDS under Value Field (in this case either the mean dual view SST (m_dual_vw) of the mean nadir SST (m_nad)) using the drop-down box.
- Specify the Record at which the plot should start and the number of Records/Plot and press Enter
- Adjust the colour settings/reset the zoom as per the standard EnviView procedures.

1.2.1.3 Instrument specific software tools

MERIS/(A)ATSR Toolbox

Overview

The Basic ERS & Envisat (A)ATSR and Meris Toolbox (BEAM) is a collection of executable tools and an application programming interface (API) which has been developed to facilitate the utilisation, viewing and processing of ESA MERIS, (A)ATSR and ASAR data. The purpose of BEAM is not to duplicate existing commercial packages, but to complement them with functions dedicated to the handling of ENVISAT MERIS and

AATSR products. The main components of the BEAM are:

- VISAT - A visualization, analyzing and processing software, entirely written in Java.
- A set of scientific tools running either from the command line or invoked by VISAT, also entirely written in Java.
- The BEAM Java API provides software frameworks and helpers for application development and new extension modules.
- ENVISAT MERIS/AATSR Product Access API for ANSI C allowing reading access to these data products using a simple programming model.

The development of the BEAM software is targeted as an open source project and comes with full source code. BEAM is available at: http://earth.esa.int/services/beam/

Architectural Design Goals

The primary design features of the BEAM are:

- Extendibility through software frameworks with dedicated plug-in points for extended functionality. This will allow for easy integration of new algorithms, new data product I/O formats and much more.
- An open source design which allows for distributed development resulting in a faster rate of growth, flexibility and stability.
- Portability through platform-independent design for use on all major operating systems. All components of the toolbox (except ANSI C library) are programmed in Java. The alpha release was tested successfully on Windows 95/98/NT4/2000, Linux, Solaris and MacOS X. The ANSI C API shall compile on any system with an ANSI-C compliant C compiler.
- High performance achieved by using optimized algorithms and frameworks. Image processing based on Java Advanced Imaging API (JAI).

More information is available from the envisat web site at http://envisat.esa.int/beam

1.3 Further Reading

Further information on the AATSR instrument can be found on the AATSR web page at http://www.leos.le.ac.uk/home/aatsr/, and on the ATSR-1 and ATSR-2 instruments at the Rutherford Appleton Laboratory web page at http://www.atsr.rl.ac.uk/.

Listed below are the documents referenced elsewhere in the handbook. For access to these documents please contact EOHelp@esa.int.

Ref 1.1
AATSR Commissioning Plan, PO-PL-RAL-AT-0501, Issue 1.3, 22 February 2001

Ref 1.2
AATSR Field of View Test Report, PO-TR-RAL-AT-0022, Issue 1, 26 March 1999

Ref 1.3
AATSR Flight Operation and Data Plan, PO-PL-ESA-AT-0152, Issue 2 Revision 5, 22 November 2001

Ref 1.4
AATSR Instrument Measurement Data Definition, PO-TN-MMB-AT-0038, Issue 1, December 1995

Ref 1.5
AATSR Infra-Red Radiometric Calibration Report, PO-TR-RAL-AT-0024, Issue 1, 26 May 1999

Ref 1.6
ENVISAT Mission Conventions Document, PO-IS-ESA-GS-0561

Ref 1.7
ENVISAT Product Format Guidelines, PO-TN-ESA-GS-0242

Ref 1.8
ENVISAT Product Specifications, PO-RS-MDA-GS-2009

Ref 1.9
AATSR Verification Plan, PO-PL-RAL-AT-0502, Issue 1.1, 12 September 2001

Ref 1.10
AATSR Visible Calibration Report, PO-TR-RAL-AT-0023, Issue 2, 8 July 1999

F. Martin Crespo, J.-P. Guignard, C. Garrido and M. Irie,
Ref 1.11
The Payload Data Segment, ESA Bulletin Number 106, June 2001

Ref 1.12
G. Mason, ATSR Test and Calibration Report, ER-RP-OXF-AT-0001, September 1991

Ref 1.13
J-M Melinotte, and O. Arino, The IONIA 1-km Net-Browser Experience - Quicklook Processing and Access Statistics, Earth Observation Quarterly, 50, 6-10, 1995

Ref 1.14
C.J. Merchant, A.R. Harris, M.J. Murray and A.M. Zavody. Towards the elimination of bias in satellite retrievals of sea-surface temperature. 1. Theory, modelling and interalgorithm comparison. Journal of Geophysical Research, 104 (C10), 23, 565 - 578, 1999.

Ref 1.15

R. W. Saunders, An automated scheme for the removal of cloud contamination from AVHRR radiances over Western Europe. Int. J. Remote Sensing, 7, 867 - 886, 1986

Ref 1.16
R. W. Saunders and R. T. Kriebel, An improved method for detecting clear sky and cloudy radiances from AVHRR data, Int. J. Remote Sensing, 9, 123 - 150, 1988

Ref 1.17
P.D. Watts, M.R. Allen, and T.J. Nightingale. Wind-speed effects on sea-surface emission and reflection for the Along-Track Scanning Radiometer. Journal of Atmospheric and Oceanic Technology, 13, No. 1, 126 - 141. 1996.

Ref 1.18
A.M. Zavody, C.T.Mutlow and D.T. Llewellyn-Jones. A radiative transfer model for sea-surface temperature retrieval for the Along-Track Scanning Radiometer. Journal of Geophysical Research, 100 (C1), 937 - 952, 1995.

Ref 1.19
A.M. Zavody, C.T.Mutlow and D.T. Llewellyn-Jones. Cloud Clearing over the Ocean in the Processing of Data from the Along-Track Scanning Radiometer (ATSR). Journal of Atmospheric and Oceanic Technology, 17, 595 - 615, 2000.

Ref 1.20
Routine Viscal Production, PO-TN-RAL-GS-0503

Ref 1.21
Prata, A.J. Land Surface Temperatures derived from the Advanced Very High Resolution Radiometer and the Along-Track Scanning Radiometer 2. Experimental results and validation of AVHRR algorithms. J. Geophys. Res. 99(D6), 13,025-13,058, 1994.

Ref 1.22
Land Surface Temperature Measurement from Space: AATSR Algorithm Theoretical Basis Document, Dr Fred Prata (CSIRO) 14 January 2002.

Ref 1.23
A.J. Prata, "Land surface temperatures derived from the AVHRR and the ATSR, 1, Theory," J. Geophys. Res., 98(D9), 16,689-16,702. 1993.

1.4 Image Gallery

ATSR and ATSR-2 data have been used for a number of applications. The image gallery shows a selected number of images covering different applications. More examples can be found at http://www.atsr.rl.ac.uk/images/index.html

and http://www.leos.le.ac.uk/home/aatsr/

1.4.1 Spatially Averaged Global SST, September 1993

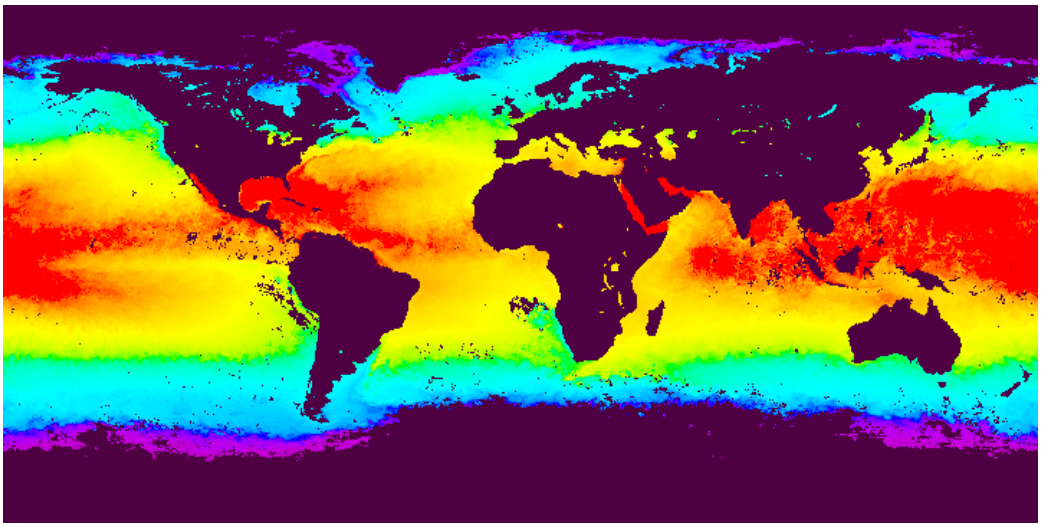

Figure 1.4 Spatially Averaged Global SST, September 1993

Spatially averaged, global sea surface temperature imagery for September 1993, derived from ATSR data. The temperatures are represented on a scale from purple/blue (coldest) through green to red (warmest). To the east of the USA, a thin tongue of warm water can be seen stretching northwards, the Gulf Stream.

1.4.2 Deforestation in Brazil

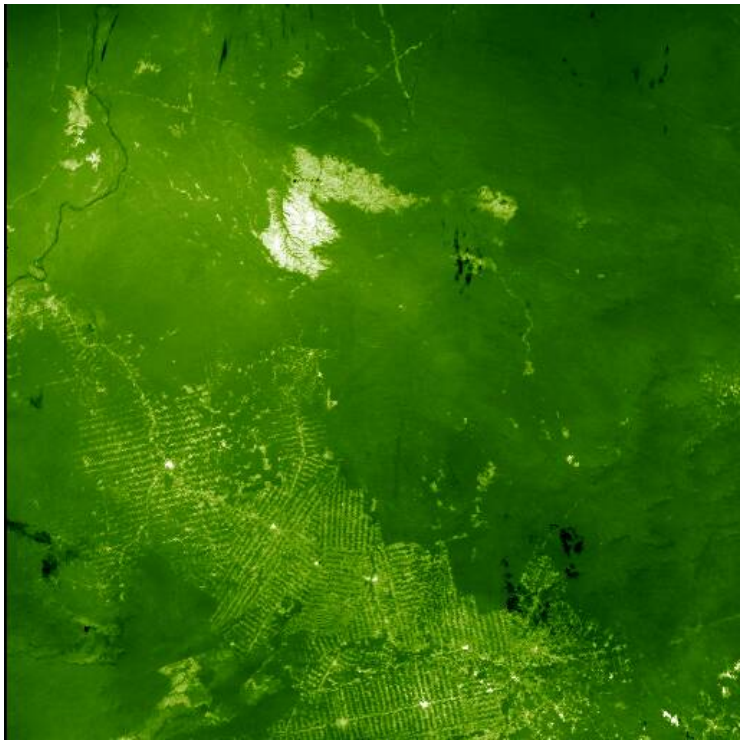

Figure 1.5 Deforestation in Brazil

Estimation of rainforest cover at the sub-pixel using ATSR-2 images of the Rondonia Province in Brazil. In this thermal ATSR-2 image of Rondonia, higher temperatures are represented by light green, decreasing to dark green. The lighter, 'lined' regions in the lower half are roads of deforestation, visible as higher temperature areas.

1.4.3 Mutsu Bay, Japan

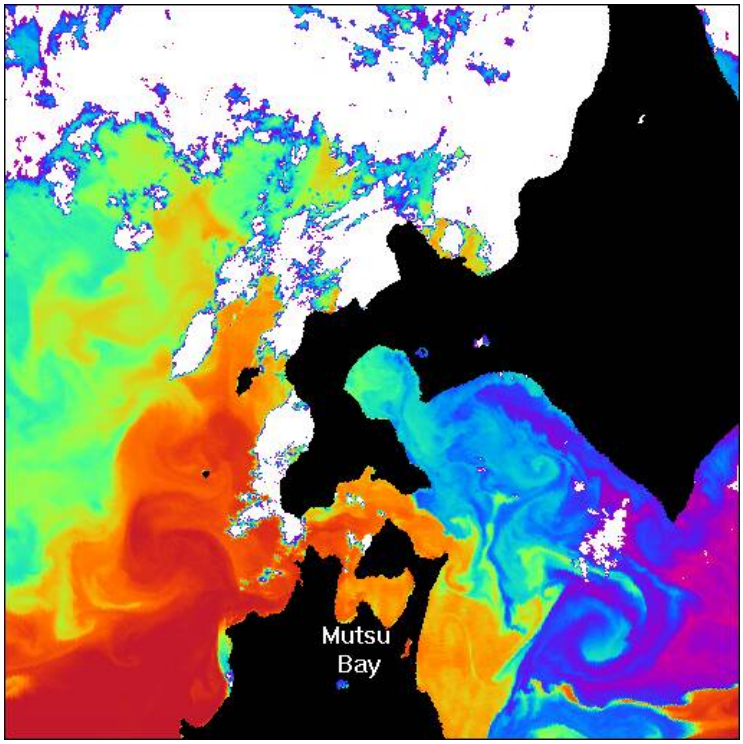

Figure 1.6 Mutsu Bay, Japan

This shows the relationship between radiometric measurements and the state of the ocean/atmosphere interface. In this thermal satellite image of northern Japan, the land has been masked in black and the clouds in white. Temperature patterns can clearly be seen on the surface of the ocean, with strong temperature gradients occurring over relatively small distances (few km). ATSR nadir view, 11µm brightness temperature histogram equalised between 274 (purple) and 284 (red) kelvin.

1.4.4 Typhoon Saomai

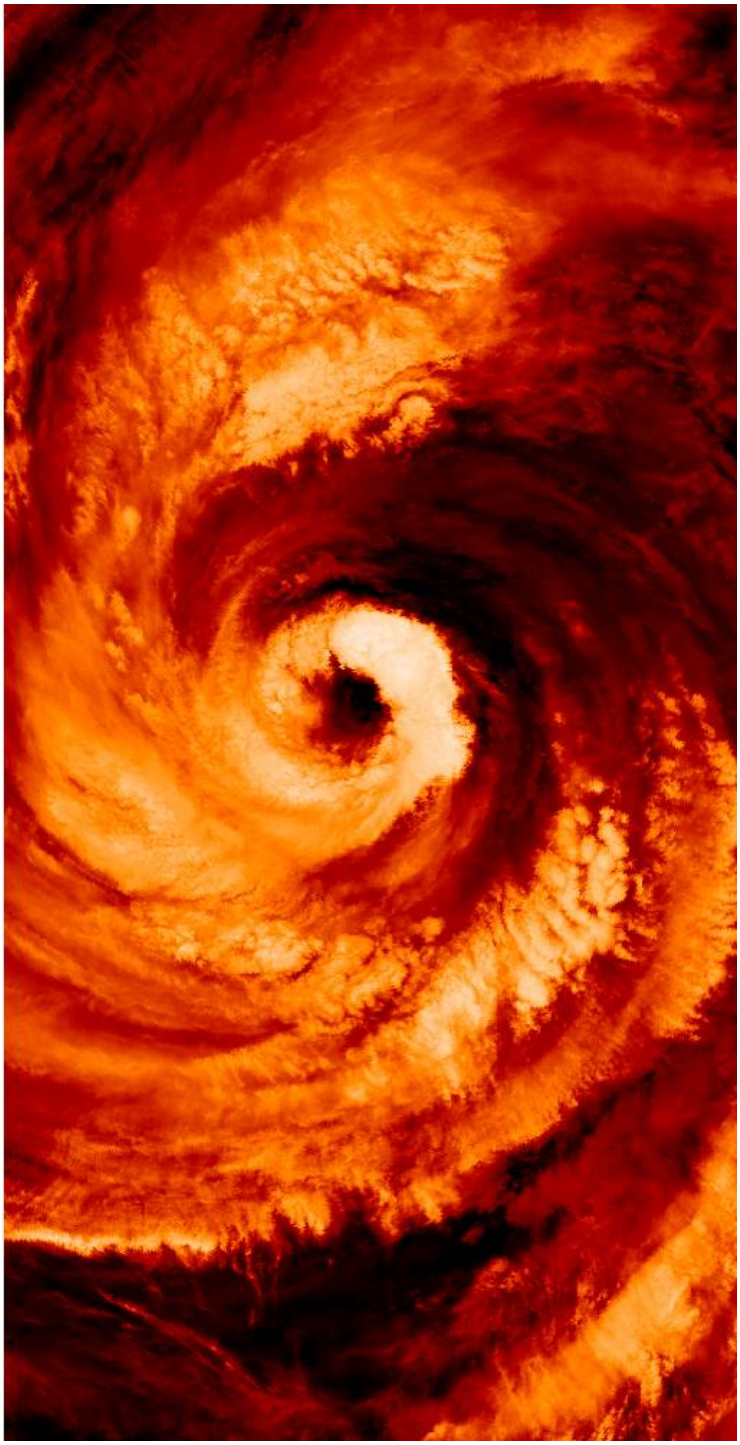

Figure 1.7 Typhoon Saomai

This is a night-time 11 μm false colour image, showing Typhoon Saomai over the East China Sea, heading north towards the Korean Peninsula. It was taken on the 13th September 2000.

1.4.5 Land cover in the Middle East

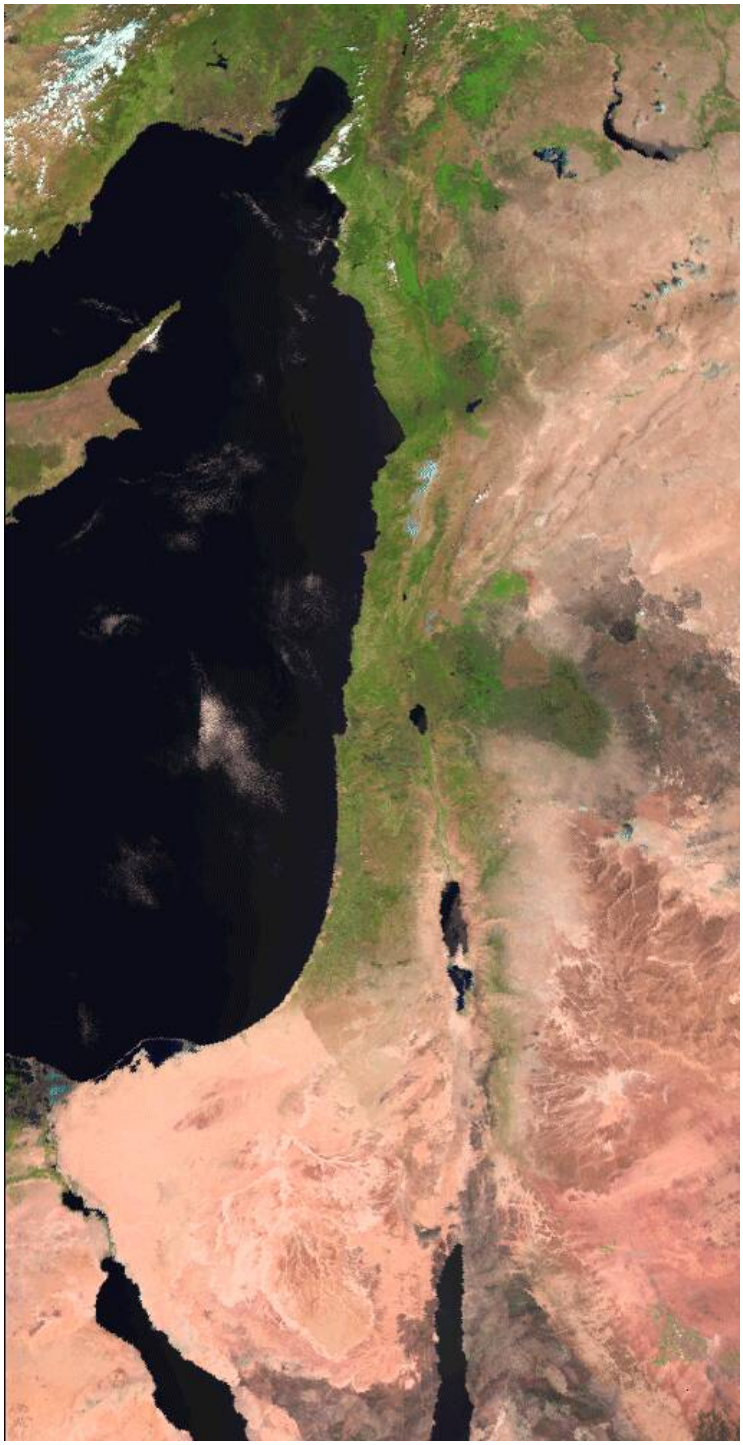

Figure 1.8 Land Cover in the Middle East

This image is a false colour composite, produced by combining uncalibrated detector counts from two of ATSR-2's visible wavelength detectors and the near infrared detector. The image was obtained from ATSR-2's nadir view, during a daytime pass of the Mediterranean Sea, and shows Cyprus, Israel and the Sinai Peninsula. The distinction between land cover change in Israel and Sinai can be clearly seen towards the bottom of the image.

1.4.6 Breakup of the Ross Ice Shelf

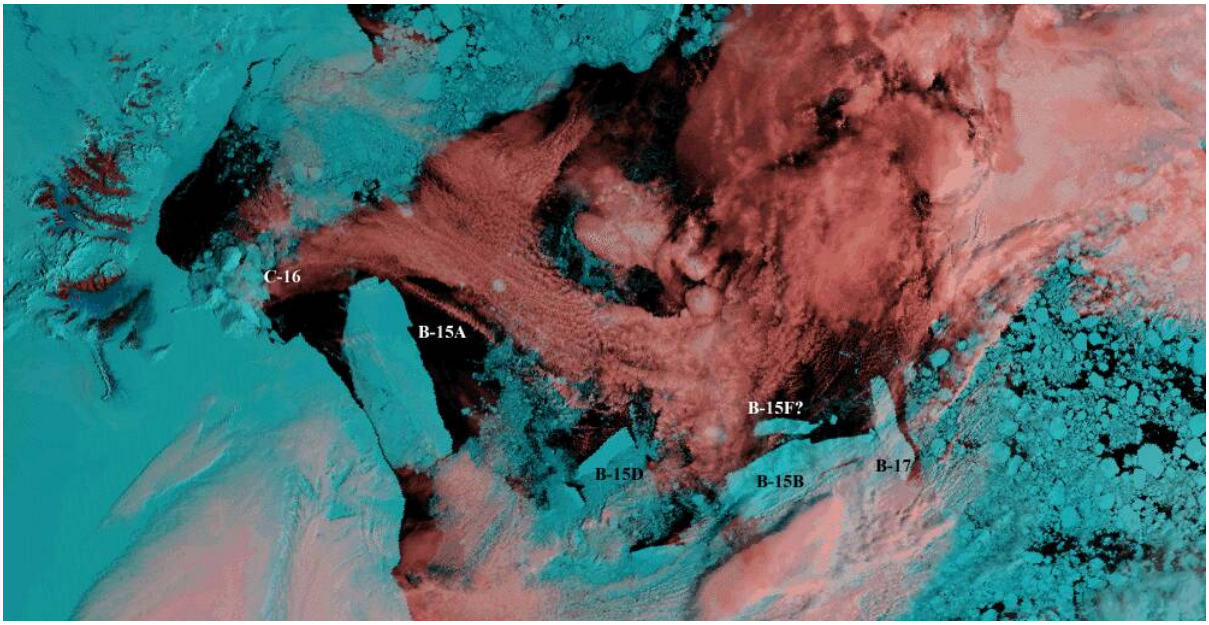

Figure 1.9 Breakup of the Ross Ice Shelf

Images collected at the Rutherford Appleton Laboratory show the breakup of the Ross Ice Shelf in the Autumn of 2000. This image was taken on the 7th December 2000, and shows the icebergs breaking away from the main ice sheet. The image is a visible day time image combining the 1.6, 0.87 and 0.67 μm wavebands.

Chapter 2

AATSR Products and Algorithms

This section of the AATSR Reference Guide provides detailed information on the AATSR instrument products and the data processing algorithms used to generate them. This information is broken down into the following sub-sections:

2.1 Introduction

The design of the ENVISAT Payload Data Segment (PDS) is summarised in 'The Payload Data Segment', ESA Bulletin Number 106, June 2001 Ref. [1.11].

2.1.1 Data Processing Centres

In common with data from other ENVISAT instruments, AATSR products generated in Near Real Time (NRT) will be processed at the Payload Data Handling Stations (PDHS) co-located with the various ENVISAT acquisition stations. Off-line processing and archiving of Level 1b (L1b) data will take place at the ENVISAT Low-rate Reference Archive Centre (LRAC) in Kiruna, followed by Level 2 (L2) processing at the Processing and Archiving Centre located in the UK (UK-PAC).

The target times for production of NRT and off-line products are given in section 2.10. .

2.1.2 Data Processing Software

All of the above centres will run the same version of the AATSR Instrument Processor Facility (IPF) software, thus ensuring that all centres use identical processing algorithms and product formats. The AATSR IPF is provided as an ENVISAT "Generic Element" which can be installed on the Processing Facility Host Structure (PFHS) at each centre. The AATSR IPF has been developed as part of the ENVISAT PDS Prime Contract, based on detailed specifications provided by the AATSR instrument provider, the UK Department for Environment, Food and Rural Affairs (DEFRA). The same specifications have also been implemented within a Prototype Processor (PP) operated by DEFRA. Test Data Sets (TDS) from the PP have been used to validate the operational IPF. All future updates to the IPF will also be verified against PP TDS. The PP may also be used in the future as a test bed for new or improved AATSR algorithms.

2.1.3 Heritage

The processing algorithms for AATSR are based on those developed for ATSR-1 and ATSR-2, and use the ATSR SADIST (Synthesis of ATSR Data Into Surface Temperatures) software as a basis. This has essentially been re-engineered for AATSR, to allow it to be integrated into the wider ENVISAT PDS architecture. However, algorithms used within SADIST have been directly re-used for AATSR wherever possible to maintain consistency across the three missions.

The differences between ATSR and AATSR products are therefore primarily in the area of product format and structure rather than scientific content. Many of these differences arise from requirements imposed by the ENVISAT project to ensure a uniform product structure across all instruments. See section (Chapter 6.) for detailed product format information.

For AATSR, a number of enhancements to the original ATSR products have also been introduced. These include:

- The use of more accurate ellipsoidal, rather than spherical, geometry in the geolocation scheme (see section 2.6.1.1.5.);
- A change in the along-track sampling of the image grid from a fixed spacing of 1 km to sampling equally spaced in time (see section 2.6.1.1.7.);
- Use of generic ENVISAT routines for time correlation, orbit propagation and geolocation, to ensure coherence between all ENVISAT instruments;
- Operational calibration of the AATSR visible channels (see section 2.6.1.1.3.);
- The inclusion of a topographic correction to the latitude and longitude of pixels over land (see section 2.6.1.1.5.4. - this algorithm description needs to be expanded eventually);
- The introduction of a Normalized Difference Vegetation Index (NDVI) retrieval over land (see section 2.7.1.2.).

2.2 Organisation of Products

2.2.1 ENVISAT Product Organisation

ENVISAT PDS files fall into the following 5 distinct classes:

- Level 0 products - raw data source packets from the satellite, wrapped in a PDS-compatible file structure;
- Level 1B products - calibrated and geolocated engineering units, with auxiliary data separated from measurements;
- Level 2 products - geolocated geophysical products in which L1B data has been transformed through higher-level processing into geophysical quantities;

- Browse products - low resolution overviews of L1B or L2 image products provided for catalogue browsing;
- Auxiliary products - external data used at various stages of the ground processing, including instrument characterisation measurements, calibration settings and meteorological and orbit predictions.

The naming convention for ENVISAT products is summarised as follows.

filename = <product_ID> <processing_stage_flag> <originator_ID><start_day> <"_"> <start_time> <"_"> <duration> <phase> <cycle> <"_"> <relative_orbit> <"_"> <absolute_orbit> <"_"><counter> <"."> <satellite_ID> <.extension>

These fields are described in detail below, with reference to the following example AATSR file:

ATS_MET_2PNPDK20050301_094558_000066812035_00108_15693_2654.N1.gz

Product ID (ATS_MET_2P)

10 character string identifying sensor, processing level and type of product (P = parent, C = child).

Processing Stage Flag (N)

Set to "N" for Near Real Time product

Set to "V" for fully validated (consolidated) product

Set to "T" for test product

Set to "S" for a special product.

Letters between N and V are assigned in order of level of consolidation (i.e., closer to V = better consolidated)

Originator ID (PDK)

Identifies the centre that generated the file. The 3-character code may be one of the following:

PDK = PDHS-K

PDE = PDHS-E

LRA = LRAC

PDC = PDCC

FOS = FOS-ES

PDA = PDAS-F

U-P = UK-PAC

D-P = D-PAC

I-P = I-PAC

F-P = F-PAC

S-P = S-PAC

E-P = E-PAC

ECM = ECMWF

Start Day (20050301)

The start day of the product from the UTC time of the first DSR. The format is YYYYMMDD.

Start Time (094558)

The start time of the product from the UTC time of the first DSR. The format is HHMMSS.

Duration (00006681)

Time coverage of the product expressed in seconds. If the duration of a product is not relevant information, it will be set to "00000000".

Phase (2)

Mission phase identifier.

Cycle (035)

Cycle number within the mission phase.

Relative Orbit (00108)

Relative orbit number within the cycle at the beginning of the product.

Absolute Orbit (15693)

Absolute orbit at the beginning of the product.

Counter (2654)

Numerical wrap-around counter for quick file identification. For a given product type the counter is incremented by 1 for each new product generated by the product originator.

Satellite ID (.N1)

E1 = ERS-1, E2 = ERS-2, N1 = ENVISAT-1

Extension(.gz)

Optional field. Used only for distribution to users to indicate common archiving and compression standards if used (e.g., .gz, .Z,.tar, .tarZ, .gif, .jpeg, etc.).

All products in the above categories conform to the following structure:

- A Main Product Header (MPH);
- A Specific Product Header (SPH), including a number of Data Set Descriptors (DSDs) which provide a directory of the remaining data sets in the file;
- Measurements Data Sets (MDS);
- Annotation Data Sets (ADS);
- Global Annotation Data Sets (GADS).

The format of the MPH is identical for all products. The SPH is specific to each product or group of related products. The MPH and SPH are written in plain ASCII text. The rest of the file is in binary format, except for a few products (none from AATSR) that also have ASCII ADS or MDS.

Each MDS, ADS or GADS consists of a sequence of data set records, containing one or more fields of data. The format of all data sets for all instruments is described in the ENVISAT Product Specifications document (PO-RS-MDA-GS-2009) Ref. [1.8] and can also be displayed via EnviView.

A MDS contains data derived from instrument measurements and related processing or instrument information. Every MDS has a time stamp indication the time of the measurement. An ADS contains processing information related to measurements such as geolocation, or quality parameters, and is also time-stamped with the time of the related measurements. The GADS contain processing configuration data that apply to the entire product and are not related to individual measurements, and hence have no time stamp.

2.2.2 AATSR Product Organisation

The AATSR products available from the PDS and their respective processing levels are summarised in table 2.1 .

Table 2.1 AATSR Products and Processing Levels

Level	Product	Product ID	Contents
0	Level 0 2.5.4.1.	ATS_NL_0P	Instrument Source Packets
1B	Gridded Brightness Temperature/Reflectance Product (GBTR)	ATS_TOA_1P	Full (1 km) resolution TOA BT/reflectance for all channels and both views
1B	Browse Product	ATS_AST_BP	3 band colour composite image derived from nadir only GBTR product, 4 x 4 km sampling
2	Gridded Surface Temperature Product (GST)	ATS_NR_2P	Full (1 km) resolution geophysical parameters over sea, land and cloud
2	Averaged Surface Temperature (AST)	ATS_AR_2P	Spatially averaged ocean, land and cloud parameters, plus spatially averaged BT/reflectance Averaged over 10 and 30 arc minute and 17 and 50 km cells
2	Meteo Product	ATS_MET_2P	SST and averaged BT for all clear pixels in 10 arc min cells

Product sizes and processing latency are discussed in section 2.10. .

The AATSR Prototype Processor (PP) operated by DEFRA also generates two internal products (table 2.2) mid-way through the L1b processing. These are not official ESA products and are not available through the PDS. These products are principally used by the instrument science and engineering teams to monitor instrument performance and internal data processing parameters.

Table 2.2 AATSR Internal Ungridded Products

Level	Product	Product ID	Contents
1	Ungridded Counts (UCOUNTS) 2.6.2.2.1.	N/A	Unpacked raw detector counts in each channel, plus calibration data and auxiliary telemetry
1	Ungridded BT/Reflectance (UBTR) 2.6.2.2.2.	N/A	Calibrated measurement data in instrument scan geometry, plus target lat/long and ground track x/y coordinates for each pixel

AATSR products are of two types: full resolution products, and averaged products. The full resolution products are image products based on a rectangular grid of 1 km nominal resolution, centered on the satellite ground track. Because of the conical scanning geometry of AATSR, the pixels measured by the instrument fall on curved scan lines, and must be re-sampled onto a rectangular grid.

This is done by migrating each pixel to the nearest grid point. This process will not completely account for every grid point, since in some parts of the scan the density of

measured scan pixels is lower than the grid point density, so to allow for this a cosmetic fill operation is then carried out. The net result is that each MDS pixel is a measured scan pixel, but displaced in position. If a pixel within the grid has been cosmetically filled, this is indicated in the corresponding confidence word, in which bit 1 will be set.

Averaged quantities in the AST product are provided at two different resolutions, and with respect to two different averaging schemes as described in Section 2.7.1.3. (Half-Degree cells) and Section 2.7.1.4. (50 km cells)

Averaged brightness temperatures and reflectances are generated from the Level 1B regridded brightness temperatures and visible channel reflectances. Two different averaging schemes are used. For the first of these, the globe is imagined to be divided into cells 0.5° in latitude by 0.5° in longitude, and these cells are further subdivided into 9 sub-cells extending 10 arcmin in latitude by 10 arcmin in longitude. Averaged brightness temperatures and reflectances are derived, for cloud-free and cloudy pixels separately, by averaging the data over these cells and sub-cells.

Each cell is further subdivided into 9 sub-cells each extending 10 arc minutes in latitude by 10 arc minutes in longitude. Similar spatially averaged quantities, averaged over cells and sub-cells of nominal dimensions 50 km by 50 km and 17 km by 17 km respectively, are derived to give an alternative averaged product based on equal area cells.

All archived AATSR products will be orbit-based (unlike full resolution ATSR-2 products, which are scene based) and will conform to the common ENVISAT product structure described above. The data sets may include both Measurement Data Sets (MDS), containing instrument data, and Annotation Data Sets (ADS), containing auxiliary data. An AATSR product data set record corresponds to an across-track image row in the full resolution products, or to a cell in the Level 2 averaged product.

2.2.3 Relationship Between AATSR and ATSR Products

The relationship between the AATSR and ATSR product sets is shown in table 2.3 .

Table 2.3 Relationship Between AATSR and ATSR-2 Products

Product ID	AATSR Product	Equivalent SADIST-2 Product
ATS_TOA_1P	Gridded Brightness Temperature and Reflectance Product (GBTR)	GBT
ATS_AST_BP	Browse Product	New product - no SADIST equivalent (NOT equivalent to the GBROWSE)
ATS_NR__2P	Gridded Surface Temperature Product (GST)	GSST
ATS_AR__2P	Averaged Surface Temperature Product (AST)	Combines elements of ASST, ABT and ACLOUD
ATS_MET_2P	Spatially Averaged BT and SST for Meteo users (Meteo)	NRT only. Derived from AST Product

NB: The internal UCOUNTS and UBTR products generated by the PP are the equivalents of the ATSR UCOUNTS and UBT.

2.3 Definitions and Conventions

2.3.1 Definitions

Across-track band: The instrument swath is imagined as divided into 10 bands of width 50 km parallel to the ground track. The bands are symmetrically arranged on either side of the ground track, so that for example Band 0 covers the range -250 < x < -200 km, and Band 5 covers the range 0 < x < 50 km. Historically these were originally defined as part of an earlier ATSR SST retrieval algorithm. In this role they are now obsolete, but the structure of the across track bands are still used internally by processor, in particular in relation to the cloud clearing algorithms, and the solar and viewing angles are sampled at the band edges.

Cell (AST): An area spanning 0.5 degree in latitude by 0.5 degree in longitude or 50km by 50km depending on the data set in question, within which pixels contribute to the averaged product.

Granule: A subdivision of the AATSR image. In general 1 granule corresponds to 32 image rows, although the Summary Quality ADS is based on a 512 row granule. In general, a granule is a group of consecutive records in a Measurement Data Set; the number of such records is instrument dependent. Thus for the AATSR full resolution products, the granule is 32 records. It is intended to be the minimum increment used to define the limits of a child product. With the exception of the Summary Quality ADS, all Annotation Data Sets in the AATSR products contain 1 record per granule.

Image pixel: Image pixels are samples of the full resolution product.

Image row: A row of image pixels orthogonal to the satellite ground track. AATSR images are regridded onto a rectangular grid of image pixels centred on the satellite ground track. The image row comprises 512 image pixels.

Instrument pixel: The AATSR scan mirror rotates clockwise (as seen from above) at a uniform rate of 400 revolutions per minute, and so making one rotation in 150 ms. The instrument channels are sampled 2000 times per rotation at equal intervals of time. The instrument thus measures 2000 instrument pixels at equal angular intervals around the scan. Not all of these samples represent a valid measurement, however, since for parts of the scan the instrument is observing parts of the instrument housing.

For this reason not all of these samples are returned in the telemetry. The instrument source packet contains 974 samples (instrument pixels) in 5 groups of contiguous pixels corresponding to the 5 views; VISCAL, nadir view, +X black body, forward view, -X black body (section 3.1.3. and figure 3.8).

Pixel selection map The pixel selection map defines which of the 2000 pixel samples are actually transmitted to the ground. Strictly it is an array within the DEU with an entry for each pixel to indicate whether or not to format science data for that pixel (Reference: AATSR Instrument Measurement Data Definition Ref. [1.4], PO-TN-MMB-AT-0038). It is possible to update the pixel selection map in flight by macrocommand.

The pixel selection map in use, which is required to unpack the pixel counts in the ground processing, is defined by parameters in the auxiliary data block of the instrument source packet. These parameters are as follows.

Table 2.4 Auxiliary data items defining the pixel selection map

Telemetry mnemonic	Telemetry identifier	Telemetry description
A2200	IDF20	Pixel Map Readout (VISCAL Start pixel number)
A2210	IDF21	Pixel Map Readout (VISCAL End pixel number)
A2220	IDF22	Pixel Map Readout (Nadir Start pixel number)
A2230	IDF23	Pixel Map Readout (Nadir End pixel number)
A2240	IDF24	Pixel Map Readout (+XBB Start pixel number)
A2250	IDF25	Pixel Map Readout (+XBB End pixel number)
A2260	IDF26	Pixel Map Readout (Along Track Start pixel number)
A2270	IDF27	Pixel Map Readout (Along Track End pixel number)
A2280	IDF28	Pixel Map Readout (-XBB Start pixel number)
A2290	IDF29	Pixel Map Readout (-XBB End pixel number)

Since pixel numbering is contiguous in each scan section, it is always possible to determine the pixel number of a given pixel in any of the scan sections from these values. (Pixel numbering starts at 1 rather than 0.)

The default pixel selection map includes 555 nadir view pixels, 371 forward view pixels, sixteen pixels for each of the two black bodies, and sixteen VISCAL pixels.

Instrument scan: The locus of the line of sight of the scan mirror on the Earth's surface. It is the intersection of the scan cone with the surface, and is approximately elliptical in shape. An instrument scan corresponds to a single telemetry source packet in the Level 0 data.

Sub-cell (AST): An area spanning 10 arc minutes of latitude by 10 arc minutes of longitude or 17km by 17km depending on the data set in question, within which pixels contribute to the averaged product. A sub-cell is one-ninth of an AST cell (q.v.). The sub-cells within each cell are identified by an index in the range 0 to 8 as follows:

Table 2.5 Sub-cell indices within a cell

6	7	8
3	4	5
0	1	2

Unfilled pixel: An image pixel to which no instrument pixel is mapped by the regridding and cosmetic fill processes. Unfilled pixels fall outside the image swath, or beyond the limits of the instrument data that contributed to the product. This is a purely geometrical property of the pixel. Thus an unfilled pixel is to be distinguished from an invalid pixel; the latter is associated with an invalid measurement, while an unfilled pixel is not associated with any measurement.

Definition of cell and sub-cell: To be completed

2.3.2 Conventions

The x and y axes of the image plane are defined as follows.

The x axis is directed in the across-track direction, at right angles to the satellite ground track, and is directed towards the right of the track viewed in the direction of satellite motion. The ground track defines the origin of the x co-ordinate.

The y axis is tangent to the satellite ground track, in the direction of satellite motion.

The relationship of some of these concepts to the surface projection of the scanning geometry is illustrated in figure. 2.1

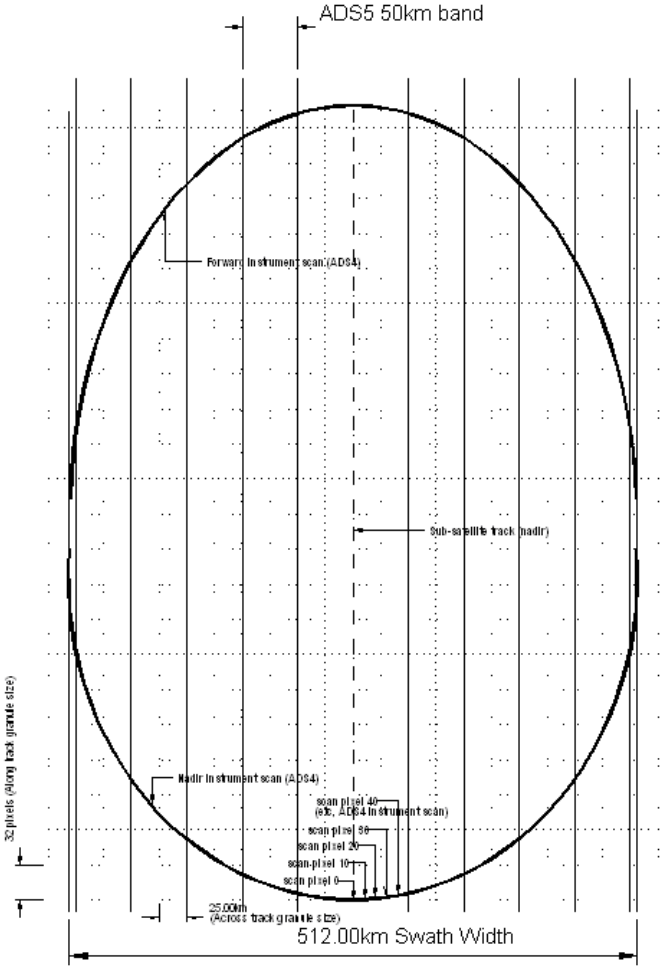

Figure 2.1 Image Concepts and their Relationship to the Surface Projection of the Scan

Bit numbering. Bits within a 2-byte product field are numbered from bit 15 (most significant bit) to bit 0 (least significant bit) (reference ENVISAT Product Specifications Ref. [1.8], PO-RS-MDA-GS-2009).

Relationship between nadir time (record time tag) and measurement time.

The ENVISAT Product Format Guidelines Ref. [1.7] (Document Ref. PO-TN-ESA-GS-0242) require that all data records in a product be provided with a time tag. However, because of the curved scanning geometry of AATSR, a given MDS record will contain pixels from a range of instrument source packets (corresponding to instrument scans). For example, each record of a full resolution product, corresponding to an image row, will contain pixels from some 100 source packets covering 15 seconds of measurement time.

Similarly each cell and sub-cell of an averaged product will contain pixels from a range of source packets. The following conventions are therefore adopted:

•

Full resolution products: The time associated with each record is the time at which the satellite ground track intersects the image row; this is the time at which the satellite was vertically overhead at the centre of the row. This is described as the 'nadir UTC time' in product descriptions, and corresponds to the scan time of the nadir pixel.

Note that the earliest pixels in time to contribute to a row of the nadir view image are those at the edge of the measurement swath. The time stored with each record of the forward view image is the nadir time of the corresponding nadir view image, although the forward view pixels that contribute to a given row are measured up to 135 seconds earlier than the corresponding nadir view pixels. Essentially, therefore, the nadir time associated with an image row is the time of the latest instrument scan to contribute to the row.

- Averaged products: The time associated with each record is the instrument scan time of the first nadir view pixel to fall within the cell or sub-cell, as appropriate. In this definition the first pixel means the first pixel encountered in the product processing, not the first pixel in time. Usually it will be one of the corner pixels, although which one will depend on the local geometrical relationship between the cell or sub-cell and the image axes.

Image co-ordinates and mapping:

AATSR images are samples on a rectangular array of pixels uniformly spaced in the x and y image co-ordinates. The x co-ordinate of an image point is the distance between the pixel and the ground track, measured along the normal section through the pixel that intersects the ground track at right angles. If the pixel is at point P and the intersection is at point Q, this is the distance PQ. (Strictly the normal section referred to here is the section that is normal to the ellipsoid at the point of intersection Q, not at P. See the fuller discussion in Section 2.6.1.1.5.2.1.1.)

The y co-ordinate is the distance measured along the satellite ground track to the point of intersection Q from an origin that depends on the product. In the case of consolidated products the origin is the ascending node of the orbit on the equator, but in the case of NRT products the origin may be an arbitrary point at the start of the product.

The across-track sampling interval Δ_x is 1 km. The along track sampling interval Δ_y = v x dt where v is the speed of the sub-satellite point along the ground track and dt = 0.150s is the AATSR scan period. The interval Δ_y varies around the orbit because v does. This equal time interval sampling means that the along track interval between image rows is that same as that between instrument scans.

Instrument pixels are located on the image grid by taking the integer part of their x and y co-ordinates (the latter in terms of the local sampling interval relative to a nearby tie point) and assigning the pixel to the corresponding image point. It follows that the co-ordinates assigned to an image pixel refer to the lower left corner of the pixel, thought of as a rectangular area.

Note that this is true of the latitude and longitude co-ordinates as well as the xy co-ordinates. In particular the ground track may be imagined to lie along the boundary between the 256th and 257th pixels in each image scan, and the latitude and longitude assigned to the 257th image pixel refers to a point on the ground track.

Instrument scan tie pixels:

The scan and pixel number ADS in the gridded AATSR products (ATS_TOA_1P and ATS_NR__2P) contain the x and y co-ordinates of original instrument pixels. Unlike the contents of other gridded product ADS, these values are not sampled with respect to the grid of image pixels, but refer to specific tie pixels on particular instrument scans.

Values are provided for every 32nd instrument scan, and each record of the ADS corresponds to one such scan. The x and y co-ordinates of intermediate pixels can be found from these ADS values using bilinear interpolation with respect to scan number and pixel index. Indices of the tie pixels within each scan are provided in the Specific Product Header, in the fields designated 'xy tie points'. A value is provided for every tenth pixel, with the proviso that where the final pixel of a view is not a multiple of 10, a value for this last pixel is provided.

Nadir and forward pixels are indexed separately, the nadir view pixels from 0 to 574, and the forward pixels from 0 to 390, giving 59 and 40 tie pixels respectively, and it is this relative index that is shown in the product header. This is also the index that is given in the scan and pixel number ADS.

The relationship between the relative pixel index and the absolute scan pixel number (which is proportional to the rotation angle of the scan) can be found using the auxiliary parameters first_nadir_pixel_number and first_forward_pixel_number found in the auxiliary file of Level 1b Characterisation Data ATS_CH1_AX. For nadir view pixels,

absolute pixel number = relative pixel index + first_nadir_pixel_number,

and for the forward view

absolute pixel number = relative pixel index + first_forward_pixel_number .

2.4 Product Evolution History

February 2002 V5.01

Launch version.

June 2002 IPF V5.02

Scan jitter error corrected. The IPF wrongly treated scans affected by scan mirror jitter as invalid, resulting in missing scans on images.

Browse algorithm modified to provide visual improvements. Histogram equalisation was removed from the daytime algorithm and the night-time algorithm concept was simplified.

July 2002 IPF V5.52

Internal change (i.e. not affecting the processing algorithms) to address an overflow problem with the variable SAT_BINARY_TIME.

Date TBD – auxiliary data update

New ATS_VC1_AX file supplied to correct scaling errors in pre-launch file (shortlty after, replaced by daily VC1 files provided by the AATSR Flight Operations Support Team).

October 2002 – auxiliary data update

New ATS_INS_AX supplied to prevent spurious BBU temperature validation warnings (internal issue, not visible in delivered data).

November 2002 – auxilliary data update

New ATS_CH1_AX file submitted to the PDS containing updated misalignment parameters, AOCS parameters and regridding tolerances. This improved the co-location between the forward and nadir views.

February 2003 IPF V5.55

Update containing modifications to the VISCAL algorithm (and associated ATS_PC1_AX auxiliary file). The original VISCAL algorithm did not work with real AATSR data because of undocumented differences in VISCAL monitor sampling between ATSR-2 (from which all test data were derived) and AATSR. The VISCAL GADS in all L1b data generated prior to this date were missing.

March 2004 IPF V5.58

Update containing:

- a new L2 LST retrieval algorithm (only applied within the ATS_NR__2P product, not available in ATS_AR__2P);
- a further modification to the VISCAL search algorithm to allow it to search backwards from the time of the OSV in the MPH (required for NRT data which is not partitioned from ANX to ANX and where the VISCAL peak may precede the OSV).

July 2004 IPF V5.59

Update containing:

- a change to the facility responsible for setting the REF_DOC field in the MPH (from PFHS to IPF);
- a change to the internal handling of CFI warning messages.

Neither of these changes have any impact on the delivered data.

August 2004 – auxiliary data update

New ATS_PC1_AX file supplied, updated with revised solar irradiance data (carried through into the output VISCAL GADS in the L1b product.

December 2004 – auxiliary data update

New ATS_GC1_AX file supplied, to correct the application of the 1.6 micron non-linearity correction.

2.5 Level 0 Products

2.5.1 AATSR Instrument Source Packet

The format and contents of the AATSR Instrument Source Packet (ISP) is summarised in figure 2.2 .

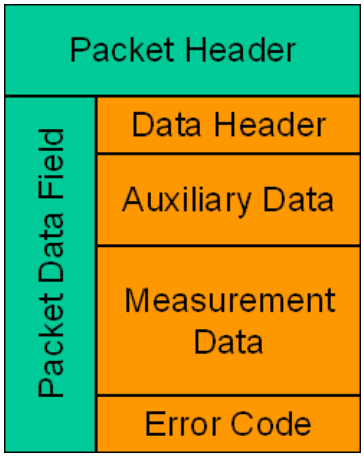

Figure 2.2 AATSR Instrument Source Packet Contents

Each packet has a fixed length and format and contains:

- Packet header information (packet ID, packet number, packet length);
- Instrument mode, On-Board Time (OBT), Redundancy information;
- Auxiliary data;
- Measurement Data:
  - Pixel data for each channel;
  - Blanking pulse data for each pixel;
- Packet error check (cyclic redundancy check).

2.5.2 Differences Between ATSR-2 and AATSR Source Packets

The AATSR instrument generates a single packet for each rotation of the scan mirror. This contains the 974 pixels selected by the pixel map for each channel at 12-bit digitisation and a complete set of housekeeping data.

In contrast to this, due to the limited bandwidth available on ERS-2, ATSR-2 has two packet formats, Low-Rate (LR) and High-Rate (HR). In LR format, the pixel data is compressed and the housekeeping data is sub-commutated over 8 consecutive scans. Some visible channel data is not included in the packet due to the size of the data buffer. The data to be included in the packet is determined by different pixel maps and by the compression mode used. HR format includes all 974 pixels and updates the housekeeping data every scan. This is more like AATSR, but in the ATSR-2 case the data are split over 2 consecutive packets.

2.5.3 Acquisition and On-Board Data Processing

Acquisition of data and on-board data processing, including construction of the source packet, are discussed in section 3.1.3. , internal data flow.

2.5.4 The Level 0 Product

Once received on ground, the ISPs are converted into a Level 0 product. The Level 0 product contains Annotated Instrument Source Packets (AISPs). These are ISPs as received from the instrument with a header and associated quality information attached by the PDS Front End Processor (FEP). Each MDS record also contains a time stamp in MJD 2000 format (as converted from the Satellite Binary Time (SBT) counter embedded in each ISP), which gives the on-board sensing time of the ISP that it contains.

2.5.4.1 ATS_NL_OP

As AATSR has only one nominal operating mode, there is only one Level 0 product (ATS_NL__0P). The structure of this product comprises a single MPH, a single SPH 5.1. and a single MDS containing the instrument source packet data, as shown in table 2.6 .

Table 2.6 AATSR L0 Product Structure

L0 Product Section	Record
MPH	MPH Record
SPH	SPH Record DSD for MDS #1 DSD for L0 Processor Configuration File used to create product DSD for Orbit State Vectors File used to create product DSD Spare
MDS #1	MDS Record #1 MDS Record #2 MDS Record #n

Each MDS record consists of a single annotated ISP with the structure shown in table 2.7 .

Table 2.7 Contents of AATSR L0 MDS Records

Field	Description	Units	Size (bytes)	Fields/record
1	ISP Sensing Time	MJD	12	1
2	FEP Annotations*	N/A	20	1
3	Packet ID	N/A	2	1
4	Packet Sequence Count	N/A	2	1
5	Packet Length	N/A	2	1
6	Data Field Header Length	N/A	2	1
7	Instrument Mode	N/A	2	1
8	ICU on-board time	N/A	4	1
9	Redundancy Vector	N/A	2	1
10	Auxiliary Data	N/A	2	390
11	Science (pixel) data	N/A	2	5357
12	CRC Error code for packet	N/A	2	1

* The FEP annotations describe the quality of the ISP reconstruction process and contain the following:

- MJD 2000 Time Stamp - Ground Station Reference Time of reception;
- Length of ISP;
- Number of Virtual Channel Data Units (VCDUs) in the ISP which contain a Cyclic Redundancy Check (CRC) error -; as identified by a failed Cyclic Redundancy Code check;
- Number of VCDUs in the ISP for which a Reed-Solomon error correction was performed.

2.5.5 Availability

Level 0 products are not routinely available to users.

2.6 Level 1B Products and Algorithms

Details of how to order AATSR data are given in Section 1.1.

The following sections describe the AATSR L1B processing algorithms, and the products they produce, in more detail:

- Level 1B Algorithms 2.6.1.
- Level 1B Products 2.6.2.

A short summary of the processing applied to each product, and a discussion of the AATSR ungridded products, is provided below.

Disclaimers addressing issues affecting AATSR L1b product quality are published at http://envisat.esa.int/dataproducts/availability/ .

ATS_TOA_1P (GBTR)

The primary Level 1B product comprises calibrated and geolocated images of brightness temperature (for the three infra-red channels) or reflectance (for the near-visible and visible channels), together with cloud and land identification. This product is used as the starting point of scientific processing to produce the Level 2 product. The processes required to generate the Level 1B product are as follows.

- First, source packets are processed to unpack and validate the science and auxiliary data that they contain. Calibration coefficients for the instrument channels are derived using the data from the on-board calibration targets and auxiliary temperature data.
- Signal calibration uses these calibration coefficients to convert the science data in each channel to units of brightness temperature or reflectance, as appropriate.
- Geolocation makes use of orbit propagation software in conjunction with available satellite orbit state vectors to determine the position on the Earth's surface of each instrument pixel.
- Because the conical scan images the Earth in a sequence of curved lines, it is necessary to rectify the data into a rectangular grid. This is done by assimilating each pixel of the instrument scan onto the nearest point of a Cartesian grid having the y axis aligned to the satellite along track direction and the x-axis aligned to the across track direction, using the pixel co-ordinates derived at the Geolocation stage. The same grid is used for both the nadir and forward view images, and therefore the collocation of the two images is ensured. This process may lead to gaps in the image, particularly in the forward view, where the density of instrument pixels is lower than the density of points on the Cartesian grid. A process of cosmetic filling of these gaps using the nearest neighbour method is therefore also applied.
- Finally, land flagging and cloud clearing algorithms are applied to the images to distinguish pixels over land from those over sea, and to identify those regions of the image that contain cloud.

The high level organisation of this product is described in section 2.6.2.1.1. .

ATS_AST_BP (Browse)

The Browse product provides the user with a quick-look illustrating the contents of the data from which it is derived, to assist users with product selection. It is a sub-sampled image at 4 km x 4 km resolution, based on the Level 1B nadir view brightness temperature and reflectance data. The product is partitioned into a day form in which different bands from the ATS_TOA_1P product are chosen to form a colour composite image showing the key features of the data, and a night form derived using the 11 micron channel brightness temperatures only. The latter image is essentially monochromatic, and transition processing is applied to the day time data at low solar elevations to minimise the visual discontinuity at the day-night transition.

The high level organisation of this product is described in section 2.6.2.1.2. .

AATSR Ungridded Products

The AATSR ungridded products (UCOUNTS and UBTR) are provided to support instrument commissioning activities, and to provide any users wishing to do their own regridding of the data with ungridded data.

The high level organisation of the UCOUNTS and UBTR products is described in section 2.6.2.2.1. and section 2.6.2.2.2. respectively.

2.6.1 Algorithms

The Level 1B algorithms are described in detail in the following sections:

- ATS_TOA_1P 2.6.1.1.
- ATS_AST_BP 2.6.1.2.

2.6.1.1 ATS_TOA_1P

Figure 2.3 shows an overview of the Level 1B processing.

Figure 2.3 Overview of the Level 1B processing.

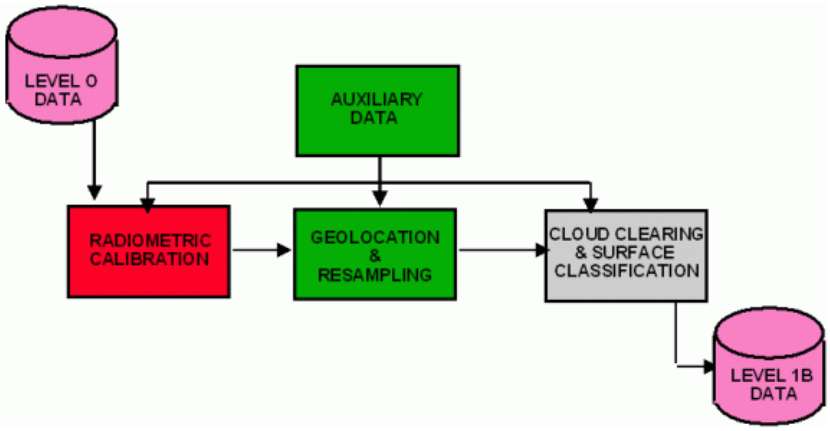

The AATSR Level 1B processor will operate on segments of AATSR Level 0 data of duration up to slightly more than one orbit.

The Level 0 data product comprises a series of records presented in chronological sequence, each of which contains a single instrument source packet. Each source packet represents a single instrument scan. For the most part (with one significant exception), the data processing up to but not including the re-gridding stage treats each source packet

independently. Thus each processing module can be regarded as a looping over a series of source packets, performing the same operations on (or in connection with) each.

The exception noted above refers to the derivation of the channel calibration coefficients. In the case of the infra-red channels, the calibration coefficients are determined by averaging calibration target data over a number of consecutive scans; the time interval containing these scans will be termed a calibration period or calibration interval. The recommended duration of the calibration interval is 10 scans; thus a new calibration interval will start at the end of the previous interval, and will continue for 10 scans or until a change in the pixel selection map is detected, whichever is the earlier.

For the visible channels, the channel offsets are derived by averaging over a calibration interval as above. The channel gains, however, are determined once per orbit, by averaging over the block of scans for which the VISCAL target is visible.

2.6.1.1.1 Source packet Processing

Initial processing must convert the data into the appropriate form for the higher levels of processing that geolocate the data and generate the products. The main functions can be summarised as follows:

- Perform basic quality checks on each raw packet, ensuring that only those that pass the checks continue on to the calibration process.
- Unpack all the auxiliary and housekeeping data containing the temperatures of the on-board black bodies and instrument health and status information.
- Validate the unpacked auxiliary and housekeeping data items.
- Convert the auxiliary data to engineering units where applicable.
- Validate the converted auxiliary data items, especially those which are vital to the calibration.
- Unpack and validate the science data containing the earth view and black body view pixel counts for all available channels from each packet.

2.6.1.1.2 Infra-Red Channel calibration

Derivation of the calibration parameters requires the calculation of the gain and offset values which define a linear relationship between pixel count and radiance. The gain and offset are derived for each channel, from the unpacked and validated auxiliary and pixel data averaged over a number of contiguous data packets.

The IR calibration module is a framework in which all the modules described in earlier sections are used. Up until this point all modules have been concerned with processing component data from a single source packet. The IR calibration calculations are concerned with using the unpacked, converted and validated auxiliary and pixel data generated by the modules previously described, to calculate average black body temperatures and average black body pixel counts over a series of contiguous packets. The number of packets over

which these values are averaged is called the "calibration period".

Once the average values for both black body temperatures have been calculated from the data available in the processed source packets in a calibration period, and the corresponding black body pixel counts have been similarly averaged, it is then possible to use these values to derive the gain and offset parameters which can then be used to convert pixel count to radiance for all valid pixels in all valid packets within the calibration period.

The look-up table for conversion from temperature to radiance contains a correction for detector non-linearity to ensure a linear relationship between radiance and detector counts. It is therefore possible to derive the calibration parameters for each IR channel from the straight line formula y = m.x + c. The mean (odd and even) black body pixel counts for the two black bodies are the two x axis values, and the two black body radiance values make up the corresponding y axis values.

The gain and offset values are derived for both odd and even pixel numbers, because AATSR uses two integrators; one for odd pixels and one for even pixels. The response time of a single integrator is too slow to use the same one for all pixels.

Details of the calibration algorithm are contained in the following section:

- Infra-Red Calibration 2.6.1.1.2.1.

2.6.1.1.2.1 Infra-Red Calibration

2.6.1.1.2.1.1 Physical Justification

2.6.1.1.2.1.1.1 Overview

The calibration of the thermal channels aims to characterise, for each channel separately, the relationship between the radiation incident on the detector and the detector output. The signal in counts from a radiometer channel whose spectral passband is $\Delta\nu$ observing a blackbody target at temperature T_{bb} is

$$S(T_{bb}) = GL(T_{bb}) + S_0 \qquad \text{eq 2.1}$$

where G is the radiometric gain, $L(T_{bb})$ is the radiance from a target, and S_0 is the radiometric offset of the channel. Thus radiometric calibration of the instrument consists of determining the linear relationship between the radiance and detector counts from each channel.

One way to do this might be to allow the instrument to view a zero radiance target, such as a cold space view, to determine the radiometric offset S_0 (i.e., $L(T_{bb}) = 0$). Then the radiometer views a hot calibration target to determine the radiometric gain of the channel, given by

$$G = (S_{hot} - S_0)/L_{hot} \qquad \text{eq 2.2}$$

The major limitation of this approach comes from the assumption that the radiometer's response is linear over a wide range of scene temperatures, 0 to 350K in the case of an Earth viewing instrument. In practice there is always some non-linearity that, if not treated properly in the ground processing algorithms, results in errors in calibration.

A different approach is therefore adopted for AATSR to minimise the sensitivity of the calibration to any non-linearity in the radiometer characteristics. This has been done both by careful design of the signal processing electronics and careful pre-flight determination of the non-linearity for beginning of life and end of life conditions on the satellite, and also through designing the calibration system so that the on-board calibration is optimised over the limited range of temperatures that span the expected range of SST observations. This is done by the use of two blackbody calibration targets, rather than a single target hot target and space view. One of these targets operates at a temperature lower than the lowest expected SST and the one other warmer than the highest. With this arrangement the calibration is most precise over the normal range of observed temperatures, and the effects of any non-linearity in the system are minimised because linearity is only assumed over a small range of measurement space. Outside this range the calibration is no worse than using the space view and single target approach, but the precision is concentrated into the portion of the measurement space where the most accurate measurements are required. Outside this range the precision of the observations is less critical, so the larger calibration errors resulting from extrapolation can be tolerated.

The signal from the cold blackbody is given by,

$$S_{cold} = GL_{cold} + S_0 \qquad \text{eq 2.3}$$

and that from the hot blackbody is given by,

$$S_{hot} = GL_{hot} + S_0 \qquad \text{eq 2.4}$$

Hence, the radiometric gain G is

$$G = (S_{hot} - S_{cold})/(L_{hot} - L_{cold})$$ eq 2.5

and by substituting G back into the equations the offset S_0 is

$$S_0 = S_{cold} - GL_{cold}$$ eq 2.6

Thus, by using this two blackbody calibration approach we can determine the radiometric gain and offset of each of the AATSR channels, in a way that allows us to achieve the highest accuracy in SST with minimal correction for signal channel non-linearity.

In practice the situation is slightly more complex than this. Firstly, the blackbody targets used for calibration cannot be made perfectly black so they also reflect radiation and this component of the signal must be included in the calibration. Secondly, despite the care taken in designing the signal channel electronics in AATSR there is still some non-linearity in the response of the detectors to variations in scene radiance. These problems are discussed in more detail below, where the theoretical treatment follows that developed for ATSR by Mason (1991) Ref. [1.12].

2.6.1.1.2.1.1.2 Detector Response to source radiation

The instrument fore-optics is designed to focus an image of the scene on the field stop. The dimensions of the field stop define the angular resolution, or instantaneous field of view, of the instrument (the angular width of the pixel); thus the solid angle subtended by the field stop at the primary mirror determines the solid angle Ω within which energy is accepted by the instrument. Then the energy falling on the nominal aperture A of the instrument from a scene of brightness temperature T is

$$A\Omega B(\lambda, T)d\lambda$$ eq 2.7

within a wavelength interval d λ, where B(λ, T) is the Planck function representing the radiance per unit wavelength interval of black body radiation of temperature T. In wavelength units the Planck function is

$$B(\lambda, T) = 2hc^2\lambda^{-5}/(\exp(hc/\lambda kT) - 1)$$ eq 2.8

Ideally all this energy should be focused on the detector; in practice the energy reaching the

detector is reduced by absorption at the surfaces of the scan and primary mirrors, by diffraction at the field stop, and by absorption within the focal plane assembly (FPA). The energy entering the FPA, in the wavelength interval d λ, is

$$d\Phi_\lambda = \varepsilon_\lambda A\Omega\tau_{Rh}^2 B(\lambda,T)d\lambda \qquad \text{eq 2.9}$$

where τ_{Rh}^2 is the square of the reflectivity of the Rhodium coating of the mirrors and where the product $\varepsilon_\lambda A\Omega$ represents the throughput of the spectral channel λ. Note that throughout this discussion the use of λ as a suffix labels the AATSR channel; the use in any other context denotes a frequency dependence. ε_λ represents the factor by which the instrument throughput in the channel is reduced below its nominal value (A Ω) owing to diffraction at the field stop and to any reduction in the aperture of the parabolic mirror below the nominal value A. A corresponding amount of radiation (1 - $\varepsilon_\lambda A\Omega$) originating from the paraboloid surround thus enters the FPA, and contributes to the radiometric offset.

We now introduce the quantity $R_\lambda(\lambda)$ representing the spectral response of the channel λ; $R_\lambda(\lambda)$ is the detector response to monochromatic incident energy at wavelength λ, normalised to a peak value of unity. It is determined for each channel by laboratory measurements on the FPA during ground characterisation of the instrument. Then the response of the detector to the incident scene energy is proportional to

$$\Phi_\lambda = \tau_{FPA}\varepsilon_\lambda A\Omega\tau_{Rh}^2 \int R_\lambda(\lambda)B(\lambda,T)d\lambda \qquad \text{eq 2.10}$$

where τ_{FPA} is the transmission of the FPA at the peak of the spectral response of the channel.

The expression (10) is proportional to the photon flux incident on the detectors. For a given channel the integral

$$L_\lambda(T) = \int R_\lambda(\lambda)B(\lambda,T)d\lambda \qquad \text{eq 2.11}$$

is a function of the scene brightness temperature only; we may term it the scene radiance. [Strictly speaking it is not a true radiance, because the detectors act as photon counters rather than as thermal detectors, and our definition of R takes account of this. If the detectors responded to incident energy, R should represent the optical transmission of the components of the FPA, and the expression would be a true radiance. As it is, R also incorporates a term proportional to wavelength, to transform the energy in an elementary wavelength interval into the number of photons. Nevertheless, the effect of this is very small over the narrow bandwidths of the AATSR channels; moreover as we have defined it, with the normalisation of R, it has the dimensions of a radiance, and following Mason (1991) Ref. [1.12] we shall refer to it as such.]

The total photon flux falling on the detectors can thus be written

$$\Phi_{\lambda} = \tau_{\text{optics}} s_{\lambda} A\Omega \tau_{12}^{2} L_{\lambda}(T) + \Phi_{\text{back}\,\lambda}$$ eq 2.12

where $\Phi_{\text{back}\,\lambda}$ represents the background signal that results from energy originating within the instrument reaching the detectors, including emissions from the scan and primary mirrors and from the paraboloid surround. It depends on the temperature of the instrument components and can be assumed to be constant over the period of validity of a calibration.

2.6.1.1.2.1.1.3 Effect of signal channel processing circuits

The signal output from each detector is amplified within a preamplifier stage and passed to a signal channel processing (SCP) subsystem located within the Instrument Electronics Unit 3.1.2.2. (IEU). The input stage of each SCP channel incorporates a digitally controlled variable offset, and is followed by further amplification the gain of which is also under digital control. These variable gain and offset functions permit the signal levels entering the digitisation stage to be adjusted to permit the full dynamic range of the digitisers to be used. The control words that determine the gain and offset are provided by the DEU. The gain and offset are generally controlled by a feedback loop (the so-called 'autocal loop') operating within the DEU, which monitors the black-body temperatures and operates to maintain the output counts in each channel at predetermined optimum levels. Alternatively the loop may be disabled and the gain and offset set by command. In either case the output signal is a linear function of the input.

After amplification the signal in each channel is integrated for 75 μs; owing to the short integration times used two integrators are provided for each channel; these operate alternately so that one is read out and reset while the other is integrating. The integrator outputs are then digitised with 12 bit resolution, and the resulting samples passed to the telemetry. The sampled signal (in counts) in channel λ is given by

$$S_{\lambda}(T) = g_{\lambda}\Phi_{\lambda} + V_{\text{off},\lambda}$$ eq 2.13

where g_{λ} and $V_{\text{off},\lambda}$ represent the SCP gain and offset of channel λ respectively. Introducing equation eq. 2.12 and gathering together the constant terms we can write

$$S_{\lambda}(T) = G_{\lambda}L_{\lambda}(T) + S_{0,\lambda}$$ eq 2.14

where G_{λ} and $S_{0,\lambda}$ are constants characteristic of the channel.

2.6.1.1.2.1.1.4 Determination of the calibration coefficients

Equation eq. 2.14 can be inverted to

$$L_\lambda(T) = A_\lambda S_\lambda(T) + L_{0,\lambda} \qquad \text{eq 2.15}$$

where $A_\lambda = 1/G_\lambda$ and $L_{0,\lambda}$ are constants. If these constants are known, then equation eq. 2.15 can be used to convert the measured pixel counts into the scene radiance L(T); T can then be recovered by inverting equation eq. 2.11 . Note that once the spectral response function R has been determined for a given channel, the radiance function (eq. 2.11 (and its inverse can be computed as look-up tables that can be used to convert from radiance to brightness temperature and vice versa.

The linear relationship eq. 2.15 is be defined if two points on the line are known. These points in turn are defined by the two black body calibration targets.

Figure 2.4 Radiance versus Counts

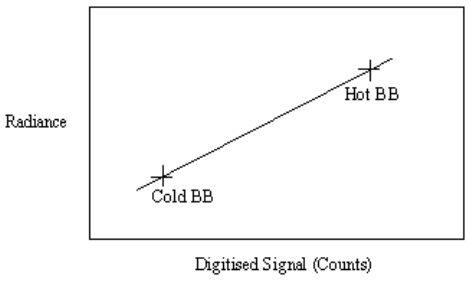

In the case of AATSR each calibration black body has 5 platinum resistance thermometers (PRT) mounted on the base, and a additional PRT on the shroud. The temperature of each black body can be determined using these. Given the temperatures of the two black bodies, their radiances can be determined; hence given a simultaneous measurement of the detector counts from the black body pixels, we can plot the points on the characteristic curve. The two black bodies taken together allow us to determine the bias and slope of the calibration characteristic.

Suppose that the radiances of the cold and hot black bodies are L_1 and L_2 respectively, and the corresponding counts are S_1 and S_2. Then

$$A_1 = (L_2 - L_1)/(S_2 - S_1)$$ eq 2.16

and

$$L_{1,2} = (L_1 S_2 - L_2 S_1)/(S_2 - S_1)$$ eq 2.17

Note that these expressions are unchanged if the suffixes 1 and 2 are interchanged; it is thus not necessary to specify explicitly which is the hot black body and which is the cold. The same expressions would have been obtained if we had defined L_1 to be the radiance of the hot black body, and L_2 that of the cold black body. In practice the choice of which black body is to be the cold and which the hot target can be determined by macro-command; however, because of the above invariance we do not need to know which selection has been made at the time of the analysis. We can redefine L_1 as the radiance of (say) the +X black body, and L_2 that of the -X black body[1], and still use these equations to determine the calibration coefficients. This is the approach that is adopted in the analysis.

([1] The two black bodies are conventionally known as the +X black body and the -X black body. This identifies them by their position in the satellite reference frame.)

If the calibration target were an ideal black body, its radiance would be given by evaluating equation eq. 2.11 at the physical temperature of the target. In practice this is not so; if the emissivity of the black body j (j = 1, 2) in the channel of wavelength λ is $\varepsilon_{j,\lambda}$, assumed constant across the bandwidth of the channel, then the corresponding calibration signal is

$$L_j = \varepsilon_{j,\lambda} L_\lambda(T_j) + (1 - \varepsilon_{j,\lambda}) L_\lambda(T_{inst})$$ eq 2.18

where T_j and T_{inst} represent the temperatures of the black body j and the instrument environment respectively.

A number of practical points arise. Firstly, the odd and even pixels are measured with different amplifier chains. Since the calibration includes the gain of the amplifier electronics, this has the consequence that separate calibration coefficients are required for the odd and even channels. Thus odd and even black body pixels are analysed separately to give the two calibrations.

Both the pixel counts and the PRT temperatures are averaged over a suitable calibration interval to reduce their respective noise levels; this is currently 10 scans. Thus for each black body and each pixel parity (that is, for the odd and even pixels separately) the pixel counts are averaged over the scans in the chosen calibration interval to give a mean count. The platinum resistance thermometer values are averaged over the same interval to give the corresponding temperatures T_j.

2.6.1.1.2.1.1.5 Signal Channel Calibration

Once the slope and intercept (the coefficients of equation eq. 2.15) are known, pixel calibration for the corresponding channel is accomplished by the use of equation eq. 2.15 . Given the measured the counts for each channel, we derive the incident energy (radiance) from this equation directly. Then we derive the corresponding brightness temperature by inverting equation eq. 2.11 . In practice this is accomplished with a look-up table that inverts the equation.

2.6.1.1.2.1.1.6 Detector non-linearity

In the description of the calibration scheme above, we have assumed that each detector output depends linearly on the scene radiance within its operating range. This is not strictly true. The 11 and 12 μm channels of AATSR use photoconductive cadmium mercury teluride (CdHgTe) detectors, and these show small but detectable non-linearity. This is accommodated within the calibration scheme by modifying the look-up tables using pre-flight characterisation measurements of the detector response. We have assumed that the detector output is proportional to the scene radiance, whereas in fact it depends on a non-linear function f{L}. If the look-up table representing the radiance function L(T) is replaced by one representing the composite function f{L(T)} then it is evident that the scheme outlined above would work equally well.

A complication is introduced when the non-zero reflectivity of the actual calibration targets is taken into account. In this case the calibration signal from the black body target j is given by

$$f\{L_j\} = f\{\varepsilon_{j,\lambda} L_\lambda(T_j) + (1-\varepsilon_{j,\lambda}) L_\lambda(T_{inst})\} \qquad \text{eq 2.19}$$

in place of equation eq. 2.18 , and, because the function f is by definition non-linear, it is not strictly possible to decompose this expression into a form that can be represented exactly by a simple look-up table. The equation eq. 2.19 is a function of two arguments T_j and T_{inst}, and to evaluate it exactly it would be necessary either to use a table with two arguments, or to have two tables to represent the functions f and T separately, rather than a single table. In practice this complication is not necessary, because of the small value of $\varepsilon_{j,\lambda}$ and the relatively slight non-linearity in question; to a sufficient approximation we can write

$$f\{L_j\} = \varepsilon_{j,\lambda} f\{L_\lambda(T_j)\} + (1-\varepsilon_{j,\lambda}) f\{L_\lambda(T_{inst})\} \qquad \text{eq 2.20}$$

as the counterpart of equation eq. 2.18 . In other words we can still base the calculation on the single modified look-up table. This is discussed in more detail below.

2.6.1.1.2.1.1.7 Derivation of the look-up tables

The derivation of a table representing the radiance as a function of brightness temperature is straightforward; given measured values of the spectral response function R, for a channel the integral eq. 2.18 can be evaluated for any temperature T using standard techniques of numerical quadrature. In order to correct the resulting tables for detector non-linearity in the case of the 11 and 12 μm channels, the following approach, originally developed for ATSR by (Mason 1991 Ref. [1.12]), is adopted.

The detector output is measured during ground characterisation in an environmental test facility with reference to external black bodies of known temperature and emissivity. The (normalised) detector output is plotted against the calculated radiance of the external targets. A straight line is then fitted to the data points of low radiance and this fitted line is regarded as the ideal detector characteristic, it being assumed that the detector response is linear at low incident radiance. The ratio of the actual detector response to the response predicted by using this fitted line is then calculated as a function of the source radiance; this quantity, the 'fractional fall-off' of the detector characteristic, is a measure of the non-linearity of the response.

In order to give an analytic representation of the fractional fall-off, a quadratic function of the normalised source radiance

$$g_\lambda = Z_{0,\lambda} + Z_{1,\lambda}\left(\frac{L_\lambda(T)}{L_\lambda(320\,K)}\right) + Z_{2,\lambda}\left(\frac{L_\lambda(T)}{L_\lambda(320\,K)}\right)^2 \qquad \text{eq 2.21}$$

is fitted to the fractional fall-off data. The radiance is normalised to that at 320 K for the purposes of determining the coefficients. Table 2.8 gives the numerical values of the coefficients for the 11 and 12 micron channels for AATSR.

Table 2.8 Coefficients for the calculation of fractional fall-off for AATSR

Coefficient	11 μm	12 μm
$Z_{0,\lambda}$	TBD	TBD
$Z_{1,\lambda}$	TBD	TBD
$Z_{2,\lambda}$	TBD	TBD

It is now a simple matter to apply the non-linearity correction to the look-up table; given the true radiance calculated for the tabular value T, $L^{\lambda}(T)$, the fractional fall-off can be calculated using equation eq. 2.21 above. The corrected radiance for the same tabular temperature is then given by the product

$$g_{\lambda} L_{\lambda}(T) \qquad \text{eq 2.22}$$

[Note to be added on non-linearity of 3.7 μm channel.]

2.6.1.1.2.1.2 Algorithm Description

The calculation of the calibration parameters for the infra-red channels involves the calculation of the slope and offset for each channel separately, from the unpacked and validated data in the processed instrument source packets. It averages the necessary values over the number of packets in a calibration period. A calibration period comprises a block of consecutive source packets, each of which corresponds to an instrument scan; the number of source packets that make up a calibration period is defined by a parameter in the auxiliary Processor Configuration File 6.5.6. . The nominal value is 10 scans.

In the event that a change to the 'autocal' loop or the Pixel Selection Map is detected within the calibration period, the calibration period is terminated and the derived coefficients are based on the data preceding the change.

The following five steps are applied to all packets in a calibration period, provided that the user's option for calibration while other instruments are operational is compatible with the state of the blanking pulse flags for selected pixels (see note below).
Step 1. Derive mean BB temperatures.

The weighted mean PRT values are calculated for both hot and cold black bodies, from all valid BB PRT values from one packet. This is repeated for all packets in the calibration period. The component means are summed, and a single mean is derived for each BB over the calibration period.

The mean background (fore-optics) temperature is also derived from valid data over the same period.
Step 2. Convert the mean BB temperatures to radiance.

The weighted mean PRT temperatures for each BB are converted to a radiance value for each IR channel. This is achieved by means of a look up table converting temperature to radiance, with one look up table for each IR channel. The look-up tables are found in the auxiliary file of General Calibration Data 6.5.4. . They are sampled to allow linear interpolation between points.
Step 3. Correct the BB radiance values.

Each black body radiance value is now corrected, using the mean background temperature derived in step 1, and the emissivity constants for each IR channel, according to equation eq. 2.18 and equation eq. 2.22 . (Note that the non-linearity corrections are included in the look-up tables.)
Step 4. Derive the mean BB pixel count for each BB over the calibration period.

These values are calculated for odd and even pixels, for both hot and cold black bodies, and for all channels, from all valid BB pixels in the calibration period. The mean (odd and even) pixel counts for each channel is derived from the valid BB pixel data in each packet. This is repeated for all packets in the calibration period, and a mean BB pixel count over the calibration period is derived, for odd and even pixels, for each BB, and for each IR channel. For a pixel to count as valid in this step, its associated blanking pulse flags must be compatible with the selected option as described in the note below.
Step 5. Calculate the gains and offsets from BB counts and BB radiance.

The gains and offsets for the calibration period, for odd and even pixels, for each black body, and for each IR channel, are derived using equation eq. 2.16 and equation eq. 2.17 .
Note: Treatment of blanking pulse flags.

Two blanking pulse (BP) flags are associated with each pixel in the AATSR source packet. Each flag is associated with one of the radar instruments aboard ENVISAT (RA-2 and ASAR), and is set if the corresponding radar was transmitting at the time the pixel was measured. The purpose of these flags is to guard against the possibility of cross-coupling or interference between the radar transmitters and the AATSR signal channel processing electronics; the flags permit pixels to be excluded from the calibration if one or other radar is transmitting, in case there is any interference from the radar.

Whether or not pixels are included in the calibration depends upon a parameter, the blanking pulse calibration flag (pulse_cal) in the Level 1B Processor Configuration File (ATS_PC1_AX). Pixels are always included in the calibration if both BP flags are off. Otherwise, pixels are included or not according to the setting of this parameter as follows.

Case 101 (pulse_cal = flag_off_bthbp): Both BP flags off: Pixel is included in the calibration only if both flags are off.

Case 102 (pulse_cal = flag_off_asar): ASAR only flag off: Pixel is included in the calibration only if the ASAR flag is off. (The RA flag is ignored).

Case 103 (pulse_cal = flag_off_onlyra): RA only flag off: Pixel is included in the calibration only if the RA flag is off. (The ASAR flag is ignored).

Case 104 (pulse_cal = flag_on_bthbp): Both BP flags on: Pixel is included irrespective of the flag setting. (Either or both flags may be on.) This is the nominal setting.

Thus in Step 4 above, only pixels for which the associated blanking pulse flags are be compatible with the selected option are treated as valid and included in the averages.

2.6.1.1.2.1.3 Accuracies

TBD

2.6.1.1.3 Visible Channel Calibration

This module unpacks the VISCAL data once per orbit (if present), when it is detected that the VISCAL unit is in sunlight. (The VISCAL data is used as a reference for the calculation of the calibration parameters for the visible channels.) In addition, it calculates calibration parameters for all visible channels. These calibration parameters are not used to calibrate the science data in the visible channels for the current orbit, but are written to the Visible Calibration Coefficients ADS in the GBTR product.

Determination of the calibration parameters for the AATSR visible channels involves two main stages. The offset value for each channel is derived by averaging the black body pixel counts in the channel over a calibration period in a similar way to the derivation of the mean black body counts for the infra-red channels during the infra-red channel calibration. The slope value for the channel is derived from the on-board visible calibration system as described below.

Two on-board sources are used to calibrate the AATSR visible/near infra-red channels. The upper reflectance measurement is provided by the visible calibration unit, VISCAL, which gives a signal corresponding to ~ 15% spectral albedo at full solar illumination. The reflectance_factor for each channel are obtained from the pre-launch calibration of the VISCAL.

The zero reflectance signal is derived from one of the on-board black bodies, used also for the thermal calibration. The data from these sources are used to derive the calibration slopes for each channel using (in the case that the MXBB (Minus X Black Body) is used as the reference black body).

Calibration_Slope[chan] = Reflectance_Factor[chan]*Gain[chan] /

(Average_VISCAL_Pixel_Counts[chan]- Average_MXBB_Pixel_Counts[chan])

where the VISCAL and MXBB pixel counts are averaged only during the period when the VISCAL is at full solar illumination. The pixel counts are normalised to unit detector gain to allow for gain changes during an orbit. The Calibration_Slope is then used to convert pixel counts to top-of-atmosphere reflectance by

Pixel_Reflectance[chan] = Calibration_Slope[chan]*

(Pixel_Count[chan] - Average_MXBB_Pixel_Counts[chan])/ Gain[chan]

where the MXBB pixel counts are taken from the same scan as the pixel counts being calibrated. This scheme is modified in the case of the 1.6 μm channel to correct for measured detector nonlinearity.

More detail on the visible calibration will be added in a future issue.

2.6.1.1.4 Satellite Time Calibration

For each scan, the Satellite Binary Time (taken from the source packet) is converted to UTC. The conversion uses a linear relationship between SBT and UTC, defined by parameters taken from the SBT to UTC Conversion Information section of the Main Product Header (MPH) of the product model.

2.6.1.1.5 Geolocation

This heading covers a number of different steps as follows.

- Instrument pixel geolocation: The latitude and longitude co-ordinates of the instrument pixels are determined. This is an intermediate step the output of which is used by the next stage.
- Mapping to a cartesian image grid: Image co-ordinates are determined for each instrument pixel. These co-ordinates are used in the regridding stage. The tie point x and y co-ordinates appear in the output product, in the Scan Pixel x and y ADS 6.6.44. .
- Image pixel geolocation: The latitude and longitude co-ordinates of the image pixels are determined. This process is distinct from the instrument pixel geolocation; the co-ordinates of the image pixels appear in the product in the Geolocation (Grid Pixel Latitude and Longitude) ADS 6.6.43. .

The following parameters are also derived as part of Geolocation:

- Solar and viewing angles;
- Topographic correction.

These topics are covered in the following sections.

- Instrument Pixel geolocation. 2.6.1.1.5.1.
- Image Pixel geolocation. 2.6.1.1.5.2.

2.6.1.1.5.1 Instrument Pixel Geolocation

2.6.1.1.5.1.1 Physical Justification

The objective of geolocation is to determine the co-ordinates on the Earth's surface corresponding to the centre of each scan pixel. The required co-ordinates are the latitude and longitude of the pixel on the reference ellipsoid. (The radial co-ordinate is then automatically known from the definition of the ellipsoid.)

The co-ordinates of the scan pixel correspond to the intersection of the line of sight (the direction of the instantaneous optic axis as it leaves the scan mirror) with the reference ellipsoid. The problem, then, is to determine this point of intersection, given the satellite position and attitude and the orientation of the scan mirror.

2.6.1.1.5.1.1.1 Co-ordinates of the scan pixel

To determine the co-ordinates of the scan pixel, we work in an Earth-fixed reference frame. This is a right-handed Cartesian frame of reference having its origin at the centre of the Earth. The Z axis is directed along the rotation axis towards the North pole, and the X and Y axes lie in the plane of the equator; the X axis lies in the plane of the Greenwich meridian, and the Y axis completes the right-handed set.

Suppose that at some instant of time t, the co-ordinates of the satellite in the earth-fixed reference frame are X_S , Y_S , and Z_S , and that the instantaneous line of sight of the ATSR optical system is defined relative to the same frame by the direction cosines l, m and n. The line of sight is then described by the equations

$$X = X_s + l\alpha \qquad \text{eq 2.23}$$

$$Y = Y_s + m\alpha \qquad \text{eq 2.24}$$

$$Z = Z_s + n\alpha \qquad \text{eq 2.25}$$

where the parameter α represents the distance between the satellite and the point (X, Y, Z).

The equation of the reference ellipsoid is given by

$$\frac{X^2}{a^2} + \frac{Y^2}{a^2} + \frac{Z^2}{b^2} = 1 \qquad \text{eq 2.26}$$

Here a is the semi-major axis of the ellipsoid (the equatorial radius of the Earth) and b is the semi-minor axis (the polar radius of the Earth).

The point of intersection is easily found by solving the simultaneous equations as follows. Substitution of the parametric equations of the line (5.3.1 - 3) in (5.3.4) gives

$$\frac{(X_s + l\alpha)^2}{a^2} + \frac{(Y_s + m\alpha)^2}{a^2} + \frac{(Z_s + n\alpha)^2}{b^2} = 1 \qquad \text{eq 2.27}$$

This is a simple quadratic equation in the parameter α; multiplying out gives

$$A\alpha^2 + B\alpha + C = 0 \qquad \text{eq 2.28}$$

where

$$A = (l^2 + m^2)b^2 + n^2a^2 \qquad \text{eq 2.29}$$

$$B = 2\left((lX_s + mY_s)b^2 + nZ_sa^2\right) \qquad \text{eq 2.30}$$

$$C = (X_s^2 + Y_s^2)b^2 + Z_s^2a^2 - a^2b^2 \qquad \text{eq 2.31}$$

The equation has two solutions

$$\alpha = \frac{-B \pm \sqrt{B^2 - 4AC}}{2A} \qquad \text{eq 2.32}$$

Provided the argument of the square root is positive, which will always be the case in practice, both solutions are real and positive, and the one that we require is the smaller of the two, which we denote by α_{min}; this will be the one corresponding to the negative sign. The other solution then defines the point of emergence of the line of sight at the far side of the earth. (If the quantity under the square root is negative, the solutions of the equation are complex. This case would arise if the line of sight did not intersect the ellipsoid, and will never occur in the normal course of geolocation of AATSR data with the satellite in yaw steering mode.)

The pixel co-ordinates are then given by

$$X_p = X_s + l\alpha_{\min} \quad \text{eq 2.33}$$

$$Y_p = Y_s + m\alpha_{\min} \quad \text{eq 2.34}$$

$$Z_p = Z_s + n\alpha_{\min} \quad \text{eq 2.35}$$

From the Cartesian co-ordinates of the pixel we can derive its longitude:

$$\lambda = \arctan(Y_p / X_p) \quad \text{eq 2.36}$$

and its geodetic latitude

$$\varphi = (1 - e^2)^{-1} \arctan(Z_p / U_p) \quad \text{eq 2.37}$$

where

$$U_p^2 = X_p^2 + Y_p^2 \quad \text{eq 2.38}$$

This procedure solves for the intersection point exactly.

2.6.1.1.5.1.1.2 Line of sight in the satellite reference frame

In order to calculate the pixel co-ordinates as above, we must determine the direction cosines of the line of sight relative to the Earth-fixed frame of reference X, Y, Z. This calculation must be repeated for each pixel for which geolocation is required. (Note that strictly, the X, Y, Z co-ordinates of the origin of the line of sight should coincide with the centre of the scan mirror. In practice the satellite centre of mass is used. The error, in terms of displacement on the surface, is negligible.)

To determine the direction cosines of the line of sight, we proceed in two main stages. First,

from knowledge of the angle through which the scan mirror has rotated, we determine the direction of the line of sight relative to a frame of reference fixed in the satellite; then we use the attitude steering law of the satellite and knowledge of its position in its orbit to relate the direction to the Earth-fixed frame of reference. These two aspects are discussed in this and the following sections.

2.6.1.1.5.1.1.2.1 AATSR Scan geometry

Imagine a Cartesian frame of reference fixed in the AATSR instrument, and orientated so that in the nominal flight attitude the Z axis points towards nadir, and the -Y axis is directed parallel to the satellite velocity vector, in the direction of satellite motion. We shall denote this frame of reference by the subscript b. Note that relative to the flight direction, the Y_b axis points backwards. The essential features of the AATSR scan geometry are expressed in terms of this frame.

In this reference frame, the rotation axis of the scan mirror, which points forward in flight, lies in the (-Y, +Z) quadrant of the Y, Z plane of this reference frame, and is inclined at an angle κ to the Z_b axis.

Define a second reference frame, the scan reference frame, as the frame of reference derived from the first by a rotation about the common X axes through the angle κ necessary to bring the Z axis parallel to the instrument scan axis. It will be denoted by the subscript a.

The viewing direction may be defined with respect to this frame as follows. The viewing direction rotates in a positive sense about the Z_a axis, to which it is inclined at angle κ. This means that the scan on the surface is traced in a clockwise direction, as seen from above. Let the scan rotation angle be φ, defined to be zero when the scan direction is in the X_a - Z_a plane. With respect to the scan reference frame, the direction cosines of the line of sight are then

eq 2.39

$$\lambda_a = \sin\kappa \cos\varphi$$

$$\mu_a = \sin\kappa \sin\varphi$$

$$\nu_a = \cos\kappa$$

The components of any vector defined in X_a , Y_a , Z_a are related to those of the same vector defined with respect to the instrument axes X_b , Y_b , Z_b by a linear transformation M_{ab} ($-\kappa$). The equations of this transformation are as follows.

Suppose that x_a , y_a , z_a are the components of a vector x relative to the scan reference frame, and that x_b , y_b , z_b are the components of the same vector relative to the instrument reference frame. M_{ab} ($-\kappa$) is a rotation of $-\kappa$ about the common X_a , X_b axes (figure 2.5), and

so the components are related by

$$x_b = x_a$$
$$y_b = y_a \cos\kappa - z_a \sin\kappa$$
$$z_b = y_a \sin\kappa + z_a \cos\kappa$$

eq 2.40

Therefore

$$M_{ab}(-\kappa) = \begin{pmatrix} 1 & 0 & 0 \\ 0 & \cos\kappa & -\sin\kappa \\ 0 & \sin\kappa & \cos\kappa \end{pmatrix}$$

eq 2.41

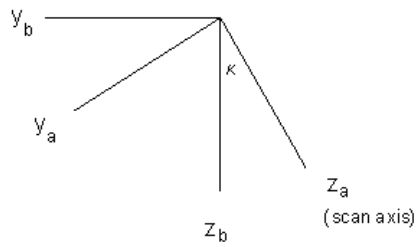

Figure 2.5

Thus relative to the instrument reference frame, the direction cosines of the line of sight are

$$\begin{pmatrix} \lambda_b \\ \mu_b \\ \nu_b \end{pmatrix} = M_{ab}(-\kappa) \begin{pmatrix} \lambda_a \\ \mu_a \\ \nu_a \end{pmatrix}$$

eq 2.42

2.6.1.1.5.1.1.2.2 Instrument misalignment

Imagine a set of Cartesian axes X_p , Y_p , Z_p fixed with respect to the satellite. We assume that the directions of these axes are defined with respect to the structure of the satellite, but in such a way that in flight, when the satellite is being yaw-steered, the axis Z_p is nominally directed towards nadir, $-Y_p$ is parallel to the satellite ground trace, and X_p completes the

right-handed set. This defines the platform reference frame (p).

The reference frame X_b , Y_b , Z_b defined above is defined with respect to the instrument. The nominal orientation of the AATSR instrument should be such that, when ENVISAT is flying in its nominal attitude in yaw steering mode, the Z_b axis points towards the true nadir and the $-Y_b$ axis. In other words the instrument reference frame should be parallel to the platform frame after integration of the instrument into the satellite. However in practice the two frames may differ by small misalignment angles. The misalignments are defined by the transformation between the instrument reference frame and the platform frame.

Quite generally, the relationship between two different sets of Cartesian axes can be expressed in terms of three consecutive rotations about different axes. Define linear transformations $M_z(\zeta)$, $M_y(\eta)$, $M_x(\xi)$, as follows:

$$M_z(\zeta) = \begin{pmatrix} \cos\zeta & \sin\zeta & 0 \\ -\sin\zeta & \cos\zeta & 0 \\ 0 & 0 & 1 \end{pmatrix} \qquad \text{eq 2.43}$$

$$M_y(\eta) = \begin{pmatrix} \cos\eta & 0 & -\sin\eta \\ 0 & 1 & 0 \\ \sin\eta & 0 & \cos\eta \end{pmatrix} \qquad \text{eq 2.44}$$

$$M_x(\xi) = \begin{pmatrix} 1 & 0 & 0 \\ 0 & \cos\xi & \sin\xi \\ 0 & -\sin\xi & \cos\xi \end{pmatrix} \qquad \text{eq 2.45}$$

$M_z(\zeta)$, $M_y(\eta)$, $M_x(\xi)$ represent elementary rotations of ζ, η, ξ about the z, y and x axes respectively. The transformation between instrument and platform frames is represented by the product of these elementary transformations. Thus the components of the line of sight vector expressed with reference to the platform frame are

$$\begin{pmatrix} \lambda_p \\ \mu_p \\ \nu_p \end{pmatrix} = M_x(\Delta x) M_y(\Delta y) M_z(\Delta z) \begin{pmatrix} \lambda_b \\ \mu_b \\ \nu_b \end{pmatrix} \qquad \text{eq 2.46}$$

This equation can be regarded as defining the misalignment angles Δ x, Δ y, Δ z. (We adopt the convention that the rotations are to be applied in that order to give the total transformation to the platform frame. Strictly speaking the matrices representing elementary rotations about different axes do not commute, and so we should specify the order in which

they are to be applied. In practice the angles are sufficiently small that any errors from this source are small in relation to the overall attitude error budget and the matrices can be regarded as commuting to a sufficient accuracy.)

In the above discussion we have used frames of reference in which the Z axes point downwards. This is convenient for a nadir viewing instrument; however in order to discuss the attitude transformations and to relate our frames of reference to those defined in the Mission Conventions Document we need to transform to a frame in which the Z axis point upwards.

Finally, the matrix M_{ps} transforms the vector to the satellite frame of reference. It represents a simple rotation of 180° about the common Y_s , Y_p axes to bring the Z axis parallel to the outward vertical. Relative to the satellite frame of reference the components of x are

$$x_s = -x_p$$
$$y_s = y_p$$
$$z_s = -z_p$$

eq 2.47

so that

$$M_{ps} = \begin{pmatrix} -1 & 0 & 0 \\ 0 & 1 & 0 \\ 0 & 0 & -1 \end{pmatrix}$$

eq 2.48

The direction cosines with respect to the satellite frame are therefore obtained by multiplying the starting vector by the matrix product

$$\begin{pmatrix} \lambda_s \\ \mu_s \\ \nu_s \end{pmatrix} = M_{ps} M_x(\Delta x) M_y(\Delta y) M_z(\Delta z) \begin{pmatrix} \lambda_0 \\ \mu_0 \\ \nu_0 \end{pmatrix}$$

eq 2.49

The satellite frame that we have defined here is equivalent to the Satellite Relative Actual Reference Frame defined in the mission conventions document, except that the frame here is explicitly imagined as fixed in the satellite. Note that we ignore mispointing throughout.)

2.6.1.1.5.1.1.3 Attitude Transformations

The Local Orbital Reference Frame is the reference frame with respect to which the attitude of the satellite is described. It is defined in the ENVISAT Mission Conventions Document

Ref. [1.6] (PO-IS-ESA-GS-0561); its origin is the centre of mass of the satellite and its basis vectors are the three unit vectors L, R, and T as follows.

- The unit vector L is directed along the outward radius from the centre of the earth to the satellite centre of mass. It is the yaw axis.
- The unit vector R is perpendicular to L, in the plane containing L and the instantaneous inertial velocity vector of the satellite, and is directed forwards, approximately in the direction of motion of the satellite. It represents the roll axis.
- Unit vector T completes the right-handed set, so that T = R x L. T is in the cross-track direction, and represents the pitch axis.

This frame is defined with respect to the orbit, not the structure of the satellite. It is an instantaneous frame; that is, it is defined at a particular instant of time.

The attitude of the satellite is specified relative to the Local Orbital Reference Frame by means of three angles ρ, τ, λ. These angles define the rotations about the roll, pitch and yaw axes respectively which, if applied in sequence to the TRL frame, would bring its axes parallel to the satellite frame. The sign of each rotation is to be interpreted so that a positive angle means that a positive rotation about the relevant axis, in the conventional right-handed sense, is required to bring the initial axes into coincidence with the derived set. Rotations about different axes do not commute, and so it is strictly necessary to define the order in which the rotations are to be applied. We adopt the convention that the rotations are to be applied in the order roll, pitch, yaw.

Suppose that (t, r, l) are the components of a vector in relative to the TRL axes, and that (t´, r´, l´) are the components of the same vector in the transformed system, which we may denote by T´R´L´. (The frame T´R´L´ is essentially the 'Local Relative Yaw Steering Orbital Reference Frame' defined in the Mission Conventions Document Ref. [1.6].) The rotation matrices in pitch, roll and yaw are identical to those defined above for rotations about X, Y and Z axes respectively. Thus the overall transformation can be expressed as

$$\begin{pmatrix} t' \\ r' \\ l' \end{pmatrix} = M_z(\lambda) M_x(\tau) M_y(\rho) \begin{pmatrix} t \\ r \\ l \end{pmatrix} \qquad \text{eq 2.50}$$

From our definition of the satellite attitude, the transformed attitude frame will be coincident with the satellite fixed frame, apart from a fixed rotation. The latter appears because we have defined the local orbital reference frame so that the roll axis R points forward, but the satellite frame is defined so that the corresponding axis points backwards. (We have simply followed the definitions adopted by ESA for these reference frames.) Comparison of the definitions of the two frames shows that the transformed frame T´R´L´ is related to the satellite frame by a rotation through 180 degrees about the z (L) axis. Specifically,

$$t' = -x_s ; r' = -y_s ; l' = z_s \qquad \text{eq 2.51}$$

We can introduce the matrix M_{SA} to represent this transformation:

$$M_{SA} = \begin{pmatrix} -1 & 0 & 0 \\ 0 & -1 & 0 \\ 0 & 0 & 1 \end{pmatrix} \quad \text{eq 2.52}$$

so that

$$\begin{pmatrix} t' \\ r' \\ l' \end{pmatrix} = M_{SA} \begin{pmatrix} x_s \\ y_s \\ z_s \end{pmatrix} \quad \text{eq 2.53}$$

We now have all the components of the transformation from the satellite reference frame to the TRL frame. Equation eq. 2.32 defines the transformation from TRL to T´R´L´. The reverse transformation is easily written

$$\begin{pmatrix} t \\ r \\ l \end{pmatrix} = M_y(-\rho) M_x(-\tau) M_z(-\lambda) \begin{pmatrix} t' \\ r' \\ l' \end{pmatrix} \quad \text{eq 2.54}$$

This follows because each of the matrices M_y , M_x , M_z represents a pure rotation, and the operation inverse to any rotation is a rotation equal in magnitude but of opposite sign about the same axis. Therefore from equation eq. 2.53 we have

$$\begin{pmatrix} t \\ r \\ l \end{pmatrix} = M_y(-\rho) M_x(-\tau) M_z(-\lambda) M_{SA} \begin{pmatrix} x_s \\ y_s \\ z_s \end{pmatrix} \quad \text{eq 2.55}$$

where M_{SA} is the matrix given by equation eq. 2.52 . The matrix M_{SA} represents a rotation about the vertical (L´) axis. It therefore reverses the direction of the orthogonal (R´ and T´) axes, while leaving the L´ axis unchanged. Moreover it must commute with the matrix $M_L(\lambda)$, since this also represents a rotation about the L´ axis, and rotations about a common axis commute. It is easy to verify this directly.

However, M_{SA} does not commute with the other two rotation matrices. Evidently a rotation of τ about the T´ axis is equivalent to a rotation of $-\tau$ about the -T´ axis, and similarly for rotations about R. (It is perhaps easier to visualise this if an active interpretation of the rotations is adopted, rather than the passive interpretation that is strictly applicable the

present discussion.) Thus one can verify by direct multiplication that

eq 2.56

$$M_{AS}\, M_X(\tau) = M_X(-\tau)\, M_{AS}$$

and similarly that

eq 2.57

$$M_{AS}\, M_Y(\rho) = M_Y(-\rho)\, M_{AS}$$

Hence

eq 2.58

$$\begin{pmatrix} t \\ r \\ l \end{pmatrix} = M_{SA} M_y(\rho) M_x(\tau) M_z(-\lambda) \begin{pmatrix} x_s \\ y_s \\ z_s \end{pmatrix}$$

In equation eq. 2.58 the sign of λ is negative, while the signs of the other two attitude angles are positive. This is a consequence of the co-ordinate rotation represented by M_{SA} .

Finally, we must relate the line of sight vector to the inertial frame. Suppose that the x, y, and z components of T are t_x , t_y , t_z respectively, and that the components of R and L are (r_x , r_y , r_z) and (l_x , l_y , l_z) respectively. If the components of the vector in TRL are t, r and l then the vector is

eq 2.59

$$t\,T + r\,R + l\,L$$

In the inertial frame this becomes, in component form

eq 2.60

$$\begin{pmatrix} x \\ y \\ z \end{pmatrix} = \begin{pmatrix} t_x & r_x & l_x \\ t_y & r_y & l_y \\ t_z & r_z & l_z \end{pmatrix} \begin{pmatrix} t \\ r \\ l \end{pmatrix}$$

The matrix is orthogonal because the individual vectors T, R, L are normalized to unit length. Note that the explicit form of this matrix depends on the position and velocity of the satellite at the time it is evaluated. If we are given the direction cosines of the line of sight with respect to TRL, then we can evaluate the matrix equation to derive the direction cosines of the line of sight with respect to the inertial frame.

Nothing prevents us from choosing the inertial frame as that whose axes instantaneously coincide with the earth-fixed reference frame at the time in question, in which case we can equate the inertial co-ordinates that we have derived to the geostationary co-ordinates.

2.6.1.1.5.1.2 Algorithm Description

2.6.1.1.5.1.2.1 Summary

The geolocation algorithm calculates the latitude and longitude of each instrument pixel. In principle this would be done by applying the transformations of section 2.6.1.1.5.1.1.1. to each pixel. In practice, to reduce the processing overhead, they are carried out for a subset of tie point pixels, and the coordinates of intermediate pixels are determined by linear interpolation in scan number and scan angle. That is, the pixel latitude and longitude are regarded as functions of scan number and pixel number, and are interpolated accordingly.

As discussed above, the transformation between the scan frame and the Earth-fixed frame can be expressed in terms of a series of consecutive matrix transformations applied to the line of sight vector. However, the implementation of this algorithm can take advantage of the fact that some of these are catered for by the ESA software target.

For each tie point pixel p in each scan s the direction of the line of sight is determined in the scan reference frame. The corresponding direction cosines are determined, transformed to the satellite reference frame, and converted back to define an azimuth and elevation. The TARGET subroutine is used to derive the pixel co-ordinates on the ellipsoid.

Given the pixel co-ordinates of the tie point pixels, linear interpolation with respect to pixel number is used to define the co-ordinates of the intermediate pixels on the scan. The process is repeated for both forward and nadir view scans.

2.6.1.1.5.1.2.2 Algorithm Definition

The following steps are carried out for each tie point pixel on each scan $s_t \in \{0, INT\_S, 2*INT\_S, ...\}$. In the general case these points are

$$p_t^n \in \{0, INT\_P, 2*INT\_P, ..., MAX\_NADIR\_PIXELS - 1\} \quad \text{eq 2.61}$$

on the nadir scan, and

$$p_t^f \in \{0, INT\_P, 2*INT\_P, ..., MAX\_FRWRD\_PIXELS - 1\} \quad \text{eq 2.62}$$

on the forward scan. The parameters MAX_NADIR_PIXELS and MAX_FRWRD_PIXELS are found in the Level 1B Processor Configuration File 6.6.40. . The interpolation intervals INT_P and INT_S are defined in the Level 1B Characterisation Data File 6.6.15. . The adopted value of INT_P is 10, and so in practice the tie points are

$$p_t^n \in \{0, 10, 20, 30, ..., MAX\_NADIR\_PIXELS - 1\} \quad \text{eq 2.63}$$

on the nadir scan, and

$$p_t^f \in \{0, 10, 20, 30, ..., MAX\_FRWRD\_PIXELS - 1\} \quad \text{eq 2.64}$$

on the forward scan.

For each scan s_t and for each tie point pixel p_t from the above sets, the following steps are executed:

1. Determine line of sight and its direction cosines in the scan reference frame.

The absolute pixel number p is calculated from

$$p = p_t^n + FIRST\_NADIR\_PIXEL\_NUMBER \quad \text{eq 2.65}$$

or

$$p = p_t^f + FIRST\_FORWARD\_PIXEL\_NUMBER \quad \text{eq 2.66}$$

as appropriate, where the values FIRST_NADIR_PIXEL_NUMBER, FIRST_FORWARD_PIXEL_NUMBER are found also in the Level 1B Characterisation Data File 6.6.15. . The scan angle is determined from

$$\phi_p = 2\pi \cdot p / 2000 + \varphi_0 \quad \text{eq 2.67}$$

and this value is substituted in Equation (5.3.18) to determine the unit vector along the line of sight.

2. Transform to satellite frame.

The direction cosines of the line of sight are transformed to the platform frame according to

$$\begin{pmatrix} \lambda_p \\ \mu_p \\ \nu_p \end{pmatrix} = M_x(\Delta x) M_y(\Delta y) M_z(\Delta z) M_{ab}(-\kappa) \begin{pmatrix} \lambda_a \\ \mu_a \\ \nu_a \end{pmatrix}$$ eq 2.68

where the half-angle of the scan cone κ and the misalignment correction angles Δx, Δy, Δz are taken from the Level 1B Characterisation Data File 6.6.15. . The interface to the target subroutine requires us to use a slightly different set of satellite axes to that defined in Section 2.6.1.1.5.1.1. Instead of Equation (5.3.27) we therefore define

$$M_{ps} = \begin{pmatrix} 0 & -1 & 0 \\ 1 & 0 & 0 \\ 0 & 0 & 1 \end{pmatrix}$$ eq 2.69

and

$$\begin{pmatrix} \lambda_s \\ \mu_s \\ \nu_s \end{pmatrix} = M_{ps} \begin{pmatrix} \lambda_p \\ \mu_p \\ \nu_p \end{pmatrix}$$ eq 2.70

The azimuth and elevation of the line of sight are calculated with respect to this frame by inverting the equations

λ_s = cos (elevation) cos (azimuth)

μ_s = cos (elevation) sin (azimuth)

ν_s = sin (elevation)

Thus

azimuth = atan2 (μ_s, λ_s)

elevation = atan2 (ν_s, sqrt($\lambda_s^2 + \mu_s^2$))

If azimuth < 0.0 then azimuth = azimuth + 360.0.

Here atan2 represents the arc tangent function of two arguments defined in the conventional way, atan2(y, x) being the angle whose tangent is (y/x) and whose quadrant is defined by the signs of x and y.

3. Use the subroutine target to determine the geolocation parameters.

The subroutine target is entered, with the line of sight direction determined by the azimuth and elevation parameters defined above, and with the orbital parameters evaluated for the time of the scan, to determine the latitude and longitude of the tie point pixels. The required outputs are the geodetic pixel co-ordinates taken from the results vector.

The longitude is converted to lie in the range -180 to 180 by the subtraction or addition of 360 if necessary.

2.6.1.1.5.1.2.3 Interpolation

The steps above have determined the co-ordinates of the tie point pixels. Linear interpolation is used to determine the co-ordinates of the intermediate pixels. The process is repeated for both forward and nadir views.

Linear interpolation with respect to scan number s is used to define the latitude and longitude of the intermediate pixels

$s \notin \{s_t\}$.

For each scan s, linear interpolation with respect to pixel number is used to define the latitude and longitude of the intermediate pixels

$p^n \notin \{p_t^n\}$; $p^f \notin \{p_t^f\}$.

In the case of longitude, the interpolation must take account of the fact that the 180 degree meridian may intersect the interpolation interval.

2.6.1.1.5.1.3 Accuracies

(To be added:

- Discussion of effect of attitude mispointing; constant offset indistinguishable from misalignment.
- Interpolation error; main contribution to absolute geolocation error is interpolation between tie points on same scan.)

2.6.1.1.5.2 Image Pixel Geolocation

2.6.1.1.5.2.1 Physical Justification

2.6.1.1.5.2.1.1 The Image Co-ordinates used for AATSR

The scanning geometry of AATSR is such that measured pixels lie on a sequence of curved instrument scans. In order to present undistorted images, and to ensure collocation of the forward and nadir views, the measured instrument pixels must be mapped onto a uniform grid. Instrument pixels are mapped onto a rectangular x-y grid aligned to the instrument swath.

This process requires that the relationship between the map co-ordinates of the pixel and its latitude and longitude be defined. If the co-ordinates of the pixel with respect to rectangular axes are x and y, the relationship of x and y to the pixel latitude and longitude defines the projection in use. In theory one could adopt any map projection one chose. In practice a projection is defined for AATSR that is related to the AATSR swath.

Over a small area we may regard the surface of the Earth as a plane, and can define Cartesian axes x and y in the surface so that the y axis is tangent to the satellite ground track. The x co-ordinate of a pixel within the area is then given by its normal distance from the y axis (the ground track), while the y co-ordinate is measured along the ground track from the origin to the foot of the normal from the pixel.

Over the wider area of the AATSR swath we cannot ignore the curvature of the Earth. However the same principle is adopted to define pixel x and y co-ordinates. We can still define a curve of constant y co-ordinate, that intersects the ground track at right angles, through any pixel.

For any pixel P that is sufficiently close [1] to the satellite ground track there will be a unique point Q on the ground track such that the vertical plane through Q whose intersection on the ellipsoid crosses the ground track at right angles also passes through the pixel. By vertical we mean that the plane includes the normal to the ellipsoid at the intersection point Q. The plane thus defines a normal section (in the sense to be defined below) at Q, and it intersects the ellipsoid in a curve that both passes through the pixel and crosses the ground track at right angles. The azimuth of the curve where it crosses the ground track is the normal section azimuth of the pixel measured at Q.

([1] If the point P is sufficiently far from the ground track on the 'concave' side, then Q is not unique.)

This curve is defined as the curve of constant y co-ordinate through the pixel. The x co-ordinate of the pixel is then the distance of the pixel from the ground track measured along this curve, while the y co-ordinate is given by the distance of the intersection point Q from the origin, measured along the ground track. The origin of the y co-ordinate is defined to be the ascending node of the orbit on the equator. In this way a coordinate system is defined that is centred on the satellite ground track.

The resultant projection does not correspond to one of the standard projections of cartography, and it is not orthomorphic (that is to say, away from the ground track the scales in the x and y directions are not exactly the same). Moreover the scale in the y direction, which varies with distance from the ground track, does not do so in a way that is precisely symmetrical about the ground track (because the ground track is curved, in the sense that it is not a geodesic on the surface). Nevertheless these effects are quantitatively small, while the mapping is conveniently matched to the instrument swath. Furthermore the mapping is unambiguously defined, and this is sufficient to ensure proper collocation of the forward and nadir views.

2.6.1.1.5.2.1.2 Geometrical Relationships on the Ellipsoid

The system of co-ordinates must take account of true distances on the ellipsoid, so that the map scale (the relationship between the nominal and true distance between the image samples) is uniform across the Earth, instead of showing a dependence on latitude.

This section gives for reference a number of standard geometrical relationships relating to the ellipsoid. Most are given without proof, but can be found in standard texts such as Bomford, G. Geodesy (4th edition), Clarendon Press, Oxford.

2.6.1.1.5.2.1.2.1 The Reference Ellipsoid

The reference ellipsoid is the ellipsoid of revolution formed by rotating an ellipse about its semi-minor axis (which will coincide with the axis of rotation of the Earth). The cross-section of the surface in any plane containing the axis of rotation will be an ellipse. If we define axes x and y to coincide with, respectively, the semi-major and semi-minor axes of this ellipse, we can write its equation in the standard form

$$\frac{x^2}{a^2} + \frac{y^2}{b^2} = 1 \qquad \text{eq 2.71}$$

where a is the semi-major axis and b is the semi-minor axis. The ratio (a - b)/a is the flattening, f. It is related to the eccentricity e by

$$(1-f)^2 = (1-e^2)$$ eq 2.72

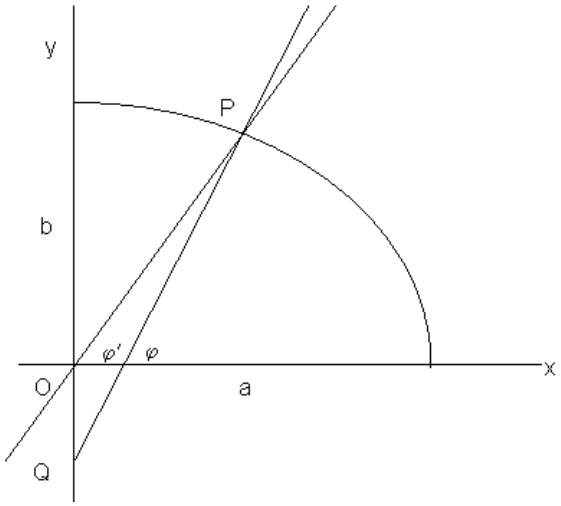

Figure 2.6

Figure 2.6 shows a point P (x', y') on the surface. The angle φ' is the geocentric latitude of P given by

$$\tan\varphi' = y'/x'$$ eq 2.73

The line PQ is the normal to the surface at P. The angle φ that this makes with the x axis (or the equatorial plane) is the geodetic latitude of P; it is related to the co-ordinates by

$$\tan\varphi' = (1-f)^2 \tan\varphi = (1-e^2)\tan\varphi$$ eq 2.74

The radius of curvature of the surface in the meridional plane at point P is given by

$$R = \frac{a(1-e^2)}{(1-e^2\sin^2\varphi)^{3/2}}$$ eq 2.75

The radius of curvature in the vertical plane orthogonal to the meridional plane (in figure 2.6 , the plane containing PQ and normal to the plane of the diagram) is

$$N = \frac{a}{\sqrt{1 - e^2 \sin^2 \varphi}} \qquad \text{eq 2.76}$$

This is sometimes termed the radius of curvature in prime vertical. The point Q is the common intersection of the surface normals at points on the parallel of latitude through P, and the length PQ can be shown to equal the normal radius of curvature N. Thus the centre of curvature in prime vertical lies on the minor axis of the ellipse. Note that the alternative notation ν, ρ is often used in the literature for the radii of curvature N, R respectively, and we shall use this notation below.

The equation of the line PQ is

$$(y - y') = (x - x')\tan \varphi \qquad \text{eq 2.77}$$

and its intercept Q at x = 0 is

$$y = y' - x' \tan \varphi = -y' e^2 / (1 - e^2) \qquad \text{eq 2.78}$$

Thus the projection of PQ onto the y axis is

$$N \sin \varphi = y' + y' e^2 / (1 - e^2) = y' / (1 - e^2) \qquad \text{eq 2.79}$$

and finally we have an expression for the coordinates of P in terms of N and φ

$$x' = N \cos \varphi \,,\; y' = N(1 - e^2) \sin \varphi \qquad \text{eq 2.80}$$

Define a right-handed set of cartesian axes X, Y, Z with origin at the centre of the Earth, with Z directed northwards along the axis of rotation, and with X in the plane of the prime meridian. The XY plane is therefore the plane of the equator. If figure 2.6 represents the meridional plane at longitude λ, the X, Y, Z coordinates of a point (x, y) in the plane are

$$X = x \cos \lambda;\; Y = x \sin \lambda;\; Z = y \qquad \text{eq 2.81}$$

and so the geocentric Cartesian coordinates (X, Y, Z) of the point P are

eq 2.82

$$X = N\cos\varphi\cos\lambda$$

$$Y = N\cos\varphi\sin\lambda$$

$$Z = N(1-e^2)\sin\varphi$$

2.6.1.1.5.2.1.2.2 Length and azimuth on the ellipsoid

We also require formulae for the length and azimuth of the curves joining two points 1 and 2 on the ellipsoid. Firstly it is necessary to be clear as to what is meant, since three different curves are in question. The geodesic is the unique curve of shortest length between the two points 1 and 2; however, many of the standard formulae refer not to the geodesic but to one of the two normal sections between the points.

The geodesic does not lie in a plane, nor does its azimuth α coincide with the bearing of point 2 that would be measured with a levelled theodolite at point 1, although the deviations will be very small for short lines. There are an infinity of plane sections through the ellipsoid including points 1 and 2. In particular we can consider two; the intersection of the ellipsoid with the plane containing point 2 and the normal to the surface at point 1, which we may call S_1, and the intersection with the plane containing point 1 and the normal to the surface at point 2, which we may call S_2. These are the normal sections, and their azimuths, measured at the points at which the plane section contains the normal to the surface, are the normal section azimuths. Thus the angle between the curve S_1 and the meridian plane through point 1 is the normal section azimuth of point 2 measured from point 1, and this angle is the bearing of point 2 that would be measured with a levelled theodolite at point 1.

The geodesic S lies between these two arcs S_1 and S_2, somewhat as shown in figure 2.7 . The angles between these curves are very small.

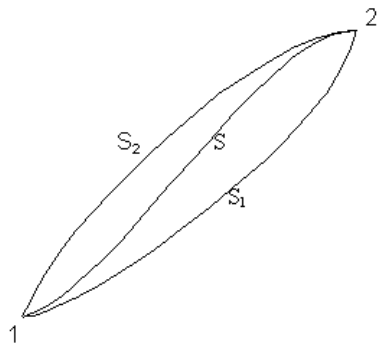

Figure 2.7

It is possible to give an exact expression for the normal section azimuth if the latitude and longitude of the two points are known. Let the two points be P and Q, and let their geodetic latitude and longitude be (φ_1, λ_1) and (φ_2, λ_2) respectively. Consider a sphere with its centre at O', the intersection of the normal through P with the axis of rotation. This sphere is tangent to the ellipsoid at the parallel of latitude through P, but does not otherwise coincide with it. Consider the spherical triangle NPQ' drawn on this sphere (Figure 2.9), where N is the intersection of the axis with the sphere, and Q' is the intersection of the line O'Q with the sphere. Then the plane O'PQ', which also contains point Q, is the normal section at P containing Q, and the normal section azimuth of Q measured from P is the angle at P (NPQ'). In the triangle, the angle N is known, since it is given by the difference in the longitudes of Q and P. The sides NP and NQ are also known, so that the triangle can be solved for angle P. NP is the geodetic co-latitude of point P. The calculation of the arc NQ is more complicated.

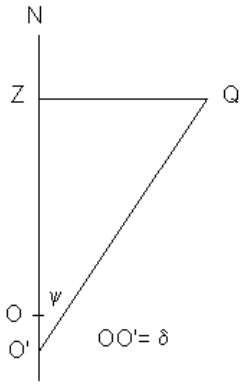

Figure 2.8

Suppose O is the centre of the Earth. We know that the z coordinate of O' is

$$\delta = -e^2 N_1 \sin \varphi_1$$

At the same time the z coordinate of Q is (Equation eq. 2.82 12)

$$N_2 (1 - e^2) \sin \varphi_2$$

Thus in figure 2.8 , which shows the meridian plane through Q, the length O'Z (where Z is the projection of Q on the polar axis) is

eq 2.83

$$N_2 (1 - e^2) \sin \varphi_2 + e^2 N_1 \sin \varphi_1$$

(Note the subscripts 1 and 2 refer to the points P and Q respectively.) The length ZQ is

$N_2 \cos \varphi_2$

and so we have

$$\tan \psi = \cos \varphi_2 / ((1 - e^2) \sin \varphi_2 + e^2(N_1/N_2) \sin \varphi_1) \qquad \text{eq 2.84}$$

from which the angle ψ can be determined.

Now consider the spherical triangle PNQ' (Figure 2.9), in which the angle A is the azimuth of the normal section PQ at P. From the standard formulae of spherical trigonometry we can obtain explicit expressions for sin A and cos A in terms of known quantities and of the unknown angle χ.

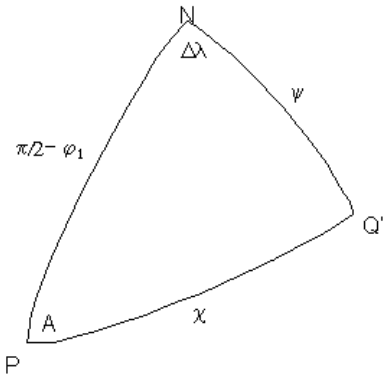

Figure 2.9

From the sine rule we get

$$\sin A = \sin \Delta\lambda \sin \psi \operatorname{cosec} \chi \qquad \text{eq 2.85}$$

Two applications of the cosine rule give

$\cos A = [\cos \psi \cos \varphi_1 - \sin \varphi_1 \sin \psi \cos \Delta\lambda] \operatorname{cosec} \chi$

Elimination of χ

$$\cot A = \operatorname{cosec} \Delta\lambda \, [\cot\psi \cos\varphi_1 - \sin\varphi_1 \cos\Delta\lambda] \qquad \text{eq 2.86}$$

$$= \sin\varphi_1 \operatorname{cosec}\Delta\lambda \, [\cot\psi / \tan\varphi_1 - \cos\Delta\lambda]$$

where

$$\cot\psi = \Lambda_{12} \tan\varphi_1 \qquad \text{eq 2.87}$$

and

$$\Lambda_{12} = (1-e^2)\frac{\tan\varphi_2}{\tan\varphi_1} + e^2\left(\frac{\nu_1}{\nu_2}\right)\frac{\cos\varphi_1}{\cos\varphi_2} \qquad \text{eq 2.88}$$

from Equation eq. 2.84 . This is Cunningham's Azimuth formula (Bomford).

An exact form for the length of the normal section is given by Bomford. Various approximate forms are also available, and will be discussed below.

2.6.1.1.5.2.1.2.3 Arc length on the ellipsoid

To define the geolocation grid (to determine the latitude and longitude of a general grid point), we first defined the latitude and longitudes of a series of points on the ground track. Then we determined the co-ordinates of the other grid points on the assumption that each lay on a line through a ground track point, at a given azimuth and at a given distance (the grid x co-ordinate) from the point.

This is an example of one of the general problems that arises in surveying and geodesy, to find the co-ordinates of a point given that it is at a known distance, along a line at a known azimuth, from a point whose co-ordinates are known. Suppose that the two points are P_1 and P_2, and that their geodetic latitude and longitude are respectively (φ_1, λ_1), (φ_2, λ_2). The problem is to find (φ_2, λ_2) given the distance L between P_1 and P_2, and the azimuth measured from North at P_1, together with the latitude and longitude of P_1. A formula that gives (φ_2, λ_2) in terms of the known quantities is a direct formula.

To determine the x and y co-ordinates of a point given its latitude and longitude, we require the inverse relationship, that gives the length and azimuth of the line between two points on the ellipsoid, as a function of the co-ordinates (latitude and longitude) of the two points. An inverse formula for the distance (though not the azimuth) is also needed to generate the

table of ground track points.

A variety of different geodetic formulae exist, of varying degrees of complexity and accuracy. The present discussion is based on the formulae of Clarke and Robbins; Robbins's formula is essentially the inverse of that of Clarke, and we consider it first.

Suppose that the co-ordinates (latitude and longitude) of two points P and Q are known. Given these quantities, the normal section azimuth of Q measured at P can be computed using Cunningham's azimuth formula (above). In the same spherical triangle (See figure 2.9) the angular distance χ (arc PQ measured at the centre of curvature in prime vertical at P, or O' in figure 2.8 can also be derived from equation eq. 2.85 , equation eq. 2.86 and equation eq. 2.87 . The corresponding length on the auxiliary sphere centred at O' is ($\nu_1 \chi$). For small separations PQ it is clear that this length is very close to the desired length of the normal section PQ, so that the latter can be derived by the application of a small correction to χ. In effect this is what Robbins's formula does.

The radii of curvature in prime vertical at the points P, Q are as follows:

$$\nu_1 = a/(1-e^2\sin(\varphi_1))^{1/2} \qquad \text{eq 2.89}$$

$$\nu_2 = a/(1-e^2\sin(\varphi_2))^{1/2} \qquad \text{eq 2.90}$$

where a is the semi-major axis (the equatorial radius) of the Earth; cf. equation eq. 2.76 . We can then calculate the angle Ψ as in equation eq. 2.84 :

$$S_\psi = (1-e^2)\sin\varphi_2 + (\nu_1/\nu_2)e^2\sin\varphi_1 \qquad \text{eq 2.91}$$

$$C_\psi = \cos\varphi_2 \qquad \text{eq 2.92}$$

$$\Psi = \text{arc cot}(S_\psi / C_\psi) \qquad \text{eq 2.93}$$

Calculate the geodetic correction coefficients

$$g = \varepsilon\sin\varphi_1\cos\varphi_1\cos A \qquad \text{eq 2.94}$$

$$h = \varepsilon \cos^2 \varphi_1 \cos^2 A \qquad \text{eq 2.95}$$

where

$$\varepsilon = e^2/(1-e^2) \qquad \text{eq 2.96}$$

The line segment between points P and Q is then given as a function of the angle χ:

$$L = \nu_1 \chi \left[1 - \frac{\chi^2}{6} h(1-h) + \frac{\chi^3}{8} g(1-2h) + K \right] \qquad \text{eq 2.97}$$

plus terms in higher powers of χ.

Clarke's direct formula, which we quote without proof, is then given as follows. Suppose we are given the latitude and longitude of point P (represented by subscript 1), and the length L of the arc PQ and the normal section azimuth A of point Q;

Calculate

$$r_2 = -\varepsilon \cos^2 \varphi_1 \cos^2 A \qquad \text{eq 2.98}$$

$$r_3 = 3\varepsilon(1-r_2) \cos \varphi_1 \sin \varphi_1 \cos A \qquad \text{eq 2.99}$$

Calculate the radius in prime vertical at latitude φ_1,

$$\nu_1 = a/\left(1 - e^2 \sin(\varphi_1)\right)^{1/2} \qquad \text{eq 2.100}$$

Then

$$\vartheta = \frac{L}{\nu_1} \left[1 - \frac{r_2(1+r_2)}{6} \left(\frac{L}{\nu_1}\right)^2 - \frac{r_3(1+3r_2)}{24} \left(\frac{L}{\nu_1}\right)^3 \right] \qquad \text{eq 2.101}$$

Refer again to figure 2.9 . The quantity just calculated is the angular distance PQ' (χ in the diagram). Once this is known, the triangle can be solved by standard techniques for the longitude difference $\Delta\lambda$ and for the angle ψ. Finally the latitude of Q can be determined from the latter as follows.

$$\rho = 1 - \tfrac{1}{2} r_2 \vartheta^2 - \tfrac{1}{6} r_3 \vartheta^3 \qquad \text{eq 2.102}$$

$$S_2 = \cos\psi - e^2 \rho \sin\varphi_1 \qquad \text{eq 2.103}$$

$$C_2 = (1 - e^2)\sin\psi \qquad \text{eq 2.104}$$

$$\tan\varphi_2 = S_2 / C_2 \qquad \text{eq 2.105}$$

Equation eq. 2.102 to equation eq. 2.105 are essentially a variant of Cunningham's formula, but adapted to the context that ν_2, the radius of curvature at point Q, is not known.

How many terms is it necessary to take in the series (enclosed in square brackets) in Robbins's formula eq. 2.97 to ensure a given degree of accuracy? Table 2.9 below gives an upper limit on the magnitude of each term, including some we have not quoted explicitly, for three different line lengths; 25 km (corresponding to the interval between along-track points used in computing the tables of along track distance), 32 km (ditto for a larger granule size) and 275 km, corresponding to the maximum across-track distance computed during the generation of the reference grid.

Table 2.9 Magnitude of terms in Robbins's Formula. (Terms in mm.)

Term	L = 25 km	32 km	275 km
χ^2	0.427 mm	0.895 mm	568.0 mm
χ^3	1.25 e-3	3.37 e-3	18.37
χ^4	6.57 e-7	2.25 e-6	0.106
χ^5	3.21 e-9	1.41 e-8	5.69 e-3

Clearly it is sufficient for our purposes to take only the first two terms. Table 2.10 shows the similar terms in Clarke's formula eq. 2.101 .

Table 2.10 Magnitude of terms in Clarke's Formula. (Terms in mm.)

Term	L = 25 km	32 km	275 km
$(L/\nu_1)^2$	0.427 mm	0.895 mm	568.0 mm
$(L/\nu_1)^3$	1.25 e-3	3.37 e-3	18.37

2.6.1.1.5.2.1.2.4 Solution of Ellipsoidal triangles

Finally, we require a method for the solution of a triangle on the ellipsoid. There are no exact formulae for treating this case, and so the solution adopted must be based on an approximation. The approximation used here is based on Legendre's theorem, or more strictly on its extension to the ellipsoid.

Legendre's Theorem proper is a result relating to spherical triangles. It is well known, and is not difficult to prove, that the area of a spherical triangle is proportional to the spherical excess of the triangle; this is the amount by which the sum of its three angles exceeds π radians (180°). Thus, suppose ABC is a triangle drawn on a sphere of radius R. The sum of the angles A, B and C will exceed π by the amount

eq 2.106

$$E = (A + B + C) - \pi$$

Then the area of the triangle ABC is ER2, where E is in radians. This result is exact.

Let the sides of the triangle ABC be a, b, c and consider the auxiliary plane triangle A'B'C' that has sides of the same length as ABC. The angles of A'B'C' will of course add up to π ;

eq 2.107

$$A' + B' + C' = \pi$$

Legendre's theorem states that to a good approximation for sufficiently small triangles the area of the auxiliary plane triangle A'B'C' is the same as that of the spherical triangle ABC, and that each of its angles can be derived by reducing the corresponding angle of the spherical triangle by one-third of the spherical excess. Thus

eq 2.108

$$A' = A - E/3$$

and similarly

eq 2.109

$$B' = B - E/3$$

eq 2.110

$$C' = C - E/3.$$

It follows that any problem in spherical trigonometry can be reduced to an equivalent problem in plane trigonometry by reducing the angles according to the above equations.

It can further be shown (Bomford) that Legendre's theorem can be extended to triangles on the ellipsoid. Thus the statements above are true (to an appropriate approximation) if the triangle ABC is drawn on the ellipsoid, and the sides of the triangle are defined as the geodesics joining the vertices A, B, C. In this case the area of the triangle is given by the expression ER^2 as above provided a suitable value for the radius is given. Bomford gives the mean radius

eq 2.111

$$R = \left\{\tfrac{1}{3}\left(1/(\rho_1 v_1) + 1/(\rho_2 v_2) + 1/(\rho_3 v_3)\right)\right\}^{-1/2}$$

where the subscripts 1, 2 and 3 refer to the three vertices A, B and C, and gives higher order terms for this case. Thus:

1. Any trigonometric calculation on the ellipsoid may be reduced to a plane calculation if desired, by correcting the angles by E/3 as above.
2. Because the relationship of the angles of the spheroidal triangle to those of the auxiliary plane triangle are the same as those of the angles of a spherical triangle having the same sides on a sphere of radius R, then to the extent that the higher order terms are negligible, we may use the formulae of spherical trigonometry to solve the spheroidal triangle, if we work with the corrected angles.

The algorithm is based on these statements.

2.6.1.1.5.2.1.3 Calculation of Image co-ordinates of Scan Pixel

Both the calculation of the image co-ordinates of a scan pixel and the image pixel geolocation (next section) make use of a pre-calculated table of the positions of a series of points along the ground track, spaced by 1 image granule (32 image rows, corresponding to approximately 32 km). Thus the table consists of the geodetic latitude and longitude of a series of points i. The table is derived with the aid of the orbit propagator.

Consider a pixel P. If a geodesic is drawn through P to meet the ground track at a right angle in point X, the point X will lie between the tabular points Q[i] and Q[i+1], as shown schematically in figure 1. The triangle PQ[i]Q[i+1] is completely determined if the latitudes and longitudes of its vertices are known, so the angle at Q[i] and Q[i+1] can be determined and the lengths PX and XQ[i] can be determined.

The x co-ordinate of the pixel is then taken to be the distance PX of the pixel from the ground-track. The y co-ordinate is determined from the distance, measured along the ground-track, between the i'th tabular point and the point X, which represents the difference between the y co-ordinate of X (and hence of P) and that of the i'th tabular point. Thus the distance Q[i]X is added to the Y co-ordinate of Q[i] to give the y coordinate of P.

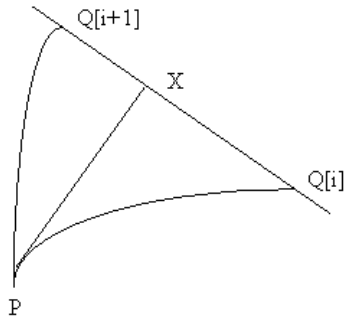

Figure 2.10

For the purposes of this calculation, the ground track between points Q[i] and Q[i+1] is regarded as approximated by the normal section between them. This is justified by the short length (32 km) of the segment; the ground track is not a geodesic, and cannot be approximated by a normal section over long distances. The definition of the table of ground track points is essentially a means to by which the ground track is approximated by a piecewise continuous curve made up of 32 km normal sections.

2.6.1.1.5.2.1.4 Image Pixel geolocation

The generation of the latitude and longitude as a function of x and y makes use of the table of ground track points defined above. Each ground track point represents the centre of an image row.

Consider a point Qi, corresponding to along-track co-ordinate y. The azimuth A of the ground track at this point can be determined, and the azimuth of the image row through Qi is

therefore A + 90°. A direct geodetic formula can therefore be used to determine the latitude and longitude of any image pixel at a distance x along the image row. Details are given in the Algorithm Description (following).

2.6.1.1.5.2.2 Algorithm Description

2.6.1.1.5.2.2.1 Summary

2.6.1.1.5.2.2.1.1 Generate Geolocation Arrays

An initial module generates look-up tables for use in the subsequent geolocation and image pixel co-ordinate determination modules. The tables comprise:

1. Tables of the latitude, longitude, and y co-ordinate of a series of sub-satellite points; these points are equally spaced in time, at an interval corresponding to 1 product granule (32 scan lines), and extend for sufficient time to cover the whole of the data to be processed. They define the satellite ground track, for use in the calculation of the pixel x and y co-ordinates and start sufficiently far south of the ascending node to permit the regridding of scans that are north of the equator in the forward view although the sub-satellite point is south of the equator. This table is derived with the aid of the ENVISAT orbit propagation subroutine.
2. Tables of the latitudes and longitudes of a rectangular grid of points covering the satellite swath. These points are spaced by 25 km across-track, and at the granule interval defined above in the along-track direction. Thus the points in the centre of the column coincide with those described at (1) above, while there are 23 points in the across-track direction. Thus in the across-track direction the points extend 275 km on either side of the ground track. The co-ordinates of the image pixels for land flagging are derived by linear interpolation in this table, and the table forms the basis of the grid pixel latitude and longitude ADS. The grid begins at the start of the first granule of the product (y coordinate 0) and ends sufficiently far beyond the end of data to ensure that the last instrument scan can be fully geolocated.

2.6.1.1.5.2.2.1.2 Calculate Pixel x and y co-ordinates

The x-y (across-track and along-track) coordinates of each tie point pixel are derived from the instrument pixel latitude and longitude.

The x and y co-ordinates may in principle be calculated for each scan pixel, but in practice they are only directly calculated for a series of tie points. The co-ordinates of the remaining points are then determined by linear interpolation between these tie points in a later module

(Interpolate Pixel Positions).

The calculation makes use of a pre-calculated table giving the latitudes and longitudes of a series of points along the ground track, equally spaced in time at an interval corresponding to 1 granule. This table is derived with the aid of the orbit propagator in an earlier module.

2.6.1.1.5.2.2.1.3 Image Pixel Positions

Linear interpolation is performed to determine the latitude and longitude coordinates of the grid pixels for use in the subsequent stages. These interpolated co-ordinates are used for internally by the processor but are not transmitted to the output product, and so this interpolation will not be described in detail here.

2.6.1.1.5.2.2.2 Image Pixel Geolocation

2.6.1.1.5.2.2.2.1 Along-track look-up tables

The orbit propagator is used to generate the look-up table that define a series of points on the ground track separated by a fixed time interval Δ T. The time step Δ T is chosen to correspond to one product granule; that is, to 32 image rows. The image rows are spaced in time by the duration of 1 instrument scan, which is 0.15 s, so that Δ T = 4.8 s.

Thus the orbit propagator is used to determine the latitude and longitude of the sub-satellite point at a sequence of times

$$t(k) = T0 + (k - K)\Delta T,\ k \in \{0, 1, 2, 3, \ldots\} \qquad \text{eq 2.112}$$

where the time origin T0 is defined by the product limits. (It will usually correspond to the ascending node of the orbit). K is a constant offset to ensure that the table extends far enough south of the equator to permit the full geolocation of forward view scans.

The ground trace velocity components are also determined at each tabular point, from which the azimuth of the ground track can be determined.

Given the latitude and longitude of each ground track point k, the interval ds(k) between points k, k + 1 is calculated by an application of Robbins formula (See 2.6.1.1.5.2.1.2.2.)

The along-track co-ordinate of each tabular point is determined from

$$s(0) = 0.0 \quad \text{eq 2.113}$$

$$s(k) = s(k-1) + ds(k),\ k \in \{1, 2, 3, \ldots\} \quad \text{eq 2.114}$$

$$y(k) = s(k) - s(K),\ k \in \{1, 2, 3, \ldots\} \quad \text{eq 2.115}$$

The final step merely redefines the origin of the y co-ordinate to be the tabular point corresponding to T0. (The image scan y co-ordinate field in each product ADS records is derived from the quantity y(k).)

2.6.1.1.5.2.2.2.2 Reference Grid of Image Pixel Co-ordinates

The latitude and longitude are calculated for a series of tie points in the image plane. The principle of the calculation is that for any point Q on the ground track, we can construct the normal section through Q that intersects the ground track at right angles. All points on the normal section have the same y co-ordinate, which is the y co-ordinate of Q. If G is any point on the normal section, the distance QG is equal by definition to the image x co-ordinate of G, and if the geodetic latitude and longitude of Q are known, the geodetic latitude and longitude of G can be derived from the known x co-ordinate and azimuth using Clarke's formula.

Each tabular point on the satellite ground track correspond to the centre of an image row. Image pixel co-ordinates are now computed for a series of 23 tie points on the image row (including the centre point). The tie points are 25 km apart, and range from x = -275 km to x = 275 km. Let the tie points be indexed by j, $j \in \{0, 1, 2, \ldots 22\}$. Then the ground track point itself corresponds to j = 11.

For each k we then have

$$grid\_lat(k - K, 11) = track\_lat[k] \quad \text{eq 2.116}$$

$$grid\_long(k - K, 11) = track\_long[k] \quad \text{eq 2.117}$$

The azimuth A of the image row is determined from the ground trace velocities.

The azimuth of the ground track at Q is β' (measured clockwise from the meridian; note the sign convention here is opposite to that we have used elsewhere). the latitudes and longitudes of 11 points to the left and right of the sub-satellite point are calculated, again using an interval of exactly 25.0 km between the points. These points are in the across-track direction, and lie on the normal section locally orthogonal to the sub-satellite track. The azimuth of this section is $\beta' - \pi/2$.

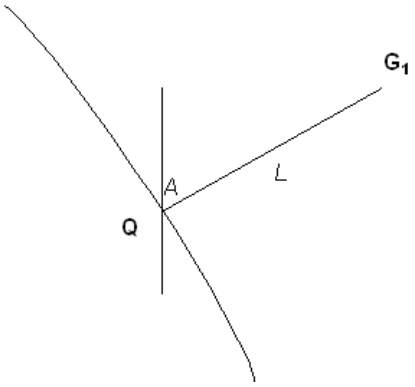

Figure 2.11

In Figure 2.11 , Q is the tabular point just calculated and G_j is the tie point at distance, L = 25 (j - 11) km from Q along the normal section at azimuth $A = \beta' - \pi/2$. Given that both A and L are known together with the co-ordinates of Q, the co-ordinates of tie point G_j can be determined using Clarke's formula.

This procedure can then be repeated on the other side of the track. The along-track coordinate of all 23 points in the across-track direction are the same as that of the sub-satellite point through which the normal section is drawn (by definition).

2.6.1.1.5.2.2.3 Image co-ordinates of the scan pixel

The x and y co-ordinates may in principle be calculated for any scan pixel, but in practice the co-ordinates are only directly calculated for a series of tie points, represented by every tenth pixel along each scan.

The first step is to identify the value of i corresponding to the interval within which the arc from P intersects the ground track at right angles. The angle between the ground track and the arc PX varies continuously as the point X moves along the ground track, and therefore the correct interval is identified using the criterion that the angle of intersection passes

through 90° within the interval.

2.6.1.1.5.2.2.3.1 Calculation of the sides of the triangle

Once the correct interval Q_1Q_2 has been identified, the co-ordinates are calculated by trigonometry. The latitude and longitude of each point P, Q_1 and Q_2 are known, and therefore the length of each side of the triangle PQ_1Q_2 can be determined by means of Robbins' formula eq. 2.97 (above). This process is applied in turn to each of the three sides of the triangle PQ_1Q_2. The triangle is then fully determined and any of its angles can be found.

Thus far our calculation has been exact, to the extent that sufficient terms of the expansion in equation eq. 2.97 have been used, given that the lengths so determined will be normal section lengths.

However, we know that the length of the normal section differs from that of the geodesic by a negligible amount for sufficiently short lines, and so we can regard the lengths calculated above as geodesic lengths, and can regard them as the lengths of the auxiliary plane triangle. We can therefore use Legendre's theorem to derive the angles of the geodesic triangle PQ_1Q2.

2.6.1.1.5.2.2.3.2 The angle at Q

The next step is therefore to compute the angle at Q_2.

The area of the auxiliary plane triangle is given exactly by a standard formula of plane trigonometry:

$$s = (s_{12} + s_{2p} + s_{p1}) / 2 \qquad \text{eq 2.118}$$

$$A = \sqrt{s(s - s_{12})(s - s_{2p})(s - s_{p1})} \qquad \text{eq 2.119}$$

and so the spherical excess is E = A/R2

By plane trigonometry the angle at Q_2' in the plane triangle is

$$Q_2' = \arctan\left\{\sqrt{\frac{(s - s_{12})(s - s_{2p})}{s(s - s_{p1})}}\right\} \qquad \text{eq 2.120}$$

hence the angle at Q_2 is this + E/3.

2.6.1.1.5.2.2.3.3 The x and y co-ordinates

The formulae of spherical trigonometry are used to to calculate the x and y co-ordinates.

Given the side Q_2P (q_1) and the angle Q_2, the right-angled triangle PQ_2X (See figure 2.10) is fully determined, and the arcs PX and Q_2X can be calculated. The arc PX is determined by an application of the sine rule.

$$\sin (PX) = \sin (PQ_2) \sin Q_2 \qquad \text{eq 2.121}$$

The side Q_2X is determined by an application of the cosine rule to the right-angled triangle.

$$\cos (PQ_2) = \cos (PX) \cos (Q_2X) \qquad \text{eq 2.122}$$

so

$$\cos (Q_2X) = \cos (PQ_2) / \cos (PX) \qquad \text{eq 2.123}$$

The arc lengths ξ, η are determined by multiplying the angular lengths PX and Q_2X respectively by the radius of the earth:

$$\xi = R (PX) \qquad \text{eq 2.124}$$

$$\eta = R (Q_2X) \qquad \text{eq 2.125}$$

The sign of the x co-ordinate of P is determined by inspecting the sign of the angle (β - ε) derived at the last value of i above. Then the x and y co-ordinates of P, expressed in km, are

$$x = (\text{sign of } x)\, \xi \qquad \text{eq 2.126}$$

$$y = 25i + (25 - \eta) \qquad \text{eq 2.127}$$

One final correction must be made. All the geolocation calculations have been based on the satellite co-ordinates and other parameters evaluated at the time of the scan time tag. This time corresponds to the start of the scan; as the scan proceeds the satellite moves, and at the end of the scan it will have moved approximately 1 km. The movement is in the y co-ordinate; thus the true y co-ordinate of a pixel measured time Δt later than the start of the scan will be $v\Delta t$ greater than that calculated, where v is the ground trace speed. This correction is added to the y co-ordinate calculated for each tie point pixel.

2.6.1.1.5.2.2.4 Accuracies

2.6.1.1.5.3 Calculate Solar Angles

Solar and viewing angles required for cloud clearing are also determined at this stage. The angles are calculated at a series of tie points across the scan at increments of 25 km in the across-track co-ordinate x; these values are required for internal use within the processor, although only values at 50 km intervals are output to the product.

The following angles are calculated:

- The azimuth of the sun at the pixel;
- The elevation of the sun as seen from the pixel;
- The azimuth of the sub-satellite point measured at the pixel.
- The elevation of the satellite as seen from the pixel.

These quantities are required for use by the 1.6 micron cloud clearing test, to identify situations in which sun-glint might be present, while the solar elevation is also used to distinguish day and night measurements in cloud clearing and level 2 processing. The satellite azimuth and elevation are also used in the calculation of the topographic correction.

The solar and viewing angles are calculated at the centres and edges of the across-track bands defined in Section 2.3.1. . These correspond to a series of across-track positions separated by 25 km. Thus if we define an index k, the solar angles are calculated for nominal across-track co-ordinates

$x = 25(k - 10)$ km

for $k = 0, 20$. In this formulation even values of k correspond to the band edges, and odd values of k to the band-centres. Internally within the processor values are calculated for both band centres and band edges and for every instrument scan, but only the band edge values on the granule rows are output to the product ADS.

Although defined at the nominal positions in the equation above, in practice the angles are calculated for specific instrument pixels. For each view and for every tenth instrument scan, and for each value of k, the instrument pixel whose across-track co-ordinate is closest to the nominal value given by equation (3.1) is identified, and its line of sight azimuth and elevation (measured at the satellite) are derived using the same algebra as in Section 2.6.1.1.5.1.1. . The calculation of the angles is then carried out using the standard ENVISAT mission CFI subroutine pp_target (Reference: Document PO-IS-GMV-GS-0559, PPF_POINTING Software User Manual) with the scan time and the line of sight azimuth and elevation as parameters.

Results for intermediate instrument scans are calculated by linear interpolation with respect to scan number for each across-track distance, and the results are regridded to the image rows in a similar way to the pixel data.

2.6.1.1.5.4 Calculate Topographic Corrections

For those scan pixels that coincide with tie points for which topographic corrections are required, and that are over land, the topographic height is determined from a digital terrain model and topographic corrections to the latitude and longitude are calculated.

2.6.1.1.5.4.1 Theoretical Basis

The pixel geolocation described in Section 2.6.1.1.5.1. finds the intersection of the line of sight from the instrument with the reference ellipsoid. If the land surface is elevated by an amount H above the reference surface, the intersection of the line of sight with the land surface, which is the true pixel position, is displaced towards the satellite in the direction of the projected line of sight by an amount that is proportional to the elevation H.

Let the unit vector from the pixel to the satellite be k = (kx, ky, kz). If the azimuth and elevation of the line of sight at the pixel are a, e respectively, then the components of the unit vector k are

$$k_x = \cos\varepsilon \sin\alpha \qquad \text{eq 2.128}$$

$$k_y = \cos\varepsilon \cos\alpha \qquad \text{eq 2.129}$$

$$k_z = \sin\varepsilon \qquad \text{eq 2.130}$$

expressed in a local co-ordinate system in which the x axis is directed to the east, the y axis is directed to the north parallel to the local meridian, and the z axis is vertical.

The pixel position is displaced by linear amounts

$$dx = H(k_x/k_z) = H \cot\varepsilon \sin\alpha \qquad \text{eq 2.131}$$

$$dy = H(k_y/k_z) = H \cot\varepsilon \cos\alpha \qquad \text{eq 2.132}$$

The corrections in latitude dφ and longitude dλ are the corresponding angular displacements:

$$d\varphi = dy / R \qquad \text{eq 2.133}$$

,

$$d\lambda = dx/(N\cos\varphi) \qquad \text{eq 2.134}$$

,

where φ is the latitude of the pixel. Here R and N are the two orthogonal radii of curvature of the Earth at latitude φ; N and R are the radii of curvature in prime vertical and in the meridian respectively, given by

$$C = EARTH\_MAJOR\_AXIS/\left(1-e^2\right)^{1/2} \qquad \text{eq 2.135}$$

,

$$N = C/\left(1+\varepsilon_2\cos^2\varphi\right)^{1/2} \qquad \text{eq 2.136}$$

,

$$R = N/\left(1+\varepsilon_2\cos^2\varphi\right) \qquad \text{eq 2.137}$$

,

where e is the eccentricity of the reference ellipsoid, and the geodetic constant

$$\varepsilon_2 = e^2/(1-e^2) \qquad \text{eq 2.138}$$

.

The quantity N cos φ is the radius of the parallel of latitude at φ.

2.6.1.1.5.4.2 Algorithm Description

The topographic corrections are computed for the same tie points as the image pixel latitude and longitude. This method makes use of the satellite viewing angles for the appropriate view and tie point previously computed. The topographic height is determined from a digital elevation model.

The nominal tie points are at across-track distances x = {-275, -250, -225, ... 275} km, corresponding to an across-track index k through x = 25(k – 11) km, k = (0, ... 22). However, if k = 0 or k = 22, no viewing angles will be available from the solar and viewing angles calculation, and so these cases are omitted.

The algorithm is applied to both nadir and forward view instrument scans. For each scan, the algorithm steps are as follows.

- For each across-track distance for which a correction is required, the index p of the instrument pixel is found whose across-track co-ordinate is closest to the required across-track distance. The latitude φ and longitude λ of this pixel are found.
- The local altitude (over land) or bathymetry (over sea), H, at latitude φ and longitude λ is extracted from the digital elevation model.
- The pixel is regridded to the appropriate image row. Steps 4 and 5 are performed only if the pixel regrids to a tie row.
- If H < 0 (note this includes the case that the pixel is over sea), the latitude and longitude corrections are set to zero and Step 5 is omitted.
- If H ³ 0 the satellite azimuth and elevation corresponding to the pixel, calculated in the solar and viewing angles module (Section 2.6.1.1.5.3), are extracted and converted to radians, and the latitude and longitude corrections d φ, d λ are calculated using equations (eq. 2.131) to (eq. 2.138) in Section 2.6.1.1.5.4.1. above.

Note that the corrections are the quantities to be added to the nominal latitude and longitude to give the topographically corrected values.

2.6.1.1.6 Signal Calibration

Uncalibrated scan pixels are calibrated using calibration coefficients derived earlier. Pixel calibration uses these calibration coefficients to convert the pixel data to brightness temperature, in the case of the infra-red channels, or to reflectance in the case of the visible and near-visible channels.

In the case of the infra-red channels, this process makes use of look-up tables for the conversion of radiance to brightness temperature. Thus for each pixel and channel, the detector count from the source packet is converted to a radiance using the linear calibration law, and the resulting radiance is used to enter a look-up table from which the brightness temperature of the pixel is derived.

In the case of the visible channels, the linear calibration law gives a calibrated reflectance directly. Calibration parameters to be used by the current module for the visible channels are read from an input file.

Each channel within each view is calibrated independently, and separate calibration parameters (slope and offset) are used for odd and even numbered pixels within the scan.

If valid calibration parameters for a given scan, parity and channel are not available, or if the derived channel values are out of range, the pixel is flagged by an exceptional value. If the input channel count is negative, this implies that the channel is invalid; it has already been flagged by an exceptional value, and is output from the module unchanged.

2.6.1.1.7 Regrid Pixels

Calibrated AATSR pixels are regridded into co-located forward and nadir images, onto a 1 km grid (modified to allow for equal time sampling along-track), using the pixel x and y coordinates derived above.

2.6.1.1.8 Cosmetic Fill

Grid pixels which remain unfilled by the regridding process are filled by copying the value in their nearest unfilled neighbour. This process has the effect of approximately reconstituting original pixel sizes. Filling occurs only where actual pixels are large, and therefore widely spaced, but have been artificially forced into 1 x 1 km boxes. Nearest neighbour copying reverses this process and allows pixels to expand to a more representative size.

2.6.1.1.9 Determine Land-Sea Flag

Given the image pixel latitude and longitude, the surface type for each image pixel is derived using land/sea mask information from an external auxiliary file.

2.6.1.1.10 Cloud Clearing

The process of cloud-clearing, or the identification of cloud affected pixels, is accomplished by applying in turn a series of tests to the brightness temperature data in the 12, 11 and 3.7 μm channels, and to the reflectance data in the 1.6 μm channel. The pixel is flagged as cloudy if any one of the tests indicates the presence of cloud. Table 2.11 below lists the cloud clearing tests that are applied. All of the tests are of course conditional on the appropriate infra-red or 1.6 μm data being available.

Table 2.11 Cloud Clearing Tests

Test	Comments
gross cloud test	applied to nadir and forward views separately
thin cirrus test	applied to nadir and forward views separately
medium/high level cloud test	applied to nadir and forward views separately
fog/low stratus test	applied to nadir and forward views separately
11 μm spatial coherence test	applied to nadir and forward views separately
1.6 μm histogram test	applied to nadir and forward views separately
11/12 μm nadir/forward test	uses both views
11/3.7 μm nadir/forward test	uses both views
infra-red histogram test	applied to nadir and forward views separately

The tests are applied in the order in which they appear in table 2.11 . Although the order in which they are applied is not critical in all cases, some of the tests depend on the results of tests performed previously. The 1.6 μm test operates only on pixels not previously flagged as cloudy by the gross cloud test, the thin cirrus test or the 11 μm spatial coherence test (these are the other single view tests that operate on daytime data), and must therefore follow these. The infrared histogram test is always applied last, and only uses those pixels that have not been flagged as cloudy by any of the preceding tests.

The 1.6 μm test operates on daytime data only. The tests involving the 3.7 μm channel, on the other hand, are only applied to night-time data, because reflected solar radiation may be significant in this channel during the day. Those tests that involve only the 11 and 12 μm channels are applicable to both daytime and night-time data. Not all of the tests are implemented over land.

A series of cloud state flags is defined for each pixel and for the forward and nadir view separately. The flags are listed in table 2.12 .

Table 2.12 Cloud-clearing/land flagging flags (nadir or forward view).

#	Meaning if set
0	Pixel is over land
1	Pixel is cloudy (result of all cloud tests)
2	Sunglint detected in pixel
3	1.6 μm reflectance histogram test shows pixel cloudy (day-time only)
4	1.6 μm spatial coherence test shows pixel cloudy (day-time only)
5	11 μm spatial coherence test shows pixel cloudy
6	12 μm gross cloud test shows pixel cloudy
7	11/12 μm thin cirrus test shows pixel cloudy
8	3.7/12 μm medium/high level test shows pixel cloudy (night-time only)
9	11/3.7 μm fog/low stratus test shows pixel cloudy (night-time only)
10	11/12 μm view-difference test shows pixel cloudy
11	3.7/11 μm view-difference test shows pixel cloudy(night-time only)
12	11/12 μm thermal histogram test shows pixel cloudy

These flags are set according to the results of the tests. Thus if one of the flags numbered 3 to 12 is set, this means that the corresponding test has indicated the presence of cloud. If on completion of the cloud-clearing sequence any of these flags is not set, it may mean either that the test did not indicate the presence of cloud, or that the test was not applied because suitable data was lacking.

Each test makes use of a look-up table of parameters with which the brightness temperature or reflectance data is compared. Where tests are applied to forward and nadir view images separately, the parameters may be defined separately for the two cases. More generally, the comparison parameters may depend on the air mass in the line of sight, and this is implemented by allowing the tabular parameters to depend upon the across-track band. For the purposes of cloud clearing and Level 2 processing, the (512 km) AATSR swath is imagined as divided into 10 bands parallel to the satellite ground track. These bands are numbered from 0 to 9, and each is 50 km wide except that the outer two are 56 km wide.

2.6.1.1.10.1 Gross cloud test

The gross cloud test uses the 12 μm channel, and is applied to single pixels for both day and night-time conditions. It is based on the principle that the temperature of the atmosphere falls with altitude, so that the brightness temperature of an optically thick cloud at high altitude will be significantly is less than the surface temperature. The test then consists of comparing the 12 μm brightness temperature with a threshold value that is set to be lower than the brightness temperature expected from the surface. If the 12 μm brightness temperature is lower than the threshold, the pixel is flagged as cloudy. The 12 μm channel is used because the optical depths of the clouds tend to be greater here than at shorter wavelengths.

Clearly the threshold value must be chosen with care. The appropriate threshold will depend

on whether the pixel is over land or over sea, on the time of year, and on the geographic region. In principle the threshold might depend on angle of incidence; in practice the dependence of brightness temperature with incidence angle is sufficiently slow that it is sufficient to have a different set of thresholds for the forward and nadir views. Changes in the angle of incidence within the view (which might be applied by varying the threshold with across-track band) are not regarded as significant.

The choice of a suitable threshold is easier over sea than over land, since sea surface temperature in a given region varies only slowly during the year. Therefore the present algorithm applies the test to data over the sea only. The test uses a look-up table with values of the threshold tabulated at intervals of 1 ° of latitude for each view (forward and nadir), and for each calendar month.

Each pixel is examined separately. If the pixel is valid and if the 12 μm brightness temp

$$I(ir12, v; i, j) < gross\_cloud\_threshold \qquad \text{eq 2.139}$$

where gross_cloud_threshold is the appropriate threshold value from the 12 μm gross cloud test LUT 6.6.21. , for the latitude and month of observation, the pixel is flagged as cloudy.

2.6.1.1.10.2 Thin cirrus test

The thin cirrus test uses the differences between the measured brightness temperatures at 11 and 12 μm; this difference may be large over optically thin cirrus cloud owing to emissivity differences at the two wavelengths (Saunders and Kriebel 1988 Ref. [1.16]).

The brightness temperature difference is calculated for each pixel and compared with a tabulated threshold value; if the difference exceeds the threshold, the pixel is flagged as cloudy.

The threshold for this test is a function of both the brightness temperature at 11 μm and the air mass in the line of sight; the latter is represented by the across-track band number. The look-up table then consists of values for each view separately, for each across-track band, and for temperature values at 1 K intervals between 250 and 310 K. In order to enter the table, a brightness temperature index is defined as the integer part of (T-250), in units of K.

The test uses a look-up table that defines a threshold thin_cirrus_threshold for the nadir and forward views separately, for each across-track band and for values of the brightness temperature index from 0 to 60 inclusive. It is applied to the forward and nadir views separately. For each pixel, if the difference

$$I(ir11, v; i, j) - I(ir12, v; i, j) > thin\_cirrus\_threshold(bt\_index, band\_no) \qquad \text{eq 2.140}$$

for the appropriate view, the pixel is flagged as cloudy. The appropriate value of the quantity thin_cirrus_threshold is taken from the thin cirrus cloud LUT 6.6.24. .

2.6.1.1.10.3 Medium/high level cloud test

This test uses the difference between the 3.7 and 12 μm channel brightness temperatures. This difference is calculated for each pixel and, if it is greater than a threshold value, the pixel is flagged as cloudy (Saunders and Kriebel 1988 Ref. [1.16]). The threshold value in this case is a function of the 12 μm brightness temperature, and is tabulated with a resolution of 0.5 K. Separate tables are defined for the forward and nadir views.

The test uses a look-up table that defines a threshold med_high_level_thresh for the nadir and forward views separately, for values of the brightness temperature index from 0 to 120 inclusive. The brightness temperature index is defined as the integer part of (T-250), in units of K. The test is applied to the forward and nadir views separately. If the 3.7 and 12 μm brightness temperatures are valid, and the difference

$$I(ir37, v; i, j) - I(ir12, v; i, j) > med\_high\_level\_thresh(bt\_index) \qquad \text{eq 2.141}$$

for the appropriate view, then the pixel is flagged as cloudy. The test is only performed for night-time data; specifically, it is only performed for pixels on image rows such that at each end of the row, the band centre solar elevation for the view in question is less than 5°. The appropriate value of the quantity med_high_level_threshold is taken from the med/high level cloud LUT 6.6.23. .

2.6.1.1.10.4 Fog/low stratus test

At night the difference between the brightness temperatures at 11 and 3.7 μm may be used as a sensitive indicator of fog or low stratus cloud (Saunders and Kriebel 1988 Ref. [1.16]), because the emissivity of such cloud is lower at 3.7 μm than at 11 μm.

The brightness temperature difference is calculated for each pixel and compared with a threshold; if the measured difference exceeds the threshold, the pixel is flagged as cloudy. The threshold depends on the air mass in the line of sight, and so different thresholds are defined for each across-track band, and for the nadir and forward view images separately. The test uses a look-up table that defines a threshold fog_low_stratus_threshold for the nadir and forward views separately, for each across-track band.

The test is only performed for pixels on image rows such that at each end of the row, the band centre solar elevation for the view in question is less than 5°, so excluding day-time data. For such pixels, if the difference

I(ir11, v; i, j) - I(ir37, v; i, j) > fog_low_stratus_threshold(band_no) eq 2.142

for the appropriate view then the pixel is flagged as cloudy. The appropriate value of the quantity fog_low_stratus_threshold is taken from the fog/low stratus LUT 6.6.22. .

2.6.1.1.10.5 Spatial coherence test (11 um)

The spatial coherence test actually comprises two tests, the small-scale and the large-scale tests. It is applied to the 11 µm image, and can be used for both day and night-time conditions. The 11 µm channel is used in preference to either the 3.7 µm or the 12 µm channel in this test because it is available in both day and night-time and, for ATSR and ATSR-2 operating with L-rate telemetry, its digitisation accuracy was better, or as good, as that of the other channels. The latter consideration does not apply to AATSR, but the test is unchanged to ensure continuity with the earlier instruments.

The small-scale spatial coherence test determines whether the variability of the 11 µm brightness temperature is greater than would be expected for clear conditions; if so, it assumes that cloud is present. To apply the test, the standard deviation of a 3 x 3 array of pixels is calculated and compared with a pre-defined threshold; cloud is flagged if the threshold is exceeded. The test can be applied over both land and sea surfaces, but different thresholds are used for the two cases. In particular a lower standard deviation threshold is used for land data at night than during the day, because the variability of the land surface temperature is found to be lower at night.

The test is only applied to 3 x 3 arrays of pixels that are all over sea, or all over land. It is not applied to mixed or coastal regions, where surface temperature variations may be large (Saunders and Kriebel 1988).

A refinement has been added to the basic small-scale test as defined by Saunders and Kriebel (1988) to allow for the possibility that the observed spatial variability may result from ocean fronts rather than cloud. This uses the difference between the 11 and 12 µm channels as a marker. It is assumed that this difference is insensitive to surface temperature variations, but will be sensitive to the presence of cloud. Thus if a group of 9 pixels have been flagged as cloudy by the basic test of spatial variability, they are further tested as follows. The average difference between the 11 and 12 µm channel brightness temperatures for the array of pixels is calculated, and compared with the same average calculated for the neighbouring cloud-free pixels. If the two averages differ by less than a pre-defined threshold, the pixels of the original group are 'unflagged'; that is, the flags representing the outcome of the test are reset to clear. The neighbouring cloud-free pixels in this case are the members of the eight surrounding 3 x 3 groups of pixels that have been flagged as clear by the basic spatial variability test.

The test is performed separately for the nadir and forward views. The nadir view 12 µm and

11 μm data are used in the nadir view test and the forward nadir view 12 μm and 11 μm data are used in the forward view test. It is assumed that the along-track size of a view is 512 km. That is, the orbit is imagined as tiled with 512 by 512 pixel images, each of which is treated separately. If an incomplete image is encountered at the end of data, the image is filled up to 512 by 512 pixels with unfilled pixels.

The small scale spatial coherence test uses a square array of 3 x 3 pixels.

The large-scale spatial coherence test is applied after the unflagging stage of the small-scale test has been completed, over open ocean only. It is logically a separate test, although it is defined as part of the same algorithm module, and as currently implemented only one flag is used to record the combined result of the small-scale and large-scale tests. Thus you cannot tell, if the flag is set, which of the two tests (if not both) has actually detected cloud.

The large-scale spatial coherence test is designed to detect low-lying marine stratiform cloud. The small-scale spatial coherence test is ineffective over uniform stratus cloud by reason of its very uniformity, and indeed this type of cloud is difficult to detect by any of the cloud tests, particularly if it is low-lying, so that the temperature differential between the cloud and clear sea is small.

The physical concept underlying the test is similar to that of the gross cloud test, that clouds are cooler than sea. However, in these circumstances it is difficult if not impossible to set a suitable threshold to differentiate between cloud and clear sea. This is particularly the case where there are significant gradients of SST; the physical basis of the test is that cloud is colder than clear sea, so that if a threshold were set that was valid at a particular place, then in the presence of temperature gradients, clear sea pixels would be rejected in colder regions, while in an area that was fully cloud covered, in warmer regions cloudy pixels might be passed as warmer than the threshold.

The detailed rationale for this test is described by Zavody et al (Zavody, A.M, Mutlow, C.T. and Llewellyn-Jones, D.T. Journal of Atmospheric and Oceanic Technology, 17, 595 – 615, 2000). The test attempts to overcome these problems by setting a dynamic threshold adapted to local conditions. The test works with rectangular areas of fixed size (the size is set by an auxiliary parameter, and in practice is 128 by 128 km), and the threshold used within a particular area is based on conditions in the neighbouring areas that surround it.

In order to set a realistic threshold for a given area, the clear sea pixels in the neighbouring areas are examined. In each area the maximum 11 micron BT of the cloud-free pixels in the area is determined. This is assumed to be representative of clear sea in the area, while the distribution of the BTs from the set of neighbouring areas is assumed to be representative of the distribution at 128 km resolution. It is then assumed that if the smallest of these representative temperatures is selected, the probability that the temperature of clear sea in the central region is lower than this is itself low. The dynamic threshold is then set on the basis of this temperature.

The large-scale spatial coherence test uses data from sub-areas of COH_AREA_SIZE x COH_AREA_SIZE. The value of COH_AREA_SIZE must be chosen so that it is a factor of 512. Its current value is 128 km.

The Small-Scale Spatial Coherence Test

The small and large-scale spatial coherence tests are applied to an image array of 512 by 512 pixels. Let the pixels be identified by indices i, j in the along-track and across-track directions respectively, where $0 \leq i < 512$ and $0 \leq j < 512$.

The small-scale spatial coherence test operates on arrays of 3 by 3 pixels, known as pixel groups. The 512 by 512 pixel image is divided into 171 by 171 such groups; let the groups be indexed by i_group and j_group, where $0 \leq i\_group < 171$ and $0 \leq j\_group < 171$. In general, the pixel indexed by (i, j) falls in the group indexed by i_group = int[i/3], j_group = int[j/3].

However, because the image size is not a multiple of 3, this rule is modified at the edges of the image. The pixels that fall within the group defined by (i_group, j_group) are those whose indices satisfy

$$i_0 \leq i \leq i_0 + 2 \ , \ j_0 \leq j \leq j_0 + 2 \ ,$$

where i_0 is the smaller of (3i_group + 1, 509) and j_0 is the smaller of (3j_group + 1, 509). Thus the last group in each row consists of the pixels having j = 509, 510, 511. If we denote the set of pixels comprising the group indexed by (i_group, j_group) by G(i_group, j_group) then

G(i_group, j_group) = $\{i, j; i_0 \leq i \leq i_0 + 2 \ , \ j_0 \leq j \leq j_0 + 2 \}$ where i_0 and j_0 are as defined as above. This implies that the last two groups in each row or column overlap, so that any pixel having either i = 509 or j = 509 falls into two adjacent groups.

The auxiliary parameters used in this test are listed in Table 1.1. They are taken from the auxiliary file of Cloud Look-up Table Data ATS_CL1_AX.

Table 2.13 Auxiliary parameters used by small-scale spatial coherence test

Parameter	Value
SEA_MAX_DEV	20
LAND_DAY_MAX_DEV	150
LAND_NIGHT_MAX_DEV	100
COHERENCE_RESET_THRESH	10

The same parameters are used for both nadir and forward view image.

The test is performed separately for the nadir and forward view image. For each image, and for each group of 3 x 3 pixels within the image, do the following steps.

1) Determine the solar elevation corresponding to the across-track band containing the group.

2) Determine whether all the valid pixels in the group are over land or over sea. Set the group_land_flag if any pixels within the group are land pixels. Proceed to the next group if the set contains a mix of land and sea pixels, or if there are 2 or fewer valid pixels.

3) Calculate the mean and standard deviation of the 11μm brightness temperatures for the valid pixels in the group, excluding cosmetic fill pixels.

4) Select the appropriate threshold. If the pixel group is over sea set the threshold to SEA_MAX_DEV. If the group is over land, inspect the solar elevation angle determined in Step 1. If the solar elevation is greater than 5° set the threshold to the daytime value LAND_DAY_MAX_DEV; otherwise set the threshold to the night-time value LAND_NIGHT_MAX_DEV.

5) If the standard deviation is greater than the selected threshold, flag the group as cloudy and proceed to step 6, otherwise continue to the next 3 x 3 group of pixels.

6) In a second pass over the image, investigate whether the spatial variation may result from ocean gradients rather than cloud:

6.1) If 4 or more of the surrounding 8 pixel groups have been flagged as clear and the group contains more than 2 valid pixels proceed to Step 6.2; otherwise move to the next group.

6.2) Calculate the average difference between the 11 and 12 micron channel brightness temperatures for the central (cloudy) group and for those of the surrounding groups that are clear. If the absolute value of the difference between the averages for cloudy and clear groups is less than COHERENCE_RESET_THRESH, then clear the flags for all pixels of the group.

The Large-Scale Spatial Coherence Test

For the large-scale test, the image is sub-divided into n by n square sub-areas whose size is defined by an auxiliary parameter COH_AREA_SIZE, such that n = 512/COH_AREA_SIZE. In practice COH_AREA_SIZE = 128, so that there are 16 sub-areas of nominal size 128 by 128 km. The sub-areas may be indexed by i_sub, j_sub, $0 \leq$ i_sub $<$ n and $0 \leq$j_sub $<$ n.

The large-scale spatial coherence test operates the pixel groups, not on individual pixels. Because the sub-area size is not divisible by three, the relationship between the pixel groups and the sub-areas is complex. The groups for the sub-area indexed by i_sub, j_sub, are defined by the limits

jx1 = INT((j_sub x COH_AREA_SIZE)/3)

jx2 = INT(((j_sub + 1) x COH_AREA_SIZE)/3) - 1

iy1 = INT((i_sub x COH_AREA_SIZE)/3)

iy2 = INT(((i_sub + 1) x COH_AREA_SIZE)/3) – 1.

Here INT denotes the integer part function.

Pixel groups are associated with the sub-areas as follows. The set of groups that corresponds to the sub-area indexed by i_sub, j_sub comprises those groups whose indices i_group, j_group satisfy

$(i\_group, j\_group) \in A(i\_sub, j\_sub)$,

where the set of index pairs A(i_sub, j_sub) is formally defined by

$A(i\_sub, j\_sub) = \{(i\_group, j\_group): jx1 \leq j\_group \leq jx2;$

$iy1 \leq i\_group \leq iy2\}$

Since the number of groups is not a multiple of n, the sets A(i_sub, j_sub) do not each contain the same number of groups.

The large-scale test uses the additional auxiliary parameters listed in Table 1.2. They are taken from the auxiliary file of Cloud Look-up Table Data ATS_CL1_AX. The detailed structure of the algorithm is as follows.

Table 2.14 Additional auxiliary parameters used by the large-scale spatial coherence test

Parameter	Value
COH_AREA_SIZE	128
COH_FRACTION_PASSED	0.005
COH_ADJ_THRESH_LAND	400
COH_ADJ_DIF_LAND	0.20
COH_AREA_DIF_NV	25
COH_AREA_DIF_FV	35
COH_MIN_DIF_NV	-15
COH_MIN_DIF_FV	-15
COH_AREA_THR_NV	200
COH_AREA_THR_FV	250
CLOUDY_BOX_THRESH	-1

1. Flag groups in coastal regions

1) By reference to the group_land_flag determined at Step 2 of the small-scale spatial coherence test, flag all groups near to land, and all land groups. For each group set an extended_land_flag(j_group, i_group) if

ΣΣgroup_land_flag(i, j) > 0

where the summations extends over indices in the ranges of

j_group - 3 < i < j_group + 3,

i_group - 3 < j < i_group + 3.

i and j must also be in the range of 0 to 170.

2. Find maximum brightness temperature (BT) and BT differences in sub-area

2) For each sub-area, find the group(s) with the highest average 11-mm brightness temperature, and the average (11-μm – 12-μm) brightness temperature difference(s) of these:

2.1) Find the highest average 11mm brightness temperature in the sub-area (max_bt_11) and its/their coordinates. Use only valid groups, where a valid group is one that satisfies the following conditions:

- its extended_land_flag is not set;
- it has passed the small-scale coherence test; that is, its group_cloud_flag is not set;
- it has not been shown to contain significant cloud by any previous test;
- it contains at least 3 natural pixels having valid 11 micron and 12 micron brightness temperatures and so is able to contribute to the computation of the average (11 micron - 12 micron) brightness temperature difference at 2.2) below. (A natural pixel is one that is neither cosmetically filled nor unfilled). In the following the number of such pixels is denoted by valid_pixel_pairs.

The flag previous_tests(j_group, i_group) is determined as follows:

If the auxiliary parameter CLOUDY_BOX_THRESH = -1, the flag is determined by inspecting only the central pixel of the group; previous_tests(j_group, i_group) is set if the pixel (i, j) was flagged by the gross cloud test, the thin cirrus test, the medium-high level cloud test, or the fog – low stratus test, where i is the lesser of (3i_group + 1, 510) and j is the lesser of (3j_group + 1, 510); i and j index the central pixel of the group.

If CLOUDY_BOX_THRESH > 0, the value of previous_tests(j_group, i_group) is determined by inspecting all pixels of the group: it is set if (n_cloudy ^{3} CLOUDY_BOX_THRESH), where n_cloudy is the total number of pixels from the group defined by the index set in G(i_group, j_group) that have been flagged as cloudy by one of the above cloud tests.

Then max_bt_11 is maximum value of the average 11 micron brightness temperature

(determined at Step 3 of the small scale spatial coherence test above) over the set of indices

$(j\_group, i\_group) \in A_{valid}(j\_sub, i\_sub)$

The set $A_{valid}(j\_sub, i\_sub)$ is the set of indices of valid groups within the sub-area, and is defined by

$A_{valid}(j\_sub, i\_sub) = \{j\_group, i\_group: (j\_group, i\_group) \in A(j\_sub, i\_sub)$

and NOT group_cloud_flag(j_group, i_group)

and NOT extended_land_flag(j_group, i_group)

and NOT previous_tests(j_group, i_group)

and (valid_pixel_pairs(j_group, i_group) ³ 3)}

Set

sub_area_max_11(j_sub, i_sub) = max_bt_11.

2.2) Calculate the average brightness temperature difference(s) $T_{11} - T_{12}$ using valid pixel pairs (as defined above) for the groups with max_bt_11).

If a single group has the average 11μm brightness temperature value of max_bt_11 then assign its brightness temperature difference value to sub_area_di(j_sub, i_sub) f.

If more than one group in the sub-area has the same max_bt_11 value then find the highest of these differences, and assign this value to sub_area_dif(j_sub, i_sub).

2.3) It is possible that there are no valid groups; that A_{valid} is an empty set. In this case sub_area_max_11(j_sub, i_sub) and sub_area_dif(j_sub, i_sub) should each be set to an exceptional value (≤ 0) to ensure that they are ignored in Step 5 below.

3. Identify sub-areas containing land

3) Set the land_sub_area flag to 1 for all sub-areas in which one or more groups are over or near land. The flag is set if

Σextended_land_flag(j_group, i_group) > 0

where the sum includes all index pairs $(j\_group, i\_group) \in A(j\_sub, i\_sub)$.

4. Identify valid sub-areas

4) Set the flag valid_sub_area_flag to 1 for all sub-areas for which the number of clear sea groups is greater than a fraction COH_FRACTION_PASSED of the total number, i.e.

S (1-group_cloud_flag(j_group, i_group)) x (1-extended_land_flag(j_group, i_group)) /

$(COH\_AREA\_SIZE/3)^2$ > COH_FRACTION_PASSED,

where the sum includes all (j_group, i_group) $\in$ A(j_sub, i_sub),

and sub_area_dif(j_sub, i_sub) is greater than COH_MIN_DIF. COH_MIN_DIF should take the value COH_MIN_DIF_NV for the nadir view, or COH_MIN_DIF_FV for the forward view, as appropriate.

5. Determine and apply dynamic threshold

5) Process each sub-area in turn. For invalid sub-areas, set the 11mm brightness temperature threshold (threshold_11) to 32000 cK i.e. to an unrealistically high value, so that all the sea pixels in these sub-areas are flagged, as cloudy and omit Steps (5.1) to (5.7). For sub-areas that are valid, determine threshold_11 as follows (Steps (5.1) to (5.7)):

5.1) Select the up to 9 sub-areas (valid or not) centred on the one being investigated. These are the sub-areas whose indices fall in the set

S(p, q) = {(j_sub, i_sub): $0 \le$ j_sub $<$ n, $0 \le$ i_sub $<$ n,

p - 1 $\le$ j_sub $\le$ p + 1, q - 1 $\le$ i_sub $\le$ q + 1}

where p, q, $0 \le p < n$, $0 \le q < n$, are the indices of the sub-area currently under consideration.

5.2) Set the flag land_in_areas if one or more of the sub-areas selected has land, that is if, for any (j_sub, i_sub) $\in$ S(p, q), land_sub_area(j_sub, i_sub) is set.

5.3) Find bt_dif_max, the highest value of sub_area_dif, for valid selected sub-areas:

bt_dif_max = max(sub_area_dif(j_sub, i_sub)),

over the set of all index pairs (j_sub, i_sub) $\in$ S(p, q) that identify valid sub-areas. (At least one sub-area, the central one, must be valid, so this operation is always possible.)

5.4) Calculate the difference threshold given by:

difference_threshold = COH_AREA_DIF*(1 + land_in_areas x COH_ADJ_DIF_LAND)

COH_AREA_DIF should take the value COH_AREA_DIF_NV for the nadir view, or COH_AREA_DIF_FV for the forward view, as appropriate.

Identify those values of sub_area_max_11 for which the corresponding sub_area_dif is within difference_threshold of bt_dif_max found in Step 5.3, that is, for which

sub_area_dif(j_sub, i_sub) > bt_dif_max - difference_threshold.

5.5) Find the lowest maximum brightness temperature of those sub-areas identified in step 5.4. Set lowest_max_bt to the minimum value of sub_area_max_11(j_sub, i_sub) over the set of index pairs (j_sub, i_sub) $\in$ S(p, q) for which the sub-area is valid, and sub_area_dif(j_sub, i_sub) satisfies the test in Step 5.4.

5.6) Calculate threshold_11 for the sub-area investigated:

threshold_11 = lowest_max_bt - COH_AREA_THRESH

- land_in_areas x COH_ADJ_THRESH_LAND.

COH_AREA_THRESH should take the value COH_AREA_THR_NV for the nadir view, or COH_AREA_THR_FV for the forward view, as appropriate

5.7) If only one valid sub-area was selected at step 5.4, and the land_in_area flag is set, lower threshold_11 by 200 cK.

5.8) Flag all sea pixels in the sub-area investigated in those groups for which the average 11 micron brightness temperature (determined at Step 3 of the small scale spatial coherence test above) is below threshold_11 determined in Steps 5.1 to 5.7 above.

2.6.1.1.10.6 Histogram test (1.6 um)

2.6.1.1.10.7 11/12 um and 11/3.7 um nadir/forward tests

Atmospheric absorption in the 11 and 12 μm window channels is dominated by water vapour. The effect is stronger in the 12 μm channel than in the 11μm channel and hence the differences in brightness temperatures in the two channels also vary in an almost linear way with the atmospheric water vapour loading.

For either channel, the total effect is also roughly proportional to the amount of water vapour in the path, and hence it is greater for the forward-view than for the nadir view.

It follows from the above that there is a fairly well defined relationship between, for example, the nadir view 11 μm minus 12 μm brightness temperature differences and the nadir view minus forward view 11 μm brightness temperature differences. Both differences increase with atmospheric water.

The relationships derived for cloud-free atmospheres do not necessarily hold if there is a uniform cloud layer in the path. Also, owing to the stereoscopic effect, clouds with spatial

dimensions of less than roughly their height above sea level affect the brightness temperature from a sea pixel in only one of the views and hence the relationship between the two differences is even more likely to differ from that for the clear atmosphere.

The test, therefore, consists of comparing the observed 11 μm (nadir-view - forward-view) differences with those expected on the basis of the relationship (derived from modelling) given the (11 μm - 12 μm) differences in the nadir view. If the discrepancy between the two is significant (greater than some threshold), the pixel is flagged as cloudy.

The effects of clouds on the 3.7 μm channel differ from those in the 11 and 12 μm window channels and hence at night it is useful to do the test with the 3.7 μm brightness temperature. For the case of clear atmospheres, the nadir-view minus forward view differences are small in this case, and vary in a non-linear way with the 3.7 μm minus 11 μm brightness temperature differences. A quadratic relationship is used to test the data.

These tests are not reliable over land for the following reasons:

- The pixels are only collocated at sea level hence, over land, the brightness temperatures measured in the nadir view and forward view do not necessarily originate on the same land pixel. As land temperatures can have strong spatial variability over distances of a few kilometers, the brightness temperature differences in the two views from non-collocated pixels is often meaningless.
- The emissivities for the different channels vary with the nature of the terrain and hence there is no unique relationship between the differences in two channels and the differences in the two views.

2.6.1.1.10.7.1 11/12 um nadir/forward test

The nadir-forward tests (Zavody et al, 2000) are based on the idea that for clear sea pixels there should be a correlation between the difference in brightness temperature between the nadir and forward view measurements at 11 microns and the difference between the nadir view 11 and 12 micron brightness temperatures, since both depend on the atmospheric characteristics, principally the water vapour loading. This relationship has been determined using radiative transfer modelling applied to an ensemble of atmospheric profiles. For each pixel the difference T11 - T12 is determined, and used to predict the view difference using this relationship. The actual view difference is compared with the prediction, and if they differ by more than a threshold, the pixel is assumed to be cloudy.

This test is only applied to sea pixels. It loops through the pixels in the 10 across-bands of an image and checks the relationship between the measured brightness temperature differences for each pixel, using the appropriate parameters and threshold. It uses the nadir view 12 μm and 11 μm brightness temperatures, and the forward view 11m brightness temperatures.

For each sea pixel the following steps are executed

1) The (11um - 12um) BT difference dif_11_12 = $T_{11} - T_{12}$ is derived.

2) The 11um (nadir-view - forward-view) BT difference dif_nv_fv is derived.

3 Using the coefficients appropriate for the across-track band in which the pixel falls, the expected view difference is computed:

$exp\_dif\_nv\_fv = a_0 + a_1 \times dif\_11\_12$

4) If the difference abs(exp_dif_nv_fv - dif_nv_fv) is greater than the threshold value, the pixel is flagged as cloudy.

The coefficients a_0 and a_1 for each across-track band, and the threshold value, are taken from the auxiliary file of Cloud Look-up Table Data ATS_CL1_AX.

2.6.1.1.10.7.2 11/3.7 um nadir/forward test

This test is similar to the preceding test but uses the 37 micron and 11 micron brightness temperatures instead of the brightness temperatures in the 11 and 12 micron channels, and is used at night when the 3.7 micron data are available. The theoretical relationship between the view difference and the nadir view channel difference is slightly more complex in this case than in the preceding test, being quadratic rather than linear.

The test uses the nadir view 11 μm and 3.7 μm brightness temperatures and the forward view 3.7 μm brightness temperatures with the appropriate parameters and threshold. Like the preceding test, it is only applied to sea pixels.

The test is applied to all sea pixels measured at night, for which the 3.7um channel is available. For each such pixel the following steps are executed.

1) The (3.7um - 11um) BT difference $dif\_37\_11 = T_{37} - T_{11}$ is derived.

2) The 3.7um (nadir-view - forward-view) BT difference (dif_nv_fv) is derived.

3) Using the coefficients appropriate for the across-track band in which the pixel falls, the expected view difference is computed:

$exp\_dif\_nv\_fv = a_0 + (a_1 + a_2 \times dif\_37\_11) \times dif\_37\_11$

4) If the difference abs(exp_dif_nv_fv - dif_nv_fv) is greater than the threshold value, the pixel is flagged as cloudy.

The coefficients a_0, a_1 and a_2 for each across-track band, and the threshold value, are taken from the auxiliary file of Cloud Look-up Table Data ATS_CL1_AX.

2.6.1.1.10.8 Infrared histogram test

This is the last of the cloud tests performed and it is applied only to those pixels that have passed all the previous cloud tests. It uses the 11 μm and 12 μm channels, and relies mostly on the following:

1. The difference between brightness temperatures measured in different channels is almost entirely determined by the atmospheric characteristics.

2. The atmospheric variability is usually small over the area of an AATSR image product. It follows that even when strong temperature gradients are present in the sea, the brightness temperature differences form a fairly tight cluster for the clear pixels.

3. Low stratus clouds, the most likely contamination to have escaped detection by the other tests, affect the brightness temperatures differently from the clear atmosphere. There are two effects:

a. The infrared radiation detected originates from a height above sea level and hence the lowest layer of the troposphere is only partially traversed by the radiation. As it is this layer that contains most of the atmospheric water vapour, which is the major source of the difference between the 11 μm and 12 μm brightness temperatures, these differences are reduced over clouds.

b. Low clouds have a slightly higher emissivity in the 12 μm channel than in the 11 μm channel. It follows that the proportion of reflected cold radiation is less for the 12 μm channel as for the 11 μm channel and hence the 12 μm brightness temperature over this type of cloud, compared with the 11 μm brightness temperature, is not as cold as over the clear sea.

The 12 μm brightness temperature is almost always lower than the 11 μm brightness temperature owing to the water vapour absorption. Both the above effects reduce the difference found over clear sea.

4. If the water vapour column amounts are not uniform over an image, and the sea surface temperature is constant, then the lowest brightness temperatures originate from pixels having the highest water vapour loadings and hence the highest (11 μm minus 12 μm) brightness temperature differences. It follows that, in this case, the brightness temperatures and the brightness temperature differences are negatively correlated for clear pixels and positively correlated for cloudy pixels. (N.B. Although this is generally true there are exceptions. A positive correlation in SST with water vapour loading, or lower tropospheric air warmer than the SST, can reduce the correlation or even change its sign.)

The test relies mostly on effects 1 - 3 listed above, with the correlation effect used as an additional check.

The histogram test operates on a 512 by 512 pixel image segment, so the orbit is divided into image segments of this size and imagined as 'tiled' with 512 row image segments. If (at the end of an orbit or at the end of a segment in stripline processing) the data is insufficient to form a complete image segment of 512 rows the histogram can be based on an incomplete image segment. Because histograms are made up of those pixels that are valid sea pixels, if an image is largely over land, one has an incomplete image anyway. Provided the number of pixels exceeds a minimum threshold number for this test, the test can be applied.

The auxiliary parameters used in this test are listed in Table 3. They are taken from the auxiliary file of Cloud Look-up Table Data ATS_CL1_AX.

Table 2.15 Auxiliary parameters used by the infrared histogram test

MIN_FOR_11_12_HISTOGRAM	100.00
PEAK_FRAC_MIN	0.51
LATITUDE_THRESHOLD	40.0
SECOND_LOW_FRACTION	0.50
HALF_WIDTH_M_NV	0.5
HALF_WIDTH_B_NV	25.0
HALF_WIDTH_M_FV	1.0
HALF_WIDTH_B_FV	15.0
MAX_DIF_AVE_CHAN_1	100.0
MAX_DIF_PEAK_CHAN_1	50.0
RATIO_B	4.0
IR_SPREAD_NV	60.0
IR_SPREAD_FV	80.0
SLOPE_MAX_ALLOWED	10.0
IR_PEAK_MIN	25000.0

Determination of the Difference Threshold

Thus the overall objective of the algorithm is simple, to determine a dynamic threshold against which the brightness temperature differences can be compared to differentiate cloudy from clear pixels. The determination of this threshold is based on the histogram of the distribution of the differences in brightness temperature between the 11 and 12 micron channels. In the presence of undetected cloud, the histogram is expected to be the superposition of two peaks, representing the distribution of the brightness temperature differences of clear sea and of cloudy pixels respectively.

The algorithm attempts to identify the presence of the two peaks, and to identify which one represents clear sea. In the simplest terms, the clear sea pixels should show a narrower and more regular distribution, at a higher brightness temperature difference, than the cloudy pixels. However, the peaks cannot be distinguished by their relative height, since the height of each peak depends on the number of contributing pixels, which is arbitrary and simply

reflects the area of clear sea or undetected cloud as appropriate. Moreover, the peaks may overlap.

Therefore the peaks are tested against various criteria to identify a valid peak, that is, a peak that shows the characteristics characteristic of the distribution of clear sea pixels. If a valid peak is identified, a threshold is set on its lower edge, and all pixels having a brightness temperature difference less than this threshold are flagged as cloudy.

The procedure involves the following stages.

1 A histogram representing the frequency distribution of the brightness temperature difference ($T_{11} - T_{12}$) is prepared over all the sea pixels that have not been flagged as cloudy by any previous test. At the same time, for each histogram bin, the cumulative brightness temperature in the 12 micron channel is calculated over all the pixels that contribute to each bin.

The histogram is generated of the brightness temperature difference $T_{diff} = (T_{11} - T_{12})$ in the range -20.0 K $T_{diff} < 80.0$ K with a bin size dT = 0.1 K. If the histogram bins are indexed by k (0 k < 1000) then the lower limit of bin k corresponds to T = k x dT - 20.0 K. The corresponding histogram value h(k) represents the number of clear sea pixels for which

k x dT - 20.0 $(T_{11} - T_{12}) <$ (k + 1) x dT - 20.0

The cumulative brightness temperature for bin k is S T_{12}, where the sum is over all contributing pixels that fall in bin k.

2 The maximum value of the histogram is found, and its position is taken to represent the principal peak of the histogram. The extent of this peak is determined, and the parameters, height, width and position that describe the peak are calculated.

The maximum of the histogram defines the principal peak, referred to in the following as the major peak, and corresponds to the mode of the frequency distribution. If the bin index corresponding to the maximum is peak_interval[MAJOR], then the maximum value is

peak_value[MAJOR] = h(peak_interval[MAJOR]).

The extent of the peak is determined by finding the first local minimum or zero value, whichever is found first, on either side of the peak. The indices of these bins are lower_limit[MAJOR] and higher_limit[MAJOR].

3 The peak is tested against certain criteria to determine whether or not it is valid, that is, possesses the characteristics likely to represent clear pixels.

The peak is flagged as invalid if it corresponds to a difference value less than zero, that is, peak_interval[MAJOR] < 200, unless the absolute latitude at the centre of the image segment exceeds a threshold LATITUDE_THRESHOLD (currently set at 40 degrees) or the number of pixels peak_value[MAJOR] exceeds a threshold IR_PEAK_MIN (currently 25000). Otherwise it is flagged as valid.

If the histogram represents a night-time scene and if the peak has passed the previous tests, so is flagged as valid, a further test is applied to verify that the histogram is not the sum of a clear and a cloudy histogram and hence excessively broad.

Firstly, a more accurate value of the histogram peak is determined, by fitting a quadratic curve to the peak value and the adjacent histogram values on either side. If the histogram peak and its neighbours are

h0 = h(peak_interval[MAJOR] - 1)

h1 = h(peak_interval[MAJOR])

h2 = h(peak_interval[MAJOR] + 1),

then the quadratic function is

h(x) = 0.5x(x-1)h0 - (x - 1)(x + 1)h1 + 0.5x(x + 1)h2

= 0.5x^2(h0 - 2h1 + h2) + 0.5x(h2 - h0) + h1,

where x is a normalised abscissa co-ordinate measured from peak_interval. The maximum of this function occurs at

x = 0.5(h0 - h2)/(h0 - 2h1 + h2).

Thus provided the denominator of this expression is not zero, which can only occur if all three ordinates are the same, improved values of the histogram peak and its position are found. The improved peak value exact_peak_value is obtained by evaluating equation () at the value of x given by equation (), while the new position is

exact_peak_interval = (peak_interval + x)

ir11_ir12_diff_at_peak = (exact_peak_interval - 200)*dT

Next, the width of the histogram at half-height is computed to sub-bin accuracy by interpolation between the two histogram values bracketing the 50% peak values defined by 0.5* exact_peak_value and differencing the abscissae. A half-width threshold is computed from

half_width_threshold = M x ir11_ir12_diff_at_peak + B,

where M and B are constants defined in the auxiliary file of cloud LUT data, ATS_CL1_AX. (These constants have different values for the forward and nadir views.)

The peak is flagged as invalid if

half_width[MAJOR] > half_width_threshold.

4 A new histogram is determined by removing the peak just found (the major peak) by setting to zero the histogram values in the open interval between the upper and lower limits of the peak determined in (2) above. The maximum of the new histogram is found, and its position defines the secondary (or minor) peak. This is tested and flagged in the same way as the major peak.

The new maximum represents the largest secondary peak, and will be designated the minor peak in the following. The same validity tests are applied to it as are described above for the major peak.

6 The two peaks are now further tested in relation to one another. These tests may result in a hitherto valid peak being flagged as invalid. In detail the tests are as set out in the detailed description of the algorithm below, but the main new element here is to use the averaged 12 micron brightness temperatures in the peak to refine the discrimination; if the mean brightness temperature for the rightmost peak exceeds that for the other by more than a threshold MAX_DIF_PEAK_CHAN_1, the left-hand peak is flagged as invalid. At the same time, if the peaks overlap, the upper limit of the left-most peak is refined by extrapolation, and the lower limit of the rightmost peak (which may for the basis of the threshold determination) is then adjusted upwards to match the extrapolated limit. (This makes for a more conservative detection.)

7 The difference threshold is now set. If only one peak is valid, the difference threshold is set to the lower limit of the valid peak. If both peaks are flagged as valid, that at the lower abscissa is selected and its lower limit is used. If neither peak is valid, all pixels are flagged as cloudy.

8 The correlation property described in paragraph 4 of section (2.6.1.1.10.8) above is used to validate and, in the case of night-time scenes, refine the threshold just derived. The average 12 micron brightness temperature associated with each histogram box is calculated, using

Tmean(k) = sigma (T_{12})/h(k), where the sum is over all pixels contributing to box k. (The calculation uses the histogram associated with the chosen peak; thus if the minor peak was valid and selected, the histogram after removal of the major peak is used.) The histogram bin corresponding to the maximum brightness temperature is identified, and the slope of the averaged brightness temperature with Bt difference is computed. If this slope exceeds a value SLOPE_MAX_ALLOWED, all pixels are flagged as cloudy.

If the histogram represents a night time scene, the average 12 micron BT are used to refine the threshold just derived. If the position of the chosen histogram peak is to the right of the BT maximum, the threshold is increased until the histogram value at the threshold exceeds a given fraction (1/RATIO_B) of that at the position of the maximum BT. If the position of the chosen histogram peak is to the left of the BT maximum, the threshold is increased until either the histogram peak is reached, or a bin is found at which the 12 micron average exceeds the highest average BT less MAX_DIF_AVE_CHAN - 1 and the slope is lower than SLOPE_MAX_ALLOWED.

9 Finally, all so far clear sea pixels having a brightness temperature difference less than the

threshold are flagged as cloudy. If the number of clear pixels that remain is less than the threshold MIN_FOR_11_12_HISTOGRAM, these pixels are also flagged as cloudy.

The detailed algorithm follows.

a) The following steps (b) to (m) are applied to the nadir and forward views separately. Some of the cloud detection parameters provided in the auxiliary file of Cloud Look-up Table Data ATS_CL1_AX differ for the two views, and where applicable those appropriate to the view being processed should be used.

b) The 11um minus 12um brightness temperature differences ($T_{11} - T_{12}$) are calculated for those pixels that have not been flagged by any of the previous cloud tests and are not over land. The histogram of these differences is generated with a bin size of 0.1 K. For each histogram bin the cumulative brightness temperature in the 12 micron channel is calculated for all the pixels that contribute to each bin.

c) If the number of pixels contributing to the histogram is less than the auxiliary value MIN_FOR_11_12_HISTOGRAM, all the pixels are flagged as cloud no further processing is applied to this view. (If the scene is less than 512 rows in length, the above threshold is scaled in proportion.)

d) The position of the histogram peak, and the histogram value at the peak, are determined. If possible, the position of the peak of the distribution is derived to sub-box accuracy by fitting a quadratic function to the histogram values at the peak and in the two adjacent boxes, and computing the position and ordinate of the maximum of the quadratic. The peak determined at this step will be termed in the following the major peak.

e) The extent of the peak is determined by finding the position of a local minimum or of an empty histogram box on each side of the peak.

e.1) Starting at the histogram peak and working to the left, inspect each histogram bin until either a bin value of zero or a local minimum is found.

e.2) Check if possible that the trough found is genuine by testing that the histogram value at the local minimum found in e.1 is greater than 10% of the peak value and that the value in the second bin from the minimum in the direction away from the peak is not lower than the local minimum value. If neither of these conditions is true then the search is continued as in e.1. (This step is done only once.)

e.3) The higher limit is found in a similar way but working to the right of the peak (to higher bin numbers).

Note: It is possible, although unlikely, that an upper or lower limit cannot be found at this step. In this case the present implementation will terminate the processing if the current view here.

f) If the number of pixels contributing to the histogram peak is less than the auxiliary value IR_PEAK_MIN, the brightness temperature difference at the histogram peak is less than

zero, and the absolute latitude of the image centre is greater than 40 degrees, then the peak is flagged as INVALID. If any of these three conditions do not apply, the peak is flagged as VALID.

Note: the current value of IR_PEAK_MIN is 25000. If the peak value of the histogram is greater than this, the peak will be flagged as VALID.

g) The average 12um brightness temperature for the pixels that fall in the histogram bin containing the most pixels (the histogram peak) is computed from the cumulative sum calculated at step (b).

h) If the major peak is VALID, and the solar elevation at the centre of the scene is less than 5 degrees, so that the histogram represents a night-time scene, the following tests are applied to verify that the histogram is not the sum of a clear and a cloudy histogram and hence excessively broad.

h.1) The width of the histogram at half-height is computed to sub-box accuracy by interpolation, using the two values bracketing the 50% peak values.

h.2) A half-width threshold is calculated from the auxiliary parameters appropriate to the view. These parameters define the threshold as a linear function of the (11um - 12um) difference value at the histogram peak.

h.3) If the half width found at (h.1) exceeds than half-width threshold from (h.2) the peak is flagged INVALID.

i) A new histogram is generated by setting to zero the histogram values in the open interval between the upper and lower limits of the major peak. The peak of this histogram, which is a secondary peak of the original histogram, and which in the following will be called the minor peak, is found and tested for validity as follows. If the number of pixels contributing to the new histogram is less than threshold used in Step (c), the minor peak is flagged as INVALID. Otherwise:

i.1) Steps (d) to (h) are repeated to determine the position of the minor peak and its limits.

If the histogram peak is at a difference value less than zero, and the (absolute) latitude of the image centre is greater than 40 degrees, then flag the minor peak as INVALID.

i.2) The minor peak is flagged as INVALID if any of the following conditions apply:

i.2.1) The difference between the higher and lower limits is 20 cK or less;

i.2.2) The major peak is highly likely to be cloudy, and the minor peak is not sufficiently distinct from the major peak:

- The box number of the minor peak is at a greater difference value

than that of the major peak, AND

- The average 12um BT at the minor peak is greater than that

at the major peak by more than threshold MAX_DIF_PEAK_CHAN_1,

AND

- the lower limit of the minor histogram is less than the higher limit of the major histogram, AND

- the value of the major peak at its higher limit is greater than half the minor peak

i.2.3) The minor peak is highly likely to be cloudy:

- The box number of the minor peak is smaller than that of the major peak, AND

- The average 12um BT at the minor peak is less than that at the major peak by more than threshold MAX_DIF_PEAK_CHAN_1

i.3) It is possible that there are no empty histogram boxes between the minor and major histogram peaks. In this case, if the major peak is likely to be cloudy, an extrapolation is used to find the intersect of the falling edge of the major peak and the x axis to refine the limits.

(i.3.1) If the minor histogram is valid and to the right of the major, the higher limit of the major histogram is adjusted by extrapolation:

(i.3.1.1) If the lower limit of the minor histogram is less than the higher limit of the major, then it is reset to the higher limit of the major histogram.

i.3.1.2) If the difference between the box numbers for the major peak and the high interval for the major peak is greater than 3 then extrapolate using the major peak box number and value, and the box number and value of the box at (high interval minus 1).

i.3.1.3) If the difference between the box numbers for the major peak and the high interval for the major peak is not greater than 3 then extrapolate using the major peak box number and value, and the box number and value of the box at high interval.

(i.3.1.4) If the lower limit of the minor histogram is less than the adjusted higher limit of the major, then it is reset to the higher limit of the major histogram. If this adjustment results in a lower limit that is not less than the minor peak position, the lower limit is further reset to the peak position - 1.

i.4) If the minor peak is at a higher difference value than the major peak, AND its average 12um brightness temperature is greater by threshold MAX_DIF_PEAK_CHAN_1 than that of the major peak, then flag the major peak as INVALID.

(i.4.1) If the minor peak is invalid and is to the left of the major histogram

(i.4.1.1) Re-adjust by crude extrapolation the minor high limit using the values of the

histogram mode and the bin second to the left of the old limit

(i.4.1.2) Re-adjust by crude extrapolation the minor high limit using the values of the histogram mode and the bin immediately adjacent to the old limit

(i.5) If the minor peak is to the right of the major peak and its average brightness temperature is at a certain value greater than the average brightness temperature of the major peak, then flag the major peak as invalid

j) Choose between the lower limits of the major and the minor peaks, if necessary:

If both peaks are VALID then choose the lower value.

If there is only one VALID peak then choose its lower limit.

If there is no VALID peak then flag all pixels as cloudy and exit.

k) If the lower limit was successfully determined in (i) then check the way the 12um brightness temperature varies with the (11um minus 12um) difference. Under normal conditions, it decreases as the difference increases.

k.1) Average the 12um brightness temperature values for the pixels in each

(11um minus 12um) difference histogram box

k.2) Find the (11um minus 12um) difference value that has the highest average 12um brightness temperature.

k.3) Compute the slope of the (average 12um BT) with respect to the (11um minus 12um) difference, at this point.

k.4) If the slope exceeds threshold SLOPE_MAX_ALLOWED then flag all pixels as cloudy, and exit.

k.5) At night, use the 12um average BTs to tighten the lower limit, if necessary.

k.5.1) If the peak position from the (11um minus 12um) histogram is at a higher difference value than the difference value from k.2 then, starting with the lower limit calculated above, increase its value until the histogram reaches a certain fraction (1/RATIO_B) of the peak value.

k.5.2) If the peak position from the (11um minus 12um) histogram is at a lower difference value than the difference value from k.2 then

k.5.2.1) Generate slopes of delta(12um BT) / delta(11um-12um BT) for each non-empty histogram box

k.5.2.2) Starting with the lower limit calculated above, increase its value until, at lower limit,

the (12um average plus threshold MAX_DIF_AVE_CHAN_1) value exceeds the highest average 12um brightness temperature determined in (k.2), and the value of the slope here is less than threshold SLOPE_MAX_ALLOWED

l) Flag as cloudy all formerly clear pixels with a (11um minus 12um) difference value less than the value of lower limit, determined above.

m) If the number of clear pixels remaining is less than a threshold, then flag all the remaining clear pixels as cloudy.

m.1) Calculate the number of clear) pixels remaining;

m.2) If the total is less than threshold value MIN_FOR_11_12_HISTOGRAM then flag all clear pixels as cloudy.

2.6.1.2 ATS_AST_BP

2.6.1.2.1 Physical Justification

The AATSR BROWSE product is a false-colour image generated from the AATSR data, and is intended to provide the user with a quick look view of the image contents. The browse product shows a sub-sampled image at 4 km resolution; the sub-sampling scheme consists of selecting every fourth pixel on every fourth image row.

Two different schemes are used to define the browse product. In the illuminated part of the orbit a coding scheme is used to derive a 3-colour composite image from the nadir view brightness temperature and reflectance images from the GBTR product. For the night-time arc the 11 μm channel brightness temperatures are used to produce a monochromatic infra-red image. Transition processing applied to the day time data at low solar elevations minimises the visual discontinuity at the transition between these forms.

2.6.1.2.1.1 Day-time browse product

Several different channel combinations might be used to generate the daytime browse product, but for the sake of compatibility with existing systems run at ESRIN, the scheme used in the IONIA AVHRR browser described by Melinotte and Arino (1995) has been adopted.

This scheme generates a three-colour composite of two AATSR visible channels and one infra-red channel; the red channel is derived from the 0.67 μm channel, the green channel from the 0.87 μm channel, and the blue band is the inverted 11 μm channel (i.e. light is cold

and dark is hot). These data are translated via look-up tables (one for each colour) to corresponding values of red, green and blue (RGB). In the IONIA scheme these LUTS have been chosen to enhance certain features of the data. They are basically a series of linear ramps between specified knots. Each colour table is interpolated between the knots (so that there may be discontinuous changes of gradient across the knots).

2.6.1.2.1.2 Night-time browse product

The night-time browse product is based on the AATSR 11 μm channel. The same look-up table is used to generate a grey-scale image from the single infra-red channel.

2.6.1.2.1.3 Transition processing

The day-time browse product is a false colour image, but the night-time processing generates a grey-scale image. The transition between day-time and night-time processing occurs at the point at which the solar elevation at the centre of the image scan is 5 degrees, that is, the day-time algorithm is only applied to scans for which the solar elevation at nadir exceeds 5 degrees. In order to reduce the visual discontinuity between the two types of image, transition processing is applied to scans at solar elevations between 5 and 6 degrees. The RGB colour triplet is transformed into a different colour representation, the HSV (Hue, Saturation, Value) model. The saturation is scaled by a factor that varies linearly with solar elevation from unity at 6 degrees to zero at 5 degrees (the transition point), and the HSV colour triplet so modified is transformed back into the RGB colour space.

The effect is to reduce the saturation of the day-time image as the day-night transition is approached, so that at the transition point the saturation is zero and the image is monochromatic.

2.6.1.2.2 Algorithm Description

The nadir view data is extracted from each granule in turn until the complete orbit has been processed. The steps described below are applied to each granule.

2.6.1.2.2.1 Image sub-sampling

The browse product is generated from a sub-sampled image obtained by selecting every 4th pixel from the nadir image from every 4th image record in granule. In the following we denote the image pixel value (brightness temperature or reflectance) in each wavelength channel by I(ch , view; i´, j´), where the codes ch and view indicate the wavelength channel

and view respectively, and ; i´, j´, index the image pixels within the granule: i´ ∈{0, 1, ... 31} indexes the image rows counting from the first row of the granule, and j´ ∈{0, 1, ... 511} indexes the pixels within each row.

Thus the sub-sampled image arrays are

$$IB[ir11; i, j] = I(ir11, n; 4i, 4j) \quad \} \qquad \text{eq 2.143}$$

$$IB[v670; i, j] = I(v670, n; 4i, 4j) \quad \}$$

$$IB[v870; i, j] = I(v870, n; 4i, 4j)$$

for i ∈ {0, 1, ... 7} and j ∈ {0, 1, ... 127}. (Note: n indicates nadir view.)

2.6.1.2.2.2 Day time processing

Day time processing generates a false colour composite from 2 visible channels plus one infrared. This processing is applied to each scan of the sub-sampled image for which the solar elevation at centre of the scan is ≥ 5.0 degrees.

2.6.1.2.2.2.1 Generation of RGB Values

Initial red, green and blue channel intensities are derived from the 0.67 µm reflectance, 0.87 µm reflectance and 11 µm brightness temperature respectively, using the pre-defined reflectance/temperature lookup tables from the auxiliary Browse Daytime Colour LUT GADS 6.6.14. .

$$R[i, j] = F_{red}\{IB[v670; i, j]\} \quad \} \qquad \text{eq 2.144}$$

$$G[i, j] = F_{green}\{IB[v870; i, j]\} \quad \}$$

$$B[i, j] = F_{blue}\{IB[ir11; i, j]\} \quad \}$$

Here the functions F_{red} , F_{green} and F_{blue} are the colour conversion functions defined by the lookup tables. For each colour (e.g. red) the look-up table provides a set of N_<colour> coefficient pairs (knots) as follows:

V_ref(index) = reference brightness temperature/reflectance, as appropriate;

coeff(index) = corresponding colour value; eq 2.145

for i = 0, N_<colour> - 1.

The functions F_{red} , F_{green} and F_{blue} are defined by piecewise linear interpolation between the knots in the corresponding tables; interpolated values are rounded to nearest integer. If the input value V is out of range of the table, the result is set to

coeff(0) if V ≤ V_ref(0) eq 2.146

and to

coeff(N_<colour>-1) if V > V_ref(N_<colour>-1) eq 2.147

Note that the blue conversion table applied to the 11 μm channel includes an inversion; the LUT gives light for T_MIN and dark for T_MAX.

These calculations are usually performed only if the three channel values are valid. However, since saturation of the 11 micron channel is relatively common in day-time data over land, the processing is modified in this case. If the 11 micron channel is saturated, the blue channel value is set equal to zero (B[i, j] = 0), while the red and green values are calculated as above.

2.6.1.2.2.3 Night-time processing

Night time processing is based on use of the 11 μm channel information. It is applied to each scan of the sub-sampled image for which the solar elevation at the centre of the scan is < 5.0 degrees

Provided it is valid, the 11 micron is converted into a colour value using the same look-up table F_{blue} as is used for the same channel in daytime processing, and the red, green and blue channels are each set to this value.Thus

$$R[i,j] = G[i,j] = B[i,j] = F_{blue}\{IB[ir11;i,j]\} \quad \text{eq 2.148}$$

The result is a monochromatic image in which the temperature values are inverted, so low temperatures appear in light tones.

2.6.1.2.2.4 Transition processing

In order to reduce the visible discontinuity between the day and night time images, transition processing is applied to scans having solar elevations between 5 and 6 degrees. This processing comprises transforming the RGB colour triplet into a different colour model; the HSV (Hue, Saturation, Value) coding. The saturation is multiplied by a scale factor that varies linearly with solar elevation from 1 at 6 degrees to 0 at the transition point of 5 degrees, and the HSV colour triplet so modified is transformed back into RGB colour space.

The three colour values R, G, B can be regarded as the co-ordinates of a point in a three-dimensional colour space. As with any co-ordinate system, these co-ordinates can be transformed into other representations, representing different colour models. One such representation is the HSV (Hue, Saturation, Value) model.

2.6.1.2.2.4.1 The RGB to HSV transformation

The transformation from the RGB to the HSV representation is as follows. (Reference: Foley, J.D., van Dam, A., Feiner, S.K. and Hughes, J.F. Computer Graphics, Principles and Practice, 2nd Edition, Addison-Wesley, 1990.) The RGB colour values, normalised to lie in the range (0, 1), are represented by r, g, b. Let the maximum and minimum values from the triplet r, g, b be represented by max and min respectively. Then

$$v = max \quad \} \qquad \text{eq 2.149}$$

$$s = (max - min)/max \text{ if } max \neq 0\}$$

$$s = 0 \text{ if } max = 0 \}$$

Note that the saturation s is zero if and only if all three colour values r, g, b are the same. The hue h is undefined if $s = 0$, otherwise its value depends on which of the three values r, g, b is the greatest.

$$delta = max - min \qquad \text{eq 2.150}$$

$$h = 60 \times (g - b)/delta \text{ if } (r = max) \} \qquad \text{eq 2.151}$$

$$h = 60 \times (2 + (b - r)/delta) \text{ if } (g = max) \}$$

h = 60 x (4 + (r - g)/delta) if (b = max) }

The hue h is considered to be an angular co-ordinate representing the angular position of the colour in the conventional colour circle, and the multiplication by 60 converts h into units of degrees. If h as given by the above equations is negative, it is converted to a positive number in the range 0 to 360 by the addition of 360.

2.6.1.2.2.4.2 The HSV to RGB transformation

The inverse transformation from the HSV to the RGB representation is as follows. (Reference: Foley, J.D., van Dam, A., Feiner, S.K. and Hughes, J.F. Computer Graphics, Principles and Practice, 2nd Edition, Addison-Wesley, 1990.)

If s = 0 then

r=g=b = v. eq 2.152

Otherwise the transformation depends on which 60 degree sector h lies in. Let i be the largest integer less than or equal to (h/60). Then

f = h - i eq 2.153

p = v x (1 - s) eq 2.154

q = v x (1 - (s x f)) eq 2.155

t = v x (1 - (s x (1 - f))) eq 2.156

(r, g, b) = (v, t, p) if i = 0 eq 2.157

(r, g, b) = (q, v, p) if i = 0 eq 2.158

$$(r, g, b) = (p, v, t) \text{ if } i = 0 \qquad \text{eq 2.159}$$

$$(r, g, b) = (p, q, v) \text{ if } i = 0 \qquad \text{eq 2.160}$$

$$(r, g, b) = (t, p, v) \text{ if } i = 0 \qquad \text{eq 2.161}$$

$$(r, g, b) = (v, p, q) \text{ if } i = 0 \qquad \text{eq 2.162}$$

Note that although for clarity we have presented the transformations in terms of normalised colour values, the values s and h are calculated as ratios, and so the transformation remains reversible under an arbitrary positive scaling of the RGB values. Thus it is not actually necessary to rescale the values in the implementation, even though the IONIA colour tables give values in the range 0 to 255.

2.6.1.2.2.4.3 Pixel processing in the transition region

The transition processing is then as follows. For each scan for which the solar elevation ε at the mid-point lies in the range $5 \leq \varepsilon \leq 6$ degrees, the pixel RGB colour values from the day-time processing are converted to the HSV system using the above transformation.

The weight factor

$$w = \varepsilon - 5, \qquad \text{eq 2.163}$$

where $(0 \leq w \leq 1)$, is calculated, and the saturation is scaled using

$$s' = w \times s. \qquad \text{eq 2.164}$$

The triplet (h, s´, v) is transformed back to the RGB system as above, and the resulting RGB colour triplet for each pixel represents its value in the browse image.

2.6.2 Level 1B Products

2.6.2.1 Structure of AATSR gridded products

Although the scanning geometry of AATSR is such that measured pixels lie on a sequence of curved instrument scans, AATSR image data is presented on a rectangular grid of points centered on the satellite ground track and of approximately 1 km resolution (but spaced by equal time intervals along-track).

To be precise, the sampling interval between grid points ('image pixels') is 1 km in the across-track (x) direction, but in the along track (y) direction it is equal to the distance moved by the sub-satellite point in one scan interval of 150 ms. This is approximately equal to 1 km, but varies around the orbit with the satellite velocity.

This sampling scheme differs from that used in ATSR and ATSR-2 processing by the introduction of equal time interval sampling. The move to equal time interval sampling was motivated in part by the change to orbit based products (ATSR and ATSR-2 products are based on 512 km square images). Equal time interval sampling permits (though it does not guarantee) continuity of sampling in the overlap region. It also permits the revised regridding scheme to operate with minimal impact on the cosmetic fill algorithm.

The standard AATSR image grid is 512 km wide, so that each row of the image contains 512 pixels. The AATSR image products at both Level 1B and Level 2 are structured so that each Measurement data record corresponds to one image row of 512 pixels.

2.6.2.1.1 ATS_TOA_1P

The Gridded Brightness Temperature/Reflectance (GBTR) product is the single Level 1B product from AATSR. It contains top of atmosphere (TOA) brightness temperature (BT) values for the three infra-red channels and reflectance values for the 1.6 μm and visible channels. Values for each channel and for the nadir and forward views occupy separate measurement data sets as shown in [Formats 6.2.1.]. Additional MDS contain cloud and land/sea flags and confidence flags for each image pixel.

The product contains the following measurement data sets.

Table 2.16 Level 1B (GBTR) Product

MDS	Channel/μm	View	Application
1	12.0	nadir	Surface temperature, cloud clearing
2	11.0	nadir	Surface temperature, cloud clearing
3	3.7	nadir	Surface temperature, cloud clearing
4	1.6	nadir	Cloud clearing
5	0.87	nadir	Vegetation index
6	0.67	nadir	Vegetation index
7	0.55	nadir	Chlorophyll
8	12.0	forward	Surface temperature, cloud clearing
9	11.0	forward	Surface temperature, cloud clearing
10	3.7	forward	Surface temperature, cloud clearing
11	1.6	forward	Cloud clearing
12	0.87	forward	Vegetation index
13	0.67	forward	Vegetation index
14	0.55	forward	Chlorophyll
15	all	nadir	Confidence words
16	all	forward	Confidence words
17	all	nadir	Cloud and land/sea flags
18	all	forward	Cloud and land/sea flags

Each measurement data set has a similar structure, in which four header fields precede 512 fields of image row data:

- Nadir time field;
- Record quality indicator;
- Spare field; three spare bytes to ensure that subsequent data fields are aligned on a 4-byte boundary;
- Image scan y co-ordinate.

The nadir time field contains the time tag assigned to the record. Because of the curved scan geometry of AATSR, the pixels making up a gridded record are measured at a wide range of times, and it is not possible to assign a single time that applies to the record as a whole. The time shown here is that which applies to the pixel at the centre of the scan (which is in fact the latest to be measured) and is calculated as the time at which the sub-satellite point coincided with the along-track pixel of the scan. The time tag assigned to a forward view record is the same as that of the corresponding nadir view record, hence the designation 'nadir time'. This ensures that coincident records have the same time field. (The forward view of a given region is measured some 2.5 minutes earlier than the nadir view because of the conical scan geometry.

The record quality indicator is a flag that is set to -1 if the record contains no valid data, and to 0 otherwise. This definition is generic, and applies to all ENVISAT instruments. In the particular case of AATSR, the curved scan geometry is such that each record may contain pixels from 100 or more instrument scans. In addition, pixels that represent an invalid measurement are set to an exception value that gives information about the precise reason that the datum is invalid. Exception values convey information, and (except for null pixels) are therefore considered to be valid data in the context of this flag. For both of these reasons it is therefore unlikely that a record will contain no valid data, and the record quality indicator will only be set in a substantial data gap.

Image scan y co-ordinate: Image pixels in the AATSR products are described by their co-ordinates in a quasi-Cartesian XY system, in which the Y axis is tangent to the satellite ground track at any point. The Image Scan Y co-ordinate is the along-track Y co-ordinate of

all the pixels on the image row contained in the record. It is the along-track distance, in metres, of the image scan measured along the sub-satellite track from an origin which depends on the product. In the case of consolidated products the origin is the ascending node of the orbit on the equator, but in the case of NRT products the origin is an arbitrary point at the start of the product, measured in km.

The remainder of the record provides the pixel value or corresponding flags word, depending on the MDS. For those MDS that contain the measured pixel, data, the pixel value represents the brightness temperature in units of 0.01K for the thermal infra-red channels, or the calibrated reflectance in units of 0.01% for the 1.6 micron and visible channels. It is possible that a valid physical measurement is not available for some pixels; in these cases the pixel is replaced by an exception value, which is a small negative number the value of which gives information about the particular fault encountered. Some of the exception conditions will only affect a particular channel; for example a particular channel may saturate, or may have no signal, while the other channels give a valid measurement. Other exception conditions may affect all channels, as when an instrument scan is missing or could not be decompressed because of CRC errors.

The exception values used to indicate faulty pixel data are shown in Table 2.17 . Note that some but not all of the exception conditions will apply to all channels. That is, if the exception value appears in one channel for a given pixel, it will apply to all, for example if the scan is not decompressed. On the other hand, a condition such as saturation or no signal in channel may affect on channel bit not the others.

Table 2.17 also gives the corresponding confidence word bit in each case.

Table 2.17 Pixel exception values in GBTR MDS #1 to MDS #14

Exception Value	Meaning	confidence word bit
-1	Scan Absent (null packet)	2
-2	Pixel Absent	3
-3	Not decompressed	4
-4	No signal in channel	5
-5	Saturation in channel	6
-6	Derived radiance outside Calibration	7
-7	Calibration Parameters unavailable	8
-8	Unfilled Pixel (set by cosmetic fill algorithm)	9

The confidence words contain a series of flags for each pixel. Separate flags are provided for the nadir and forward views. The GBTR confidence flags are listed in Table 2.18 .

The blanking pulse flag (bit 1) indicates that one of the radar instruments was transmitting at the time of the pixel measurement. It is provided so that if there were any interference between the radar s and AATSR it would be possible to identify affected pixels.

Bit 2 is set to indicate a cosmetic fill pixel. Note that the allocation of cosmetic fill pixels is determined entirely on geometrical considerations, so that a cosmetic fill pixel may show an exception value if the neighbouring pixel from which it is copied does.

Bits 2 - 9 are derived from the pixel exception values. In each case the bit is set if the corresponding exception value is set for any of the channels. Thus in cases where only one value is affected by the exception value, the bit may be set even though some of the channels contain valid data.

Table 2.18 GB TR Confidence Flags (nadir or forward view)

.

Bit	Meaning if set
0	Blanking Pulse
1	Cosmetic Fill Pixel
2	Entire scan absent from telemetry
3	Pixel absent from telemetry
4	Pixel not decompressed owing to error in packet validation
5	No signal in some channel (zero count)
6	Saturation in some channel (maximum count)
7	Derived radiance of some channel outside range of calibration
8	Calibration Parameters unavailable for pixel
9	Pixel unfilled (cosmetic fill algorithm unable to find nearest neighbour pixel)
10 - 15	Unused

Note: Bits are numbered from ms bit 15, ls bit 0

The cloud / land flag words contain the cloud and land flags for each pixel. Separate flags are provided for the nadir and forward views, since several of the cloud tests are applied to the forward and nadir view images separately, and may give different results for any pixel. These flags are listed in Table; their meaning is largely self-explanatory.

Table 2.19 GBTR Cloud-clearing/land flagging flags (nadir or forward view)

.

Bit	Meaning if set
0	Pixel is over land
1	Pixel is cloudy (result of all cloud tests)
2	Sunglint detected in pixel
3	1.6 micron reflectance histogram test shows pixel cloudy (day-time only)
4	1.6 micron spatial coherence test shows pixel cloudy (day-time only)
5	11 micron spatial coherence test shows pixel cloudy
6	12 micron gross cloud test shows pixel cloudy

7	11/12 micron thin cirrus test shows pixel cloudy
8	3.7/12 micron medium/high level test shows pixel cloudy (night-time only)
9	11/3.7 micron fog/low stratus test shows pixel cloudy (night-time only)
10	11/12 micron view-difference test shows pixel cloudy
11	3.7/11 micron view-difference test shows pixel cloudy(night-time only)
12	11/12 micron thermal histogram test shows pixel cloudy
13-15	Unused

Note: Bits are numbered from ms bit 15, ls bit 0

Full details of the format are here 6.2.1. .

The Level 1B annotation data sets include geolocation data (pixel latitude and longitude), topographic data, solar and viewing angles, and data to show the mapping between the image and instrument pixels.

The format of the Summary Quality ADS is described here 6.6.45. .

The remaining ADS contain one record per granule in the along track direction and are conceived so that interpolation error should not be a significant problem.

ADS 1 and ADS 2 are provided so that the original scan positions can be recovered if required. They are an FODP Ref. [1.3] Annex B requirement.

ADS 3 6.6.43. contains grid pixel latitude and longitude. These do not need to be much better than the equivalent of 1 km (the nominal pixel size).

ADS 4 6.6.44. contains scan pixel x and y. These are of supplied for specialist users who want to know by how much the pixels have been displaced in the regridding.

ADS 5 and ADS 6 contain solar and viewing angles for pixels in the nadir and forward view respectively. These are calculated once for each across-track band (i.e. with an across-track sampling of about 50 km).

Finally, a Visible Calibration GADS 6.6.51. contains calibration data for the visible channel, derived from the current orbit. (Note that this is not the calibration data that has been applied to the visible channel pixels of the current orbit; that will have derived from an earlier orbit.)

More information on the sampling schemes used in the ADSs listed above can be found in section 2.12.1.3.1. , Hints and Algorithms on Data Use.

2.6.2.1.2 ATS_AST_BP

The AATSR Browse Product ATS_AST_BP 6.3.1. is a 3 colour image product derived from the Level 1B product. It is sub-sampled at 4 km resolution. The product contains 2 ADS and

1 MDS.

The Browse Summary Quality ADS 6.6.45. is essentially identical to that of the Level 1B GBTR product.

ADS 1 6.6.11. contains the geolocation information from the corresponding Level 1B ADS. It is sampled at 1 record per granule, and on the same across-track tie points as the corresponding Level 1B ADS. Note that because the Browse product is sub-sampled at 4 km nominal resolution, 1 granule corresponds to 8 Browse MDS records.

The single Browse MDS 6.6.12. contains RGB image data for 128 across-track pixels.

2.6.2.2 Structure of AATSR Ungridded Products

2.6.2.2.1 UCOUNTS

The UCOUNTS product provides raw detector output (counts) in each waveband, for both thermal infrared and reflectance channels, together with calibration data from both thermal and reflectance calibration sources. End-users are unlikely to be interested in this product, it is primarily a tool for AATSR instrument scientists and engineers. Unlike the ATSR-2 UCOUNTS product, no geolocation information is provided in this product. When geolocation information is required in an ungridded product, it can be found in the UBTR.

The format and contents of the UCOUNTS product are shown in table 2.20 to table 2.22 . There are no ADS defined for the UCOUNTS product. All MDS records for all 7 channels share the same data set structure as shown in table 2.21 . The size of the UCOUNTS product is approximately 645 Mbyte/orbit.

Table 2.20 Product Structure

Data Set	Data Set Records	Contents
MPH	MPH Record	Main Product Header
SPH	SPH Record DSD for MDS #1 ... DSD for MDS #7	Specific Product Header
MDS #1	MDS Record #1 ... MDS Record n	12 µm detector record
MDS #2	MDS Record #1 ... MDS Record n	11 µm detector record
MDS #3	MDS Record #1 ... MDS Record n	3.7 µm detector record

MDS #4	MDS Record #1 ... MDS Record n	1.6 µm detector record
MDS #5	MDS Record #1 ... MDS Record n	0.87 µm detector record
MDS #6	MDS Record #1 ... MDS Record n	0.67 µm detector record
MDS #7	MDS Record #1 ... MDS Record n	0.55 µm detector record

Table 2.21 Data Sets Structure MDS #1 - #7

Field Number	Field Description	Units	Size
1	UTC nadir time 1	days	4 bytes
2	UTC nadir time 2	s	4 bytes
3	UTC nadir time 3	µs	4 bytes
4	spare		4 bytes
5-579	nadir view pixel detector counts	counts	575 x 2
580-970	forward view detector counts	counts	391 x 2
	plus black body (+bb) detector	counts	36 x 2
	minus black body (-bb) detector	counts	36 x 2
	VISCAL unit detector counts	counts	36 x 2
	VISCAL monitor diode signal		2
	mean cold black body radiance		2
	measured +bb temperatures	0.001K	7 x 4
	measured -bb temperatures	0.001K	7 x 4
	SCP gain (mantissa)		4
	SCP gain (exponent)		2
	SCP offset (mantissa)		4
	SCP offset (exponent)		2
	IDF scan count when SCP gain/offset last changed		4
	calibration gain mantissa (even pix)		4
	calibration gain exponent (even pix)		2
	calibration gain mantissa (odd pix)		4
	calibration gain exponent (odd pix)		2
	calibration offset mantissa (even pix)		4
	calibration offset exponent (even pix)		2
	calibration offset mantissa (odd pix)		4
	calibration offset exponent (odd pix)		2
	packet sequence count		4
	source packet validation result		2
	ICU on-board time		4
	IDF scan count		4
	spare		13 x 2

Table 2.22 UCOUNTS Exception Values

Parameter	Value	Meaning
Detector Counts	-1	Entire scan absent from telemetry
	-2	Pixel count initial value
	-3	Source packet failed basic validation
	-4	No signal in channel (zero counts)

	-5	Saturation in channel (maximum counts)

2.6.2.2.2 UBTR

The UBTR (Ungridded Brightness Temperature/Reflectance) product provides calibrated thermal infrared and reflectance channel data, preserving the instrument scan geometry, but providing target lattitude/longitude and ground track x/y co-ordinates for each instrument scan sample or "pixel".

The format and contents of the UBTR product are shown in table to table 2.28 . The product is comprised of 10 ADS (table 2.24 to table 2.26) and 7 MDS (table 2.27). All MDS records for all 7 channels share the same data set structure, with the exception that the thermal channel data sets contain values of BT and the visible and NIR channels contain percentage reflectance. The size of the UCOUNTS product is approximately 665 Mbyte/orbit.

Table 2.23 Product Structure

Data Set	Data Set Records	Contents
MPH	MPH Record	Main Product Header
SPH	SPH Record DSD for ADS #1 ... DSD for ADS #10 DSD for MDS #1 ... DSD for MDS #7	Specific Product Header
ADS #1	ADS Record #1 ... ADS Record n	latitudes of nadir view pixels
ADS #2	ADS Record #1 ... ADS Record n	latitudes of forward view pixels
ADS #3	ADS Record #1 ... ADS Record n	longitudes of nadir view pixels
ADS #4	ADS Record #1 ... ADS Record n	longitudes of forward view pixels
ADS #5	ADS Record #1 ... ADS Record n	x co-ordinates of nadir view pixels
ADS #6	ADS Record #1 ... ADS Record n	x co-ordinates of forward view pixels
ADS #7	ADS Record #1 ... ADS Record n	y co-ordinates of nadir view pixels
ADS #8	ADS Record #1 ... ADS Record n	y co-ordinates of forward view pixels
ADS #9	ADS Record #1 ... ADS Record n	nadir view solar and viewing angles
ADS #10	ADS Record #1 ... ADS Record n	forward view solar and viewing angles

MDS #1	MDS Record #1 ... MDS Record n	12 µm detector record
MDS #2	MDS Record #1 ... MDS Record n	11 µm detector record
MDS #3	MDS Record #1 ... MDS Record n	3.7 µm detector record
MDS #4	MDS Record #1 ... MDS Record n	1.6 µm detector record
MDS #5	MDS Record #1 ... MDS Record n	0.87 µm detector record
MDS #6	MDS Record #1 ... MDS Record n	0.67 µm detector record
MDS #7	MDS Record #1 ... MDS Record n	0.55 µm detector record

Table 2.24 Data Set Structure: ADS #1 - #4

Field Number	Field Description	Units	Size
1	UTC nadir time 1	days	4 bytes
2	UTC nadir time 2	s	4 bytes
3	UTC nadir time 3	µs	4 bytes
	pixel latitude or longitude	deg/1000	575 x 4 (nadir) 391 x 4 (forward)

Table 2.25 Data Set Structure: ADS #5 - #8

Field Number	Field Description	Units	Size
1	UTC nadir time 1	days	4 bytes
2	UTC nadir time 2	s	4 bytes
3	UTC nadir time 3	µs	4 bytes
	pixel x or y co-ordinate	meters	575 x 4 (nadir) 391 x 4 (forward)

Table 2.26 Data Set Structure: ADS #9 - #10

Field Number	Field Description	Units	Size
1	UTC nadir time 1	days	4 bytes
2	UTC nadir time 2	s	4 bytes
3	UTC nadir time 3	µs	4 bytes
6 - 50	solar elevation	degs	11 x 4
51 - 94	satellite elevation	degs	11 x 4
95 - 138	solar azimuth	degs	11 x 4
139 - 182	satellite azimuth	degs	11 x 4

Note: The solar and viewing angles are provided once per granule, for the following tie point pixels:

- nadir view pixels: 574, 516, 459, 401, 344, 287, 229, 172, 114, 57, 0
- forward view pixels: 0, 39, 78, 117, 156, 195, 234, 273, 312, 351, 390

The nadir pixels are provided in reverse order since AATSR scans the nadir view right-to-left, and the forward view left-to-right (as the scan rotates clockwise). This approach means that the angles given in these ADS are given from left-to-right, for both views.

Table 2.27 Data Set Structure MDS #1 - #7

Field Number	Field Description	Units	Size
1	UTC nadir time 1	days	4 bytes
2	UTC nadir time 2	s	4 bytes
3	UTC nadir time 3	μs	4 bytes
4	spare		4 bytes
5-516	nadir view pixel brightness temp. or reflectance	0.01K (BT) %/100 (refl.)	575 x 2
	forward view pixel brightness temp. or reflectance	0.01K (BT) %/100 (refl.)	391 x 2
	plus black body (+bb) detector	counts	36 x 2
	minus black body (-bb) detector	counts	36 x 2
	VISCAL unit detector counts	counts	36 x 2
	VISCAL monitor diode signal		2
	mean cold black body radiance		2
	measured +bb temperatures	0.001K	7 x 4
	measured -bb temperatures	0.001K	7 x 4
	SCP gain (mantissa)		4
	SCP gain (exponent)		2
	SCP offset (mantissa)		4
	SCP offset (exponent)		2
	IDF scan count when SCP gain/offset last changed		4
	calibration gain mantissa (even pix)		4
	calibration gain exponent (even pix)		2
	calibration gain mantissa (odd pix)		4
	calibration gain exponent (odd pix)		2
	calibration offset mantissa (even pix)		4
	calibration offset exponent (even pix)		2
	calibration offset mantissa (odd pix)		4
	calibration offset exponent (odd pix)		2
	packet sequence count		4
	source packet validation result		2
	ICU on-board time		4
	IDF scan count		4
	spare		13 x 2

Table 2.28 UBTR Exception Values

Parameter	Value	Meaning
BT/Reflectance	-1	Entire scan absent from telemetry
	-2	Pixel count initial value

	-3	Source packet failed basic validation
	-4	No signal in channel (zero counts)
	-5	Saturation in channel (maximum counts)
	-6	Derived radiance outside calibration range
	-7	Calibration unavailable for pixel
	-8	Pixel unfilled

2.7 Level 2 Products

Details of how to order AATSR data are given in Section 1.1.

The following sections describe the AATSR L2 processing algorithms, and the products they produce, in more detail:

- Level 2 Algorithms 2.7.1.
- Level 2 Products 2.7.2.

A short summary of the processing applied to each product is also provided below.

Disclaimers addressing issues affecting AATSR L2 product quality are published at http://envisat.esa.int/dataproducts/availability/ .

ATS_NR__2P (GST) and ATS_AR__2P (AST)

The main AATSR Level 2 processing encompasses the derivation of the ATS_NR__2P (GST) and ATSR_AR__2P (AST) products from the ATS_TOA_1P (GBTR) product output by the Level 1B processing.

The main steps in the production of the Level 2 products are as follows:

- Derivation of Sea Surface Temperature (SST) and other parameters from the GBTR regridded brightness temperatures.
- Generation of averaged brightness temperatures and reflectances from the GBTR regridded brightness temperatures and visible channel reflectances.
- Derivation of averaged SST from the averaged brightness temperatures, and of NDVI from the averaged reflectances.

The high level organisation of the GST and AST products is described in section 2.7.2.1. and section 2.7.2.2. respectively.

ATS_MET_2P (Meteo)

The AATSR Meteo product contains spatially averaged SST and Brightness Temperature data in 10 arc minute cells over sea. These data are extracted from the ATS_AR__2P (AST) product. It is intended for near-real time use by meteorological agencies.

The high level organisation of this product is described in section 2.7.2.3. .

2.7.1 Level 2 Algorithms

The AATSR Level 2 processing steps are summarised in figure 2.12 . The main steps are also outlined below.

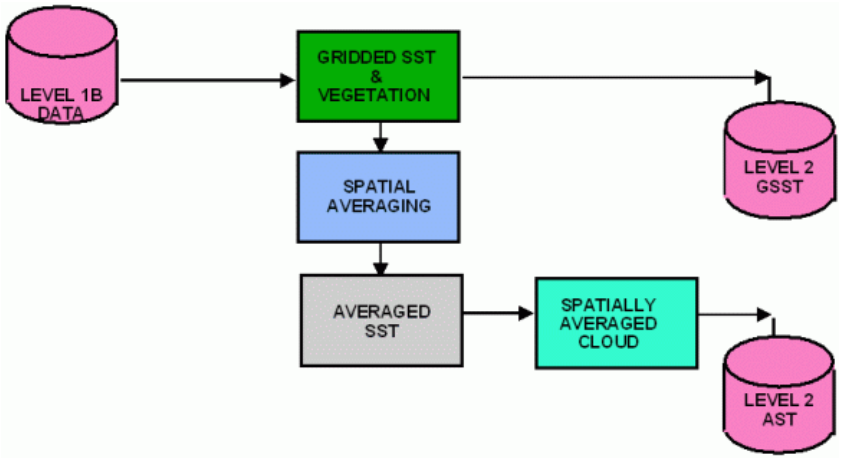

Figure 2.12 Overview of the Level 2 processing.

2.7.1.1 Prepare Inputs

Before averaged BTs and reflectances can be derived from the input GBTR product, the relevant measurement and annotation data must be extracted from the L1B product as follows.

2.7.1.1.1 Input Annotation Data Sets

The Annotation Data Sets of the GBTR product that are required for Level 2 Processing are read in and converted into appropriate units where necessary.

2.7.1.1.2 Assemble Regridded Brightness Temperature Arrays

Grid co-ordinates and channel brightness temperatures / reflectances for forward and nadir views are read in from the appropriate MDS of the GBTR product and arranged in the required memory configuration.

2.7.1.1.3 Interpolate Solar Angles

The solar azimuth and elevation and satellite azimuth and elevation, all measured at the pixel, are available for a series of uniformly spaced tie point pixels in ADS #5 of the GBTR product for the nadir view and in ADS #6 for the forward view images. This step derives those angles that are required for level 2 processing at every scan, and at the bound edges of the bands, by linear interpolation, between these tie points. Only the solar elevation is required for Level 2 processing as presently defined.

2.7.1.1.4 Interpolate Image Pixel position

The (geodetic) latitudes and longitudes of a series of uniformly space tie point pixels are available in ADS #3 of the GBTR. This module derives the latitude and longitude of each image pixel by linear interpolation, in two dimensions, between these tie points.

2.7.1.2 Derive Gridded Product

This step derives the contents of the GST product at 1 km resolution from the infra-red brightness temperatures. It derives the sea surface temperature (SST) or, over land, the vegetation index (NDVI), at 1 km resolution, using cloud free data.

The derivation of SSTs uses the 11 and 12 μm channels for day time data and for night time data the 11, 12 and 3.7 μm channels. For each 1 km resolution element two results are obtained, one using the combined nadir and forward views and the other using the nadir view alone.

The SSTs are calculated using preset retrieval coefficients. These coefficients are provided for both nadir only and combined view SSTs and are a function of latitude and viewing angle. Smoothing is applied by smoothing the difference between the calculated SST and the 11 μm brightness temperature. The effect is to smooth the atmospheric correction.

Details of the SST retrieval algorithm are contained in the following section:

- SST Retrieval 2.7.1.2.1.

The NDVIs are calculated using the nadir 0.67 and 0.87 μm channels and the results are

returned in the combined image land pixels.

In order to provide completely filled images the 11 μm brightness temperature is returned in the nadir image field when over land. In cloudy conditions the cloud top temperature is returned in the nadir image field and the cloud top height in the combined view image field (see section 2.12.1.5. concerning placeholders).

2.7.1.2.1 SST Retrieval

2.7.1.2.1.1 Physical Justification

2.7.1.2.1.1.1 Introduction

Infrared radiation emitted by the surface is modified by its passage through the atmosphere as a result of absorption by atmospheric gases and absorption and scattering by liquid and solid particles. Accurate measurements of SST from space are only possible when the particle effects are small, when clouds and fog are absent, and when the reflected/scattered solar component of the signal is negligible (i.e., 3.7 μm night). In these conditions the total upwelling infrared radiance L total(ν) observed at a given wavenumber ν by the satellite at an altitude Z is the sum of three components:

- the radiation emitted by the surface $L_s(\nu)$;
- the radiation emitted by the atmosphere L a(ν); and
- the atmospheric radiation L ar(ν) reflected from the surface back to space.

Thus

$$L_{total}(\nu) = L_s(\nu) + L_a(\nu) + L_{ar}(\nu) \qquad \text{eq 2.165}$$

The three terms in Equation (1.1) are as follows;

$$L_s(\nu) = \varepsilon_s(\nu) B(\nu, T_s) \tau(\nu, 0, Z) \qquad \text{eq 2.166}$$

$$L_a(\nu) = \int_0^Z \varepsilon_a(\nu, z) B\left(\nu, T_a(z)\right) \tau(\nu, z, Z) dz \qquad \text{eq 2.167}$$

$$L_{sw}(\nu) = (1-\varepsilon_s(\nu))\tau(\nu,0,Z)\int_0^Z \varepsilon_a(\nu,z)B(\nu,T_a(z))\tau(\nu,z,0)dz \qquad \text{eq 2.168}$$

where εs is the surface emissivity, T s the surface temperature, τ(ν, 0, Z) is the transmission of the atmosphere from the surface to the satellite at height Z, εa is the emissivity of the atmosphere at height z, τ(ν, z, Z) is the transmission of the atmosphere from height z to the satellite, and τ(ν, z, 0) is the transmission of the atmosphere from the height z to the surface. B(ν, T) is the Planck Function, given by the expression

$$B(\nu,T) = C_1\nu^3/(\exp(C_2\nu/T)-1) \qquad \text{eq 2.169}$$

where C1 and C2 are the first and second radiation constants, respectively.

The observed radiance in the channel of width Dν can be expressed in terms of the brightness temperature of the scene T:

$$L_{total} = \int_{\Delta\nu} L(\nu)d\nu = \int_{\Delta\nu} B(\nu,\overline{T})d\nu \qquad \text{eq 2.170}$$

This equation can be solved to give the brightness temperature T corresponding to the observed radiance.

In the absence of the atmosphere the brightness temperature is a direct measurement of the radiating surface temperature of the Earth. Therefore, in a world without atmosphere, accurate SST could be obtained from a single brightness temperature, provided the surface emissivity were known. However, the presence of the real atmosphere complicates the retrieval of SST, and it is necessary to make measurements at a number of different of wavelengths in parts of the spectrum where the effects of the atmosphere differ; this is known as the multi-channel or multi-spectral approach to atmospheric correction.

The most commonly used multi-channel method is the 'split window' method, in which the 10 - 13 μm atmospheric window is divided into two spectral bands in which the atmospheric effects are markedly different. The two split window channels are at 11 μm and 12 μm respectively; the atmospheric effect in this part of the spectrum is mainly due to water vapour and is much stronger at 12 μmm than at the shorter wavelength. Thus, by using the two split window brightness temperatures it is possible to provide a correction for the effects of the atmospheric water vapour and therefore to retrieve a more accurate SST.

AATSR uses the 11/12 μm split window, and has a further channel at 3.7 μm. This improves the retrieval, as it provides an additional atmospheric measurement and a more accurate determination of temperature because of the stronger temperature dependence of the Planck function at the shorter wavelength. The SST is retrieved using an algorithm that

combines the brightness temperatures T_i from each channel in the following way:

$$T_{sst} = a_0 + \sum_{i=1}^{N} a_i T_i \qquad \text{eq 2.171}$$

In addition to the multi-channel approach, AATSR employs along track scanning to provide a further improvement in the atmospheric correction. The dual angle data are used in the retrieval in the same way as the other brightness temperatures.

$$T_{sst} = a_0 + \sum_{i=1}^{N} a_i^n T_i^n + \sum_{j=1}^{N} a_j^f T_j^f \qquad \text{eq 2.172}$$

where the subscript i is the spectral channel identifier, and the superscripts n and f are the nadir and forward view brightness temperature data from each channel, respectively. The coefficients in and represent an optimum linear relationship between true sea surface temperature and the measured channel brightness temperatures.

2.7.1.2.1.1.2 Channel selection

The objective of the algorithm is to use the measured infrared brightness temperature values to determine, for each cloud-free pixel over sea, the best estimate of the Sea Surface Temperature (SST) of the pixel, to form an SST image at 1 km resolution.

In practice the derivation of SST makes use of either 2 infra-red channels (11 micron and 12 micron), or of all three infra-red channels (3.7 micron, 11 micron and 12 micron), and may use either one or both views. The selection of the set of channels to be used depends on the availability of the data.

Whenever possible, both the nadir view and forward view pixels are used. Cloud contamination for the forward view pixels is more likely than for the nadir view owing to the larger sampling area in the former, so the possibility of using the brightness temperatures from the nadir view only is also catered for. (It would be possible in theory to derive retrieval coefficients for the case of a forward view image only, but this is not done in practice.)

From eq. 2.171 , the algorithms using the nadir view only are given by

$$T_{sst,i}^{nadir} = a_0 + a_1 T_{ir11}^n + a_2 T_{ir12}^n \qquad \text{eq 2.173}$$

or

$$T_{sst,i}^{nadir} = b_0 + b_1 T_{ir11}^{n} + b_2 T_{ir12}^{n} + b_3 T_{ir37}^{n} \qquad \text{eq 2.174}$$

When both views are used (eq. 2.172), the corresponding equations are

$$T_{sst,i}^{dual} = c_0 + c_1 T_{ir11}^{n} + c_2 T_{ir12}^{n} + c_3 T_{ir11}^{f} + c_4 T_{ir12}^{f} \qquad \text{eq 2.175}$$

or

$$T_{sst,i}^{dual} = d_0 + d_1 T_{ir11}^{n} + d_2 T_{ir12}^{n} + d_3 T_{ir37}^{n} + d_4 T_{ir11}^{f} + d_5 T_{ir12}^{f} + d_6 T_{ir37}^{f} \qquad \text{eq 2.176}$$

respectively.

The coefficients a, b, c, d for use in the above equations are pre-determined by means of a radiative transfer modelling calculation. A radiative transfer model (RTM) is used to derive the expected brightness temperatures, essentially by evaluating eq. 2.165 to eq. 2.170 for each of a representative ensemble of atmospheric states and SST values. From the results the coefficients of the linear regression between SST and the measured brightness temperatures are derived. The RTM, and the method of deriving the coefficients, is described in Zavody et al, 1995 1.3. in the context of the ATSR instrument. The derivation of the AATSR coefficients proceeded along similar lines, but with the following differences;

- The version of the RTM used incorporated certain improvements;
- Aerosol robust coefficients for the dual view retrieval were derived using the method described by Merchant et al, 1999 1.3. ;
- A modified across-track banding scheme was used, as described below.

Preset coefficients are specified for each of three geographical regions: tropical, mid-latitude and polar (note that in practice the aerosol-robust dual view coefficients for AATSR are global: that is the same coefficients are defined for each of the three latitude zones). The coefficients also depend on the viewing geometry, and so the across-track distance of the pixel determines the set of coefficients to be used for a given pixel in a given region. In total, 38 different sets of coefficients are given for each geographical region; these represent 38 different across-track distances and correspond to 38 approximately equally spaced air masses across the instrument swath. These issues are discussed in 2.7.1.1.3. and 2.7.1.1.4. following.

2.7.1.2.1.1.3 Latitude zones

The latitude of the pixel governs whether the coefficients for the tropical, temperate, or polar regions are to be used. Three zonal limits are defined, TROPICAL_INDEX, TEMPERATE_INDEX, and POLAR_INDEX. Numerical values are given in .

Table 2.29 Latitude Limits

Index	Value
TROPICAL_INDEX	12.5°
TEMPERATE_INDEX	37.0°
POLAR_INDEX	70.0°

The latitude and across-track band number of the pixel determine the usage of the retrieval coefficients as follows. If the absolute value of the latitude is less than TROPICAL_INDEX, the retrieval coefficients for the tropical zone and for the appropriate across-track distance are used. Similarly if the absolute value of the latitude is greater than or equal to POLAR_INDEX the retrieval coefficients for the polar or high-latitude region and for the appropriate across-track distance are used.

If the pixel lies in the mid-latitude zone, a slightly more complex calculation is undertaken to ensure that the retrieval varies smoothly with latitude. In these cases two retrievals are computed, and the final SST is obtained by linear interpolation between them with respect to latitude. If the absolute value of the latitude is less than TEMPERATE_INDEX but is not less than TROPICAL_INDEX, two retrievals are made using the retrieval coefficients for both the tropical and mid-latitude zones. If these two retrievals are $T_{tropical}$ and $T_{temperate}$ respectively, the final value for the retrieved SST is given by

$$T_{sst} = T_{tropical} + w(T_{temperate} - T_{tropical}) \qquad \text{eq 2.177}$$

where

$$w = \frac{(ABS(latitude) - TROPICAL\_INDEX)}{(TEMPERATE\_INDEX - TROPICAL\_INDEX)} \qquad \text{eq 2.178}$$

and latitude is the latitude of the pixel.

Similarly if the absolute value of the latitude is less than POLAR_INDEX but not less than TEMPERATE_INDEX, two retrievals are made using the retrieval coefficients for the

high-latitude and mid-latitude regions. If these two retrievals are T_{polar} and $T_{temperate}$ respectively, the final value for the retrieved SST is given by

$$T_{sst} = T_{temperate} + w(T_{polar} - T_{temperate}) \quad \text{eq 2.179}$$

where

$$w = \frac{(ABS(latitude) - TEMPERATE\_INDEX)}{(POLAR\_INDEX - TEMPERATE\_INDEX)} \quad \text{eq 2.180}$$

In each of the above cases of course the relevant retrieval coefficients appropriate for the across-track distance of the pixel are used.

This approach ensures that the retrievals do not show discontinuities at latitudes equal to one of the values TROPICAL_INDEX, TEMPERATE_INDEX, or POLAR_INDEX. Note that because the retrieval equations are themselves linear, the method of linear interpolation described above is equivalent to assuming that the individual retrieval coefficients vary linearly with latitude in the ranges TROPICAL_INDEX < latitude < TEMPERATE_INDEX and TEMPERATE_INDEX < latitude < POLAR_INDEX.

2.7.1.2.1.1.4 Across-Track Bands

In the first instance, coefficients are derived off-line for two across-track positions, corresponding to the swath centre and swath edge. To derive retrieval coefficients for intermediate across-track positions, it is assumed that the coefficients should be proportional to the air mass through which the pixel is viewed, and the coefficients for intermediate positions are derived by linear interpolation with respect to nadir air mass between the centre and edge values.

Interpolated coefficients are derived for a set of 38 equally spaced air mass values, which correspond to the centres of 38 bands parallel to the swath on each side of the ground track. The same coefficients are used for all pixels that fall within a band, and the separation between the bands is sufficiently small that perceptible discontinuities are not introduced at the band edges.

The air mass is proportional to secθ, where θis the angle of incidence of the line of sight to the pixel. 2.13 shows the relationship between the normalized air mass secθand the across-track co-ordinate x for the nadir view, and for the nominal scan geometry.

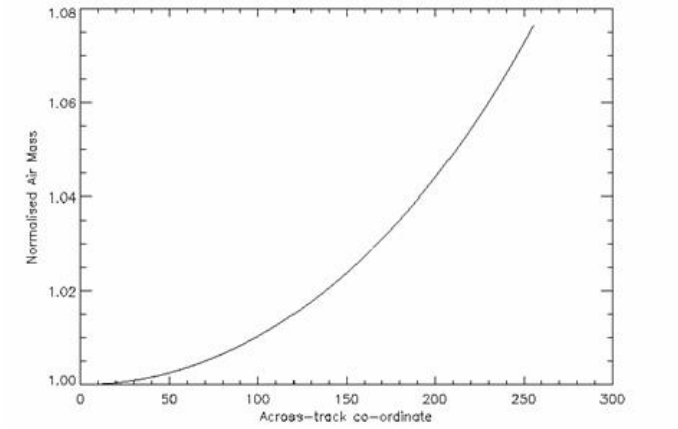

Figure 2.13 Normalized air mass versus across-track position (km)

Suppose the pixels are indexed in an across-track direction by j ($0 \leq j < 512$). The across-track co-ordinate x, measured from the centre of the swath, of the mid-point of pixel j is then given by

$$x = (j - 256) + 0.5\text{km}. \qquad \text{eq 2.181}$$

Let k ($0 \leq k < 38$) be an index to the across-track bands. The bands are defined so that pixel j falls in band k where

$$1 + \Delta/2 + (k - 1)\,\Delta < \sec\theta_j \leq 1 + \Delta/2 + k\Delta \qquad \text{eq 2.182}$$

for general k, or

$$0 < \sec\theta_j \leq 1 + \Delta/2 \qquad \text{eq 2.183}$$

in the special case k = 0. Here θ_j is the angle of incidence at pixel j, and Δ is the selected air mass increment (strictly the increment in secθ), which defines the width of the bands. The adopted value of the increment Δ is 0.00207186.

2.14 shows the relationship between band and pixel number. Note that band 0 is centred on the ground track and that the bands are arranged symmetrically about the ground track. The precise mapping between band and pixel numbers is defined in the auxiliary Across-track Band Mapping Look-up Table, which is contained in the SST Retrieval Coefficient Data File (ATS_SST_AX) 6.5.8. .

2.7.1.2.1.1.5 Smoothing

Finally, in the case of the full resolution (gridded) product smoothing is applied to the derived temperature images. This step is required because, although the derived temperatures are valid estimates of the true SST, they are affected by noise to a greater degree than the measured brightness temperatures themselves, because the coefficients multiplying the brightness temperatures in equations (eq. 2.173 - eq. 2.176) may exceed unity, and combine to yield a net increase in variance.

The smoothing technique adopted uses the difference between the derived SST image and the nadir-view 11 micron brightness temperature image. If there were no atmosphere, the 11 micron brightness temperature at near normal incidence would be a very good approximation to the SST (differing only because the emissivity of the sea surface viewed at normal incidence differs slightly from unity). Thus the difference between the retrieved SST and the nadir-view 11 micron brightness temperature is a good measure of the atmospheric attenuation in the 11 micron channel, and might be expected to show only small spatial variations over distances of a few kilometres. Thus if this difference is smoothed, the result may be added to the nadir-view 11 micron brightness temperature to give the smoothed SST.

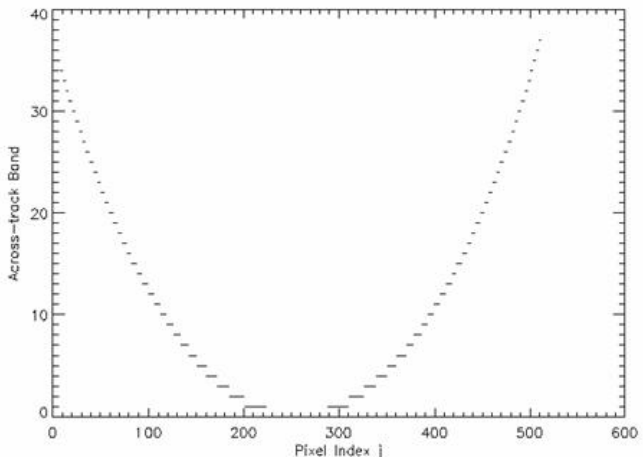

Figure 2.14 The across-track band number as a function of pixel index

The difference is averaged over square blocks of n by n pixels, the pixels corresponding to

valid retrievals being included in the average with equal weight. The size n of the smoothing block is defined by a parameter in the auxiliary file of Processor Configuration Data (ATS_PC2_AX 6.5.7.). The nominal value of n is 3, so that up to 9 pixels contribute to each average. The smoothed difference is then added to the nadir-view 11 micron brightness temperature to give the final retrieved SST value. If no valid pixels contribute to the average, or if there is no valid nadir view SST, a corrected SST is not calculated and the smoothed SST value is set to - 1. (Note that this over-rides the setting to the 11 micron temperature for invalid SST retrievals noted above.) The smoothing is carried out separately for the nadir and dual view images.

The smoothing takes account of cloud flagging; that is, pixels flagged as cloudy are not included in the average, or an increased variance of the smoothed SST in cloudy areas would result.

The smoothing step is not required in the case of the averaged (AST) product.

2.7.1.2.1.2 Algorithm Description

2.7.1.2.1.2.1 Full resolution (gridded) Surface Temperature Image Product

The AATSR full resolution geophysical product (ATS_NR__2P) contains a single Measurement Data Set (MDS), the contents of which are switchable; that is to say, the content of each pixel field depends on the surface type. Specifically, the content of each data field depends on the setting of the forward and nadir cloud flags and the land flag. Thus the processor must check the flag settings for each pixel before selecting the appropriate procedure for the surface type. These checks are integral to the logical structure of the algorithm, and so are shown in the algorithm description that follows, although the emphasis is on the detailed derivation of SST for clear sea pixels.

In the following, a pixel value is invalid if it does not represent a valid brightness temperature. This is indicated when the numerical value corresponds to an exception value; otherwise the pixel is valid.

The appropriate across-track band index corresponding to an image pixel is obtained by entering the auxiliary Across-track Band Mapping Look-up Table (from the auxiliary file ATS_SST_AX 6.5.8.) with the across-track index of the pixel. This value is used to index the set of coefficients to extract the set corresponding to the correct air mass value.

The logic of the procedure used for deriving the GSST product at 1 km resolution is as follows. Initially, the GSST confidence word flags nadir_image_valid and combined_image_valid associated with each image pixel are initialised to the value FALSE. The nadir image field is also set to the 11 micron brightness temperature; this is the default if

a valid retrieval is not achieved.

Steps 1 to 3 below are executed for each image scan, then Step 4 is executed to smooth the SST image.

1) Calculate the nadir-view image. For each pixel in the scan, the procedure is as follows:

The surface type flags (cloud flag and land/sea flag) associated with each pixel are inspected.

If the pixel is over land, a land surface temperature (LST) retrieval is attempted (see later section). If this is successful, the nadir image valid flag in the confidence word is set to TRUE.

If the pixel is cloudy, the nadir view field is set to the 11 micron brightness temperature, as an estimate of the cloud top temperature, and the nadir image valid flag in the confidence word is set to TRUE.

Otherwise the pixel is a clear sea pixel, and an SST retrieval is attempted.

The nadir-view 11 and 12 micron brightness temperatures are inspected to ensure that both are valid. If either is invalid, an SST cannot be retrieved and processing continues at the next pixel.

If both are valid, an SST retrieval is attempted using either a 2-channel algorithm or a 3 channel algorithm. If the solar elevation is negative (indicating a night-time pixel) and the 3.7 micron brightness temperature is valid, a 3 channel algorithm (Equation) is used, otherwise a two-channel retrieval (Equation) is used. If the 3.7 μm brightness temperature is valid, the corresponding flag of the confidence word is set accordingly. In either case the retrieval is performed using the coefficients for the appropriate across-track band index and taking account of the geographic zone as described below.

1.1) If the pixel lies within the tropical region (latitude < TROPICAL_INDEX) or if the pixel lies within the polar region (pixel latitude = POLAR INDEX), then the SST is calculated using the retrieval coefficients for that region and for the for the appropriate across-track band index. Equation is used if a two-channel retrieval was specified, or Equation is used if a three-channel retrieval was specified.

1.2) If the pixel lies within the temperate region, then the SST value is calculated using the coefficients for the temperate region, and a second SST value is calculated using the coefficients for the polar or tropical region. The coefficients for the tropical region are used if the pixel latitude is less than TEMPERATE_INDEX, otherwise the coefficients for the polar region are used. In either case the retrieval coefficients for the appropriate across-track band index are used, with Equation if a two-channel retrieval was specified, or Equation if a three-channel retrieval was specified. A linear interpolation with latitude is used to obtain the SST value from those calculated for the two regions, using Equation or Equation as appropriate.

1.3) In either case the 'nadir-only SST is valid flag' of the confidence word is set.

2) Calculate the dual-view image. For each pixel in the scan the dual-view SST is calculated as follows:

The surface type flags (cloud flag and land/sea flag) associated with the pixel in each view are inspected.

If the pixel is over land, and the 0.87 and 0.67 micron channel reflectances are valid, the NDVI is computed and assigned to the combined image field, and the combined image valid flag in the confidence word is set to TRUE.

If the pixel is cloudy, the combined image field is set to zero, and the combined image valid flag in the confidence word is set to FALSE. (The combined image field is reserved for the cloud top height value in a future revision of the processor.)

Otherwise the pixel is a clear sea pixel, and an SST retrieval is attempted.

If the 11 or 12 micron brightness temperature values of the pixel for either view are invalid, an SST cannot be retrieved and processing continues at the next pixel.

If all are valid, an SST retrieval is attempted using either a 4-channel algorithm or a 6-channel algorithm. If the solar elevation is negative (indicating a night-time pixel) and the 3.7 micron brightness temperature is valid in both views, a 6-channel algorithm (Equation) is used, otherwise a four-channel retrieval (Equation) is used. If the 3.7 μm data is valid, the corresponding flag of the confidence word is set accordingly. In either case the retrieval is performed using the coefficients for the appropriate across-track band index and taking account of the geographic zone as described below.

2.1) If the pixel lies within the tropical region (latitude < TROPICAL_INDEX) or if the pixel lies within the polar region (latitude = POLAR_INDEX), then the SST is calculated using the retrieval coefficients for that region and for the appropriate across-track band index. Equation is used if a four-channel retrieval was specified, or Equation if a six-channel retrieval was specified.

2.2) If the pixel lies within the temperate region, then the SST value is calculated using the coefficients for the temperate region, and a second SST value is calculated using the coefficients for the polar or tropical region. The coefficients for the tropical region are used if the pixel latitude is less than TEMPERATE_INDEX, otherwise the coefficients for the polar region are used. In each case the retrieval coefficients for the appropriate across-track band index are to be used, with Equation if a four-channel retrieval was specified, or Equation if a six-channel retrieval was specified. A linear interpolation with latitude is used to obtain the SST value from those calculated for the two regions, using Equation or Equation as appropriate.

2.3) In each case the combined image valid flag of the confidence word is set.

3) The confidence word flags that relate to cloud, blanking pulses, and cosmetic fill are set appropriately.

4) Finally, the SST image is smoothed as described in section 2.7.1.2.1.1.5. above

2.7.1.2.2 Land Surface Temperature Retrieval

2.7.1.2.2.1 Physical Justification

The definition [3] of the LST algorithm selected for AATSR is based on work by Prata [1, 2] to develop algorithms to retrieve land surface temperature (LST) from ATSR and AVHRR data. These algorithms are based on radiative transfer theory applied to the exchange of radiation between the surface and atmosphere, and have been subjected to extensive validation using a network of ground-truth sites across Australia.

The algorithm for LST retrieval is based on a split-window algorithm similar to that used for two-channel nadir-only SST retrieval:

$$LST = a_0 + b_0 T_{11} + c_0 T_{12} \qquad \text{eq 2.184}$$

where a_0 , b_0 and c_0 are coefficients that depend on the land surface characteristics, viewing angle, and atmospheric water vapour, and T_{11} and T_{12} represent the brightness temperatures in the 11 and 12 micron channels respectively. In order to permit an additional tuning of the algorithm, a weak non-linearity is introduced by replacing Equation eq. 2.184 by

$$LST = a_0 + b_0 (T_{11} - T_{12})^n + (b_0 + c_0) T_{12} \qquad \text{eq 2.185}$$

where the index n depends on the incidence angle θ as follows:

$$n = 1/\cos(\theta / m) \qquad \text{eq 2.186}$$

Here m is an empirical constant. Currently, the value m = 5 is adopted. Equation eq. 2.185 reduces to Equation eq. 2.184 when n = 1. If $T_{11} - T_{12}$ is negative, then the term $(T_{11} - T_{12})^n$ in Equation eq. 2.185 is in general complex. This case can certainly arise in practice, and the solution adopted is to set n = 1 if $T_{11} < T_{12}$; in other words, to revert to Equation eq. 2.184 in this case. The value n = 1 is also adopted in the case of inland lakes.

2.7.1.2.2.1.1 Retrieval Coefficients

The essence of the algorithm is to apply Equation eq. 2.184 above to the 11 and 12 micron brightness temperatures in the nadir view. The retrieval coefficients a_0, b_0, c_0, depend on surface characteristics and atmospheric water vapour. Their values must reflect the complex variability of the surface, and this is achieved by means of look-up tables read from the auxiliary files. These define the local characteristics of the surface, and the local climatology, at a resolution of 0.5° in latitude by 0.5° in longitude.

Let the latitude and longitude of the pixel indexed by [i, j] be represented by φ(i, j), λ(i, j) respectively, with the conventions that

$$-90.0 \le \varphi \le +90.0 \qquad \text{eq 2.187}$$

, and

$$-180.0 \le \lambda < 180.0 \qquad \text{eq 2.188}$$

It is convenient to redefine the origin of latitude and longitude so that both are positive. We thus define the shifted co-ordinates

$$\hat{\varphi} = \varphi + 90.0$$
$$\hat{\lambda} = \lambda + 180.0 \qquad \text{eq 2.189}$$

The auxiliary files define the surface class and vegetation fraction in cells of dimension 0.5° in latitude by 0.5° in longitude. Suppose that each cell is identified by the co-ordinates of its origin, defined to be its lower left-hand (i.e. south-west) corner. The cells form a two dimensional array indexed by latitude and longitude indices lat_index and lon_index, such that the origin of the cell indexed by lat_index and lon_index is

$$\hat{\varphi}_0 = lat\_index \times \Delta\varphi$$
$$\hat{\lambda}_0 = lon\_index \times \Delta\lambda \qquad \text{eq 2.190}$$

where Δj, Δl are the cell dimensions in latitude and longitude respectively. In the present case

$$\Delta\phi = \Delta\lambda = 0.5\,degrees \qquad \text{eq 2.191}$$

,

and so the indices of the cell containing the point (φ, λ) are

$$lat\_index = \text{int}[2\varphi(i,j) + 180.0],$$
$$lon\_index = \text{int}[2\lambda(i,j) + 360.0].$$ eq 2.192

For each cell, entries in a look-up table [LUT] define the following quantities:

- The surface type classification within the cell. The cell is assigned to one of 14 surface types represented by an integer in the range 1 to 14. The surface types adopted comprise 13 land cover classes or biomes together with an additional class representing inland lakes, and are listed in Table 1. In the following the surface type classification will be represented by the symbol class.
- The vegetation fraction f ($0 < f < 1$) representative of the cell. This quantity has a seasonal variation that is represented in the tables by defining 12 values of f, one for each calendar month. The basis of the definition of this variation is defined in [3].
- The monthly mean precipitable water at the centre of the cell. Again 12 values are given, one for each month, to represent the seasonal variation.

A further table defines four sets of regression coefficients a, b and c for each surface type, corresponding to vegetation and bare soil, and to day and night conditions.

Table 2.30 The land type classification used by the AATSR LST algorithm.

Type	Description	Type	Description
1	Broadleaf evergreen trees	8	Broadleaf shrubs with groundcover
2	Broadleaf deciduous trees	9	Broadleaf shrubs with bare soil
3	Broadleaf and needleleaf trees	10	Dwarf trees, shrubs with groundcover
4	Needleleaf evergreen trees	11	Bare soil
5	Needleleaf deciduous trees	12	Broadleaf deciduous trees with winter wheat
6	Broadleaf trees with groundcover	13	Perennial land ice
7	Groundcover	14	Permanent inland lakes

Thus for a given pixel, its latitude and longitude define the 0.5° ´ 0.5° cell within which the pixel falls according to the equations eq. 2.192 . The surface type for this cell, and the vegetation fraction for the current month and for the same cell, are extracted from the look-up tables.

The vegetation fraction is used to take account of the seasonal variation of vegetation cover, and the consequent effect on the retrieved surface temperature. For each surface type, and for day and night conditions separately, two sets of regression coefficients are provided, representing bare soil and vegetated surfaces. The coefficients used for the retrieval are derived as a linear combination of these with the relative weights determined by the

vegetation fraction.

Thus given the surface type, the table of coefficients is entered to extract the two sets of regression coefficients a, b and c for this surface class for both vegetation and bare soil. The day or night-time coefficients, as appropriate, are extracted, and the following linear combinations are derived from the mean of the vegetation and bare soil values, weighted by f, (1 - f) respectively. Thus we have

$$a_f(class) = f * a(class, \nu) + (1.0 - f) * a(class, s) \quad \text{eq 2.193}$$

$$b_o(class) = f * b(class, \nu) + (1.0 - f) * b(class, s) \quad \text{eq 2.194}$$

$$c_o(class) = f * c(class, \nu) + (1.0 - f) * c(class, s) \quad \text{eq 2.195}$$

In these equations the indices v, s designate vegetation and bare soil respectively, so that for example a(class, v) represents the coefficient a applicable to a vegetated surface of surface type class, and so on. Finally, before eq. 2.184 is evaluated, a correction is applied to the coefficient a_0 that depends on the precipitable water.

$$a_o = a_f + d * (cosec(\pi * satelev/180.0) - 1.0) * pw \quad \text{eq 2.196}$$

In this equation sat_elev represents the satellite elevation as seem from the pixel, in degrees,, and pw represents the total precipitable water (in units of cm) at the position of the pixel. This is derived from the tabulated values using a bilinear interpolation. The look-up table of precipitable water values is valid everywhere; that is, it includes a value for each cell, including sea and coastal cells as well as land cells; there are no invalid values. The coefficients a_0, b_0 and c_0 given by equations , and are the required retrieval coefficients.

In the case of the inland lake surface type, class = 14, the two sets of coefficients for vegetation and bare soil are identical, so the coefficients are independent of vegetation fraction, and the precipitable water correction of equation is not applied, equivalent to setting d = 0.

In the above we have not specified the units in which temperature is expressed, but the retrieval coefficients have been developed with all temperatures expressed in degrees Celsius. If temperatures are expressed in Kelvin, then in place of Equation eq. 2.184 we have the following equation for the LST in K:

$$LST = a_0 + b_0(T_{11} - T_{12})^n + (b_0 + c_0)(T_{12} - T_0) + T_0 \quad \text{eq 2.197}$$

This is the equation actually used for the LST retrieval. In it, T_0 is the temperature in Kelvin at 0°C.

The LST is stored in the product as a 16-bit short integer in units of 0.01K, and it is possible that the retrieval will give a result that exceeds the maximum value that can be represented in this way. In this case, if the retrieved LST (in units of 0.01K) exceeds 32767.5, then the output LST is set to 32767 and the nadir image valid flag is set to false, to indicate an out-of-range value. Otherwise the LST is rounded to the nearest integer and the nadir image valid flag is set to true.

As well as the quantities described above, a topographic variance flag field is defined for each cell in a further LUT. This is a two-bit field that is not used by the processing, but is passed to the product confidence word as a guide to the quality of the retrieved LST. The topographic variance field indicates the surface height range within the cell; a low topographic variance is likely to be associated with greater homogeneity of the surface type within the cell, and so a better quality LST. Reference [3] defines the meaning of the topographic variance field values as follows.

Value	Meaning
0	Extremely flat ground (very high confidence)
1	Some topographic variation (good confidence)
2	Significant topographic variation (low confidence)
3	Extreme topographic variation (no confidence)

The topographic variance flag values have been derived from a digital elevation model.

2.7.1.2.2.1.2 Interpolation of precipitable water

The water vapour sample indexed by lat_index, lon_index and corresponding to the cell whose origin is at $\hat{\varphi}_0, \hat{\lambda}_0$ is taken to refer to the point at the centre of the half-degree cell, whose (shifted) co-ordinates are $\hat{\varphi}_0 + \Delta\varphi/2, \hat{\lambda}_0 + \Delta\lambda/2$, and so the water vapour samples form a grid whose origin is at the point $\Delta\varphi/2, \Delta\lambda/2$.

For example, the cell at 58N, 7E extends over the latitude range 58.0 to 58.5 and the longitude range 7.0 to 7.5, and is indexed by lat_index = 296, lon_index = 374, and the surface class and vegetation fraction associated with this cell are taken to apply to all pixels within the specified range. However, the precipitable water value is taken to refer to the centre of the cell. Thus the precipitable water value associated with the cell [296][374] refers to the point at latitude 58.25 N, longitude 7.25 E. This must be taken into account in the interpolation of precipitable water. The centre points of the cells are the grid points for the interpolation of the precipitable water pw.

The precipitable water is interpolated to the position of the pixel using a bilinear interpolation between the four points of this grid that surround the pixel. These are the corner points of a quadrilateral enclosing the pixel.

The origin of this quadrilateral is not necessarily the sample point corresponding to the cell in which the pixel falls. The grid defined by the water vapour sample points divides the cell at (φ_0, λ_0) into four quadrants, each of which falls in a different interpolation quadrilateral. The quadrant into which the pixel (φ, λ) falls defines the interpolation quadrilateral, and its origin is calculated as follows.

The pixel (φ, λ) falls within the cell (φ_0, λ_0), as given by the equations and above. The nearest water vapour sample to the pixel is that which falls within the same cell, at co-ordinates ($\Delta\varphi/2$, $\Delta\lambda/2$) relative to the origin of the cell, and this sample is one of the corner points of the interpolation quadrilateral. The co-ordinates of the pixel relative to the cell origin are

$$d\phi = \phi - \phi_o \qquad \text{eq 2.198}$$

$$d\lambda = \lambda - \lambda_o \qquad \text{eq 2.199}$$

and relative to the centre point (the precipitable water sample) its position is

$$d\phi - \Delta\phi/2 = \eta\Delta\phi \qquad \text{eq 2.200}$$

$$d\lambda - \Delta\lambda/2 = \epsilon\Delta\lambda \qquad \text{eq 2.201}$$

with $-0.5 \leq \varepsilon, \eta < 0.5$.

The relative indices of the origin of the interpolation quadrilateral are given by the fractional parts, algebraically defined, of the displacements e, h.

Thus

$$jx = \begin{cases} -1 \text{ if } d\lambda < \Delta\lambda/2 \\ 0 \text{ if } d\lambda \geq \Delta\lambda/2 \end{cases} \qquad \text{eq 2.202}$$

$$iy = \begin{cases} -1 \text{ if } d\varphi < \Delta\varphi/2 \\ 0 \text{ if } d\varphi \geq \Delta\varphi/2 \end{cases} \qquad \text{eq 2.203}$$

The indices of the cell containing the origin of the interpolation quadrilateral are lat_index + iy, lon_index + ix. If the array of precipitable water samples for the current month is pw_table(lat_index, lon_index), we then have

$$pw00 = pw_table(lat_index + iy, lon_index + jx) \text{ eq 2.204}$$

$$pw01 = pw_table(lat_index + iy + 1, lon_index + jx) \text{ eq 2.205}$$

$$pw10 = pw_table(lat_index + iy, lon_index + jx + 1) \text{ eq 2.206}$$

$$pw11 = pw_table(lat_index + iy + 1, lon_index + jx + 1) \text{ eq 2.207}$$

Note the table must wrap round when the longitude index exceeds 719, so that lon_{index} = 720 is interpreted as lon_{index} = 0 (i.e. the longitude index is interpreted modulo 720).

The fractional displacements of the pixel relative to the origin of the interpolation quadrilateral are

$$q = \eta - iy$$

$$p = \epsilon - ix$$

The interpolated precipitable water value at the pixel is then given by

$$pw = 0.001 * ((1-p)(1-q)pw00 + (1-p)q * pw01 + p(1-q)pw10 + pq * pw11) \text{ eq 2.208}$$

2.7.1.2.2.2 Algorithm Description

The following steps are carried out for each pixel for which the 11 and 12 micron nadir view brightness temperatures (T_{11} and T_{12}) are both valid. If either of these brightness temperatures in the nadir view is invalid, no retrieval is attempted for that pixel, and the nadir image valid flag remains FALSE. Otherwise the calculation proceeds as follows.

1. Latitude and longitude indices are derived from the pixel latitude and longitude according to the equations (eq. 2.192).

2. The solar elevation at the centre of the across-track band in which the pixel falls is inspected. If it is positive, a day/night flag is set to indicate day-time observations, otherwise the flag is set to indicate night.
3. A linear interpolation is used to determine the satellite elevation at the pixel from the band edge satellite elevation values. If $T_{11} > T_{12}$ the non-linear exponent n is calculated using equation (eq. 2.186), otherwise n is set to 1.
4. The retrieval coefficients to be used for this pixel are determined, using the latitude and longitude indices determined at Step 1 to extract the vegetation fraction f and surface classification class appropriate for this cell from the look-up tables. The precipitable water pw is calculated by linear interpolation as in (2.7.1.2.2.1.2.). If class < 1 or class > NCLASS (the number of valid surface types) then the class index is out of range; the calculation for this pixel is abandoned and the nadir_image_valid flag remains false. Otherwise the retrieval coefficients are calculated using equations (eq. 2.193 , eq. 2.194 , eq. 2.195 , eq. 2.196). If class = 14, n = 1.
5. The land surface temperature is calculated using Equation (), trapping the condition that the resulting LST is out of range.
6. The topographic variance flag for the pixel is set to the value appropriate to the half-degree cell, taken from the table. Note that this is a two-bit flag.

2.7.1.3 Derive Averaged Product (Half-Degree cells)

Averaged BTs and reflectances, and then averaged SST and NDVI are derived for the half-degree cells via the following steps.

2.7.1.3.1 Spatial Averaging

For the averaged products in half-degree cells, the globe is imagined as divided into cells 0.5° in latitude by 0.5° in longitude, and these cells are further subdivided into 9 sub-cells extending 10 arcmin in latitude by 10 arcmin in longitude. For each channel, the average brightness temperature (for the infra-red channels) or reflectance (for the visible channels) is averaged over all pixels of each type that fall within each sub-cell, to give distributions of a brightness temperature and radiance at 10 arc minute resolution. Averages are performed for the forward and nadir views separately, and a separate average is performed for each surface type (land and sea) and cloud state (clear or cloudy). There are thus 4 averages per channel per view. The mean across-track pixel number in each cell is also derived, for use by the averaged SST algorithm.

2.7.1.3.2 Averaged SST Retrieval

The Averaged Surface Temperature (AST) Product ATS_AR_2P contains averaged

geophysical quantities at two different resolutions, and with respect to two different averaging schemes.

Measurement Data Sets at resolutions of 0.5° by 0.5° and 10 by 10 arc minutes with respect to a latitude / longitude grid provide continuity with existing ATSR-2 products. Other data sets contain data averaged over equal area cells of 50 by 50 km and 17 by 17 km aligned with the satellite ground track.

In the first averaging scheme, the globe is imagined to be divided into cells 0.5° in latitude by 0.5° in longitude, and each of these cells is further subdivided into 9 sub-cells extending 10 arcmin in latitude by 10 arcmin in longitude. Averaged brightness temperatures and reflectances are derived, for cloud-free and cloudy pixels separately, by averaging the data over these cells and sub-cells. For those sub-cells containing clear sea pixels, an averaged sea surface temperature is derived from the averaged brightness temperature as described below. Finally the averaged SST for each 0.5° cell is derived by averaging the valid SST values for the component sub-cells.

The sub-cells within each cell are identified by an index in the 0 to 8 as follows:

6	7	8
3	4	5
0	1	2

Further notes on AST product structure are given in Section 2.7.2.2. below.

The derivation of averaged SST is in principle the same as that described above for gridded SST, but with the following practical differences:

- The retrieval is based on the average brightness temperature for clear sea pixels within a sub-cell;
- Appropriate new criteria for the validity of brighness temperatures are introduced;
- Different retrieval coefficients are used.

In the following, the notation M(ch , v) is used to denote the number of valid clear sea pixels for channel ch and view v (v = nadir ¦ forward) that fall within the 10 arc minute sub-cell under consideration.

The appropriate across-track band index corresponding to a sub-cell is obtained by entering the auxiliary Across-track Band Mapping Look-up Table 6.5.8. with the mean across-track pixel number for the sub-cell. This value is used to index the table of coefficients to extract those corresponding to the correct air mass value.

The logic of the procedure used for deriving the averaged SST for the AST product is as follows. Steps 1 and 2 below are executed for each sub-cell in a half-degree cell, then Step 3 is executed to determine averaged quantities for the whole cell.

1) Calculate the nadir-view retrieval.

The minimum number of pixels required for the cell in the nadir view is determined;

minpn= 340 * NADIR_PIXELS_THRESH * cos ((π/180)x latitude) + 1,

where latitude is the latitude of the sub-cell, in degrees. The value NADIR_PIXELS_THRESH is taken from the auxiliary file of Level 2 Processor Configuration Data(ATS_PC2_AX) 6.5.7. .

The number of pixels that have contributed to the average clear sea nadir brightness temperature in each of the 11 and 12 micron channels is inspected. If this is less that minpn for either channel, an SST cannot be retrieved, and the AST field is set to an exception value of –1.

Otherwise, if M(ir12, n) ≥ minpn and M(ir11, n) ≥ minpn, an SST retrieval is attempted, using either a 2- channel algorithm or a 3 channel algorithm. If the solar elevation associated with the parent cell (not the sub-cell) is negative (indicating a night-time measurement) and a valid 3.7 micron brightness temperature average is available, a 3 channel algorithm (Equation) is used, otherwise a two-channel retrieval (Equation) is used.

For night-time data the 3.7 micron brightness temperature average is considered to be valid if the ratio of the number of contributing pixels at 3.7 microns to the number at 11 microns,

float{M(ir37, n)} / float{M(ir11, n)} ≥ IR37_THRESH.

If the ratio is less than IR37_THRESH the two-channel algorithm is used. The two-channel algorithm is always used for day-time data. The parameter IR37_THRESH is taken from the auxiliary file of Level 2 Processor Configuration Data 6.5.7. .

If a three-channel retrieval is possible, the corresponding flag of the confidence word is set accordingly. In either case the retrieval is performed using the coefficients for the appropriate across-track band index and taking account of the geographic zone as described below.

1.1) If the sub-cell falls in the tropical region (latitude < TROPICAL_INDEX) or if it falls in the polar region (latitude = POLAR INDEX), then the SST is calculated using the retrieval coefficients for that region and for the appropriate across-track band index. Equation is used if a two-channel retrieval is required, or Equation is used for a three-channel retrieval.

1.2) Otherwise the sub-cell lies within the temperate region. Two SST values are calculated, one using the coefficients for the temperate region, and the second using the coefficients for the polar or tropical region. The coefficients for the tropical region are used if the subcell latitude is less than TEMPERATE_INDEX, otherwise the coefficients for the polar region are used. In each case the retrieval coefficients for the appropriate across-track band index are used, with Equation if a two-channel retrieval is required, or Equation if a three-channel retrieval is required. A linear interpolation with respect to latitude is then used to obtain the final SST value from the two regional values, using Equation or Equation as appropriate.

2) Calculate the dual-view retrieval.

The minimum number of pixels required for the cell in the forward view is determined;

minpf= 340 * FRWRD_PIXELS_THRESH * cos ((π/180) x latitude) + 1,

where latitude is the latitude of the sub-cell, in degrees. The value FRWRD_PIXELS_THRESH is taken from the auxiliary file of Level 2 Processor Configuration Data (ATS_PC2_AX) 6.5.7. .

For each view, and for each of the 11 and 12 micron channels, the number of pixels that have contributed to the corresponding average clear sea brightness temperature in the sub-cell is inspected. If this is less than minpn or minpf, as appropriate, for either channel in either view, an SST cannot be retrieved, and the AST field is set to an exception value of –1.

Otherwise, if

M(ir12, n) ≥ minpnand M(ir11, n) ≥ minpn

and

M(ir12, f) ≥ minpfand M(ir11, f) ≥ minpf

an SST retrieval is attempted, using either a 4-channel algorithm or a 6-channel algorithm. If the solar elevation associated with the parent cell (again not the sub-cell) is negative (indicating a night-time measurement) in each view, and if valid 3.7 micron brightness temperature averages are available for both the nadir and the forward views, a 6-channel algorithm (Equation) is used, otherwise a 4-channel retrieval (Equation) is used.

For night-time data the 3.7 micron brightness temperature average is considered to be valid if the ratio of the total number of contributing pixels in the two views at 3.7 microns to that at 11 microns,

float{M(ir37, n) + M(ir37, f)} / float{M(ir11, n) + M(ir11, f)} ≥ IR37_THRESH.

If the ratio is less than IR37_THRESH the two-channel algorithm is used. The two-channel algorithm is always used for day-time data.

If a 3 channel retrieval is possible, the corresponding flag of the confidence word is set accordingly. In either case the retrieval is performed using the coefficients for the appropriate across-track band index and taking account of the geographic zone as described below.

2.1 If the sub-cell falls in the tropical region (latitude < TROPICAL_INDEX) or if it falls in the polar region (pixel latitude = POLAR INDEX), then the SST is calculated using the retrieval coefficients for that region and for the for the appropriate across-track band index. Equation is used if a 4-channel retrieval was specified, or Equation if a 6-channel retrieval

was specified.

2.2) Otherwise the sub-cell lies within the temperate region. Two SST values are calculated, one using the coefficients for the temperate region, and the second using the coefficients for the polar or tropical region. The coefficients for the tropical region are used if the sub-cell latitude is less than TEMPERATE_INDEX, otherwise the coefficients for the polar region are used. In each case the retrieval coefficients for the appropriate across-track band index are used, with Equation if a 4-channel retrieval is required, or Equation if a 6-channel retrieval is required. A linear interpolation with latitude is then used to obtain the final SST value from the two regional values, using Equation or Equation as appropriate.

3) Calculate cell averages.

When the nadir and dual view SST values have been calculated for each of the sub-cells that contribute to a cell, average nadir and dual view SST values are calculated for the cell.

For up to nine 10-arcmin cells within the half-degree cell, the mean nadir view SST for the half-degree cell is derived.

$$T_{nadir}(cell) = \frac{1}{\mu_1}\sum_k T_{nadir}(k, cell)$$

This is repeated for the dual-view retrieval.

$$T_{dual}(cell) = \frac{1}{\mu_2}\sum_k T_{dual}(k, cell)$$

where $k \in \{0 \le k \le 8\}$ is an index to the sub-cells and in each case the sum is over all values of k for which the respective sub-cell temperature is valid (i.e. has a positive value), and where μ_1 and μ_2 are the numbers of such valid temperatures in the nadir and forward views, respectively. If either of the values μ_1 or μ_2 is zero, the corresponding temperature is set to -1.

The standard deviations of the 10-arcmin SST values are also calculated, as is the mean across-track pixel number to be associated with the 30 arc minute SST:

sst_mean_pixel (cell) = $\frac{1}{\mu_1}\sum_k across\_track\_mean(k, cell)$ if $\mu_1 > 0$

sst_mean_pixel (cell) = -1 if $\mu_1 = 0$

where the sum is over all $k \in \{0 \le k \le 8\}$ for which corresponding SST T nadir(k, cell) is valid ($\neq$-1.)

2.7.1.3.3 Averaged NDVI and LST Retrieval

The NDVI is calculated for each sub-cell for which average reflectances over land have been calculated. The averaged NDVI over all the subcells, and its standard deviation, are also computed.

The algorithm for Averaged LST retrieval is essentially the same as that described in Section 2.7.1.2.2. above, but applied to the averaged brightness temperature values for clear pixels within the cell in place of the pixel brightness temperatures.

2.7.1.3.4 Spatially Averaged Cloud Parameters

This step provides physical information on the cloud state additional to the results of the cloud flagging provided by the cloud clearing algorithms. The product is based on the same half-degree cells defined above. The frequency distribution of brightness temperature for the cloudy pixels within the cell is given together with representative parameters and an estimate of the cloud-top temperature. The latter is interpreted as the mean brightness temperature of the coldest 25% of the cloudy pixels in the cell.

For each half-degree cell, information is given for the nadir and forward views separately. The information consists of the number of cloudy and cloud-free pixels falling within the cell, a histogram of the 11 μm brightness temperatures of the cloudy pixels, and various statistical parameters derived from the histogram. The 11 μm channel is used as the basis of the product following the practice of ATSR and ATSR-2.

The product is generated as follows. Two histograms are generated of the frequency distribution of 11 μm brightness temperature, for cloudy pixels over sea and land respectively. The histograms represent the brightness temperature at 0.1 K resolution between 190 K and 290 K. Thus each contains 1000 bins where the first bin contains the number of pixels with temperatures in the range 190.0 to 190.1 K, and the last bin contains the number of pixels with temperatures in the range 289.9 to 290.0 K. The cloud state of each filled pixel falling within the cell is inspected. If it is clear, a count of the number of clear pixels is incremented; if it is cloudy, the 11 μm channel BT is inspected and the count in the appropriate histogram bin is incremented. Note that cosmetic fill pixels are included in the processing.

As each pixel is inspected, a test is made to determine whether its 11 μm BT is lower than the lowest value previously encountered, and if so to store the location of the pixel. Then when the histogram is complete the identity of the minimum pixel will be known, and can be used to extract its channel values.

Once the histogram is complete for a given cell, that is once all the pixels falling within the cell have been inspected, the cloud temperature and coverage results are derived from it. Firstly the total number of cloudy pixels detected is computed by summing the histogram samples. If this total is less than 20 no further derivations are performed. If 20 or more cloudy pixels have been identified and included in the histogram, the mean 11 μm brightness

temperature and its standard deviation are calculated from the histogram.

The histogram is searched for the lowest temperature represented by the histogram. This is the temperature corresponding to the first non-zero bin of the histogram. Next, the cloud-top temperature is estimated. The histogram bin containing the 25th percentile is identified; this is the first bin (as the histogram is searched in the direction of ascending temperature) for which the cumulative total of the bins up to and including itself exceeds 25% of the total number of cloudy pixels. The mean temperature represented by the bins up to and including this bin is calculated.

[Note that the cloud top temperature so derived may represent the mean of slightly more than 25% of the cloudy pixels, since the cumulative total including the 25th percentile bin may exceed 25%.]

Finally the percentage cloud cover is calculated from the ratio of cloudy pixels to total pixels.

2.7.1.4 Derive Averaged Product (50 km cells)

For this part of the product, averaged BTs, reflectances, SST and NDVI are derived using the same method as in section 2.7.1.3.1. to section 2.7.1.3.4. , but averaged over cells and sub-cells of nominal dimensions 50 km x 50 km and 17 x 17 km respectively.

The SST retrieval algorithm used for 50 / 17 km resolution is essentially the same as that for the half-degree cells described in Section 2.7.1.3. except that the latitude dependence is omitted from the calculation of the validity thresholds minpn etc., because the cell and sub-cell areas are independent of latitude in this case.

2.7.2 Level 2 Products

2.7.2.1 ATS_NR_2P

The Gridded Surface Temperature (GST) Product is the Level 2 full resolution geophysical product. It contains a single MDS 6.6.39. the contents of which are switchable, that is to say, the content of each pixel field will depend on the surface type. Specifically, the contents of the data fields will depend on the setting of the forward and nadir cloud flags and the land flag as shown in Table 2.31 .

Table 2.31 Contents of the Data Fields

Nadir View Cloud Flag	Forward View Cloud Flag	Land Flag	Nadir Field	Combined Field
0	0	0	Nadir only SST	Dual-view SST
0	1	0	Nadir only SST	11 μm BT
1	0/1	0/1	CTT (currently 11 μm BT)	CTH (currently set to zero)
0	0/1	1	LST	NDVI

Each record contains header data followed by three data fields for each pixel. The header fields are the same as those in the level IB product:

- Nadir time field;
- Record quality indicator;
- Spare field; three spare bytes to ensure that subsequent data fields are aligned on a 4-byte boundary;
- Image scan y co-ordinate.

The three data fields are the confidence word, the nadir field, and the combined field.

The confidence word contains the flags listed in Table. As noted above, the cloud and land flags (bits 4, 5 and 8) within the confidence words determine the contents of the other two fields, which are switchable.

Bit	Meaning if set
0	Nadir-only SST is valid
1	Nadir-only SST retrieval includes 3.7 micron channel
2	Dual-view SST is valid
3	Dual-view SST retrieval includes 3.7 micron channel
4	Pixel is over land
5	Nadir-view pixel is cloudy
6	Nadir-view pixel has blanking pulse
7	Nadir-view pixel is cosmetic fill
8	Forward-view pixel is cloudy
9	Forward-view pixel has blanking pulse
10	Forward-view pixel is cosmetic fill
11	One or both views flagged cloudy by 1.6 micron test (daytime only)
12	Cloud flagged by 11 micron/12 micron nadir - forward test
13	One or both views flagged cloudy by infra-red histogram test
14 - 15	Topographic variance flags for LST retrieval

Note: Bits are numbered from ms bit 15, ls bit 0

Bit 0 is set if the nadir field contains a valid datum, and Bit 2 is set if th ecombined field contains a valid datum. This is true regardless of the surface type. Thus although bit 0 is described as 'nadir only SST is valid' here and elsewhere in the AATSR documentation, this is a misnomer, because it implies that the bit is not used if the pixel is not clear sea. It should properly be called 'nadir image valid' to imply that regardless of surface type the value in the nadir image field contains a valid datum appropriate to the surface type. If the pixel were a land pixel, bit 0 would be set to indicate that the nadir field contains a valid LST. In a similar way bit 2 should be called 'combined image valid', not 'dual view SST is valid'.

(The description 'nadir only SST is valid' is historical; it comes from the SADIST-2 GSST

product, which did not have fields whose meaning depended on surface type in the same way. Bit 0 does not have the same meaning in the AATSR product as in the SADIST product.)

Bits 1 and 3 are used only if the pixel is over clear sea and so contains valid nadir-only and dual view SST values. These bits are set to indicate that the 3.7 micron channel data was used in the retrieval of the corresponding nadir-only or dual view SST. (Thus typically these bits will be set for night-time data, but not for data measured during the day.)

Bit 4 is set to indicate a land pixel; it is a copy of the corresponding land flag from the Level 1B product.

Bits 5 – 10 are copies of the corresponding nadir and forward view cloud and confidence flags from the Level 1B product. Bits 11 - 13 are derived from the corresponding Level 1B cloud flags; bit 12 is a copy of the Level 1B 11 / 12 micron nadir-forward cloud test, while bits 11 and 13 are the OR of the nadir and forward view flags for the 1.6 micron and infrared histogram tests.

Finally, bits 14 and 15 form the topographic variance flag for the LST.

The principal annotation data sets from the GBTR product from which the GST is derived are also included in this product. The Annotation Data Sets are as follows.

- The format of the Summary Quality ADS 6.6.37. is similar to that of the Level 1B product, but contains four additional fields.
- The remaining ADS are identical to those of the corresponding GBTR product.
- ADS 1 and ADS 2 are provided so that the original scan positions can be recovered if required.
- ADS 3 6.6.43. contains grid pixel latitude and longitude.
- ADS 4 6.6.44. contains scan pixel x and y.
- ADS 5 and ADS 6 contain solar and viewing angles for pixels in the nadir and forward view respectively.

The structure of this product is shown in the formats 6.1.3. section.

2.7.2.2 ATS_AR_2P

The Averaged Surface Temperature (AST) Product contains averaged geophysical at two different resolutions, and with respect to two different averaging schemes. Measurement data sets at resolutions of 0.5° by 0.5° and 10 by 10 arcmin with respect to a latitude/longitude grid provide continuity with existing ATSR-2 products. Other data sets contain data averaged over equal area cells of 50 by 50 km and 17 by 17 km aligned with the satellite ground track. Both top-of-atmosphere and surface data sets are provided. The surface temperature data sets provide, for sea cells, nadir and dual view sea surface temperatures, and for land cells, land surface temperature (currently set to the 11 μm BT) and NDVI. Cloud data is also included. No ADS are included in the AST product; auxiliary data is contained within the MDS. The data sets of the AST product are arranged by surface type and resolution as shown in the formats 6.1.1. section.

Because the cells and sub-cells are defined with respect to their geographic co-ordinates, there is no simple relationship between the cell positions and the satellite ground track. There is therefore no unambiguous natural way to order the cells and sub-cells in the output product. Also the edges of the cells are not in general parallel to the instrument swath, and cells may be intersected by the swath edge. Thus they may no contain complete data.

The AST product contains 8 MDS at 10 / 30 arc minute resolutions, comprising Surface Temperature and Brightness Temperature / Reflectance MDS for each resolution and for each surface type (land and sea).

The basic unit is the 30 arc minute cell. If any pixel falls within the bounds of a 30 arc-minute cell, a data structure is created for this cell, and this will contain sub-structures for each of the nine 10 arc minute sub-cells contained in the cell, into which will be assembled all the relevant data for the 8 MDS. The algorithm for output of the data then provides as follows.

- If a 30 arc minute cell contains any data, a record corresponding to this cell will be output to each 30 arc minute MDS, and records corresponding to each of the nine 10 arc minute sub-cells will be output to each of the 10 arc minute MDS.

Although the 30 arc minute cell contains data, there may not be any valid pixels to contribute to particular sub-cells or MDs records. For example:

- If a cell consists entirely of land pixels, there will be not data in the corresponding sea records (and vice versa).
- If a 30 arc minute cell is intersected by the swath edge, some of the sub-cells may fall outside the swath, and contain no measured pixels. In this case the 10 arc minute MDS records corresponding to these sub-cells will contain no valid data.

The Record Quality Indicator is used to flag cells which contain no pixels of the corresponding surface type. (The Attachment Flag is not used in the AST product because there are no ADS, and no definition of a granule.) In addition, other exception values will appear in the relevant data fields.

The basis of the Record Quality Indicator setting is as follows. For each 10 arc minute sub-cell the processor calculates the total number of pixels in each view, and in each of the categories defined by the land/sea and cloud/clear flags that fall within the sub-cell. From these one can calculate the total number of land and sea pixels in each view that fall within the sub-cell. (Note that the two views would give identical counts if we are dealing with land and sea pixels, since the pixels in the views are co-located. But this may not be true if there are different numbers of unfilled pixels in the two views.) The record Quality Indicator is then set if the corresponding count in each view is zero. (In this case of course all the data will contribute to the corresponding land MDS.)

Spatially averaged quantities, averaged over cells and sub-cells of nominal dimensions 50 km by 50 km and 17 km by 17 km respectively, are derived to give an alternative averaged product based on equal area cells. The relationship between the cells and the swath is simpler in this case, since the cell boundaries are parallel to the instrument swath, but the same principles of data selection apply.

The AST confidence flags are shown in Table 2.32 . Currently only four flags are used. Bits 0 and 1 are used only for the Sea records, and are set to indicate that the 3.7 micron channel data was used in the retrieval of the nadir-only or dual view SST. (Thus typically these bits will be set for night-time data, but not for data measured during the day.)

Bits 2 and 3 are set to indicate that the nadir and forward views respectively contain day-time data, and thus that the nadir only and dual view SST retrievals will include such data. Clearly it will generally be the case that these bits will be set when bits 0 and 1 are clear, and vice versa, although this is not an invariable rule.)

Table 2.32 AST confidence word

bit	meaning if set.
0	Sea MDS: Nadir-only SST retrieval used 3.7 micron channel Land MDS: Reserved
1	Sea MDS: Dual-view SST retrieval used 3.7 micron channel Land MDS: Reserved
2	Nadir view contains day-time data
3	Forward view contains day-time data
4 - 31	Unused

2.7.2.3 ATS_MET_2P

The Meteo product is a fast delivery product designed for use by meteorological offices, and contains averaged BT and SST at 10 arc minute resolution. The single MDS 6.6.35. of this product comprises the fields of MDS#3 (SST record, 10 arc min cell) of the AST product, with the addition of Average Brightness Temperature (ABT) fields (BT/TOA sea record, 10 arc min cell) to make it more self-contained.

The structure of this product is shown in the formats 6.1.2. section.

In the AST product (from which the Meteo product is derived), all cells are present regardless of surface type. Specifically every 10 arc minute cell is represented by two records - a land record and a sea record, and all are physically present even if they are empty (e.g. land records for cells that are entirely sea, and vice versa). If a cell is entirely over sea, the sea record will contain valid data, and the land record will not. If a cell is intersected by coastline then both records will contain valid data, representing / derived from the averaged brightness temperatures of the land and sea pixels respectively.

The Meteo product contains only the sea records, but it contains all of them, including those that are wholly over land (which are empty) or partly over land (which contain averages derived from only the sea pixels in the cell).

2.8 Instrument Specific Topics

This section will be expanded in a later issue. For now, a number of instrument-specific topics are discussed in section 1.2. of the User Guide, How to use AATSR Data 1.2. .

2.9 Auxiliary products

A key component of the AATSR data processing system is the set of auxiliary data products used. These are described further in the following sub-sections:

- Summary 2.9.1.
- Level 1B Processing 2.9.2.
- Level 2 Processing 2.9.3.
- Common Auxiliary Data Sets 2.9.4.

2.9.1 Summary of auxiliary data sets

2.9.1.1 Definition

Auxiliary data files are all those files used to produce a product, other than the direct measurements of the instrument. Most auxiliary files are specific to individual instruments. However, there are also a number of files that are common across several instrument processors.

- L1B Processing 2.9.2.
- L2 Processing 2.9.3.
- Common Auxiliary Data Sets 2.9.4.

2.9.1.2 Structure

Auxiliary files follow the same format guidelines as the PDS products. Every auxiliary file

contains an MPH, SPH and one or more data sets. Product headers are in plain ASCII text, with all other data sets in binary format.

2.9.1.3 Files Used in AATSR Processing

The files used in AATSR processing are summarised in table 2.33 below.

Table 2.33 AATSR Auxiliary Data Files

Product ID	Approx. Size (MB)	Update Rate	Type	Processing Level	Comment
ATS_INS_AX	0.2	Infrequent	AATSR	L1B	AATSR Instrument Characterisation File
ATS_PC1_AX	0.002	Infrequent	AATSR	L1B	AATSR L1B Processor Configuration File
ATS_VC1_AX	0.002	Once per day	AATSR	L1B	Visible Calibration File
ATS_GC1_AX	0.2	Infrequent	AATSR	L1B	General Calibration File
ATS_CH1_AX	0.002	Infrequent	AATSR	L1B	L1B Characterisation File
ATS_CL1_AX	0.01	Infrequent	AATSR	L1B	Cloud Test LUTs
ATS_BRW_AX	0.002	Infrequent	AATSR	L1B	Browse LUT
ATS_PC2_AX	0.002	Infrequent	AATSR	L2	AATSR L2 Processor Configuration File
ATS_SST_AX	0.1	Infrequent	AATSR	L2	SST Retrieval Coefficients
ATS_LST_AX	12.8	Infrequent	AATSR	L2	LST Retrieval Data
AUX_DEM_AX	36	Infrequent	Common	L1B	Digital Elevation Model
AUX_LSM_AX	12	Infrequent	Common	L1B	Land/Sea mask
AUX_FPO_AX	1.01	Once per day	Common	L1B	FOS Predicted Orbit State Vectors
AUX_FRO_AX	0.2	Once per day	Common	L1B	FOS Restituted Orbit State Vectors
AUX_TIM_AX	0.002	Once per orbit	Common	L1B	UTC/SBT Time Conversion File

2.9.1.4 Information and Availability

The version number of the auxiliary files used during processing will be shown in the SPH of each product.

Auxiliary products can be ordered from the PDS via the USF, in the same way as ordering data products.

2.9.2 Auxiliary Data Sets for Level 1B processing

All of the following AATSR-specific L1B auxiliary files will be maintained by the

Announcement of Opportunity Instrument Provider (AOIP), with the exception of ATS_BRW_AX. This file will be maintained by ESA.

Clicking on the links provided will take the reader to the Data Formats section of this handbook, which contains a description of each field within each data set.

AATSR L1B Processor Configuration File (ATS_PC1_AX) 6.5.6.
Use/Contents
Used throughout the L1B processing, this file consists of a single data set containing constants and internal instrument and data processing parameters.
Source
AATSR processing architecture and instrument characterisation data.
Update
Optimised during L1B algorithm verification. Likely to remain unchanged from then on.

AATSR Instrument Characterisation File (ATS_INS_AX) 6.5.5.
Use/Contents
Used to unpack and validate the AATSR measurement and auxiliary telemetry, this file contains 6 data sets:

- General parameters for unpacking source packet auxiliary data.
- Master Unpacking Definition Table (MUDT) for unpacking auxiliary data.
- Parameters to convert unpacked auxiliary items.
- Parameters to perform limit checks on the unpacked auxiliary items.
- Surveillance limits for checks on converted auxiliary items.
- Validation parameters for specialised checks of converted auxiliary items.

Source
Instrument telemetry definition, instrument characterisation data and Instrument Operations Manual (IOM).
Update
These instrument parameters will be scrutinised as part of the instrument Switch On and Data Acquisition Phase (SODAP) test programme. Once completed, they are expected to remain relatively stable throughout the mission. Any changes to surveillance limits will be identified as part of routine instrument performance monitoring by the Flight Operations Support team.

Visible Calibration File (ATS_VC1_AX) 6.5.9.
Use/Contents
Contains a single data set of visible channel calibration parameters.
Source
New calibration parameters are calculated and submitted to the PDS once per day based on the observed signal from the AATSR VISCAL unit from previous orbits.
Update
Daily (see section 2.11. for further details).

General Calibration File (ATS_GC1_AX) 6.5.4.
Use/Contents
Consists of 4 data sets containing parameters used in the calibration of the infrared channels:

- General parameters for IR calibration
- Temperature to radiance LUT
- Radiance to Brightness Temperature LUT
- 1.6 μm channel non-linearity correction LUT

Source

Calculated from instrument characterisation data, including channel filter profiles and non-linearity measurements. This process is discussed further in section 2.6.1.1.2. and section 2.6.1.1.3.

Update

Verified during AATSR Switch-On and Data Acquisition Phase (SODAP). Any future updates are expected to be infrequent.

L1B Characterisation File (ATS_CH1_AX) 6.5.2.

Use/Contents

A single data set containing several categories of parameter: instrument alignment parameters related to the satellite geolocation model, AOCS and geodetic constants (e.g. parameters of the reference ellipsoid) and parameters relating to the pixel map and regridding. Used primarily for geolocation and regridding.

Source

Instrument characterisation data, physical constants and internal processing parameters.

Update

Instrument alignment parameters will require verification in-flight during the SODAP. Further tuning may be necessary during algorithm verification. Subsequent updates will be infrequent. All other data will be stable prior to launch.

Cloud Test LUTs (ATS_CL1_AX) 6.5.3.

Use/Contents

9 data sets, containing coefficients and thresholds for the 9 tests used by the cloud-clearing algorithm. (Zavody et al, 2000 Ref. [1.19]):

- 1.6 μm histogram test LUT
- 11 μm spatial coherence test LUT
- 12 μm gross cloud test LUT
- Thin cirrus test LUT
- Medium/high level cloud test LUT
- Fog/low stratus test LUT
- 11/12 μm nadir/forward test LUT
- 11/3.7 μm nadir/forward test LUT
- Infra-red histogram test LUT

Source

Some tables are based on Radiative Transfer (RT) modelling. Others are derived on a more empirical basis by inspection of images. Many have been passed directly from ATSR-2 to AATSR.

For the 2 view-difference tests, coefficients were fitted to BT data derived from RT modelling. The thresholds for these tests remain the same as for ATSR-2.

Thresholds for the 11/12 micron thin cirrus test and the medium/high level cloud test represent an envelope enclosing the data on a corresponding scatter diagram. New

thresholds were derived for AATSR by applying a differential correction to those in the ATSR-2 table, the magnitude of which is derived from RT modelling.

All other tables are those used with ATSR-2. In most of these cases, the tables for ATSR-1 and ATSR-2 were identical, and no basis for a differential correction was identified.
Update
Certain LUT parameters may be adjusted on an empirical basis with respect to real data during the commissioning phase, however there are no plans for a thorough review of the AATSR cloud tests. The RT modelling for cloud clearing is similar to that required for the derivation of SST retrieval coefficients. Therefore, any update to those files requiring RT modelling is likely to coincide with a new RT modelling exercise for the SST coefficients.

Browse LUT (ATS_BRW_AX) 6.5.1.
Use/Contents
Colour LUT used during production of the daytime part of the AATSR Browse product to convert the 0.67, 0.87 and 11 μm channel values to values of red, green and blue.
Source
IONIA AVHRR Browser scheme (Melinotte et al,1995 Ref. [1.13]). This LUT has been developed to enhance specific features of the data.
Update
Infrequent. Most likely during the early months of the mission, to optimise the performance of the Browse product. Will remain stable from that point on.

2.9.3 Auxiliary Data Sets for Level 2 processing

AATSR only uses 2 auxiliary files in its L2 processing. Both L2 auxiliary files are maintained by DEFRA.

Clicking on the links provided will take the reader to the Data Formats section, which contains a description of each field within each data set.

AATSR Level 2 Processor Configuration File (ATS_PC2_AX) 6.5.7.
Use/Contents
A single data set containing miscellaneous configuration parameters including brightness temperature thresholds for the AST product and parameters defining the geometry of the averaged product.
Source
Based on requirements of AATSR processor design.
Update
To be optimised as part of AATSR L2 algorithm verification. Unlikely to change beyond this point.

SST Retrieval Coefficients (ATS_SST_AX) 6.5.8.
Use/Contents
Used to retrieve full resolution (see section 2.7.1.2.) and spatially averaged (see section

2.7.1.3.) SST from L1B BTs. The file contains 3 data sets:

- Across-track band mapping LUT (defines the relationship between pixel across-track co-ordinate and across-track band number).
- SST retrieval coefficients (for the 1 km gridded SST retrieval).
- Averaged SST retrieval coefficients (for the averaged SST retrieval).

Source

The coefficients represent a linear regression of SST on brightness temperature. Regression is based on model brightness temperatures derived from an ensemble of atmospheric profiles using a Radiative Transfer (RT) model. (A)ATSR coefficients are based on the model RADGEN from the Rutherford Appleton Laboratory. See below for further details.

Update

Infrequent. As these coefficients are derived on the basis of RT modelling and are not subject to empirical adjustment, any changes to this file will be the result of a new RT calculation. Such an exercise might be undertaken to apply new physical parameters or modelling as the result of detailed product validation.

LST Retrieval Coefficients (ATS_LST_AX)

Use/Contents:

Used to retrieve full resolution LST from L1b BTs. The file contains 6 data sets comprising a short GADS of general parameters, four LUT GADS of vegetation class, vegetation fraction, climatology and topographic variance data, and one LST Retrieval Coefficient LUT GADS:

- General Parameters for LST Retrieval
- Index Data for LST Retrieval
- Vegetation Fraction for LST Retrieval
- Climatology Records for LST Retrieval
- Topographic variance flag for LST retrieval
- LST Retrieval Coefficients

Source:

See Land Surface Temperature Measurement from Space: AATSR Algorithm Theoretical Basis Document, Jan 2002 1.3. .

Update:

Infrequent.

Generation of Retrieval Coefficient Sets for (A)ATSR

The original ATSR coefficients were based on the work of Zavody et al, 1995 Ref. [1.18], using a scheme with 10 across-track bands. However, they have recently been updated to take account of new developments in coefficient generation, including an improved stratospheric aerosol treatment developed by Merchant et al, 1999 Ref. [1.14], which uses 38 bands to reduce discontinuities at the band edges.

Coefficient derivation involves 3 steps:

- Generate a statistically representative ensemble of atmospheric profiles;
- Run radiative transfer model (RADGEN) to derive brightness temperatures for each profile;
- Derive regression coefficients of surface temperature vs. brightness temperature.

The derivation is therefore dependent on a) the ensemble of atmospheric profiles used, b)

the version of RADGEN used, and c) the auxiliary data used in this process.

The recent update to RADGEN was designed to address the following requirements:

- Ability to read atmospheric profiles derived from ECMWF data

The original ATSR coefficients were based on a set of 158 radiosonde profiles provided by the UK Met Office. However, Merchant et al introduced a new set of profiles based on ECMWF re-analysis data. Therefore the code had to be modified to accept these new profiles.

- Enhanced tropospheric aerosol model

The modifications to the tropospheric aerosol subroutine included the optional implementation of a 'hybrid' scattering model, the addition of asymmetry coefficients (from Shettle and Fenn, 1979) and the removal of redundant scaling. Modifications to the main programme included the optional inclusion of 'constant number density' scaling as alternative to 'constant visibility' scaling, and the introduction of exponential aerosol height distribution, in place of the original distribution, which was uniform below 1 km height.

- Revised air mass and emissivity definitions to accommodate revised across-track banding scheme

The original across-track banding scheme used interpolation between 5 standard air mass values computed by RADGEN. The new scheme requires air mass values at swath centre and swath edge in each view.

- Inclusion of parameterised wind speed effects in the forward view.

This scheme modifies surface reflectivity and emissivity to account for roughness effects in the forward view (Watts et al 1996 Ref. [1.17]), depending on wind speed.

- Improved portability of the code.

LST Retrieval Coefficients

The auxiliary file designated ATS_LST_AX contains the look-up tables and retrieval coefficients used by the LST algorithm. It includes the data sets listed in table.

Table 2.34 Data sets included in the LST auxiliary file ATS_LST_AX

Description of data set	Contents
General parameters for LST retrieval	3 parameters d, m, NCLASS
Surface type classification	720 x 360 array
Vegetation fraction	720 x 360 x 12 array
Precipitable water	720 x 360 x 12 array
Topographic variance flag	720 x 360 array

LST retrieval coefficients	16 x 2 (vegetation / soil) x 2 (night/day) coefficient sets

The auxiliary files define the surface class and vegetation fraction with a resolution of 0.5 degrees. Thus for each cell of 0.5 degrees in latitude by 0.5 degrees in longitude a surface class and vegetation fraction are defined, that are taken to apply to the whole cell. The arrays are indexed using the latitude and longitude indices lat_index and lon_index defined in Section 2.7.1.2.2.1.1. , and the array values are ordered so that the longitude index varies most rapidly.

2.9.4 Common Auxiliary data sets

Common auxiliary files are files provided by the ENVISAT ground segment for use by all ENVISAT instruments (link to generic section on common aux files) . The common ENVISAT auxiliary files used by AATSR are listed below. Maintenance of these files is the responsibility of the ENVISAT Programme.

Digital Elevation Model File (AUX_DEM_AX)
Use/Contents
Contains a world Digital Elevation Model (DEM). Used by AATSR to calculate the topographic correction to pixel latitude and longitude over land in the L1B and L2 1 km gridded products (see section 2.6.1.1.5.4.). Elevation values are provided over a regular grid. The coverage of the grid is from 180 + 1/24 W to 180 - 1/24 E degrees in longitude and from -90 + 1/24 to 90 - 1/24 degrees in latitude. The resolution of the grid is 1/12 degrees in longitude and 1/12 degrees in latitude. One value is recorded at each grid point. The file contains two data sets:

- General GADS (containing information describing the file)
- DEM GADS (containing the values of ocean depth or land elevation)

Source
TerrainBase CD-ROM Release 1.1, NOAA NESDIS National Geophysical Data Centre (www.ngdc.noaa.gov)
Update
Infrequent. Most likely to be triggered by availability of improved DEM.

Land Sea Mask (AUX_LSM_AX)
Use/Contents
A file classifying points on the Earth's surface as land/sea or coastline. Information is provided in 6 data sets at different resolutions. Used to set the AATSR land/sea flag associated with each pixel (see section 2.6.1.1.9.).

- 1 degree resolution surface GADS
- 0.1 degree resolution surface GADS
- 0.01 degree resolution surface GADS
- 1 degree resolution coastline GADS
- 0.1 degree resolution coastline GADS

- 0.01 degree resolution coastline GADS

Source
Rutherford Appleton Laboratory, Space Science and Technology Department, ATSR Project.
Update
Infrequent

FOS Predicted Orbit State Vectors (AUX_FPO_AX) and FOS Restituted Orbit State Vectors (AUX_FRO_AX)
Use/Contents
Input to the ENVISAT orbit propagator software (link to generic section on ENVISAT CFIs) used for geolocation. Includes orbit number and satellite X, Y and Z position and velocity relative to the Earth fixed reference frame. The Preliminary and Precise Orbit State Vectors supplied by the DORIS instrument (link to DORIS handbook) can also be used for this purpose.
Source
ENVISAT Flight Operations Segment (FOS)
Update
Once per day

UTC/SBT Time Conversion (AUX_TIM_AX)
Use/Contents
Input to the ENVISAT UTC/SBT Time Conversion software (link to generic section on ENVISAT CFIs) used throughout the ground segment
Source
ENVISAT FOS (TBC)
Update
Once per orbit

2.10 Latency, Throughput and Data Volume

2.10.1 Latency

AATSR acquires data continuously around the orbit, in all channels. At night, the visible channels continue to operate even though the data they acquire contain zero signal.

AATSR products will be provided in their unconsolidated form in NRT, and as consolidated products when processed off-line. Unconsolidated data are processed from dump to dump. Consolidated data are time-ordered, with no overlaps or data gaps and processed from ANX to ANX.

NRT and off-line products will be identical, but for their level of consolidation and the auxiliary files used in their production. Updates to most AATSR auxiliary files will be infrequent, with the exception of the ATS_VC1_AX file containing visible channel calibration coefficients. The version of this file used for NRT processing will not contain the exact coefficients for that orbit. A file from one or two days previous to the acquisition of the orbit in question will be used instead. Under normal circumstances VC1 files used for off-line processing should be no more that 1 day old. For more information on this, see Section 2.9.2 on L1b Auxiliary Files and Section 2.11.2 on Characterisation and Calibration. NRT data will also be processed with predicted rather than restituted Orbit State Vectors.

AATSR processing does not use any auxiliary files sourced externally to the PDS (e.g. ECMWF files). Therefore, the time required to receive these files does not represent a potential block to AATSR processing.

Column 4 of Table 2.35 shows the time between acquisition and availability to end-users for all AATSR products.

2.10.2 Throughput

An AATSR product is generally considered to represent one whole orbit, and one instance of each product type (TOA, NR, AR etc.) is generated per orbit. Under normal circumstances, data will not be processed in small segments. Processing will take place on whole orbits, and segments of processed data can then be extracted from the archived orbit product.

AATSR products will be processed straight through from L0 to L2 during NRT product generation, but processing will be split between L1B and L2 for off-line products. In this case, processing from L0 to L1B will take place at the LRAC. This L1B data will then be passed on to the UK-PAC for onward processing to L2.

2.10.3 Data Volume

Column 5 of table 2.35 shows the approximate file size for each full orbit product. These sizes have been calculated on the basis that one orbit comprises approximately 40,000 image scans. The size of child products will vary depending on the geographical area and data sets chosen.

Table 2.35 AATSR Product Size and Availability

Level	Product	Product ID	Availability	Approx. Size Mbytes/orbit
L0	Instrument Source Packet Data 2.5.4.1.	ATS_NR__0P	NRT: 1 day Off-line: 2 weeks	490
L1B	Gridded Brightness Temperature/Reflectance (GBTR)	ATS_TOA_1P	NRT: 3 hours Off-line: 2 weeks	729
L1B	Browse	ATS_AST_BP	NRT: 3 hrs to 3 days Off-line: 3 days	5
L2	Gridded Surface Temperature (GST)	ATS_NR__2P	NRT: 1 to 3 days Off-line: 2 weeks	126
L2	Averaged Surface Temperature (AST)	ATS_AR__2P	NRT: 3 hours Off-line: 2 weeks	63
L2	Meteo	ATS_MET_2P	NRT: 3 hours	5

2.11 Characterisation and Calibration

2.11.1 Introduction

Some ENVISAT instruments use a set of characterisation and calibration algorithms that are run on acquired data outside of the PDS. These are then used to provide auxiliary files back to the IPFs within the PDS. This section is intended to describe these algorithms. However, AATSR is essentially a self-calibrating instrument, deriving calibration coefficients for the thermal and visible channels via its on-board calibration targets. Therefore, there are no specific external calibration algorithms involved.

There is, however, a monitoring function related to the calibration of the visible channels that is executed outside the processing chain. This is described below.

2.11.2 Monitoring of AATSR VISCAL Parameters

For ATSR-2, no routine calibration is performed on the visible and near-infrared image data supplied to users. Instead, this must be done explicitly by the user, using the calibration tables provided on the ATSR Project Web site. For AATSR however, a calibration is routinely applied to the visible and NIR channels as part of the L1B product generation.

During processing, the calibration parameters used for AATSR are taken from an auxiliary file, ATS_VC1_AX, which is based on calibration data taken from a previous orbit. Therefore, the processing chain does not directly apply calibration data from the orbit being processed. This is because the point at which the VISCAL unit is illuminated by the Sun

occurs in the middle of the orbit, and the initial processing steps are applied on a scan-by-scan basis. This means that these VISCAL parameters could only be applied by making two passes over the orbit, one to extract the VISCAL signal and a second to apply the calibration, and this is not possible in the current processing scenario. Consequently the L1b process includes a step to extract and calculate the VISCAL parameters for each orbit (see section 2.6.1.1.3.), but these are only written into the product (into ADS 7, Visible Calibration Coefficients ADS), and are not applied to that particular orbit.

The ATS_VC1_AX file will be monitored and updated daily to ensure that an optimum set of calibration data are available for off-line processing. Whilst NRT processing will use the latest available ATS_VC1_AX file available within the PDS, it is important that off-line processing uses a file as close as possible to the time of acquisition, to minimise the effect of the build-up of condensation on the FPA relay lens (see Section 1.1.3.2. and Section 3.2.2.2.1.). The monitoring activity will take place according to the following procedure:

1. Under normal circumstances between 1 and 4 orbits of L0 data are received by the FOS team each day. These are processed to derive the exact visible channel calibration coefficients for each of these orbits. This is effectively a repeat of the IPF processing described in Section 2.6.1.1.3. . If no Level 0 data are received, NRT VC1 file.
2. Each day produces between 1 and 4 NRT VC1 files. Each file generated is checked for discontinuities with respect to the recent trends in slope and noise. The last file in the sequence is delivered to the IECF for onward distribution to the PDS. In addition, VISCAL history files based on the results of the L0 processing are maintained by the FOS team and long-term plots are made available for relevant meetings and reviews.
3. The selected file is transferred to the PDS, where it will be made available for off-line processing.
4. NRT processing will use the closest possible ATS_VC1_AX file from those already in the PDS archive.
5. Details of the monitoring and quality assurance procedures applied to the AATSR visible channel calibration parameters can be found in Technical Note PO-TN-RAL-GS-0503 "Routine VISCAL Production" Ref. [1.20].

2.12 Data Handling Cookbook

This section is designed as a repository for miscellaneous information on how to handle and interpret AATSR data. The first sub-section contains advice relating to the standard AATSR products available from the ESA PDS. The second sub-section covers the processing of these standard products into higher-level products.

- Hints and Algorithms for Data Use 2.12.1.
- Hints and Algorithms for Higher Level Processing 2.12.2.

2.12.1 Hints and Algorithms for Data Use

As noted in section 1.2. of the AATSR User Guide, there are a number of important concepts associated with the AATSR products that should be understood before proceeding with reading and interpret the data.

The following list of topics is by no means complete. Additional hints and explanations will be added in subsequent issues of this handbook, based on the problems experienced by and the feedback received from users during the mission.

2.12.1.1 Granules

Certain parameters within the products are calculated per granule, rather than for every individual pixel. A granule represents a sub-division of the product, which can be of variable size depending on the parameter in question. In general the along-track dimension of a granule corresponds to 32 image rows. However, the Summary Quality ADS in the GBTR product is based on a 512-row granule.

2.12.1.2 Tie Points

Tie point pixels are pixels associated with specific points equally spaced across a single image or instrument scan. A series of tie points can be defined for every image row, or at specific intervals in the along-track direction, thus forming the across-track dimension to a granule.

2.12.1.3 Relationship Between Measurement Data and Annotation Data in the Gridded Products

2.12.1.3.1 ATS_TOA_1P

Further information on the interpolation of pixel geolocation in the AATSR full resolution products can be found in the following document HERE.

The AATSR MDS records are re-sampled to a 1 km grid, and every pixel in every row of that grid is written into the MDS. However, the corresponding ADSs are sub-sampled with

respect to this grid. Therefore, users must employ an interpolation scheme to retrieve annotation data for each pixel.

The sub-sampling schemes used in each ADS are summarised below.

ADS 0, the Summary Quality ADS (SQADS), contains one record per set of 512 image rows.

ADS 1 and 2, containing scan and pixel numbers for the nadir and forward views, are provided at points every 32 rows along track and for every pixel across track. To derive the scan number of each pixel in the rows between the along-track tie points, take the scan number of the current tie point, and increment by 1 for every subsequent row until the next tie row is reached.

ADS 3 , latitude, longitude and topographic correction, contains these parameters every 32 rows along track and every 25 km across track. Note that in this case, this set of tie points include points at the edges of the scan, at (±275 km), which may lie outside the instrument swath. This results in 23 array elements per record. Latitudes and longitudes for these tie points are simple to calculate, since this is a matter of pure geometry given the position of the tie point.

Linear interpolation should be used to establish the latitude and longitude values for the pixels lying between the tie points. For this reason, the provision of tie points outside the swath was necessary to ensure that there are always two points to interpolate between to derive the latitude and longitude of the edge pixels. Care should be taken whilst doing this interpolation in regions that cross the 180 degree meridian.

It is not appropriate to attempt to interpolate values of topography at this sampling rate, as topography does not change at a uniform rate.

ADS 4 provides the x and y co-ordinates of the INSTRUMENT (as opposed to image) pixels, before regridding onto the image grid, therefore it is arranged in terms of instrument scans instead of image rows. One scan includes pixels from both the nadir and forward views. Therefore scan pixel x and y co-ordinates are not separated into different data sets for the nadir and forward views.

These co-ordinates are provided for every 32^{nd} instrument scan, and for every 10^{th} pixel around the scan. The instrument pixel number of each of these tie points is given in the SPH of the product.

Note also that because this ADS is based in instrument scans, the corresponding time tag represents the time of the instrument scan derived from the telemetry source packet and reflects the start of the instrument scan, rather than the nadir time (i.e. the time at which the middle pixel of the nadir view was beneath the sub-satellite point) used in the other ADS and MDS records.

Linear interpolation should be used to derive scan pixel x and y co-ordinates of the pixels between the tie points.

ADS 5 and 6, solar and viewing angles for the nadir and forward views, are provided every 32 rows along track and every 50km across track (i.e. for the image pixel closest to the 25 km point across-track).

Linear interpolation can be used to derive the solar and viewing angles of the pixels between the tie points, although care must be taken when the azimuth angle passes through 180 degrees.

ADS 7, the visible calibration coefficients ADS, is a Global Annotation Data Set, and therefore contains only one record per product.

2.12.1.3.2 ATS_NR_2P

The ADSs from the L1B product are carried forward into the Level 2 full resolution product, with the exception of ADS 7. The ADSs in the L2 product use exactly the same sub-sampling as for the L1b ADSs above.

2.12.1.3.3 ATS_AR_2P

The AATSR spatially averaged product does not contain any annotation data.

2.12.1.4 The Switchable Product Concept

The GST product (ATS_NR_2P) is switchable, meaning that the content of the MDS depends on the settings of the land/cloud flags for each pixel. The MDS also contains 2 image fields, the Nadir Field and the Combined Field. The contents of these fields, as reflected in the current version of AATSR GST product, are defined as shown in table 2.36 .

Table 2.36 Contents of ATS_NR_2P Distributed Product MDS

Nadir View Cloud Flag	Forward View Cloud Flag	Surface Type	Nadir Field	Combined Field
Clear	Clear	Sea	Nadir only SST	Dual-view SST
Clear	Cloudy	Sea	Nadir only SST	11 μm BT
Cloudy	Cloudy or clear	Land or sea	CTT (currently 11 μm BT)	CTH (currently set to zero)
Clear	Cloudy or clear	Land	LST	NDVI

2.12.1.5 Placeholders

The following placeholders are currently used in certain fields of the Level 2 AATSR products to allow for the development of new or improved retrieval algorithms over a longer timescale.

2.12.1.5.1 GST Product (ATS_NR_2P)

Table 2.37 ATS_NR_2P Placeholders

Parameter Name	Current Field Contents (i.e. placeholder)
Cloud Top Temperature	11 µm Brightness Temperature
Cloud Top Height	zero

2.12.1.5.2 AST Product (ATS_AR_2P)

Table 2.38 ATS_AR_2P Placeholders

Parameter Name	Current Field Contents (i.e. placeholder)
Averaged Land Surface Temperature	11 µm average Brightness Temperature
Averaged Cloud Top Temperature	mean BT of coldest 25%of cloud pixels in cell

2.12.1.6 Visualising Spatially Averaged Cells

The AST product contains spatially averages surface parameters for two different cell grids and two different cell sizes: 10 arc minute and 30 arc minute, and 17 km and 50 km. The larger cells are derived by averaging over a group of 9 small cells.

The 10 and 30 arc minute cells are not aligned to the 1 km grid of the input GST product from which they are derived. Put very simply, the processing for this product involves creating a 10 arc minute cell, assigning pixels to that cell, and closing and outputting the cell when this process is complete. Due to the misalignment between the two grids, it may be

necessary to create a new cell for a pixel that falls outside the boundary of the old cell, before the old cell is completely full. Similarly, it is possible for cell #2 to fill up and be output before cell #1. Therefore, these cells are not output from the processor in a natural grid pattern and should not be treated as a standard array. Instead they should be displayed on a map projection, according to the latitude and longitude co-ordinates associated with each cell.

The 17 km cells are aligned directly with the input 1 km grid and the pixels contributing to each cell are allocated on a systematic basis. Therefore each cell is filled up and output one after the other. The 17 and 50 km cells should therefore be treated just like the 1 km cells in the GST and GBTR products. They can be read into a 2-D raster grid in a systematic order from bottom left to top right.

2.12.1.6.1 Spatially Averaged Cell Latitude and Longitude

The latitude and longitude given for each spatially averaged cell represents that of the lower left-hand corner of the cell.

In 50/17 km cells, this coincides with the first nadir pixel contributing to the cell. In the case of the 50/17 km cells, the cell boundaries are aligned with the image rows and columns, and so the pixels can be systematically assigned to cells from left to right. In this case the first pixel to be assigned to the cell is the lower left corner pixel. The cell time tag is taken as the scan time of the same pixel. In this case 'lower left' means in relation to the conventional image orientation, with the y axis in the direction of satellite motion. This is the south-west corner on ascending arcs, but the north-east corner on descending arcs.

In the case of the 30/10 arc minute cells, the cell latitude and longitude refer to the geometrical co-ordinates of the south-west corner of the cell, and are always multiples of the cell size. This point does not necessarily coincide with an image pixel, and the first pixel to fall in the cell does not usually fall in this corner of the cell. The image rows are oblique with respect to the cell boundaries, and because the orbit is retrograde the cells will fill from east to west. The first pixel to be assigned to the cell, again the pixel which defines the time tag of the cell, is likely to fall in the south-east corner on ascending arcs and the north-east corner on descending arcs.

2.12.1.6.2 Confidence Words and Exception Values

The confidence words and exception values used in the AATSR products are listed in section 2.6.2.1.1. , section 2.7.2.1. and section 2.7.2.2. .

Confidence words provide, on a pixel-by-pixel basis, a bit setting for a particular condition that has occurred in one or more channels of the pixel in question. For example, if the nadir confidence word bit 6 is set, this means that saturation occurred in the pixel and the exception value -5 would be expected in one or more of the channel pixel values.

This is the case for NATURAL pixels. The exception values are set, corresponding to the various error conditions, as these conditions are encountered during pixel processing. In some cases (e.g. Scan Absent; Not Decompressed), the error condition will occur in all 7 channels if it occurs in any. In other cases, (e.g. Saturation in Channel; Calibration Parameters Unavailable), only one channel may be affected. For each view, however, there is only one confidence word per pixel, so the confidence word does not necessarily indicate how many of the channels are affected. It is set if any one or more of the channels show the exception condition. To find which ones, the individual channel images must be inspected.

In the case of COSMETIC pixels, the confidence word bits are not set to match any exception values that may occur. The confidence flags are set during pixel regridding. As each pixel is regridded, the flags that will comprise the relevant confidence word are set. No confidence flags are created at this stage for pixels that are at that time unfilled. This includes pixels that may afterwards be cosmetically filled.

During the cosmetic fill process, adjacent pixel values are copied into the unfilled pixels wherever possible. However, cosmetic fill is based entirely on geometric considerations; i.e., each channel of the cosmetically filled pixel is set to the corresponding value of the neighbouring pixel regardless of whether or not the latter is an exception value. The cosmetic fill flag is then set, but no other flags are. If the pixel remains unfilled, the unfilled pixel flag is set. It therefore follows that for the case of a cosmetically filled pixel, only the cosmetic fill flag in the confidence word is set, even if the actual pixel values are set to exception values.

2.12.1.6.3 Topographic Correction

There will be a narrow strip at the edge of the swath for which no topographic correction is calculated. The topographic corrections are calculated at the same tie points as the image pixel latitude and longitude, so that they can occupy the same ADS. However, as already stated above, this scheme includes tie points outside the instrument swath. The topographic corrections depend on the direction of view, and it is not meaningful to define a view direction for a pixel that is not observed. The topographic corrections are therefore calculated in a similar manner to the solar and viewing angles, for the measured instrument pixel closest to the required tie point. If there is no such pixel, then this tie point will contain an exception value.

A topographic correction is not calculated for land below sea level. It is, however, calculated for lakes above sea level. This is because the current algorithm sets the latitude and longitude corrections to zero if the height value read in from the DEM is negative (i.e. the condition height < 0 is used as a test for sea, and the possibility that a land surface may be below sea level is ignored). The topographic correction is set to zero for these areas.

2.12.1.7 Implications of true IFOV on LST measurements (based on Notes from E. Noyes, University of Leicester, August 2005)

Although data from the AATSR is re-gridded onto a regular 1 km grid, the instrument field of view (FOV) actually extends beyond the edges of the 1 km image pixels on the ground. In addition, the FOV is not uniform. As the viewing angles deviate from true nadir (0º zenith), the FOV on the ground becomes distorted. This is particularly apparent in the forward view, where the instrument pixel size approaches 2.5 km^2 on the ground due to the increase in zenith angle. Figure 2.15 illustrates the approximate FOV for the 11 µm channel image pixels at the centre and edges of the swath in both the nadir and forward views. Different FOV maps are produced for each of the seven AATSR channels.

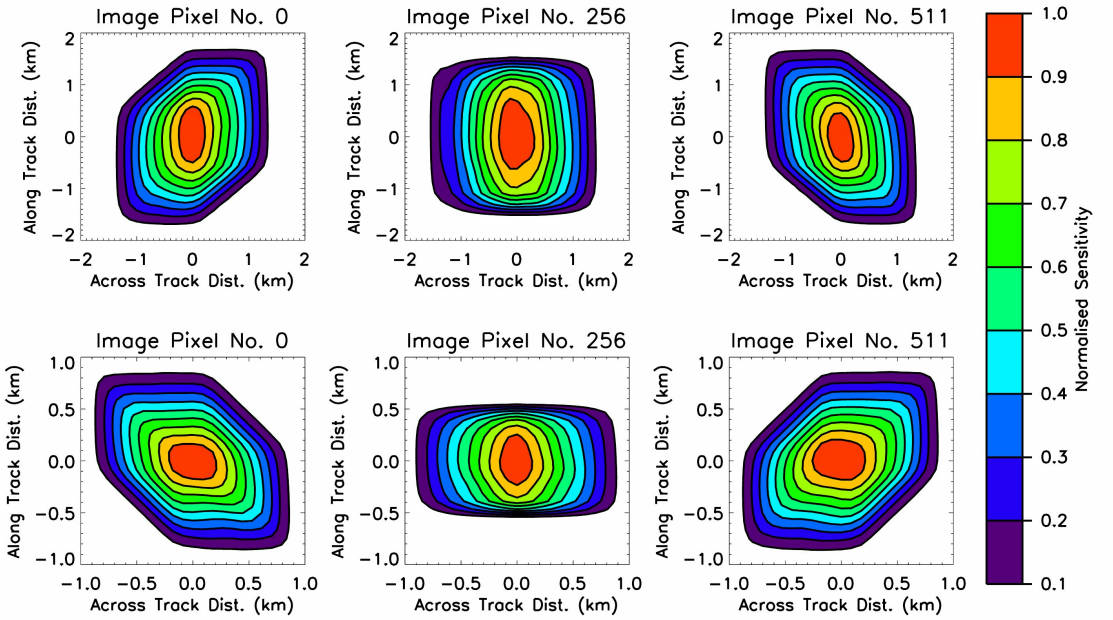

Figure 2.15

If the Earth's surface is completely uniform over the entire instantaneous FOV of the AATSR, the nature of the true FOV is not important. However, for much of the earth, the surface is heterogeneous on the scale of an AATSR pixel. For example, variations of Land Surface Temperature (LST) of the order of 10 K have been observed over the scale of a few metres (Prata, 1994).

It has been demonstrated that biases of the order of several tenths of a degree can result in LSTs obtained over a heterogeneous site, if the true FOV of the AATSR is not considered.

From a users point of view, the surface measurements provided by the AATSR may not represent what users believe they represent. There will be a tendency for users to consider the AATSR data as an average value over the 1x1 km image pixel, whereas in reality, the quantity measured may be affected strongly by the FOV. Further information on this effect

can be obtained from the University of Leicester or the AATSR team at the Rutherford Appleton Laboratory (initial contact to be made through EOHelp@esa.int).

2.12.2 Hints and Algorithms for Higher Level Processing

Areas of interest for AATSR Level 3 processing include cloud parameter retrieval, SST skin/bulk conversion and the development of user-defined binning schemes for the 1 km gridded products. At present there are no algorithms specifically recommended by the AATSR Project for higher level processing, however these topics are the subject of ongoing research, and this section will be updated in subsequent issues of this handbook, throughout the exploitation phase of the mission.

Note that spatially averaged BT and reflectance values have been included in the AATSR L2 averaged product, ATS_AR_2P, specifically to allow users to develop and/or apply their own geophysical parameter retrievals on a global basis, without having to revert to the full resolution L1B product ATS_TOA_1P.

Chapter 3

The AATSR Instrument

This section of the AATSR reference guide provides details about the instrument's design and its performance:

- Instrument Description 3.1.
- Instrument Characteristics and Performance 3.2.

3.1 Instrument Description

The Advanced Along Track Scanning Radiometer (AATSR) is the third in a series of instruments, continuing from ATSR-1 launched on ERS-1 in July 1991 and ATSR-2 launched on ERS-2 in April 1995. The instruments have a common heritage, although certain aspects of instrument design have evolved and improved and a summary of the major differences between the instruments is included in the FAQ, section.

The subsections below describe the components of AATSR and how the instrument works:

- Payload Description, position on the platform 3.1.1.
- Instrument Functionality 3.1.2.
- Internal data flow 3.1.3.

3.1.1 Payload description, position on the platform

The AATSR instrument is an imaging radiometer, sensing at thermal infra-red, reflected infra-red and visible wavelengths. The main part of AATSR, the Infrared and Visible Radiometer (IVR) 3.1.2.1. , is mounted on the right-hand end panel of ENVISAT, with the Digital Electronics Unit (DEU) 3.1.2.3. mounted on an Earth facing panel. Figure 3.1 below highlights the location of AATSR on ENVISAT.

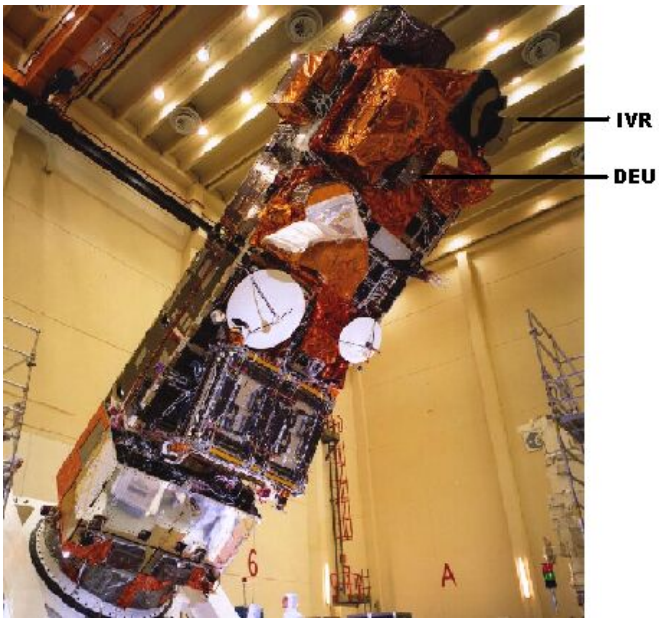

Figure 3.1 The location of AATSR on ENVISAT

The next section 3.1.2. also includes a drawing 3.4 which shows the locations of the components of AATSR on ENVISAT.

3.1.2 Instrument Functionality

Figure 3.2 below shows the functions of AATSR. In summary, AATSR operates by reflecting infrared and visible energy from either the Earth or calibration targets off the rotating Scan Mirror onto a Paraboloid Mirror. The energy is then focused and reflected into the infrared and visible Focal Plane Assemblies (FPA) where detectors convert the radiant energy into electrical signals. The low level signals from the FPA are then amplified by a Signal Pre-Amplifier (SPA) before undergoing signal processing (including digitisation) and data formatting. The data are then passed onto other systems on ENVISAT for storage and transmission back to the Earth. The next sections describe how these functions are mapped to the individual units in AATSR and section 3.1.3. discusses the instrument's internal data flow.

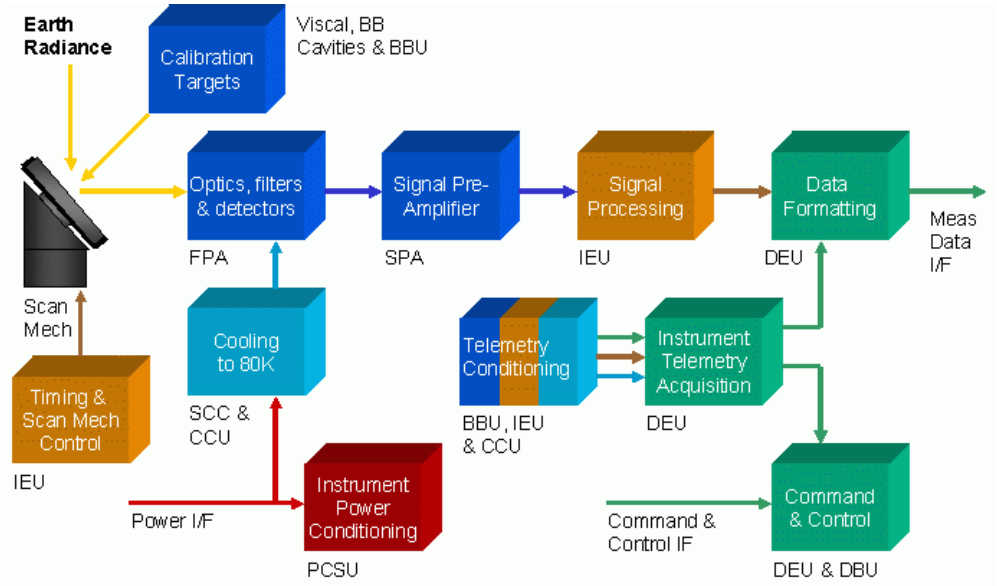

Figure 3.2 AATSR Functional Schematic

The functions are assigned to units and assemblies as shown in figure 3.3 below.

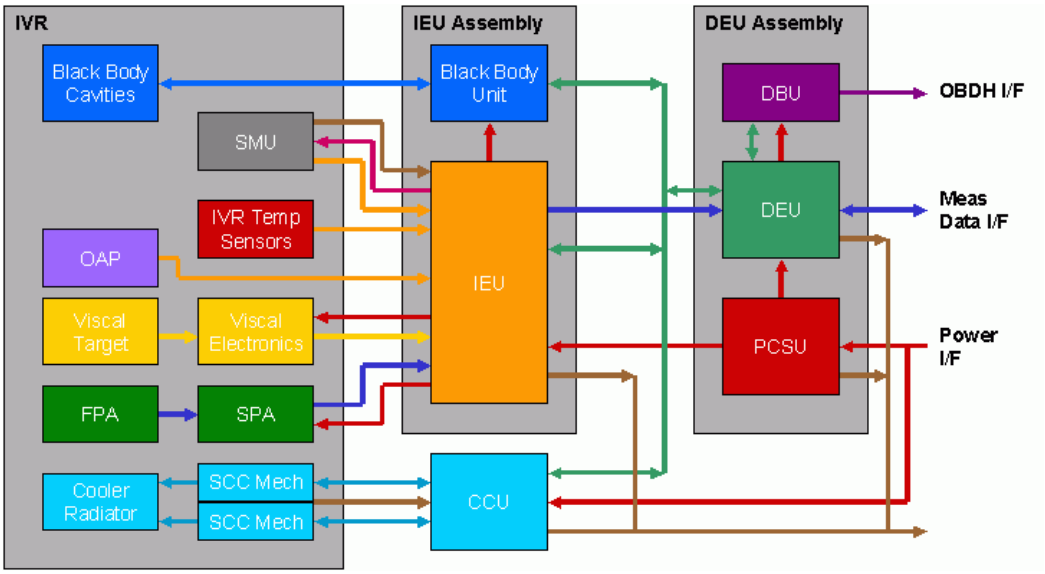

Figure 3.3 AATSR Hardware Architecture

The components of AATSR

Figure 3.4 shows the major components of AATSR in their relative positions on ENVISAT. If ENVISAT is in flight, this is looking from the right hand side of the satellite, with ENVISAT moving from left to right in the diagram.

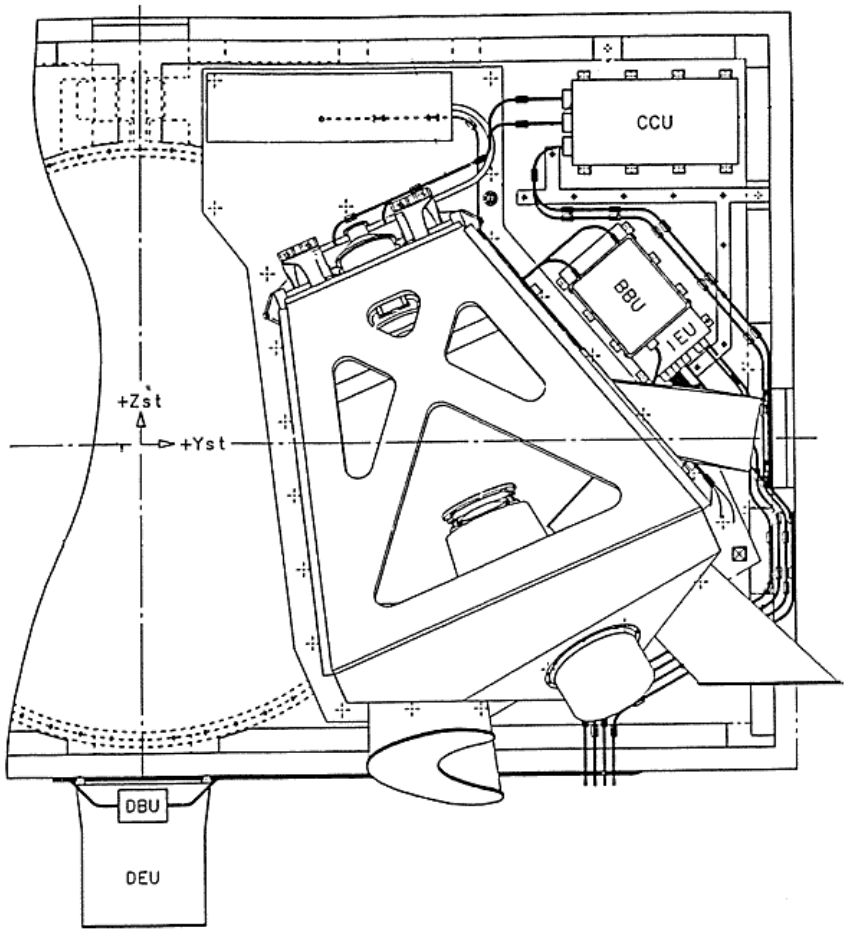

Figure 3.4 AATSR's Major Components and their Locations

The AATSR instrument consists of the following discrete items:

1. The instrument itself, known as the Infrared and Visible Radiometer (IVR) 3.1.2.1.
2. The Instrument Electronics Unit (IEU) 3.1.2.2. , providing the signal channel processing function, the scan mirror drive control and temperature sensor conditioning. The Black Body Electronics Unit (BBU) 3.1.2.2. is mounted on top, and provides the control of the black body heaters and collects temperature sensor data.
3. The Digital Electronics Unit (DEU)/Power Conditioning and Switching Unit (PCSU)/Digital Bus Unit (DBU) 3.1.2.3. for instrument control, data formatting and power control functions.
4. The Cooler Control Unit 3.1.2.4. which controls the Stirling cycle coolers (SCC).
5. The Instrument Harness 3.1.2.5. , which electrically connects the above items.

These are described in more detail in the sections which follow.

3.1.2.1 Infrared and Visible Radiometer Assembly

The Flight Model IVR can be seen in figure 3.5 below. This photograph shows the IVR with the thermal blankets present.

Figure 3.5 AATSR Flight Model IVR

This view is looking up the along-track (forward view) baffle. The nadir view baffle is to the left and the two cylinders at the top and bottom of the picture between the baffles are the Black Body cavities. The baffle on the right face of the IVR is for the VISCAL.

The main features of the IVR are shown in figure 1.2 in the user guide. Figure 3.6 below shows an alternative view of the IVR, looking from the Earth-viewing side of the instrument.

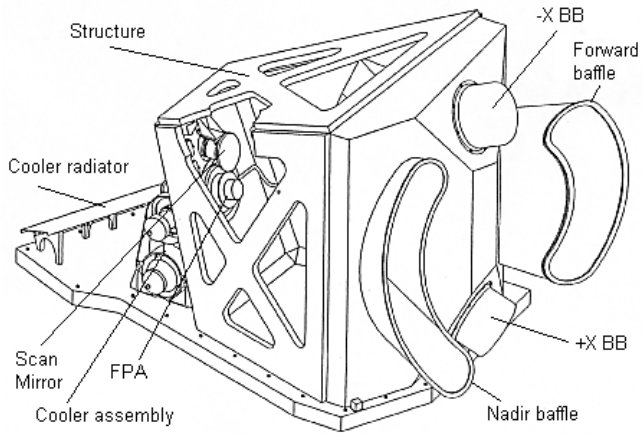

Figure 3.6 AATSR IVR

The Infrared and Visible Radiometer is made up of a number of units:

•

The IVR structure provides physical support and mechanical interfaces for other AATSR components and ensures stable alignment for AATSR's optics. Baffles keep direct sunlight out of the IVR during normal instrument operation.

•

The Scan Mirror Unit (SMU) provides the required positioning and rotation of the Scan Mirror. The plane inclined Scan Mirror reflects the radiation from the Earth's surface or calibration sources onto the Paraboloid Mirror (figure 3.8 shows the scan cycle). The control of the mechanism is performed by the Instrument Electronics Unit 3.1.2.2.1. .

•

The Paraboloid Mirror Assembly (PMA) provides the support for the off-axis paraboloid mirror and the aperture stop. The mirror focuses the reflected radiation from the Scan Mirror into the Focal Plane Assembly.

•

The Focal Plane Assembly (FPA) includes the detectors which convert the radiation into electrical signals and the optical components necessary to select the seven spectral ranges of interest. The FPA consists of two parts, one, the Infrared FPA (IRFPA), for the four infrared detectors, which are cooled to 80K, and the other, the Visible FPA (VFPA), for the three visible detectors. The VFPA is not cooled. The IRFPA contains the single field stop, which defines AATSR's Instantaneous Field of View (IFOV) for all the detectors. Details of the IFOV and AATSR's sampling around the scan are contained in section 3.2.1.2.1. .

•

The Signal Preamplifier (SPA)amplifies each of the detector signals from the FPA, before they are passed on to the Instrument Electronics Unit 3.1.2.2.1. for processing.

•

A pair of Black Body cavities (BBCs) provide a hot (at approximately 305K) and cold (at approximately 265K) calibration reference for the infrared detectors on every scan, as well as

a zero radiance reference for the visible detectors. They are controlled by the Black Body Electronics unit (BBU) 3.1.2.2.2. . On AATSR, there are 6 temperature sensors on each of the BBCs, compared to the 7 on each for ATSR-1 and ATSR-2. Five of the temperature sensors are mounted on the base of the cavity, with the sixth on the wall.

- The VISCAL unit is the "bright" calibration source for the visible channels on AATSR (one of the BBCs is used as the "dark" calibration source). The VISCAL provides an approximately 16% radiance calibration reference signal when illuminated by the sun for approximately 34 seconds once per orbit near sunrise.
- The Cooler Mechanism Assembly provides mechanical support for, and includes, the pair of Stirling cycle coolers (SCC) which cool the IRFPA detectors. The structural attachment to the FPA is decoupled by a pair of bellows, while the thermal attachment is via a pair of flexible braids. The coolers are controlled by the Cooler Control Unit 3.1.2.4. .
- The heat dissipated by the coolers is radiated into space by a thermal radiator, which is connected to the Cooler Mechanism Assembly by a heatpipe.
- The IVR also has thermal hardware (i.e. multi-layer insulation blankets, temperature sensors), to ensure that the component temperatures are maintained within safe limits and that performance of the radiometer is not compromised.
- The electrical connections between items on the IVR are provided by the IVR harness.

3.1.2.2 Instrument Electronics Unit/Black Body Electronics Unit

The radiometer electronics are contained in the Instrument Electronics Unit (IEU). The Black Body electronics (BBU) are in a separate unit which is mounted on the top of the IEU. Power and the instrument's Command and Telemetry Bus are routed through the IEU to the BBU.

3.1.2.2.1 Instrument Electronics Unit

The IEU forms a part of the electronics subsystem for the AATSR Instrument. As shown in figure 3.3 , it interfaces with the Digital Electronics Unit (DEU) and Power Conditioning and Switching Unit (PCSU) 3.1.2.3. , the Signal Preamplifier (SPA), the Scan Mirror Unit (SMU), the BBU 3.1.2.2.2. , and the Infrared Visible Radiometer (IVR) 3.1.2.1. itself.

The IEU houses the electronics for processing the analogue signals from the detectors in the Focal Plane Assembly (FPA) after they have been amplified by the SPA, for temperature sensors and analogue monitors and for driving the SMU.

The interfaces to the DEU/PCSU are for the transfer of command, telemetry and science

data and for the supply to the IEU of regulated power.

The electronic system in the IEU are subdivided into the sub-systems listed below:
(1) Signal Channel Processing
There are seven Signal Channel Processors (SCP) which receive the analogue inputs from the FPA's detectors after they have been amplified by the SPA. The SCPs scale and convert the analogue inputs to serial digital words. Scaling is performed under control of the DEU 3.1.2.3. 's Auto Gain/Offset and Auto Offset software.
(2) Scan Mirror Drive
The IEU includes the control system for the SMU. The performance of the SMU and its control system is described in section 3.2.1.3.2. .
(3) Temperature Sensors
The IEU conditions and digitises integrated circuit temperature sensors mounted on the instrument structure, SMU, VFPA and visible calibration target assembly. It also provides these functions for the cryogenic temperature sensors in the IRFPA.
(4) Visible Calibration Monitor
The VISCAL includes a monitor circuit which measures the radiance of the VISCAL source. The monitor output is conditioned and digitised by the IEU.

3.1.2.2.2 Black Body Electronics Unit

The Black Body electronics Unit (BBU) has the following main functions:
(1) Heater control
The BBU selects the BBC to be heated and the heater level under command of the DEU 3.1.2.3. . Only one BBC can be heated at a time and the main heater has three power settings, of which the intermediate level is normally used.
(2) Temperature Sensors
The temperature sensors (6 platinum resistance thermomeneters on each CBB and a temperature sensor in the BBU) are sampled by the BBU on request of the DEU 3.1.2.3. .

3.1.2.3 Digital Electronics Unit/Power Conditioning and Switching Unit

The Digital Electronics Unit/Power Conditioning and Switching Unit (DEU/PCSU) assembly consists of two units:

•

The DEU contains the Instrument Control Unit (ICU) function and the function to format the detector and other data from the IEU. The ICU receives telecommands from the ground via the Payload Module Computer and sends telemetry back. The ICU includes software to control the instrument as well as for monitoring housekeeping parameters for out of limits conditions. The ICU software is stored in Electrically Eraseable Programmable Read-Only Memory (EEPROM) and can be updated in flight.

The data formatter
includes the pixel selection function based on a programmable pixel map and the hardware

to assemble the science data and auxiliary data to make up the instrument source packets for transmission to the spacecraft's High Speed Multiplexer. On AATSR (unlike ATSR-1 and ATSR-2), the source packet contains all 12 bits for each pixel in the Earth and calibration targets for all channels all the time. Therefore, the pixel map will not be routinely varied in flight after it has been optimised during commissioning (see section 3.2.2.1.). The pixel map is discussed in more detail in section.

- The assembly includes the PCSU, which provides all secondary regulated and unregulated supplies to the AATSR instrument.

The DEU interfaces to the spacecraft's Onboard Data Handling bus via the Digital Bus Unit, supplied by ESA.

3.1.2.4 Cooler Control Unit

The Cooler Control Unit (CCU) controls the two Stirling cycle coolers in response to commands from the DEU 3.1.2.3. . The CCU commands the coolers' operation and continuously monitors appropriate parameters to monitor their operation. The cooler subsystem ensures that the IRFPA detectors are maintained at a stable cryogenic temperature (80K nominally), around the orbit and over longer time periods.

3.1.2.5 Instrument Harness

The instrument harness electrically connects the AATSR assemblies. It also includes electrical bonding straps from the IVR and electronics units to the ENVISAT ground reference rail.

3.1.3 Internal Data Flow

Figure 3.7 shows the acquisition and flow sequence for AATSR observation and calibration data.

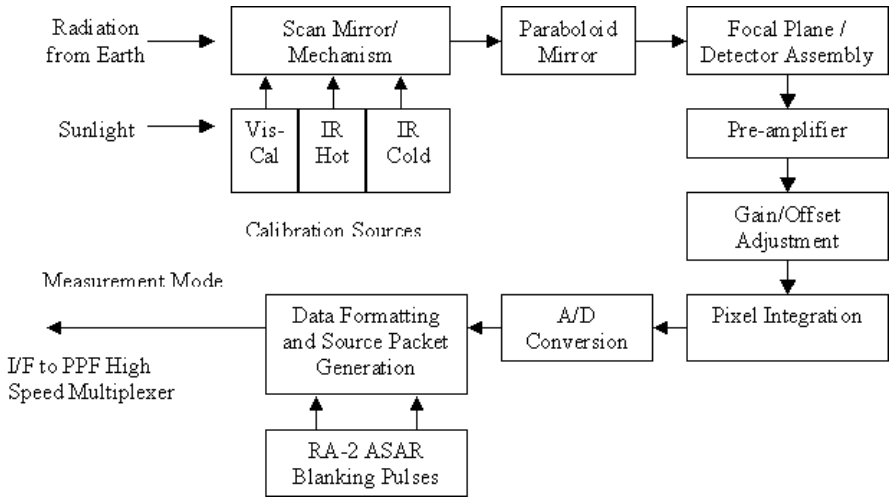

Figure 3.7 ATSR acquisition and flow sequence for instrument observation and calibration data

The data flow for AATSR is as follows:

•

Infrared radiation and visible illumination from two views of the Earth is incident on the plane inclined Scan Mirror which rotates and performs a conical scan 1.1.3.1. of the instrument IFOV.

•

The hot and cold black body targets and the visible calibration target also provide radiance which are in the conical path swept out by the scan mirror (see Figure 3.8 below).

Figure 3.8 AATSR San Cycle

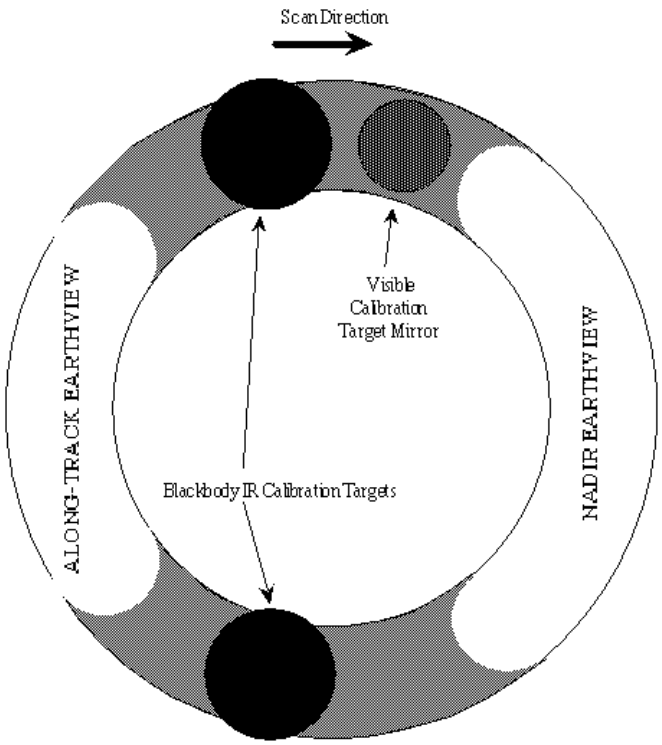

(This is an image map, so clicking on a part of AATSR will take you to detailed information about it)

•

The radiation is focussed onto the cooled Focal Plane Assembly by the instrument optics and beamsplitters. The low level signals which are proportional to the radiation intensity are amplified by a Signal Preamplifier.

•

These signals are in turn passed to the Instrument Electronics Unit 3.1.2.2.1. (IEU) where the signals have gain and offset adjustments made. The gain and offset adjustments are made autonomously by the ICU for the IR channels (Auto Gain/Offset (AGO)) by sampling the digital data within the Digital Electronics Unit 3.1.2.3. (DEU) corresponding to the hot and cold calibration target radiances for each IR channel. For the visible channels, offset adjustments are made autonomously by the ICU by sampling the digital data within the DEU corresponding to the cold calibration target radiances for each visible channel (Auto Offset). Visible channel gain adjustments are made by macrocommand following analysis of the ground processed source packet data at the time of sun illumination of the visible calibrator.

•

The signals for each channel are then integrated over sample periods, each of 75µs, by a pair of integrators operating alternately. This integration provides a total of 2000 pixels per revolution (scan) of the scan mirror. Each of the integrated data samples is then converted from analogue to 12 bit digital data. In order to distinguish between the 2000 pixels in a scan, the clock generator electronics (in the IEU 3.1.2.2.1.) produces a 'Scan Sync' pulse synchronised to pixel location 1 and a 'Pixel Sync' pulse for each of the 2000 pixels.

•

The 12 bit data from each signal channel are passed serially to the DEU 3.1.2.3. where the

pixel data are selected for formatting in accordance with a pixel map held in a dedicated non-volatile memory within the DEU. The map is a look up table with one entry for each of the 2000 pixels in a scan. The map identifies whether or not to format science data for each pixel. Of the 2000 pixels in a 360° rotation of the instrument scan mirror, 974 of these pixels contain useful data i.e. Earth viewing and calibration source radiances. Some pixels represent views of the instrument housing/structure and are therefore discarded. Table 3.1 below shows the pixel selection map at launch - this may be updated during commissioning (see section 3.2.2.1.).

Table 3.1 Pixel Selection Map at Launch

Region	Used Pixels
Viscal	75-90
Nadir View	224-778
+X BB	1074-1089
Forward View	1316-1686
-X BB	1913-1928

•

Two bits of blanking pulse data, one from each of Radar Altimeter-2 (RA-2) and the Advanced Synthetic Aperture radar (ASAR) instruments, are merged with the selected pixel data. Blanking pulses only occur in the merged data for those pixels which were being integrated during the occurrence of a blanking pulse and are included to allow possible data discrepancies to be tied in with transmissions from the RA-2 and the ASAR.
The observation and calibration data are combined with blanking pulse data, additional header data and auxiliary data to produce a packet of information in a predetermined format, known as a source packet 2.2 . Each source packet has a length of 5756 x 16 bits. These packets are automatically transferred every 150ms at a clock rate of 625 kbits/s to the spacecraft's High Speed Multiplexer (HSM) for onward transmission to the ground.

3.2 Instrument Characteristics and Performance

This section describes the characteristics and performance of AATSR. It is split into two sections:

- section 3.2.1. describes the pre-flight characteristics and expected performance.
- section 3.2.2. describes the way in which AATSR's performance will be verified in-flight.

3.2.1 Pre-flight characteristics and expected performance

This section describes the pre-flight characteristics and expected performance of AATSR in the following areas:

- Spectral 3.2.1.1.
- Spatial 3.2.1.2.
- Pointing 3.2.1.3.
- Radiometric 3.2.1.4.
- Stability 3.2.1.5.

These subsections rely on the results of the pre-launch testing and analysis of AATSR, as well as AATSR's specifications, to describe the expected performance.

3.2.1.1 Spectral

3.2.1.1.1 Specifications

The choice of wavebands for AATSR was derived from the scientific requirements for sea surface temperature and land surface mapping (for more detail, see section 1.1.2.). For continuity of the SST and land surface reflectance data sets, which commenced with ATSR-1 and ATSR-2, the channel responses of the AATSR 0.55 µm, 0.66 µm, 0.87 µm, 1.6 µm, 3.7 µm, 11 µm and 12 µm channels were specified to have similar spectral shapes to those on ATSR-1 and ATSR-2.

The AATSR signal channel end-to-end response characteristics as specified for AATSR are shown in table 3.2 .

Table 3.2 AATSR Specified Spectral Responses

Channel / µm	Centre Wavelength / µm	50% of Peak / µm	Error on 50% Points / µm	Slope 5% - 80% / µm	<1 % of Peak / µm
0.55	0.555	0.545 - 0.565	± 0.003	< 0.008	0.530 - 0.580
0.66	0.659	0.649 - 0.669	± 0.003	< 0.008	0.634 - 0.684
0.87	0.865	0.855 - 0.875	± 0.003	< 0.008	0.840 - 0.890
1.6	1.61	1.58 - 1.64	+ 0.01/- 0.04	< 0.30	1.52 - 1.70
3.7	3.70	3.55 - 3.93	± 0.06	< 0.12	3.40 - 4.12
11	10.85	10.40 - 11.30	± 0.09	< 0.34	9.80 - 11.90
12	12.00	11.50 - 12.50	± 0.09	< 0.37	10.90 - 13.10

In addition to the specifications in table 3.2 , requirements were set for the out of band response for each AATSR channel. The peak out of band response was specified as less than 10^{-4} of the peak in-band response and the out of band response for each channel was specified as contributing less than 1 part in 4095 of the total signal integrated over

wavelength.

From ATSR-2 experience, it was understood that for the 0.55 µm, 0.66 µm and 0.87 µm channels, the tolerances of the half power points given in table 3.2 are not independent for each edge. In order to meet the spectral width specification, a further requirement was necessary, to specify that the difference between the half power points (i.e. the width) for the 0.55 µm, 0.66 µm and 0.87 µm channels needs to be 20 nm, with a tolerance of -0/+2 nm.

3.2.1.1.2 Measurements

Measurements of the spectral responses were made for the Focal Plane Assembly and generally the above specifications were met. The full set of spectral response measurements can be downloaded here. The measured response curves for the AATSR channels can also be seen in the plots below. Click on each plot to view a larger version.

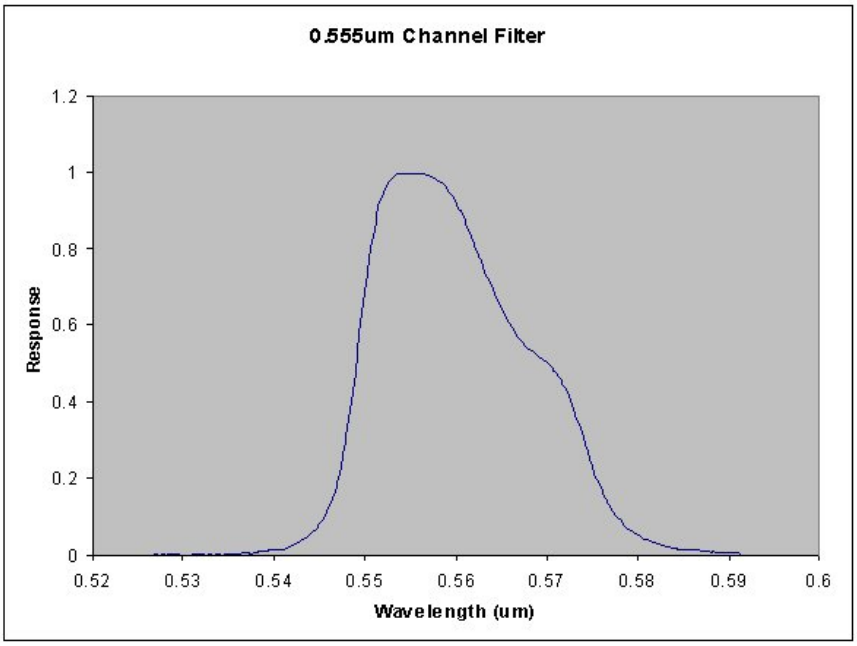

Figure 3.9

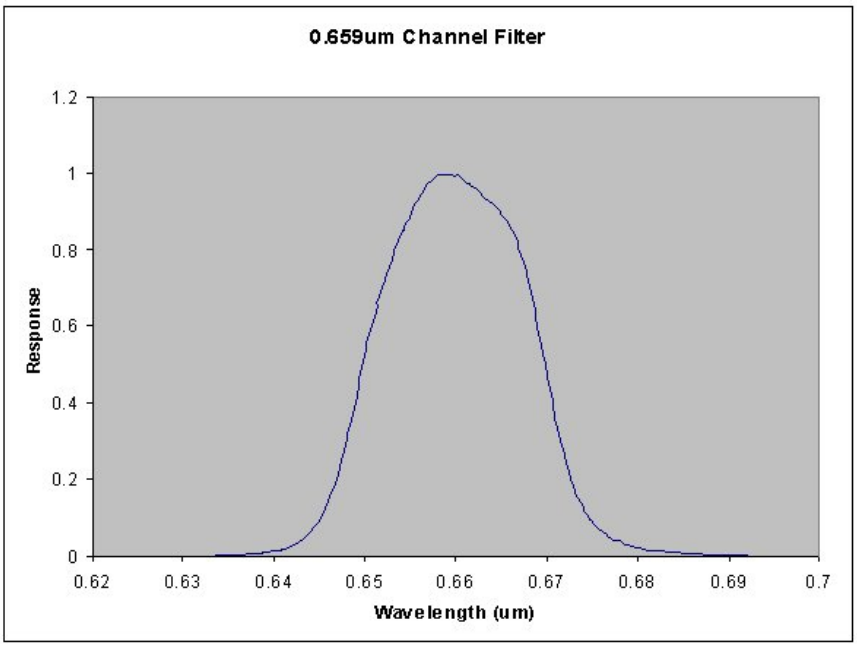

Figure 3.10

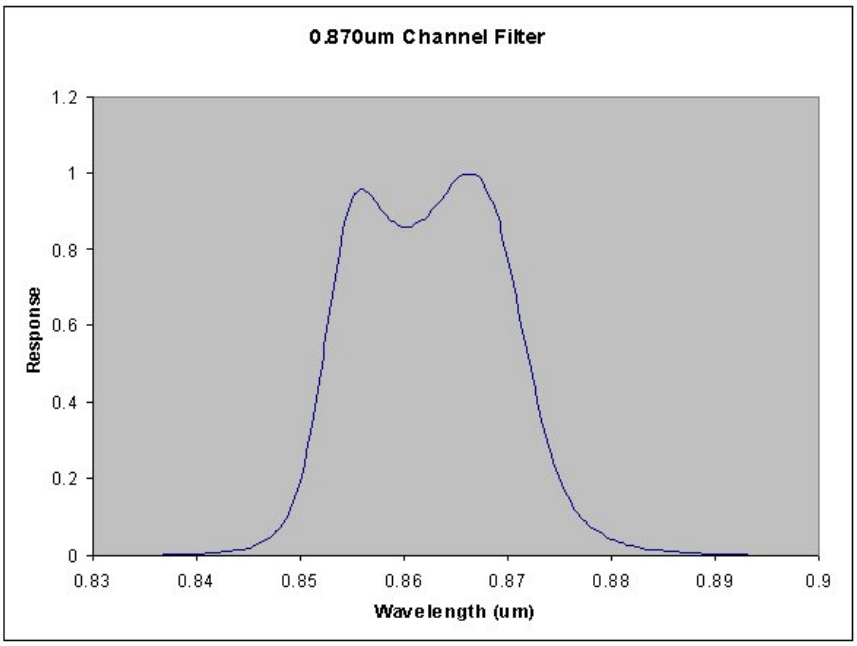

Figure 3.11

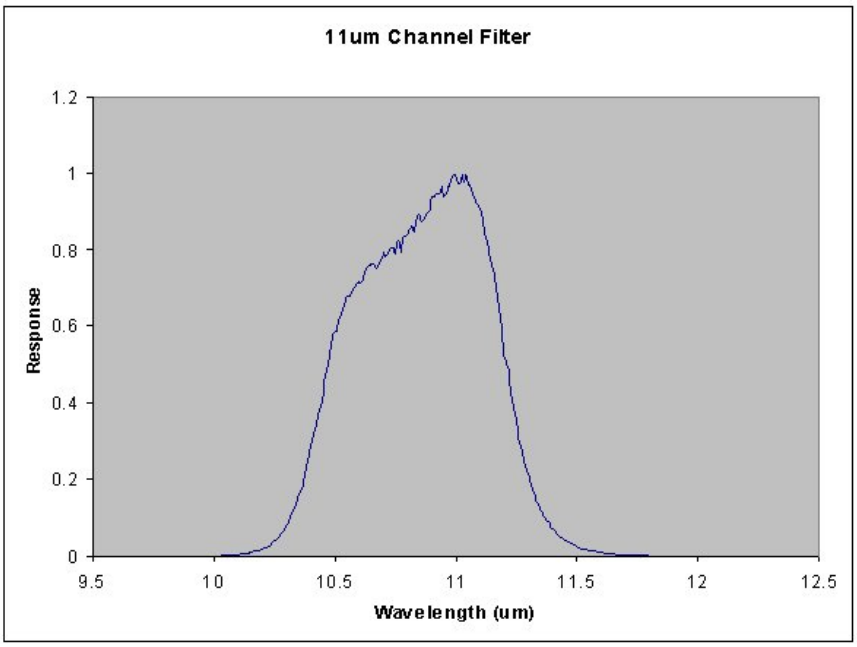

Figure 3.12

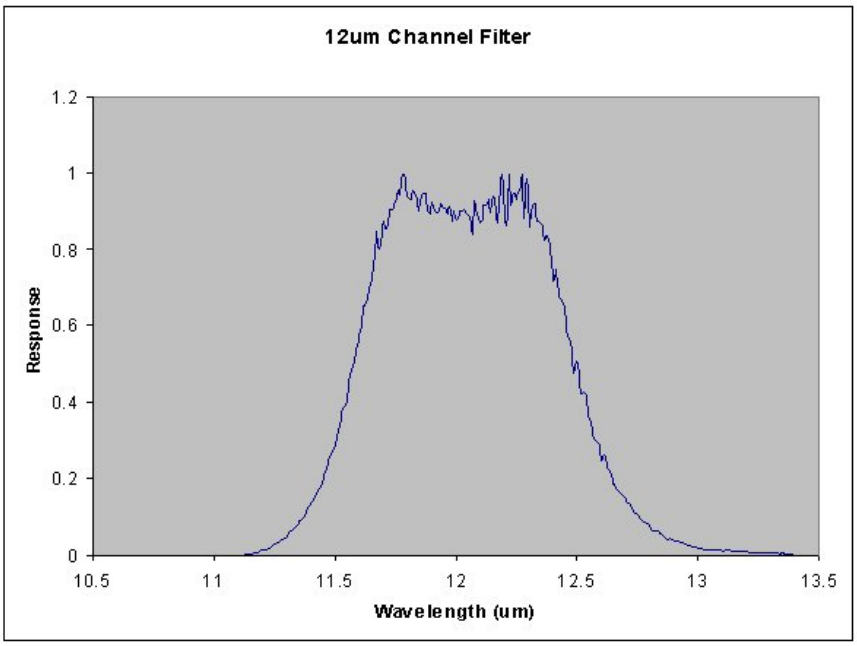

Figure 3.13

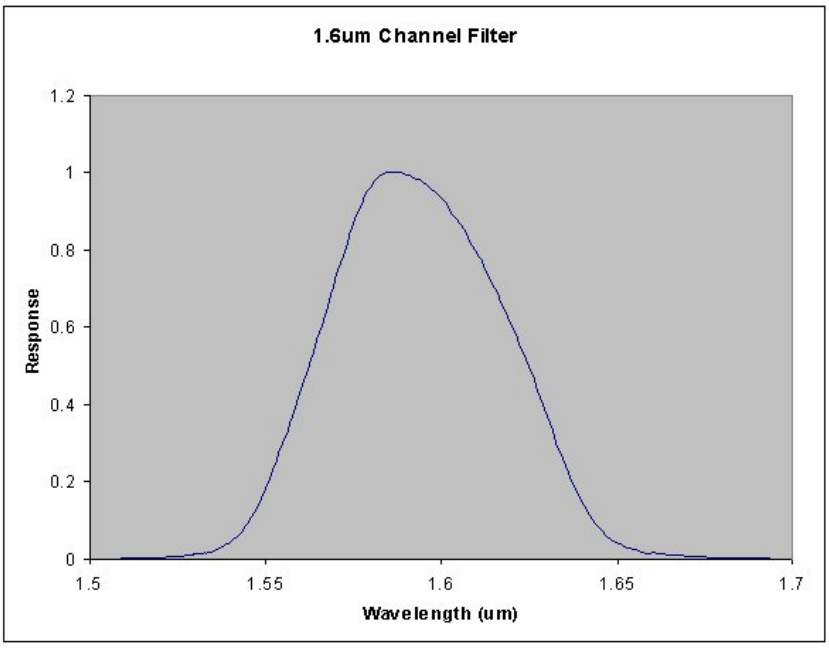

Figure 3.14

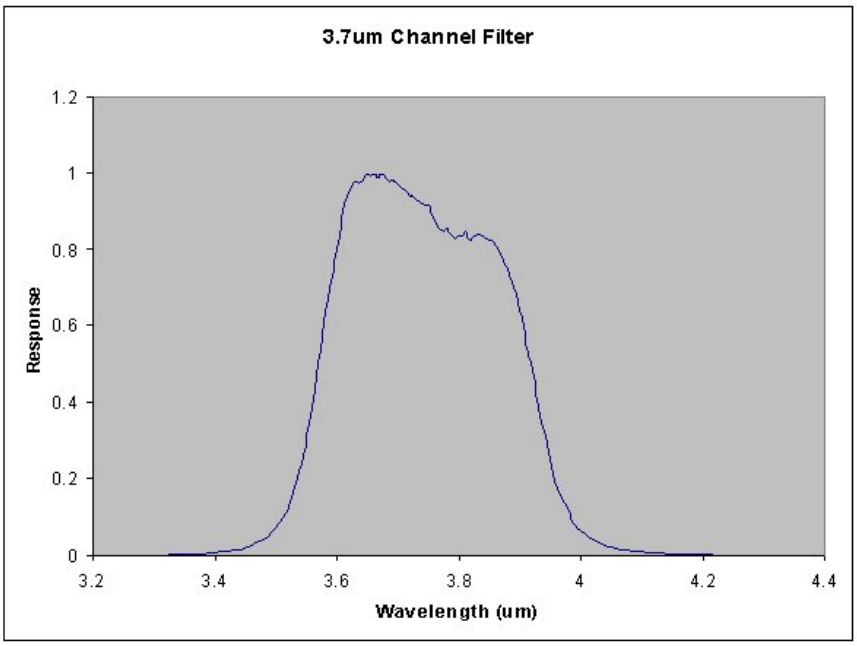

Figure 3.15

The out of band response proved difficult to measure and quantify accurately, but the results showed that generally the out of band responses were less than 10^{-3} of peak response.

Further details of the AATSR spectral characterisation are available on request from the Rutherford Appleton Laboratory (initial contact to be made via EOHelp@esa.int).

3.2.1.2 Spatial

3.2.1.2.1 Description and Specifications

AATSR has two ~500 km wide curved swaths, with 555 pixels across the nadir swath and 371 pixels across the forward swath (see figure 1.1 in the User Guide). Each pixel (or sample) is defined by integrating the detector signals over 75 ±0.75 µs as the scan mirror rotates, thus giving 2000 samples per 150 ms scan (only the useful samples of the earth views and calibration sources are transmitted to the ground, and are selected using a pixel map).

The nominal Instantaneous Field of View (IFOV)
is specified to be 1 x 1 km at the centre of the nadir swath. With ENVISAT orbiting at 800 km, the angular IFOV set at the field stop in the Focal Plane Assembly (FPA) is specified to be a square 1/777 rad (265 arc seconds) ±1.44% by 1/777 rad (265 arc seconds) ±1.44%, which gives a surface projected IFOV at nadir of 1.03 km by 1.03 km.

The varying viewing angle to the Earth's surface which results from AATSR's conical scan 1.1.3. affects the projection of the IFOV on the ground. As already described, at nadir, the projection of the IFOV is 1 x 1 km, but at the centre of the forward view, it is 1.5 x 2 km.

The Field of View (FOV) along-track has a response shape like the IFOV, varying from a 1 km length at nadir to 2 km length at the centre of the forward view due to the angle it is projected onto the Earth (see figure 1.1 in the User Guide). Around the scan (which is across-track at nadir and at the centre of the along-track view - see figure 1.3 in the User Guide), the FOV is the IFOV convolved with itself for its displacement during one 75 µs integration. Thus, assuming that the response across the IFOV is uniform, the FOV in the around-scan direction has an approximately triangular shape. As the nominal sampling distance is approximately 1 km, at nadir the FOV is a 1 km wide half-height triangle, with a base width of 2 km. Figure 3.16 illustrates the calculation and shape of the FOV around the scan.

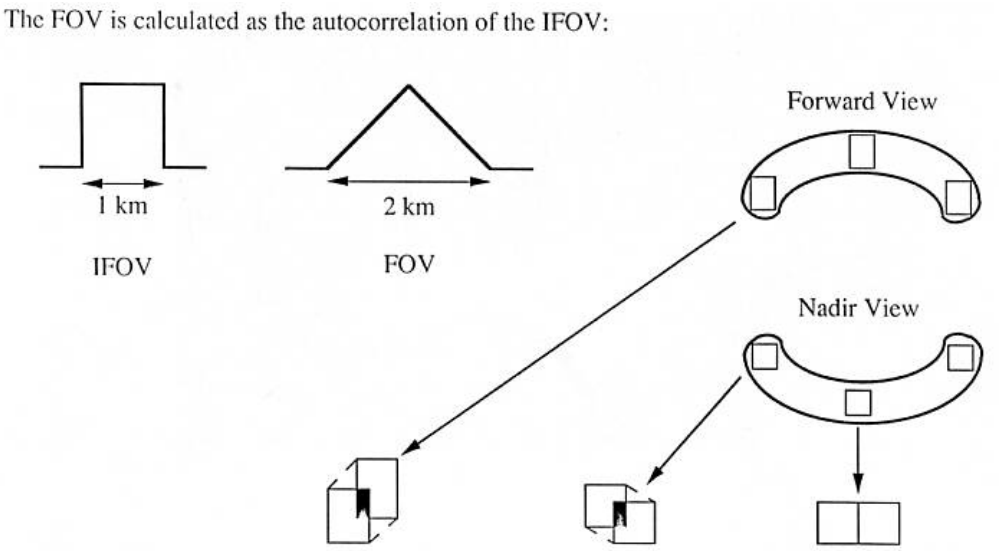

Figure 3.16 Calculation of the FOV from the IFOV around the scan

Co-registration of the different spectral channels is important, and the specification is for errors in optical and electrical alignment between channels not to exceed 0.1 sample distance at nadir. This is helped by having a single field stop, but the integration periods for each channel must also be accurately synchronised.

One specific difference in AATSR's FOV from ATSR-1 and ATSR-2 results from a change to the orientation of the 11 µm and 12µm detectors. It is known from previous ATSR missions that the detectors used for these channels have a response variation across their sensitive areas, which is related to electrical bias. This causes a variation in the response over the IFOV in one dimension. In previous ATSRs, this response variation was imaged along-track. For AATSR, the construction of the detectors has been altered to minimise the inherent variation and the detectors are oriented so that the variation now appears in the across-track direction.

3.2.1.2.2 Measurements

The instrument level measurements of the IFOV (which were made at RAL) are described here.

The objectives of the tests were:

- To map out the IFOV of each signal channel to a resolution of better than 10% of a pixel.
- To measure the relative alignment of each channel.

- To determine and quantify the effect on the IFOV due to significant distortion of the instrument's fore optics as a result of changes in the thermal environment between BOL and EOL thermal conditions.
- To determine whether the instrument optical alignment is affected by outgassing of the carbon fibre structure.

The IFOV of each channel was mapped out by scanning the image of a point source across the instrument's field stop and recording the detector's response as a function of position.

Two methods for mapping the IFOV were used:

- A 'static' method where the instrument's scan mirror is kept stationary and the image of the point source is steered across the field stop in both azimuth and elevation.
- A 'dynamic' method, where the instrument's scan mirror is rotating, using a gimbal mounted mirror to move the image in the along-track direction and the scan mirror to move the image in the across-track direction.

The results of the measurements are described in detail in RAL's FOV Test Report Ref. [1.2] and are summarised below. The static IFOV measurements are shown in figure 3.17 and figure 3.18 and summarised in table 3.3 , with the dynamic measurements shown in figure 3.19 .

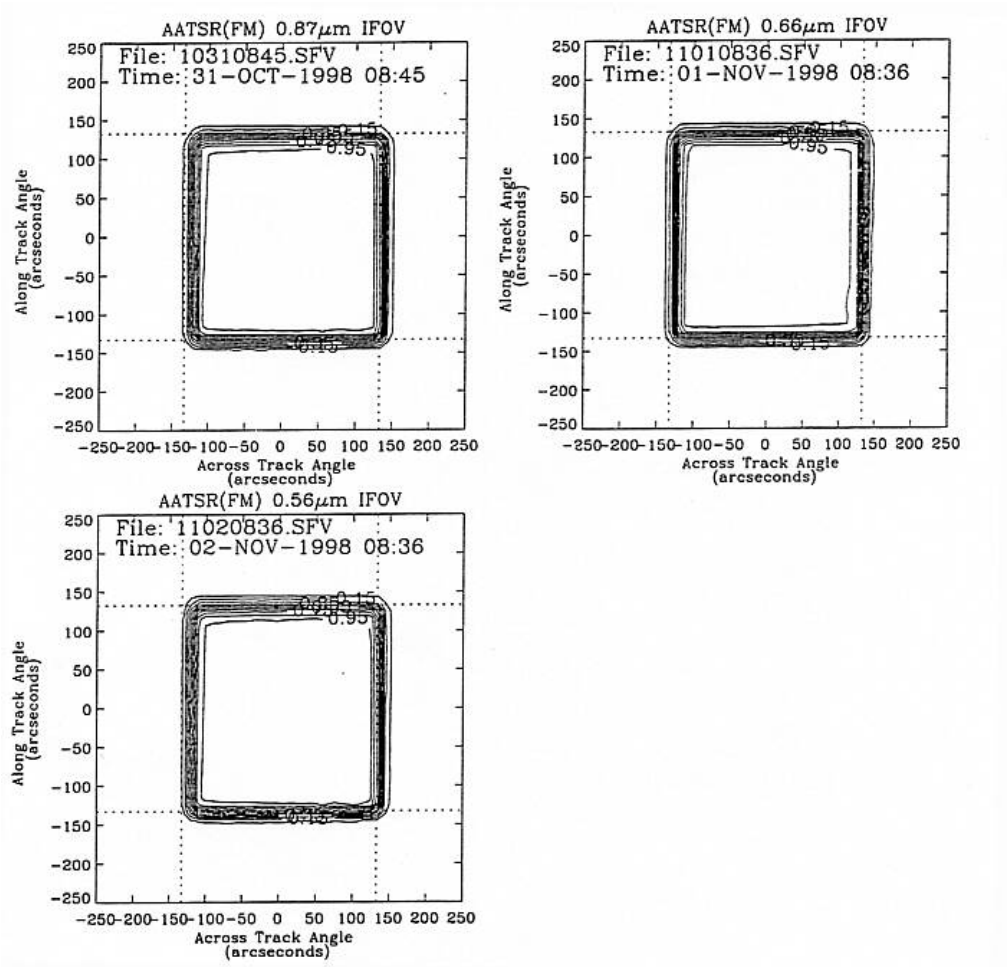

Figure 3.17 IFOV maps for 0.87 μm, 0.66 μm and 0.56 μm channels in air (the dashed lines show the nominal IFOV as defined by the FPA's field stop)

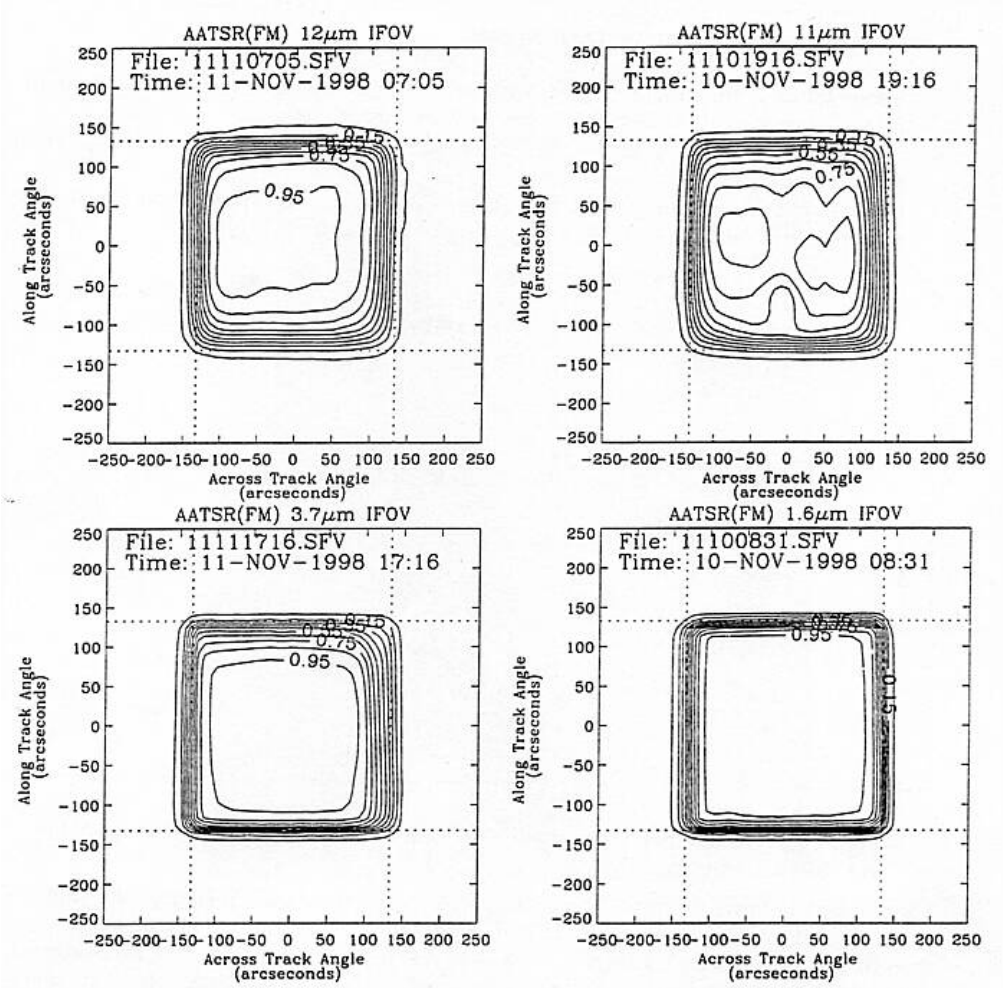

Figure 3.18 IFOV maps for 12 μm, 11 μm, 3.7 μm and 1.6 μm channels in air (the dashed lines show the nominal IFOV as defined by the FPA's field stop)

Table 3.3 Widths and centre (relative to 0.87μm co-alignment scans) of AATSR static IFOV maps

Channel	Width of IFOV (arc seconds)		Centre of IFOV (arc seconds)	
	Along-Track	Across-Track	Along-Track	Across-Track
12μm	235	245	6	-5
11μm	223	235	-1	-3
3.7μm	246	253	-6	6
1.6μm	259	259	1	-3
0.87μm	261	258	0	0
0.66μm	262	255	-2	5
0.56μm	263	256	-1	8

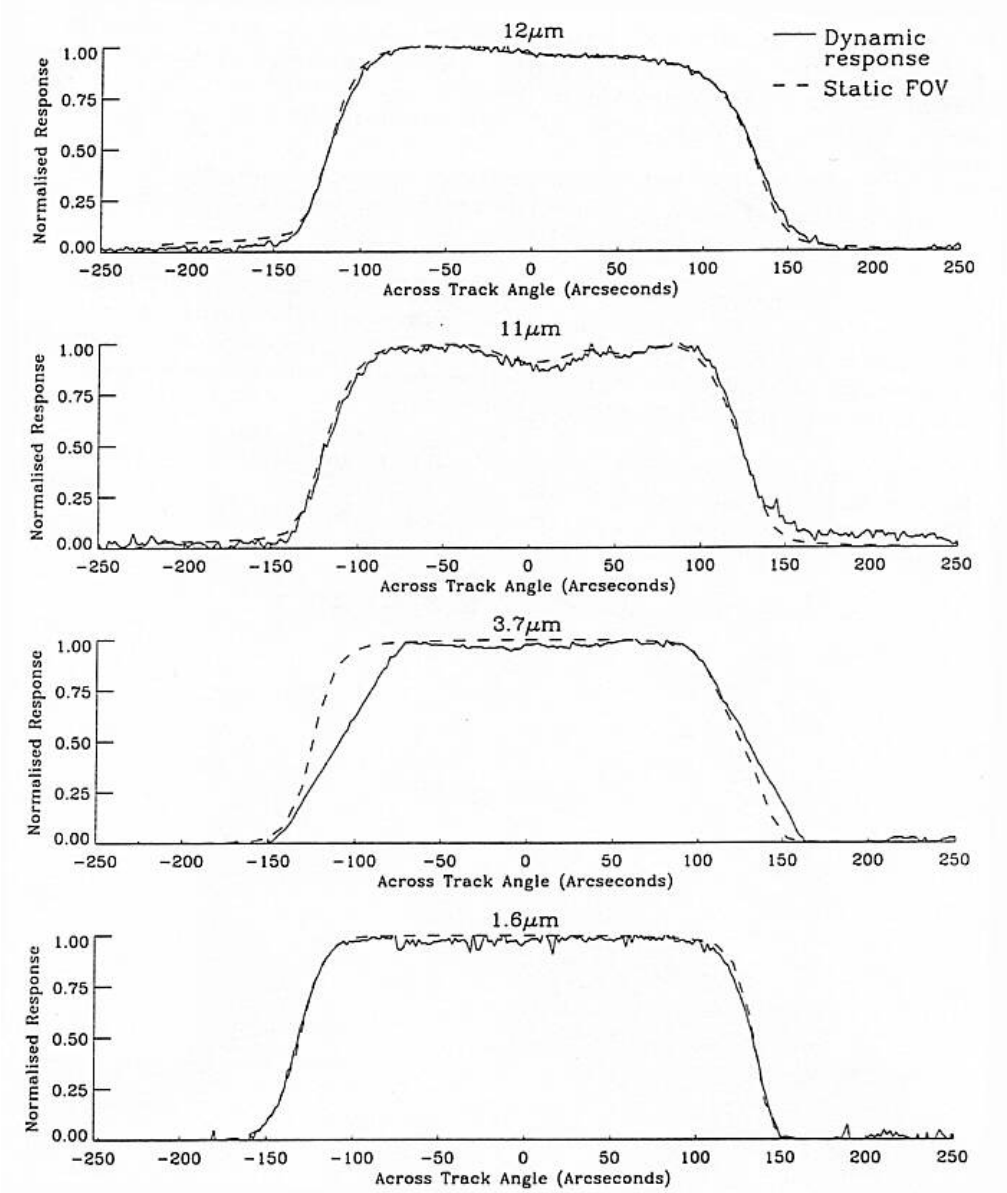

Figure 3.19 Dynamic response measurement for the IR channels (solid lines). These are compared against the integrated, static IFOVs in the across-track direction (dashed lines)

In conclusion, the results of the measurements at RAL (see RAL's FOV Test Report Ref. [1.2]) showed that the centres of the IFOVs for all AATSR channels agree to within 5% of a sample period. The widths of the 3.7 μm, 1.6 μm, 0.87 μm, 0.66 μm and 0.55 μm channels are within 10% of the expected IFOV defined by the field stop. The 12 μm and 11 μm channels are also well centred but were smaller in area. This is due to the smaller active areas of the detectors.

The IFOV map of the 0.87 µm channel did not show any significant differences between ambient, BOL or EOL conditions.

The drift in alignment between ambient and BOL conditions is less than 0.1 pixel in the along-track direction and 1 pixel in the across-track direction. This will have no effect on the beam clearance. Between BOL and EOL, there was a 60% shift in the across-track direction. However, the drifts induced under normal orbital variations will be much less and should have a minimal effect on geolocation.

The dynamic response tests demonstrated that there were no observable effects on the IFOVs of the 12 µm, 11 µm and 1.6 µm channels. The 3.7 µm channel does show some slight difference just as for ATSR-2, which may be the result of a longer time constant in the detector/preamplifier combination.

RAL and the Principal Investigator concluded that the IFOV results were acceptable for flight.

Further comments on the implication of the true FOV on the exploitation of AATSR data, particularly over land, are given in Section 2.12.1. .

3.2.1.3 Pointing

3.2.1.3.1 Alignment and platform pointing

AATSR's pointing has to be known and stable. Thus, the angle of the scan cone for AATSR is specified to be 46.90° (tolerance ±1.0 arc minutes), with one cone side including the nadir, and the cone axis pointing 23.45° (tolerance ±0.5 arc minutes) forward from nadir. The Scan Mirror normal is, therefore, inclined at an angle of 11.725° (tolerance ±0.25 arc minutes). These angles are shown in figure 3.20 below. AATSR also has an alignment cube, so that AATSR's alignment can be referenced to the spacecraft alignment and pointing.

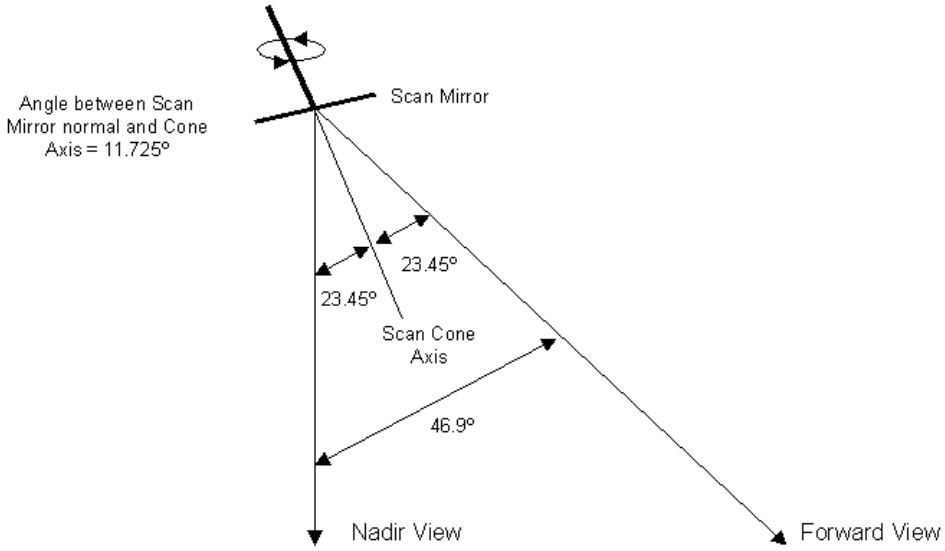

Figure 3.20 Scan Cone Characteristics

Measurements have shown that the scan cone axis deviates slightly outside specification as it lies within 2.5 arc minutes of the ideal position at 23.478°. The measurements of the scan cone characteristics and the alignment between AATSR and the platform are used in AATSR data processing (see section).

ENVISAT's pointing accuracy and stability (add link to satellite-level information) do not present any constraints on AATSR's performance (e.g. for geolocation).

3.2.1.3.2 Pointing performance of the scan mechanism

AATSR uses the same technique as ATSR-1 and ATSR-2 of using a scan reference pulse, provided once per scan, in conjunction with the difference from the time of the pulse to work out where the scan mirror is pointing on the ground at any time around the scan. Therefore, the scan mechanism must rotate uniformly, so as not to introduce errors in the pointing for an individual sample.

To give an example, imagine that the scan mechanism runs very slightly slow. Thus, the instrument is actually viewing a point on the scan slightly behind where it would be expected to be if the mechanism was running at the correct speed. Using the time since the scan reference pulse to locate the sample would thus introduce a pointing error. Unfortunately, ATSR-2's scan mechanism has suffered problems with minor rotation speed variations or "jitter", which can affect the products. Extensive effort has gone into AATSR to reduce the possibilities of similar problems to those experienced at times with ATSR-2.

To minimise the pointing errors introduced by non-constant scan mechanism rotation, AATSR is specified such that the scan mechanism shall rotate at a sufficiently uniform angular velocity that its maximum positional error in angle of rotation, from that implied by assuming a uniform rate, shall be less than 5 arc minutes at any position around the scan, when measured in air. This performance in air is expected to be equivalent to an error of 1 arc min (i.e. 0.09 sample distance) (1 sigma RMS) in vacuum. Test results have shown that the worst case normal mode error budget is ±2.4 arc minutes.

The AATSR scan mechanism had backup systems introduced after the problems experienced in-flight with ATSR-2. The pointing performance of the backup Phase Locked Loop mode is not as good as that of the main system, with the worst case backup mode error budget being ±4.8 arc minutes.

The stability of the sample spacing around the scan could also be affected by mechanical disturbances from AATSR mechanisms (other than the scan mechanism) and any satellite mechanisms. Thus, AATSR is specified such that mechanisms shall affect the pointing of the scan vector by less than 0.1 sample distance.

3.2.1.4 Radiometric

3.2.1.4.1 Specifications

From the scientific requirements for SST and land surface mapping, the dynamic range and noise performance required for the AATSR channels have been derived and are shown in table 3.4 .

Table 3.4 Dynamic Range and Noise Performance for a Single Calibrated AATSR Sample

Channel/µm	Nominal Working Range	NEΔT at 270K/K	S/N at 0.5% Albedo
0.55	0 - 50 mW cm^{-2} µm^{-1} sr^{-1}	N/A	20:1
0.66	0 - 45 mW cm^{-2} µm^{-1} sr^{-1}	N/A	20:1
0.87	0 - 30 mW cm^{-2} µm^{-1} sr^{-1}	N/A	20:1
1.6	0 - 7 mW cm^{-2} µm^{-1} sr^{-1}	N/A	20:1
3.7	0 - 311 K	0.08	N/A
11	200 - 321 K *	0.05	N/A
12	200 - 318 K *	0.05	N/A

* - Extended range or low gain mode (previously known as forest fire mode on ATSR-2) can extend these to higher values (see section of the User Guide), although it is not part of baseline planning to use this mode.

AATSR has 12 bit digitisation, with the full range downlinked for all channels all of the time.

So that AATSR can extract the maximum performance from each channel's detector/preamplifier combination, the instrument includes a system to automatically optimise the signal channel offsets for all channels, with the gain of the thermal channels also automatically optimised. Visible channel gains are commanded manually. The gain and offset for all channels is set up using the onboard calibration systems.

Responsivity can be affected by the polarisation of the radiance, and AATSR was specified so that the difference in response between any two orthogonal polarisations was to be not more than 4% for the thermal channels and 6% for the reflection channels. In addition, for all channels, the response variation with plane of polarisation was specified to be known to better than 0.5%. Unfortunately, the specification was not met, and the actual performance is described below.

3.2.1.4.2 Measurements

3.2.1.4.2.1 Polarisation

Polarisation measurements were made at FPA level and instrument level. Concerning the FPA level measurements, some non-compliances with the polarisation specification were found and the results are summarised in table 3.5 .

Table 3.5 FPA-level Measurements of Variation in Response with Polarisation

Channel/μm	Variation in Response with Polarisation
0.55	1-2%
0.66	14-15%
0.87	3.5-4.5%
1.6	33-35%
3.7	3-5%
11	3.5-7%
12	0-6%

Ref. [1.10] Polarisation measurements were also performed at instrument level for the visible and 1.6 μm channels (see RAL's Visible Calibration Report) and the results are summarised in table 3.6 .

Table 3.6 Instrument-level Measurements of Variation in Response with Polarisation

Channel/µm	Variation in Response with Polarisation
0.55	2%
0.66	15%
0.87	10%
1.6	40%

The magnitude of the polarisation variation is in good agreement with the FPA-level measurements, with the main difference being that the 0.87 µm channel appears to be slightly more sensitive.

3.2.1.4.2.2 Instrument-level visible channel results

The objectives of the Visible Calibration were:

- Measure the normalised detector response as a function of input intensity over the expected operational range to better than 5%.
- Determine and measure any scan dependent effects by measuring the response at all points around the nadir and along track views and VISCAL opal.
- Characterise the variation of the normalised radiometric response due to polarisation to better than 0.5% (the results are discussed above).
- Measure the radiometric noise.

The test results are discussed below (details are provided in RAL's Visible Calibration Report Ref. [1.10]).

The tests showed that the 0.87 µm, 0.66 µm and 0.55 µm channel responses were linear with input radiance, whereas the 1.6 µm channel was found to have a significantly non-linear response (13.4% for radiances corresponding to full albedo). The non-linearity of the 1.6 µm channel has been quantified and a calibration algorithm derived for use within the Level 1B processing (see section). The radiometric responses of the other VNIR channels are assumed to be linear in the data processing. Measurements of the radiometric responses with the FPA evacuated and with the IRFPA at ambient temperatures have been selected for use in the data processing as representing the conditions seen at the start of the mission. The errors in the radiometric response measurements are summarised in table 3.7 .

Table 3.7 Errors in Radiometric Response Results

Channel/µm	Error in Radiometric Response Measurements
0.55	3.9%
0.66	3.4%
0.87	3.6%
1.6	9.0%

The measured signal-to-noise ratios are summarised in table 3.8 .

Table 3.8 Signal-to-Noise Ratio Results

Channel/μm	S/N Ratio at 0.5% albedo
0.55	25:1
0.66	28:1
0.87	25:1
1.6	31:1

Variations in the radiometric calibration around the scan were <1%, although it is likely that the observed variations were caused by inaccuracy in positioning the source.

The reflectance factor of the VISCAL was measured for all channels and was found to be in good agreement with prediction. An interesting result was the 10% variation of signal across the VISCAL in the 1.6μm channel, which was very similar to in-flight data from ATSR-2. This does not arise from features of the VISCAL, but is caused by non-uniform response across the main aperture, and will not affect the in-flight calibration of the channel. The predictions and measurements are summarised in table 3.9 .

Table 3.9 Measured VISCAL Reflectance Factors compared with the expected values calculated from the geometry and optical properties

Channel/μm	VISCAL Reflectance Factor	
	Measured	Expected
0.55	0.163±0.004	0.165±0.003
0.66	0.163±0.005	0.163±0.003
0.87	0.154±0.003	0.156±0.004
1.6	0.191±0.006	0.192±0.005

In conclusion, the measurements showed that the visible channels meet the performance requirements.

3.2.1.4.2.3 Instrument-level infra-red results

The principles behind the calibration of the thermal infrared channels are the same as those for the calibration tests performed on ATSR-1 and 2. These are to:

- Verify the 'on-board' radiometric calibration for a range of target temperatures between 210K and 310K.
- Measure any detector non-linearities and make appropriate corrections.
- Verify that the different channels produce self consistent results.
- Measure the radiometric noise.
- Measure the effect on the radiometric calibration with the detectors operating at an

increased temperature.
- Verify the calibration with the on-board black bodies set at different power levels.
- Investigate the radiometric performance under different thermal conditions.
- Determine and measure any scan dependent variation in the radiometric performance.
- Determine and measure radiometric leaks.
- Verify the calibration under simulated orbital transient thermal conditions.

The test results are discussed below (details are provided in RAL's Infra-red Radiometric Calibration Report Ref. [1.5]).

The calibration of the 3.7µm, 11µm and 12µm channels was verified against precision black body targets having an accuracy of ±0.037K. The thermometer, resistance and emissivity calibrations of these targets can be traced to international standards. In particular, the rhodium-iron resistance thermometers have been calibrated to the International Temperature Scale of 1990 (ITS90).

The main radiometric calibration was performed with the instrument operating under Beginning-of-Life thermal balance conditions, for target temperatures between 210K and 315K. The initial results showed that the detectors had non-linear responses similar to those observed on ATSR-2. These data were used to derive non-linearity corrections for the Level 1B processing (see section).

Measurements taken with the external black bodies matched to the on-board target temperatures revealed an emissivity error at 3.7 µm. It was concluded that the true emissivities of the on-board black bodies were best represented by calculated values based on reflectance measurements of witness samples.

After applying the corrections, the brightness temperatures at 270K were within 30 mK of the target temperatures measured by the RIRTs. These results and the NEΔT measurements are summarised in table.
T for a target temperature of 270K with the FPA at 80K" rel="eph_tab">

Channel/µm	T_{AATSR}-T_{RIRT} / K	NEΔT / K (FPA at 80K)
3.7	-0.014	0.037
11	-0.030	0.025
12	-0.020	0.025

The calibration was also performed at all points around the nadir and along-track swaths (see figure 1.3 in the User Guide for the swath pattern), under different thermal environments and different on-board black-body power settings. The results showed that there were no significant scan dependent effects or radiometric leaks.

Although the orbital simulations did not return data under the planned conditions, the full sequence of orbits was carried out and the results show that the calibration was not affected by the transient thermal environment of the tests.

In conclusion, the measurements showed that the 3.7 µm, 11 µm and 12 µm channels meet the performance requirements.

3.2.1.5 Stability

AATSR's responses need to be stable on a number of timescales, from around the scan right up to the mission duration.

To minimise the possibilities of stray signals reaching the detectors around the scan, view baffles are necessary to keep out all direct sunlight during normal instrument operation. Similarly, the instrument enclosure must also be light-tight (other than for necessary apertures) and internally must be generally of low reflectivity to minimise the possibility of stray signals reaching the detectors at any point around the scan. The scan mirror is also sufficiently specular so that no significant signals from outside the telescope beam are passed back to the detectors. The mirror's scattering caused by surface roughness is less than 0.05% for the shortest wavelength AATSR channel. Verification that AATSR's measurements did not vary around the scan took place during radiometric calibration 3.2.1.4.2. , with no problems being observed.

The response of the thermal channels
has to be stable over the period between forward and nadir views of the Earth's surface, so as not to introduce large errors into forward/nadir differencing algorithms. Items of the instrument which are "visible" to the detectors must remain stable in temperature over the time period between forward and nadir views. Each of the items was assigned an error budget of 0.02K over the two minutes between views, assuming that the 12µm channel is viewing a 265K scene and the instrument is at 264K. From the ATSR-1/2 design, this corresponded to stability requirements on the paraboloid mirror aperture stop of 0.2K/120s and on the focal plane assembly baffle of 0.8K/120s. Modelling, correlated with test results, has shown that the temperature stability requirements should all be comfortably met.

The onboard calibration sources are also designed to be stable
. Uncertainties in the black body calibration source radiance must not exceed the equivalent of 100mK temperature error so that the overall SST accuracy requirements to be met. The SST retrieval algorithms also require that the radiances of the BBCs are stable over the period between nadir and forward views (approximately two minutes). Therefore, the BBCs are designed so that their temperatures are stable to better than 0.03K over a two minute period and have been shown to meet this requirement.

For land reflectance measurements, the stability of the reflection channel gains has to be to 0.1% over the time between forward and nadir views and 1% around the orbit.

AATSR is also designed so that the linearity of the electronics for each signal channel is not expected to change by >0.5LSB between pre-launch beginning of life (BOL) non-linearity assessment and end of life (EOL) flight performance.

3.2.2 In-flight performance verification

3.2.2.1 Commissioning

AATSR undergoes commissioning shortly after launch which brings the instrument through to nominal operations. As part of this, a number of performance checks are carried out and the instrument operation is optimised. AATSR commissioning includes initial verification of the operation of the instrument and an optimisation phase. Details of commissioning are contained in the AATSR Commissioning Plan Ref. [1.1], but, in summary, the following major optimisation steps are performed after initial verification of AATSR's operation:

- Optimisation of the coolers' operating configuration;
- Checkout of the scan mechanism, in particular, assessment of 'jitter';
- A Black Body cross-over test, during which the radiometric signals from each blackbody when they are at the same temperature are compared to make an estimate of the relative accuracy. Any significant difference in signal would imply a drift in the temperature sensors' calibration or change in emissivity.
- Checks of thermal stability of important items;
- The pixel map will be optimised and the instrument's optical alignment will be verified by checking the positions of the edges of clear views of the earth views and calibration targets;
- The gains and offsets for the visible and 1.6 μm channels will be optimised to ensure that the dynamic range fully covers the darkest and brightest likely scene types;
- The operation of the auto gain-offset loop will be optimised;
- The performance of AATSR's low gain mode will be tested;
- The source packets will be checked for anomalies (this will identify problems in the instrument or the ground processing transcription);
- After optimisation of the main subsystems, science data will be analysed to assess the performance of the signal channels. Checks will be made on the radiometric noise, dynamic range, digitisation 3.2.1.4. and stability 3.2.1.5. to verify that the performance is acceptable;
- The initial performance of the VISCAL unit will be assessed by analysing science data to check that the signal from the unit at full solar illumination agrees with expected levels, the diffuser is uniformly illuminated and the signal is stable.
- Science data will be examined to investigate any evidence of stray light contamination in-flight;
- The receipt of blanking pulses and any effect on AATSR data from the RA-2 and the Advanced Synthetic Aperture radar (ASAR) instruments will be tested.

Further testing may be required during the remainder of the commissioning phase dependent upon the results of the above activities.

3.2.2.2 Routine Verification

The performance of the instrument will continue to be assessed during routine operations throughout the duration of the mission. Routine monitoring will include assessment of daily and long term housekeeping trend plots, monitoring the scan mechanism, Black Body, VISCAL, signal channel (radiometric noise, dynamic range and digitisation 3.2.1.4.) and cooler performance, Level 0 2.5.4.1. data quality checks and production of regular reports on instrument health (Information on the instrument status and performance will be made available to users on the AATSR Engineering Data System web site, accessible from the AATSR Operations website) .

More details of verification are contained in the AATSR Verification Plan Ref. [1.9].

The specific topic of outgassing is discussed in more detail below, as this affects data availability.

3.2.2.2.1 Outgassing

Some water and other materials are inevitably carried into space with the satellite, so when the IRFPA is cooled there will be a build up of condensation affecting the cooler performance and the optical throughput. It will be necessary to warm the IRFPA periodically to allow the condensate to evaporate and thus allow the instrument performance to recover.

From experience of ATSR-1 and ATSR-2, the frequency of outgassing is likely to be:

- 2-3 weeks after the initial cool down;
- 3 months after, depending on condensation rates;
- 6 months thereafter.

In practice, most out-gassings on ATSR-1 and ATSR-2 occurred opportunistically when the instrument was forced into standby mode (and hence for the IRFPA to warm up) due to a platform or payload anomaly, and therefore it has only been necessary to perform a few scheduled outgassings.

During a scheduled outgassing, the instrument will still be operating, but with the IRFPA above its nominal working temperature, and although no useful data will be available from the IRFPA channels (i.e. the 1.6 μm, 3.7 μm, 11 μm and 12 μm), data will be available from the visible channels (i.e. the 0.55 μm, 0.66 μm and 0.87 μm channels). However, there is a caveat over the calibration of the VFPA channels which applied to the products during outgassings and this is discussed in of the User Guide.

Chapter 4

Frequently Asked Questions

The AATSR Frequently Asked Questions document can be downloaded HERE

Chapter 5

Glossary

5.1 Acronyms and Abbreviations

Table 5.1

AATSR	Advanced Along Track Scanning Radiometer
(A)ATSR	The ATSR and AATSR family of instruments
ADS	Annotation Data Set
AGO	Auto Gain/Offset
AISP	Annotated Instrument Source Packet
AO	Announcement of Opportunity
AOIP	Announcement of Opportunity Instrument Provider
AOCS	Attitude and Orbit Control System

AST	Averaged Surface Temperature
ATSR	Along Track Scanning Radiometer
ATSR-1	Along Track Scanning Radiometer - 1
ATSR-2	Along Track Scanning Radiometer - 2
AVHRR	Advanced Very High Resolution Radiometer
BBC	Black Body Cavity
BBU	Black Body electronics Unit
BOL	Beginning of Life
BPU	Blanking Pulse Unit
BT	Brightness Temperature
CATSA	Calibration And Thermal Simulation Assembly
CCU	Cooler Control Unit
CGU	Clock Generator Unit
CMT	Cadmium Mercury Telluride
COTS	Commercial Off the Shelf (tools)
CRC	Cyclic Redundancy Check
CTB	Command and Telemetry Bus
CTH	Cloud Top Height
CTP	Cryogenic Temperature Sensor Processing
CTT	Cloud Top Temperature
DBU	Digital Bus Unit
DEFRA	Department for Environment, Food and Rural Affairs
DEM	Digital Elevation Model
DSD	Data Set Descriptor
DEU	Digital Electronics Unit
ECMWF	European Centre for Medium range Weather Forecasting
EMI	Electromagnetic Interference
ENVI	Environment for Visualising Images
ENVISAT	Environmental Satellite
EOL	End Of Life
ERS-1	European Remote Sensing Satellite - 1
ERS-2	European Remote Sensing Satellite - 2
ESA	European Space Agency
FEP	Front End Processor
FOS	Flight Operations Segment (ENVISAT) or Flight Operations Support (AATSR)
FPA	Focal Plane Assembly
FWHM	Full Width Half Maximum
GADS	Global Annotation Data Set
GBTR	Gridded Brightness Temperature/Reflectance
GST	Gridded Surface Temperature
HDF	Hierarchical Data Format
HSM	High Speed Multiplexer
HSU	Heater Switching Unit
ICU	Instrument Control Unit
IDL	Interactive Data Language
IEU	Instrument Electronics Unit
IFOV	Instantaneous Field Of View
IOM	Instrument Operations Manual
IPF	Instrument Processor Facility
IRFPA	Infrared Focal Plane Assembly
ISP	Instrument Source Packet
IVR	Infrared Visible Radiometer
JFET	Junction Field Effect Transistor
K	kelvin
L0	Level 0
L1B	Level 1B
L2	Level 2
LRAC	Low Rate Reference Archive Centre
LSB	Least Significant Bit
LSM	Land-Sea mask
LST	Land Surface Temperature
LUT	Look Up Table
MDS	Measurement Data Set
MJD	Modified Julian Date
MLI	Multi Layer Insulation
MPH	Main Product Header
MSS	Multi-Spectral Scanner
MXBB	-X Black Body
NDVI	Normalised Difference Vegetation Index
NIR	Near Infrared
NOAA	National Oceanic and Atmospheric Administration
NRT	Near Real Time
OBDH	On Board Data Handling System
OBT	On Board Time
OSV	Orbit State Vector

PAC	Processing and Archiving Centre
PCSU	Power Conditioning and Switching Unit
PDHS	Payload Data Handling Stations
PDS	Payload Data Segment
PEB	Payload Equipment Bay
PFHS	Processing Facility Host Structure
PL-PDU	Payload Power Distribution Unit
PMA	Paraboloid Mirror Assembly
PP	Prototype Processor
PRT	Platinum Resistance Thermometer
PSF	Point Spread Function
PXBB	+X Black Body
RA	Radar Altimeter
RAL	Rutherford Appleton Laboratory
RIRT	Rhodium Iron Resistance Thermometer
RT	Radiative Transfer
SADIST	Synthesis of ATSR Data Into Sea-surface Temperature
SBT	Satellite Binary Time
SCC	Stirling Cycle Cooler
SCP	Signal Channel Processor
SM	Service Module or Scan Mirror
SMD	Scan Mirror Drive
SMU	Scan Mirror Unit
SODAP	Switch-On and Data Acquisition Phase
SOT	Select on Test
SPA	Signal Preamplifier Assembly
SPH	Specific Product Header
SST	Sea Surface Temperature
TCS	Thermal Control Subsystem
TDS	Test Data Set
TIR	Thermal Infrared
TM	Thematic Mapper or Telemetry
TOA	Top Of Atmosphere
TSAD	Temperature Sensor A/D converter
TSM	Temperature Sensor Multiplexer
TVCI	Temperature sensor and Viscal monitor CTB Interface
UK-PAC	United Kingdom Processing and Archiving Centre
USF	User Service Facility
UTC	Universal Time Coordinated
VCDU	Virtual Channel Data Unit
VFPA	Visible Focal Plane Assembly
VisCal	Visible Calibration system
VNIR	Visible and Near InfraRed

5.2 Glossary

The Instantaneous Field of View (IFOV) is defined as the solid angle over which an optical system is sensitive to incoming radiation at an instant in time. The IFOV, in the AATSR Instrument Performance Requirements, is taken to be defined by an optical field stop. Optical effects such as diffraction and defocusing are excluded from this definition of the IFOV.

Note: Certain specific terms relating to the AATSR data processing algorithms are also defined in Section 2.3. Definitions and Conventions

Chapter 6

AATSR Data Formats Products

6.1 Level 2 Products

Table 6.1

6.1.1 ATS_AR__2P: AATSR averaged geophysical product

Table 6.2

ATS_AR__2P

AATSR averaged geophysical product

File Structure

Data Sets 18

MPH 6.6.1.	Envisat MPH
SPH 6.6.10.	Level 2 SPH
SEA_ST_50_KM_CELL_MDS 6.6.8.	SST record 30 arc minute cell MDS
SEA_ST_17_KM_CELL_MDS 6.6.9.	SST record 10 arc minute cell MDS
LAND_ST_50_KM_CELL_MDS 6.6.4.	LST record 30 arc minute cell MDS
LAND_ST_17_KM_CELL_MDS 6.6.5.	LST record 10 arc minute cell MDS
BT_TOA_LAND_50_KM_CELL_MDS 6.6.2.	BT/TOA Land record 30 arc minute cell MDS
BT_TOA_LAND_17_KM_CELL_MDS 6.6.3.	BT/TOA Land record 10 arc minute cell MDS
BT_TOA_SEA_50_KM_CELL_MDS 6.6.6.	BT/TOA Sea record 30 arc minute cell MDS
BT_TOA_SEA_17_KM_CELL_MDS 6.6.7.	BT/TOA Sea record 10 arc minute cell MDS
SEA_ST_10_MIN_CELL_MDS 6.6.9.	SST record 10 arc minute cell MDS
SEA_ST_30_MIN_CELL_MDS 6.6.8.	SST record 30 arc minute cell MDS
LAND_ST_10_MIN_CELL_MDS 6.6.5.	LST record 10 arc minute cell MDS
LAND_ST_30_MIN_CELL_MDS 6.6.4.	LST record 30 arc minute cell MDS
BT_TOA_LAND_10_MIN_CELL_MDS 6.6.3.	BT/TOA Land record 10 arc minute cell MDS
BT_TOA_LAND_30_MIN_CELL_MDS 6.6.2.	BT/TOA Land record 30 arc minute cell MDS
BT_TOA_SEA_10_MIN_CELL_MDS 6.6.7.	BT/TOA Sea record 10 arc minute cell MDS
BT_TOA_SEA_30_MIN_CELL_MDS 6.6.6.	BT/TOA Sea record 30 arc minute cell MDS

Format Version 114.0

6.1.2 ATS_MET_2P: AATSR Spatially Averaged Sea Surface Temperature for Meteo Users

Table 6.3

ATS_MET_2P

AATSR Spatially Averaged Sea Surface Temperature for Meteo Users

File Structure

Data Sets 3

MPH 6.6.1.	Envisat MPH
SPH 6.6.36.	SPH
SEA_ST_10_MIN_CELL_MDS 6.6.35.	10-arcminute mds

Format Version 114.0

6.1.3 ATS_NR__2P: AATSR geophysical product (full resolution)

Table 6.4

ATS_NR__2P

AATSR geophysical product (full resolution)

File Structure

Data Sets 10

MPH 6.6.1.	Envisat MPH
SPH 6.6.38.	Level 2 SPH
GEOLOCATION_ADS 6.6.43.	Grid pixel latitude and longtitude, topographic corrections ADS
SCAN_PIXEL_X_AND_Y_ADS 6.6.44.	Scan pixel x and y ADS
DISTRIB_SST_CLOUD_LAND_MDS 6.6.39.	Distributed product MDS
SUMMARY_QUALITY_ADS 6.6.37.	Summary Quality ADS
NADIR_VIEW_SOLAR_ANGLES_ADS 6.6.64.	Forward view solar angles ADS
FWARD_VIEW_SOLAR_ANGLES_ADS 6.6.64.	Forward view solar angles ADS
NADIR_VIEW_SCAN_PIX_NUM_ADS 6.6.62.	Scan and pixel number forward view ADS
FWARD_VIEW_SCAN_PIX_NUM_ADS 6.6.62.	Scan and pixel number forward view ADS

Format Version 114.0

6.2 Level 1 Products

Table 6.5

6.2.1 ATS_TOA_1P: AATSR Gridded brightness temperature and reflectance

Table 6.6

ATS_TOA_1P

AATSR Gridded brightness temperature and reflectance

File Structure

Data Sets 28

MPH 6.6.1.	Envisat MPH
SPH 6.6.50.	Level 1B SPH
SUMMARY_QUALITY_ADS 6.6.45.	Summary Quality ADS
GEOLOCATION_ADS 6.6.43.	Grid pixel latitude and longtitude, topographic corrections ADS
SCAN_PIXEL_X_AND_Y_ADS 6.6.44.	Scan pixel x and y ADS
NADIR_VIEW_SOLAR_ANGLES_ADS 6.6.64.	Forward view solar angles ADS
FWARD_VIEW_SOLAR_ANGLES_ADS 6.6.64.	Forward view solar angles ADS
VISIBLE_CALIB_COEFS_GADS 6.6.51.	Visible channel calibration parameters GADS
NADIR_VIEW_SCAN_PIX_NUM_ADS 6.6.62.	Scan and pixel number forward view ADS
FWARD_VIEW_SCAN_PIX_NUM_ADS 6.6.62.	Scan and pixel number forward view ADS
11500_12500_NM_NADIR_TOA_MDS 6.6.47.	3.7 micron nadir view MDS
10400_11300_NM_NADIR_TOA_MDS 6.6.47.	3.7 micron nadir view MDS
03505_03895_NM_NADIR_TOA_MDS 6.6.47.	3.7 micron nadir view MDS
01580_01640_NM_NADIR_TOA_MDS 6.6.49.	0.55 micron nadir view MDS
00855_00875_NM_NADIR_TOA_MDS 6.6.49.	0.55 micron nadir view MDS
00649_00669_NM_NADIR_TOA_MDS 6.6.49.	0.55 micron nadir view MDS
00545_00565_NM_NADIR_TOA_MDS 6.6.49.	0.55 micron nadir view MDS

11500_12500_NM_FWARD_TOA_MDS 6.6.46.	3.7 micron forward view MDS
10400_11300_NM_FWARD_TOA_MDS 6.6.46.	3.7 micron forward view MDS
03505_03895_NM_FWARD_TOA_MDS 6.6.46.	3.7 micron forward view MDS
01580_01640_NM_FWARD_TOA_MDS 6.6.48.	0.55 micron forward view MDS
00855_00875_NM_FWARD_TOA_MDS 6.6.48.	0.55 micron forward view MDS
00649_00669_NM_FWARD_TOA_MDS 6.6.48.	0.55 micron forward view MDS
00545_00565_NM_FWARD_TOA_MDS 6.6.48.	0.55 micron forward view MDS
NADIR_VIEW_CONFIDENCE_MDS 6.6.65.	Confidence words forward view MDS
FWARD_VIEW_CONFIDENCE_MDS 6.6.65.	Confidence words forward view MDS
NADIR_VIEW_CLOUD_MDS 6.6.63.	Cloud flag forward view MDS
FWARD_VIEW_CLOUD_MDS 6.6.63.	Cloud flag forward view MDS

Format Version 114.0

6.3 Browse Products

Table 6.7

6.3.1 ATS_AST_BP: AATSR browse image

Table 6.8

ATS_AST_BP

AATSR browse image

File Structure

Data Sets 5

MPH 6.6.1.	Envisat MPH
SPH 6.6.13.	Browse SPH
SUMMARY_QUALITY_ADS 6.6.45.	Summary Quality ADS
GEOLOCATION_ADS 6.6.11.	Grid pixel latitude and longtitude,topographic correction ADS

BROWSE_MDS 6.6.12.	Browse MDS

Format Version 114.0

6.4 Level 0 Products

Table 6.9

6.4.1 ATS_NL__0P: AATSR Level 0 product

Table 6.10

ATS_NL__0P

AATSR Level 0 product

File Structure

Data Sets 3

MPH 6.6.1.	Envisat MPH
SPH 6.6.54.	Level 0 SPH
AATSR_SOURCE_PACKETS 6.6.53.	Level 0 MDSR

Format Version 114.0

6.5 Auxilliary Products

Table 6.11

6.5.1 ATS_BRW_AX: Browse Product LUT data

Table 6.12

ATS_BRW_AX

Browse Product LUT data

File Structure

Data Sets 3

MPH 6.6.1.	Envisat MPH
SPH 6.6.52.	Auxiliary Data SPH with N=1 DSD:DSD (G)
Browse Day Colour LUT GADS 6.6.14.	Browse Day_Time Colour LUT GADS

Format Version 114.0

6.5.2 ATS_CH1_AX: Level-1B Characterization data

Table 6.13

ATS_CH1_AX

Level-1B Characterization data

File Structure

Data Sets 3

MPH 6.6.1.	Envisat MPH
SPH 6.6.52.	Auxiliary Data SPH with N=1 DSD:DSD (G)
Characterisation Table 6.6.15.	Characterisation GADS

Format Version 114.0

6.5.3 ATS_CL1_AX: Cloud LUT data

Table 6.14

ATS_CL1_AX

Cloud LUT data

File Structure

Data Sets 11

MPH 6.6.1.	Envisat MPH
SPH 6.6.52.	Auxiliary Data SPH with N=1 DSD:DSD (G)
1.6 micron histogram LUT 6.6.19.	1.6 Micron Histogram Test LUT GADS
11 micron spatial coh LUT 6.6.18.	11 Micron Spatial Coherence Test LUT GADS
12 micron gross cloud LUT 6.6.21.	12 Micron Gross Cloud Test LUT GADS
thin cirrus cloud LUT 6.6.24.	Thin Cirrus Test LUT GADS
med/high level cloud LUT 6.6.23.	Medium/High Level Test LUT GADS
fog/low stratus 6.6.22.	Fog/low Stratus Test LUT GADS

11/12 micron ndr/frwrd LUT 6.6.16.	11/12 Micron Nadir/Forward Test LUT GADS
11/37 micron ndr/frwrd LUT 6.6.17.	11/3.7 Micron Nadir/Forward Test LUT GADS
infra-red histogram LUT 6.6.20.	Infrared Histogram Test LUT GADS

Format Version 114.0

6.5.4 ATS_GC1_AX: General Calibration data

Table 6.15

ATS_GC1_AX

General Calibration data

File Structure

Data Sets 6

MPH 6.6.1.	Envisat MPH
SPH 6.6.52.	Auxiliary Data SPH with N=1 DSD:DSD (G)
General parameters for IR 6.6.25.	General Parameters GADS
Temperature to radiance LUT 6.6.28.	Temperature to Radiance LUT GADS
Radiance to temperature LUT 6.6.27.	Radiance to Brightness Temperature LUT GADS
1.6 micron LUT 6.6.26.	1.6 micron Non-Linearity Correction LUT GADS

Format Version 114.0

6.5.5 ATS_INS_AX: AATSR Instrument data

Table 6.16

ATS_INS_AX

AATSR Instrument data

File Structure

Data Sets 8

MPH 6.6.1.	Envisat MPH
SPH 6.6.52.	Auxiliary Data SPH with N=1 DSD:DSD (G)
General parameters 6.6.29.	General Parameters GADS
Master unpacking table 6.6.33.	Master Unpacking Definition Table GADS
Conversion parameters 6.6.31.	Conversion Parameters GADS
Validation limit checks 6.6.32.	Limits GADS
Surveillance limit checks 6.6.34.	Surveillance Limits GADS
Specialised limit checks 6.6.30.	Validation Parameters GADS

Format Version 114.0

6.5.6 ATS_PC1_AX: Level-1B Processing configuration data

Table 6.17

ATS_PC1_AX

Level-1B Processing configuration data

File Structure

Data Sets 3

MPH 6.6.1.	Envisat MPH
SPH 6.6.52.	Auxiliary Data SPH with N=1 DSD:DSD (G)
Processor config data 6.6.40.	Processor configuration GADS

Format Version 114.0

6.5.7 ATS_PC2_AX: Level-2 Processor Configuration data

Table 6.18

ATS_PC2_AX

Level-2 Processor Configuration data

File Structure

Data Sets 3

MPH 6.6.1.	Envisat MPH
SPH 6.6.52.	Auxiliary Data SPH with N=1 DSD:DSD (G)
PROCESSOR_CONFIG 6.6.41.	Configuration Data GADS

Format Version 114.0

6.5.8 ATS_SST_AX: SST Retrieval Coeficients data

Table 6.19

ATS_SST_AX

SST Retrieval Coeficients data

File Structure

Data Sets 5

MPH 6.6.1.	Envisat MPH
SPH 6.6.52.	Auxiliary Data SPH with N=1 DSD:DSD (G)

BAND_LUT 6.6.42.	Across-track Band Mapping Look-up Table
GRIDDED_LUT 6.6.61.	Average SST Retrieval Coefficients GADS
AVERAGE_LUT 6.6.61.	Average SST Retrieval Coefficients GADS

Format Version 114.0

6.5.9 ATS_VC1_AX: Visible Calibration data

Table 6.20

ATS_VC1_AX

Visible Calibration data

File Structure

Data Sets 3

MPH 6.6.1.	Envisat MPH
SPH 6.6.52.	Auxiliary Data SPH with N=1 DSD:DSD (G)
Visible Calibration Data 6.6.51.	Visible channel calibration parameters GADS

Format Version 114.0

6.6 Records

6.6.1 Main Product Header

Table 6.21 Main Product Header

Envisat MPH

#	Description	Units	Count	Type	Size
Data Record					
0	product_name_title PRODUCT=	keyword	1	AsciiString	8 byte(s)
1	quote_1 quotation mark (""")	ascii	1	AsciiString	1 byte(s)
2	product Product File name	ascii	1	AsciiString	62 byte(s)
3	quote_2 quotation mark (""")	ascii	1	AsciiString	1 byte(s)
4	newline_char_1 newline character	terminator	1	AsciiString	1 byte(s)
5	processing_stage_title PROC_STAGE=	keyword	1	AsciiString	11 byte(s)
6	proc_stage Processing Stage FlagN = Near Real Time, T = test product, V= fully validated (fully consolidated) product, S = special product. Letters between N and V (with the exception of T and S) indicate steps in the consolidation process, with letters closer to V	ascii	1	AsciiString	1 byte(s)
7	newline_char_2 newline character	terminator	1	AsciiString	1 byte(s)
8	reference_doc_title REF_DOC=	keyword	1	AsciiString	8 byte(s)
9	quote_3 quotation mark (""")	ascii	1	AsciiString	1 byte(s)
10	ref_doc Reference Document Describing Product AA-BB-CCC-DD-EEEE_V/I?? (23 characters, including blank space characters) where AA-BB-CCC-DD-EEEE is the ESA standard document no. and V/I is the Version / Issue. If the reference document is the Products Specifications PO-RS-MDA-GS-2009, the version and revision have to refer to the volume 1 of the document, where the status (version/revision) of all volumes can be found. If not used, set to ??????????????????????	ascii	1	AsciiString	23 byte(s)
11	quote_4 quotation mark (""")	ascii	1	AsciiString	1 byte(s)
12	newline_char_3 newline character	terminator	1	AsciiString	1 byte(s)
13	spare_1 Spare	-	1	SpareField	41 byte(s)
14	acquisition_station_id_title ACQUISITION_STATION=	keyword	1	AsciiString	20 byte(s)
15	quote_5 quotation mark (""")	ascii	1	AsciiString	1 byte(s)
16	acquisition_station Acquisition Station ID (up to 3 codes) If not used, set to ??????????????????	ascii	1	AsciiString	20 byte(s)
17	quote_6 quotation mark (""")	ascii	1	AsciiString	1 byte(s)
18	newline_char_5 newline character	terminator	1	AsciiString	1 byte(s)
19	processing_center_title PROC_CENTER=	keyword	1	AsciiString	12 byte(s)
20	quote_7 quotation mark (""")	ascii	1	AsciiString	1 byte(s)
21	proc_center Processing Center ID which generated current product If not used, set to ??????	ascii	1	AsciiString	6 byte(s)
22	quote_8	ascii	1	AsciiString	1 byte(s)

#	Description	Units	Count	Type	Size
	quotation mark (""")				
23	newline_char_6 newline character	terminator	1	AsciiString	1 byte(s)
24	processing_time_title PROC_TIME=	keyword	1	AsciiString	10 byte(s)
25	quote_9 quotation mark (""")	ascii	1	AsciiString	1 byte(s)
26	proc_time UTC Time of Processing (product generation time)UTC Time format. If not used, set to ??????????????????????????????.	UTC	1	UtcExternal	27 byte(s)
27	quote_10 quotation mark (""")	ascii	1	AsciiString	1 byte(s)
28	newline_char_7 newline character	terminator	1	AsciiString	1 byte(s)
29	software_version_title SOFTWARE_VER=	keyword	1	AsciiString	13 byte(s)
30	quote_11 quotation mark (""")	ascii	1	AsciiString	1 byte(s)
31	software_ver Software Version number of processing softwareFormat: Name of processor (up to 10 characters)/ version number (4 characters) -- left justified (any blanks added at end). If not used, set to ??????????????.e.g. MIPAS/2.31????	ascii	1	AsciiString	14 byte(s)
32	quote_12 quotation mark (""")	ascii	1	AsciiString	1 byte(s)
33	newline_char_8 newline character	terminator	1	AsciiString	1 byte(s)
34	spare_2 Spare	-	1	SpareField	41 byte(s)
35	sensing_start_title SENSING_START=	keyword	1	AsciiString	14 byte(s)
36	quote_13 quotation mark (""")	ascii	1	AsciiString	1 byte(s)
37	sensing_start UTC start time of data sensing (first measurement in first data record) UTC Time format. If not used, set to ??????????????????????????????.	UTC	1	UtcExternal	27 byte(s)
38	quote_14 quotation mark (""")	ascii	1	AsciiString	1 byte(s)
39	newline_char_10 newline character	terminator	1	AsciiString	1 byte(s)
40	sensing_stop_title SENSING_STOP=	keyword	1	AsciiString	13 byte(s)
41	quote_15 quotation mark (""")	ascii	1	AsciiString	1 byte(s)
42	sensing_stop UTC stop time of data sensing (last measurements last data record) UTC Time format. If not used, set to ??????????????????????????????.	UTC	1	UtcExternal	27 byte(s)
43	quote_16 quotation mark (""")	ascii	1	AsciiString	1 byte(s)
44	newline_char_11 newline character	terminator	1	AsciiString	1 byte(s)
45	spare_3 Spare	-	1	SpareField	41 byte(s)
46	phase_title PHASE=	keyword	1	AsciiString	6 byte(s)
47	phase Phasephase letter. If not used, set to X.	ascii	1	AsciiString	1 byte(s)
48	newline_char_13 newline character	terminator	1	AsciiString	1 byte(s)
49	cycle_title CYCLE=	keyword	1	AsciiString	6 byte(s)
50	cycle CycleCycle number. If not used, set to +000.	-	1	AsciiIntegerAuc	4 byte(s)
51	newline_char_14 newline character	terminator	1	AsciiString	1 byte(s)
52	relative_orbit_title REL_ORBIT=	keyword	1	AsciiString	10 byte(s)
53	rel_orbit Start relative orbit number If not used, set to +00000	-	1	As	6 byte(s)
54	newline_char_15 newline character	terminator	1	AsciiString	1 byte(s)
55	absolute_orbit_title ABS_ORBIT=	keyword	1	AsciiString	10 byte(s)

#	Description	Units	Count	Type	Size
56	abs_orbit Start absolute orbit number.If not used, set to +00000.	-	1	As	6 byte(s)
57	newline_char_16 newline character	terminator	1	AsciiString	1 byte(s)
58	state_vector_time_title STATE_VECTOR_TIME=	keyword	1	AsciiString	18 byte(s)
59	quote_17 quotation mark (""")	ascii	1	AsciiString	1 byte(s)
60	state_vector_time UTC of ENVISAT state vector. UTC time format. If not used, set to ??????????????????????????.	UTC	1	UtcExternal	27 byte(s)
61	quote_18 quotation mark (""")	ascii	1	AsciiString	1 byte(s)
62	newline_char_17 newline character	terminator	1	AsciiString	1 byte(s)
63	delta_ut1_title DELTA_UT1=	keyword	1	AsciiString	10 byte(s)
64	delta_ut1 DUT1=UT1-UTC. If not used, set to +.000000.	s	1	Ado06	8 byte(s)
65	delta_ut1_units <s>	units	1	AsciiString	3 byte(s)
66	newline_char_18 newline character	terminator	1	AsciiString	1 byte(s)
67	x_position_title X_POSITION=	keyword	1	AsciiString	11 byte(s)
68	x_position X Position in Earth-Fixed reference. If not used, set to +0000000.000.	m	1	Ado73	12 byte(s)
69	x_position_units <m>	units	1	AsciiString	3 byte(s)
70	newline_char_19 newline character	terminator	1	AsciiString	1 byte(s)
71	y_position_title Y_POSITION=	keyword	1	AsciiString	11 byte(s)
72	y_position Y Position in Earth-Fixed reference. If not used, set to +0000000.000.	m	1	Ado73	12 byte(s)
73	y_position_units <m>	units	1	AsciiString	3 byte(s)
74	newline_char_20 newline character	terminator	1	AsciiString	1 byte(s)
75	z_position_title Z_POSITION=	keyword	1	AsciiString	11 byte(s)
76	z_position Z Position in Earth-Fixed reference. If not used, set to +0000000.000.	m	1	Ado73	12 byte(s)
77	z_position_units <m>	units	1	AsciiString	3 byte(s)
78	newline_char_21 newline character	terminator	1	AsciiString	1 byte(s)
79	x_velocity_title X_VELOCITY=	keyword	1	AsciiString	11 byte(s)
80	x_velocity X velocity in Earth fixed reference. If not used, set to +0000.000000.	m/s	1	Ado46	12 byte(s)
81	x_velocity_units <m/s>	units	1	AsciiString	5 byte(s)
82	newline_char_22 newline character	terminator	1	AsciiString	1 byte(s)
83	y_velocity_title Y_VELOCITY=	keyword	1	AsciiString	11 byte(s)
84	y_velocity Y velocity in Earth fixed reference. If not used, set to +0000.000000.	m/s	1	Ado46	12 byte(s)
85	y_velocity_units <m/s>	units	1	AsciiString	5 byte(s)
86	newline_char_23 newline character	terminator	1	AsciiString	1 byte(s)
87	z_velocity_title Z_VELOCITY=	keyword	1	AsciiString	11 byte(s)
88	z_velocity Z velocity in Earth fixed reference. If not used, set to +0000.000000.	m/s	1	Ado46	12 byte(s)
89	z_velocity_units <m/s>	units	1	AsciiString	5 byte(s)
90	newline_char_24	terminator	1	AsciiString	1 byte(s)

#	Description	Units	Count	Type	Size
	newline character				
91	vector_source_title VECTOR_SOURCE=	keyword	1	AsciiString	14 byte(s)
92	quote_19 quotation mark (""")	ascii	1	AsciiString	1 byte(s)
93	vector_source Source of Orbit Vectors	ascii	1	AsciiString	2 byte(s)
94	quote_20 quotation mark (""")	ascii	1	AsciiString	1 byte(s)
95	newline_char_25 newline character	terminator	1	AsciiString	1 byte(s)
96	spare_4 Spare	-	1	SpareField	41 byte(s)
97	utc_sbt_time_title UTC_SBT_TIME=	keyword	1	AsciiString	13 byte(s)
98	quote_21 quotation mark (""")	ascii	1	AsciiString	1 byte(s)
99	utc_sbt_time UTC time corresponding to SBT below(currently defined to be given at the time of the ascending node state vector). If not used, set to ??????????????????????????????.	UTC	1	UtcExternal	27 byte(s)
100	quote_22 quotation mark (""")	ascii	1	AsciiString	1 byte(s)
101	newline_char_28 newline character	terminator	1	AsciiString	1 byte(s)
102	sat_binary_time_title SAT_BINARY_TIME=	keyword	1	AsciiString	16 byte(s)
103	sat_binary_time Satellite Binary Time (SBT) 32bit integer time of satellite clock. Its value is unsigned (=>0). If not used, set to +0000000000.	-	1	AsciiIntegerAul	11 byte(s)
104	newline_char_29 newline character	terminator	1	AsciiString	1 byte(s)
105	clock_step_title CLOCK_STEP=	keyword	1	AsciiString	11 byte(s)
106	clock_step Clock Step Sizeclock step in picoseconds. Its value is unsigned (=>0). If not used, set to +0000000000.	psec.	1	AsciiIntegerAul	11 byte(s)
107	clock_step_units <ps>	units	1	AsciiString	4 byte(s)
108	newline_char_30 newline character	terminator	1	AsciiString	1 byte(s)
109	spare_5 Spare	-	1	SpareField	33 byte(s)
110	leap_utc_title LEAP_UTC=	keyword	1	AsciiString	9 byte(s)
111	quote_23 quotation mark (""")	ascii	1	AsciiString	1 byte(s)
112	leap_utc UTC time of the occurrence of the Leap SecondSet to ?????????????????????????????? if not used.	UTC	1	UtcExternal	27 byte(s)
113	quote_24 quotation mark (""")	ascii	1	AsciiString	1 byte(s)
114	newline_char_302 newline character	terminator	1	AsciiString	1 byte(s)
115	leap_sign_title LEAP_SIGN=	keyword	1	AsciiString	10 byte(s)
116	leap_sign Leap second sign(+001 if positive Leap Second, -001 if negative)Set to +000 if not used.	s	1	Ac	4 byte(s)
117	newline_char_303 newline character	terminator	1	AsciiString	1 byte(s)
118	leap_err_title LEAP_ERR=	keyword	1	AsciiString	9 byte(s)
119	leap_err Leap second errorif leap second occurs within processing segment = 1, otherwise = 0If not used, set to 0.	ascii	1	AsciiString	1 byte(s)
120	newline_char_304 newline character	terminator	1	AsciiString	1 byte(s)
121	spare_6 Spare	-	1	SpareField	41 byte(s)
122	product_err_title PRODUCT_ERR=	keyword	1	AsciiString	12 byte(s)

#	Description	Units	Count	Type	Size
123	product_err 1 or 0. If 1, errors have been reported in the product. User should then refer to the SPH or Summary Quality ADS of the product for details of the error condition. If not used, set to 0.	ascii	1	AsciiString	1 byte(s)
124	newline_char_33 newline character	terminator	1	AsciiString	1 byte(s)
125	total_size_title TOT_SIZE=	keyword	1	AsciiString	9 byte(s)
126	tot_size Total Size Of Product (# bytes DSR + SPH+ MPH)	bytes	1	Ad	21 byte(s)
127	total_size_units <bytes>	units	1	AsciiString	7 byte(s)
128	newline_char_34 newline character	terminator	1	AsciiString	1 byte(s)
129	sph_size_title SPH_SIZE=	keyword	1	AsciiString	9 byte(s)
130	sph_size Length Of SPH(# bytes in SPH)	bytes	1	Al	11 byte(s)
131	sph_size_units <bytes>	units	1	AsciiString	7 byte(s)
132	newline_char_35 newline character	terminator	1	AsciiString	1 byte(s)
133	number_of_dsd_title NUM_DSD=	keyword	1	AsciiString	8 byte(s)
134	num_dsd Number of DSDs(# DSDs)	-	1	Al	11 byte(s)
135	newline_char_36 newline character	terminator	1	AsciiString	1 byte(s)
136	size_of_dsd_title DSD_SIZE=	keyword	1	AsciiString	9 byte(s)
137	dsd_size Length of Each DSD(# bytes for each DSD, all DSDs shall have the same length)	-	1	Al	11 byte(s)
138	size_of_dsd_units <bytes>	units	1	AsciiString	7 byte(s)
139	newline_char_37 newline character	terminator	1	AsciiString	1 byte(s)
140	number_of_ds_att_title NUM_DATA_SETS=	keyword	1	AsciiString	14 byte(s)
141	num_data_sets Number of DSs attached(not all DSDs have a DS attached)	-	1	Al	11 byte(s)
142	newline_char_38 newline character	terminator	1	AsciiString	1 byte(s)
143	spare_7 Spare	-	1	SpareField	41 byte(s)

Record Length : 1247

DS_NAME : Envisat MPH

Format Version 114.0

6.6.2 BT/TOA Land record 50 km cell MDS

Table 6.22 BT/TOA Land record 50 km cell MDS

BT/TOA Land record 30 arc minute cell MDS

#	Description	Units	Count	Type	Size
Data Record					
0	dsr_time Nadir UTC time in MJD format The (nadir and forward view) instrument data contributing to a given cell or sub-cell may cover a range of up to 150 seconds of measurement times. It is therefore not possible to assign a unique time tag to an AST record, and the time tag is therefore arbitrarily assigned as follows. The nadir time associated with a given AST record represents the scan time of a nadir pixel contributing to the record. In general this is the time of the first filled pixel encountered during processing that falls within the geometrical boundary of the cell or sub-cell (see link), although exception cases may arise. Because the cell boundaries bear no clear geometrical relationship to the AATSR instrument scan it is not possible to state in general that this corresponds to a particular corner of the cell or sub-cell. Note also that if a cell is intersected by coastline, so that it contains both land and sea pixels, the time tag of a given record does not necessarily correspond to a pixel of the same surface type.	MJD	1	mjd	12 byte(s)
1	quality_flag Quality Indicator (-1 for blank MDSR, 0 otherwise) This field is set to -1 if all the measurement values in the record are invalid, and is set to 0 otherwise.	flag	1	BooleanFlag	1 byte(s)
2	spare_1 Spare	-	1	SpareField	3 byte(s)
3	lat Latitude of cell The latitude of the lower left-hand corner of the cell, in units of micro-degrees. The latitude is defined in the range -90 degrees to +90 degrees. If the cell contains no valid data, this field may be set to the exceptional value -399,999,999.	(1e-6) degrees	1	GeoCoordinate	4 byte(s)
4	lon Longitude of cell The longitude of the lower left-hand corner of the cell, in units of micro-degrees. The longitude is defined in the range -180 degrees to +180 degrees. If the cell contains no valid data, this field may be set to the exceptional value -399,999,999.	(1e-6) degrees	1	GeoCoordinate	4 byte(s)
5	m_actrk_pix_num Mean across-track pixel number The average pixel index to be associated with the land/sea pixels that contribute to the cell averages. It is the unweighted average of the sub-cell mean across-track pixel number for the contributing sub-cells (those containing at least one valid pixel). The pixel index, in the range 0 to 511 inclusive, is the across-track index of the pixel in the image, and ids linearly related to the X co-ordinate by X = j - 256 km. The mean across-track pixel index is thus a measure of the mean X co-ordinate of the of the distribution of clear land/sea pixels that contribute to the ABT determination.	-	1	ss	2 byte(s)
6	pix_nad Number of filled pixels in cell, nadir view The total number of filled pixels, measured in the nadir view, that fall within the cell, regardless of surface type. This differs from the total number of pixels which fall within the cell by the number of unfilled pixels. In the case of 30 arc minute cells the area of the cell, and hence the number of pixels that fall within it, is a function of the latitude..	-	1	ss	2 byte(s)
7	pix_ls_nad Number of filled pixels in cell over land surface, nadir view The total number of filled pixels over land, measured in the nadir view, that fall within the cell, irrespective of cloud state. It is thus the sum of the numbers of clear land and cloudy land pixel in the cell.	-	1	ss	2 byte(s)
8	perc_cl_pix_ls_nad Percentage of cloudy pixels in cell over land surface, nadir view The percentage of the total number of land pixels within the cell and measured in the nadir view that are cloudy, expressed as an integer in units of 0.01%.	-	1	ss	2 byte(s)
9	lat_corr_nad Topographic latitude correction, nadir view The geolocation of the AATSR pixels assumes that the surface is at mean sea level. This will give rise to errors in the case of elevated land. This field is intended to contain the mean geolocation error in latitude over the cell from this cause, for the nadir view, based on surface elevations taken from a standard DTM. The correction is in units of microdegrees, in the sense true minus nominal latitude. Currently this field is undefined.	(1e-6) degrees	1	sl	4 byte(s)
10	long_corr_nad Topographic longitude correction, nadir view The geolocation of the AATSR pixels assumes that the surface is at mean sea level. This will give rise to errors in the case of elevated land. This field is intended to contain the mean geolocation error in longitude over the cell from this cause, for the nadir view, based on surface elevations taken from a standard DTM. The correction is in units of microdegrees, in the sense true minus nominal longitude.	(1e-6) degrees	1	sl	4 byte(s)

#	Description	Units	Count	Type	Size
	Currently this field is undefined.				
11	sa_12bt_clr_nad Spatially averaged 12 micron BT of all clear pixels (nadir view) The mean calibrated brightness temperature in the 12 micron channel of all the valid clear pixels over land, measured in the nadir view, that fall within the cell. This is an unweighted mean of the corresponding average BT over the sub-cells within the cell that contain at least one valid pixel. The brightness temperature is expressed as a long (32 bit) integer in units of 0.001 K. Valid mean brightness temperatures will be positive numbers in the range 170,000 to 321,000. If no valid clear land pixels fall within the sub-cell, the field will be set to an exceptional value of -1.	K/1000	1	sl	4 byte(s)
12	sd_12bt_clr_nad Standard deviation of above The standard deviation of the sub-cell brightness temperatures that contribute to the spatially averaged 12 micron BT of all clear nadir view pixels.	K/1000	1	sl	4 byte(s)
13	sa_11bt_clr_nad Spatially averaged 11 micron BT of all clear pixels (nadir view) The mean calibrated brightness temperature in the 11 micron channel of all the valid clear pixels over land, measured in the nadir view, that fall within the cell. This is an unweighted mean of the corresponding average BT over the sub-cells within the cell that contain at least one valid pixel. The brightness temperature is expressed as a long (32 bit) integer in units of 0.001 K. Valid mean brightness temperatures will be positive numbers in the range 170,000 to 321,000. If no valid clear land pixels fall within the sub-cell, the field will be set to an exceptional value of -1.	K/1000	1	sl	4 byte(s)
14	sd_11bt_clr_nad Standard deviation of above The standard deviation of the sub-cell brightness temperatures that contribute to the spatially averaged 11 micron BT of all clear nadir view pixels.	K/1000	1	sl	4 byte(s)
15	sa_37bt_clr_nad Spatially averaged 3.7 micron BT of all clear pixels (nadir view) The mean calibrated brightness temperature in the 3.7 micron channel of all the valid clear pixels over land, measured in the nadir view, that fall within the cell. This is an unweighted mean of the corresponding average BT over the sub-cells within the cell that contain at least one valid pixel. The brightness temperature is expressed as a long (32 bit) integer in units of 0.001 K. Valid mean brightness temperatures will be positive numbers in the range 195,000 to 321,000. If no valid clear land pixels fall within the sub-cell, the field will be set to an exceptional value of -1.	K/1000	1	sl	4 byte(s)
16	sd_37bt_clr_nad Standard deviation of above The standard deviation of the sub-cell brightness temperatures that contribute to the spatially averaged 3.7 micron BT of all clear nadir view pixels.	%/1000	1	sl	4 byte(s)
17	sa_16toa_clr_nad Spatially averaged 1.6 micron TOA reflectance of all clear pixels (nadir view) The mean calibrated reflectance in the 1.6 micron channel of all the valid clear pixels over land, measured in the nadir view, that fall within the cell. This is an unweighted mean of the corresponding average TOA reflectance over the sub-cells within the cell that contain at least one valid pixel. The reflectance is expressed as a short (16 bit) integer in units of 0.01 %. Valid reflectance values will be positive numbers in the range 0 to 10,000. If no valid clear land pixels fall within the cell, the field will be set to an exceptional value of -1.	%/100	1	ss	2 byte(s)
18	sd_16toa_clr_nad Standard deviation of above The standard deviation of the sub-cell reflectance values that contribute to the spatially averaged 1.6 micron TOA reflectance of all clear nadir view pixels.	%/100	1	ss	2 byte(s)
19	sa_87toa_clr_nad Spatially averaged 0.87 micron TOA reflectance of all clear pixels (nadir view) The mean calibrated brightness temperature in the 0.87 micron channel of all the valid clear pixels over land, measured in the nadir view, that fall within the cell. This is an unweighted mean of the corresponding average BT over the sub-cells within the cell that contain at least one valid pixel. The brightness temperature is expressed as a long (32 bit) integer in units of 0.001 K. Valid mean brightness temperatures will be positive numbers in the range 195,000 to 321,000. If no valid clear land pixels fall within the sub-cell, the field will be set to an exceptional value of -1.	%/100	1	ss	2 byte(s)
20	sd_87toa_clr_nad Standard deviation of above The standard deviation of the sub-cell reflectance values that contribute to the spatially averaged 0.87 micron TOA reflectance of all clear nadir view pixels.	%/100	1	ss	2 byte(s)
21	sa_67toa_clr_nad Spatially averaged 0.67 micron TOA reflectance of all clear pixels (nadir view) The mean calibrated brightness temperature in the 0.67 micron channel of all the valid clear pixels over land, measured in the nadir view, that fall within the cell. This is an unweighted mean of the corresponding average BT over the sub-cells within the cell that contain at least one valid pixel. The brightness temperature is expressed as a long (32 bit) integer in units of 0.001 K. Valid mean brightness temperatures will be positive numbers in the range 195,000 to 321,000. If no valid clear land pixels fall within the sub-cell, the field will be set to an exceptional value of -1.	%/100	1	ss	2 byte(s)
22	sd_67toa_clr_nad Standard deviation of above The standard deviation of the sub-cell reflectance values that contribute to the spatially averaged 0.67 micron TOA reflectance of all clear nadir view pixels.	%/100	1	ss	2 byte(s)

#	Description	Units	Count	Type	Size
23	sa_55toa_clr_nad Spatially averaged 0.55 micron TOA reflectance of all clear pixels (nadir view) The mean calibrated brightness temperature in the 0.55 micron channel of all the valid clear pixels over land, measured in the nadir view, that fall within the cell. This is an unweighted mean of the corresponding average BT over the sub-cells within the cell that contain at least one valid pixel. The brightness temperature is expressed as a long (32 bit) integer in units of 0.001 K. Valid mean brightness temperatures will be positive numbers in the range 195,000 to 321,000. If no valid clear land pixels fall within the sub-cell, the field will be set to an exceptional value of -1.	%/100	1	ss	2 byte(s)
24	sd_55toa_clr_nad Standard deviation of above The standard deviation of the sub-cell reflectance values that contribute to the spatially averaged 0.55 micron TOA reflectance of all clear nadir view pixels.	%/100	1	ss	2 byte(s)
25	sa_12bt_cl_nad Spatially averaged 12 micron BT of all cloudy pixels (nadir view) The mean calibrated brightness temperature in the 12 micron channel of all the valid cloudy pixels over land, measured in the nadir view, that fall within the cell. This is an unweighted mean of the corresponding average BT over the sub-cells within the cell that contain at least one valid pixel. The brightness temperature is expressed as a long (32 bit) integer in units of 0.001 K. Valid mean brightness temperatures will be positive numbers in the range 170,000 to 321,000. If no valid cloudy land pixels fall within the sub-cell, the field will be set to an exceptional value of -1.	K/1000	1	sl	4 byte(s)
26	sd_12bt_cl_nad Standard deviation of above The standard deviation of the sub-cell brightness temperatures that contribute to the spatially averaged 12 micron BT of all cloudy nadir view pixels.	K/1000	1	sl	4 byte(s)
27	sa_11bt_cl_nad Spatially averaged 11 micron BT of all cloudy pixels (nadir view) The mean calibrated brightness temperature in the 11 micron channel of all the valid cloudy pixels over land, measured in the nadir view, that fall within the cell. This is an unweighted mean of the corresponding average BT over the sub-cells within the cell that contain at least one valid pixel. The brightness temperature is expressed as a long (32 bit) integer in units of 0.001 K. Valid mean brightness temperatures will be positive numbers in the range 170,000 to 321,000. If no valid cloudy land pixels fall within the sub-cell, the field will be set to an exceptional value of -1.	K/1000	1	sl	4 byte(s)
28	sd_11bt_cl_nad Standard deviation of above The standard deviation of the sub-cell brightness temperatures that contribute to the spatially averaged 11 micron BT of all cloudy nadir view pixels.	K/1000	1	sl	4 byte(s)
29	sa_37bt_cl_nad Spatially averaged 3.7 micron BT of all cloudy pixels (nadir view) The mean calibrated brightness temperature in the 3.7 micron channel of all the valid cloudy pixels over land, measured in the nadir view, that fall within the cell. This is an unweighted mean of the corresponding average BT over the sub-cells within the cell that contain at least one valid pixel. The brightness temperature is expressed as a long (32 bit) integer in units of 0.001 K. Valid mean brightness temperatures will be positive numbers in the range 195,000 to 321,000. If no valid cloudy land pixels fall within the sub-cell, the field will be set to an exceptional value of -1.	K/1000	1	sl	4 byte(s)
30	sd_37bt_cl_nad Standard deviation of above The standard deviation of the sub-cell brightness temperatures that contribute to the spatially averaged 3.7 micron BT of all cloudy nadir view pixels.	%/1000	1	sl	4 byte(s)
31	sa_16toa_cl_nad Spatially averaged 1.6 micron TOA reflectance of all cloudy pixels (nadir view) The mean calibrated reflectance in the 1.6 micron channel of all the valid cloudy pixels over land, measured in the nadir view, that fall within the cell. This is an unweighted mean of the corresponding average TOA reflectance over the sub-cells within the cell that contain at least one valid pixel. The reflectance is expressed as a short (16 bit) integer in units of 0.01 %. Valid reflectance values will be positive numbers in the range 0 to 10,000. If no valid cloudy land pixels fall within the cell, the field will be set to an exceptional value of -1.	%/100	1	ss	2 byte(s)
32	sd_16toa_cl_nad Standard deviation of above The standard deviation of the sub-cell reflectance values that contribute to the spatially averaged 1.6 micron TOA reflectance of all cloudy nadir view pixels.	%/100	1	ss	2 byte(s)
33	sa_87toa_cl_nad Spatially averaged 0.87 micron TOA reflectance of all cloudy pixels (nadir view) The mean calibrated brightness temperature in the 0.87 micron channel of all the valid cloudy pixels over land, measured in the nadir view, that fall within the cell. This is an unweighted mean of the corresponding average BT over the sub-cells within the cell that contain at least one valid pixel. The brightness temperature is expressed as a long (32 bit) integer in units of 0.001 K. Valid mean brightness temperatures will be positive numbers in the range 195,000 to 321,000. If no valid cloudy land pixels fall within the sub-cell, the field will be set to an exceptional value of -1.	%/100	1	ss	2 byte(s)
34	sd_87toa_cl_nad Standard deviation of above The standard deviation of the sub-cell reflectance values that contribute to the spatially averaged 0.87 micron TOA reflectance of all cloudy nadir view pixels.	%/100	1	ss	2 byte(s)

#	Description	Units	Count	Type	Size
35	sa_67toa_cl_nad Spatially averaged 0.67 micron TOA reflectance of all cloudy pixels (nadir view) The mean calibrated brightness temperature in the 0.67 micron channel of all the valid cloudy pixels over land, measured in the nadir view, that fall within the cell. This is an unweighted mean of the corresponding average BT over the sub-cells within the cell that contain at least one valid pixel. The brightness temperature is expressed as a long (32 bit) integer in units of 0.001 K. Valid mean brightness temperatures will be positive numbers in the range 195,000 to 321,000. If no valid cloudy land pixels fall within the sub-cell, the field will be set to an exceptional value of -1.	%/100	1	ss	2 byte(s)
36	sd_67toa_cl_nad Standard deviation of above The standard deviation of the sub-cell reflectance values that contribute to the spatially averaged 0.67 micron TOA reflectance of all cloudy nadir view pixels.	%/100	1	ss	2 byte(s)
37	sa_55toa_cl_nad Spatially averaged 0.55 micron TOA reflectance of all cloudy pixels (nadir view) The mean calibrated brightness temperature in the 0.55 micron channel of all the valid cloudy pixels over land, measured in the nadir view, that fall within the cell. This is an unweighted mean of the corresponding average BT over the sub-cells within the cell that contain at least one valid pixel. The brightness temperature is expressed as a long (32 bit) integer in units of 0.001 K. Valid mean brightness temperatures will be positive numbers in the range 195,000 to 321,000. If no valid cloudy land pixels fall within the sub-cell, the field will be set to an exceptional value of -1.	%/100	1	ss	2 byte(s)
38	sd_55toa_cl_nad Standard deviation of above The standard deviation of the sub-cell reflectance values that contribute to the spatially averaged 0.55 micron TOA reflectance of all cloudy nadir view pixels	%/100	1	ss	2 byte(s)
39	fail_flag_nad Pixel threshold failure flags for averages, nadir view A 16 bit word of quality flags for the nadir view data. Each of bits 0 to 13 of the word is a flag that corresponds to one of the channel/cloud flag combinations (i.e. to one of the nadir view spatially averaged fields of the product), which if set indicates that the number of pixels contributing to the corresponding cell average is less than a pre-defined quality threshold. The meanings of the flags are tabulated below.	-	1	us	2 byte(s)
40	pix_for Number of filled pixels in cell, forward view The total number of filled pixels, measured in the forward view, that fall within the cell, regardless of surface type. This differs from the total number of pixels which fall within the cell by the number of unfilled pixels. In the case of 30 arc minute cells the area of the cell, and hence the number of pixels that fall within it, is a function of the latitude..	-	1	ss	2 byte(s)
41	pix_ls_for Number of filled pixels in cell over land surface, forward view The total number of filled pixels over land, measured in the forward view, that fall within the cell, irrespective of cloud state. It is thus the sum of the numbers of clear land and cloudy land pixel in the cell.	-	1	ss	2 byte(s)
42	perc_cl_pix_ls_for Percentage of cloudy pixels in cell over land surface, forward view The percentage of the total number of land pixels within the cell and measured in the forward view that are cloudy, expressed as an integer in units of 0.01%.	-	1	ss	2 byte(s)
43	lat_corr_for Topographic latitude correction, forward view The geolocation of the AATSR pixels assumes that the surface is at mean sea level. This will give rise to errors in the case of elevated land. This field is intended to contain the mean geolocation error in latitude over the cell from this cause, for the forward view, based on surface elevations taken from a standard DTM. The correction is in units of microdegrees, in the sense true minus nominal latitude. Currently this field is undefined.	(1e-6) degrees	1	sl	4 byte(s)
44	long_corr_for Topographic longitude correction, forward view The geolocation of the AATSR pixels assumes that the surface is at mean sea level. This will give rise to errors in the case of elevated land. This field is intended to contain the mean geolocation error in longitude over the cell from this cause, for the forward view, based on surface elevations taken from a standard DTM. The correction is in units of microdegrees, in the sense true minus nominal longitude. Currently this field is undefined.	(1e-6) degrees	1	sl	4 byte(s)
45	sa_12bt_clr_for Spatially averaged 12 micron BT of all clear pixels (forward view) The mean calibrated brightness temperature in the 12 micron channel of all the valid clear pixels over land, measured in the forward view, that fall within the cell. This is an unweighted mean of the corresponding average BT over the sub-cells within the cell that contain at least one valid pixel. The brightness temperature is expressed as a long (32 bit) integer in units of 0.001 K. Valid mean brightness temperatures will be positive numbers in the range 170,000 to 321,000. If no valid clear land pixels fall within the sub-cell, the field will be set to an exceptional value of -1.	K/1000	1	sl	4 byte(s)
46	sd_12bt_clr_for Standard deviation of above The standard deviation of the sub-cell brightness temperatures that contribute to the spatially averaged 12 micron BT of all clear forward view pixels.	K/1000	1	sl	4 byte(s)
47	sa_11bt_clr_for	K/1000	1	sl	4 byte(s)

#	Description	Units	Count	Type	Size
	Spatially averaged 11 micron BT of all clear pixels (forward view) The mean calibrated brightness temperature in the 11 micron channel of all the valid clear pixels over land, measured in the forward view, that fall within the cell. This is an unweighted mean of the corresponding average BT over the sub-cells within the cell that contain at least one valid pixel. The brightness temperature is expressed as a long (32 bit) integer in units of 0.001 K. Valid mean brightness temperatures will be positive numbers in the range 170,000 to 321,000. If no valid clear land pixels fall within the sub-cell, the field will be set to an exceptional value of -1.				
48	sd_11bt_clr_for Standard deviation of above The standard deviation of the sub-cell brightness temperatures that contribute to the spatially averaged 11 micron BT of all clear forward view pixels.	K/1000	1	sl	4 byte(s)
49	sa_37bt_clr_for Spatially averaged 3.7 micron BT of all clear pixels (forward view) The mean calibrated brightness temperature in the 3.7 micron channel of all the valid clear pixels over land, measured in the forward view, that fall within the cell. This is an unweighted mean of the corresponding average BT over the sub-cells within the cell that contain at least one valid pixel. The brightness temperature is expressed as a long (32 bit) integer in units of 0.001 K. Valid mean brightness temperatures will be positive numbers in the range 195,000 to 321,000. If no valid clear land pixels fall within the sub-cell, the field will be set to an exceptional value of -1.	K/1000	1	sl	4 byte(s)
50	sd_37bt_clr_for Standard deviation of above The standard deviation of the sub-cell brightness temperatures that contribute to the spatially averaged 3.7 micron BT of all clear forward view pixels.	K/1000	1	sl	4 byte(s)
51	sa_16toa_clr_for Spatially averaged 1.6 micron TOA reflectance of all clear pixels (forward view) The mean calibrated reflectance in the 1.6 micron channel of all the valid clear pixels over land, measured in the forward view, that fall within the cell. This is an unweighted mean of the corresponding average TOA reflectance over the sub-cells within the cell that contain at least one valid pixel. The reflectance is expressed as a short (16 bit) integer in units of 0.01 %. Valid reflectance values will be positive numbers in the range 0 to 10,000. If no valid clear land pixels fall within the cell, the field will be set to an exceptional value of -1.	%/100	1	ss	2 byte(s)
52	sd_16toa_clr_for Standard deviation of above The standard deviation of the sub-cell reflectance values that contribute to the spatially averaged 1.6 micron TOA reflectance of all clear forward view pixels.	%/100	1	ss	2 byte(s)
53	sa_87toa_clr_for Spatially averaged 0.87 micron TOA reflectance of all clear pixels (forward view) The mean calibrated brightness temperature in the 0.87 micron channel of all the valid clear pixels over land, measured in the forward view, that fall within the cell. This is an unweighted mean of the corresponding average BT over the sub-cells within the cell that contain at least one valid pixel. The brightness temperature is expressed as a long (32 bit) integer in units of 0.001 K. Valid mean brightness temperatures will be positive numbers in the range 195,000 to 321,000. If no valid clear land pixels fall within the sub-cell, the field will be set to an exceptional value of -1.	%/100	1	ss	2 byte(s)
54	sd_87toa_clr_for Standard deviation of above The standard deviation of the sub-cell reflectance values that contribute to the spatially averaged 0.87 micron TOA reflectance of all clear forward view pixels.	%/100	1	ss	2 byte(s)
55	sa_67toa_clr_for Spatially averaged 0.67 micron TOA reflectance of all clear pixels (forward view) The mean calibrated brightness temperature in the 0.67 micron channel of all the valid clear pixels over land, measured in the forward view, that fall within the cell. This is an unweighted mean of the corresponding average BT over the sub-cells within the cell that contain at least one valid pixel. The brightness temperature is expressed as a long (32 bit) integer in units of 0.001 K. Valid mean brightness temperatures will be positive numbers in the range 195,000 to 321,000. If no valid clear land pixels fall within the sub-cell, the field will be set to an exceptional value of -1.	%/100	1	ss	2 byte(s)
56	sd_67toa_clr_for Standard deviation of above The standard deviation of the sub-cell reflectance values that contribute to the spatially averaged 0.67 micron TOA reflectance of all clear forward view pixels.	%/100	1	ss	2 byte(s)
57	sa_55toa_clr_for Spatially averaged 0.55 micron TOA reflectance of all clear pixels (forward view) The mean calibrated brightness temperature in the 0.55 micron channel of all the valid clear pixels over land, measured in the forward view, that fall within the cell. This is an unweighted mean of the corresponding average BT over the sub-cells within the cell that contain at least one valid pixel. The brightness temperature is expressed as a long (32 bit) integer in units of 0.001 K. Valid mean brightness temperatures will be positive numbers in the range 195,000 to 321,000. If no valid clear land pixels fall within the sub-cell, the field will be set to an exceptional value of -1.	%/100	1	ss	2 byte(s)
58	sd_55toa_clr_for Standard deviation of above The standard deviation of the sub-cell reflectance values that contribute to the spatially averaged 0.55 micron TOA reflectance of all clear forward view pixels.	%/100	1	ss	2 byte(s)
59	sa_12bt_cl_for Spatially averaged 12 micron BT of all cloudy pixels (forward view)	K/1000	1	sl	4 byte(s)

#	Description	Units	Count	Type	Size
	The mean calibrated brightness temperature in the 12 micron channel of all the valid cloudy pixels over land, measured in the forward view, that fall within the cell. This is an unweighted mean of the corresponding average BT over the sub-cells within the cell that contain at least one valid pixel. The brightness temperature is expressed as a long (32 bit) integer in units of 0.001 K. Valid mean brightness temperatures will be positive numbers in the range 170,000 to 321,000. If no valid cloudy land pixels fall within the sub-cell, the field will be set to an exceptional value of -1.				
60	sd_12bt_cl_for Standard deviation of above The standard deviation of the sub-cell brightness temperatures that contribute to the spatially averaged 12 micron BT of all cloudy forward view pixels.	K/1000	1	sl	4 byte(s)
61	sa_11bt_cl_for Spatially averaged 11 micron BT of all cloudy pixels (forward view) The mean calibrated brightness temperature in the 11 micron channel of all the valid cloudy pixels over land, measured in the forward view, that fall within the cell. This is an unweighted mean of the corresponding average BT over the sub-cells within the cell that contain at least one valid pixel. The brightness temperature is expressed as a long (32 bit) integer in units of 0.001 K. Valid mean brightness temperatures will be positive numbers in the range 170,000 to 321,000. If no valid cloudy land pixels fall within the sub-cell, the field will be set to an exceptional value of -1.	K/1000	1	sl	4 byte(s)
62	sd_11bt_cl_for Standard deviation of above The standard deviation of the sub-cell brightness temperatures that contribute to the spatially averaged 11 micron BT of all cloudy forward view pixels.	K/1000	1	sl	4 byte(s)
63	sa_37bt_cl_for Spatially averaged 3.7 micron BT of all cloudy pixels (forward view) The mean calibrated brightness temperature in the 3.7 micron channel of all the valid cloudy pixels over land, measured in the forward view, that fall within the cell. This is an unweighted mean of the corresponding average BT over the sub-cells within the cell that contain at least one valid pixel. The brightness temperature is expressed as a long (32 bit) integer in units of 0.001 K. Valid mean brightness temperatures will be positive numbers in the range 195,000 to 321,000. If no valid cloudy land pixels fall within the sub-cell, the field will be set to an exceptional value of -1.	K/1000	1	sl	4 byte(s)
64	sd_37bt_cl_for Standard deviation of above The standard deviation of the sub-cell brightness temperatures that contribute to the spatially averaged 3.7 micron BT of all cloudy forward view pixels.	K/1000	1	sl	4 byte(s)
65	sa_16toa_cl_for Spatially averaged 1.6 micron TOA reflectance of all cloudy pixels (forward view) The mean calibrated reflectance in the 1.6 micron channel of all the valid cloudy pixels over land, measured in the forward view, that fall within the cell. This is an unweighted mean of the corresponding average TOA reflectance over the sub-cells within the cell that contain at least one valid pixel. The reflectance is expressed as a short (16 bit) integer in units of 0.01 %. Valid reflectance values will be positive numbers in the range 0 to 10,000. If no valid cloudy land pixels fall within the cell, the field will be set to an exceptional value of -1.	%/100	1	ss	2 byte(s)
66	sd_16toa_cl_for Standard deviation of above The standard deviation of the sub-cell reflectance values that contribute to the spatially averaged 1.6 micron TOA reflectance of all cloudy forward view pixels.	%/100	1	ss	2 byte(s)
67	sa_87toa_cl_for Spatially averaged 0.87 micron TOA reflectance of all cloudy pixels (forward view) The mean calibrated brightness temperature in the 0.87 micron channel of all the valid cloudy pixels over land, measured in the forward view, that fall within the cell. This is an unweighted mean of the corresponding average BT over the sub-cells within the cell that contain at least one valid pixel. The brightness temperature is expressed as a long (32 bit) integer in units of 0.001 K. Valid mean brightness temperatures will be positive numbers in the range 195,000 to 321,000. If no valid cloudy land pixels fall within the sub-cell, the field will be set to an exceptional value of -1.	%/100	1	ss	2 byte(s)
68	sd_87toa_cl_for Standard deviation of above The standard deviation of the sub-cell reflectance values that contribute to the spatially averaged 0.87 micron TOA reflectance of all cloudy forward view pixels.	%/100	1	ss	2 byte(s)
69	sa_67toa_cl_for Spatially averaged 0.67 micron TOA reflectance of all cloudy pixels (forward view) The mean calibrated brightness temperature in the 0.67 micron channel of all the valid cloudy pixels over land, measured in the forward view, that fall within the cell. This is an unweighted mean of the corresponding average BT over the sub-cells within the cell that contain at least one valid pixel. The brightness temperature is expressed as a long (32 bit) integer in units of 0.001 K. Valid mean brightness temperatures will be positive numbers in the range 195,000 to 321,000. If no valid cloudy land pixels fall within the sub-cell, the field will be set to an exceptional value of -1.	%/100	1	ss	2 byte(s)
70	sd_67toa_cl_for Standard deviation of above The standard deviation of the sub-cell reflectance values that contribute to the spatially averaged 0.67 micron TOA reflectance of all cloudy forward view pixels.	%/100	1	ss	2 byte(s)
71	sa_55toa_cl_for Spatially averaged 0.55 micron TOA reflectance of all cloudy pixels (forward view) The mean calibrated brightness temperature in the 0.55 micron channel of all the	%/100	1	ss	2 byte(s)

#	Description	Units	Count	Type	Size
	valid cloudy pixels over land, measured in the forward view, that fall within the cell. This is an unweighted mean of the corresponding average BT over the sub-cells within the cell that contain at least one valid pixel. The brightness temperature is expressed as a long (32 bit) integer in units of 0.001 K. Valid mean brightness temperatures will be positive numbers in the range 195,000 to 321,000. If no valid cloudy land pixels fall within the sub-cell, the field will be set to an exceptional value of -1.				
72	sd_55toa_cl_for Standard deviation of above The standard deviation of the sub-cell reflectance values that contribute to the spatially averaged 0.55 micron TOA reflectance of all cloudy forward view pixels	%/100	1	ss	2 byte(s)
73	fail_flag_for Pixel threshold failure flags for averages, forward view A 16 bit word of quality flags for the forward view data. Each of bits 0 to 13 of the word is a flag that corresponds to one of the channel/cloud flag combinations (i.e. to one of the forward view spatially averaged fields of the product), which if set indicates that the number of pixels contributing to the corresponding cell average is less than a pre-defined quality threshold. The meanings of the flags are tabulated below.	-	1	us	2 byte(s)
74	pix_nsig_nad Number of filled pixels (N-Sigma), nadir view Reserved: this field is currently undefined and is set to zero.	-	1	ss	2 byte(s)
75	pix_ss Percentage filled pixels over land surface Reserved: this field is currently undefined and is set to zero.	%/100	1	ss	2 byte(s)
76	low_11bt_cl_nad Lowest 11 micron BT of all cloudy pixels, nadir view The minimum brightness temperature in the 11 micron channel of all valid cloudy land pixels measured in the nadir view and falling within the cell, in units of 0.01K. A pixel is valid in this sense if its 11 micron brightness temperature falls between 190K and 290 K.	K/100	1	ss	2 byte(s)
77	corr_12bt_nad Corresponding 12 micron BT, nadir view The brightness temperature in the 12 micron nadir view channel, in units of 0.01K, of the cloudy land pixel (above) having the minimum brightness temperature measured in the 11 micron channel.	K/100	1	ss	2 byte(s)
78	corr_37bt_nad Corresponding 3.7 micron BT, nadir view The brightness temperature in the 3.7 micron nadir view channel, in units of 0.01K, of the cloudy land pixel (above) having the minimum brightness temperature measured in the 11 micron channel.	K/100	1	ss	2 byte(s)
79	corr_16ref_nad Corresponding 1.6 micron reflectance, nadir view The reflectance at 1.6 micron wavelength, in units of 0.01%, of the nadir view cloudy land pixel (above) having the minimum brightness temperature measured in the 11 micron channel.	%/100	1	ss	2 byte(s)
80	corr_87ref_nad Corresponding 0.87 micron reflectance, nadir view The reflectance at 0.87 micron wavelength, in units of 0.01%, of the nadir view cloudy land pixel (above) having the minimum brightness temperature measured in the 11 micron channel.	%/100	1	ss	2 byte(s)
81	corr_67ref_nad Corresponding 0.67 micron reflectance, nadir view The reflectance at 0.67 micron wavelength, in units of 0.01%, of the nadir view cloudy land pixel (above) having the minimum brightness temperature measured in the 11 micron channel.	%/100	1	ss	2 byte(s)
82	corr_55ref_nad Corresponding 0.55 micron reflectance, nadir view The reflectance at 0.55 micron wavelength, in units of 0.01%, of the nadir view cloudy land pixel (above) having the minimum brightness temperature measured in the 11 micron channel.	%/100	1	ss	2 byte(s)
83	low_11bt_cl_for Lowest 11 micron BT of all cloudy pixels, forward view The minimum brightness temperature in the 11 micron channel of all valid cloudy land pixels measured in the forward view and falling within the cell, in units of 0.01K. A pixel is valid in this sense if its 11 micron brightness temperature falls between 190K and 290 K.	K/100	1	ss	2 byte(s)
84	corr_12bt_for Corresponding 12 micron BT, forward view The brightness temperature in the 12 micron forward view channel, in units of 0.01K, of the cloudy land pixel (above) having the minimum brightness temperature measured in the 11 micron channel.	K/100	1	ss	2 byte(s)
85	corr_37bt_for Corresponding 3.7 micron BT, forward view The brightness temperature in the 3.7 micron forward view channel, in units of 0.01K, of the cloudy land pixel (above) having the minimum brightness temperature measured in the 11 micron channel.	K/100	1	ss	2 byte(s)
86	corr_16ref_for Corresponding 1.6 micron reflectance, forward view The reflectance at 1.6 micron wavelength, in units of 0.01%, of the forward view	%/100	1	ss	2 byte(s)

#	Description	Units	Count	Type	Size
	cloudy land pixel (above) having the minimum brightness temperature measured in the 11 micron channel.				
87	corr_87ref_for Corresponding 0.87 micron reflectance, forward view The reflectance at 0.87 micron wavelength, in units of 0.01%, of the forward view cloudy land pixel (above) having the minimum brightness temperature measured in the 11 micron channel.	%/100	1	ss	2 byte(s)
88	corr_67ref_for Corresponding 0.67 micron reflectance, forward view The reflectance at 0.67 micron wavelength, in units of 0.01%, of the forward view cloudy land pixel (above) having the minimum brightness temperature measured in the 11 micron channel.	%/100	1	ss	2 byte(s)
89	corr_55ref_for Corresponding 0.55 micron reflectance, forward view The reflectance at 0.55 micron wavelength, in units of 0.01%, of the forward view cloudy land pixel (above) having the minimum brightness temperature measured in the 11 micron channel.	%/100	1	ss	2 byte(s)

Record Length : 250

DS_NAME : BT/TOA Land record 30 arc minute cell MDS

Format Version 114.0

The following table defines the contents of the pixel threshold failure flags word.

Table 6.23 Pixel threshold failure flags (nadir or forward view)

Bit	Meaning if set
0	Number of clear pixels contributing to average is less than threshold, 12 micron channel
1	Number of clear pixels contributing to average is less than threshold, 11 micron channel
2	Number of clear pixels contributing to average is less than threshold, 3.7 micron channel
3	Number of clear pixels contributing to average is less than threshold, 1.6 micron channel
4	Number of clear pixels contributing to average is less than threshold, 0.870 micron channel
5	Number of clear pixels contributing to average is less than threshold, 0.670 micron channel
6	Number of clear pixels contributing to average is less than threshold, 0.555 micron channel
7	Number of cloudy pixels contributing to average is less than threshold, 12 micron channel
8	Number of cloudy pixels contributing to average is less than threshold, 11 micron channel
9	Number of cloudy pixels contributing to average is less than threshold, 3.7 micron channel
10	Number of cloudy pixels contributing to average is less than threshold, 1.6 micron channel
11	Number of cloudy pixels contributing to average is less than threshold, 0.870 micron channel
12	Number of cloudy pixels contributing to average is less than threshold, 0.670 micron channel
13	Number of cloudy pixels contributing to average is less than threshold, 0.555 micron channel
14	View contains day-time data
15	Unused

Note: Bits are numbered from ms bit 15 to ls bit 0.

6.6.3 BT/TOA Land record 17 km cell MDS

Table 6.24 BT/TOA Land record 17 km cell MDS

BT/TOA Land record 10 arc minute cell MDS

#	Description	Units	Count	Type	Size
Data Record					
0	dsr_time Nadir UTC time in MJD format The (nadir and forward view) instrument data contributing to a given cell or sub-cell may cover a range of up to 150 seconds of measurement times. It is therefore not possible to assign a unique time tag to an AST record, and the time tag is therefore arbitrarily assigned as follows. The nadir time associated with a given AST record represents the scan time of a nadir pixel contributing to the record. In general this is the time of the first filled pixel encountered during processing that falls within the geometrical boundary of the cell or sub-cell (see link), although exception cases may arise. Because the cell boundaries bear no clear geometrical relationship to the AATSR instrument scan it is not possible to state in general that this corresponds to a particular corner of the cell or sub-cell. Note also that if a cell is intersected by coastline, so that it contains both land and sea pixels, the time tag of a given record does not necessarily correspond to a pixel of the same surface type.	MJD	1	mjd	12 byte(s)
1	quality_flag Quality Indicator (-1 for blank MDSR, 0 otherwise) This field is set to -1 if all the measurement values in the record are invalid, and is set to 0 otherwise.	flag	1	BooleanFlag	1 byte(s)
2	spare_1 Spare	-	1	SpareField	3 byte(s)
3	lat Latitude of cell The latitude of the lower left-hand corner of the sub-cell, in units of micro-degrees. The latitude is defined in the range -90 degrees to +90 degrees. If the cell contains no valid data, this field may be set to the exceptional value -399,999,999.	(1e-6) degrees	1	GeoCoordinate	4 byte(s)
4	lon Longitude of cell The longitude of the lower left-hand corner of the sub-cell, in units of micro-degrees. The longitude is defined in the range -180 degrees to +180 degrees. If the cell contains no valid data, this field may be set to the exceptional value -399,999,999.	(1e-6) degrees	1	GeoCoordinate	4 byte(s)
5	m_actrk_pix_num Mean across-track pixel number The average pixel index of the nadir view clear sea pixels that fall within the sub-cell. The pixel index, in the range 0 to 511 inclusive, is the across-track index of the pixel in the image, and is linearly related to the X co-ordinate by X = j - 256 km. The mean across-track pixel index is thus a measure of the X co-ordinate of the centroid of the distribution of clear sea pixels that will contribute to the SST determination. It may be used to select SST retrieval coefficients for the cell.	-	1	ss	2 byte(s)
6	pix_nad Number of filled pixels in cell, nadir view The total number of filled pixels, measured in the nadir view, that fall within the sub-cell, regardless of surface type. This differs from the total number of pixels which fall within the sub-cell by the number of unfilled pixels. In the case of 10 arc minute cells the area of the cell, and hence the number of pixels that fall within it, is a function of the latitude.	-	1	ss	2 byte(s)
7	pix_ls_nad Number of filled pixels in cell over land surface, nadir view The total number of filled pixels over land, measured in the nadir view, that fall within the sub-cell, irrespective of cloud state. It is thus the sum of the numbers of clear land and cloudy land pixel in the sub-cell.	-	1	ss	2 byte(s)

#	Description	Units	Count	Type	Size
8	perc_cl_pix_ls_nad Percentage of cloudy pixels in cell over land surface, nadir view The percentage of the total number of land pixels within the sub-cell and measured in the nadir view that are cloudy, expressed as an integer in units of 0.01%.	-	1	ss	2 byte(s)
9	lat_corr_nad Topographic latitude correction, nadir view The geolocation of the AATSR pixels assumes that the surface is at mean sea level. This will give rise to errors in the case of elevated land. This field is intended to contain the mean geolocation error in latitude over the sub-cell from this cause, for the nadir view, based on surface elevations taken from a standard DTM. The correction is in units of microdegrees, in the sense true minus nominal latitude. Currently this field is undefined.	(1e-6) degrees	1	sl	4 byte(s)
10	long_corr_nad Topographic longitude correction, nadir view The geolocation of the AATSR pixels assumes that the surface is at mean sea level. This will give rise to errors in the case of elevated land. This field is intended to contain the mean geolocation error in longitude over the sub-cell from this cause, for the nadir view, based on surface elevations taken from a standard DTM. The correction is in units of microdegrees, in the sense true minus nominal longitude. Currently this field is undefined.	(1e-6) degrees	1	sl	4 byte(s)
11	sa_12bt_clr_nad Spatially averaged 12 micron BT of all clear pixels (nadir view) The mean calibrated brightness temperature in the 12 micron channel of all the valid clear pixels over land, measured in the nadir [forward] view, that fall within the sub-cell. The brightness temperature is expressed as a long (32 bit) integer in units of 0.001 K. Valid mean brightness temperatures will be positive numbers in the range 170,000 to 321,000. If no valid clear land pixels fall within the sub-cell, the field will be set to an exceptional value of -1.	K/1000	1	sl	4 byte(s)
12	sa_11bt_clr_nad Spatially averaged 11 micron BT of all clear pixels (nadir view) The mean calibrated brightness temperature in the 11 micron channel of all the valid clear pixels over land, measured in the nadir view, that fall within the sub-cell. The brightness temperature is expressed as a long (32 bit) integer in units of 0.001 K. Valid mean brightness temperatures will be positive numbers in the range 170,000 to 321,000. If no valid clear land pixels fall within the sub-cell, the field will be set to an exceptional value of -1.	K/1000	1	sl	4 byte(s)
13	sa_37bt_clr_nad Spatially averaged 3.7 micron BT of all clear pixels (nadir view) The mean calibrated brightness temperature in the 3.7 micron channel of all the valid clear pixels over land, measured in the nadir view, that fall within the sub-cell. The brightness temperature is expressed as a long (32 bit) integer in units of 0.001 K. Valid mean brightness temperatures will be positive numbers in the range 195,000 to 321,000. If no valid clear land pixels fall within the sub-cell, the field will be set to an exceptional value of -1.	K/1000	1	sl	4 byte(s)
14	sa_16toa_clr_nad Spatially averaged 1.6 micron TOA reflectance of all clear pixels (nadir view) The mean calibrated reflectance in the 1.6 micron channel of all the valid clear pixels over land, measured in the nadir view, that fall within the sub-cell. The reflectance is expressed as a short (16 bit) integer in units of 0.01 %. Valid mean reflectances will be positive numbers in the range 0 to 10,000. If no valid clear land pixels fall within the sub-cell, the field will be set to an exceptional value of -1.	%/100	1	ss	2 byte(s)
15	sa_87toa_clr_nad Spatially averaged 0.87 micron TOA reflectance of all clear pixels (nadir view) The mean calibrated reflectance in the 0.87 micron channel of all the valid clear pixels over land, measured in the nadir view, that fall within the sub-cell. The reflectance is expressed as a short (16 bit) integer in units of 0.01 %. Valid mean reflectances will be positive numbers in the range 0 to 10,000. If no valid clear land pixels fall within the sub-cell, the field will be set to an exceptional value of -1.	%/100	1	ss	2 byte(s)
16	sa_67toa_clr_nad Spatially averaged 0.67 micron TOA reflectance of all clear pixels (nadir view) The mean calibrated reflectance in the 0.67 micron channel of all the valid clear pixels over land, measured in the nadir view, that fall within the sub-cell. The reflectance is expressed as a short (16 bit) integer in units of 0.01 %. Valid mean reflectances will be positive numbers in the range 0 to 10,000. If no valid clear land pixels fall within the sub-cell, the field will be set to an exceptional value of -1.	%/100	1	ss	2 byte(s)
17	sa_55toa_clr_nad Spatially averaged 0.55 micron TOA reflectance of all clear pixels (nadir view) The mean calibrated reflectance in the 0.55 micron channel of all the valid clear pixels over land, measured in the nadir view, that fall within the sub-cell. The reflectance is expressed as a short (16 bit) integer in units of 0.01 %. Valid mean reflectances will be positive numbers in the range 0 to 10,000. If no valid clear land pixels fall within the sub-cell, the field will be set to an exceptional value of -1.	%/100	1	ss	2 byte(s)
18	sa_12bt_cl_nad Spatially averaged 12 micron BT of all cloudy pixels (nadir view) The mean calibrated brightness temperature in the 12 micron channel of all the valid cloudy pixels over land, measured in the nadir view, that fall within the sub-cell. The brightness temperature is expressed as a long (32 bit) integer in units of 0.001 K. Valid mean brightness temperatures will be positive numbers in the range 170,000 to 321,000. If no valid cloudy land pixels fall within the sub-cell, the field will be set to an exceptional value of -1.	K/1000	1	sl	4 byte(s)
19	sa_11bt_cl_nad Spatially averaged 11 micron BT of all cloudy pixels (nadir view) The mean calibrated brightness temperature in the 11 micron channel of all the	K/1000	1	sl	4 byte(s)

#	Description	Units	Count	Type	Size
	valid cloudy pixels over land, measured in the nadir view, that fall within the sub-cell. The brightness temperature is expressed as a long (32 bit) integer in units of 0.001 K. Valid mean brightness temperatures will be positive numbers in the range 170,000 to 321,000. If no valid cloudy land pixels fall within the sub-cell, the field will be set to an exceptional value of -1.				
20	sa_37bt_cl_nad Spatially averaged 3.7 micron BT of all cloudy pixels (nadir view) The mean calibrated brightness temperature in the 3.7 micron channel of all the valid cloudy pixels over land, measured in the nadir view, that fall within the sub-cell. The brightness temperature is expressed as a long (32 bit) integer in units of 0.001 K. Valid mean brightness temperatures will be positive numbers in the range 195,000 to 321,000. If no valid cloudy land pixels fall within the sub-cell, the field will be set to an exceptional value of -1.	K/1000	1	sl	4 byte(s)
21	sa_16toa_cl_nad Spatially averaged 1.6 micron TOA reflectance of all cloudy pixels (nadir view) The mean calibrated reflectance in the 1.6 micron channel of all the valid cloudy pixels over land, measured in the nadir view, that fall within the sub-cell. The reflectance is expressed as a short (16 bit) integer in units of 0.01 %. Valid mean reflectances will be positive numbers in the range 0 to 10,000. If no valid cloudy land pixels fall within the sub-cell, the field will be set to an exceptional value of -1.	%/100	1	ss	2 byte(s)
22	sa_87toa_cl_nad Spatially averaged 0.87 micron TOA reflectance of all cloudy pixels (nadir view) The mean calibrated reflectance in the 0.87 micron channel of all the valid cloudy pixels over land, measured in the nadir view, that fall within the sub-cell. The reflectance is expressed as a short (16 bit) integer in units of 0.01 %. Valid mean reflectances will be positive numbers in the range 0 to 10,000. If no valid cloudy land pixels fall within the sub-cell, the field will be set to an exceptional value of -1.	%/100	1	ss	2 byte(s)
23	sa_67toa_cl_nad Spatially averaged 0.67 micron TOA reflectance of all cloudy pixels (nadir view) The mean calibrated reflectance in the 0.67 micron channel of all the valid cloudy pixels over land, measured in the nadir view, that fall within the sub-cell. The reflectance is expressed as a short (16 bit) integer in units of 0.01 %. Valid mean reflectances will be positive numbers in the range 0 to 10,000. If no valid cloudy land pixels fall within the sub-cell, the field will be set to an exceptional value of -1.	%/100	1	ss	2 byte(s)
24	sa_55toa_cl_nad Spatially averaged 0.55 micron TOA reflectance of all cloudy pixels (nadir view) The mean calibrated reflectance in the 0.55 micron channel of all the valid cloudy pixels over land, measured in the nadir view, that fall within the sub-cell. The reflectance is expressed as a short (16 bit) integer in units of 0.01 %. Valid mean reflectances will be positive numbers in the range 0 to 10,000. If no valid cloudy land pixels fall within the sub-cell, the field will be set to an exceptional value of -1.	%/100	1	ss	2 byte(s)
25	fail_flag_nad Pixel threshold failure flags for averages, nadir view A 16 bit word of quality flags for the nadir view data. Each of bits 0 to 13 of the word is a flag that corresponds to one of the channel/cloud flag combinations (i.e. to one of the nadir view spatially averaged fields of the product), which if set indicates that the number of pixels contributing to the corresponding average is less than a pre-defined quality threshold. The meanings of the flags are tabulated below.	-	1	us	2 byte(s)
26	pix_for Number of filled pixels in cell, forward view The total number of filled pixels, measured in the forward view, that fall within the sub-cell, regardless of surface type. This differs from the total number of pixels which fall within the sub-cell by the number of unfilled pixels. In the case of 10 arc minute cells the area of the cell, and hence the number of pixels that fall within it, is a function of the latitude.	-	1	ss	2 byte(s)
27	pix_ss_for Number of filled pixels in cell over land surface, forward view The total number of filled pixels over land, measured in the forward view, that fall within the sub-cell, irrespective of cloud state. It is thus the sum of the numbers of clear land and cloudy land pixel in the sub-cell.	-	1	ss	2 byte(s)
28	perc_cl_pix_ss_for Percentage of cloudy pixels in cell over land surface, forward view The percentage of the total number of land pixels within the sub-cell and measured in the forward view that are cloudy, expressed as an integer in units of 0.01%.	-	1	ss	2 byte(s)
29	lat_corr_for Topographic latitude correction, forward view The geolocation of the AATSR pixels assumes that the surface is at mean sea level. This will give rise to errors in the case of elevated land. This field is intended to contain the mean geolocation error in latitude over the sub-cell from this cause, for the forward view, based on surface elevations taken from a standard DTM. The correction is in units of microdegrees, in the sense true minus nominal latitude. Currently this field is undefined.	(1e-6) degrees	1	sl	4 byte(s)
30	long_corr_for Topographic longitude correction, forward view The geolocation of the AATSR pixels assumes that the surface is at mean sea level. This will give rise to errors in the case of elevated land. This field is intended to contain the mean geolocation error in longitude over the sub-cell from this cause, for the forward view, based on surface elevations taken from a standard DTM. The correction is in units of microdegrees, in the sense true minus nominal longitude. Currently this field is undefined.	(1e-6) degrees	1	sl	4 byte(s)
31	sa_12bt_clr_for Spatially averaged 12 micron BT of all clear pixels (forward view)	K/1000	1	sl	4 byte(s)

#	Description	Units	Count	Type	Size
	The mean calibrated brightness temperature in the 12 micron channel of all the valid clear pixels over land, measured in the forward [forward] view, that fall within the sub-cell. The brightness temperature is expressed as a long (32 bit) integer in units of 0.001 K. Valid mean brightness temperatures will be positive numbers in the range 170,000 to 321,000. If no valid clear land pixels fall within the sub-cell, the field will be set to an exceptional value of -1.				
32	sa_11bt_clr_for Spatially averaged 11 micron BT of all clear pixels (forward view) The mean calibrated brightness temperature in the 11 micron channel of all the valid clear pixels over land, measured in the forward view, that fall within the sub-cell. The brightness temperature is expressed as a long (32 bit) integer in units of 0.001 K. Valid mean brightness temperatures will be positive numbers in the range 170,000 to 321,000. If no valid clear land pixels fall within the sub-cell, the field will be set to an exceptional value of -1.	K/1000	1	sl	4 byte(s)
33	sa_37bt_clr_for Spatially averaged 3.7 micron BT of all clear pixels (forward view) The mean calibrated brightness temperature in the 3.7 micron channel of all the valid clear pixels over land, measured in the forward view, that fall within the sub-cell. The brightness temperature is expressed as a long (32 bit) integer in units of 0.001 K. Valid mean brightness temperatures will be positive numbers in the range 195,000 to 321,000. If no valid clear land pixels fall within the sub-cell, the field will be set to an exceptional value of -1.	K/1000	1	sl	4 byte(s)
34	sa_16toa_clr_for Spatially averaged 1.6 micron TOA reflectance of all clear pixels (forward view) The mean calibrated reflectance in the 1.6 micron channel of all the valid clear pixels over land, measured in the forward view, that fall within the sub-cell. The reflectance is expressed as a short (16 bit) integer in units of 0.01 %. Valid mean reflectances will be positive numbers in the range 0 to 10,000. If no valid clear land pixels fall within the sub-cell, the field will be set to an exceptional value of -1.	%/100	1	ss	2 byte(s)
35	sa_87toa_clr_for Spatially averaged 0.87 micron TOA reflectance of all clear pixels (forward view) The mean calibrated reflectance in the 0.87 micron channel of all the valid clear pixels over land, measured in the forward view, that fall within the sub-cell. The reflectance is expressed as a short (16 bit) integer in units of 0.01 %. Valid mean reflectances will be positive numbers in the range 0 to 10,000. If no valid clear land pixels fall within the sub-cell, the field will be set to an exceptional value of -1.	%/100	1	ss	2 byte(s)
36	sa_67toa_clr_for Spatially averaged 0.67 micron TOA reflectance of all clear pixels (forward view) The mean calibrated reflectance in the 0.67 micron channel of all the valid clear pixels over land, measured in the forward view, that fall within the sub-cell. The reflectance is expressed as a short (16 bit) integer in units of 0.01 %. Valid mean reflectances will be positive numbers in the range 0 to 10,000. If no valid clear land pixels fall within the sub-cell, the field will be set to an exceptional value of -1.	%/100	1	ss	2 byte(s)
37	sa_55toa_clr_for Spatially averaged 0.55 micron TOA reflectance of all clear pixels (forward view) The mean calibrated reflectance in the 0.55 micron channel of all the valid clear pixels over land, measured in the forward view, that fall within the sub-cell. The reflectance is expressed as a short (16 bit) integer in units of 0.01 %. Valid mean reflectances will be positive numbers in the range 0 to 10,000. If no valid clear land pixels fall within the sub-cell, the field will be set to an exceptional value of -1.	%/100	1	ss	2 byte(s)
38	sa_12bt_cl_for Spatially averaged 12 micron BT of all cloudy pixels (forward view) The mean calibrated brightness temperature in the 12 micron channel of all the valid cloudy pixels over land, measured in the forward view, that fall within the sub-cell. The brightness temperature is expressed as a long (32 bit) integer in units of 0.001 K. Valid mean brightness temperatures will be positive numbers in the range 170,000 to 321,000. If no valid cloudy land pixels fall within the sub-cell, the field will be set to an exceptional value of -1.	K/1000	1	sl	4 byte(s)
39	sa_11bt_cl_for Spatially averaged 11 micron BT of all cloudy pixels (forward view) The mean calibrated brightness temperature in the 11 micron channel of all the valid cloudy pixels over land, measured in the forward view, that fall within the sub-cell. The brightness temperature is expressed as a long (32 bit) integer in units of 0.001 K. Valid mean brightness temperatures will be positive numbers in the range 170,000 to 321,000. If no valid cloudy land pixels fall within the sub-cell, the field will be set to an exceptional value of -1.	K/1000	1	sl	4 byte(s)
40	sa_37bt_cl_for Spatially averaged 3.7 micron BT of all cloudy pixels (forward view) The mean calibrated brightness temperature in the 3.7 micron channel of all the valid cloudy pixels over land, measured in the forward view, that fall within the sub-cell. The brightness temperature is expressed as a long (32 bit) integer in units of 0.001 K. Valid mean brightness temperatures will be positive numbers in the range 195,000 to 321,000. If no valid cloudy land pixels fall within the sub-cell, the field will be set to an exceptional value of -1.	K/1000	1	sl	4 byte(s)
41	sa_16toa_cl_for Spatially averaged 1.6 micron TOA reflectance of all cloudy pixels (forward view) The mean calibrated reflectance in the 1.6 micron channel of all the valid cloudy pixels over land, measured in the forward view, that fall within the sub-cell. The reflectance is expressed as a short (16 bit) integer in units of 0.01 %. Valid mean reflectances will be positive numbers in the range 0 to 10,000. If no valid cloudy land pixels fall within the sub-cell, the field will be set to an exceptional value of -1.	%/100	1	ss	2 byte(s)
42	sa_87toa_cl_for Spatially averaged 0.87 micron TOA reflectance of all cloudy pixels (forward view) The mean calibrated reflectance in the 0.87 micron channel of all the valid cloudy pixels over land, measured in the forward view, that fall within the sub-cell. The	%/100	1	ss	2 byte(s)

#	Description	Units	Count	Type	Size
	reflectance is expressed as a short (16 bit) integer in units of 0.01 %. Valid mean reflectances will be positive numbers in the range 0 to 10,000. If no valid cloudy land pixels fall within the sub-cell, the field will be set to an exceptional value of -1.				
43	sa_67toa_cl_for Spatially averaged 0.67 micron TOA reflectance of all cloudy pixels (forward view) The mean calibrated reflectance in the 0.67 micron channel of all the valid cloudy pixels over land, measured in the forward view, that fall within the sub-cell. The reflectance is expressed as a short (16 bit) integer in units of 0.01 %. Valid mean reflectances will be positive numbers in the range 0 to 10,000. If no valid cloudy land pixels fall within the sub-cell, the field will be set to an exceptional value of -1.	%/100	1	ss	2 byte(s)
44	sa_55toa_cl_for Spatially averaged 0.55 micron TOA reflectance of all cloudy pixels (forward view) The mean calibrated reflectance in the 0.55 micron channel of all the valid cloudy pixels over land, measured in the forward view, that fall within the sub-cell. The reflectance is expressed as a short (16 bit) integer in units of 0.01 %. Valid mean reflectances will be positive numbers in the range 0 to 10,000. If no valid cloudy land pixels fall within the sub-cell, the field will be set to an exceptional value of -1	%/100	1	ss	2 byte(s)
45	fail_flag_for Pixel threshold failure flags for averages, forward view A 16 bit word of quality flags for the forward view data. Each of bits 0 to 13 of the word is a flag that corresponds to one of the channel/cloud flag combinations (i.e. to one of the forward view spatially averaged fields of the product), which if set indicates that the number of pixels contributing to the corresponding average is less than a pre-defined quality threshold. The meanings of the flags are tabulated below.	-	1	us	2 byte(s)

Record Length : 138

DS_NAME : BT/TOA Land record 10 arc minute cell MDS

Format Version 114.0

The following table defines the contents of the pixel threshold failure flags word.

Table 6.25

Bit	Meaning if set
0	Number of clear pixels contributing to average is less than threshold, 12 micron channel
1	Number of clear pixels contributing to average is less than threshold, 11 micron channel
2	Number of clear pixels contributing to average is less than threshold, 3.7 micron channel
3	Number of clear pixels contributing to average is less than threshold, 1.6 micron channel
4	Number of clear pixels contributing to average is less than threshold, 0.870 micron channel
5	Number of clear pixels contributing to average is less than threshold, 0.670 micron channel
6	Number of clear pixels contributing to average is less than threshold, 0.555 micron channel
7	Number of cloudy pixels contributing to average is less than threshold, 12 micron channel
8	Number of cloudy pixels contributing to average is less than threshold, 11 micron channel
9	Number of cloudy pixels contributing to average is less than threshold, 3.7 micron channel
10	Number of cloudy pixels contributing to average is less than threshold, 1.6 micron channel
11	Number of cloudy pixels contributing to average is less than threshold, 0.870 micron channel
12	Number of cloudy pixels contributing to average is less than threshold, 0.670 micron channel
13	Number of cloudy pixels contributing to average is less than threshold, 0.555 micron channel
14	View contains day-time data
15	Unused

Pixel threshold failure flags (nadir or forward view).

Note: Bits are numbered from ms bit 15 to ls bit 0.

6.6.4 LST record 50 km cell MDS

Table 6.26 LST record 50 km cell MDS

LST record 30 arc minute cell MDS

#	Description	Units	Count	Type	Size
Data Record					
0	dsr_time Nadir UTC time in MJD format The (nadir and forward view) instrument data contributing to a given cell or sub-cell may cover a range of up to 150 seconds of measurement times. It is therefore not possible to assign a unique time tag to an AST record, and the time tag is therefore arbitrarily assigned as follows. The nadir time associated with a given AST record represents the scan time of a nadir pixel contributing to the record. In general this is the time of the first filled pixel encountered during processing that falls within the geometrical boundary of the cell or sub-cell (see link), although exception cases may arise. Because the cell boundaries bear no clear geometrical relationship to the AATSR instrument scan it is not possible to state in general that this corresponds to a particular corner of the cell or sub-cell. Note also that if a cell is intersected by coastline, so that it contains both land and sea pixels, the time tag of a given record does not necessarily correspond to a pixel of the same surface type.	MJD	1	mjd	12 byte(s)
1	quality_flag Quality Indicator (-1 for blank MDSR, 0 otherwise) This field is set to -1 if all the measurement values in the record are invalid, and is set to 0 otherwise.	flag	1	BooleanFlag	1 byte(s)
2	spare_1 Spare	-	1	SpareField	3 byte(s)
3	lat Latitude of cell The latitude of the lower left-hand corner of the cell, in units of micro-degrees. The latitude is defined in the range -90 degrees to +90 degrees. [If the cell contains no valid data, this field may be set to the exceptional value -399,999,999.?? This case may not arise for the full cell.]	(1e-6) degrees	1	GeoCoordinate	4 byte(s)
4	lon Longitude of cell The longitude of the lower left-hand corner of the cell, in units of micro-degrees. The longitude is defined in the range -180 degrees to +180 degrees.	(1e-6) degrees	1	GeoCoordinate	4 byte(s)
5	m_actrk_pix_num Mean across-track pixel number A weighted mean pixel index of the nadir view clear land pixels that fall within the cell and contribute to the average. This quantity is derived by averaging the mean across-track pixel number (q.v.) over those sub-cells which contain sufficient valid pixels to contribute to the averaged LST in the cell.	-	1	ss	2 byte(s)
6	m_lst mean land surface temperature (ST) The mean land surface temperature (LST) for the cell derived using only data in the nadir view. It is derived by averaging the mean nadir-only LST (q.v.) for each of the (up to) 9 sub-cells that fall within the cell and that contain more than a minimum number of valid clear sea pixels. If none of the contributing sub-cells contains sufficient valid pixels, the field is set to the exceptional value -1.	K/100	1	ss	2 byte(s)

#	Description	Units	Count	Type	Size
7	sd_lst standard deviation of land ST The standard deviation of the mean nadir-only LST of the contributing sub-cells.	K/100	1	ss	2 byte(s)
8	pix_lst Number of pixels in land surface temperature average The number of valid 11 and 12 micron pixels contributing to the ABT determination in the cell. This will usually be the same as the number of valid 11 and 12 micron pixels contributing to the mean nadir-only LST determination in the cell, although if any sub-cells contain too few valid pixels to contribute to the averaged LST, the numbers may differ. In general the numbers of valid pixels in the 11 and 12 micron channels are expected to be the same; if they differ, the lower is given here.	-	1	us	2 byte(s)
9	m_ndvi mean NDVI The mean Normalised Difference Vegetation Index (NDVI) for the cell derived using data from both nadir and forward views. It is derived by averaging the sub-cell NDVI (q.v.) for each of the (up to) 9 sub-cells that fall within the cell and that contain more than a minimum number of valid clear land pixels. If none of the contributing sub-cells contains sufficient valid pixels, the field is set to the exceptional value -1.	-	1	ss	2 byte(s)
10	sd_ndvi standard deviation of NDVI The standard deviation of the mean NDVI of the contributing sub-cells.	-	1	ss	2 byte(s)
11	pix_ndvi Number of pixels in NDVI average The number of valid 0.87 and 0.67 micron pixels contributing to the ABT determination in the cell. This will usually be the same as the number of valid pixels contributing to the mean NDVI determination in the cell, although if any sub-cells contain too few valid pixels to contribute to the NDVI, these numbers may differ. The numbers of valid pixels in the different channel and view combinations are not necessarily equal. When they differ, the lowest is given here.	-	1	us	2 byte(s)
12	ast_conf_flags AST confidence word A 16-bit word containing confidence flags for the record. The detailed interpretation of these bits is defined in the table below. Bits 4 to 31 are currently unused.	flags	2	us	2*2 byte(s)
13	cl_top_temp_nad Cloud-top temperature, nadir view An estimate of the cloud-top temperature in the half-degree cell. This estimate is derived by generating a histogram of the 11 micron brightness temperatures of cloudy land pixels within the cell in the nadir view, and averaging the brightness temperatures of the lowest quartile. The estimate is derived from land pixels only.	K/100	1	ss	2 byte(s)
14	perc_cl_cov_nad Percentage cloud-cover, nadir view The fraction of nadir view land pixels within the cell that are cloudy, expressed as a percentage in units of 0.01%.	%/100	1	ss	2 byte(s)
15	cl_top_temp_for Cloud-top temperature, forward view An estimate of the cloud-top temperature in the half-degree cell. This estimate is derived by generating a histogram of the 11 micron brightness temperatures of cloudy land pixels within the cell in the forward view, and averaging the brightness temperatures of the lowest quartile. The estimate is derived from land pixels only.	K/100	1	ss	2 byte(s)
16	perc_cl_cov_for Percentage cloud-cover, forward view The fraction of forward view land pixels within the cell that are cloudy, expressed as a percentage in units of 0.01%.	%/100	1	ss	2 byte(s)

Record Length : 50

DS_NAME : LST record 30 arc minute cell MDS

Format Version 114.0

The table below lists the confidence flags in the AST Confidence Word.

Table 6.27

bit	meaning if set.
0	Sea MDS: Nadir-only SST retrieval used 3.7 micron channel Land MDS: Reserved
1	Sea MDS: Dual-view SST retrieval used 3.7 micron channel Land MDS: Reserved
2	Nadir view contains day-time data
3	Forward view contains day-time data
4 - 31	Unused

AST confidence word

6.6.5 LST record 17 km cell MDS

Table 6.28 LST record 17 km cell MDS

LST record 10 arc minute cell MDS

#	Description	Units	Count	Type	Size
Data Record					
0	dsr_time Nadir UTC time in MJD format The (nadir and forward view) instrument data contributing to a given cell or sub-cell may cover a range of up to 150 seconds of measurement times. It is therefore not possible to assign a unique time tag to an AST record, and the time tag is therefore arbitrarily assigned as follows. The nadir time associated with a given AST record represents the scan time of a nadir pixel contributing to the record. In general this is the time of the first filled pixel encountered during processing that falls within the geometrical boundary of the cell or sub-cell (see link), although exception cases may arise. Because the cell boundaries bear no clear geometrical relationship to the AATSR instrument scan it is not possible to state in general that this corresponds to a particular corner of the cell or sub-cell. Note also that if a cell is intersected by coastline, so that it contains both land and sea pixels, the time tag of a given record does not necessarily correspond to a pixel of the same surface type.	MJD	1	mjd	12 byte(s)
1	quality_flag Quality Indicator (-1 for blank MDSR, 0 otherwise) This field is set to -1 if all the measurement values in the record are invalid, and is set to 0 otherwise.	flag	1	BooleanFlag	1 byte(s)
2	spare_1 Spare	-	1	SpareField	3 byte(s)
3	lat Latitude of cell The latitude of the lower left-hand corner of the sub-cell, in units of micro-degrees. The latitude is defined in the range -90 degrees to +90 degrees. If the cell contains no valid data, this field may be set to the exceptional value -399,999,999.	(1e-6) degrees	1	GeoCoordinate	4 byte(s)
4	lon Longitude of cell The longitude of the lower left-hand corner of the sub-cell, in units of micro-degrees. The longitude is defined in the range -180 degrees to +180 degrees. If the cell contains no valid data, this field may be set to the exceptional	(1e-6) degrees	1	GeoCoordinate	4 byte(s)

#	Description	Units	Count	Type	Size
	value -399,999,999.				
5	m_actrk_pix_num Mean across-track pixel number The average pixel index of the nadir view clear land pixels that fall within the sub-cell. The pixel index, in the range 0 to 511 inclusive, is the across-track index of the pixel in the image, and is linearly related to the X co-ordinate by X = j - 256 km. The mean across-track pixel index is thus a measure of the X co-ordinate of the centroid of the distribution of clear land pixels that will contribute to the LST determination.	-	1	ss	2 byte(s)
6	m_lst mean land ST in cells The mean land surface temperature (LST) derived using only data in the nadir view. The LST is derived from the mean brightness temperatures in the 11 and 12 micron infra-red channels, averaged over the valid clear land pixels in the sub-cell.	K/100	1	ss	2 byte(s)
7	pix_lst Number of pixels in land surface temperature average The number of valid 11 and 12 micron pixels contributing to the LST determination in the cell. In general the numbers of valid pixels in the 11 and 12 micron channels are expected to be the same; if they differ, the lower is given here.	-	1	us	2 byte(s)
8	m_ndvi mean NDVI The mean Normalised Difference Vegetation Index (NDVI), derived from the calibrated reflectances in the 0.87 and 0.67 micron nadir channels, averaged over the valid clear sea pixels in the sub-cell.	-	1	ss	2 byte(s)
9	pix_ndvi Number of pixels in NDVI average The number of valid 11 and 12 micron pixels contributing to the NDVI determination in the cell. In general the numbers of valid pixels in the two contributing channels are expected to be the same. When the numbers of valid pixels in the different channel and view combinations differ, the lowest is given here.	-	1	us	2 byte(s)
10	ast_conf_flags AST confidence word A 16-bit word containing confidence flags for the record. Bits 0 to 3 are set to indicate whether or not 3.7 micron channel data was used in the SST retrieval, and whether or not day-time data contributes to the retrieved temperatures. The detailed interpretation of these bits is defined in the table below. Bits 4 to 31 are currently unused.	flags	2	us	2*2 byte(s)

Record Length : 38

DS_NAME : LST record 10 arc minute cell MDS

Format Version 114.0

Table 6.29

The table below lists the confidence flags in the AST Confidence Word.

bit	meaning if set.
0	Sea MDS: Nadir-only SST retrieval used 3.7 micron channel Land MDS: Reserved
1	Sea MDS: Dual-view SST retrieval used 3.7 micron channel Land MDS: Reserved
2	Nadir view contains day-time data
3	Forward view contains day-time data
4 - 31	Unused

AST confidence word

6.6.6 BT/TOA Sea record 50 km cell MDS

Table 6.30 BT/TOA Sea record 50 km cell MDS

BT/TOA Sea record 30 arc minute cell MDS

#	Description	Units	Count	Type	Size
Data Record					
0	dsr_time Nadir UTC time in MJD format The (nadir and forward view) instrument data contributing to a given cell or sub-cell may cover a range of up to 150 seconds of measurement times. It is therefore not possible to assign a unique time tag to an AST record, and the time tag is therefore arbitrarily assigned as follows. The nadir time associated with a given AST record represents the scan time of a nadir pixel contributing to the record. In general this is the time of the first filled pixel encountered during processing that falls within the geometrical boundary of the cell or sub-cell (see link), although exception cases may arise. Because the cell boundaries bear no clear geometrical relationship to the AATSR instrument scan it is not possible to state in general that this corresponds to a particular corner of the cell or sub-cell. Note also that if a cell is intersected by coastline, so that it contains both land and sea pixels, the time tag of a given record does not necessarily correspond to a pixel of the same surface type.	MJD	1	mjd	12 byte(s)
1	quality_flag Quality Indicator (-1 for blank MDSR, 0 otherwise) This field is set to -1 if all the measurement values in the record are invalid, and is set to 0 otherwise.	flag	1	BooleanFlag	1 byte(s)
2	spare_1 Spare	-	1	SpareField	3 byte(s)
3	lat Latitude of cell The latitude of the lower left-hand corner of the cell, in units of micro-degrees. The latitude is defined in the range -90 degrees to +90 degrees. If the cell contains no valid data, this field may be set to the exceptional value -399,999,999.	(1e-6) degrees	1	GeoCoordinate	4 byte(s)
4	lon Longitude of cell The longitude of the lower left-hand corner of the cell, in units of micro-degrees. The longitude is defined in the range -180 degrees to +180 degrees. If the cell contains no valid data, this field may be set to the exceptional value -399,999,999.	(1e-6) degrees	1	GeoCoordinate	4 byte(s)
5	m_actrk_pix_num Mean across-track pixel number The average pixel index to be associated with the land/sea pixels that contribute to the cell averages. It is the unweighted average of the sub-cell mean across-track pixel number for the contributing sub-cells (those containing at least one valid pixel). The pixel index, in the range 0 to 511 inclusive, is the across-track index of the pixel in the image, and ids linearly related to the X co-ordinate by X = j - 256 km. The mean across-track pixel index is thus a measure of the mean X co-ordinate of the of the distribution of clear land/sea pixels that contribute to the ABT determination.	-	1	ss	2 byte(s)
6	pix_nad Number of filled pixels in cell, nadir view The total number of filled pixels, measured in the nadir view, that fall within the cell, regardless of surface type. This differs from the total number of pixels which fall within the cell by the number of unfilled pixels. In the case of 30 arc minute cells the area of the cell, and hence the number of pixels that fall within it, is a function of the latitude..	-	1	ss	2 byte(s)
7	pix_ss_nad Number of filled pixels in cell over sea surface, nadir view	-	1	ss	2 byte(s)

#	Description	Units	Count	Type	Size
	The total number of filled pixels over sea, measured in the nadir view, that fall within the cell, irrespective of cloud state. It is thus the sum of the numbers of clear sea and cloudy sea pixel in the cell.				
8	clpix_ss_nad Percentage of cloudy pixels in cell over sea surface, nadir view The percentage of the total number of sea pixels within the cell and measured in the nadir view that are cloudy, expressed as an integer in units of 0.01%.	-	1	ss	2 byte(s)
9	sa_12bt_clr_nad Spatially averaged 12 micron BT of all clear pixels (nadir view) The mean calibrated brightness temperature in the 12 micron channel of all the valid clear pixels over sea, measured in the nadir view, that fall within the cell. This is an unweighted mean of the corresponding average BT over the sub-cells within the cell that contain at least one valid pixel. The brightness temperature is expressed as a long (32 bit) integer in units of 0.001 K. Valid mean brightness temperatures will be positive numbers in the range 170,000 to 321,000. If no valid clear sea pixels fall within the sub-cell, the field will be set to an exceptional value of -1.	K/1000	1	sl	4 byte(s)
10	sd_12bt_clr_nad Standard deviation of above The standard deviation of the sub-cell brightness temperatures that contribute to the spatially averaged 12 micron BT of all clear nadir view pixels.	K/1000	1	sl	4 byte(s)
11	sa_11bt_clr_nad Spatially averaged 11 micron BT of all clear pixels (nadir view) The mean calibrated brightness temperature in the 11 micron channel of all the valid clear pixels over sea, measured in the nadir view, that fall within the cell. This is an unweighted mean of the corresponding average BT over the sub-cells within the cell that contain at least one valid pixel. The brightness temperature is expressed as a long (32 bit) integer in units of 0.001 K. Valid mean brightness temperatures will be positive numbers in the range 170,000 to 321,000. If no valid clear sea pixels fall within the sub-cell, the field will be set to an exceptional value of -1.	K/1000	1	sl	4 byte(s)
12	sd_11bt_clr_nad Standard deviation of above The standard deviation of the sub-cell brightness temperatures that contribute to the spatially averaged 11 micron BT of all clear nadir view pixels.	K/1000	1	sl	4 byte(s)
13	sa_37bt_clr_nad Spatially averaged 3.7 micron BT of all clear pixels (nadir view) The mean calibrated brightness temperature in the 3.7 micron channel of all the valid clear pixels over sea, measured in the nadir view, that fall within the cell. This is an unweighted mean of the corresponding average BT over the sub-cells within the cell that contain at least one valid pixel. The brightness temperature is expressed as a long (32 bit) integer in units of 0.001 K. Valid mean brightness temperatures will be positive numbers in the range 195,000 to 321,000. If no valid clear sea pixels fall within the sub-cell, the field will be set to an exceptional value of -1.	K/1000	1	sl	4 byte(s)
14	sd_37bt_clr_nad Standard deviation of above The standard deviation of the sub-cell brightness temperatures that contribute to the spatially averaged 3.7 micron BT of all clear nadir view pixels.	K/1000	1	sl	4 byte(s)
15	sa_16toa_clr_nad Spatially averaged 1.6 micron TOA reflectance of all clear pixels (nadir view) The mean calibrated reflectance in the 1.6 micron channel of all the valid clear pixels over sea, measured in the nadir view, that fall within the cell. This is an unweighted mean of the corresponding average TOA reflectance over the sub-cells within the cell that contain at least one valid pixel. The reflectance is expressed as a short (16 bit) integer in units of 0.01 %. Valid reflectance values will be positive numbers in the range 0 to 10,000. If no valid clear sea pixels fall within the cell, the field will be set to an exceptional value of -1.	%/100	1	ss	2 byte(s)
16	sd_16toa_clr_nad Standard deviation of above The standard deviation of the sub-cell reflectance values that contribute to the spatially averaged 1.6 micron TOA reflectance of all clear nadir view pixels.	%/100	1	ss	2 byte(s)
17	sa_87toa_clr_nad Spatially averaged 0.87 micron TOA reflectance of all clear pixels (nadir view) The mean calibrated brightness temperature in the 0.87 micron channel of all the valid clear pixels over sea, measured in the nadir view, that fall within the cell. This is an unweighted mean of the corresponding average BT over the sub-cells within the cell that contain at least one valid pixel. The brightness temperature is expressed as a long (32 bit) integer in units of 0.001 K. Valid mean brightness temperatures will be positive numbers in the range 195,000 to 321,000. If no valid clear sea pixels fall within the sub-cell, the field will be set to an exceptional value of -1.	%/100	1	ss	2 byte(s)
18	sd_87toa_clr_nad Standard deviation of above The standard deviation of the sub-cell reflectance values that contribute to the spatially averaged 0.87 micron TOA reflectance of all clear nadir view pixels.	%/100	1	ss	2 byte(s)
19	sa_67toa_clr_nad Spatially averaged 0.67 micron TOA reflectance of all clear pixels (nadir view) The mean calibrated brightness temperature in the 0.67 micron channel of all the valid clear pixels over sea, measured in the nadir view, that fall within the cell. This is an unweighted mean of the corresponding average BT over the sub-cells within the cell that contain at least one valid pixel. The brightness temperature is expressed as a long (32 bit) integer in units of 0.001 K. Valid mean brightness temperatures will be positive numbers in the range 195,000 to 321,000. If no valid	%/100	1	ss	2 byte(s)

#	Description	Units	Count	Type	Size
	clear sea pixels fall within the sub-cell, the field will be set to an exceptional value of -1.				
20	sd_67toa_clr_nad Standard deviation of above The standard deviation of the sub-cell reflectance values that contribute to the spatially averaged 0.67 micron TOA reflectance of all clear nadir view pixels.	%/100	1	ss	2 byte(s)
21	sa_55toa_clr_nad Spatially averaged 0.55 micron TOA reflectance of all clear pixels (nadir view) The mean calibrated brightness temperature in the 0.55 micron channel of all the valid clear pixels over sea, measured in the nadir view, that fall within the cell. This is an unweighted mean of the corresponding average BT over the sub-cells within the cell that contain at least one valid pixel. The brightness temperature is expressed as a long (32 bit) integer in units of 0.001 K. Valid mean brightness temperatures will be positive numbers in the range 195,000 to 321,000. If no valid clear sea pixels fall within the sub-cell, the field will be set to an exceptional value of -1.	%/100	1	ss	2 byte(s)
22	sd_55toa_clr_nad Standard deviation of above The standard deviation of the sub-cell reflectance values that contribute to the spatially averaged 0.55 micron TOA reflectance of all clear nadir view pixels.	%/100	1	ss	2 byte(s)
23	sa_12bt_cl_nad Spatially averaged 12 micron BT of all cloudy pixels (nadir view) The mean calibrated brightness temperature in the 12 micron channel of all the valid cloudy pixels over sea, measured in the nadir view, that fall within the cell. This is an unweighted mean of the corresponding average BT over the sub-cells within the cell that contain at least one valid pixel. The brightness temperature is expressed as a long (32 bit) integer in units of 0.001 K. Valid mean brightness temperatures will be positive numbers in the range 170,000 to 321,000. If no valid cloudy sea pixels fall within the sub-cell, the field will be set to an exceptional value of -1.	K/1000	1	sl	4 byte(s)
24	sd_12bt_cl_nad Standard deviation of above The standard deviation of the sub-cell brightness temperatures that contribute to the spatially averaged 12 micron BT of all cloudy nadir view pixels.	K/1000	1	sl	4 byte(s)
25	sa_11bt_cl_nad Spatially averaged 11 micron BT of all cloudy pixels (nadir view) The mean calibrated brightness temperature in the 11 micron channel of all the valid cloudy pixels over sea, measured in the nadir view, that fall within the cell. This is an unweighted mean of the corresponding average BT over the sub-cells within the cell that contain at least one valid pixel. The brightness temperature is expressed as a long (32 bit) integer in units of 0.001 K. Valid mean brightness temperatures will be positive numbers in the range 170,000 to 321,000. If no valid cloudy sea pixels fall within the sub-cell, the field will be set to an exceptional value of -1.	K/1000	1	sl	4 byte(s)
26	sd_11bt_cl_nad Standard deviation of above The standard deviation of the sub-cell brightness temperatures that contribute to the spatially averaged 11 micron BT of all cloudy nadir view pixels.	K/1000	1	sl	4 byte(s)
27	sa_37bt_cl_nad Spatially averaged 3.7 micron BT of all cloudy pixels (nadir view) The mean calibrated brightness temperature in the 3.7 micron channel of all the valid cloudy pixels over sea, measured in the nadir view, that fall within the cell. This is an unweighted mean of the corresponding average BT over the sub-cells within the cell that contain at least one valid pixel. The brightness temperature is expressed as a long (32 bit) integer in units of 0.001 K. Valid mean brightness temperatures will be positive numbers in the range 195,000 to 321,000. If no valid cloudy sea pixels fall within the sub-cell, the field will be set to an exceptional value of -1.	K/1000	1	sl	4 byte(s)
28	sd_37bt_cl_nad Standard deviation of above The standard deviation of the sub-cell brightness temperatures that contribute to the spatially averaged 3.7 micron BT of all cloudy nadir view pixels.	K/1000	1	sl	4 byte(s)
29	sa_16toa_cl_nad Spatially averaged 1.6 micron TOA reflectance of all cloudy pixels (nadir view) The mean calibrated reflectance in the 1.6 micron channel of all the valid cloudy pixels over sea, measured in the nadir view, that fall within the cell. This is an unweighted mean of the corresponding average TOA reflectance over the sub-cells within the cell that contain at least one valid pixel. The reflectance is expressed as a short (16 bit) integer in units of 0.01 %. Valid reflectance values will be positive numbers in the range 0 to 10,000. If no valid cloudy sea pixels fall within the cell, the field will be set to an exceptional value of -1.	%/100	1	ss	2 byte(s)
30	sd_16toa_cl_nad Standard deviation of above The standard deviation of the sub-cell reflectance values that contribute to the spatially averaged 1.6 micron TOA reflectance of all cloudy nadir view pixels.	%/100	1	ss	2 byte(s)
31	sa_87toa_cl_nad Spatially averaged 0.87 micron TOA reflectance of all cloudy pixels (nadir view) The mean calibrated brightness temperature in the 0.87 micron channel of all the valid cloudy pixels over sea, measured in the nadir view, that fall within the cell. This is an unweighted mean of the corresponding average BT over the sub-cells within the cell that contain at least one valid pixel. The brightness temperature is expressed as a long (32 bit) integer in units of 0.001 K. Valid mean brightness temperatures will be positive numbers in the range 195,000 to 321,000. If no valid cloudy sea pixels fall within the sub-cell, the field will be set to an exceptional	%/100	1	ss	2 byte(s)

#	Description	Units	Count	Type	Size
	value of -1.				
32	sd_87toa_cl_nad Standard deviation of above The standard deviation of the sub-cell reflectance values that contribute to the spatially averaged 0.87 micron TOA reflectance of all cloudy nadir view pixels.	%/100	1	ss	2 byte(s)
33	sa_67toa_cl_nad Spatially averaged 0.67 micron TOA reflectance of all cloudy pixels (nadir view) The mean calibrated brightness temperature in the 0.67 micron channel of all the valid cloudy pixels over sea, measured in the nadir view, that fall within the cell. This is an unweighted mean of the corresponding average BT over the sub-cells within the cell that contain at least one valid pixel. The brightness temperature is expressed as a long (32 bit) integer in units of 0.001 K. Valid mean brightness temperatures will be positive numbers in the range 195,000 to 321,000. If no valid cloudy sea pixels fall within the sub-cell, the field will be set to an exceptional value of -1.	%/100	1	ss	2 byte(s)
34	sd_67toa_cl_nad Standard deviation of above The standard deviation of the sub-cell reflectance values that contribute to the spatially averaged 0.67 micron TOA reflectance of all cloudy nadir view pixels.	%/100	1	ss	2 byte(s)
35	sa_55toa_cl_nad Spatially averaged 0.55 micron TOA reflectance of all cloudy pixels (nadir view) The mean calibrated brightness temperature in the 0.55 micron channel of all the valid cloudy pixels over sea, measured in the nadir view, that fall within the cell. This is an unweighted mean of the corresponding average BT over the sub-cells within the cell that contain at least one valid pixel. The brightness temperature is expressed as a long (32 bit) integer in units of 0.001 K. Valid mean brightness temperatures will be positive numbers in the range 195,000 to 321,000. If no valid cloudy sea pixels fall within the sub-cell, the field will be set to an exceptional value of -1.	%/100	1	ss	2 byte(s)
36	sd_55toa_cl_nad Standard deviation of above The standard deviation of the sub-cell reflectance values that contribute to the spatially averaged 0.55 micron TOA reflectance of all cloudy nadir view pixels	%/100	1	ss	2 byte(s)
37	fail_flag_nad Pixel threshold failure flags for averages, nadir view A 16 bit word of quality flags for the nadir view data. Each of bits 0 to 13 of the word is a flag that corresponds to one of the channel/cloud flag combinations (i.e. to one of the nadir view spatially averaged fields of the product, which if set indicates that the number of pixels contributing to the corresponding cell average is less than a pre-defined quality threshold. The meanings of the flags are tabulated below.	-	1	us	2 byte(s)
38	pix_for Number of filled pixels in cell, forward view The total number of filled pixels, measured in the forward view, that fall within the cell, regardless of surface type. This differs from the total number of pixels which fall within the cell by the number of unfilled pixels. In the case of 30 arc minute cells the area of the cell, and hence the number of pixels that fall within it, is a function of the latitude..	-	1	ss	2 byte(s)
39	pix_ss_for Number of filled pixels in cell over sea surface, forward view The total number of filled pixels over sea, measured in the forward view, that fall within the cell, irrespective of cloud state. It is thus the sum of the numbers of clear sea and cloudy sea pixel in the cell.	-	1	ss	2 byte(s)
40	perc_cl_pix_ss_for Percentage of cloudy pixels in cell over sea surface, forward view The percentage of the total number of sea pixels within the cell and measured in the forward view that are cloudy, expressed as an integer in units of 0.01%.	-	1	ss	2 byte(s)
41	sa_12bt_clr_for Spatially averaged 12 micron BT of all clear pixels (forward view) The mean calibrated brightness temperature in the 12 micron channel of all the valid clear pixels over sea, measured in the forward view, that fall within the cell. This is an unweighted mean of the corresponding average BT over the sub-cells within the cell that contain at least one valid pixel. The brightness temperature is expressed as a long (32 bit) integer in units of 0.001 K. Valid mean brightness temperatures will be positive numbers in the range 170,000 to 321,000. If no valid clear sea pixels fall within the sub-cell, the field will be set to an exceptional value of -1.	K/1000	1	sl	4 byte(s)
42	sd_12bt_clr_for Standard deviation of above The standard deviation of the sub-cell brightness temperatures that contribute to the spatially averaged 12 micron BT of all clear forward view pixels.	K/1000	1	sl	4 byte(s)
43	sa_11bt_clr_for Spatially averaged 11 micron BT of all clear pixels (forward view) The mean calibrated brightness temperature in the 11 micron channel of all the valid clear pixels over sea, measured in the forward view, that fall within the cell. This is an unweighted mean of the corresponding average BT over the sub-cells within the cell that contain at least one valid pixel. The brightness temperature is expressed as a long (32 bit) integer in units of 0.001 K. Valid mean brightness temperatures will be positive numbers in the range 170,000 to 321,000. If no valid clear sea pixels fall within the sub-cell, the field will be set to an exceptional value of -1.	K/1000	1	sl	4 byte(s)
44	sd_11bt_clr_for Standard deviation of above	K/1000	1	sl	4 byte(s)

#	Description	Units	Count	Type	Size
	The standard deviation of the sub-cell brightness temperatures that contribute to the spatially averaged 11 micron BT of all clear forward view pixels.				
45	sa_37bt_clr_for Spatially averaged 3.7 micron BT of all clear pixels (forward view) The mean calibrated brightness temperature in the 3.7 micron channel of all the valid clear pixels over sea, measured in the forward view, that fall within the cell. This is an unweighted mean of the corresponding average BT over the sub-cells within the cell that contain at least one valid pixel. The brightness temperature is expressed as a long (32 bit) integer in units of 0.001 K. Valid mean brightness temperatures will be positive numbers in the range 195,000 to 321,000. If no valid clear sea pixels fall within the sub-cell, the field will be set to an exceptional value of -1.	K/1000	1	sl	4 byte(s)
46	sd_37bt_clr_for Standard deviation of above The standard deviation of the sub-cell brightness temperatures that contribute to the spatially averaged 3.7 micron BT of all clear forward view pixels.	K/1000	1	sl	4 byte(s)
47	sa_16toa_clr_for Spatially averaged 1.6 micron TOA reflectance of all clear pixels (forward view) The mean calibrated reflectance in the 1.6 micron channel of all the valid clear pixels over sea, measured in the forward view, that fall within the cell. This is an unweighted mean of the corresponding average TOA reflectance over the sub-cells within the cell that contain at least one valid pixel. The reflectance is expressed as a short (16 bit) integer in units of 0.01 %. Valid reflectance values will be positive numbers in the range 0 to 10,000. If no valid clear sea pixels fall within the cell, the field will be set to an exceptional value of -1.	%/100	1	ss	2 byte(s)
48	sd_16toa_clr_for Standard deviation of above The standard deviation of the sub-cell reflectance values that contribute to the spatially averaged 1.6 micron TOA reflectance of all clear forward view pixels.	%/100	1	ss	2 byte(s)
49	sa_87toa_clr_for Spatially averaged 0.87 micron TOA reflectance of all clear pixels (forward view) The mean calibrated brightness temperature in the 0.87 micron channel of all the valid clear pixels over sea, measured in the forward view, that fall within the cell. This is an unweighted mean of the corresponding average BT over the sub-cells within the cell that contain at least one valid pixel. The brightness temperature is expressed as a long (32 bit) integer in units of 0.001 K. Valid mean brightness temperatures will be positive numbers in the range 195,000 to 321,000. If no valid clear sea pixels fall within the sub-cell, the field will be set to an exceptional value of -1.	%/100	1	ss	2 byte(s)
50	sd_87toa_clr_for Standard deviation of above The standard deviation of the sub-cell reflectance values that contribute to the spatially averaged 0.87 micron TOA reflectance of all clear forward view pixels.	%/100	1	ss	2 byte(s)
51	sa_67toa_clr_for Spatially averaged 0.67 micron TOA reflectance of all clear pixels (forward view) The mean calibrated brightness temperature in the 0.67 micron channel of all the valid clear pixels over sea, measured in the forward view, that fall within the cell. This is an unweighted mean of the corresponding average BT over the sub-cells within the cell that contain at least one valid pixel. The brightness temperature is expressed as a long (32 bit) integer in units of 0.001 K. Valid mean brightness temperatures will be positive numbers in the range 195,000 to 321,000. If no valid clear sea pixels fall within the sub-cell, the field will be set to an exceptional value of -1.	%/100	1	ss	2 byte(s)
52	sd_67toa_clr_for Standard deviation of above The standard deviation of the sub-cell reflectance values that contribute to the spatially averaged 0.67 micron TOA reflectance of all clear forward view pixels.	%/100	1	ss	2 byte(s)
53	sa_55toa_clr_for Spatially averaged 0.55 micron TOA reflectance of all clear pixels (forward view) The mean calibrated brightness temperature in the 0.55 micron channel of all the valid clear pixels over sea, measured in the forward view, that fall within the cell. This is an unweighted mean of the corresponding average BT over the sub-cells within the cell that contain at least one valid pixel. The brightness temperature is expressed as a long (32 bit) integer in units of 0.001 K. Valid mean brightness temperatures will be positive numbers in the range 195,000 to 321,000. If no valid clear sea pixels fall within the sub-cell, the field will be set to an exceptional value of -1.	%/100	1	ss	2 byte(s)
54	sd_55toa_clr_for Standard deviation of above The standard deviation of the sub-cell reflectance values that contribute to the spatially averaged 0.55 micron TOA reflectance of all clear forward view pixels.	%/100	1	ss	2 byte(s)
55	sa_12bt_cl_for Spatially averaged 12 micron BT of all cloudy pixels (forward view) The mean calibrated brightness temperature in the 12 micron channel of all the valid cloudy pixels over sea, measured in the forward view, that fall within the cell. This is an unweighted mean of the corresponding average BT over the sub-cells within the cell that contain at least one valid pixel. The brightness temperature is expressed as a long (32 bit) integer in units of 0.001 K. Valid mean brightness temperatures will be positive numbers in the range 170,000 to 321,000. If no valid cloudy sea pixels fall within the sub-cell, the field will be set to an exceptional value of -1.	K/1000	1	sl	4 byte(s)
56	sd_12bt_cl_for Standard deviation of above The standard deviation of the sub-cell brightness temperatures that contribute to	K/1000	1	sl	4 byte(s)

#	Description	Units	Count	Type	Size
	the spatially averaged 12 micron BT of all cloudy forward view pixels.				
57	sa_11bt_cl_for Spatially averaged 11 micron BT of all cloudy pixels (forward view) The mean calibrated brightness temperature in the 11 micron channel of all the valid cloudy pixels over sea, measured in the forward view, that fall within the cell. This is an unweighted mean of the corresponding average BT over the sub-cells within the cell that contain at least one valid pixel. The brightness temperature is expressed as a long (32 bit) integer in units of 0.001 K. Valid mean brightness temperatures will be positive numbers in the range 170,000 to 321,000. If no valid cloudy sea pixels fall within the sub-cell, the field will be set to an exceptional value of -1.	K/1000	1	sl	4 byte(s)
58	sd_11bt_cl_for Standard deviation of above The standard deviation of the sub-cell brightness temperatures that contribute to the spatially averaged 11 micron BT of all cloudy forward view pixels.	K/1000	1	sl	4 byte(s)
59	sa_37bt_cl_for Spatially averaged 3.7 micron BT of all cloudy pixels (forward view) The mean calibrated brightness temperature in the 3.7 micron channel of all the valid cloudy pixels over sea, measured in the forward view, that fall within the cell. This is an unweighted mean of the corresponding average BT over the sub-cells within the cell that contain at least one valid pixel. The brightness temperature is expressed as a long (32 bit) integer in units of 0.001 K. Valid mean brightness temperatures will be positive numbers in the range 195,000 to 321,000. If no valid cloudy sea pixels fall within the sub-cell, the field will be set to an exceptional value of -1.	K/1000	1	sl	4 byte(s)
60	sd_37bt_cl_for Standard deviation of above The standard deviation of the sub-cell brightness temperatures that contribute to the spatially averaged 3.7 micron BT of all cloudy forward view pixels.	K/1000	1	sl	4 byte(s)
61	sa_16toa_cl_for Spatially averaged 1.6 micron TOA reflectance of all cloudy pixels (forward view) The mean calibrated reflectance in the 1.6 micron channel of all the valid cloudy pixels over sea, measured in the forward view, that fall within the cell. This is an unweighted mean of the corresponding average TOA reflectance over the sub-cells within the cell that contain at least one valid pixel. The reflectance is expressed as a short (16 bit) integer in units of 0.01 %. Valid reflectance values will be positive numbers in the range 0 to 10,000. If no valid cloudy sea pixels fall within the cell, the field will be set to an exceptional value of -1.	%/100	1	ss	2 byte(s)
62	sd_16toa_cl_for Standard deviation of above The standard deviation of the sub-cell reflectance values that contribute to the spatially averaged 1.6 micron TOA reflectance of all cloudy forward view pixels.	%/100	1	ss	2 byte(s)
63	sa_87toa_cl_for Spatially averaged 0.87 micron TOA reflectance of all cloudy pixels (forward view) The mean calibrated brightness temperature in the 0.87 micron channel of all the valid cloudy pixels over sea, measured in the forward view, that fall within the cell. This is an unweighted mean of the corresponding average BT over the sub-cells within the cell that contain at least one valid pixel. The brightness temperature is expressed as a long (32 bit) integer in units of 0.001 K. Valid mean brightness temperatures will be positive numbers in the range 195,000 to 321,000. If no valid cloudy sea pixels fall within the sub-cell, the field will be set to an exceptional value of -1.	%/100	1	ss	2 byte(s)
64	sd_87toa_cl_for Standard deviation of above The standard deviation of the sub-cell reflectance values that contribute to the spatially averaged 0.87 micron TOA reflectance of all cloudy forward view pixels.	%/100	1	ss	2 byte(s)
65	sa_67toa_cl_for Spatially averaged 0.67 micron TOA reflectance of all cloudy pixels (forward view) The mean calibrated brightness temperature in the 0.67 micron channel of all the valid cloudy pixels over sea, measured in the forward view, that fall within the cell. This is an unweighted mean of the corresponding average BT over the sub-cells within the cell that contain at least one valid pixel. The brightness temperature is expressed as a long (32 bit) integer in units of 0.001 K. Valid mean brightness temperatures will be positive numbers in the range 195,000 to 321,000. If no valid cloudy sea pixels fall within the sub-cell, the field will be set to an exceptional value of -1.	%/100	1	ss	2 byte(s)
66	sd_67toa_cl_for Standard deviation of above The standard deviation of the sub-cell reflectance values that contribute to the spatially averaged 0.67 micron TOA reflectance of all cloudy forward view pixels.	%/100	1	ss	2 byte(s)
67	sa_55toa_cl_for Spatially averaged 0.55 micron TOA reflectance of all cloudy pixels (forward view) The mean calibrated brightness temperature in the 0.55 micron channel of all the valid cloudy pixels over sea, measured in the forward view, that fall within the cell. This is an unweighted mean of the corresponding average BT over the sub-cells within the cell that contain at least one valid pixel. The brightness temperature is expressed as a long (32 bit) integer in units of 0.001 K. Valid mean brightness temperatures will be positive numbers in the range 195,000 to 321,000. If no valid cloudy sea pixels fall within the sub-cell, the field will be set to an exceptional value of -1.	%/100	1	ss	2 byte(s)
68	sd_55toa_cl_for Standard deviation of above The standard deviation of the sub-cell reflectance values that contribute to the spatially averaged 0.55 micron TOA reflectance of all cloudy forward view pixels	%/100	1	ss	2 byte(s)

#	Description	Units	Count	Type	Size
69	fail_flag_for Pixel threshold failure flags for averages, foward view A 16 bit word of quality flags for the forward view data. Each of bits 0 to 13 of the word is a flag that corresponds to one of the channel/cloud flag combinations (i.e. to one of the forward view spatially averaged fields of the product, which if set indicates that the number of pixels contributing to the corresponding cell average is less than a pre-defined quality threshold. The meanings of the flags are tabulated below.	-	1	us	2 byte(s)
70	pix_nsig_nad Number of filled pixels (N-Sigma), nadir view Reserved: this field is currently undefined and is set to zero.	-	1	ss	2 byte(s)
71	pix_ss Percentage filled pixels over sea surface Reserved: this field is currently undefined and is set to zero.	%/100	1	ss	2 byte(s)
72	low_11bt_cl_nad Lowest 11 micron BT of all cloudy pixels, nadir view The minimum brightness temperature in the 11 micron channel of all valid cloudy sea pixels measured in the nadir view and falling within the cell, in units of 0.01K. A pixel is valid in this sense if its 11 micron brightness temperature falls between 190K and 290 K.	K/100	1	ss	2 byte(s)
73	corr_12bt_nad Corresponding 12 micron BT, nadir view The brightness temperature in the 12 micron nadir view channel, in units of 0.01K, of the cloudy sea pixel (above) having the minimum brightness temperature measured in the 11 micron channel.	K/100	1	ss	2 byte(s)
74	corr_37bt_nad Corresponding 3.7 micron BT, nadir view The brightness temperature in the 3.7 micron nadir view channel, in units of 0.01K, of the cloudy sea pixel (above) having the minimum brightness temperature measured in the 11 micron channel.	K/100	1	ss	2 byte(s)
75	corr_16ref_nad Corresponding 1.6 micron reflectance, nadir view The reflectance at 1.6 micron wavelength, in units of 0.01%, of the nadir view cloudy sea pixel (above) having the minimum brightness temperature measured in the 11 micron channel.	%/100	1	ss	2 byte(s)
76	corr_87ref_nad Corresponding 0.87 micron reflectance, nadir view The reflectance at 0.87 micron wavelength, in units of 0.01%, of the nadir view cloudy sea pixel (above) having the minimum brightness temperature measured in the 11 micron channel.	%/100	1	ss	2 byte(s)
77	corr_67ref_nad Corresponding 0.67 micron reflectance, nadir view The reflectance at 0.67 micron wavelength, in units of 0.01%, of the nadir view cloudy sea pixel (above) having the minimum brightness temperature measured in the 11 micron channel.	%/100	1	ss	2 byte(s)
78	corr_55ref_nad Corresponding 0.55 micron reflectance, nadir view The reflectance at 0.55 micron wavelength, in units of 0.01%, of the nadir view cloudy sea pixel (above) having the minimum brightness temperature measured in the 11 micron channel.	%/100	1	ss	2 byte(s)
79	low_11bt_cl_for Lowest 11 micron BT of all cloudy pixels, forward view The minimum brightness temperature in the 11 micron channel of all valid cloudy sea pixels measured in the forward view and falling within the cell, in units of 0.01K. A pixel is valid in this sense if its 11 micron brightness temperature falls between 190K and 290 K.	K/100	1	ss	2 byte(s)
80	corr_12bt_for Corresponding 12 micron BT, forward view The brightness temperature in the 12 micron forward view channel, in units of 0.01K, of the cloudy sea pixel (above) having the minimum brightness temperature measured in the 11 micron channel.	K/100	1	ss	2 byte(s)
81	corr_37bt_for Corresponding 3.7 micron BT, forward view The brightness temperature in the 3.7 micron forward view channel, in units of 0.01K, of the cloudy sea pixel (above) having the minimum brightness temperature measured in the 11 micron channel.	K/100	1	ss	2 byte(s)
82	corr_16ref_for Corresponding 1.6 micron reflectance, forward view The reflectance at 1.6 micron wavelength, in units of 0.01%, of the forward view cloudy sea pixel (above) having the minimum brightness temperature measured in the 11 micron channel.	%/100	1	ss	2 byte(s)
83	corr_87ref_for Corresponding 0.87 micron reflectance, forward view The reflectance at 0.87 micron wavelength, in units of 0.01%, of the forward view cloudy sea pixel (above) having the minimum brightness temperature measured in the 11 micron channel.	%/100	1	ss	2 byte(s)
84	corr_67ref_for Corresponding 0.67 micron reflectance, forward view The reflectance at 0.67 micron wavelength, in units of 0.01%, of the forward view cloudy sea pixel (above) having the minimum brightness temperature measured in	%/100	1	ss	2 byte(s)

#	Description	Units	Count	Type	Size
	the 11 micron channel.				
85	corr_55ref_for Corresponding 0.55 micron reflectance, forward view The reflectance at 0.55 micron wavelength, in units of 0.01%, of the forward view cloudy sea pixel (above) having the minimum brightness temperature measured in the 11 micron channel.	%/100	1	ss	2 byte(s)

Record Length : 234

DS_NAME : BT/TOA Sea record 30 arc minute cell MDS

Format Version 114.0

The following table defines the contents of the pixel threshold failure flags word.

Table 6.31

Bit	Meaning if set
0	Number of clear pixels contributing to average is less than threshold, 12 micron channel
1	Number of clear pixels contributing to average is less than threshold, 11 micron channel
2	Number of clear pixels contributing to average is less than threshold, 3.7 micron channel
3	Number of clear pixels contributing to average is less than threshold, 1.6 micron channel
4	Number of clear pixels contributing to average is less than threshold, 0.870 micron channel
5	Number of clear pixels contributing to average is less than threshold, 0.670 micron channel
6	Number of clear pixels contributing to average is less than threshold, 0.555 micron channel
7	Number of cloudy pixels contributing to average is less than threshold, 12 micron channel
8	Number of cloudy pixels contributing to average is less than threshold, 11 micron channel
9	Number of cloudy pixels contributing to average is less than threshold, 3.7 micron channel
10	Number of cloudy pixels contributing to average is less than threshold, 1.6 micron channel
11	Number of cloudy pixels contributing to average is less than threshold, 0.870 micron channel
12	Number of cloudy pixels contributing to average is less than threshold, 0.670 micron channel
13	Number of cloudy pixels contributing to average is less than threshold, 0.555 micron channel
14	View contains day-time data
15	Unused

Pixel threshold failure flags (nadir or forward view).

Note: Bits are numbered from ms bit 15 to ls bit 0.

6.6.7 BT/TOA Sea record 17 km cell MDS

Table 6.32 BT/TOA Sea record 17 km cell MDS

BT/TOA Sea record 10 arc minute cell MDS

#	Description	Units	Count	Type	Size
Data Record					
0	dsr_time Nadir UTC time in MJD format The (nadir and forward view) instrument data contributing to a given cell or sub-cell may cover a range of up to 150 seconds of measurement times. It is therefore not possible to assign a unique time tag to an AST record, and the time tag is therefore arbitrarily assigned as follows. The nadir time associated with a given AST record represents the scan time of a nadir pixel contributing to the record. In general this is the time of the first filled pixel encountered during processing that falls within the geometrical boundary of the cell or sub-cell (see link), although exception cases may arise. Because the cell boundaries bear no clear geometrical relationship to the AATSR instrument scan it is not possible to state in general that this corresponds to a particular corner of the cell or sub-cell. Note also that if a cell is intersected by coastline, so that it contains both land and sea pixels, the time tag of a given record does not necessarily correspond to a pixel of the same surface type.	MJD	1	mjd	12 byte(s)
1	quality_flag Quality Indicator (-1 for blank MDSR, 0 otherwise) This field is set to -1 if all the measurement values in the record are invalid, and is set to 0 otherwise.	flag	1	BooleanFlag	1 byte(s)
2	spare_1 Spare	-	1	SpareField	3 byte(s)
3	lat Latitude of cell The latitude of the lower left-hand corner of the sub-cell, in units of micro-degrees. The latitude is defined in the range -90 degrees to +90 degrees. If the cell contains no valid data, this field may be set to the exceptional value -399,999,999.	(1e-6) degrees	1	GeoCoordinate	4 byte(s)
4	lon Longitude of cell The longitude of the lower left-hand corner of the sub-cell, in units of micro-degrees. The longitude is defined in the range -180 degrees to +180 degrees. If the cell contains no valid data, this field may be set to the exceptional value -399,999,999.	(1e-6) degrees	1	GeoCoordinate	4 byte(s)
5	m_actrk_pix_num Mean across-track pixel number The average pixel index of the nadir view clear sea pixels that fall within the sub-cell. The pixel index, in the range 0 to 511 inclusive, is the across-track index of the pixel in the image, and is linearly related to the X co-ordinate by X = j - 256 km. The mean across-track pixel index is thus a measure of the X co-ordinate of the centroid of the distribution of clear sea pixels that will contribute to the SST determination. It may be used to select SST retrieval coefficients for the cell.	-	1	ss	2 byte(s)
6	pix_nad Number of filled pixels in cell, nadir view The total number of filled pixels, measured in the nadir view, that fall within the sub-cell, regardless of surface type. This differs from the total number of pixels which fall within the sub-cell by the number of unfilled pixels. In the case of 10 arc minute cells the area of the cell, and hence the number of pixels that fall within it, is a function of the latitude.	-	1	ss	2 byte(s)
7	pix_ss_nad Number of filled pixels in cell over sea surface, nadir view The total number of filled pixels over sea, measured in the nadir view, that fall within the sub-cell, irrespective of cloud state. It is thus the sum of the numbers of clear sea and cloudy sea pixel in the sub-cell.	-	1	ss	2 byte(s)
8	clpix_ss_nad Percentage of cloudy pixels in cell over sea surface, nadir view The percentage of the total number of sea pixels within the sub-cell and measured in the nadir view that are cloudy, expressed as an integer in units of 0.01%.	-	1	ss	2 byte(s)
9	sa_12bt_clr_nad Spatially averaged 12 micron BT of all clear pixels (nadir view) The mean calibrated brightness temperature in the 12 micron channel of all the valid clear pixels over sea, measured in the nadir [forward] view, that fall within	K/1000	1	sl	4 byte(s)

#	Description	Units	Count	Type	Size
	the sub-cell. The brightness temperature is expressed as a long (32 bit) integer in units of 0.001 K. Valid mean brightness temperatures will be positive numbers in the range 170,000 to 321,000. If no valid clear sea pixels fall within the sub-cell, the field will be set to an exceptional value of -1.				
10	sa_11bt_clr_nad Spatially averaged 11 micron BT of all clear pixels (nadir view) The mean calibrated brightness temperature in the 11 micron channel of all the valid clear pixels over sea, measured in the nadir view, that fall within the sub-cell. The brightness temperature is expressed as a long (32 bit) integer in units of 0.001 K. Valid mean brightness temperatures will be positive numbers in the range 170,000 to 321,000. If no valid clear sea pixels fall within the sub-cell, the field will be set to an exceptional value of -1.	K/1000	1	sl	4 byte(s)
11	sa_37bt_clr_nad Spatially averaged 3.7 micron BT of all clear pixels (nadir view) The mean calibrated brightness temperature in the 3.7 micron channel of all the valid clear pixels over sea, measured in the nadir view, that fall within the sub-cell. The brightness temperature is expressed as a long (32 bit) integer in units of 0.001 K. Valid mean brightness temperatures will be positive numbers in the range 195,000 to 321,000. If no valid clear sea pixels fall within the sub-cell, the field will be set to an exceptional value of -1.	K/1000	1	sl	4 byte(s)
12	sa_16toa_clr_nad Spatially averaged 1.6 micron TOA reflectance of all clear pixels (nadir view) The mean calibrated reflectance in the 1.6 micron channel of all the valid clear pixels over sea, measured in the nadir view, that fall within the sub-cell. The reflectance is expressed as a short (16 bit) integer in units of 0.01 %. Valid mean reflectances will be positive numbers in the range 0 to 10,000. If no valid clear sea pixels fall within the sub-cell, the field will be set to an exceptional value of -1.	%/100	1	ss	2 byte(s)
13	sa_87toa_clr_nad Spatially averaged 0.87 micron TOA reflectance of all clear pixels (nadir view) The mean calibrated reflectance in the 0.87 micron channel of all the valid clear pixels over sea, measured in the nadir view, that fall within the sub-cell. The reflectance is expressed as a short (16 bit) integer in units of 0.01 %. Valid mean reflectances will be positive numbers in the range 0 to 10,000. If no valid clear sea pixels fall within the sub-cell, the field will be set to an exceptional value of -1.	%/100	1	ss	2 byte(s)
14	sa_67toa_clr_nad Spatially averaged 0.67 micron TOA reflectance of all clear pixels (nadir view) The mean calibrated reflectance in the 0.67 micron channel of all the valid clear pixels over sea, measured in the nadir view, that fall within the sub-cell. The reflectance is expressed as a short (16 bit) integer in units of 0.01 %. Valid mean reflectances will be positive numbers in the range 0 to 10,000. If no valid clear sea pixels fall within the sub-cell, the field will be set to an exceptional value of -1.	%/100	1	ss	2 byte(s)
15	sa_55toa_clr_nad Spatially averaged 0.55 micron TOA reflectance of all clear pixels (nadir view) The mean calibrated reflectance in the 0.55 micron channel of all the valid clear pixels over sea, measured in the nadir view, that fall within the sub-cell. The reflectance is expressed as a short (16 bit) integer in units of 0.01 %. Valid mean reflectances will be positive numbers in the range 0 to 10,000. If no valid clear sea pixels fall within the sub-cell, the field will be set to an exceptional value of -1.	%/100	1	ss	2 byte(s)
16	sa_12bt_cl_nad Spatially averaged 12 micron BT of all cloudy pixels (nadir view) The mean calibrated brightness temperature in the 12 micron channel of all the valid cloudy pixels over sea, measured in the nadir view, that fall within the sub-cell. The brightness temperature is expressed as a long (32 bit) integer in units of 0.001 K. Valid mean brightness temperatures will be positive numbers in the range 170,000 to 321,000. If no valid cloudy sea pixels fall within the sub-cell, the field will be set to an exceptional value of -1.	K/1000	1	sl	4 byte(s)
17	sa_11bt_cl_nad Spatially averaged 11 micron BT of all cloudy pixels (nadir view) The mean calibrated brightness temperature in the 11 micron channel of all the valid cloudy pixels over sea, measured in the nadir view, that fall within the sub-cell. The brightness temperature is expressed as a long (32 bit) integer in units of 0.001 K. Valid mean brightness temperatures will be positive numbers in the range 170,000 to 321,000. If no valid cloudy sea pixels fall within the sub-cell, the field will be set to an exceptional value of -1.	K/1000	1	sl	4 byte(s)
18	sa_37bt_cl_nad Spatially averaged 3.7 micron BT of all cloudy pixels (nadir view) The mean calibrated brightness temperature in the 3.7 micron channel of all the valid cloudy pixels over sea, measured in the nadir view, that fall within the sub-cell. The brightness temperature is expressed as a long (32 bit) integer in units of 0.001 K. Valid mean brightness temperatures will be positive numbers in the range 195,000 to 321,000. If no valid cloudy sea pixels fall within the sub-cell, the field will be set to an exceptional value of -1.	K/1000	1	sl	4 byte(s)
19	sa_16toa_cl_nad Spatially averaged 1.6 micron TOA reflectance of all cloudy pixels (nadir view) The mean calibrated reflectance in the 1.6 micron channel of all the valid cloudy pixels over sea, measured in the nadir view, that fall within the sub-cell. The reflectance is expressed as a short (16 bit) integer in units of 0.01 %. Valid mean reflectances will be positive numbers in the range 0 to 10,000. If no valid cloudy sea pixels fall within the sub-cell, the field will be set to an exceptional value of -1.	%/100	1	ss	2 byte(s)
20	sa_87toa_cl_nad Spatially averaged 0.87 micron TOA reflectance of all cloudy pixels (nadir view) The mean calibrated reflectance in the 0.87 micron channel of all the valid cloudy pixels over sea, measured in the nadir view, that fall within the sub-cell. The reflectance is expressed as a short (16 bit) integer in units of 0.01 %. Valid mean reflectances will be positive numbers in the range 0 to 10,000. If no valid cloudy	%/100	1	ss	2 byte(s)

#	Description	Units	Count	Type	Size
	sea pixels fall within the sub-cell, the field will be set to an exceptional value of -1.				
21	sa_67toa_cl_nad Spatially averaged 0.67 micron TOA reflectance of all cloudy pixels (nadir view) The mean calibrated reflectance in the 0.67 micron channel of all the valid cloudy pixels over sea, measured in the nadir view, that fall within the sub-cell. The reflectance is expressed as a short (16 bit) integer in units of 0.01 %. Valid mean reflectances will be positive numbers in the range 0 to 10,000. If no valid cloudy sea pixels fall within the sub-cell, the field will be set to an exceptional value of -1.	%/100	1	ss	2 byte(s)
22	sa_55toa_cl_nad Spatially averaged 0.55 micron TOA reflectance of all cloudy pixels (nadir view) The mean calibrated reflectance in the 0.55 micron channel of all the valid cloudy pixels over sea, measured in the nadir view, that fall within the sub-cell. The reflectance is expressed as a short (16 bit) integer in units of 0.01 %. Valid mean reflectances will be positive numbers in the range 0 to 10,000. If no valid cloudy sea pixels fall within the sub-cell, the field will be set to an exceptional value of -1.	%/100	1	ss	2 byte(s)
23	fail_flag_nad Pixel threshold failure flags for averages, nadir view A 16 bit word of quality flags for the nadir view data. Each of bits 0 to 13 of the word is a flag that corresponds to one of the channel/cloud flag combinations (i.e. to one of the nadir view spatially averaged fields of the product), which if set indicates that the number of pixels contributing to the corresponding average is less than a pre-defined quality threshold. The meanings of the flags are tabulated below.	-	1	us	2 byte(s)
24	pix_for Number of filled pixels in cell, forward view The total number of filled pixels, measured in the forward view, that fall within the sub-cell, regardless of surface type. This differs from the total number of pixels which fall within the sub-cell by the number of unfilled pixels. In the case of 10 arc minute cells the area of the cell, and hence the number of pixels that fall within it, is a function of the latitude.	-	1	ss	2 byte(s)
25	pix_ss_for Number of filled pixels in cell over sea surface, forward view The total number of filled pixels over sea, measured in the forward view, that fall within the sub-cell, irrespective of cloud state. It is thus the sum of the numbers of clear sea and cloudy sea pixel in the sub-cell.	-	1	ss	2 byte(s)
26	perc_cl_pix_ss_for Percentage of cloudy pixels in cell over sea surface, forward view The percentage of the total number of sea pixels within the sub-cell and measured in the forward view that are cloudy, expressed as an integer in units of 0.01%.	-	1	ss	2 byte(s)
27	sa_12bt_clr_for Spatially averaged 12 micron BT of all clear pixels (forward view) The mean calibrated brightness temperature in the 12 micron channel of all the valid clear pixels over sea, measured in the forward [forward] view, that fall within the sub-cell. The brightness temperature is expressed as a long (32 bit) integer in units of 0.001 K. Valid mean brightness temperatures will be positive numbers in the range 170,000 to 321,000. If no valid clear sea pixels fall within the sub-cell, the field will be set to an exceptional value of -1.	K/1000	1	sl	4 byte(s)
28	sa_11bt_clr_for Spatially averaged 11 micron BT of all clear pixels (forward view) The mean calibrated brightness temperature in the 11 micron channel of all the valid clear pixels over sea, measured in the forward view, that fall within the sub-cell. The brightness temperature is expressed as a long (32 bit) integer in units of 0.001 K. Valid mean brightness temperatures will be positive numbers in the range 170,000 to 321,000. If no valid clear sea pixels fall within the sub-cell, the field will be set to an exceptional value of -1.	K/1000	1	sl	4 byte(s)
29	sa_37bt_clr_for Spatially averaged 3.7 micron BT of all clear pixels (forward view) The mean calibrated brightness temperature in the 3.7 micron channel of all the valid clear pixels over sea, measured in the forward view, that fall within the sub-cell. The brightness temperature is expressed as a long (32 bit) integer in units of 0.001 K. Valid mean brightness temperatures will be positive numbers in the range 195,000 to 321,000. If no valid clear sea pixels fall within the sub-cell, the field will be set to an exceptional value of -1.	K/1000	1	sl	4 byte(s)
30	sa_16toa_clr_for Spatially averaged 1.6 micron TOA reflectance of all clear pixels (forward view) The mean calibrated reflectance in the 1.6 micron channel of all the valid clear pixels over sea, measured in the forward view, that fall within the sub-cell. The reflectance is expressed as a short (16 bit) integer in units of 0.01 %. Valid mean reflectances will be positive numbers in the range 0 to 10,000. If no valid clear sea pixels fall within the sub-cell, the field will be set to an exceptional value of -1.	%/100	1	ss	2 byte(s)
31	sa_87toa_clr_for Spatially averaged 0.87 micron TOA reflectance of all clear pixels (forward view) The mean calibrated reflectance in the 0.87 micron channel of all the valid clear pixels over sea, measured in the forward view, that fall within the sub-cell. The reflectance is expressed as a short (16 bit) integer in units of 0.01 %. Valid mean reflectances will be positive numbers in the range 0 to 10,000. If no valid clear sea pixels fall within the sub-cell, the field will be set to an exceptional value of -1.	%/100	1	ss	2 byte(s)
32	sa_67toa_clr_for Spatially averaged 0.67 micron TOA reflectance of all clear pixels (forward view) The mean calibrated reflectance in the 0.67 micron channel of all the valid clear pixels over sea, measured in the forward view, that fall within the sub-cell. The reflectance is expressed as a short (16 bit) integer in units of 0.01 %. Valid mean reflectances will be positive numbers in the range 0 to 10,000. If no valid clear sea pixels fall within the sub-cell, the field will be set to an exceptional value of -1.	%/100	1	ss	2 byte(s)

#	Description	Units	Count	Type	Size
33	sa_55toa_clr_for Spatially averaged 0.55 micron TOA reflectance of all clear pixels (forward view) The mean calibrated reflectance in the 0.55 micron channel of all the valid clear pixels over sea, measured in the forward view, that fall within the sub-cell. The reflectance is expressed as a short (16 bit) integer in units of 0.01 %. Valid mean reflectances will be positive numbers in the range 0 to 10,000. If no valid clear sea pixels fall within the sub-cell, the field will be set to an exceptional value of -1.	%/100	1	ss	2 byte(s)
34	sa_12bt_cl_for Spatially averaged 12 micron BT of all cloudy pixels (forward view) The mean calibrated brightness temperature in the 12 micron channel of all the valid cloudy pixels over sea, measured in the forward view, that fall within the sub-cell. The brightness temperature is expressed as a long (32 bit) integer in units of 0.001 K. Valid mean brightness temperatures will be positive numbers in the range 170,000 to 321,000. If no valid cloudy sea pixels fall within the sub-cell, the field will be set to an exceptional value of -1.	K/1000	1	sl	4 byte(s)
35	sa_11bt_cl_for Spatially averaged 11 micron BT of all cloudy pixels (forward view) The mean calibrated brightness temperature in the 11 micron channel of all the valid cloudy pixels over sea, measured in the forward view, that fall within the sub-cell. The brightness temperature is expressed as a long (32 bit) integer in units of 0.001 K. Valid mean brightness temperatures will be positive numbers in the range 170,000 to 321,000. If no valid cloudy sea pixels fall within the sub-cell, the field will be set to an exceptional value of -1.	K/1000	1	sl	4 byte(s)
36	sa_37bt_cl_for Spatially averaged 3.7 micron BT of all cloudy pixels (forward view) The mean calibrated brightness temperature in the 3.7 micron channel of all the valid cloudy pixels over sea, measured in the forward view, that fall within the sub-cell. The brightness temperature is expressed as a long (32 bit) integer in units of 0.001 K. Valid mean brightness temperatures will be positive numbers in the range 195,000 to 321,000. If no valid cloudy sea pixels fall within the sub-cell, the field will be set to an exceptional value of -1.	K/1000	1	sl	4 byte(s)
37	sa_16toa_cl_for Spatially averaged 1.6 micron TOA reflectance of all cloudy pixels (forward view) The mean calibrated reflectance in the 1.6 micron channel of all the valid cloudy pixels over sea, measured in the forward view, that fall within the sub-cell. The reflectance is expressed as a short (16 bit) integer in units of 0.01 %. Valid mean reflectances will be positive numbers in the range 0 to 10,000. If no valid cloudy sea pixels fall within the sub-cell, the field will be set to an exceptional value of -1.	%/100	1	ss	2 byte(s)
38	sa_87toa_cl_for Spatially averaged 0.87 micron TOA reflectance of all cloudy pixels (forward view) The mean calibrated reflectance in the 0.87 micron channel of all the valid cloudy pixels over sea, measured in the forward view, that fall within the sub-cell. The reflectance is expressed as a short (16 bit) integer in units of 0.01 %. Valid mean reflectances will be positive numbers in the range 0 to 10,000. If no valid cloudy sea pixels fall within the sub-cell, the field will be set to an exceptional value of -1.	%/100	1	ss	2 byte(s)
39	sa_67toa_cl_for Spatially averaged 0.67 micron TOA reflectance of all cloudy pixels (forward view) The mean calibrated reflectance in the 0.67 micron channel of all the valid cloudy pixels over sea, measured in the forward view, that fall within the sub-cell. The reflectance is expressed as a short (16 bit) integer in units of 0.01 %. Valid mean reflectances will be positive numbers in the range 0 to 10,000. If no valid cloudy sea pixels fall within the sub-cell, the field will be set to an exceptional value of -1.	%/100	1	ss	2 byte(s)
40	sa_55toa_cl_for Spatially averaged 0.55 micron TOA reflectance of all cloudy pixels (forward view) The mean calibrated reflectance in the 0.55 micron channel of all the valid cloudy pixels over sea, measured in the forward view, that fall within the sub-cell. The reflectance is expressed as a short (16 bit) integer in units of 0.01 %. Valid mean reflectances will be positive numbers in the range 0 to 10,000. If no valid cloudy sea pixels fall within the sub-cell, the field will be set to an exceptional value of -1	%/100	1	ss	2 byte(s)
41	fail_flag_for Pixel threshold failure flags for averages, foward view A 16 bit word of quality flags for the forward view data. Each of bits 0 to 13 of the word is a flag that corresponds to one of the channel/cloud flag combinations (i.e. to one of the forward view spatially averaged fields of the product), which if set indicates that the number of pixels contributing to the corresponding average is less than a pre-defined quality threshold. The meanings of the flags are tabulated below.	-	1	us	2 byte(s)

Record Length : 122

DS_NAME : BT/TOA Sea record 10 arc minute cell MDS

Format Version 114.0

The following table defines the contents of the pixel threshold failure flags word.

Table 6.33

Bit	Meaning if set
0	Number of clear pixels contributing to average is less than threshold, 12 micron channel
1	Number of clear pixels contributing to average is less than threshold, 11 micron channel
2	Number of clear pixels contributing to average is less than threshold, 3.7 micron channel
3	Number of clear pixels contributing to average is less than threshold, 1.6 micron channel
4	Number of clear pixels contributing to average is less than threshold, 0.870 micron channel
5	Number of clear pixels contributing to average is less than threshold, 0.670 micron channel
6	Number of clear pixels contributing to average is less than threshold, 0.555 micron channel
7	Number of cloudy pixels contributing to average is less than threshold, 12 micron channel
8	Number of cloudy pixels contributing to average is less than threshold, 11 micron channel
9	Number of cloudy pixels contributing to average is less than threshold, 3.7 micron channel
10	Number of cloudy pixels contributing to average is less than threshold, 1.6 micron channel
11	Number of cloudy pixels contributing to average is less than threshold, 0.870 micron channel
12	Number of cloudy pixels contributing to average is less than threshold, 0.670 micron channel
13	Number of cloudy pixels contributing to average is less than threshold, 0.555 micron channel
14	View contains day-time data
15	Unused

Pixel threshold failure flags (nadir or forward view).

Note: Bits are numbered from ms bit 15 to ls bit 0.

6.6.8 SST record 50 km cell MDS

Table 6.34 SST record 50 km cell MDS

SST record 30 arc minute cell MDS

#	Description	Units	Count	Type	Size
Data Record					

#	Description	Units	Count	Type	Size
0	dsr_time Nadir UTC time in MJD format The (nadir and forward view) instrument data contributing to a given cell or sub-cell may cover a range of up to 150 seconds of measurement times. It is therefore not possible to assign a unique time tag to an AST record, and the time tag is therefore arbitrarily assigned as follows. The nadir time associated with a given AST record represents the scan time of a nadir pixel contributing to the record. In general this is the time of the first filled pixel encountered during processing that falls within the geometrical boundary of the cell or sub-cell (see link), although exception cases may arise. Because the cell boundaries bear no clear geometrical relationship to the AATSR instrument scan it is not possible to state in general that this corresponds to a particular corner of the cell or sub-cell. Note also that if a cell is intersected by coastline, so that it contains both land and sea pixels, the time tag of a given record does not necessarily correspond to a pixel of the same surface type.	MJD	1	mjd	12 byte(s)
1	quality_flag Quality Indicator (-1 for blank MDSR, 0 otherwise) This field is set to -1 if all the measurement values in the record are invalid, and is set to 0 otherwise.	flag	1	BooleanFlag	1 byte(s)
2	spare_1 Spare	-	1	SpareField	3 byte(s)
3	lat Latitude of cell The latitude of the lower left-hand corner of the cell, in units of micro-degrees. The latitude is defined in the range -90 degrees to +90 degrees. [If the cell contains no valid data, this field may be set to the exceptional value -399,999,999.?? This case may not arise for the full cell.]	(1e-6) degrees	1	GeoCoordinate	4 byte(s)
4	lon Longitude of cell The longitude of the lower left-hand corner of the cell, in units of micro-degrees. The longitude is defined in the range -180 degrees to +180 degrees.	(1e-6) degrees	1	GeoCoordinate	4 byte(s)
5	m_actrk_pix_num Mean across-track pixel number A weighted mean pixel index of the nadir view clear sea pixels that fall within the cell and contribute to the average. This quantity is derived by averaging the mean across-track pixel number (q.v.) over those sub-cells which contain sufficient valid pixels to contribute to the averaged SST in the cell.	-	1	ss	2 byte(s)
6	m_nad mean nadir-only SST The mean sea surface temperature (SST) for the cell derived using only data in the nadir view. It is derived by averaging the mean nadir-only SST (q.v.) for each of the (up to) 9 sub-cells that fall within the cell and that contain more than a minimum number of valid clear sea pixels. If none of the contributing sub-cells contains sufficient valid pixels, the field is set to the exceptional value -1.	K/100	1	ss	2 byte(s)
7	sd_nad standard deviation of nadir-only SST The standard deviation of the mean nadir-only SST of the contributing sub-cells.	K/100	1	ss	2 byte(s)
8	pix_nad Number of pixels in nadir-only average The number of valid 11 and 12 micron pixels contributing to the ABT determination in the cell. This will usually be the same as the number of valid 11 and 12 micron pixels contributing to the mean nadir-only SST determination in the cell, although if any sub-cells contain too few valid pixels to contribute to the averaged SST, the numbers may differ. In general the numbers of valid pixels in the 11 and 12 micron channels are expected to be the same; if they differ, the lower is given here.	-	1	us	2 byte(s)
9	m_dual_vw mean dual-view SST The mean sea surface temperature (SST) for the cell derived using data from both nadir and forward views. It is derived by averaging the mean dual view SST (q.v.) for each of the (up to) 9 sub-cells that fall within the cell and that contain more than a minimum number of valid clear sea pixels. If none of the contributing sub-cells contains sufficient valid pixels, the field is set to the exceptional value -1.	K/100	1	ss	2 byte(s)
10	sd_dual_vw standard deviation of dual-view SST The standard deviation of the mean dual view SST of the contributing sub-cells.	K/100	1	ss	2 byte(s)
11	pix_dual_vw Number of pixels in dual view average The number of valid 11 and 12 micron pixels contributing to the ABT determination in the cell. This will usually be the same as the number of valid 11 and 12 micron pixels contributing to the mean nadir-only SST determination in the cell, although if any sub-cells contain too few valid pixels to contribute to the averaged SST, the numbers may differ. The numbers of valid pixels in the different channel and view combinations are not necessarily equal. When they differ, the lowest is given here.	-	1	us	2 byte(s)
12	ast_conf_flags AST confidence word A 16-bit word containing confidence flags for the record. Bits 0 to 3 are set to indicate whether or not 3.7 micron channel data was used in the SST retrieval, and whether or not day-time data contributes to the retrieved temperatures. The detailed interpretation of these bits is defined in the table below. Bits 4 to 31 are currently unused.	flags	2	us	2*2 byte(s)
13	cl_top_temp_nad	K/100	1	ss	2 byte(s)

#	Description	Units	Count	Type	Size
	Cloud-top temperature, nadir view An estimate of the cloud-top temperature in the half-degree cell. This estimate is derived by generating a histogram of the 11 micron brightness temperatures of cloudy sea pixels within the cell in the nadir view, and averaging the brightness temperatures of the lowest quartile. The estimate is derived from sea pixels only.				
14	perc_cl_cov_nad Percentage cloud-cover, nadir view The fraction of nadir view sea pixels within the cell that are cloudy, expressed as a percentage in units of 0.01%.	%/100	1	ss	2 byte(s)
15	cl_top_temp_for Cloud-top temperature, forward view An estimate of the cloud-top temperature in the half-degree cell. This estimate is derived by generating a histogram of the 11 micron brightness temperatures of cloudy sea pixels within the cell in the forward view, and averaging the brightness temperatures of the lowest quartile. The estimate is derived from sea pixels only.	K/100	1	ss	2 byte(s)
16	perc_cl_cov_for Percentage cloud-cover, forward view The fraction of forward view sea pixels within the cell that are cloudy, expressed as a percentage in units of 0.01%.	%/100	1	ss	2 byte(s)

Record Length : 50

DS_NAME : SST record 30 arc minute cell MDS

Format Version 114.0

The table below lists the confidence flags in the AST Confidence Word.

Table 6.35

bit	meaning if set.
0	Sea MDS: Nadir-only SST retrieval used 3.7 micron channel Land MDS: Reserved
1	Sea MDS: Dual-view SST retrieval used 3.7 micron channel Land MDS: Reserved
2	Nadir view contains day-time data
3	Forward view contains day-time data
4 - 31	Unused

AST confidence word

6.6.9 SST record 17 km cell MDS

Table 6.36 SST record 17 km cell MDS

SST record 10 arc minute cell MDS

#	Description	Units	Count	Type	Size
Data Record					
0	dsr_time Nadir UTC time in MJD format The (nadir and forward view) instrument data contributing to a given cell or sub-cell may cover a range of up to 150 seconds of measurement times. It is therefore not possible to assign a unique time tag to an AST record, and the time tag is therefore arbitrarily assigned as follows. The nadir time associated with a given AST record represents the scan time of a nadir pixel contributing to the record. In general this is the time of the first filled pixel encountered during processing that falls within the geometrical boundary of the cell or sub-cell (see link), although exception cases may arise. Because the cell boundaries bear no clear geometrical relationship to the AATSR instrument scan it is not possible to state in general that this corresponds to a particular corner of the cell or sub-cell. Note also that if a cell is intersected by coastline, so that it contains both land and sea pixels, the time tag of a given record does not necessarily correspond to a pixel of the same surface type.	MJD	1	mjd	12 byte(s)
1	quality_flag Quality Indicator (-1 for blank MDSR, 0 otherwise) This field is set to -1 if all the measurement values in the record are invalid, and is set to 0 otherwise.	flag	1	BooleanFlag	1 byte(s)
2	spare_1 Spare	-	1	SpareField	3 byte(s)
3	lat Latitude of cell The latitude of the lower left-hand corner of the sub-cell, in units of micro-degrees. The latitude is defined in the range -90 degrees to +90 degrees. If the cell contains no valid data, this field may be set to the exceptional value -399,999,999.	(1e-6) degrees	1	GeoCoordinate	4 byte(s)
4	lon Longitude of cell The longitude of the lower left-hand corner of the sub-cell, in units of micro-degrees. The longitude is defined in the range -180 degrees to +180 degrees. If the cell contains no valid data, this field may be set to the exceptional value -399,999,999.	(1e-6) degrees	1	GeoCoordinate	4 byte(s)
5	m_actrk_pix_num Mean across-track pixel number The average pixel index of the nadir view clear sea pixels that fall within the sub-cell. The pixel index, in the range 0 to 511 inclusive, is the across-track index of the pixel in the image, and ids linearly related to the X co-ordinate by X = j - 256 km. The mean across-track pixel index is thus a measure of the X co-ordinate of the centroid of the distribution of clear sea pixels that will contribute to the SST determination. It is used to select the SST retrieval coefficients for the cell.	-	1	ss	2 byte(s)
6	m_nad mean nadir-only SST The mean sea surface temperature (SST) derived using only data in the nadir view. The SST is derived from the mean brightness temperatures in the three infra-red channels, averaged over the valid clear sea pixels in the sub-cell. The SST determination uses retrieval coefficients optimised for averaged data. Day-time retrievals use the 11 and 12 micron channels only; night-time determinations will also use valid 3.7 micron data.	K/100	1	ss	2 byte(s)
7	pix_nad Number of pixels in nadir-only average The number of valid 11 and 12 micron pixels contributing to the nadir-only SST determination in the cell. In general the numbers of valid pixels in the 11 and 12 micron channels are expected to be the same; if they differ, the lower is given here.	-	1	us	2 byte(s)
8	m_dual_vw mean dual-view SST The mean sea surface temperature (SST) derived using data from both nadir and forward views. The SST is derived from the mean brightness temperatures in the three infra-red channels, averaged over the valid clear sea pixels in the sub-cell. The SST determination uses retrieval coefficients optimised for averaged data. Day-time retrievals use the 11 and 12 micron channels only; night-time determinations will also use valid 3.7 micron data.	K/100	1	ss	2 byte(s)
9	pix_dual_vw Number of pixels in dual-view average The number of valid 11 and 12 micron pixels contributing to the dual view SST determination in the cell. In general the numbers of valid pixels in the 11 and 12 micron channels in a given view are expected to be the same. However, they may differ, and in a cloudy scene the number of valid pixels in the nadir and forward views may differ. When the numbers of valid pixels in the different channel and view combinations differ, the lowest is given here.	-	1	us	2 byte(s)
10	ast_conf_flags AST confidence word	flags	2	us	2*2 byte(s)

#	Description	Units	Count	Type	Size
	A 16-bit word containing confidence flags for the record. Bits 0 to 3 are set to indicate whether or not 3.7 micron channel data was used in the SST retrieval, and whether or not day-time data contributes to the retrieved temperatures. The detailed interpretation of these bits is defined in the table below. Bits 4 to 31 are currently unused.				

Record Length : 38

DS_NAME : SST record 10 arc minute cell MDS

Format Version 114.0

The table below lists the confidence flags in the AST Confidence Word.

Table 6.37

bit	meaning if set.
0	Sea MDS: Nadir-only SST retrieval used 3.7 micron channel Land MDS: Reserved
1	Sea MDS: Dual-view SST retrieval used 3.7 micron channel Land MDS: Reserved
2	Nadir view contains day-time data
3	Forward view contains day-time data
4 - 31	Unused

6.6.10 Level 2 SPH

Table 6.38 Level 2 SPH

Level 2 SPH

#	Description	Units	Count	Type	Size
Data Record					
0	sph_descriptor_title SPH_DESCRIPTOR=	keyword	1	AsciiString	15 byte(s)
1	quote_1 quotation mark (""")	ascii	1	AsciiString	1 byte(s)
2	sph_descriptor	ascii	1	AsciiString	28 byte(s)

#	Description	Units	Count	Type	Size
	SPH Descriptor ASCII string describing the product.				
3	quote_2 quotation mark (""")	ascii	1	AsciiString	1 byte(s)
4	newline_char_1 newline character	terminator	1	AsciiString	1 byte(s)
5	stripline_cont_ind_title STRIPLINE_CONTINUITY_INDICATOR=	keyword	1	AsciiString	31 byte(s)
6	stripline_continuity_indicator Value: 0= No stripline continuity, the product is a complete segment. Other: Stripline Counter	-	1	Ac	4 byte(s)
7	newline_char_2 newline character	terminator	1	AsciiString	1 byte(s)
8	slice_pos_title SLICE_POSITION=	keyword	1	AsciiString	15 byte(s)
9	slice_position Value: +001 to NUM_SLICES. Default value if no stripline continuity = +001	-	1	Ac	4 byte(s)
10	newline_char_3 newline character	terminator	1	AsciiString	1 byte(s)
11	num_slices_title NUM_SLICES=	keyword	1	AsciiString	11 byte(s)
12	num_slices Number of slices in this striplineDefault value if no continuity = +001	-	1	Ac	4 byte(s)
13	newline_char_4 newline character	terminator	1	AsciiString	1 byte(s)
14	first_ln_time_title FIRST_LINE_TIME=	keyword	1	AsciiString	16 byte(s)
15	quote_3 quotation mark (""")	ascii	1	AsciiString	1 byte(s)
16	first_line_time Azimuth time first line of product. UTC Time of first range line in the MDS of this product. UTC time format contained within quotation marks.	UTC	1	UtcExternal	27 byte(s)
17	quote_4 quotation mark (""")	ascii	1	AsciiString	1 byte(s)
18	newline_char_5 newline character	terminator	1	AsciiString	1 byte(s)
19	last_ln_time_title LAST_LINE_TIME=	keyword	1	AsciiString	15 byte(s)
20	quote_5 quotation mark (""")	ascii	1	AsciiString	1 byte(s)
21	last_line_time Azimuth time last line of product. Time of last range line in the MDS of this product. UTC time format contained within quotation marks.	UTC	1	UtcExternal	27 byte(s)
22	quote_6 quotation mark (""")	ascii	1	AsciiString	1 byte(s)
23	newline_char_6 newline character	terminator	1	AsciiString	1 byte(s)
24	first_first_lat_title FIRST_FIRST_LAT=	keyword	1	AsciiString	16 byte(s)
25	first_first_lat Geodetic Latitude of the first sample of the first line. A negative value denotes south latitude, a positive value denotes North latitude	(1e-6) degrees	1	AsciiGeoCoordinate	11 byte(s)
26	first_first_lat_units <10-6degN>	units	1	AsciiString	10 byte(s)
27	newline_char_7 newline character	terminator	1	AsciiString	1 byte(s)
28	first_first_long_title FIRST_FIRST_LONG=	keyword	1	AsciiString	17 byte(s)
29	first_first_long East geodetic longitude of the first sample of the first line. Positive values East of Greenwich, negative values west of Greenwich.	(1e-6) degrees	1	AsciiGeoCoordinate	11 byte(s)
30	first_first_long_units <10-6degE>	units	1	AsciiString	10 byte(s)
31	newline_char_8 newline character	terminator	1	AsciiString	1 byte(s)
32	first_mid_lat_title FIRST_MID_LAT=	keyword	1	AsciiString	14 byte(s)
33	first_mid_lat Geodetic Latitude of the middle sample of the first line. A negative value denotes south latitude, a positive value denotes North latitude	(1e-6) degrees	1	AsciiGeoCoordinate	11 byte(s)
34	first_mid_lat_units <10-6degN>	units	1	AsciiString	10 byte(s)
35	newline_char_9	terminator	1	AsciiString	1 byte(s)

#	Description	Units	Count	Type	Size
	newline character				
36	first_mid_long_title FIRST_MID_LONG=	keyword	1	AsciiString	15 byte(s)
37	first_mid_long East geodetic longitude of the middle sample of the first line. Positive values East of Greenwich, negative values west of Greenwich.	(1e-6) degrees	1	AsciiGeoCoordinate	11 byte(s)
38	first_mid_long_units <10-6degE>	units	1	AsciiString	10 byte(s)
39	newline_char_10 newline character	terminator	1	AsciiString	1 byte(s)
40	first_last_lat_title FIRST_LAST_LAT=	keyword	1	AsciiString	15 byte(s)
41	first_last_lat Geodetic Latitude of the last sample of the first line. A negative value denotes south latitude, a positive value denotes North latitude	(1e-6) degrees	1	AsciiGeoCoordinate	11 byte(s)
42	first_last_lat_units <10-6degN>	units	1	AsciiString	10 byte(s)
43	newline_char_11 newline character	terminator	1	AsciiString	1 byte(s)
44	first_last_long_title FIRST_LAST_LONG=	keyword	1	AsciiString	16 byte(s)
45	first_last_long East geodetic longitude of the last sample of the first line. Positive values East of Greenwich, negative values west of Greenwich.	(1e-6) degrees	1	AsciiGeoCoordinate	11 byte(s)
46	first_last_long_units <10-6degE>	units	1	AsciiString	10 byte(s)
47	newline_char_12 newline character	terminator	1	AsciiString	1 byte(s)
48	last_first_lat_title LAST_FIRST_LAT=	keyword	1	AsciiString	15 byte(s)
49	last_first_lat Geodetic Latitude of the first sample of the last line. A negative value denotes south latitude, a positive value denotes North latitude	(1e-6) degrees	1	AsciiGeoCoordinate	11 byte(s)
50	last_first_units <10-6degN>	units	1	AsciiString	10 byte(s)
51	newline_char_13 newline character	terminator	1	AsciiString	1 byte(s)
52	last_first_long_title LAST_FIRST_LONG=	keyword	1	AsciiString	16 byte(s)
53	last_first_long East geodetic longitude of the first sample of the last line. Positive values East of Greenwich, negative values west of Greenwich.	(1e-6) degrees	1	AsciiGeoCoordinate	11 byte(s)
54	last_first_long_units <10-6degE>	units	1	AsciiString	10 byte(s)
55	newline_char_14 newline character	terminator	1	AsciiString	1 byte(s)
56	last_mid_lat_title LAST_MID_LAT=	keyword	1	AsciiString	13 byte(s)
57	last_mid_lat Geodetic Latitude of the middle sample of the last line. A negative value denotes south latitude, a positive value denotes North latitude	(1e-6) degrees	1	AsciiGeoCoordinate	11 byte(s)
58	last_mid_lat_units <10-6degN>	units	1	AsciiString	10 byte(s)
59	newline_char_15 newline character	terminator	1	AsciiString	1 byte(s)
60	last_mid_long_title LAST_MID_LONG=	keyword	1	AsciiString	14 byte(s)
61	last_mid_long East geodetic longitude of the middle sample of the last line. Positive values East of Greenwich, negative values west of Greenwich.	(1e-6) degrees	1	AsciiGeoCoordinate	11 byte(s)
62	last_mid_long_units <10-6degE>	units	1	AsciiString	10 byte(s)
63	newline_char_16 newline character	terminator	1	AsciiString	1 byte(s)
64	last_last_lat_title LAST_LAST_LAT=	keyword	1	AsciiString	14 byte(s)
65	last_last_lat Geodetic Latitude of the last sample of the last line. A negative value denotes south latitude, a positive value denotes North latitude	(1e-6) degrees	1	AsciiGeoCoordinate	11 byte(s)
66	last_last_lat_units <10-6degN>	units	1	AsciiString	10 byte(s)
67	newline_char_17	terminator	1	AsciiString	1 byte(s)

#	Description	Units	Count	Type	Size
	newline character				
68	last_last_long_title LAST_LAST_LONG=	keyword	1	AsciiString	15 byte(s)
69	last_last_long East geodetic longitude of the last sample of the last line. Positive values East of Greenwich, negative values west of Greenwich.	(1e-6) degrees	1	AsciiGeoCoordinate	11 byte(s)
70	last_last_long_units <10-6degE>	units	1	AsciiString	10 byte(s)
71	newline_char_18 newline character	terminator	1	AsciiString	1 byte(s)
72	spare_1 Spare	-	1	SpareField	51 byte(s)
73	min_fpp_basep_temp_title MIN_FPP_BASEPLATE_TEM=	keyword	1	AsciiString	22 byte(s)
74	min_fpp_baseplate_tem Minimum FPP baseplate temperature The minimum physical temperature of the instrument Focal Plane Assembly baseplate during the orbit, taken from the on-board telemetry (identifier A5061).	K	1	Afl	15 byte(s)
75	min_fpp_basep_temp_units <K>	units	1	AsciiString	3 byte(s)
76	newline_char_20 newline character	terminator	1	AsciiString	1 byte(s)
77	min_12_mic_temp_title MIN_12_MICRON_DETECTOR_TEMP=	keyword	1	AsciiString	28 byte(s)
78	min_12_micron_detector_temp Minimum 12 micron detector temperature The minimum physical temperature of the 12 micron detector within the product duration, taken from the on-board telemetry (identifier A5061).	K	1	Afl	15 byte(s)
79	min_12_mic_temp_units <K>	units	1	AsciiString	3 byte(s)
80	newline_char_21 newline character	terminator	1	AsciiString	1 byte(s)
81	min_11_mic_temp_title MIN_11_MICRON_DETECTOR_TEMP=	keyword	1	AsciiString	28 byte(s)
82	min_11_micron_detector_temp Minimum 11 micron detector temperature The minimum physical temperature of the 11 micron detector within the product duration, taken from the on-board telemetry (identifier A5061).	K	1	Afl	15 byte(s)
83	min_11_mic_temp_units <K>	units	1	AsciiString	3 byte(s)
84	newline_char_22 newline character	terminator	1	AsciiString	1 byte(s)
85	min_37_mic_temp_title MIN_3_7_MICRON_DETECTOR_TEMP=	keyword	1	AsciiString	29 byte(s)
86	min_3_7_micron_detector_temp Minimum 3.7 micron detector temperature The minimum physical temperature of the 3.7 micron detector within the product duration, taken from the on-board telemetry (identifier A5061).	K	1	Afl	15 byte(s)
87	min_37_mic_temp_units <K>	units	1	AsciiString	3 byte(s)
88	newline_char_23 newline character	terminator	1	AsciiString	1 byte(s)
89	min_16_mic_temp_title MIN_1_6_MICRON_DETECTOR_TEMP=	keyword	1	AsciiString	29 byte(s)
90	min_1_6_micron_detector_temp Minimum 1.6 micron detector temperature The minimum physical temperature of the 1.6 micron detector within the product duration, taken from the on-board telemetry (identifier A5061).	K	1	Afl	15 byte(s)
91	min_16_mic_temp_units <K>	units	1	AsciiString	3 byte(s)
92	newline_char_24 newline character	terminator	1	AsciiString	1 byte(s)
93	min_087_mic_temp_title MIN_0_87_MICRON_DETECTOR_TEMP=	keyword	1	AsciiString	30 byte(s)
94	min_0_87_micron_detector_temp Minimum 0.87 micron detector temperature The minimum physical temperature of the 0.87 micron detector within the product duration, taken from the on-board telemetry (identifier A5061).	K	1	Afl	15 byte(s)
95	min_087_mic_temp_units <K>	units	1	AsciiString	3 byte(s)
96	newline_char_25 newline character	terminator	1	AsciiString	1 byte(s)

#	Description	Units	Count	Type	Size
97	max_fpp_basep_temp_title MAX_FPP_BASEPLATE_TEM=	keyword	1	AsciiString	22 byte(s)
98	max_fpp_baseplate_tem Maximum FPP baseplate temperature The maximum physical temperature of the instrument Focal Plane Assembly baseplate during the orbit, taken from the on-board telemetry (identifier A5061).	K	1	Afl	15 byte(s)
99	max_fpp_basep_temp_units <K>	units	1	AsciiString	3 byte(s)
100	newline_char_26 newline character	terminator	1	AsciiString	1 byte(s)
101	max_12_mic_temp_title MAX_12_MICRON_DETECTOR_TEMP=	keyword	1	AsciiString	28 byte(s)
102	max_12_micron_detector_temp Maximum 12 micron detector temperature The maximum physical temperature of the 12 micron detector within the product duration, taken from the on-board telemetry (identifier A5061).	K	1	Afl	15 byte(s)
103	max_12_mic_temp_units <K>	units	1	AsciiString	3 byte(s)
104	newline_char_27 newline character	terminator	1	AsciiString	1 byte(s)
105	max_11_mic_temp_title MAX_11_MICRON_DETECTOR_TEMP=	keyword	1	AsciiString	28 byte(s)
106	max_11_micron_detector_temp Maximum 11 micron detector temperature The maximum physical temperature of the 11 micron detector within the product duration, taken from the on-board telemetry (identifier A5061).	K	1	Afl	15 byte(s)
107	max_11_mic_temp_units <K>	units	1	AsciiString	3 byte(s)
108	newline_char_28 newline character	terminator	1	AsciiString	1 byte(s)
109	max_37_mic_temp_title MAX_3_7_MICRON_DETECTOR_TEMP=	keyword	1	AsciiString	29 byte(s)
110	max_3_7_micron_detector_temp Maximum 3.7 micron detector temperature The maximum physical temperature of the 3.7 micron detector within the product duration, taken from the on-board telemetry (identifier A5061).	K	1	Afl	15 byte(s)
111	max_37_mic_temp_units <K>	units	1	AsciiString	3 byte(s)
112	newline_char_29 newline character	terminator	1	AsciiString	1 byte(s)
113	max_16_mic_temp_title MAX_1_6_MICRON_DETECTOR_TEMP=	keyword	1	AsciiString	29 byte(s)
114	max_1_6_micron_detector_temp Maximum 1.6 micron detector temperature The maximum physical temperature of the 1.6 micron detector within the product duration, taken from the on-board telemetry (identifier A5061).	K	1	Afl	15 byte(s)
115	max_16_mic_temp_units <K>	units	1	AsciiString	3 byte(s)
116	newline_char_30 newline character	terminator	1	AsciiString	1 byte(s)
117	max_087_mic_temp_title MAX_0_87_MICRON_DETECTOR_TEMP=	keyword	1	AsciiString	30 byte(s)
118	max_0_87_micron_detector_temp Maximum 0.87 micron detector temperature The maximum physical temperature of the 0.87 micron detector within the product duration, taken from the on-board telemetry (identifier A5061).	K	1	Afl	15 byte(s)
119	max_087_mic_temp_units <K>	units	1	AsciiString	3 byte(s)
120	newline_char_31 newline character	terminator	1	AsciiString	1 byte(s)
121	spare_2 Spare	-	1	SpareField	51 byte(s)
122	dsd_spare_3 DSD Spare	-	1	dsd_sp	0 byte(s)
123	dsd_spare_4 DSD Spare	-	1	dsd_sp	0 byte(s)

Record Length : 1315

DS_NAME : Level 2 SPH

Format Version 114.0

6.6.11 Grid pixel latitude and longtitude topographic correction ADS

Table 6.39 Grid pixel latitude and longtitude topographic correction ADS

Grid pixel latitude and longtitude,topographic correction ADS

#	Description	Units	Count	Type	Size
Data Record					
0	dsr_time Nadir UTC time in MJD format The nadir time associated with a given record, or image row, is the time at which the sub-satellite point intersects the image row, or the time at which the satellite is vertically overhead at the centre of the row. It corresponds to the measurement time at which the pixels in the centre of the row (the nadir pixels) are measured. Because of the curvature of the instrument scans, the measurement time at the extremities of the row may differ from the nadir time by up to 15 seconds. Similarly the measurement time of a forward view image will differ by approximately 135 seconds (2.25 minutes) from the measurement time of the corresponding nadir scan. The relationship between nadir time and measurement time is explained in more detail in the accompanying link.	MJD	1	mjd	12 byte(s)
1	attach_flag Attachment flag(set to 1 if all MDSRs corresponding to this ADSR are zero. In accordance with ESA guidelines, this flag will be set to 1 if all of the MDS records in the granule have the record quality indicator set to -1; otherwise it is set to zero. If the flag is set to 1 the corresponding MDS records will be omitted; this mechanism allows gaps in the sequence of MDS records to be identified.	flag	1	BooleanFlag	1 byte(s)
2	spare_1 Spare	-	1	SpareField	3 byte(s)
3	img_scan_y image scan y coordinate The y co-ordinate of the image row (or image scan), in units of metres. Because the AATSR image data is sampled at equal intervals of time in the along track direction, this quantity is provided in order to define the relationship between time and image scale. The y co-ordinate is measured along the satellite ground track; the origin (in the case of consolidated data) is at the ascending node of the orbit. (Precisely, from the point corresponding to time T0, however defined.) The co-ordinate frame of the AATSR images is defined in the accompanying link.	km	1	sl	4 byte(s)
4	tie_pt_lat tie point latitudes In order to permit the geolocation of the AATSR images, the latitudes and longitudes of selected tie points (or tie pixels) on the image are provided in this ADS. These fields contain the latitude of each tie point on the granule row, in units of microdegrees. On each granule row there are 23 tie points at x co-ordinates of -275, -250, ... 275 km. Pixels are 1 km apart, and the tie point at 0 km corresponds to pixel 256, therefore an x co-ordinate of -250 km corresponds to pixel number 6, and so on. Latitudes of intermediate points may be derived by linear interpolation. Note that the extreme tie points at +/- 275 km are beyond the extremities of the image row, which extends to +/- 256 km.	(1e-6) degrees	23	GeoCoordinate	23*4 byte(s)
5	tie_pt_long tie point longitudes In order to permit the geolocation of the AATSR images, the latitudes and longitudes of selected tie points (or tie pixels) on the image are provided in this	(1e-6) degrees	23	GeoCoordinate	23*4 byte(s)

#	Description	Units	Count	Type	Size
	ADS. These fields contain the longitude of each tie point on the granule row, in units of microdegrees. On each granule row there are 23 tie points at x co-ordinates of -275, -250, ... 275 km. Pixels are 1 km apart, and the tie point at 0 km corresponds to pixel 256, therefore an x co-ordinate of -250 km corresponds to pixel number 6, and so on. Longitudes of intermediate points may be derived by linear interpolation. Note that the extreme tie points at +/- 275 km are beyond the extremities of the image row, which extends to +/- 256 km.				

Record Length : 204

DS_NAME : Grid pixel latitude and longtitude,topographic correction ADS

Format Version 114.0

6.6.12 Browse MDS

Table 6.40 Browse MDS

Browse MDS

#	Description	Units	Count	Type	Size
Data Record					
0	dsr_time Nadir UTC time in MJD format The nadir time associated with a given record, or image row, is the time at which the sub-satellite point intersects the image row, or the time at which the satellite is vertically overhead at the centre of the row. It corresponds to the measurement time at which the pixels in the centre of the row (the nadir pixels) are measured. Because of the curvature of the instrument scans, the measurement time at the extremities of the row may differ from the nadir time by up to 15 seconds. Similarly the measurement time of a forward view image will differ by approximately 135 seconds (2.25 minutes) from the measurement time of the corresponding nadir scan. The relationship between nadir time and measurement time is explained in more detail in the accompanying link.	MJD	1	mjd	12 byte(s)
1	quality_flag Quality Indicator (-1 for blank MDSR, 0 otherwise) The record quality indicator is set to -1 to indicate a blank MDS Record, to zero otherwise (I.e. if the record contains valid data).	flag	1	BooleanFlag	1 byte(s)
2	spare_1 Spare	-	1	SpareField	3 byte(s)
3	img_scan_y image scan y coordinate The y co-ordinate of the image row (or image scan), in units of metres. Because the AATSR image data is sampled at equal intervals of time in the along track direction, this quantity is provided in order to define the relationship between time and image scale. The y co-ordinate is measured along the satellite ground track; the origin (in the case of consolidated data) is at the ascending node of the orbit. (Precisely, from the point corresponding to time T0, however defined.) The co-ordinate frame of the AATSR images is defined in the accompanying link.	km	1	sl	4 byte(s)
4	rgb_pix Red, Green, Blue channel intensity for pixel 1- 128 The red, green and blue intensities are interleaved, 1 byte per channel.	intensity	128*3	uc	128*3*1 byte(s)

Record Length : 404

DS_NAME : Browse MDS

Format Version 114.0

6.6.13 Browse SPH

Table 6.41 Browse SPH

Browse SPH

#	Description	Units	Count	Type	Size
Data Record					
0	sph_descriptor_title SPH_DESCRIPTOR=	keyword	1	AsciiString	15 byte(s)
1	quote_1 quotation mark (""")	ascii	1	AsciiString	1 byte(s)
2	sph_descriptor SPH Descriptor ASCII string describing the product.	ascii	1	AsciiString	28 byte(s)
3	quote_2 quotation mark (""")	ascii	1	AsciiString	1 byte(s)
4	newline_char_1 newline character	terminator	1	AsciiString	1 byte(s)
5	stripline_cont_ind_title STRIPLINE_CONTINUITY_INDICATOR=	keyword	1	AsciiString	31 byte(s)
6	stripline_continuity_indicator Value: 0= No stripline continuity, the product is a complete segment. Other: Stripline Counter	-	1	Ac	4 byte(s)
7	newline_char_2 newline character	terminator	1	AsciiString	1 byte(s)
8	slice_pos_title SLICE_POSITION=	keyword	1	AsciiString	15 byte(s)
9	slice_position Value: +001 to NUM_SLICES. Default value if no stripline continuity = +001	-	1	Ac	4 byte(s)
10	newline_char_3 newline character	terminator	1	AsciiString	1 byte(s)
11	num_slices_title NUM_SLICES=	keyword	1	AsciiString	11 byte(s)
12	num_slices Number of slices in this striplineDefault value if no continuity = +001	-	1	Ac	4 byte(s)
13	newline_char_4 newline character	terminator	1	AsciiString	1 byte(s)
14	first_ln_time_title FIRST_LINE_TIME=	keyword	1	AsciiString	16 byte(s)
15	quote_3 quotation mark (""")	ascii	1	AsciiString	1 byte(s)
16	first_line_time	UTC	1	UtcExternal	27 byte(s)

#	Description	Units	Count	Type	Size
	Azimuth time first line of product. UTC Time of first range line in the MDS of this product. UTC time format contained within quotation marks.				
17	quote_4 quotation mark (""")	ascii	1	AsciiString	1 byte(s)
18	newline_char_5 newline character	terminator	1	AsciiString	1 byte(s)
19	last_ln_time_title LAST_LINE_TIME=	keyword	1	AsciiString	15 byte(s)
20	quote_5 quotation mark (""")	ascii	1	AsciiString	1 byte(s)
21	last_line_time Azimuth time last line of product. Time of last range line in the MDS of this product. UTC time format contained within quotation marks.	UTC	1	UtcExternal	27 byte(s)
22	quote_6 quotation mark (""")	ascii	1	AsciiString	1 byte(s)
23	newline_char_6 newline character	terminator	1	AsciiString	1 byte(s)
24	first_first_lat_title FIRST_FIRST_LAT=	keyword	1	AsciiString	16 byte(s)
25	first_first_lat Geodetic Latitude of the first sample of the first line. A negative value denotes south latitude, a positive value denotes North latitude	(1e-6) degrees	1	AsciiGeoCoordinate	11 byte(s)
26	first_first_lat_units <10-6degN>	units	1	AsciiString	10 byte(s)
27	newline_char_7 newline character	terminator	1	AsciiString	1 byte(s)
28	first_first_long_title FIRST_FIRST_LONG=	keyword	1	AsciiString	17 byte(s)
29	first_first_long East geodetic longitude of the first sample of the first line. Positive values East of Greenwich, negative values west of Greenwich.	(1e-6) degrees	1	AsciiGeoCoordinate	11 byte(s)
30	first_first_long_units <10-6degE>	units	1	AsciiString	10 byte(s)
31	newline_char_8 newline character	terminator	1	AsciiString	1 byte(s)
32	first_mid_lat_title FIRST_MID_LAT=	keyword	1	AsciiString	14 byte(s)
33	first_mid_lat Geodetic Latitude of the middle sample of the first line. A negative value denotes south latitude, a positive value denotes North latitude	(1e-6) degrees	1	AsciiGeoCoordinate	11 byte(s)
34	first_mid_lat_units <10-6degN>	units	1	AsciiString	10 byte(s)
35	newline_char_9 newline character	terminator	1	AsciiString	1 byte(s)
36	first_mid_long_title FIRST_MID_LONG=	keyword	1	AsciiString	15 byte(s)
37	first_mid_long East geodetic longitude of the middle sample of the first line. Positive values East of Greenwich, negative values west of Greenwich.	(1e-6) degrees	1	AsciiGeoCoordinate	11 byte(s)
38	first_mid_long_units <10-6degE>	units	1	AsciiString	10 byte(s)
39	newline_char_10 newline character	terminator	1	AsciiString	1 byte(s)
40	first_last_lat_title FIRST_LAST_LAT=	keyword	1	AsciiString	15 byte(s)
41	first_last_lat Geodetic Latitude of the last sample of the first line. A negative value denotes south latitude, a positive value denotes North latitude	(1e-6) degrees	1	AsciiGeoCoordinate	11 byte(s)
42	first_last_lat_units <10-6degN>	units	1	AsciiString	10 byte(s)
43	newline_char_11 newline character	terminator	1	AsciiString	1 byte(s)
44	first_last_long_title FIRST_LAST_LONG=	keyword	1	AsciiString	16 byte(s)
45	first_last_long East geodetic longitude of the last sample of the first line. Positive values East of Greenwich, negative values west of Greenwich.	(1e-6) degrees	1	AsciiGeoCoordinate	11 byte(s)
46	first_last_long_units <10-6degE>	units	1	AsciiString	10 byte(s)
47	newline_char_12 newline character	terminator	1	AsciiString	1 byte(s)
48	last_first_lat_title	keyword	1	AsciiString	15 byte(s)

#	Description	Units	Count	Type	Size
	LAST_FIRST_LAT=				
49	last_first_lat Geodetic Latitude of the first sample of the last line. A negative value denotes south latitude, a positive value denotes North latitude	(1e-6) degrees	1	AsciiGeoCoordinate	11 byte(s)
50	last_first_units <10-6degN>	units	1	AsciiString	10 byte(s)
51	newline_char_13 newline character	terminator	1	AsciiString	1 byte(s)
52	last_first_long_title LAST_FIRST_LONG=	keyword	1	AsciiString	16 byte(s)
53	last_first_long East geodetic longitude of the first sample of the last line. Positive values East of Greenwich, negative values west of Greenwich.	(1e-6) degrees	1	AsciiGeoCoordinate	11 byte(s)
54	last_first_long_units <10-6degE>	units	1	AsciiString	10 byte(s)
55	newline_char_14 newline character	terminator	1	AsciiString	1 byte(s)
56	last_mid_lat_title LAST_MID_LAT=	keyword	1	AsciiString	13 byte(s)
57	last_mid_lat Geodetic Latitude of the middle sample of the last line. A negative value denotes south latitude, a positive value denotes North latitude	(1e-6) degrees	1	AsciiGeoCoordinate	11 byte(s)
58	last_mid_lat_units <10-6degN>	units	1	AsciiString	10 byte(s)
59	newline_char_15 newline character	terminator	1	AsciiString	1 byte(s)
60	last_mid_long_title LAST_MID_LONG=	keyword	1	AsciiString	14 byte(s)
61	last_mid_long East geodetic longitude of the middle sample of the last line. Positive values East of Greenwich, negative values west of Greenwich.	(1e-6) degrees	1	AsciiGeoCoordinate	11 byte(s)
62	last_mid_long_units <10-6degE>	units	1	AsciiString	10 byte(s)
63	newline_char_16 newline character	terminator	1	AsciiString	1 byte(s)
64	last_last_lat_title LAST_LAST_LAT=	keyword	1	AsciiString	14 byte(s)
65	last_last_lat Geodetic Latitude of the last sample of the last line. A negative value denotes south latitude, a positive value denotes North latitude	(1e-6) degrees	1	AsciiGeoCoordinate	11 byte(s)
66	last_last_lat_units <10-6degN>	units	1	AsciiString	10 byte(s)
67	newline_char_17 newline character	terminator	1	AsciiString	1 byte(s)
68	last_last_long_title LAST_LAST_LONG=	keyword	1	AsciiString	15 byte(s)
69	last_last_long East geodetic longitude of the last sample of the last line. Positive values East of Greenwich, negative values west of Greenwich.	(1e-6) degrees	1	AsciiGeoCoordinate	11 byte(s)
70	last_last_long_units <10-6degE>	units	1	AsciiString	10 byte(s)
71	newline_char_18 newline character	terminator	1	AsciiString	1 byte(s)
72	spare_1 Spare	-	1	SpareField	51 byte(s)
73	min_fpp_basep_temp_title MIN_FPP_BASEPLATE_TEM=	keyword	1	AsciiString	22 byte(s)
74	min_fpp_baseplate_tem Minimum FPP baseplate temperature The minimum physical temperature of the instrument Focal Plane Assembly baseplate during the orbit, taken from the on-board telemetry (identifier A5061).	K	1	Afl	15 byte(s)
75	min_fpp_basep_temp_units <K>	units	1	AsciiString	3 byte(s)
76	newline_char_20 newline character	terminator	1	AsciiString	1 byte(s)
77	min_12_mic_temp_title MIN_12_MICRON_DETECTOR_TEMP=	keyword	1	AsciiString	28 byte(s)
78	min_12_micron_detector_temp Minimum 12 micron detector temperature The minimum physical temperature of the 12 micron detector within the product duration, taken from the on-board telemetry (identifier A5061).	K	1	Afl	15 byte(s)
79	min_12_mic_temp_units	units	1	AsciiString	3 byte(s)

#	Description	Units	Count	Type	Size
	<K>				
80	newline_char_21 newline character	terminator	1	AsciiString	1 byte(s)
81	min_11_mic_temp_title MIN_11_MICRON_DETECTOR_TEMP=	keyword	1	AsciiString	28 byte(s)
82	min_11_micron_detector_temp Minimum 11 micron detector temperature The minimum physical temperature of the 11 micron detector within the product duration, taken from the on-board telemetry (identifier A5061).	K	1	Afl	15 byte(s)
83	min_11_mic_temp_units <K>	units	1	AsciiString	3 byte(s)
84	newline_char_22 newline character	terminator	1	AsciiString	1 byte(s)
85	min_37_mic_temp_title MIN_3_7_MICRON_DETECTOR_TEMP=	keyword	1	AsciiString	29 byte(s)
86	min_3_7_micron_detector_temp Minimum 3.7 micron detector temperature The minimum physical temperature of the 3.7 micron detector within the product duration, taken from the on-board telemetry (identifier A5061).	K	1	Afl	15 byte(s)
87	min_37_mic_temp_units <K>	units	1	AsciiString	3 byte(s)
88	newline_char_23 newline character	terminator	1	AsciiString	1 byte(s)
89	min_16_mic_temp_title MIN_1_6_MICRON_DETECTOR_TEMP=	keyword	1	AsciiString	29 byte(s)
90	min_1_6_micron_detector_temp Minimum 1.6 micron detector temperature The minimum physical temperature of the 1.6 micron detector within the product duration, taken from the on-board telemetry (identifier A5061).	K	1	Afl	15 byte(s)
91	min_16_mic_temp_units <K>	units	1	AsciiString	3 byte(s)
92	newline_char_24 newline character	terminator	1	AsciiString	1 byte(s)
93	min_087_mic_temp_title MIN_0_87_MICRON_DETECTOR_TEMP=	keyword	1	AsciiString	30 byte(s)
94	min_0_87_micron_detector_temp Minimum 0.87 micron detector temperature The minimum physical temperature of the 0.87 micron detector within the product duration, taken from the on-board telemetry (identifier A5061).	K	1	Afl	15 byte(s)
95	min_087_mic_temp_units <K>	units	1	AsciiString	3 byte(s)
96	newline_char_25 newline character	terminator	1	AsciiString	1 byte(s)
97	max_fpp_basep_temp_title MAX_FPP_BASEPLATE_TEM=	keyword	1	AsciiString	22 byte(s)
98	max_fpp_baseplate_tem Maximum FPP baseplate temperature The maximum physical temperature of the instrument Focal Plane Assembly baseplate during the orbit, taken from the on-board telemetry (identifier A5061).	K	1	Afl	15 byte(s)
99	max_fpp_basep_temp_units <K>	units	1	AsciiString	3 byte(s)
100	newline_char_26 newline character	terminator	1	AsciiString	1 byte(s)
101	max_12_mic_temp_title MAX_12_MICRON_DETECTOR_TEMP=	keyword	1	AsciiString	28 byte(s)
102	max_12_micron_detector_temp Maximum 12 micron detector temperature The maximum physical temperature of the 12 micron detector within the product duration, taken from the on-board telemetry (identifier A5061).	K	1	Afl	15 byte(s)
103	max_12_mic_temp_units <K>	units	1	AsciiString	3 byte(s)
104	newline_char_27 newline character	terminator	1	AsciiString	1 byte(s)
105	max_11_mic_temp_title MAX_11_MICRON_DETECTOR_TEMP=	keyword	1	AsciiString	28 byte(s)
106	max_11_micron_detector_temp Maximum 11 micron detector temperature The maximum physical temperature of the 11 micron detector within the product duration, taken from the on-board telemetry (identifier A5061).	K	1	Afl	15 byte(s)
107	max_11_mic_temp_units <K>	units	1	AsciiString	3 byte(s)
108	newline_char_28	terminator	1	AsciiString	1 byte(s)

#	Description	Units	Count	Type	Size
	newline character				
109	max_37_mic_temp_title MAX_3_7_MICRON_DETECTOR_TEMP=	keyword	1	AsciiString	29 byte(s)
110	max_3_7_micron_detector_temp Maximum 3.7 micron detector temperature The maximum physical temperature of the 3.7 micron detector within the product duration, taken from the on-board telemetry (identifier A5061).	K	1	Afl	15 byte(s)
111	max_37_mic_temp_units <K>	units	1	AsciiString	3 byte(s)
112	newline_char_29 newline character	terminator	1	AsciiString	1 byte(s)
113	max_16_mic_temp_title MAX_1_6_MICRON_DETECTOR_TEMP=	keyword	1	AsciiString	29 byte(s)
114	max_1_6_micron_detector_temp Maximum 1.6 micron detector temperature The maximum physical temperature of the 1.6 micron detector within the product duration, taken from the on-board telemetry (identifier A5061).	K	1	Afl	15 byte(s)
115	max_16_mic_temp_units <K>	units	1	AsciiString	3 byte(s)
116	newline_char_30 newline character	terminator	1	AsciiString	1 byte(s)
117	max_087_mic_temp_title MAX_0_87_MICRON_DETECTOR_TEMP=	keyword	1	AsciiString	30 byte(s)
118	max_0_87_micron_detector_temp Maximum 0.87 micron detector temperature The maximum physical temperature of the 0.87 micron detector within the product duration, taken from the on-board telemetry (identifier A5061).	K	1	Afl	15 byte(s)
119	max_087_mic_temp_units <K>	units	1	AsciiString	3 byte(s)
120	newline_char_31 newline character	terminator	1	AsciiString	1 byte(s)
121	lat_long_tie_pt_title LAT_LONG_TIE_POINTS=	keyword	1	AsciiString	20 byte(s)
122	lat_long_tie_points x co-ordinates of lat/long tie points. The X co-ordinates of the latitude/longitude tie points used in ADS#3 (grid pixel latitude and longitude). The 23 values range from -275 km to + 275 km in steps of 25 km.	km	23	As	23*6 byte(s)
123	lat_long_tie_pt_units <km>	units	1	AsciiString	4 byte(s)
124	newline_char_32 newline character	terminator	1	AsciiString	1 byte(s)
125	view_angle_tie_pt_title VIEW_ANGLE_TIE_POINTS=	keyword	1	AsciiString	22 byte(s)
126	view_angle_tie_points x co-ordinates of solar angle tie points. The X co-ordinates of the solar and viewing angle tie points used in ADS#5 and ADS#6 (nadir and forward solar angles). The 11 values range from -250 km to + 250 km in steps of 50 km.	km	11	As	11*6 byte(s)
127	view_angle_tie_pt_units <km>	units	1	AsciiString	4 byte(s)
128	newline_char_33 newline character	terminator	1	AsciiString	1 byte(s)
129	xy_tie_pt_pix_num_title XY_TIE_POINTS_PIXEL_NUM=	keyword	1	AsciiString	24 byte(s)
130	xy_tie_points_pixel_num pixel numbers of x-y tie points The absolute instrument pixel numbers (in the range 1 to 2000) of the tie points used in ADS#4 (scan pixel x and y).	-	99	As	99*6 byte(s)
131	newline_char_34 newline character	terminator	1	AsciiString	1 byte(s)
132	spare_2 Spare	-	1	SpareField	51 byte(s)
133	dsd_spare_3 DSD Spare	-	1	dsd_sp	0 byte(s)
134	dsd_spare_4 DSD Spare	-	1	dsd_sp	0 byte(s)

Record Length : 2190

DS_NAME : Browse SPH

Format Version 114.0

6.6.14 Browse Day_Time Colour LUT GADS

Table 6.42 Browse Day_Time Colour LUT GADS

Browse Day_Time Colour LUT GADS

#	Description	Units	Count	Type	Size
Data Record					
0	no_red_coeffs Number of red coefficients in LUT	-	1	ss	2 byte(s)
1	red_reflec Red channel relectancee	0.01%	10	ss	10*2 byte(s)
2	red_coeffs red channel colour coefficients	-	10	uc	10*1 byte(s)
3	no_green_coeffs Number of green coefficients in LUT	-	1	ss	2 byte(s)
4	green_reflec Green channel relectancee	0.01%	10	ss	10*2 byte(s)
5	green_coeffs green channel colour coefficients	-	10	uc	10*1 byte(s)
6	no_blue_coeffs Number of blue coefficients in LUT	-	1	ss	2 byte(s)
7	blue_reflec Blue channel relectancee	0.01%	10	ss	10*2 byte(s)
8	blue_coeffs blue channel colour coefficients	-	10	uc	10*1 byte(s)
9	spare_1 spare	-	1	SpareField	20 byte(s)

Record Length : 116

DS_NAME : Browse Day_Time Colour LUT GADS

Format Version 114.0

6.6.15 Characterisation GADS

Characterisation GADS

This product contains miscellaneous parameters used by the Level 1B processor, including instrument and geodetic parameters and parameters required by the regridding algorithm. It comprises a Main Product Header, a standard Auxiliary Data SPH with one DSD, and the Level 1b Characterisation Data GADS as described in the following table.

Table 6.43 Characterisation GADS

Characterisation GADS

#	Description	Units	Count	Type	Size
Data Record					
0	cone_angle cone angle The apex angle of the conical scan of aatsr, in radians. This is the angle between the line of sight and the scan axis.	radians	1	fl	4 byte(s)
1	mir_off mirror offset angle The azimuthal offset of the scan from its nominal position, in radians. This is the angle between the nominal and actual mirror positions a the start of the scan.	radians	1	fl	4 byte(s)
2	x_misalign_corr x misalignment correction One of the three angles that define the misalignment between the instrument and the spacecraft. The misalignment is specified by the angular rotations about three orthogonal axes required to bring the instrument into nominal alignment with the spacecraft platform. This is the rotation about the x axis, in radians.	radians	1	fl	4 byte(s)
3	y_misalign_corr y misalignment correction One of the three angles that define the misalignment between the instrument and the spacecraft. The misalignment is specified by the angular rotations about three orthogonal axes required to bring the instrument into nominal alignment with the spacecraft platform. This is the rotation about the x axis, in radians.	radians	1	fl	4 byte(s)
4	z_misalign_corr z misalignment correction One of the three angles that define the misalignment between the instrument and the spacecraft. The misalignment is specified by the angular rotations about three orthogonal axes required to bring the instrument into nominal alignment with the spacecraft platform. This is the rotation about the x axis, in radians.	radians	1	fl	4 byte(s)
5	aocs_cx AOCS parameter Cx The AOCS rotation amplitude in pitch. This defines the rotation in pitch applied by the ENVISAT attitude control system in yaw steering mode, according to the formulae set out in the Mission Conventions Document (GS-0561).	deg.	1	db	8 byte(s)
6	aocs_cy AOCS parameter Cy The AOCS rotation amplitude in roll. This defines the rotation in roll applied by the ENVISAT attitude control system in yaw steering mode, according to the formulae set out in the Mission Conventions Document (GS-0561).	deg.	1	db	8 byte(s)
7	aocs_cz AOCS parameter Cz The AOCS rotation amplitude in yaw. This defines the rotation in yaw applied by the ENVISAT attitude control system in yaw steering mode, according to the formulae set out in the Mission Conventions Document (GS-0561).	deg.	1	db	8 byte(s)
8	aocs_pitch_mis AOCS pitch mispointing The constant component of pitch error (if any) of the ENVISAT attitude control system in yaw steering mode. This is applied as a correction during geolocation.	deg.	1	db	8 byte(s)
9	aocs_roll_mis	deg.	1	db	8 byte(s)

#	Description	Units	Count	Type	Size
	AOCS roll mispointing The constant component of roll error (if any) of the ENVISAT attitude control system in yaw steering mode. This is applied as a correction during geolocation.				
10	aocs_yaw_mis AOCS yaw mispointing The constant component of yaw error (if any) of the ENVISAT attitude control system in yaw steering mode. This is applied as a correction during geolocation.	deg.	1	db	8 byte(s)
11	earth_maj_axis EARTH_MAJOR_AXIS The semi-major axis of the geodetic reference ellipsoid used for AATSR image geolocation. For the WGS 84 ellipsoid it is 6378.137 km.	km	1	db	8 byte(s)
12	atrk_samp_int Along-track sampling interval Redundant parameter, no longer used.	km	1	db	8 byte(s)
13	uni_time Uniform time step The time interval corresponding to 1 granule, or 32 scans. This is 32 times the scan interval, or 32 times 150 ms, expressed in days. It defines the internal sampling interval used by the geolocation algorithm.	days	1	db	8 byte(s)
14	img_row Number of image rows per granule This parameter defines the length of the product granule in image rows; the adopted value is 32.	-	1	sl	4 byte(s)
15	grid_row Number of grid rows This is an upper limit on the number of product granules in an orbit, used internally by the Operational Processor to determine the range of times to be used to derive geolocation tables.	-	1	sl	4 byte(s)
16	disp_tabl Displacement of table start before ascending node Because the forward view of the AATSR instrument is displaced by approximately 900 km from the nadir view, the data processing for an orbit must start with instrument scans measured when the satellite is still some 900 km south of the equator, before the ascending node, and the internal look-up tables used by the geolocation algorithm must allow for this. This parameter defines the number of granules prior to the ascending node crossing that must be catered for by the internal tables to permit forward view data on the equator to be geolocated. The current adopted value is 30.	-	1	sl	4 byte(s)
17	ecc_ellip eccentricity of ellipsoid The eccentricity of the geodetic reference ellipsoid used for AATSR image geolocation. For the WGS 84 ellipsoid it is 0.0818191908426.	-	1	db	8 byte(s)
18	geo_para Geodetic parameter (square of second eccentricity) The square of the geodetic parameter known as the second eccentricity of the adopted reference ellipsoid. For the WGS 84 ellipsoid it is 0.00673949674227.	-	1	db	8 byte(s)
19	spare_1 Spare	-	1	SpareField	8 byte(s)
20	fst_nad_pix FIRST_NADIR_PIXEL_NUMBER Absolute pixel index corresponding to the first element of the internal pixel arrays for nadir view. This index is internal to the Operational Processor; it is not fixed by the actual pixel selection map, and does not impact on the format or scientific contents of the AATSR products.	-	1	sl	4 byte(s)
21	fst_for_pix FIRST_FORWARD_PIXEL_NUMBER Absolute pixel index corresponding to the first element of the internal pixel arrays for forward view. This index is internal to the Operational Processor; it is not fixed by the actual pixel selection map, and does not impact on the format or scientific contents of the AATSR products.	-	1	sl	4 byte(s)
22	est_scan_pos_nad Estimate of relative scan position, nadir scan The time interval (expressed in days) corresponding to the along track displacement of the nadir instrument scan at the swath edge from the sub-satellite point. (It is, in other words, the linear displacement divided by the satellite velocity.) This parameter is internal to the Operational Processor; it is used to initialise an iteration within the geolocation algorithm, and the output product should be independent of the actual value of this parameter.	days	1	db	8 byte(s)
23	est_scan_pos_for Estimate of relative scan position, forward scan The time interval (expressed in days) corresponding to the along track displacement of the nadir instrument scan at the swath edge from the sub-satellite point. (It is, in other words, the linear displacement divided by the satellite velocity.) This parameter is internal to the Operational Processor; it is used to initialise an iteration within the geolocation algorithm, and the output product should be independent of the actual value of this parameter.	days	1	db	8 byte(s)
24	algtrk_ip_int Along-track interpolation interval The along-track separation of tie points used internally for geolocation.	-	1	ss	2 byte(s)
25	acrtrk_ip_it	-	1	ss	2 byte(s)

#	Description	Units	Count	Type	Size
	Across-track interpolation interval The across-track separation of tie points used internally for geolocation				
26	eps_x Regridding perturbation (eps_x) An across-track tolerance used internally by the regridding algorithm (qv.) The value is set to optimise the efficiency of the regridding algorithm.	m	1	ss	2 byte(s)
27	eps_y Regridding perturbation (eps_y) An along-track tolerance used internally by the regridding algorithm (qv.) The value is set to optimise the efficiency of the regridding algorithm.	m	1	ss	2 byte(s)
28	long_off_flag Longitude offset flag (0=no offset) This flag is provided for system integration testing, and will be set to zero (off) in normal operational processing.	flag	1	sl	4 byte(s)
29	long_off Longitude offset (for system testing) This parameter is an offset applied to the land-sea mask if the longitude offset flag is non-zero. This parameter is provided only for use in system integration testing, and is not relevant to operational product generation.	(1e-6) degrees	1	GeoCoordinate	4 byte(s)
30	spare_2 Spare	-	1	SpareField	8 byte(s)

Record Length : 176

DS_NAME : Characterisation GADS

Format Version 114.0

6.6.16 11/12 Micron Nadir/Forward Test LUT GADS

The cloud clearing algorithm used by AATSR includes nine independent cloud tests. This Data Set contains the auxiliary parameters used by the 11/12 micron nadir-forward view difference test. This test is applied only to sea pixels; for each sea pixel it calculates the difference between the nadir and forward view 11 micron brightness temperatures and compares it with an estimate of the same difference derived from a regression on the nadir view (11 micron - 12 micron) brightness temperature difference. If the observed difference differs from that estimated from the regression by more than the specified threshold, the pixel is flagged as cloudy in both views.

Table 6.44 11/12 Micron Nadir/Forward Test LUT GADS

11/12 Micron Nadir/Forward Test LUT GADS

#	Description	Units	Count	Type	Size
Data Record					
0	diff_slope view_diff_slope[j] Constant regression coefficient (For each across-track band j = 5,...9)	-	5	fl	5*4 byte(s)
1	diff_offset view_diff_offset[j] Linear regression coefficient (For each across-track band j = 5,...9)	-	5	fl	5*4 byte(s)
2	diff_thresh ir11_ir12_view_diff_thresh Specified difference threshold.	K/100	1	ss	2 byte(s)

Record Length : 42

DS_NAME : 11/12 Micron Nadir/Forward Test LUT GADS

Format Version 114.0

6.6.17 11/3.7 Micron Nadir/Forward Test LUT GADS

The cloud clearing algorithm used by AATSR includes nine independent cloud tests. This Data Set contains the auxiliary parameters used by the 11/3.7 micron nadir-forward view difference test. This test is applied only to sea pixels; for each sea pixel it calculates the difference between the nadir and forward view 3.7 micron brightness temperatures and compares it with an estimate of the same difference derived from a regression on the nadir view (3.7 micron - 11 micron) brightness temperature difference. If the observed difference differs from that estimated from the regression by more than the specified threshold, the pixel is flagged as cloudy in both views. Because it requires the presence of uncontaminated 3.7 micron data, the test is only applied to night-time data.

Table 6.45 11/3.7 Micron Nadir/Forward Test LUT GADS

11/3.7 Micron Nadir/Forward Test LUT GADS

#	Description	Units	Count	Type	Size
Data Record					
0	const_coeff constant coefficient a0[j] Constant regression coefficient (For each across-track band j = 5,...9)	-	5	fl	5*4 byte(s)
1	lin_coeff linear coefficient a1[j] Linear regression coefficient (For each across-track band j = 5,...9)	-	5	fl	5*4 byte(s)

#	Description	Units	Count	Type	Size
2	quad_coeff quadratic coefficient a2[j] Quadratic regression coefficient (For each across-track band j = 5,...9)	-	5	fl	5*4 byte(s)
3	diff_thresh ir37_ir11_view_diff_thresh Specified difference threshold.	K/100	1	ss	2 byte(s)

Record Length : 62

DS_NAME : 11/3.7 Micron Nadir/Forward Test LUT GADS

Format Version 114.0

6.6.18 11 Micron Spatial Coherence Test LUT GADS

The cloud clearing algorithm used by AATSR includes nine independent cloud tests. This Data Set contains the auxiliary parameters used by the 11 micron spatial coherence test.

Table 6.46 11 Micron Spatial Coherence Test LUT GADS

11 Micron Spatial Coherence Test LUT GADS

#	Description	Units	Count	Type	Size
Data Record					
0	sea_max_dev sea_max_dev Standard deviation threshold for sea data. Groups whose standard deviation exceeds this value are flagged as cloudy by the small-scale test.	K/100	1	ss	2 byte(s)
1	land_day_max_dev land_day_max_dev Standard deviation threshold for daytime land data. Groups whose standard deviation exceeds this value are flagged as cloudy by the small-scale test.	K/100	1	ss	2 byte(s)
2	land_night_max_dev land_night_max_dev Standard deviation threshold for night-time land data. Groups whose standard deviation exceeds this value are flagged as cloudy by the small-scale test.	K/100	1	ss	2 byte(s)
3	coh_reset_thresh coherence_reset_thresh Reset threshold	K/100	1	ss	2 byte(s)
4	coh_area_size coh_area_size Size of sub-arrays used in the large scale spatial coherence test. In practice this test operates on sub-arrays of 128 by 128 pixels, so the adopted value is 128.	Km	1	ss	2 byte(s)
5	coh_fraction_pass coh_fraction_passed	-	1	fl	4 byte(s)

#	Description	Units	Count	Type	Size
	Validity threshold for sub-areas.				
6	coh_adj_thresh_land coh_adj_thresh_land Correction to adaptive threshold for sub-areas adjacent to land.	K/100	1	ss	2 byte(s)
7	coh_adj_dif_land coh_adj_dif_land Correction to difference threshold for sub-areas adjacent to land.	-	1	fl	4 byte(s)
8	coh_area_dif_nv coh_area_dif_nv Difference threshold for infra-red channels, nadir view.	K/100	1	ss	2 byte(s)
9	coh_area_dif_fv coh_area_dif_fv Difference threshold for infra-red channels, forward view.	K/100	1	ss	2 byte(s)
10	coh_min_dif_nv coh_min_dif_nv Selection threshold for infra-red channel differences, nadir view.	K/100	1	ss	2 byte(s)
11	coh_min_dif_fv coh_min_dif_fv Selection threshold for infra-red channel differences, forward view.	K/100	1	ss	2 byte(s)
12	coh_area_thresh_nv coh_area_thresh_nv Adaptive threshold offset, nadir view.	K/100	1	ss	2 byte(s)
13	coh_area_thresh_fv coh_area_thresh_fv Adaptive threshold offset, forward view.	K/100	1	ss	2 byte(s)
14	dep_test_flag Dependency Test flag (cloudy_box_thresh) Option flag to determine how previous tests are accounted for in the large scale spatial coherence test.	flag	1	ss	2 byte(s)

Record Length : 34

DS_NAME : 11 Micron Spatial Coherence Test LUT GADS

Format Version 114.0

6.6.19 1.6 Micron Histogram

The cloud clearing algorithm used by AATSR includes nine independent cloud tests. This Data Set contains the auxiliary parameters used by the 1.6 micron histogram test.

Table 6.47 1.6 Micron Histogram

1.6 Micron Histogram Test LUT GADS

#	Description	Units	Count	Type	Size
Data Record					
0	v16_sprd_nad Nadir view histogram spread parameter Maximum width of a valid histogram using nadir view data	%	1	fl	4 byte(s)
1	v16_sprd_for Forward view histogram spread parameter Maximum width of a valid histogram using forward view data	%	1	fl	4 byte(s)
2	v16_pk_nad Auxiliary peak height parameter, nadir view Used in identifying valid histogram of nadir view data	-	1	ss	2 byte(s)
3	v16_pk_for Auxiliary peak height parameter, forward view Used in identifying valid histogram of forward view data	-	1	ss	2 byte(s)
4	min_v16_hist Minimum pixels for a valid histogram If the number of valid pixels contributing to the histogram is less than this value, the histogram test is not attempted	-	1	ss	2 byte(s)
5	tilt_thresh Sunglint threshold If the angle (in degrees) through which a sea facet would need to be tilted away from normal to specularly reflect the sun into the instrument is less than this value, sunglint is flagged. The histogram test is not attempted, and a spatial coherence test on the 1.6 micron data is used instead.	degrees	1	fl	4 byte(s)
6	thresh_3 threshold_3	-	1	fl	4 byte(s)
7	nr_glt_rang Near glint threshold If the angle (in degrees) through which a sea facet would need to be tilted away from normal to specularly reflect the sun into the instrument is greater than the sunglint threshold (tilt_thresh) but less than this value (nr_glt_rang), the region is treated as a near glint region. An attempt is made to detrend the data to remove any residual reflected solar radiation before the histogram test is applied.	degrees	1	fl	4 byte(s)
8	min_for_pass min_for_passed	-	1	ss	2 byte(s)
9	rang_pk search_range_for_peak	%	1	fl	4 byte(s)
10	wt_limt tilt_weight_limit	degrees	1	fl	4 byte(s)
11	r_wt_limt range_weight_limit	degrees	1	fl	4 byte(s)
12	wt_fac tilt_weight_factor	-	1	fl	4 byte(s)
13	min_pk_val min_peak_value	-	1	ss	2 byte(s)
14	min_for_detr min_for_detrend	-	1	ss	2 byte(s)
15	max_glt_thresh max_glint_threshold	%	1	fl	4 byte(s)
16	spare_1 spare	-	1	SpareField	20 byte(s)

Record Length : 72

DS_NAME : 1.6 Micron Histogram Test LUT GADS

Format Version 114.0

6.6.20 Infrared Histogram Test LUT GADS

The cloud clearing algorithm used by AATSR includes nine independent cloud tests. This Data Set contains the auxiliary parameters used by the infra-red histogram test.

Table 6.48 Infrared Histogram Test LUT GADS

Infrared Histogram Test LUT GADS

#	Description	Units	Count	Type	Size
Data Record					
0	min_hist min_for_ir11_ir12_histogram	TBD	1	ss	2 byte(s)
1	pk_frac_min peak_frac_min	TBD	1	fl	4 byte(s)
2	pos_lat_thresh positive_latitude_thresh	TBD	1	fl	4 byte(s)
3	sec_low_frac second_low_fraction	TBD	1	fl	4 byte(s)
4	h_width_m1 half_width_m[1]	TBD	1	fl	4 byte(s)
5	h_width_b1 half_width_b[1]	TBD	1	fl	4 byte(s)
6	h_width_m0 half_width_m[0]	TBD	1	fl	4 byte(s)
7	h_width_b0 half_width_b[0]	TBD	1	fl	4 byte(s)
8	max_dif_ave_chan_1 max_dif_ave_chan_1	TBD	1	fl	4 byte(s)
9	max_dif_pk_chan_1 max_dif_peak_chan_1	TBD	1	fl	4 byte(s)
10	ratio_b ratio_b	TBD	1	fl	4 byte(s)
11	ir_sprd_nv ir_spread_nv	TBD	1	fl	4 byte(s)
12	ir_sprd_fv ir_spread_fv	TBD	1	fl	4 byte(s)
13	slp_max_allow slope_max_allowed	TBD	1	fl	4 byte(s)
14	ir_pk_min ir_peak_min	TBD	1	fl	4 byte(s)

Record Length : 58

DS_NAME : Infrared Histogram Test LUT GADS

Format Version 114.0

6.6.21 12 Micron Gross Cloud Test LUT GADS

The cloud clearing algorithm used by AATSR includes nine independent cloud tests. This Data Set contains the auxiliary parameters used by the 12 micron gross cloud test. This test flags those pixels as cloudy for which the 12 micron brightness temperature is less than the specified threshold. It is only applied to sea pixels.

Table 6.49 12 Micron Gross Cloud Test LUT GADS

12 Micron Gross Cloud Test LUT GADS

#	Description	Units	Count	Type	Size
Data Record					
0	thresh_nad 12 micron threshold nadir The test flags those nadir view pixels as cloudy for which the 12 micron brightness temperature is less than this value.	K/100	1	ss	2 byte(s)
1	thresh_for 12 micron threshold forward The test flags those forward view pixels as cloudy for which the 12 micron brightness temperature is less than this value.	K/100	1	ss	2 byte(s)

Record Length : 4

DS_NAME : 12 Micron Gross Cloud Test LUT GADS

Format Version 114.0

6.6.22 Fog/low Stratus Test LUT GADS

The cloud clearing algorithm used by AATSR includes nine independent cloud tests. This Data Set contains the auxiliary parameters used by the fog/low stratus test. This test flags those pixels as cloudy for which the brightness temperature difference between the 11 and 3.7 micron channels is greater than the specified threshold. Because it requires the presence

of uncontaminated 3.7 micron data, it is only applied to night-time data.

Table 6.50 Fog/low Stratus Test LUT GADS

Fog/low Stratus Test LUT GADS

#	Description	Units	Count	Type	Size
Data Record					
0	nad_thresh fog_threshold[j], nadir Threshold for nadir view pixels.	K/100	1	ss	2 byte(s)
1	for_thresh fog_threshold[j], forward Threshold for forward view pixels.	K/100	1	ss	2 byte(s)

Record Length : 4

DS_NAME : Fog/low Stratus Test LUT GADS

Format Version 114.0

6.6.23 Medium/High Level Test LUT GADS

The cloud clearing algorithm used by AATSR includes nine independent cloud tests. This Data Set contains the auxiliary parameters used by the medium/high level cloud test. This test flags those pixels as cloudy for which the brightness temperature difference between the 3.7 and 12 micron channels is greater than the specified threshold. Because it requires the presence of uncontaminated 3.7 micron data, it is only applied to night-time data.

Table 6.51 Medium/High Level Test LUT GADS

Medium/High Level Test LUT GADS

#	Description	Units	Count	Type	Size
Data Record					
0	nad_thresh med_high_level_threshold[i], nadir Threshold for nadir view pixels.	K/100	1	ss	2 byte(s)
1	for_thresh med_high_level_threshold[i], forward Threshold for forward view pixels.	K/100	1	ss	2 byte(s)

Record Length : 4

DS_NAME : Medium/High Level Test LUT GADS

Format Version 114.0

6.6.24 Thin Cirrus Test LUT GADS

The cloud clearing algorithm used by AATSR includes nine independent cloud tests. This Data Set contains the auxiliary parameters used by the thin cirrus test. This test flags those pixels as cloudy for which the brightness temperature difference between the 11 and 12 micron channels is greater than the specified threshold.

Table 6.52 Thin Cirrus Test LUT GADS

Thin Cirrus Test LUT GADS

#	Description	Units	Count	Type	Size
Data Record					
0	nad_thresh nadir_threshold[i][j] Threshold for nadir view pixels.	K/100	1	ss	2 byte(s)
1	for_thresh frwrd_threshold[i][j] Threshold for nadir view pixels.	K/100	1	ss	2 byte(s)

Record Length : 4

DS_NAME : Thin Cirrus Test LUT GADS

Format Version 114.0

6.6.25 General Parameters GADS

Table 6.53 General Parameters GADS

General Parameters GADS

#	Description	Units	Count	Type	Size
Data Record					
0	ems_mxbb_12 Emissivity factor for MXBB, 12 micron channel The emissivity of the -X black body at 12 micron wavelength, derived from ground calibration measurements.	-	1	db	8 byte(s)
1	ems_mxbb_11 Emissivity factor for MXBB, 11 micron channel The emissivity of the -X black body at 11 micron wavelength, derived from ground calibration measurements.	-	1	db	8 byte(s)
2	ems_mxbb_37 Emissivity factor for MXBB, 3.7 micron channel The emissivity of the -X black body at 3.7 micron wavelength, derived from ground calibration measurements.	-	1	db	8 byte(s)
3	ems_pxbb_12 Emissivity factor for PXBB, 12 micron channel The emissivity of the +X black body at 12 micron wavelength, derived from ground calibration measurements.	-	1	db	8 byte(s)
4	ems_pxbb_11 Emissivity factor for PXBB, 11 micron channel The emissivity of the +X black body at 11 micron wavelength, derived from ground calibration measurements.	-	1	db	8 byte(s)
5	ems_pxbb_37 Emissivity factor for PXBB, 3.7 micron channel The emissivity of the + black body at 3.7 micron wavelength, derived from ground calibration measurements.	-	1	db	8 byte(s)
6	num_temp_rad Number of entries in Temperature to Radiance LUT or size_of_LUT The number of entries (typically about 400) in the Temperature to Radiance LUT.	-	1	ss	2 byte(s)
7	inc_temp_rad Increment in Temperature to Radiance LUT The constant temperature increment (K) in the Temperature to Radiance LUT.	K	1	db	8 byte(s)
8	fst_value_temp First value in Temperature to Radiance LUT The first temperature value (K) in the Temperature to Radiance LUT.	K	1	db	8 byte(s)
9	last_val_temp Last value in Temperature to Radiance LUT The last temperature value (K) in the Temperature to Radiance LUT.	K	1	db	8 byte(s)

#	Description	Units	Count	Type	Size
10	num_radtemp_12 Number of entries in 12 micron Radiance to Temperature LUT The number of entries (typically about 4000) in the 12 micron Radiance to Brightness Temperature LUT.	-	1	ss	2 byte(s)
11	inc_rad_temp_12 Increment in 12 micron Radiance to brightness Temperature LUT The increment in the 12 micron Radiance to Brightness Temperature LUT (in radiance units W cm-2 sr-1).	Wcm-2 sr-1	1	db	8 byte(s)
12	fst_value_rad_12 First value in 12 micron Radiance to brightness Temperature LUT The radiance value corresponding to the first entry in the 12 micron Radiance to Brightness Temperature LUT (in radiance units W cm-2 sr-1).	Wcm-2 sr-1	1	db	8 byte(s)
13	last_val_rad_12 Last value in 12 micron Radiance to brightness Temperature LUT The radiance value corresponding to the last entry in the 12 micron Radiance to Brightness Temperature LUT (in radiance units W cm-2 sr-1).	Wcm-2 sr-1	1	db	8 byte(s)
14	num_radtemp_11 Number of entries in 11 micron Radiance to Temperature LUT The number of entries (typically about 4000) in the 11 micron Radiance to Brightness Temperature LUT.	-	1	ss	2 byte(s)
15	inc_rad_temp_11 Increment in 11 micron Radiance to brightness Temperature LUT The increment in the 11 micron Radiance to Brightness Temperature LUT (in radiance units W cm-2 sr-1).	Wcm-2 sr-1	1	db	8 byte(s)
16	fst_value_rad_11 First value in 11 micron Radiance to brightness Temperature LUT The radiance value corresponding to the first entry in the 11 micron Radiance to Brightness Temperature LUT (in radiance units W cm-2 sr-1).	Wcm-2 sr-1	1	db	8 byte(s)
17	last_val_rad_11 Last value in 11 micron Radiance to brightness Temperature LUT The radiance value corresponding to the last entry in the 11 micron Radiance to Brightness Temperature LUT (in radiance units W cm-2 sr-1).	Wcm-2 sr-1	1	db	8 byte(s)
18	num_radtemp_37 Number of entries in 3.7 micron Radiance to Temperature LUT The number of entries (typically about 4000) in the 3.7 micron Radiance to Brightness Temperature LUT.	-	1	ss	2 byte(s)
19	inc_rad_temp_37 Increment in 3.7 micron Radiance to brightness Temperature LUT The increment in the 3.7 micron Radiance to Brightness Temperature LUT (in radiance units W cm-2 sr-1).	Wcm-2 sr-1	1	db	8 byte(s)
20	fst_value_rad_37 First value in 3.7 micron Radiance to brightness Temperature LUT The radiance value corresponding to the first entry in the 3.7 micron Radiance to Brightness Temperature LUT (in radiance units W cm-2 sr-1).	Wcm-2 sr-1	1	db	8 byte(s)
21	last_val_rad_37 Last value in 3.7 micron Radiance to brightness Temperature LUT The radiance value corresponding to the last entry in the 3.7 micron Radiance to Brightness Temperature LUT (in radiance units W cm-2 sr-1).	Wcm-2 sr-1	1	db	8 byte(s)
22	num_nonlin_cor_16 Number of entries in 1.6 micron Non-Linearity Correction LUT The number of entries (typically about 100) in the 1.6 micron Channel Non-linearity Correction LUT.	-	1	ss	2 byte(s)
23	inc_nonlin_cor_16 Increment in 1.6 micron Non-Linearity Correction LUT The increment, in instrument counts, in the 1.6 micron Channel Non-linearity Correction LUT.	-	1	db	8 byte(s)
24	fst_nonlin_cor_16 First value in 1.6 micron Non-Linearity Correction LUT The instrument count corresponding to the first entry in the 1.6 micron Channel Non-linearity Correction LUT.	-	1	db	8 byte(s)
25	last_nonlin_cor_16 Last value in 1.6 micron Non-Linearity Correction LUT The instrument count corresponding to the last entry in the 1.6 micron Channel Non-linearity Correction LUT.	-	1	db	8 byte(s)
26	spare_1 Spare	-	1	SpareField	20 byte(s)

Record Length : 198

DS_NAME : General Parameters GADS

Format Version 114.0

6.6.26 1.6 micron Non-Linearity Correction LUT GADS

Table 6.54 1.6 micron Non-Linearity Correction LUT GADS

1.6 micron Non-Linearity Correction LUT GADS

#	Description	Units	Count	Type	Size
Data Record					
0	uncor_count Uncorrected count table entry Each record of the file contains a single table entry. This field contains the instrument count corrected for signal channel non-linearity, in the range 0 to 4095, corresponding to the table entry. The non-linearity of the channel was determined during ground characterisation.	-	1	db	8 byte(s)
1	cor_count Corrected count table entry Each record of the file contains a single table entry. This field contains the instrument count, in the range 0 to 4095, corresponding to the table entry.	-	1	db	8 byte(s)

Record Length : 16

DS_NAME : 1.6 micron Non-Linearity Correction LUT GADS

Format Version 114.0

6.6.27 Radiance to Brightness Temperature LUT GADS

Table 6.55 Radiance to Brightness Temperature LUT GADS

Radiance to Brightness Temperature LUT GADS

#	Description	Units	Count	Type	Size
Data Record					
0	temp_lut_12 temperature_lut [12 micron] This field in record j of the table contains the brightness temperature in K corresponding to the jth tabular value of the 12 micron channel integrated radiance. The tabular value for record j is given by (First value in 12 micron LUT) + (j - 1) * Increment.	K	1	db	8 byte(s)
1	temp_lut_11 temperature_lut [11 micron] This field in record j of the table contains the brightness temperature in K corresponding to the jth tabular value of the 11 micron channel integrated radiance. The tabular value for record j is given by (First value in 11 micron LUT) + (j - 1) * Increment.	K	1	db	8 byte(s)
2	temp_lut_37 temperature_lut [3.7 micron] This field in record j of the table contains the brightness temperature in K corresponding to the jth tabular value of the 3.7 micron channel integrated radiance. The tabular value for record j is given by (First value in 3.7 micron LUT) + (j - 1) * Increment.	K	1	db	8 byte(s)

Record Length : 24

DS_NAME : Radiance to Brightness Temperature LUT GADS

Format Version 114.0

6.6.28 Temperature to Radiance LUT GADS

Table 6.56 Temperature to Radiance LUT GADS

Temperature to Radiance LUT GADS

#	Description	Units	Count	Type	Size
Data Record					
0	temp temperature Each record of the file contains a single table entry. This field contains the temperature in K corresponding to the table entry.	K	1	db	8 byte(s)
1	rad_lut_12 radiance_lut [12 micron] This field contains the integrated radiance in the 12 micron channel, corrected for	Wcm-2 sr-1	1	db	8 byte(s)

#	Description	Units	Count	Type	Size
	channel non-linearity, corresponding to the table entry. The integrated radiance is expressed in units of W cm-2 sr-1.				
2	rad_lut_11 radiance_lut [11 micron] This field contains the integrated radiance in the 11 micron channel, corrected for channel non-linearity, corresponding to the table entry. The integrated radiance is expressed in units of W cm-2 sr-1.	Wcm-2 sr-1	1	db	8 byte(s)
3	rad_lut_37 radiance_lut [3.7 micron] This field contains the integrated radiance in the 3.7 micron channel, corrected for channel non-linearity, corresponding to the table entry. The integrated radiance is expressed in units of W cm-2 sr-1.	Wcm-2 sr-1	1	db	8 byte(s)

Record Length : 32

DS_NAME : Temperature to Radiance LUT GADS

Format Version 114.0

6.6.29 General Parameters GADS

Table 6.57 General Parameters GADS

General Parameters GADS

#	Description	Units	Count	Type	Size
Data Record					
0	aux_tot aux_tot: Total number of auxiliary data items in MUDT This parameter defines the number of records in the Master Unpacking Definition Table (MUDT). Each record of the MUDT defines a single auxiliary parameter.	-	1	sl	4 byte(s)
1	aux_val_tot aux_val_tot: Total number of sets of auxiliary limits data items This parameter defines the number of records in the table of validation limits for unpacked auxiliary items. It is equal to the number of auxiliary parameters for which validation limits are defined.	-	1	sl	4 byte(s)
2	n_conv n_conv: Total number of auxiliary items for conversion This parameter defines the number of records in the table of conversion parameters. It is equal to the number of auxiliary parameters for which conversions to engineering units are defined.	-	1	sl	4 byte(s)
3	s_surv n_surv_tot: Total number of surveillance limit specifications This parameter defines the number of records in the table of surveillance limits for converted auxiliary items. It is equal to the number of auxiliary parameters for which surveillance limits are defined.	-	1	sl	4 byte(s)
4	spare_1 Spare	-	1	SpareField	12 byte(s)

Record Length : 28

DS_NAME : General Parameters GADS

Format Version 114.0

6.6.30 Validation Parameters GADS

Table 6.58 Validation Parameters GADS

Validation Parameters GADS

#	Description	Units	Count	Type	Size
Data Record					
0	prt_mean_difference prt_mean_difference This value is used in a quality check of the three platinum resistance thermometer readings (PRT1, PRT2 and PRT3). These thermometers measure the temperature of the paraboloidal mirror of the AATSR telescope. If any of the readings differs from their mean by more than prt_mean_difference that reading is marked as invalid, and is not used for the instrument calibration.	Deg K	1	db	8 byte(s)
1	max_hbb_prt_mean_diff max_hbb_prt_mean_diff This value is used in a quality check of the readings of the platinum resistance thermometers that measure the temperature of the hot black body used for infra-red channel calibration. If any of the readings differs from their mean by more than max_hbb_prt_mean_diff that reading is marked as invalid, and is not used for the instrument calibration.	Deg K	1	db	8 byte(s)
2	max_cbb_prt_mean_diff max_cbb_prt_mean_diff This value is used in a quality check of the readings of the platinum resistance thermometers that measure the temperature of the cold black body used for infra-red channel calibration. If any of the readings differs from their mean by more than max_cbb_prt_mean_diff that reading is marked as invalid, and is not used for the instrument calibration.	Deg K	1	db	8 byte(s)
3	scp2_6_temp_diff scp2_6_temp_diff This value is used in a quality check of temperature readings (SCP2 to SCP6) associated with the signal channel processor (SCP) chain. If the maximum difference between the temperature readings designated SCP2 to SCP6, taken in pairs, exceeds scp2_6_temp_diff then internal error flags are set which may, if other error conditions are also present, cause the temperatures to be excluded from the calibration. (The temperatures SCP2 to SCP 5 inclusive refer to the infrared channel detectors; SCP 6 is the FPA baseplate temperature).	Deg K	1	db	8 byte(s)
4	scp7_10_temp_diff scp7_10_temp_diff This value is used in a quality check of temperature readings (SC7 to SCP10) associated with the signal channel processor (SCP) chain. If the maximum difference between the temperature readings designated SCP7 to SCP10, taken in pairs, exceeds scp7_10_temp_diff then internal error flags are set which may, if other error conditions are also present, cause the temperatures to be excluded from the calibration.	Deg K	1	db	8 byte(s)
5	prt8_fixed_val prt8_fixed_val This and the following value (prt8_variance) are used in a quality check of the	Digitised counts	1	ss	2 byte(s)

#	Description	Units	Count	Type	Size
	platinum resistance thermometer reading PRT8 (within the Instrument Electronics Unit). This check is performed on the unconverted count from the thermometer; if the unconverted count falls outside the range prt8_fixed_val ? prt8_variance then internal error flags are set which may, if other error conditions are also present, cause the baffle and paraboloid temperatures to be excluded from the calibration.				
6	prt8_variance prt8_variance See prt8_fixed_val.	Digitised counts	1	ss	2 byte(s)

Record Length : 44

DS_NAME : Validation Parameters GADS

Format Version 114.0

6.6.31 Conversion Parameters GADS

Table 6.59 Conversion Parameters GADS

Conversion Parameters GADS

#	Description	Units	Count	Type	Size
Data Record					
0	aux_id auxiliary item identifier A 5 character alphanumeric code identifying the auxiliary item. This is the Telemetry ID as defined in document PO-TN-MMB-AT-0044. Values range from A0010 to A7401.	-	5	uc	5*1 byte(s)
1	func_id function identifier A 3 character alphanumeric code identifying the generic conversion function to be applied to this parameter. The code has the form Fnn, where nn represents a two-digit integer.	-	3	uc	3*1 byte(s)
2	par_lst parameter list The numerical parameters of the generic conversion function defined in the preceding function identifier field. The number of parameters depends on the particular function.	variable	20	db	20*8 byte(s)

Record Length : 168

DS_NAME : Conversion Parameters GADS

Format Version 114.0

The type of these fields depends on context. In the majority of cases the definition 'double' is appropriate, but in certain specific cases the field is to be interpreted as an ASCII string '8*uc'. Details may be found in the Level 1B DPM/PDL Document.

6.6.32 Limits GADS

Table 6.60 Limits GADS

Limits GADS

#	Description	Units	Count	Type	Size
Data Record					
0	aux_id_limt auxiliary identifier limits The 5 character telemetry ID identifying the auxiliary item. This is the Telemetry ID as defined in document PO-TN-MMB-AT-0044. Values range from A0010 to A7401.	-	5	uc	5*1 byte(s)
1	aux_val_low_limt aux validation lower limit Lower validation limit. The unpacked data item is considered to be invalid if it falls outside the range defined by the upper and lower limits specified here.	-	1	us	2 byte(s)
2	aux_val_up_limt aux validation upper limit Upper validation limit. The unpacked data item is considered to be invalid if it falls outside the range defined by the upper and lower limits specified here.	-	1	us	2 byte(s)

Record Length : 9

DS_NAME : Limits GADS

Format Version 114.0

6.6.33 Master Unpacking Definition Table GADS

Table 6.61 Master Unpacking Definition Table GADS

Master Unpacking Definition Table GADS

#	Description	Units	Count	Type	Size
Data Record					
0	aux_id auxiliary item identifier A 5 character alphanumeric code identifying the auxiliary item. This is the Telemetry ID as defined in document PO-TN-MMB-AT-0044. Values range from A0010 to A7401.	-	5	uc	5*1 byte(s)
1	wd_num_aux word number in packet containing auxiliary item The index to the word containing the auxiliary data item within the auxiliary data area of the AATSR instrument source packet.	-	1	us	2 byte(s)
2	mask mask to extract auxiliary item from word A 16 bit binary mask to extract the auxiliary data field from the word within which it is contained.	-	1	ss	2 byte(s)
3	shft_norm shift to normalise The shift, in bits (in the range 0 to 15), to right-justify the auxiliary data field within the word.	-	1	us	2 byte(s)

Record Length : 11

DS_NAME : Master Unpacking Definition Table GADS

Format Version 114.0

The MUDT contains 1 record for each auxiliary data item within the source packet. All auxiliary data, the data item identifiers, their unpacking and conversion parameters are defined in the detailed AATSR Telemetry Specifications, from which the total number of auxiliary data items, which is less than 1000, is derived.

6.6.34 Surveillance Limits GADS

Table 6.62 Surveillance Limits GADS

Surveillance Limits GADS

#	Description	Units	Count	Type	Size
Data Record					
0	surv_limt_aux surveillance limit auxiliary identifiers The 5 character telemetry ID identifying the auxiliary item. This is the Telemetry ID as defined in document PO-TN-MMB-AT-0044. Values range from A0010 to A7401.	-	5	uc	5*1 byte(s)
1	surv_llimt surveillance lower limit Lower surveillance limit. The converted data item is considered to be invalid if it falls outside the range defined by the upper and lower limits specified here.	-	1	fl	4 byte(s)
2	surv_ulimt surveillance upper limit Upper surveillance limit. The converted data item is considered to be invalid if it falls outside the range defined by the upper and lower limits specified here.	-	1	fl	4 byte(s)

Record Length : 13

DS_NAME : Surveillance Limits GADS

Format Version 114.0

6.6.35 10-arcminute mds

Table 6.63 10-arcminute mds

10-arcminute mds

#	Description	Units	Count	Type	Size
Data Record					
0	dsr_time Nadir UTC time in MJD format The (nadir and forward view) instrument data contributing to a given cell or sub-cell may cover a range of up to 150 seconds of measurement times. It is therefore not possible to assign a unique time tag to an AST record, and the time tag is therefore arbitrarily assigned as follows. The nadir time associated with a given AST record represents the scan time of a nadir pixel contributing to the record. In general this is the time of the first filled pixel encountered during processing that falls within the geometrical boundary of the cell or sub-cell (see link), although exception cases may arise. Because the cell boundaries bear no clear geometrical relationship to the AATSR instrument scan it is not possible to state in general that this corresponds to a particular corner of the cell or sub-cell. Note also that if a cell is intersected by coastline, so that it contains both land and sea pixels, the time tag of a given record does not necessarily correspond to a pixel of the same surface type.	MJD	1	mjd	12 byte(s)
1	rec_qua_ind Record Quality indicator This field is set to -1 if all the measurement values in the record are invalid, and is set to 0 otherwise.	-	1	sc	1 byte(s)
2	spare_1 Spare	-	1	SpareField	3 byte(s)

#	Description	Units	Count	Type	Size
3	lat Latitude of 10 arcmin cell The latitude of the lower left-hand corner of the sub-cell, in units of micro-degrees. The latitude is defined in the range -90 degrees to +90 degrees. If the cell contains no valid data, this field may be set to the exceptional value -399,999,999.	(1e-6) degrees	1	GeoCoordinate	4 byte(s)
4	lon Longitude of 10 arcmin cell The longitude of the lower left-hand corner of the sub-cell, in units of micro-degrees. The longitude is defined in the range -180 degrees to +180 degrees. If the cell contains no valid data, this field may be set to the exceptional value -399,999,999.	(1e-6) degrees	1	GeoCoordinate	4 byte(s)
5	sa_12bt_clr_nad Nadir spatially averaged 12 micron BT of all clear pixels 10 arcmin cells The mean calibrated brightness temperature in the 12 micron channel of all the valid clear pixels over sea, measured in the nadir view, that fall within the sub-cell. The brightness temperature is expressed as a long (32 bit) integer in units of 0.001 K. Valid mean brightness temperatures will be positive numbers in the range 170,000 to 321,000. If no valid clear sea pixels fall within the sub-cell, the field will be set to an exceptional value of -1.	K/1000	1	sl	4 byte(s)
6	sa_11bt_clr_nad Nadir spatially averaged 11 micron BT of all clear pixels in 10 arcmin cells The mean calibrated brightness temperature in the 11 micron channel of all the valid clear pixels over sea, measured in the nadir view, that fall within the sub-cell. The brightness temperature is expressed as a long (32 bit) integer in units of 0.001 K. Valid mean brightness temperatures will be positive numbers in the range 170,000 to 321,000. If no valid clear sea pixels fall within the sub-cell, the field will be set to an exceptional value of -1.	K/1000	1	sl	4 byte(s)
7	sa_37bt_clr_nad Nadir spatially averaged 3.7 micron BT of all clear pixels in 10 arcmin cells The mean calibrated brightness temperature in the 3.7 micron channel of all the valid clear pixels over sea, measured in the nadir view, that fall within the sub-cell. The brightness temperature is expressed as a long (32 bit) integer in units of 0.001 K. Valid mean brightness temperatures will be positive numbers in the range 195,000 to 321,000. If no valid clear sea pixels fall within the sub-cell, the field will be set to an exceptional value of -1.	K/1000	1	sl	4 byte(s)
8	sa_12bt_clr_for Forward spatially averaged 12 micron BT of all clear pixels in 10 arcmin cells The mean calibrated brightness temperature in the 12 micron channel of all the valid clear pixels over sea, measured in the forward view, that fall within the sub-cell. The brightness temperature is expressed as a long (32 bit) integer in units of 0.001 K. Valid mean brightness temperatures will be positive numbers in the range 170,000 to 321,000. If no valid clear sea pixels fall within the sub-cell, the field will be set to an exceptional value of -1.	K/1000	1	sl	4 byte(s)
9	sa_11bt_clr_for Forward spatially averaged 11 micron BT of all clear pixels in 10 arcmin cells The mean calibrated brightness temperature in the 11 micron channel of all the valid clear pixels over sea, measured in the forward view, that fall within the sub-cell. The brightness temperature is expressed as a long (32 bit) integer in units of 0.001 K. Valid mean brightness temperatures will be positive numbers in the range 170,000 to 321,000. If no valid clear sea pixels fall within the sub-cell, the field will be set to an exceptional value of -1.	K/1000	1	sl	4 byte(s)
10	sa_37bt_clr_for Forward spatially averaged 3.7 micron BT of all clear pixels in 10 arcmin cells The mean calibrated brightness temperature in the 3.7 micron channel of all the valid clear pixels over sea, measured in the forward view, that fall within the sub-cell. The brightness temperature is expressed as a long (32 bit) integer in units of 0.001 K. Valid mean brightness temperatures will be positive numbers in the range 195,000 to 321,000. If no valid clear sea pixels fall within the sub-cell, the field will be set to an exceptional value of -1.	K/1000	1	sl	4 byte(s)
11	m_actrk_pix_num Mean across-track pixel number The average pixel index of the nadir view clear sea pixels that fall within the sub-cell. The pixel index, in the range 0 to 511 inclusive, is the across-track index of the pixel in the image, and ids linearly related to the X co-ordinate by X = j - 256 km. The mean across-track pixel index is thus a measure of the X co-ordinate of the centroid of the distribution of clear sea pixels that will contribute to the SST determination. It is used to select the SST retrieval coefficients for the cell.	-	1	ss	2 byte(s)
12	m_nad Mean nadir-only SST 10 arcmin cells The mean sea surface temperature (SST) derived using only data in the nadir view. The SST is derived from the mean brightness temperatures in the three infra-red channels, averaged over the valid clear sea pixels in the sub-cell. The SST determination uses retrieval coefficients optimised for averaged data. Day-time retrievals use the 11 and 12 micron channels only; night-time determinations will also use valid 3.7 micron data.	K/100	1	ss	2 byte(s)
13	pix_nad Number of pixels in nadir-only average, 10 arcmin cells The number of valid 11 and 12 micron pixels contributing to the nadir-only SST determination in the cell. In general the numbers of valid pixels in the 11 and 12 micron channels are expected to be the same; if they differ, the lower is given here.	-	1	us	2 byte(s)
14	m_dual_vw Mean dual-view SST in 10 arcmin cells The mean sea surface temperature (SST) derived using data from both nadir and	K/100	1	ss	2 byte(s)

#	Description	Units	Count	Type	Size
	forward views. The SST is derived from the mean brightness temperatures in the three infra-red channels, averaged over the valid clear sea pixels in the sub-cell. The SST determination uses retrieval coefficients optimised for averaged data. Day-time retrievals use the 11 and 12 micron channels only; night-time determinations will also use valid 3.7 micron data.				
15	pix_dual_vw Number of pixels in dual-view average, 10 arcmin cells The number of valid 11 and 12 micron pixels contributing to the dual view SST determination in the cell. In general the numbers of valid pixels in the 11 and 12 micron channels in a given view are expected to be the same. However, they may differ, and in a cloudy scene the number of valid pixels in the nadir and forward views may differ. When the numbers of valid pixels in the different channel and view combinations differ, the lowest is given here.	-	1	us	2 byte(s)
16	ast_conf_flags AST confidence word A 16-bit word containing confidence flags for the record. Bits 0 to 3 are set to indicate whether or not 3.7 micron channel data was used in the SST retrieval, and whether or not day-time data contributes to the retrieved temperatures. The detailed interpretation of these bits is defined in the table below. Bits 4 to 31 are currently unused.	flags	2	us	2*2 byte(s)

Record Length : 62

DS_NAME : 10-arcminute mds

Format Version 114.0

The table below lists the confidence flags in the AST Confidence Word.

Table 6.64

bit	meaning if set.
0	Sea MDS: Nadir-only SST retrieval used 3.7 micron channel Land MDS: Reserved
1	Sea MDS: Dual-view SST retrieval used 3.7 micron channel Land MDS: Reserved
2	Nadir view contains day-time data
3	Forward view contains day-time data
4 - 31	Unused

AST confidence word

6.6.36 SPH

Table 6.65 SPH

SPH

#	Description	Units	Count	Type	Size
Data Record					
0	sph_descriptor_title SPH_DESCRIPTOR=	keyword	1	AsciiString	15 byte(s)
1	quote_1 quotation mark (""")	ascii	1	AsciiString	1 byte(s)
2	sph_descriptor SPH Descriptor ASCII string describing the product.	ascii	1	AsciiString	28 byte(s)
3	quote_2 quotation mark (""")	ascii	1	AsciiString	1 byte(s)
4	newline_char_1 newline character	terminator	1	AsciiString	1 byte(s)
5	stripline_cont_ind_title STRIPLINE_CONTINUITY_INDICATOR=	keyword	1	AsciiString	31 byte(s)
6	stripline_continuity_indicator Value: 0= No stripline continuity, the product is a complete segment. Other: Stripline Counter	-	1	Ac	4 byte(s)
7	newline_char_2 newline character	terminator	1	AsciiString	1 byte(s)
8	slice_pos_title SLICE_POSITION=	keyword	1	AsciiString	15 byte(s)
9	slice_position Value: +001 to NUM_SLICES. Default value if no stripline continuity = +001	-	1	Ac	4 byte(s)
10	newline_char_3 newline character	terminator	1	AsciiString	1 byte(s)
11	num_slices_title NUM_SLICES=	keyword	1	AsciiString	11 byte(s)
12	num_slices Number of slices in this striplineDefault value if no continuity = +001	-	1	Ac	4 byte(s)
13	newline_char_4 newline character	terminator	1	AsciiString	1 byte(s)
14	first_ln_time_title FIRST_LINE_TIME=	keyword	1	AsciiString	16 byte(s)
15	quote_3 quotation mark (""")	ascii	1	AsciiString	1 byte(s)
16	first_line_time Azimuth time first line of product. UTC Time of first range line in the MDS of this product. UTC time format contained within quotation marks.	UTC	1	UtcExternal	27 byte(s)
17	quote_4 quotation mark (""")	ascii	1	AsciiString	1 byte(s)
18	newline_char_5 newline character	terminator	1	AsciiString	1 byte(s)
19	last_ln_time_title LAST_LINE_TIME=	keyword	1	AsciiString	15 byte(s)
20	quote_5 quotation mark (""")	ascii	1	AsciiString	1 byte(s)
21	last_line_time Azimuth time last line of product. Time of last range line in the MDS of this product. UTC time format contained within quotation marks.	UTC	1	UtcExternal	27 byte(s)
22	quote_6 quotation mark (""")	ascii	1	AsciiString	1 byte(s)
23	newline_char_6 newline character	terminator	1	AsciiString	1 byte(s)
24	first_first_lat_title FIRST_FIRST_LAT=	keyword	1	AsciiString	16 byte(s)
25	first_first_lat Geodetic Latitude of the first sample of the first line. A negative value denotes south latitude, a positive value denotes North latitude	(1e-6) degrees	1	AsciiGeoCoordinate	11 byte(s)
26	first_first_lat_units <10-6degN>	units	1	AsciiString	10 byte(s)
27	newline_char_7 newline character	terminator	1	AsciiString	1 byte(s)
28	first_first_long_title FIRST_FIRST_LONG=	keyword	1	AsciiString	17 byte(s)

#	Description	Units	Count	Type	Size
29	first_first_long East geodetic longitude of the first sample of the first line. Positive values East of Greenwich, negative values west of Greenwich.	(1e-6) degrees	1	AsciiGeoCoordinate	11 byte(s)
30	first_first_long_units <10-6degE>	units	1	AsciiString	10 byte(s)
31	newline_char_8 newline character	terminator	1	AsciiString	1 byte(s)
32	first_mid_lat_title FIRST_MID_LAT=	keyword	1	AsciiString	14 byte(s)
33	first_mid_lat Geodetic Latitude of the middle sample of the first line. A negative value denotes south latitude, a positive value denotes North latitude	(1e-6) degrees	1	AsciiGeoCoordinate	11 byte(s)
34	first_mid_lat_units <10-6degN>	units	1	AsciiString	10 byte(s)
35	newline_char_9 newline character	terminator	1	AsciiString	1 byte(s)
36	first_mid_long_title FIRST_MID_LONG=	keyword	1	AsciiString	15 byte(s)
37	first_mid_long East geodetic longitude of the middle sample of the first line. Positive values East of Greenwich, negative values west of Greenwich.	(1e-6) degrees	1	AsciiGeoCoordinate	11 byte(s)
38	first_mid_long_units <10-6degE>	units	1	AsciiString	10 byte(s)
39	newline_char_10 newline character	terminator	1	AsciiString	1 byte(s)
40	first_last_lat_title FIRST_LAST_LAT=	keyword	1	AsciiString	15 byte(s)
41	first_last_lat Geodetic Latitude of the last sample of the first line. A negative value denotes south latitude, a positive value denotes North latitude	(1e-6) degrees	1	AsciiGeoCoordinate	11 byte(s)
42	first_last_lat_units <10-6degN>	units	1	AsciiString	10 byte(s)
43	newline_char_11 newline character	terminator	1	AsciiString	1 byte(s)
44	first_last_long_title FIRST_LAST_LONG=	keyword	1	AsciiString	16 byte(s)
45	first_last_long East geodetic longitude of the last sample of the first line. Positive values East of Greenwich, negative values west of Greenwich.	(1e-6) degrees	1	AsciiGeoCoordinate	11 byte(s)
46	first_last_long_units <10-6degE>	units	1	AsciiString	10 byte(s)
47	newline_char_12 newline character	terminator	1	AsciiString	1 byte(s)
48	last_first_lat_title LAST_FIRST_LAT=	keyword	1	AsciiString	15 byte(s)
49	last_first_lat Geodetic Latitude of the first sample of the last line. A negative value denotes south latitude, a positive value denotes North latitude	(1e-6) degrees	1	AsciiGeoCoordinate	11 byte(s)
50	last_first_units <10-6degN>	units	1	AsciiString	10 byte(s)
51	newline_char_13 newline character	terminator	1	AsciiString	1 byte(s)
52	last_first_long_title LAST_FIRST_LONG=	keyword	1	AsciiString	16 byte(s)
53	last_first_long East geodetic longitude of the first sample of the last line. Positive values East of Greenwich, negative values west of Greenwich.	(1e-6) degrees	1	AsciiGeoCoordinate	11 byte(s)
54	last_first_long_units <10-6degE>	units	1	AsciiString	10 byte(s)
55	newline_char_14 newline character	terminator	1	AsciiString	1 byte(s)
56	last_mid_lat_title LAST_MID_LAT=	keyword	1	AsciiString	13 byte(s)
57	last_mid_lat Geodetic Latitude of the middle sample of the last line. A negative value denotes south latitude, a positive value denotes North latitude	(1e-6) degrees	1	AsciiGeoCoordinate	11 byte(s)
58	last_mid_lat_units <10-6degN>	units	1	AsciiString	10 byte(s)
59	newline_char_15 newline character	terminator	1	AsciiString	1 byte(s)
60	last_mid_long_title LAST_MID_LONG=	keyword	1	AsciiString	14 byte(s)

#	Description	Units	Count	Type	Size
61	last_mid_long East geodetic longitude of the middle sample of the last line. Positive values East of Greenwich, negative values west of Greenwich.	(1e-6) degrees	1	AsciiGeoCoordinate	11 byte(s)
62	last_mid_long_units <10-6degE>	units	1	AsciiString	10 byte(s)
63	newline_char_16 newline character	terminator	1	AsciiString	1 byte(s)
64	last_last_lat_title LAST_LAST_LAT=	keyword	1	AsciiString	14 byte(s)
65	last_last_lat Geodetic Latitude of the last sample of the last line. A negative value denotes south latitude, a positive value denotes North latitude	(1e-6) degrees	1	AsciiGeoCoordinate	11 byte(s)
66	last_last_lat_units <10-6degN>	units	1	AsciiString	10 byte(s)
67	newline_char_17 newline character	terminator	1	AsciiString	1 byte(s)
68	last_last_long_title LAST_LAST_LONG=	keyword	1	AsciiString	15 byte(s)
69	last_last_long East geodetic longitude of the last sample of the last line. Positive values East of Greenwich, negative values west of Greenwich.	(1e-6) degrees	1	AsciiGeoCoordinate	11 byte(s)
70	last_last_long_units <10-6degE>	units	1	AsciiString	10 byte(s)
71	newline_char_18 newline character	terminator	1	AsciiString	1 byte(s)
72	spare_1 Spare	-	1	SpareField	51 byte(s)
73	min_fpp_basep_temp_title MIN_FPP_BASEPLATE_TEM=	keyword	1	AsciiString	22 byte(s)
74	min_fpp_baseplate_tem Minimum FPP baseplate temperature The minimum physical temperature of the instrument Focal Plane Assembly baseplate during the orbit, taken from the on-board telemetry (identifier A5061).	K	1	Afl	15 byte(s)
75	min_fpp_basep_temp_units <K>	units	1	AsciiString	3 byte(s)
76	newline_char_20 newline character	terminator	1	AsciiString	1 byte(s)
77	min_12_mic_temp_title MIN_12_MICRON_DETECTOR_TEMP=	keyword	1	AsciiString	28 byte(s)
78	min_12_micron_detector_temp Minimum 12 micron detector temperature The minimum physical temperature of the 12 micron detector within the product duration, taken from the on-board telemetry (identifier A5061).	K	1	Afl	15 byte(s)
79	min_12_mic_temp_units <K>	units	1	AsciiString	3 byte(s)
80	newline_char_21 newline character	terminator	1	AsciiString	1 byte(s)
81	min_11_mic_temp_title MIN_11_MICRON_DETECTOR_TEMP=	keyword	1	AsciiString	28 byte(s)
82	min_11_micron_detector_temp Minimum 11 micron detector temperature The minimum physical temperature of the 11 micron detector within the product duration, taken from the on-board telemetry (identifier A5061).	K	1	Afl	15 byte(s)
83	min_11_mic_temp_units <K>	units	1	AsciiString	3 byte(s)
84	newline_char_22 newline character	terminator	1	AsciiString	1 byte(s)
85	min_37_mic_temp_title MIN_3_7_MICRON_DETECTOR_TEMP=	keyword	1	AsciiString	29 byte(s)
86	min_3_7_micron_detector_temp Minimum 3.7 micron detector temperature The minimum physical temperature of the 3.7 micron detector within the product duration, taken from the on-board telemetry (identifier A5061).	K	1	Afl	15 byte(s)
87	min_37_mic_temp_units <K>	units	1	AsciiString	3 byte(s)
88	newline_char_23 newline character	terminator	1	AsciiString	1 byte(s)
89	min_16_mic_temp_title MIN_1_6_MICRON_DETECTOR_TEMP=	keyword	1	AsciiString	29 byte(s)
90	min_1_6_micron_detector_temp Minimum 1.6 micron detector temperature The minimum physical temperature of the 1.6 micron detector within the product duration, taken from the on-board telemetry (identifier A5061).	K	1	Afl	15 byte(s)

#	Description	Units	Count	Type	Size
91	min_16_mic_temp_units <K>	units	1	AsciiString	3 byte(s)
92	newline_char_24 newline character	terminator	1	AsciiString	1 byte(s)
93	min_087_mic_temp_title MIN_0_87_MICRON_DETECTOR_TEMP=	keyword	1	AsciiString	30 byte(s)
94	min_0_87_micron_detector_temp Minimum 0.87 micron detector temperature The minimum physical temperature of the 0.87 micron detector within the product duration, taken from the on-board telemetry (identifier A5061).	K	1	Afl	15 byte(s)
95	min_087_mic_temp_units <K>	units	1	AsciiString	3 byte(s)
96	newline_char_25 newline character	terminator	1	AsciiString	1 byte(s)
97	max_fpp_basep_temp_title MAX_FPP_BASEPLATE_TEM=	keyword	1	AsciiString	22 byte(s)
98	max_fpp_baseplate_tem Maximum FPP baseplate temperature The maximum physical temperature of the instrument Focal Plane Assembly baseplate during the orbit, taken from the on-board telemetry (identifier A5061).	K	1	Afl	15 byte(s)
99	max_fpp_basep_temp_units <K>	units	1	AsciiString	3 byte(s)
100	newline_char_26 newline character	terminator	1	AsciiString	1 byte(s)
101	max_12_mic_temp_title MAX_12_MICRON_DETECTOR_TEMP=	keyword	1	AsciiString	28 byte(s)
102	max_12_micron_detector_temp Maximum 12 micron detector temperature The maximum physical temperature of the 12 micron detector within the product duration, taken from the on-board telemetry (identifier A5061).	K	1	Afl	15 byte(s)
103	max_12_mic_temp_units <K>	units	1	AsciiString	3 byte(s)
104	newline_char_27 newline character	terminator	1	AsciiString	1 byte(s)
105	max_11_mic_temp_title MAX_11_MICRON_DETECTOR_TEMP=	keyword	1	AsciiString	28 byte(s)
106	max_11_micron_detector_temp Maximum 11 micron detector temperature The maximum physical temperature of the 11 micron detector within the product duration, taken from the on-board telemetry (identifier A5061).	K	1	Afl	15 byte(s)
107	max_11_mic_temp_units <K>	units	1	AsciiString	3 byte(s)
108	newline_char_28 newline character	terminator	1	AsciiString	1 byte(s)
109	max_37_mic_temp_title MAX_3_7_MICRON_DETECTOR_TEMP=	keyword	1	AsciiString	29 byte(s)
110	max_3_7_micron_detector_temp Maximum 3.7 micron detector temperature The maximum physical temperature of the 3.7 micron detector within the product duration, taken from the on-board telemetry (identifier A5061).	K	1	Afl	15 byte(s)
111	max_37_mic_temp_units <K>	units	1	AsciiString	3 byte(s)
112	newline_char_29 newline character	terminator	1	AsciiString	1 byte(s)
113	max_16_mic_temp_title MAX_1_6_MICRON_DETECTOR_TEMP=	keyword	1	AsciiString	29 byte(s)
114	max_1_6_micron_detector_temp Maximum 1.6 micron detector temperature The maximum physical temperature of the 1.6 micron detector within the product duration, taken from the on-board telemetry (identifier A5061).	K	1	Afl	15 byte(s)
115	max_16_mic_temp_units <K>	units	1	AsciiString	3 byte(s)
116	newline_char_30 newline character	terminator	1	AsciiString	1 byte(s)
117	max_087_mic_temp_title MAX_0_87_MICRON_DETECTOR_TEMP=	keyword	1	AsciiString	30 byte(s)
118	max_0_87_micron_detector_temp Maximum 0.87 micron detector temperature The maximum physical temperature of the 0.87 micron detector within the product duration, taken from the on-board telemetry (identifier A5061).	K	1	Afl	15 byte(s)
119	max_087_mic_temp_units <K>	units	1	AsciiString	3 byte(s)

#	Description	Units	Count	Type	Size
120	newline_char_31 newline character	terminator	1	AsciiString	1 byte(s)
121	spare_2 Spare	-	1	SpareField	51 byte(s)
122	dsd_spare_3 DSD Spare	-	1	dsd_sp	0 byte(s)
123	dsd_spare_4 DSD Spare	-	1	dsd_sp	0 byte(s)

Record Length : 1315

DS_NAME : SPH

Format Version 114.0

6.6.37 Summary Quality ADS

Table 6.66 Summary Quality ADS

Summary Quality ADS

#	Description	Units	Count	Type	Size
Data Record					
0	dsr_time Nadir UTC time in MJD format The nadir time associated with a given record, or image row, is the time at which the sub-satellite point intersects the image row, or the time at which the satellite is vertically overhead at the centre of the row. It corresponds to the measurement time at which the pixels in the centre of the row (the nadir pixels) are measured. Because of the curvature of the instrument scans, the measurement time at the extremities of the row may differ from the nadir time by up to 15 seconds. Similarly the measurement time of a forward view image will differ by approximately 135 seconds (2.25 minutes) from the measurement time of the corresponding nadir scan. The relationship between nadir time and measurement time is explained in more detail in the accompanying link.	MJD	1	mjd	12 byte(s)
1	attach_flag Attachment flag(set to 1 if all MDSRs corresponding to this ADSR are blank, set to 0 otherwise) In accordance with ESA guidelines, this flag will be set to 1 if all of the MDS records in the granule have the record quality indicator set to -1; otherwise it is set to zero. If the flag is set to 1 the corresponding MDS records will be omitted; this mechanism allows gaps in the sequence of MDS records to be identified. In the case of the SQADS, the attachment flag will only be set if all 512 records are omitted under this provision.	flag	1	BooleanFlag	1 byte(s)
2	spare_1 Spare	-	1	SpareField	3 byte(s)
3	scan_num image scan number The number of the image scan, or image row, of the first row of the major granule corresponding to this record. This is a continuous count starting from the first row of the product.	-	1	us	2 byte(s)

#	Description	Units	Count	Type	Size
4	pv_nad_null_pac Packet Validation during nadir view number of scans null packet The number of rows of the 512 row large granule for which at least one nadir view pixel is flagged as from a null packet (a telemetry data gap).	-	1	ss	2 byte(s)
5	pv_nad_fail_val Packet Validation during nadir view number of scans failing basic validation The number of rows of the 512 row large granule for which at least one nadir view pixel is flagged 'scan failing basic validation'.	-	1	ss	2 byte(s)
6	pv_nad_fail_crc_chk Packet Validation during nadir view number of scans failing CRC check The number of rows of the 512 row large granule for which at least one nadir view pixel is flagged 'scan failed CRC check'	-	1	ss	2 byte(s)
7	pv_nad_show_buf_full Packet Validation during nadir view number of scans showing buffers full The number of rows of the 512 row large granule for which at least one nadir view pixel is flagged 'scan buffers full'.	-	1	ss	2 byte(s)
8	pv_nad_scan_jitt Packet Validation during nadir view number of scans showing scan jitter The number of rows of the 512 row large granule for which at least one nadir view pixel is flagged 'scan jitter'.	-	1	ss	2 byte(s)
9	per_cloud_pix percentage of cloudy pixels The percentage of filled image pixels in the large granule that are cloudy, expressed as a short integer in units of 0.01%.	0.01%	1	ss	2 byte(s)
10	per_ndvi_inv percentage of NDVI invalid The percentage of filled clear land pixels in the large granule for which the NDVI is invalid, expressed as a short integer in units of 0.01%.	0.01%	1	ss	2 byte(s)
11	per_sst_for_inv percentage of SST (nadir view) invalid The percentage of filled clear sea pixels in the large granule for which the nadir view SST is invalid, expressed as a short integer in units of 0.01%.	0.01%	1	ss	2 byte(s)
12	per_sst_dual_inv percentage of SST (dual view) invalid The percentage of filled clear sea pixels in the large granule for which the dual view SST is invalid, expressed as a short integer in units of 0.01%.	0.01%	1	ss	2 byte(s)
13	pv_nad_scan_error Packet Validation during nadir view number of scans - all other errors The number of rows of the 512 row large granule for which at least one nadir view pixel shows any error or exception condition not mentioned above.	-	1	ss	2 byte(s)
14	pv_for_null_pac Packet Validation during forward view number of scans null packet The number of rows of the 512 row large granule for which at least one forward view pixel is flagged as from a null packet (a telemetry data gap).	-	1	ss	2 byte(s)
15	pv_for_fail_val Packet Validation during forward view number of scans failing basic validation The number of rows of the 512 row large granule for which at least one forward view pixel is flagged 'scan failing basic validation'.	-	1	ss	2 byte(s)
16	pv_for_fail_crc_chk Packet Validation during forward view number of scans failing CRC check The number of rows of the 512 row large granule for which at least one forward view pixel is flagged 'scan failed CRC check'	-	1	ss	2 byte(s)
17	pv_for_show_buf_full Packet Validation during forward view number of scans showing buffers full The number of rows of the 512 row large granule for which at least one forward view pixel is flagged 'scan buffers full'.	-	1	ss	2 byte(s)
18	pv_for_scan_jitt Packet Validation during forward view number of scans showing scan jitter The number of rows of the 512 row large granule for which at least one forward view pixel is flagged 'scan jitter'.	-	1	ss	2 byte(s)
19	resv_char_5 reserved for future use Field is currently unused and set to zero.	-	1	ss	2 byte(s)
20	resv_char_6 reserved for future use Field is currently unused and set to zero.	-	1	ss	2 byte(s)
21	resv_char_7 reserved for future use Field is currently unused and set to zero.	-	1	ss	2 byte(s)
22	resv_char_8 reserved for future use Field is currently unused and set to zero.	-	1	ss	2 byte(s)
23	pv_for_scan_error Packet Validation during forward view number of scans - all other errors The number of rows of the 512 row large granule for which at least one forward view pixel shows any error or exception condition not mentioned above.	-	1	ss	2 byte(s)

#	Description	Units	Count	Type	Size
24	spare_2 Spare	-	1	SpareField	28 byte(s)

Record Length : 86

DS_NAME : Summary Quality ADS

Format Version 114.0

6.6.38 Level 2 SPH

Table 6.67 Level 2 SPH

Level 2 SPH

#	Description	Units	Count	Type	Size
Data Record					
0	sph_descriptor_title SPH_DESCRIPTOR=	keyword	1	AsciiString	15 byte(s)
1	quote_1 quotation mark (""")	ascii	1	AsciiString	1 byte(s)
2	sph_descriptor SPH Descriptor ASCII string describing the product.	ascii	1	AsciiString	28 byte(s)
3	quote_2 quotation mark (""")	ascii	1	AsciiString	1 byte(s)
4	newline_char_1 newline character	terminator	1	AsciiString	1 byte(s)
5	stripline_cont_ind_title STRIPLINE_CONTINUITY_INDICATOR=	keyword	1	AsciiString	31 byte(s)
6	stripline_continuity_indicator Value: 0= No stripline continuity, the product is a complete segment. Other: Stripline Counter	-	1	Ac	4 byte(s)
7	newline_char_2 newline character	terminator	1	AsciiString	1 byte(s)
8	slice_pos_title SLICE_POSITION=	keyword	1	AsciiString	15 byte(s)
9	slice_position Value: +001 to NUM_SLICES. Default value if no stripline continuity = +001	-	1	Ac	4 byte(s)
10	newline_char_3 newline character	terminator	1	AsciiString	1 byte(s)
11	num_slices_title NUM_SLICES=	keyword	1	AsciiString	11 byte(s)
12	num_slices Number of slices in this striplineDefault value if no continuity = +001	-	1	Ac	4 byte(s)
13	newline_char_4 newline character	terminator	1	AsciiString	1 byte(s)
14	first_ln_time_title	keyword	1	AsciiString	16 byte(s)

#	Description	Units	Count	Type	Size
	FIRST_LINE_TIME=				
15	quote_3 quotation mark (""")	ascii	1	AsciiString	1 byte(s)
16	first_line_time Azimuth time first line of product. UTC Time of first range line in the MDS of this product. UTC time format contained within quotation marks.	UTC	1	UtcExternal	27 byte(s)
17	quote_4 quotation mark (""")	ascii	1	AsciiString	1 byte(s)
18	newline_char_5 newline character	terminator	1	AsciiString	1 byte(s)
19	last_ln_time_title LAST_LINE_TIME=	keyword	1	AsciiString	15 byte(s)
20	quote_5 quotation mark (""")	ascii	1	AsciiString	1 byte(s)
21	last_line_time Azimuth time last line of product. Time of last range line in the MDS of this product. UTC time format contained within quotation marks.	UTC	1	UtcExternal	27 byte(s)
22	quote_6 quotation mark (""")	ascii	1	AsciiString	1 byte(s)
23	newline_char_6 newline character	terminator	1	AsciiString	1 byte(s)
24	first_first_lat_title FIRST_FIRST_LAT=	keyword	1	AsciiString	16 byte(s)
25	first_first_lat Geodetic Latitude of the first sample of the first line. A negative value denotes south latitude, a positive value denotes North latitude	(1e-6) degrees	1	AsciiGeoCoordinate	11 byte(s)
26	first_first_lat_units <10-6degN>	units	1	AsciiString	10 byte(s)
27	newline_char_7 newline character	terminator	1	AsciiString	1 byte(s)
28	first_first_long_title FIRST_FIRST_LONG=	keyword	1	AsciiString	17 byte(s)
29	first_first_long East geodetic longitude of the first sample of the first line. Positive values East of Greenwich, negative values west of Greenwich.	(1e-6) degrees	1	AsciiGeoCoordinate	11 byte(s)
30	first_first_long_units <10-6degE>	units	1	AsciiString	10 byte(s)
31	newline_char_8 newline character	terminator	1	AsciiString	1 byte(s)
32	first_mid_lat_title FIRST_MID_LAT=	keyword	1	AsciiString	14 byte(s)
33	first_mid_lat Geodetic Latitude of the middle sample of the first line. A negative value denotes south latitude, a positive value denotes North latitude	(1e-6) degrees	1	AsciiGeoCoordinate	11 byte(s)
34	first_mid_lat_units <10-6degN>	units	1	AsciiString	10 byte(s)
35	newline_char_9 newline character	terminator	1	AsciiString	1 byte(s)
36	first_mid_long_title FIRST_MID_LONG=	keyword	1	AsciiString	15 byte(s)
37	first_mid_long East geodetic longitude of the middle sample of the first line. Positive values East of Greenwich, negative values west of Greenwich.	(1e-6) degrees	1	AsciiGeoCoordinate	11 byte(s)
38	first_mid_long_units <10-6degE>	units	1	AsciiString	10 byte(s)
39	newline_char_10 newline character	terminator	1	AsciiString	1 byte(s)
40	first_last_lat_title FIRST_LAST_LAT=	keyword	1	AsciiString	15 byte(s)
41	first_last_lat Geodetic Latitude of the last sample of the first line. A negative value denotes south latitude, a positive value denotes North latitude	(1e-6) degrees	1	AsciiGeoCoordinate	11 byte(s)
42	first_last_lat_units <10-6degN>	units	1	AsciiString	10 byte(s)
43	newline_char_11 newline character	terminator	1	AsciiString	1 byte(s)
44	first_last_long_title FIRST_LAST_LONG=	keyword	1	AsciiString	16 byte(s)
45	first_last_long East geodetic longitude of the last sample of the first line. Positive values East of Greenwich, negative values west of Greenwich.	(1e-6) degrees	1	AsciiGeoCoordinate	11 byte(s)
46	first_last_long_units	units	1	AsciiString	10 byte(s)

#	Description	Units	Count	Type	Size
	<10-6degE>				
47	newline_char_12 newline character	terminator	1	AsciiString	1 byte(s)
48	last_first_lat_title LAST_FIRST_LAT=	keyword	1	AsciiString	15 byte(s)
49	last_first_lat Geodetic Latitude of the first sample of the last line. A negative value denotes south latitude, a positive value denotes North latitude	(1e-6) degrees	1	AsciiGeoCoordinate	11 byte(s)
50	last_first_units <10-6degN>	units	1	AsciiString	10 byte(s)
51	newline_char_13 newline character	terminator	1	AsciiString	1 byte(s)
52	last_first_long_title LAST_FIRST_LONG=	keyword	1	AsciiString	16 byte(s)
53	last_first_long East geodetic longitude of the first sample of the last line. Positive values East of Greenwich, negative values west of Greenwich.	(1e-6) degrees	1	AsciiGeoCoordinate	11 byte(s)
54	last_first_long_units <10-6degE>	units	1	AsciiString	10 byte(s)
55	newline_char_14 newline character	terminator	1	AsciiString	1 byte(s)
56	last_mid_lat_title LAST_MID_LAT=	keyword	1	AsciiString	13 byte(s)
57	last_mid_lat Geodetic Latitude of the middle sample of the last line. A negative value denotes south latitude, a positive value denotes North latitude	(1e-6) degrees	1	AsciiGeoCoordinate	11 byte(s)
58	last_mid_lat_units <10-6degN>	units	1	AsciiString	10 byte(s)
59	newline_char_15 newline character	terminator	1	AsciiString	1 byte(s)
60	last_mid_long_title LAST_MID_LONG=	keyword	1	AsciiString	14 byte(s)
61	last_mid_long East geodetic longitude of the middle sample of the last line. Positive values East of Greenwich, negative values west of Greenwich.	(1e-6) degrees	1	AsciiGeoCoordinate	11 byte(s)
62	last_mid_long_units <10-6degE>	units	1	AsciiString	10 byte(s)
63	newline_char_16 newline character	terminator	1	AsciiString	1 byte(s)
64	last_last_lat_title LAST_LAST_LAT=	keyword	1	AsciiString	14 byte(s)
65	last_last_lat Geodetic Latitude of the last sample of the last line. A negative value denotes south latitude, a positive value denotes North latitude	(1e-6) degrees	1	AsciiGeoCoordinate	11 byte(s)
66	last_last_lat_units <10-6degN>	units	1	AsciiString	10 byte(s)
67	newline_char_17 newline character	terminator	1	AsciiString	1 byte(s)
68	last_last_long_title LAST_LAST_LONG=	keyword	1	AsciiString	15 byte(s)
69	last_last_long East geodetic longitude of the last sample of the last line. Positive values East of Greenwich, negative values west of Greenwich.	(1e-6) degrees	1	AsciiGeoCoordinate	11 byte(s)
70	last_last_long_units <10-6degE>	units	1	AsciiString	10 byte(s)
71	newline_char_18 newline character	terminator	1	AsciiString	1 byte(s)
72	spare_1 Spare	-	1	SpareField	51 byte(s)
73	min_fpp_basep_temp_title MIN_FPP_BASEPLATE_TEM=	keyword	1	AsciiString	22 byte(s)
74	min_fpp_baseplate_tem Minimum FPP baseplate temperature The minimum physical temperature of the instrument Focal Plane Assembly baseplate during the orbit, taken from the on-board telemetry (identifier A5061).	K	1	Afl	15 byte(s)
75	min_fpp_basep_temp_units <K>	units	1	AsciiString	3 byte(s)
76	newline_char_20 newline character	terminator	1	AsciiString	1 byte(s)
77	min_12_mic_temp_title MIN_12_MICRON_DETECTOR_TEMP=	keyword	1	AsciiString	28 byte(s)
78	min_12_micron_detector_temp	K	1	Afl	15 byte(s)

#	Description	Units	Count	Type	Size
	Minimum 12 micron detector temperature The minimum physical temperature of the 12 micron detector within the product duration, taken from the on-board telemetry (identifier A5061).				
79	min_12_mic_temp_units <K>	units	1	AsciiString	3 byte(s)
80	newline_char_21 newline character	terminator	1	AsciiString	1 byte(s)
81	min_11_mic_temp_title MIN_11_MICRON_DETECTOR_TEMP=	keyword	1	AsciiString	28 byte(s)
82	min_11_micron_detector_temp Minimum 11 micron detector temperature The minimum physical temperature of the 11 micron detector within the product duration, taken from the on-board telemetry (identifier A5061).	K	1	Afl	15 byte(s)
83	min_11_mic_temp_units <K>	units	1	AsciiString	3 byte(s)
84	newline_char_22 newline character	terminator	1	AsciiString	1 byte(s)
85	min_37_mic_temp_title MIN_3_7_MICRON_DETECTOR_TEMP=	keyword	1	AsciiString	29 byte(s)
86	min_3_7_micron_detector_temp Minimum 3.7 micron detector temperature The minimum physical temperature of the 3.7 micron detector within the product duration, taken from the on-board telemetry (identifier A5061).	K	1	Afl	15 byte(s)
87	min_37_mic_temp_units <K>	units	1	AsciiString	3 byte(s)
88	newline_char_23 newline character	terminator	1	AsciiString	1 byte(s)
89	min_16_mic_temp_title MIN_1_6_MICRON_DETECTOR_TEMP=	keyword	1	AsciiString	29 byte(s)
90	min_1_6_micron_detector_temp Minimum 1.6 micron detector temperature The minimum physical temperature of the 1.6 micron detector within the product duration, taken from the on-board telemetry (identifier A5061).	K	1	Afl	15 byte(s)
91	min_16_mic_temp_units <K>	units	1	AsciiString	3 byte(s)
92	newline_char_24 newline character	terminator	1	AsciiString	1 byte(s)
93	min_087_mic_temp_title MIN_0_87_MICRON_DETECTOR_TEMP=	keyword	1	AsciiString	30 byte(s)
94	min_0_87_micron_detector_temp Minimum 0.87 micron detector temperature The minimum physical temperature of the 0.87 micron detector within the product duration, taken from the on-board telemetry (identifier A5061).	K	1	Afl	15 byte(s)
95	min_087_mic_temp_units <K>	units	1	AsciiString	3 byte(s)
96	newline_char_25 newline character	terminator	1	AsciiString	1 byte(s)
97	max_fpp_basep_temp_title MAX_FPP_BASEPLATE_TEM=	keyword	1	AsciiString	22 byte(s)
98	max_fpp_baseplate_tem Maximum FPP baseplate temperature The maximum physical temperature of the instrument Focal Plane Assembly baseplate during the orbit, taken from the on-board telemetry (identifier A5061).	K	1	Afl	15 byte(s)
99	max_fpp_basep_temp_units <K>	units	1	AsciiString	3 byte(s)
100	newline_char_26 newline character	terminator	1	AsciiString	1 byte(s)
101	max_12_mic_temp_title MAX_12_MICRON_DETECTOR_TEMP=	keyword	1	AsciiString	28 byte(s)
102	max_12_micron_detector_temp Maximum 12 micron detector temperature The maximum physical temperature of the 12 micron detector within the product duration, taken from the on-board telemetry (identifier A5061).	K	1	Afl	15 byte(s)
103	max_12_mic_temp_units <K>	units	1	AsciiString	3 byte(s)
104	newline_char_27 newline character	terminator	1	AsciiString	1 byte(s)
105	max_11_mic_temp_title MAX_11_MICRON_DETECTOR_TEMP=	keyword	1	AsciiString	28 byte(s)
106	max_11_micron_detector_temp Maximum 11 micron detector temperature The maximum physical temperature of the 11 micron detector within the product duration, taken from the on-board telemetry (identifier A5061).	K	1	Afl	15 byte(s)

#	Description	Units	Count	Type	Size
107	max_11_mic_temp_units <K>	units	1	AsciiString	3 byte(s)
108	newline_char_28 newline character	terminator	1	AsciiString	1 byte(s)
109	max_37_mic_temp_title MAX_3_7_MICRON_DETECTOR_TEMP=	keyword	1	AsciiString	29 byte(s)
110	max_3_7_micron_detector_temp Maximum 3.7 micron detector temperature The maximum physical temperature of the 3.7 micron detector within the product duration, taken from the on-board telemetry (identifier A5061).	K	1	Afl	15 byte(s)
111	max_37_mic_temp_units <K>	units	1	AsciiString	3 byte(s)
112	newline_char_29 newline character	terminator	1	AsciiString	1 byte(s)
113	max_16_mic_temp_title MAX_1_6_MICRON_DETECTOR_TEMP=	keyword	1	AsciiString	29 byte(s)
114	max_1_6_micron_detector_temp Maximum 1.6 micron detector temperature The maximum physical temperature of the 1.6 micron detector within the product duration, taken from the on-board telemetry (identifier A5061).	K	1	Afl	15 byte(s)
115	max_16_mic_temp_units <K>	units	1	AsciiString	3 byte(s)
116	newline_char_30 newline character	terminator	1	AsciiString	1 byte(s)
117	max_087_mic_temp_title MAX_0_87_MICRON_DETECTOR_TEMP=	keyword	1	AsciiString	30 byte(s)
118	max_0_87_micron_detector_temp Maximum 0.87 micron detector temperature The maximum physical temperature of the 0.87 micron detector within the product duration, taken from the on-board telemetry (identifier A5061).	K	1	Afl	15 byte(s)
119	max_087_mic_temp_units <K>	units	1	AsciiString	3 byte(s)
120	newline_char_31 newline character	terminator	1	AsciiString	1 byte(s)
121	lat_long_tie_pt_title LAT_LONG_TIE_POINTS=	keyword	1	AsciiString	20 byte(s)
122	lat_long_tie_points x co-ordinates of lat/long tie points. The X co-ordinates of the latitude/longitude tie points used in ADS#3 (grid pixel latitude and longitude). The 23 values range from -275 km to + 275 km in steps of 25 km.	km	23	As	23*6 byte(s)
123	lat_long_tie_pt_units <km>	units	1	AsciiString	4 byte(s)
124	newline_char_32 newline character	terminator	1	AsciiString	1 byte(s)
125	view_angle_tie_pt_title VIEW_ANGLE_TIE_POINTS=	keyword	1	AsciiString	22 byte(s)
126	view_angle_tie_points x co-ordinates of solar angle tie points. The X co-ordinates of the solar and viewing angle tie points used in ADS#5 and ADS#6 (nadir and forward solar angles). The 11 values range from -250 km to + 250 km in steps of 50 km.	km	11	As	11*6 byte(s)
127	view_angle_tie_pt_units <km>	units	1	AsciiString	4 byte(s)
128	newline_char_33 newline character	terminator	1	AsciiString	1 byte(s)
129	xy_tie_pt_pix_num_title XY_TIE_POINTS_PIXEL_NUM=	keyword	1	AsciiString	24 byte(s)
130	xy_tie_points_pixel_num pixel numbers of x-y tie points The absolute instrument pixel numbers (in the range 1 to 2000) of the tie points used in ADS#4 (scan pixel x and y).	-	99	As	99*6 byte(s)
131	newline_char_34 newline character	terminator	1	AsciiString	1 byte(s)
132	spare_2 Spare	-	1	SpareField	51 byte(s)
133	dsd_spare_3 DSD Spare	-	1	dsd_sp	0 byte(s)
134	dsd_spare_4 DSD Spare	-	1	dsd_sp	0 byte(s)

Record Length : 2190

DS_NAME : Level 2 SPH

Format Version 114.0

6.6.39 Distributed product MDS

Table 6.68 Distributed product MDS

Distributed product MDS

#	Description	Units	Count	Type	Size
Data Record					
0	dsr_time Nadir UTC time in MJD format The nadir time associated with a given record, or image row, is the time at which the sub-satellite point intersects the image row, or the time at which the satellite is vertically overhead at the centre of the row. It corresponds to the measurement time at which the pixels in the centre of the row (the nadir pixels) are measured. Because of the curvature of the instrument scans, the measurement time at the extremities of the row may differ from the nadir time by up to 15 seconds. Similarly the measurement time of a forward view image will differ by approximately 135 seconds (2.25 minutes) from the measurement time of the corresponding nadir scan. The relationship between nadir time and measurement time is explained in more detail in the accompanying link.	MJD	1	mjd	12 byte(s)
1	quality_flag Quality Indicator (-1 for blank MDSR, 0 otherwise) The record quality indicator is set to -1 to indicate a blank MDS Record, to zero otherwise (I.e. if the record contains valid data).	flag	1	BooleanFlag	1 byte(s)
2	spare_1 Spare	-	1	SpareField	3 byte(s)
3	img_scan_y image scan y coordinate The y co-ordinate of the image row (or image scan), in units of metres. Because the AATSR image data is sampled at equal intervals of time in the along track direction, this quantity is provided in order to define the relationship between time and image scale. The y co-ordinate is measured along the satellite ground track; the origin (in the case of consolidated data) is at the ascending node of the orbit. (Precisely, from the point corresponding to time T0, however defined.) The co-ordinate frame of the AATSR images is defined in the accompanying link.	m	1	sl	4 byte(s)
4	conf_wd_flags confidence words (Defined in Table 7.5.1.7.8 3) A 16 bit confidence word for each pixel (number 0 to 511) in the image row. Each bit of the confidence word is a flag that if set indicates a status or exception condition associated with the corresponding pixel. The meanings of the flags are tabulated below. Bits 4, 5, and 8 are of particular importance; bit 4, if set, indicates that the pixel is over land, and bits 5 and 8 , if set, indicate that the pixel is flagged as cloudy in the nadir and forward views respectively. The interpretation of the following fields depends on these bits.	flags	512	us	512*2 byte(s)
5	nad_field nadir field (Note 1) The GSST product is described as a switchable distributed product , which means that the information supplied for each pixel depends on the surface type of the pixel, and on whether or not it is cloudy. These fields contain a value for each	K/100	512	ss	512*2 byte(s)

#	Description	Units	Count	Type	Size
	pixel (0 to 511); the interpretation of the value depends on the cloud and land flags in the corresponding confidence word. If the pixel is a clear sea pixel, the field contains the sea surface temperature, retrieved from the nadir view measurements only. In other cases the field contents are as defined in the table below.				
6	comb_field combined field (Note 1) The GSST product is described as a switchable distributed product , which means that the information supplied for each pixel depends on the surface type of the pixel, and on whether or not it is cloudy. These fields contain a value for each pixel (0 to 511); the interpretation of the value depends on the cloud and land flags in the corresponding confidence word. If the pixel is a clear sea pixel, the field contains the sea surface temperature, retrieved from the combined nadir and forward view measurements only. In other cases the field contents are as defined in the table below.	See Note 1	512	ss	512*2 byte(s)

Record Length : 3092

DS_NAME : Distributed product MDS

Format Version 114.0

The following table lists the flag bits within the Level 2 GSST Confidence word.

Table 6.69 GSST Confidence Flags

The following table lists the GSST nadir and combined field contents. (IODD Table 6-12).

Table 6.70 GSST Nadir and Combined Field Contents

nadir cloud	forward cloud	land	Nadir field	combined field
0	0	0	SST nadir	SST combined
0	1	0	SST nadir	Note 2
1	0/1	0/1	cloud top temp	cloud top height
0	0/1	1	Land surface temp	NDVI

Notes

1. Bits are numbered from ms bit 15 to ls bit 0.

2. A dual view SST is calculated in this case as if the forward view were cloud-free, but the

value is excluded from the smoothing, and the corresponding confidence flag (.dual view SST valid.) is not set.

6.6.40 Processor configuration GADS

This product contains configuration data for the Level 1b AATSR Processor. It comprises a Main Product Header, a standard Auxiliary Data SPH with one DSD, and the Processor Configuration Data GADS as described in the following table. A few of the parameters in this file are steering parameters that modify product generation, but many of them are internal to the Operational Processor, and do not affect the logic of its operation, or the products generated.

Table 6.71 Processor configuration GADS

Processor configuration GADS

#	Description	Units	Count	Type	Size
Data Record					
0	pulse_cal blanking pulse calibration code: blanking_pulse_calibration_flag A parameter to determine whether or not blanking pulse flags are to affect the infra-red calibration. The parameter may take one of four possible values (see link).	-	1	sl	4 byte(s)
1	scan_cal Number of scans in calibration period This parameter defines the integration time used to determine the infra-red calibration coefficients, in terms of the number of instrument scans included in each average. The calibration period is the interval over which the black body pixels are integrated during infra-red calibration. The adopted value is 10 scans (equivalent to an interval of 1.5 seconds).	-	1	sl	4 byte(s)
2	res_vis_cal_code Reserved for visible calibration option code Parameter to select which of the on-board black bodies is to be used to determine the dark signal (offset) for the visible calibration.	-	1	sl	4 byte(s)
3	spare_1 Spare	-	1	SpareField	12 byte(s)
4	max_vis_pix max_viscal_pixels This parameter is used to dimension internal arrays. It must be equal to or greater than the number of visible calibration pixels in the pixel selection map (see link).	-	1	ss	2 byte(s)
5	max_nad_pix max_nadir_pixels This parameter is used to dimension internal arrays. It must be equal to or greater than the number of nadir view pixels in the pixel selection map (see link).	-	1	ss	2 byte(s)
6	max_pxbb_pix max_pxbb_pixels This parameter is used to dimension internal arrays. It must be equal to or greater than the number of +X black body pixels in the pixel selection map (see link).	-	1	ss	2 byte(s)
7	max_frwrd_pix max_frwrd_pixels This parameter is used to dimension internal arrays. It must be equal to or greater than the number of forward view pixels in the pixel selection map (see link).	-	1	ss	2 byte(s)
8	max_mxbb_pix	-	1	ss	2 byte(s)

#	Description	Units	Count	Type	Size
	max_mxbb_pixels This parameter is used to dimension internal arrays. It must be equal to or greater than the number of -X black body pixels in the pixel selection map (see link).				
9	spare_2 Spare	-	1	SpareField	12 byte(s)
10	flag_off_bthbp Calibration bp flag value: both bp flags off Blanking pulse flag code. If the blanking pulse calibration code is set equal to CAL_BP_BOTH_OFF, pixels contribute to the calibration only if both flags are off. The adopted value of this code is 101	-	1	ss	2 byte(s)
11	flag_off_asar Calibration bp flag value: ASAR only flag off Blanking pulse flag code. If the blanking pulse calibration code is set equal to CAL_BP_ASAR_OFF, pixels contribute to the calibration only if the ASAR flag is off. (The RA flag is ignored). The adopted value of this code is 102.	-	1	ss	2 byte(s)
12	flag_off_onlyra Calibration bp flag value: RA only flag off Blanking pulse flag code. If the blanking pulse calibration code is set equal to CAL_BP_RA_OFF, pixels contribute to the calibration only if the RA flag is off. (The ASAR flag is ignored). The adopted value of this code is 103.	-	1	ss	2 byte(s)
13	flag_on_bthbp Calibration bp flag value: both bp flags on Blanking pulse flag code. If the blanking pulse calibration code is set equal to CAL_BP_BOTH_ON, pixels contribute to the calibration irrespective of the flag setting. (Either or both flags may be on.) The adopted value of this code is 104.	-	1	ss	2 byte(s)
14	init_cal_parm INIT_CAL_PARAM This is an exception value used to initialise calibration parameters. Its use is internal to the processor, and does not appear in output products.	-	1	fl	4 byte(s)
15	spare_3 Spare	-	1	SpareField	12 byte(s)
16	vis_bb_code_px vis_bb_code_px Visible calibration option value. If the visible calibration option code is set equal to vis_bb_code_px, the visible calibration offset (dark signal) is derived from the +X black body only.	-	1	ss	2 byte(s)
17	vis_bb_code_mx vis_bb_code_mx Visible calibration option value. If the visible calibration option code is set equal to vis_bb_code_mx, the visible calibration offset (dark signal) is derived from the -X black body only.	-	1	ss	2 byte(s)
18	vis_bb_code_both vis_bb_code_both Visible calibration option value. If the visible calibration option code is set equal to vis_bb_code_both, the derivation of the visible calibration offset (dark signal) uses both black bodies.	-	1	ss	2 byte(s)
19	vis_bb_code_none vis_bb_code_none Reserved.	-	1	ss	2 byte(s)
20	spare_4 Spare	-	1	SpareField	12 byte(s)
21	pix_cnt_from_nullpacket PIXEL_COUNT_FROM_NULL_PACKET Pixel exceptional value. Negative integer used to flag invalid image pixels in the Level 1b GBTR product. This code is used to indicate that the pixel comes from a null (i.e. missing) source packet. The adopted value is -1.	-	1	ss	2 byte(s)
22	pix_cnt_int PIXEL_COUNT_INITIAL_VALUE Pixel exceptional value. Negative integer used to flag invalid image pixels in the Level 1b GBTR product. This code is used to indicate that the is missing from the instrument scan. It is most likely to occur at the edge of the instrument swath, where the regridded image extends beyond the limits of the instrument field of view. The adopted value is -2.	-	1	ss	2 byte(s)
23	pix_cnt_scidata_ndcmp PIXEL_COUNT_SCIENCE_DATA_NOT_DECOMPRESSSED Pixel exceptional value. Negative integer used to flag invalid image pixels in the Level 1b GBTR product. This code is indicates that the corresponding pixel field in the instrument source packet could not be decoded, and is most likely to occur when the corresponding source packet shows a CRC (cyclic redundancy check) error. The adopted value is -3.	-	1	ss	2 byte(s)
24	pix_cnt_zero PIXEL_COUNT_ZERO Pixel exceptional value. Negative integer used to flag invalid image pixels in the Level 1b GBTR product. This code is used to indicate that the pixel count in the instrument source packet was zero. The adopted value is -4.	-	1	ss	2 byte(s)
25	pix_cnt_sat PIXEL_COUNT_SATURATED Pixel exceptional value. Negative integer used to flag invalid image pixels in the Level 1b GBTR product. This code is used to indicate that the channel is	-	1	ss	2 byte(s)

#	Description	Units	Count	Type	Size
	saturated, that is that the pixel count in the instrument source packet has the maximum possible value. The adopted value is -5.				
26	cal_unavl_pix CALIBRATION_UNAVAILABLE_FOR_PIXEL Pixel exceptional value. Negative integer used to flag invalid image pixels in the Level 1b GBTR product. This code is used to indicate that the pixel could not be calibrated, because valid calibration coefficients could not be derived for the calibration interval. The adopted value is -7.	-	1	ss	2 byte(s)
27	pix_rad_out_cal PIXEL_RADIANCE_OUTSIDE_CALIBRATION Pixel exceptional value. Negative integer used to flag invalid image pixels in the Level 1b GBTR product. This code is used to indicate that the pixel could not be calibrated, because although valid calibration coefficients were available, the derived radiance fell outside the range of the radiance to brightness temperature table (for the thermal infra-red channels) or the non-linear correction table (1.6 micron channel). The adopted value is -6.	-	1	ss	2 byte(s)
28	pix_unfilled PIXEL_UNFILLED Pixel exceptional value. Negative integer used to flag invalid image pixels in the Level 1b GBTR product. This code is used to indicate that the cosmetic fill algorithm (see link) could not find a nearest neighbour point to fill this pixel. The adopted value is -8.	-	1	ss	2 byte(s)
29	spare_5 Spare	-	1	SpareField	12 byte(s)
30	null_pckt_err NULL PCKT ERR The use of this code is internal to the processor. It is not relevant to the interpretation of output products.	-	1	ss	2 byte(s)
31	raw_pkt_fail RAW_PKT_FAILS_BASIC_VALIDATION_ERR The use of this code is internal to the processor. It is not relevant to the interpretation of output products.	-	1	ss	2 byte(s)
32	crc_err_dect_err CRC_ERR_DETECTED_ERR The use of this code is internal to the processor. It is not relevant to the interpretation of output products.	-	1	ss	2 byte(s)
33	buf_full_chk_err BUFFERS_FULL_CHECK_ERR The use of this code is internal to the processor. It is not relevant to the interpretation of output products.	-	1	ss	2 byte(s)
34	raw_aux_proc_err RAWPKT_FAILS_AUXILIARY_DATA_PROCESSING_ERR The use of this code is internal to the processor. It is not relevant to the interpretation of output products.	-	1	ss	2 byte(s)
35	temp_out_range_err TEMP_OUT_OF_RANGE_FOR_LUT_ERR The use of this code is internal to the processor. It is not relevant to the interpretation of output products.	-	1	ss	2 byte(s)
36	pix_scan_jit_err PIX_SCAN_JITTER_ERR The use of this code is internal to the processor. It is not relevant to the interpretation of output products.	-	1	us	2 byte(s)
37	utmz_domain_err UTMZ_DOMAIN_EROR The use of this code is internal to the processor. It is not relevant to the interpretation of output products.	-	1	ss	2 byte(s)
38	tmz_atlimt_err TMZ_AT_LIMIT_ERR The use of this code is internal to the processor. It is not relevant to the interpretation of output products.	-	1	us	2 byte(s)
39	tmz_rog_prt_err TMZ_ROGUE_PRT_ERR The use of this code is internal to the processor. It is not relevant to the interpretation of output products.	-	1	us	2 byte(s)
40	tmz_cal_err TMZ_CALIBRATION_ERR The use of this code is internal to the processor. It is not relevant to the interpretation of output products.	-	1	us	2 byte(s)
41	tmz_bb_over_err TMZ_BB_OVERRANGE_ERR The use of this code is internal to the processor. It is not relevant to the interpretation of output products.	-	1	us	2 byte(s)
42	tmz_survll_err TMZ_SURVEILLANCE_ERR The use of this code is internal to the processor. It is not relevant to the interpretation of output products.	-	1	us	2 byte(s)
43	tmz_prt8_err TMZ_PRT8_ERR	-	1	us	2 byte(s)

#	Description	Units	Count	Type	Size
	The use of this code is internal to the processor. It is not relevant to the interpretation of output products.				
44	tmz_rog_scp_err TMZ_ROGUE_SCP_ERR The use of this code is internal to the processor. It is not relevant to the interpretation of output products.	-	1	us	2 byte(s)
45	tmz_bb_outlimt_err TMZ_BB_OUT_OF_LIMIT_ERR	-	1	us	2 byte(s)
46	bb_outrang_err BB_PIX_COUNT_OUT_OF_RANGE_ERR The use of this code is internal to the processor. It is not relevant to the interpretation of output products.	-	1	ss	2 byte(s)
47	bb_outrang_allchn BB_PIX_COUNT_OUT_OF_RANGE_ALL_CHANS The use of this code is internal to the processor. It is not relevant to the interpretation of output products.	-	1	ss	2 byte(s)
48	tmz_rog_bb_err TMZ_ROGUE_BB_ERR The use of this code is internal to the processor. It is not relevant to the interpretation of output products.	-	1	us	2 byte(s)
49	mon_threshold monitor threshold The visible calibration interval is determined by the value of the VISCAL monitor field in the telemetry. Only instrument scans for which the VISCAL monitor output exceeds the monitor threshold defined here are considered by the visible calibration algorithm.	-	1	ss	2 byte(s)
50	calibration_window_diff1 Calibration window diff1	-	1	ss	2 byte(s)
51	calibration_window_diff2 Calibration window diff2	-	1	ss	2 byte(s)
52	reserved Reserved field	-	1	ss	2 byte(s)
53	orbit_period orbit period The nominal orbital period of the satellite in seconds (used for estimating the time of maximum solar illumination of the visible calibration unit diffusing plate).	s	1	fl	4 byte(s)
54	time_offset time offset The time offset, in seconds, between the time at which the satellite crosses the terminator (day/night boundary) and the time of maximum solar illumination of the visible calibration unit diffusing plate.	s	1	fl	4 byte(s)
55	reflec_fact_16 1.6 microns reflectance factor The reflectance of the visible calibration unit at 1.6 micron wavelength, determined during ground calibration.	-	1	fl	4 byte(s)
56	reflec_fact_87 0.87 micron reflectance factor The reflectance of the visible calibration unit at 0.87 micron wavelength, determined during ground calibration.	-	1	fl	4 byte(s)
57	reflec_fact_67 0.67 micron reflectance factor The reflectance of the visible calibration unit at 0.67 micron wavelength, determined during ground calibration.	-	1	fl	4 byte(s)
58	reflec_fact_55 0.555 micron reflectance factor The reflectance of the visible calibration unit at 0.555 micron wavelength, determined during ground calibration.	-	1	fl	4 byte(s)
59	solar_irrad_16 1.6 micron solar irradiance The mean solar irradiance, in units of mW/cm2/micron, at 1.6 micron wavelength. This is not used directly in the visible channel calibration, but is used to derive an estimate of the solar irradiance in the channel for inclusion in the Visible Calibration Coefficients ADS.	mW/cm2/um	1	fl	4 byte(s)
60	solar_irrad_87 0.87 micron solar irradiance The mean solar irradiance, in units of mW/cm2/micron, at 0.87 micron wavelength. This is not used directly in the visible channel calibration, but is used to derive an estimate of the solar irradiance in the channel for inclusion in the Visible Calibration Coefficients ADS.	mW/cm2/um	1	fl	4 byte(s)
61	solar_irrad_67 0.67 micron solar irradiance The mean solar irradiance, in units of mW/cm2/micron, at 0.67 micron wavelength. This is not used directly in the visible channel calibration, but is used to derive an estimate of the solar irradiance in the channel for inclusion in the Visible Calibration Coefficients ADS.	mW/cm2/um	1	fl	4 byte(s)
62	solar_irrad_55 0.555 micron solar irradiance	mW/cm2/um	1	fl	4 byte(s)

#	Description	Units	Count	Type	Size
	The mean solar irradiance, in units of mW/cm2/micron, at 0.555 micron wavelength. This is not used directly in the visible channel calibration, but is used to derive an estimate of the solar irradiance in the channel for inclusion in the Visible Calibration Coefficients ADS.				
63	chan_bandw_16 1.6 micron channel bandwidth The bandwidth of the 1.6 micron channel, expressed in microns. This is used in the derivation of the estimate of the solar irradiance in the channel, included in the Visible Calibration Coefficients ADS.	um	1	fl	4 byte(s)
64	chan_bandw_87 0.87 micron channel bandwidth The bandwidth of the 0.870 micron channel, expressed in microns. This is used in the derivation of the estimate of the solar irradiance in the channel, included in the Visible Calibration Coefficients ADS	um	1	fl	4 byte(s)
65	chan_bandw_67 0.67 micron channel bandwidth The bandwidth of the 0.670 micron channel, expressed in microns. This is used in the derivation of the estimate of the solar irradiance in the channel, included in the Visible Calibration Coefficients ADS	um	1	fl	4 byte(s)
66	chan_bandw_55 0.555 micron channel bandwidth The bandwidth of the 0.555 micron channel, expressed in microns. This is used in the derivation of the estimate of the solar irradiance in the channel, included in the Visible Calibration Coefficients ADS	um	1	fl	4 byte(s)
67	window_half_width_in_min Window half width	minutes	1	fl	4 byte(s)
68	spare_6 Spare	-	1	SpareField	8 byte(s)

Record Length : 232

DS_NAME : Processor configuration GADS

Format Version 114.0

6.6.41 Configuration Data GADS

Table 6.72 Configuration Data GADS

Configuration Data GADS

#	Description	Units	Count	Type	Size
	Data Record				
0	thresh_10_nad Threshold for ABT flag, 10 arcmin cell nadir view The corresponding PFF flag in the AST product will be set to 1 if the number of valid pixels contributing to the spatial average is less than the this threshold, otherwise the flag will be set to 0.	-	1	sl	4 byte(s)
1	thresh_10_for Threshold for ABT flag, 10 arcmin cell forward view The corresponding PFF flag in the AST product will be set to 1 if the number of	-	1	sl	4 byte(s)

#	Description	Units	Count	Type	Size
	valid pixels contributing to the spatial average is less than the this threshold, otherwise the flag will be set to 0.				
2	thresh_30_nad Threshold for ABT flag, 30 arcmin cell nadir view The corresponding PFF flag in the AST product will be set to 1 if the number of valid pixels contributing to the spatial average is less than the this threshold, otherwise the flag will be set to 0.	-	1	sl	4 byte(s)
3	thresh_30_for Threshold for ABT flag, 30 arcmin cell forward view The corresponding PFF flag in the AST product will be set to 1 if the number of valid pixels contributing to the spatial average is less than the this threshold, otherwise the flag will be set to 0.	-	1	sl	4 byte(s)
4	thresh_17_nad Threshold for ABT flag, 17 km cell nadir view The corresponding PFF flag in the AST product will be set to 1 if the number of valid pixels contributing to the spatial average is less than the this threshold, otherwise the flag will be set to 0.	-	1	sl	4 byte(s)
5	thresh_17_for Threshold for ABT flag, 17 km cell forward view The corresponding PFF flag in the AST product will be set to 1 if the number of valid pixels contributing to the spatial average is less than the this threshold, otherwise the flag will be set to 0.	-	1	sl	4 byte(s)
6	thresh_50_nad Threshold for ABT flag, 50 km cell nadir view The corresponding PFF flag in the AST product will be set to 1 if the number of valid pixels contributing to the spatial average is less than the this threshold, otherwise the flag will be set to 0.	-	1	sl	4 byte(s)
7	thresh_50_for Threshold for ABT flag, 50 km cell forward view The corresponding PFF flag in the AST product will be set to 1 if the number of valid pixels contributing to the spatial average is less than the this threshold, otherwise the flag will be set to 0.	-	1	sl	4 byte(s)
8	ngrid_size NGRID or NGRANULE Granule Size The number of MDS records (or image rows) that comprise 1 product granule. The adopted value is 32.	-	1	sl	4 byte(s)
9	cell_dim AST Cell dimension The precise dimension, in km, of the nominal 50 km AST cell. (The adopted value is 51).	-	1	sl	4 byte(s)
10	trop_indx TROPICAL_INDEX The latitude, in degrees, of the tropical zone boundary. (The adopted value is 12.5.)	degrees	1	fl	4 byte(s)
11	temp_ind TEMPERATE_INDEX The nominal latitude boundary, within the temperate zone, between interpolation regions used by the SST retrieval algorithm. (The adopted value is 37.0.)	degrees	1	fl	4 byte(s)
12	pol_indx POLAR_INDEX The latitude, in degrees, of the polar zone boundary. (The adopted value is 70.0.)	degrees	1	fl	4 byte(s)
13	nad_pix_thresh NADIR-PIXELS_THRESH A spatially averaged SST will not be derived if the fraction of valid 11 or 12 micron pixels in a cell is less than this number.	-	1	fl	4 byte(s)
14	for_pix_thresh FRWRD_PIXELS_THRESH A spatially averaged dual view SST will not be derived if the fraction of valid 11 or 12 micron pixels in a cell is less than this number.	-	1	fl	4 byte(s)
15	ir37_thresh IR37_THRESH The 3.7 micron channel will not be used in the spatially averaged derivation if the ratio of valid 3.7 micron pixels to 11 micron pixels in the cell is less than this value.	-	1	fl	4 byte(s)
16	sm_scale_fac Smoothing scaling factor Retrieved gridded SST values are smoothed in groups of n x n pixels. This value is n.	-	1	ss	2 byte(s)
17	max_cells_x MAX_CELLS_X (number of 50 km cells across track) The number of across-track 50 km cells to be computed in the AST product. (Nominal value 10.)	-	1	ss	2 byte(s)
18	max_cells_y MAX_CELLS_Y (number of 50 km cells along track) Used internally by the processor.	-	1	ss	2 byte(s)
19	mx MX: across track origin of 50 km cells Defines the across-track position of the 50 km cells. The lower left corner of the	-	1	sl	4 byte(s)

#	Description	Units	Count	Type	Size
	left-hand cell has row index MX.				
20	spare_1 Spare	-	1	SpareField	12 byte(s)

Record Length : 86

DS_NAME : Configuration Data GADS

Format Version 114.0

6.6.42 Across-track Band Mapping Look-up Table

Table 6.73 Across-track Band Mapping Look-up Table

Across-track Band Mapping Look-up Table

#	Description	Units	Count	Type	Size
Data Record					
0	pixel_index Pixel index (j) Pixel index, in the range 0 to 511.	-	1	ss	2 byte(s)
1	actrk_band_index Across-track band index (map index) The across-track band number, in the range 0 to 37, corresponding to pixel index j.	-	1	ss	2 byte(s)

Record Length : 4

DS_NAME : Across-track Band Mapping Look-up Table

Format Version 114.0

The Across-track Band Mapping Look-up Table GADS defines the relationship between pixel across-track co-ordinate and across-track band number. The data set contains one entry for each value of the pixel index j = 0, 511.

6.6.43 Grid pixel latitude and longtitude topographic corrections ADS

Table 6.74 Grid pixel latitude and longtitude topographic corrections ADS

Grid pixel latitude and longtitude, topographic corrections ADS

#	Description	Units	Count	Type	Size
Data Record					
0	dsr_time Nadir UTC time in MJD format The nadir time associated with a given record, or image row, is the time at which the sub-satellite point intersects the image row, or the time at which the satellite is vertically overhead at the centre of the row. It corresponds to the measurement time at which the pixels in the centre of the row (the nadir pixels) are measured. Because of the curvature of the instrument scans, the measurement time at the extremities of the row may differ from the nadir time by up to 15 seconds. Similarly the measurement time of a forward view image will differ by approximately 135 seconds (2.25 minutes) from the measurement time of the corresponding nadir scan. The relationship between nadir time and measurement time is explained in more detail in the accompanying link.	MJD	1	mjd	12 byte(s)
1	attach_flag Attachment Flag (set to 1 if all MDSRs corresponding to this ADSR are blank, set to 0 otherwise) In accordance with ESA guidelines, this flag will be set to 1 if all of the MDS records in the granule have the record quality indicator set to -1; otherwise it is set to zero. If the flag is set to 1 the corresponding MDS records will be omitted; this mechanism allows gaps in the sequence of MDS records to be identified.	flag	1	BooleanFlag	1 byte(s)
2	spare_1 Spare	-	1	SpareField	3 byte(s)
3	img_scan_y image scan y coordinate The y co-ordinate of the image row (or image scan), in units of metres. Because the AATSR image data is sampled at equal intervals of time in the along track direction, this quantity is provided in order to define the relationship between time and image scale. The y co-ordinate is measured along the satellite ground track; the origin (in the case of consolidated data) is at the ascending node of the orbit. (Precisely, from the point corresponding to time T0, however defined.) The co-ordinate frame of the AATSR images is defined in the accompanying link.	m	1	sl	4 byte(s)
4	tie_pt_lat tie point latitudes In order to permit the geolocation of the AATSR images, the latitudes and longitudes of selected tie points (or tie pixels) on the image are provided in this ADS. These fields contain the latitude of each tie point on the granule row, in units of microdegrees. On each granule row there are 23 tie points at x co-ordinates of -275, -250, ... 275 km. Pixels are 1 km apart, and the tie point at 0 km corresponds to pixel 256, therefore an x co-ordinate of -250 km corresponds to pixel number 6, and so on. Latitudes of intermediate points may be derived by linear interpolation. Note that the extreme tie points at +/- 275 km are beyond the extremities of the image row, which extends to +/- 256 km.	(1e-6) degrees	23	GeoCoordinate	23*4 byte(s)
5	tie_pt_long tie point longitudes In order to permit the geolocation of the AATSR images, the latitudes and longitudes of selected tie points (or tie pixels) on the image are provided in this ADS. These fields contain the longitude of each tie point on the granule row, in units of microdegrees. On each granule row there are 23 tie points at x co-ordinates of -275, -250, ... 275 km. Pixels are 1 km apart, and the tie point at 0 km corresponds to pixel 256, therefore an x co-ordinate of -250 km corresponds to pixel number 6, and so on. Longitudes of intermediate points may be derived by	(1e-6) degrees	23	GeoCoordinate	23*4 byte(s)

#	Description	Units	Count	Type	Size
	linear interpolation. Note that the extreme tie points at +/- 275 km are beyond the extremities of the image row, which extends to +/- 256 km.				
6	lat_corr_nadv latitude corrections, nadir view The geolocation of the AATSR pixels assumes that the surface is at mean sea level. That is to say, the co-ordinates of the pixel in fact define the point of intersection of the line of sight with the reference ellipsoid. This approach is acceptable for points over the sea, and also for low-lying land, but will give rise to errors in the case of elevated land. This field defines the correction to be [added] to the pixel latitude to give the true latitude, based on the elevation of the pixel taken from a standard DTM. The correction is in units of microdegrees. If a valid correction is not available for the tie point, the field will contain an exceptional value of [-999,999]; this will generally occur at the edges of the swath, where a valid tie point pixel is not available.	(1e-6) degrees	23	sl	23*4 byte(s)
7	long_corr_nadv longitude corrections, nadir view As above, the geolocation of the AATSR pixels assumes that the surface is at mean sea level. This field defines the correction to be [added] to the pixel longitude for pixels over land to give the true longitude, based on the elevation of the pixel taken from a standard DTM. The correction is in units of microdegrees. If a valid correction is not available for the tie point, the field will contain an exceptional value of [-999,999]; this will generally occur at the edges of the swath, where a valid tie point pixel is not available.	(1e-6) degrees	23	sl	23*4 byte(s)
8	lat_corr_forv latitude corrections, forward view The geolocation of the AATSR pixels assumes that the surface is at mean sea level. That is to say, the co-ordinates of the pixel in fact define the point of intersection of the line of sight with the reference ellipsoid. This approach is acceptable for points over the sea, and also for low-lying land, but will give rise to errors in the case of elevated land. This field defines the correction to be added to the pixel latitude to give the true latitude, based on the elevation of the pixel taken from a standard DTM. The correction is in units of microdegrees. If a valid correction is not available for the tie point, the field will contain an exceptional value of [-999,999]; this will generally occur at the edges of the swath, where a valid tie point pixel is not available.	(1e-6) degrees	23	sl	23*4 byte(s)
9	long_corr_forv longitude corrections, forward view As above, the geolocation of the AATSR pixels assumes that the surface is at mean sea level. This field defines the correction to be added to the pixel longitude for pixels over land to give the true longitude, based on the elevation of the pixel taken from a standard DTM. The correction is in units of microdegrees. If a valid correction is not available for the tie point, the field will contain an exceptional value of [-999,999]; this will generally occur at the edges of the swath, where a valid tie point pixel is not available.	(1e-6) degrees	23	sl	23*4 byte(s)
10	topo_alt Topographic Altitude The topographic altitude of the tie pixel, in metres, taken from a standard Digital Terrain [Elevation] Model (DTM). The tie points are the same as for the pixel latitude and longitude.	metres	23	ss	23*2 byte(s)
11	spare_2 Spare	-	1	SpareField	8 byte(s)

Record Length : 626

DS_NAME : Grid pixel latitude and longtitude, topographic corrections ADS

Format Version 114.0

6.6.44 Scan pixel x and y ADS

Table 6.75 Scan pixel x and y ADS

Scan pixel x and y ADS

#	Description	Units	Count	Type	Size
Data Record					
0	dsr_time Scan UTC time in MJD format This ADS, unlike the others, is arranged in terms of instrument scans instead of image rows, and the corresponding time tag represents the time of the instrument scan, derived from the telemetry source packet. The time represents the start of the instrument scan, and is given in the standard MJD format, relative to J2000.0.	MJD	1	mjd	12 byte(s)
1	attach_flag Attachment Flag (always set to zero for this ADS) The attachment flag is always zero for this ADS.	flag	1	BooleanFlag	1 byte(s)
2	spare_1 Spare	-	1	SpareField	3 byte(s)
3	instr_scan_num instrument scan number The number of the instrument scan to which this record refers. Scan number is counted from an arbitrary origin close to he start of the product.	-	1	us	2 byte(s)
4	tie_pix_x tie pixel x coordinate This ADS gives the x and y co-ordinates of the instrument pixels, before regridding. These fields give the x co-ordinate of each tie pixel on the scan. The x co-ordinate is in units of metres, in the range -275,000 to +275,000 (-275 to + 275 km). The tie pixels are defined in the accompanying link.	m	99	sl	99*4 byte(s)
5	tie_pix_y tie pixel y coordinate This ADS gives the x and y co-ordinates of the instrument pixels, before regridding. These fields give the y co-ordinate of each tie pixel on the scan. The y co-ordinate is in units of km, measured from an origin close to the ascending node of the orbit [for consolidated data], in the range -2,000,000 to +42,000,000 (-2000 to +42000 km). The tie pixels are defined in the accompanying link.	m	99	sl	99*4 byte(s)
6	spare_2 spare	-	1	SpareField	20 byte(s)

Record Length : 830

DS_NAME : Scan pixel x and y ADS

Format Version 114.0

6.6.45 Summary Quality ADS

Table 6.76 Summary Quality ADS

Summary Quality ADS

#	Description	Units	Count	Type	Size
Data Record					
0	dsr_time Nadir UTC time in MJD format The nadir time associated with a given record, or image row, is the time at which the sub-satellite point intersects the image row, or the time at which the satellite is vertically overhead at the centre of the row. It corresponds to the measurement time at which the pixels in the centre of the row (the nadir pixels) are measured. Because of the curvature of the instrument scans, the measurement time at the extremities of the row may differ from the nadir time by up to 15 seconds. Similarly the measurement time of a forward view image will differ by approximately 135 seconds (2.25 minutes) from the measurement time of the corresponding nadir scan. The relationship between nadir time and measurement time is explained in more detail in the accompanying link.	MJD	1	mjd	12 byte(s)
1	attach_flag Attachment flag(set to 1 if all MDSRs corresponding to this ADSR are blank, set to 0 otherwise) In accordance with ESA guidelines, this flag will be set to 1 if all of the MDS records in the granule have the record quality indicator set to -1; otherwise it is set to zero. If the flag is set to 1 the corresponding MDS records will be omitted; this mechanism allows gaps in the sequence of MDS records to be identified. In the case of the SQADS, the attachment flag will only be set if all 512 records are omitted under this provision.	flag	1	BooleanFlag	1 byte(s)
2	spare_1 Spare	-	1	SpareField	3 byte(s)
3	scan_num scan number The number of the image scan, or image row, of the first row of the major granule corresponding to this record. This is a continuous count starting from the first row of the product.	-	1	us	2 byte(s)
4	pv_nad_null_pac Packet Validation during nadir view number of scans null packet The number of rows of the 512 row large granule for which at least one nadir view pixel is flagged as from a null packet (a telemetry data gap).	-	1	ss	2 byte(s)
5	pv_nad_fail_val Packet Validation during nadir view number of scans failing basic validation The number of rows of the 512 row large granule for which at least one nadir view pixel is flagged 'scan failing basic validation'.	-	1	ss	2 byte(s)
6	pv_nad_fail_crc_chk Packet Validation during nadir view number of scans failing CRC check The number of rows of the 512 row large granule for which at least one nadir view pixel is flagged 'scan failed CRC check'	-	1	ss	2 byte(s)
7	pv_nad_show_buf_full Packet Validation during nadir view number of scans showing buffers full The number of rows of the 512 row large granule for which at least one nadir view pixel is flagged 'scan buffers full'.	-	1	ss	2 byte(s)
8	pv_nad_scan_jitt Packet Validation during nadir view number of scans showing scan jitter The number of rows of the 512 row large granule for which at least one nadir view pixel is flagged 'scan jitter'.	-	1	ss	2 byte(s)
9	resv_char_1 reserved for future use Field is currently unused and set to zero.	-	1	ss	2 byte(s)
10	resv_char_2 reserved for future use Field is currently unused and set to zero.	-	1	ss	2 byte(s)
11	resv_char_3 reserved for future use Field is currently unused and set to zero.	-	1	ss	2 byte(s)
12	resv_char_4 reserved for future use Field is currently unused and set to zero.	-	1	ss	2 byte(s)
13	pv_nad_scan_error Packet Validation during nadir view number of scans - all other errors The number of rows of the 512 row large granule for which at least one nadir view pixel shows any error or exception condition not mentioned above.	-	1	ss	2 byte(s)
14	pv_for_null_pac Packet Validation during forward view number of scans null packet The number of rows of the 512 row large granule for which at least one forward view pixel is flagged as from a null packet (a telemetry data gap).	-	1	ss	2 byte(s)
15	pv_for_fail_val Packet Validation during forward view number of scans failing basic validation The number of rows of the 512 row large granule for which at least one forward view pixel is flagged 'scan failing basic validation'.	-	1	ss	2 byte(s)
16	pv_for_fail_crc_chk	-	1	ss	2 byte(s)

#	Description	Units	Count	Type	Size
	Packet Validation during forward view number of scans failing CRC check The number of rows of the 512 row large granule for which at least one forward view pixel is flagged 'scan failed CRC check'				
17	pv_for_show_buf_full Packet Validation during forward view number of scans showing buffers full The number of rows of the 512 row large granule for which at least one forward view pixel is flagged 'scan buffers full'.	-	1	ss	2 byte(s)
18	pv_for_scan_jitt Packet Validation during forward view number of scans showing scan jitter The number of rows of the 512 row large granule for which at least one forward view pixel is flagged 'scan jitter'.	-	1	ss	2 byte(s)
19	resv_char_5 reserved for future use Field is currently unused and set to zero.	-	1	ss	2 byte(s)
20	resv_char_6 reserved for future use Field is currently unused and set to zero.	-	1	ss	2 byte(s)
21	resv_char_7 reserved for future use Field is currently unused and set to zero.	-	1	ss	2 byte(s)
22	resv_char_8 reserved for future use Field is currently unused and set to zero.	-	1	ss	2 byte(s)
23	pv_for_scan_error Packet Validation during forward view number of scans - all other errors The number of rows of the 512 row large granule for which at least one forward view pixel shows any error or exception condition not mentioned above.	-	1	ss	2 byte(s)
24	spare_2 Spare	-	1	SpareField	28 byte(s)

Record Length : 86

DS_NAME : Summary Quality ADS

Format Version 114.0

6.6.46 12 micron forward view MDS

Table 6.77 12 micron forward view MDS

3.7 micron forward view MDS

#	Description	Units	Count	Type	Size
Data Record					
0	dsr_time Nadir UTC time in MJD format The nadir time associated with a given record, or image row, is the time at which the sub-satellite point intersects the image row, or the time at which the satellite is vertically overhead at the centre of the row. It corresponds to the	MJD	1	mjd	12 byte(s)

#	Description	Units	Count	Type	Size
	measurement time at which the pixels in the centre of the row (the nadir pixels) are measured. Because of the curvature of the instrument scans, the measurement time at the extremities of the row may differ from the nadir time by up to 15 seconds. Similarly the measurement time of a forward view image will differ by approximately 135 seconds (2.25 minutes) from the measurement time of the corresponding nadir scan. The relationship between nadir time and measurement time is explained in more detail in the accompanying link.				
1	quality_flag Quality Indicator (-1 for blank MDSR, 0 otherwise) The record quality indicator is set to -1 to indicate a blank MDS Record, to zero otherwise (I.e. if the record contains valid data).	flag	1	BooleanFlag	1 byte(s)
2	spare_1 Spare	-	1	SpareField	3 byte(s)
3	img_scan_y image scan y coordinate The y co-ordinate of the image row (or image scan), in units of metres. Because the AATSR image data is sampled at equal intervals of time in the along track direction, this quantity is provided in order to define the relationship between time and image scale. The y co-ordinate is measured along the satellite ground track; the origin (in the case of consolidated data) is at the ascending node of the orbit. (Precisely, from the point corresponding to time T0, however defined.) The co-ordinate frame of the AATSR images is defined in the accompanying link.	m	1	sl	4 byte(s)
4	bt_rad_pix BT or reflectance for pixel 0 - 511(Units are K/100 for BT, %/100 for reflectance). The calibrated brightness temperature of each pixel on the image row (numbers 0 to 511) in the appropriate infra-red channel, measured in the forward view. The brightness temperature is expressed as a 16 bit integer in units of 0.01 K. Valid brightness temperatures will be positive numbers in the range 17,000 to 32,100, but in the event that a valid BT is not available, the field will be set to an exceptional value that is a small negative integer. The exceptional values are tabulated and explained below.	K/100	512	ss	512*2 byte(s)

Record Length : 1044

DS_NAME : 3.7 micron forward view MDS

Format Version 114.0

The following table shows the pixel exceptional values and the corresponding flag bits in the confidence word.

Table 6.78 Pixel exception values in GBTR MDS #1 to MDS #14

Exception Value	Meaning	Confidence word bit
-1	Scan Absent (null packet)	2
-2	Pixel Absent	3
-3	Not decompressed	4
-4	No signal in channel	5
-5	Saturation in channel	6
-6	Derived radiance outside Calibration	7
-7	Calibration Parameters unavailable	8
-8	Unfilled Pixel (set in cosmetic fill)	9

6.6.47 12 micron nadir view MDS

Table 6.79 12 micron nadir view MDS

3.7 micron nadir view MDS

#	Description	Units	Count	Type	Size
Data Record					
0	dsr_time Nadir UTC time in MJD format The nadir time associated with a given record, or image row, is the time at which the sub-satellite point intersects the image row, or the time at which the satellite is vertically overhead at the centre of the row. It corresponds to the measurement time at which the pixels in the centre of the row (the nadir pixels) are measured. Because of the curvature of the instrument scans, the measurement time at the extremities of the row may differ from the nadir time by up to 15 seconds. Similarly the measurement time of a forward view image will differ by approximately 135 seconds (2.25 minutes) from the measurement time of the corresponding nadir scan. The relationship between nadir time and measurement time is explained in more detail in the accompanying link.	MJD	1	mjd	12 byte(s)
1	quality_flag Quality Indicator (-1 for blank MDSR, 0 otherwise) The record quality indicator is set to -1 to indicate a blank MDS Record, to zero otherwise (I.e. if the record contains valid data).	flag	1	BooleanFlag	1 byte(s)
2	spare_1 Spare	-	1	SpareField	3 byte(s)
3	img_scan_y image scan y coordinate The y co-ordinate of the image row (or image scan), in units of metres. Because the AATSR image data is sampled at equal intervals of time in the along track direction, this quantity is provided in order to define the relationship between time and image scale. The y co-ordinate is measured along the satellite ground track; the origin (in the case of consolidated data) is at the ascending node of the orbit. (Precisely, from the point corresponding to time T0, however defined.) The co-ordinate frame of the AATSR images is defined in the accompanying link.	m	1	sl	4 byte(s)
4	bt_rad_pix BT or reflectance for pixel 0 - 511(Units are K/100 for BT, %/100 for reflectance). The calibrated brightness temperature of each pixel on the image row (numbers 0 to 511) in the appropriate infra-red channel, measured in the nadir view. The brightness temperature is expressed as a 16 bit integer in units of 0.01 K. Valid brightness temperatures will be positive numbers in the range 17,000 to 32,100, but in the event that a valid BT is not available, the field will be set to an exceptional value that is a small negative integer. The exceptional values are tabulated and explained below.	K/100	512	ss	512*2 byte(s)

Record Length : 1044

DS_NAME : 3.7 micron nadir view MDS

Format Version 114.0

The following table shows the pixel exceptional values and the corresponding flag bits in the confidence word.

Table 6.80 Pixel exception values in GBTR MDS #1 to MDS #14.

Exception Value	Meaning	Confidence word bit
-1	Scan Absent (null packet)	2
-2	Pixel Absent	3
-3	Not decompressed	4
-4	No signal in channel	5
-5	Saturation in channel	6
-6	Derived radiance outside Calibration	7
-7	Calibration Parameters unavailable	8
-8	Unfilled Pixel (set in cosmetic fill)	9

6.6.48 1.6 micron forward view MDS

Table 6.81 1.6 micron forward view MDS

0.55 micron forward view MDS

#	Description	Units	Count	Type	Size
Data Record					
0	dsr_time Nadir UTC time in MJD format The nadir time associated with a given record, or image row, is the time at which the sub-satellite point intersects the image row, or the time at which the satellite is vertically overhead at the centre of the row. It corresponds to the measurement time at which the pixels in the centre of the row (the nadir pixels) are measured. Because of the curvature of the instrument scans, the measurement time at the extremities of the row may differ from the nadir time by up to 15 seconds. Similarly the measurement time of a forward view image will differ by approximately 135 seconds (2.25 minutes) from the measurement time of the corresponding nadir scan. The relationship between nadir time and measurement time is explained in more detail in the accompanying link.	MJD	1	mjd	12 byte(s)
1	quality_flag Quality Indicator (-1 for blank MDSR, 0 otherwise) The record quality indicator is set to -1 to indicate a blank MDS Record, to zero otherwise (i.e. if the record contains valid data).	flag	1	BooleanFlag	1 byte(s)
2	spare_1 Spare	-	1	SpareField	3 byte(s)
3	img_scan_y image scan y coordinate The y co-ordinate of the image row (or image scan), in units of metres. Because the AATSR image data is sampled at equal intervals of time in the along track direction, this quantity is provided in order to define the relationship between time and image scale. The y co-ordinate is measured along the satellite ground track; the origin (in the case of consolidated data) is at the ascending node of the	m	1	sl	4 byte(s)

#	Description	Units	Count	Type	Size
	orbit. (Precisely, from the point corresponding to time T0, however defined.) The co-ordinate frame of the AATSR images is defined in the accompanying link.				
4	bt_rad_pix BT or reflectance for pixel 0 - 511(Units are K/100 for BT, %/100 for reflectance). The calibrated reflectance of each pixel on the image row (numbers 0 to 511) in the selected visible channel, measured in the forward view. The reflectance is not corrected for solar illumination angle (see link). It is expressed as a 16 bit integer in units of 0.01 %. Valid reflectances will be positive numbers, but in the event that a valid reflectance is not available, the field will be set to an exceptional value that is a small negative integer. The exceptional values are tabulated and explained below.	%/100	512	ss	512*2 byte(s)

Record Length : 1044

DS_NAME : 0.55 micron forward view MDS

Format Version 114.0

The following table shows the pixel exceptional values and the corresponding flag bits in the confidence word.

Table 6.82 Pixel exception values in GBTR MDS #1 to MDS #14

Exception Value	Meaning	Confidence word bit
-1	Scan Absent (null packet)	2
-2	Pixel Absent	3
-3	Not decompressed	4
-4	No signal in channel	5
-5	Saturation in channel	6
-6	Derived radiance outside Calibration	7
-7	Calibration Parameters unavailable	8
-8	Unfilled Pixel (set in cosmetic fill)	9

6.6.49 1.6 micron nadir view MDS

Table 6.83 1.6 micron nadir view MDS

0.55 micron nadir view MDS

#	Description	Units	Count	Type	Size
Data Record					
0	dsr_time Nadir UTC time in MJD format The nadir time associated with a given record, or image row, is the time at which the sub-satellite point intersects the image row, or the time at which the satellite is vertically overhead at the centre of the row. It corresponds to the measurement time at which the pixels in the centre of the row (the nadir pixels) are measured. Because of the curvature of the instrument scans, the measurement time at the extremities of the row may differ from the nadir time by up to 15 seconds. Similarly the measurement time of a forward view image will differ by approximately 135 seconds (2.25 minutes) from the measurement time of the corresponding nadir scan. The relationship between nadir time and measurement time is explained in more detail in the accompanying link.	MJD	1	mjd	12 byte(s)
1	quality_flag Quality Indicator (-1 for blank MDSR, 0 otherwise) The record quality indicator is set to -1 to indicate a blank MDS Record, to zero otherwise (i.e. if the record contains valid data).	flag	1	BooleanFlag	1 byte(s)
2	spare_1 Spare	-	1	SpareField	3 byte(s)
3	img_scan_y image scan y coordinate The y co-ordinate of the image row (or image scan), in units of metres. Because the AATSR image data is sampled at equal intervals of time in the along track direction, this quantity is provided in order to define the relationship between time and image scale. The y co-ordinate is measured along the satellite ground track; the origin (in the case of consolidated data) is at the ascending node of the orbit. (Precisely, from the point corresponding to time T0, however defined.) The co-ordinate frame of the AATSR images is defined in the accompanying link.	m	1	sl	4 byte(s)
4	bt_rad_pix BT or reflectance for pixel 0 - 511(Units are K/100 for BT, %/100 for reflectance). The calibrated reflectance of each pixel on the image row (numbers 0 to 511) in the selected visible channel, measured in the nadir view. The reflectance is not corrected for solar illumination angle (see link). It is expressed as a 16 bit integer in units of 0.01 %. Valid reflectances will be positive numbers, but in the event that a valid reflectance is not available, the field will be set to an exceptional value that is a small negative integer. The exceptional values are tabulated and explained below.	%/100	512	ss	512*2 byte(s)

Record Length : 1044

DS_NAME : 0.55 micron nadir view MDS

Format Version 114.0

The following table shows the pixel exceptional values and the corresponding flag bits in the confidence word.

Table 6.84 Pixel exception values in GBTR MDS #1 to MDS #14

Exception Value	Meaning	Confidence word bit
-1	Scan Absent (null packet)	2
-2	Pixel Absent	3

-3	Not decompressed	4
-4	No signal in channel	5
-5	Saturation in channel	6
-6	Derived radiance outside Calibration	7
-7	Calibration Parameters unavailable	8
-8	Unfilled Pixel (set in cosmetic fill)	9

6.6.50 Level 1B SPH

Table 6.85 Level 1B SPH

Level 1B SPH

#	Description	Units	Count	Type	Size
Data Record					
0	sph_descriptor_title SPH_DESCRIPTOR=	keyword	1	AsciiString	15 byte(s)
1	quote_1 quotation mark (""")	ascii	1	AsciiString	1 byte(s)
2	sph_descriptor SPH Descriptor ASCII string describing the product.	ascii	1	AsciiString	28 byte(s)
3	quote_2 quotation mark (""")	ascii	1	AsciiString	1 byte(s)
4	newline_char_1 newline character	terminator	1	AsciiString	1 byte(s)
5	stripline_cont_ind_title STRIPLINE_CONTINUITY_INDICATOR=	keyword	1	AsciiString	31 byte(s)
6	stripline_continuity_indicator Value: 0= No stripline continuity, the product is a complete segment. Other: Stripline Counter	-	1	Ac	4 byte(s)
7	newline_char_2 newline character	terminator	1	AsciiString	1 byte(s)
8	slice_pos_title SLICE_POSITION=	keyword	1	AsciiString	15 byte(s)
9	slice_position Value: +001 to NUM_SLICES. Default value if no stripline continuity = +001	-	1	Ac	4 byte(s)
10	newline_char_3 newline character	terminator	1	AsciiString	1 byte(s)
11	num_slices_title NUM_SLICES=	keyword	1	AsciiString	11 byte(s)
12	num_slices Number of slices in this striplineDefault value if no continuity = +001	-	1	Ac	4 byte(s)
13	newline_char_4 newline character	terminator	1	AsciiString	1 byte(s)
14	first_ln_time_title FIRST_LINE_TIME=	keyword	1	AsciiString	16 byte(s)
15	quote_3 quotation mark (""")	ascii	1	AsciiString	1 byte(s)

#	Description	Units	Count	Type	Size
16	first_line_time Azimuth time first line of product. UTC Time of first range line in the MDS of this product. UTC time format contained within quotation marks.	UTC	1	UtcExternal	27 byte(s)
17	quote_4 quotation mark (""")	ascii	1	AsciiString	1 byte(s)
18	newline_char_5 newline character	terminator	1	AsciiString	1 byte(s)
19	last_ln_time_title LAST_LINE_TIME=	keyword	1	AsciiString	15 byte(s)
20	quote_5 quotation mark (""")	ascii	1	AsciiString	1 byte(s)
21	last_line_time Azimuth time last line of product. Time of last range line in the MDS of this product. UTC time format contained within quotation marks.	UTC	1	UtcExternal	27 byte(s)
22	quote_6 quotation mark (""")	ascii	1	AsciiString	1 byte(s)
23	newline_char_6 newline character	terminator	1	AsciiString	1 byte(s)
24	first_first_lat_title FIRST_FIRST_LAT=	keyword	1	AsciiString	16 byte(s)
25	first_first_lat Geodetic Latitude of the first sample of the first line. A negative value denotes south latitude, a positive value denotes North latitude	(1e-6) degrees	1	AsciiGeoCoordinate	11 byte(s)
26	first_first_lat_units <10-6degN>	units	1	AsciiString	10 byte(s)
27	newline_char_7 newline character	terminator	1	AsciiString	1 byte(s)
28	first_first_long_title FIRST_FIRST_LONG=	keyword	1	AsciiString	17 byte(s)
29	first_first_long East geodetic longitude of the first sample of the first line. Positive values East of Greenwich, negative values west of Greenwich.	(1e-6) degrees	1	AsciiGeoCoordinate	11 byte(s)
30	first_first_long_units <10-6degE>	units	1	AsciiString	10 byte(s)
31	newline_char_8 newline character	terminator	1	AsciiString	1 byte(s)
32	first_mid_lat_title FIRST_MID_LAT=	keyword	1	AsciiString	14 byte(s)
33	first_mid_lat Geodetic Latitude of the middle sample of the first line. A negative value denotes south latitude, a positive value denotes North latitude	(1e-6) degrees	1	AsciiGeoCoordinate	11 byte(s)
34	first_mid_lat_units <10-6degN>	units	1	AsciiString	10 byte(s)
35	newline_char_9 newline character	terminator	1	AsciiString	1 byte(s)
36	first_mid_long_title FIRST_MID_LONG=	keyword	1	AsciiString	15 byte(s)
37	first_mid_long East geodetic longitude of the middle sample of the first line. Positive values East of Greenwich, negative values west of Greenwich.	(1e-6) degrees	1	AsciiGeoCoordinate	11 byte(s)
38	first_mid_long_units <10-6degE>	units	1	AsciiString	10 byte(s)
39	newline_char_10 newline character	terminator	1	AsciiString	1 byte(s)
40	first_last_lat_title FIRST_LAST_LAT=	keyword	1	AsciiString	15 byte(s)
41	first_last_lat Geodetic Latitude of the last sample of the first line. A negative value denotes south latitude, a positive value denotes North latitude	(1e-6) degrees	1	AsciiGeoCoordinate	11 byte(s)
42	first_last_lat_units <10-6degN>	units	1	AsciiString	10 byte(s)
43	newline_char_11 newline character	terminator	1	AsciiString	1 byte(s)
44	first_last_long_title FIRST_LAST_LONG=	keyword	1	AsciiString	16 byte(s)
45	first_last_long East geodetic longitude of the last sample of the first line. Positive values East of Greenwich, negative values west of Greenwich.	(1e-6) degrees	1	AsciiGeoCoordinate	11 byte(s)
46	first_last_long_units <10-6degE>	units	1	AsciiString	10 byte(s)
47	newline_char_12 newline character	terminator	1	AsciiString	1 byte(s)

#	Description	Units	Count	Type	Size
48	last_first_lat_title LAST_FIRST_LAT=	keyword	1	AsciiString	15 byte(s)
49	last_first_lat Geodetic Latitude of the first sample of the last line. A negative value denotes south latitude, a positive value denotes North latitude	(1e-6) degrees	1	AsciiGeoCoordinate	11 byte(s)
50	last_first_units <10-6degN>	units	1	AsciiString	10 byte(s)
51	newline_char_13 newline character	terminator	1	AsciiString	1 byte(s)
52	last_first_long_title LAST_FIRST_LONG=	keyword	1	AsciiString	16 byte(s)
53	last_first_long East geodetic longitude of the first sample of the last line. Positive values East of Greenwich, negative values west of Greenwich.	(1e-6) degrees	1	AsciiGeoCoordinate	11 byte(s)
54	last_first_long_units <10-6degE>	units	1	AsciiString	10 byte(s)
55	newline_char_14 newline character	terminator	1	AsciiString	1 byte(s)
56	last_mid_lat_title LAST_MID_LAT=	keyword	1	AsciiString	13 byte(s)
57	last_mid_lat Geodetic Latitude of the middle sample of the last line. A negative value denotes south latitude, a positive value denotes North latitude	(1e-6) degrees	1	AsciiGeoCoordinate	11 byte(s)
58	last_mid_lat_units <10-6degN>	units	1	AsciiString	10 byte(s)
59	newline_char_15 newline character	terminator	1	AsciiString	1 byte(s)
60	last_mid_long_title LAST_MID_LONG=	keyword	1	AsciiString	14 byte(s)
61	last_mid_long East geodetic longitude of the middle sample of the last line. Positive values East of Greenwich, negative values west of Greenwich.	(1e-6) degrees	1	AsciiGeoCoordinate	11 byte(s)
62	last_mid_long_units <10-6degE>	units	1	AsciiString	10 byte(s)
63	newline_char_16 newline character	terminator	1	AsciiString	1 byte(s)
64	last_last_lat_title LAST_LAST_LAT=	keyword	1	AsciiString	14 byte(s)
65	last_last_lat Geodetic Latitude of the last sample of the last line. A negative value denotes south latitude, a positive value denotes North latitude	(1e-6) degrees	1	AsciiGeoCoordinate	11 byte(s)
66	last_last_lat_units <10-6degN>	units	1	AsciiString	10 byte(s)
67	newline_char_17 newline character	terminator	1	AsciiString	1 byte(s)
68	last_last_long_title LAST_LAST_LONG=	keyword	1	AsciiString	15 byte(s)
69	last_last_long East geodetic longitude of the last sample of the last line. Positive values East of Greenwich, negative values west of Greenwich.	(1e-6) degrees	1	AsciiGeoCoordinate	11 byte(s)
70	last_last_long_units <10-6degE>	units	1	AsciiString	10 byte(s)
71	newline_char_18 newline character	terminator	1	AsciiString	1 byte(s)
72	spare_1 Spare	-	1	SpareField	51 byte(s)
73	min_fpp_basep_temp_title MIN_FPP_BASEPLATE_TEM=	keyword	1	AsciiString	22 byte(s)
74	min_fpp_baseplate_tem Minimum FPP baseplate temperature The minimum physical temperature of the instrument Focal Plane Assembly baseplate during the orbit, taken from the on-board telemetry (identifier A5061).	K	1	Afl	15 byte(s)
75	min_fpp_basep_temp_units <K>	units	1	AsciiString	3 byte(s)
76	newline_char_20 newline character	terminator	1	AsciiString	1 byte(s)
77	min_12_mic_temp_title MIN_12_MICRON_DETECTOR_TEMP=	keyword	1	AsciiString	28 byte(s)
78	min_12_micron_detector_temp Minimum 12 micron detector temperature The minimum physical temperature of the 12 micron detector within the product duration, taken from the on-board telemetry (identifier A5061).	K	1	Afl	15 byte(s)

#	Description	Units	Count	Type	Size
79	min_12_mic_temp_units <K>	units	1	AsciiString	3 byte(s)
80	newline_char_21 newline character	terminator	1	AsciiString	1 byte(s)
81	min_11_mic_temp_title MIN_11_MICRON_DETECTOR_TEMP=	keyword	1	AsciiString	28 byte(s)
82	min_11_micron_detector_temp Minimum 11 micron detector temperature The minimum physical temperature of the 11 micron detector within the product duration, taken from the on-board telemetry (identifier A5061).	K	1	Afl	15 byte(s)
83	min_11_mic_temp_units <K>	units	1	AsciiString	3 byte(s)
84	newline_char_22 newline character	terminator	1	AsciiString	1 byte(s)
85	min_37_mic_temp_title MIN_3_7_MICRON_DETECTOR_TEMP=	keyword	1	AsciiString	29 byte(s)
86	min_3_7_micron_detector_temp Minimum 3.7 micron detector temperature The minimum physical temperature of the 3.7 micron detector within the product duration, taken from the on-board telemetry (identifier A5061).	K	1	Afl	15 byte(s)
87	min_37_mic_temp_units <K>	units	1	AsciiString	3 byte(s)
88	newline_char_23 newline character	terminator	1	AsciiString	1 byte(s)
89	min_16_mic_temp_title MIN_1_6_MICRON_DETECTOR_TEMP=	keyword	1	AsciiString	29 byte(s)
90	min_1_6_micron_detector_temp Minimum 1.6 micron detector temperature The minimum physical temperature of the 1.6 micron detector within the product duration, taken from the on-board telemetry (identifier A5061).	K	1	Afl	15 byte(s)
91	min_16_mic_temp_units <K>	units	1	AsciiString	3 byte(s)
92	newline_char_24 newline character	terminator	1	AsciiString	1 byte(s)
93	min_087_mic_temp_title MIN_0_87_MICRON_DETECTOR_TEMP=	keyword	1	AsciiString	30 byte(s)
94	min_0_87_micron_detector_temp Minimum 0.87 micron detector temperature The minimum physical temperature of the 0.87 micron detector within the product duration, taken from the on-board telemetry (identifier A5061).	K	1	Afl	15 byte(s)
95	min_087_mic_temp_units <K>	units	1	AsciiString	3 byte(s)
96	newline_char_25 newline character	terminator	1	AsciiString	1 byte(s)
97	max_fpp_basep_temp_title MAX_FPP_BASEPLATE_TEM=	keyword	1	AsciiString	22 byte(s)
98	max_fpp_baseplate_tem Maximum FPP baseplate temperature The maximum physical temperature of the instrument Focal Plane Assembly baseplate during the orbit, taken from the on-board telemetry (identifier A5061).	K	1	Afl	15 byte(s)
99	max_fpp_basep_temp_units <K>	units	1	AsciiString	3 byte(s)
100	newline_char_26 newline character	terminator	1	AsciiString	1 byte(s)
101	max_12_mic_temp_title MAX_12_MICRON_DETECTOR_TEMP=	keyword	1	AsciiString	28 byte(s)
102	max_12_micron_detector_temp Maximum 12 micron detector temperature The maximum physical temperature of the 12 micron detector within the product duration, taken from the on-board telemetry (identifier A5061).	K	1	Afl	15 byte(s)
103	max_12_mic_temp_units <K>	units	1	AsciiString	3 byte(s)
104	newline_char_27 newline character	terminator	1	AsciiString	1 byte(s)
105	max_11_mic_temp_title MAX_11_MICRON_DETECTOR_TEMP=	keyword	1	AsciiString	28 byte(s)
106	max_11_micron_detector_temp Maximum 11 micron detector temperature The maximum physical temperature of the 11 micron detector within the product duration, taken from the on-board telemetry (identifier A5061).	K	1	Afl	15 byte(s)
107	max_11_mic_temp_units <K>	units	1	AsciiString	3 byte(s)

#	Description	Units	Count	Type	Size
108	newline_char_28 newline character	terminator	1	AsciiString	1 byte(s)
109	max_37_mic_temp_title MAX_3_7_MICRON_DETECTOR_TEMP=	keyword	1	AsciiString	29 byte(s)
110	max_3_7_micron_detector_temp Maximum 3.7 micron detector temperature The maximum physical temperature of the 3.7 micron detector within the product duration, taken from the on-board telemetry (identifier A5061).	K	1	Afl	15 byte(s)
111	max_37_mic_temp_units <K>	units	1	AsciiString	3 byte(s)
112	newline_char_29 newline character	terminator	1	AsciiString	1 byte(s)
113	max_16_mic_temp_title MAX_1_6_MICRON_DETECTOR_TEMP=	keyword	1	AsciiString	29 byte(s)
114	max_1_6_micron_detector_temp Maximum 1.6 micron detector temperature The maximum physical temperature of the 1.6 micron detector within the product duration, taken from the on-board telemetry (identifier A5061).	K	1	Afl	15 byte(s)
115	max_16_mic_temp_units <K>	units	1	AsciiString	3 byte(s)
116	newline_char_30 newline character	terminator	1	AsciiString	1 byte(s)
117	max_087_mic_temp_title MAX_0_87_MICRON_DETECTOR_TEMP=	keyword	1	AsciiString	30 byte(s)
118	max_0_87_micron_detector_temp Maximum 0.87 micron detector temperature The maximum physical temperature of the 0.87 micron detector within the product duration, taken from the on-board telemetry (identifier A5061).	K	1	Afl	15 byte(s)
119	max_087_mic_temp_units <K>	units	1	AsciiString	3 byte(s)
120	newline_char_31 newline character	terminator	1	AsciiString	1 byte(s)
121	lat_long_tie_pt_title LAT_LONG_TIE_POINTS=	keyword	1	AsciiString	20 byte(s)
122	lat_long_tie_points x co-ordinates of lat/long tie points. The X co-ordinates of the latitude/longitude tie points used in ADS#3 (grid pixel latitude and longitude). The 23 values range from -275 km to + 275 km in steps of 25 km.	km	23	As	23*6 byte(s)
123	lat_long_tie_pt_units <km>	units	1	AsciiString	4 byte(s)
124	newline_char_32 newline character	terminator	1	AsciiString	1 byte(s)
125	view_angle_tie_pt_title VIEW_ANGLE_TIE_POINTS=	keyword	1	AsciiString	22 byte(s)
126	view_angle_tie_points x co-ordinates of solar angle tie points. The X co-ordinates of the solar and viewing angle tie points used in ADS#5 and ADS#6 (nadir and forward solar angles). The 11 values range from -250 km to + 250 km in steps of 50 km.	km	11	As	11*6 byte(s)
127	view_angle_tie_pt_units <km>	units	1	AsciiString	4 byte(s)
128	newline_char_33 newline character	terminator	1	AsciiString	1 byte(s)
129	xy_tie_pt_pix_num_title XY_TIE_POINTS_PIXEL_NUM=	keyword	1	AsciiString	24 byte(s)
130	xy_tie_points_pixel_num pixel numbers of x-y tie points The absolute instrument pixel numbers (in the range 1 to 2000) of the tie points used in ADS#4 (scan pixel x and y).	-	99	As	99*6 byte(s)
131	newline_char_34 newline character	terminator	1	AsciiString	1 byte(s)
132	spare_2 Spare	-	1	SpareField	51 byte(s)
133	dsd_spare_3 DSD Spare	-	1	dsd_sp	0 byte(s)
134	dsd_spare_4 DSD Spare	-	1	dsd_sp	0 byte(s)

Record Length : 2190

DS_NAME : Level 1B SPH

Format Version 114.0

6.6.51 Visible calibration coefficients GADS

This product comprises a Main Product Header, a standard Auxiliary Data SPH with one DSD, and the Visible Channel Calibration Parameters GADS as described in the following table. The GADS is a small file of visible channel calibration parameters used by the processor to calibrate visible channel pixel reflectance.

Table 6.86 Visible calibration coefficients GADS

Visible channel calibration parameters GADS

#	Description	Units	Count	Type	Size
Data Record					
0	dsr_time Time of cal in MJD format The calibration time given here is an estimate of the time at which the VISCAL unit is fully illuminated by the sun, based on an analytic formula for the solar declination. It defines the centre of the period which is searched for illuminated VISCAL source packets.	MJD	1	mjd	12 byte(s)
1	attach_flag Attachment flag (always set to zero for this flag)	flag	1	BooleanFlag	1 byte(s)
2	spare_1 Spare	-	1	SpareField	3 byte(s)
3	slp_16_mic 1.6 micron slope The visible calibration coefficient for the 1.6 micron channel, derived from the VISCAL data for the orbit. This is the slope of the linear relationship between reflectance and instrument count, normalised to unit channel gain, and in the case of the 1.6 micron channel, corrected for channel non-linearity.	-	1	fl	4 byte(s)
4	slp_087_mic 0.870 micron slope The visible calibration coefficient for the 0.87 micron channel, derived from the VISCAL data for the orbit. This is the slope of the linear relationship between reflectance and instrument count, normalised to unit channel gain.	-	1	fl	4 byte(s)
5	slp_067_mic 0.670 micron slope The visible calibration coefficient for the 0.67 micron channel, derived from the VISCAL data for the orbit. This is the slope of the linear relationship between reflectance and instrument count, normalised to unit channel gain.	-	1	fl	4 byte(s)
6	slp_055_mic 0.555 micron slope The visible calibration coefficient for the 0.555 micron channel, derived from the VISCAL data for the orbit. This is the slope of the linear relationship between reflectance and instrument count, normalised to unit channel gain.	-	1	fl	4 byte(s)
7	asc_time	MJD	1	mjd	12 byte(s)

#	Description	Units	Count	Type	Size
	UTC at ascending node crossing, in MJD format The UTC of the ascending node crossing for the current orbit. This is the ascending node crossing immediately preceding the VISCAL illumination period.				
8	ave_mon_cnt Average Monitor count The average count in the VISCAL monitor channel during the calibration interval (see link). VISCAL data is only included in the computation of the calibration coefficients if the monitor count exceeds a threshold (1500 counts) and a flatness condition is satisfied.	-	1	fl	4 byte(s)
9	sd_mon_cnt Standard deviation of Monitor count The standard deviation of the count in the VISCAL monitor channel during the calibration interval (see link).	-	1	fl	4 byte(s)
10	sol_irr_16 Solar irradiance (1.6 micron) An estimate of the solar irradiance in the 1.6 micron channel, in units of mW/cm2, at the time of the calibration, based on an analytic formula for the seasonal variation.	-	1	fl	4 byte(s)
11	sol_irr_087 Solar irradiance (0.870 micron) An estimate of the solar irradiance in the 0.87 micron channel, in units of mW/cm2, at the time of the calibration, based on an analytic formula for the seasonal variation.	-	1	fl	4 byte(s)
12	sol_irr_067 Solar irradiance (0.670 micron) An estimate of the solar irradiance in the 0.67 micron channel, in units of mW/cm2, at the time of the calibration, based on an analytic formula for the seasonal variation.	-	1	fl	4 byte(s)
13	sol_irr_055 Solar irradiance (0.555 micron) An estimate of the solar irradiance in the 0.555 micron channel, in units of mW/cm2, at the time of the calibration, based on an analytic formula for the seasonal variation.	-	1	fl	4 byte(s)
14	ave_vispix_16 Average VISCAL Pixel Counts (1.6 (m) The average count in the 1.6 micron signal channel when viewing the illuminated diffusing plate during the calibration interval (see link).	-	1	fl	4 byte(s)
15	ave_vispix_087 Average VISCAL Pixel Counts (0.87 (m) The average count in the 0.87 micron signal channel when viewing the illuminated diffusing plate during the calibration interval (see link).	-	1	fl	4 byte(s)
16	ave_vispix_067 Average VISCAL Pixel Counts (0.67 (m) The average count in the 0.67 micron signal channel when viewing the illuminated diffusing plate during the calibration interval (see link).	-	1	fl	4 byte(s)
17	ave_vispix_055 Average VISCAL Pixel Counts (0.55 (m) The average count in the 0.555 micron signal channel when viewing the illuminated diffusing plate during the calibration interval (see link).	-	1	fl	4 byte(s)
18	vis_pixnois_16 VISCAL Pixel Noise (1.6 micron) The standard deviation of the count in the 1.6 micron signal channel when viewing the illuminated diffusing plate during the calibration interval (see link).	-	1	fl	4 byte(s)
19	vis_pixnois_087 VISCAL Pixel Noise (0.87 micron) The standard deviation of the count in the 0.87 micron signal channel when viewing the illuminated diffusing plate during the calibration interval (see link).	-	1	fl	4 byte(s)
20	vis_pixnois_067 VISCAL Pixel Noise (0.67 micron) The standard deviation of the count in the 0.67 micron signal channel when viewing the illuminated diffusing plate during the calibration interval (see link).	-	1	fl	4 byte(s)
21	vis_pixnois_055 VISCAL Pixel Noise (0.55 micron) The standard deviation of the count in the 0.555 micron signal channel when viewing the illuminated diffusing plate during the calibration interval (see link).	-	1	fl	4 byte(s)
22	ave_xbb_16 Average -X BB Pixel Counts (1.6 (m) The average count (the dark count) in the 1.6 micron signal channel when viewing the selected black body during the calibration interval (see link).	-	1	fl	4 byte(s)
23	ave_xbb_cnt_087 Average -X BB Pixel Counts (0.87 (m) The average count (the dark count) in the 0.87 micron signal channel when viewing the selected black body during the calibration interval (see link).	-	1	fl	4 byte(s)
24	ave_xbb_cnt_067 Average -X BB Pixel Counts (0.67 (m) The average count (the dark count) in the 0.67 micron signal channel when viewing the selected black body during the calibration interval (see link).	-	1	fl	4 byte(s)
25	ave_xbb_cnt_055	-	1	fl	4 byte(s)

#	Description	Units	Count	Type	Size
	Average -X BB Pixel Counts (0.55 (m) The average count (the dark count) in the 0.555 micron signal channel when viewing the selected black body during the calibration interval (see link).				
26	xbb_nois_16 -X BB Pixel Noise (1.6 micron) The standard deviation of the count (the dark count) in the 1.6 micron signal channel when viewing the selected black body during the calibration interval (see link).	-	1	fl	4 byte(s)
27	xbb_nois_087 -X BB Pixel Noise (0.87 micron) The standard deviation of the count (the dark count) in the 0.87 micron signal channel when viewing the selected black body during the calibration interval (see link).	-	1	fl	4 byte(s)
28	xbb_nois_067 -X BB Pixel Noise (0.67 micron) The standard deviation of the count (the dark count) in the 0.67 micron signal channel when viewing the selected black body during the calibration interval (see link).	-	1	fl	4 byte(s)
29	xbb_nois_055 -X BB Pixel Noise (0.55 micron) The standard deviation of the count (the dark count) in the 0.87 micron signal channel when viewing the selected black body during the calibration interval (see link).	-	1	fl	4 byte(s)
30	parity_char (Reserved for parity indicator) At present the visible calibration algorithm, unlike that for the thermal infra-red channels, treats all pixels alike regardless of their parity. This location is provided to cater for the hypothetical possibility of an upgrade to the algorithm which would treat odd and even pixels separately and require different calibration coefficients for the two groups.	-	1	ss	2 byte(s)
31	spare_2 Spare	-	1	SpareField	20 byte(s)

Record Length : 154

DS_NAME : Visible channel calibration parameters GADS

Format Version 114.0

6.6.52 Auxilliary Data SPH with N = 1

Table 6.87 Auxilliary Data SPH with N = 1

Auxiliary Data SPH with N=1 DSD:DSD (G)

#	Description	Units	Count	Type	Size
Data Record					
0	sph_descriptor_title SPH_DESCRIPTOR=	keyword	1	AsciiString	15 byte(s)
1	quote_1 quotation mark (""")	ascii	1	AsciiString	1 byte(s)

#	Description	Units	Count	Type	Size
2	sph_descriptor SPH descriptor ASCII string describing the product	ascii	1	AsciiString	28 byte(s)
3	quote_2 quotation mark (""")	ascii	1	AsciiString	1 byte(s)
4	newline_char_1 newline character	terminator	1	AsciiString	1 byte(s)
5	spare_1 Spare	-	1	SpareField	51 byte(s)

Record Length : 97

DS_NAME : Auxiliary Data SPH with N=1 DSD:DSD (G)

Format Version 114.0

6.6.53 Level 0 MDSR

Table 6.88 Level 0 MDSR

Level 0 MDSR

#	Description	Units	Count	Type	Size
Data Record					
0	dsr_time MJD of sensing time as extracted from Aisp	MJD	1	mjd	12 byte(s)
1	gsrt Ground station reference time	MJD	1	mjd	12 byte(s)
2	isp_length Length of the isp = length of the source packet - 7 bytes	bytes	1	us	2 byte(s)
3	crc_errs Number of VCDUs in the isp which contain a CRC error	VCDU	1	us	2 byte(s)
4	rs_errs Number of VCDUs in the isp for which an RS correction was performed	VCDU	1	us	2 byte(s)
5	spare_1 spare	-	1	SpareField	2 byte(s)
6	source_packet downlinked source packet	-	1	source_packetStruct	-1.0 byte(s)
	a: Isp_Fields Instrument Source Packet	-		uc	1 byte(s)

Record Length : 31

DS_NAME : Level 0 MDSR

Format Version 114.0

6.6.54 Level 0 SPH

Table 6.89 Level 0 SPH

Level 0 SPH

#	Description	Units	Count	Type	Size
Data Record					
0	sph_descriptor_title SPH_DESCRIPTOR=	keyword	1	AsciiString	15 byte(s)
1	quote_1 quotation mark (""")	ascii	1	AsciiString	1 byte(s)
2	sph_descriptor SPH descriptor ASCII string describing the product	ascii	1	AsciiString	28 byte(s)
3	quote_2 quotation mark (""")	ascii	1	AsciiString	1 byte(s)
4	newline_char_1 newline character	terminator	1	AsciiString	1 byte(s)
5	start_lat_title START_LAT=	keyword	1	AsciiString	10 byte(s)
6	start_lat WGS84 latitude of first satellite nadir point at the sensing start time of the MPH A negative value denotes south latitude; a positive value denotes north latitude.	(1e-6) degrees	1	AsciiGeoCoordinate	11 byte(s)
7	start_lat_units <10-6degN>	units	1	AsciiString	10 byte(s)
8	newline_char_2 newline character	terminator	1	AsciiString	1 byte(s)
9	start_long_title START_LONG=	keyword	1	AsciiString	11 byte(s)
10	start_long WGS84 longitude of first satellite nadir point at the sensing start time of the MPH A positive value denotes east of Greenwich; a negative value denotes west of Greenwich.	(1e-6) degrees	1	AsciiGeoCoordinate	11 byte(s)
11	start_long_units <10-6degE>	units	1	AsciiString	10 byte(s)
12	newline_char_3 newline character	terminator	1	AsciiString	1 byte(s)
13	stop_lat_title STOP_LAT=	keyword	1	AsciiString	9 byte(s)
14	stop_lat WGS84 latitude of first satellite nadir point at the sensing stop time of the MPH A negative value denotes south latitude; a positive value denotes north latitude.	(1e-6) degrees	1	AsciiGeoCoordinate	11 byte(s)
15	stop_lat_units <10-6degN>	units	1	AsciiString	10 byte(s)
16	newline_char_4	terminator	1	AsciiString	1 byte(s)

#	Description	Units	Count	Type	Size
	newline character				
17	stop_long_title STOP_LONG=	keyword	1	AsciiString	10 byte(s)
18	stop_long WGS84 longitude of first satellite nadir point at the sensing stop time of the MPH A positive value denotes east of Greenwich; a negative value denotes west of Greenwich.	(1e-6) degrees	1	AsciiGeoCoordinate	11 byte(s)
19	stop_long_units <10-6degE>	units	1	AsciiString	10 byte(s)
20	newline_char_5 newline character	terminator	1	AsciiString	1 byte(s)
21	sat_track_title SAT_TRACK=	keyword	1	AsciiString	10 byte(s)
22	sat_track Sub-satellite track heading at the sensing start time in the MPH.	degrees	1	Afl	15 byte(s)
23	sat_track_units <deg>	units	1	AsciiString	5 byte(s)
24	newline_char_6 newline character	terminator	1	AsciiString	1 byte(s)
25	spare_1 Spare	-	1	SpareField	51 byte(s)
26	isp_errors_sig_title ISP_ERRORS_SIGNIFICANT=	keyword	1	AsciiString	23 byte(s)
27	isp_errors_significant 1 or 0.1 if number of ISPs with CRC errors exceeds threshold	ascii	1	AsciiString	1 byte(s)
28	newline_char_8 newline character	terminator	1	AsciiString	1 byte(s)
29	missing_isps_sig_title MISSING_ISPS_SIGNIFICANT=	keyword	1	AsciiString	25 byte(s)
30	missing_isps_significant 1 or 0.1 if number of missing ISPs exceeds threshold	ascii	1	AsciiString	1 byte(s)
31	newline_char_9 newline character	terminator	1	AsciiString	1 byte(s)
32	isp_discard_sig_title ISP_DISCARDED_SIGNIFICANT=	keyword	1	AsciiString	26 byte(s)
33	isp_discarded_significant 1 or 0.1 if number of ISPs discarded by the PF-HS exceeds threshold	ascii	1	AsciiString	1 byte(s)
34	newline_char_10 newline character	terminator	1	AsciiString	1 byte(s)
35	rs_sig_title RS_SIGNIFICANT=	keyword	1	AsciiString	15 byte(s)
36	rs_significant 1 or 0.1 if number of ISPs with Reed Solomon corrections exceeds threshold	ascii	1	AsciiString	1 byte(s)
37	newline_char_11 newline character	terminator	1	AsciiString	1 byte(s)
38	spare_2 Spare	-	1	SpareField	51 byte(s)
39	num_err_isps_title NUM_ERROR_ISPS=	keyword	1	AsciiString	15 byte(s)
40	num_error_isps Number of ISPs containing CRC errors as reported by the FEP	ISPs	1	Al	11 byte(s)
41	newline_char_13 newline character	terminator	1	AsciiString	1 byte(s)
42	err_isp_thresh_title ERROR_ISPS_THRESH=	keyword	1	AsciiString	18 byte(s)
43	error_isps_thresh Threshold at which number of ISPs containing CRC errors is considered significant	percent	1	Afl	15 byte(s)
44	err_isp_thresh_units <%>	units	1	AsciiString	3 byte(s)
45	newline_char_14 newline character	terminator	1	AsciiString	1 byte(s)
46	num_missing_isps_title NUM_MISSING_ISPS=	keyword	1	AsciiString	17 byte(s)
47	num_missing_isps Number of missing ISPs	ISPs	1	Al	11 byte(s)
48	newline_char_15 newline character	terminator	1	AsciiString	1 byte(s)
49	missing_isps_thresh_title MISSING_ISPS_THRESH=	keyword	1	AsciiString	20 byte(s)
50	missing_isps_thresh	percent	1	Afl	15 byte(s)

#	Description	Units	Count	Type	Size
	Threshold at which number of ISPs missing is considered significant				
51	missing_isps_thresh_units <%>	units	1	AsciiString	3 byte(s)
52	newline_char_16 newline character	terminator	1	AsciiString	1 byte(s)
53	num_discard_title NUM_DISCARDED_ISPS=	keyword	1	AsciiString	19 byte(s)
54	num_discarded_isps Number of ISPs discarded by PF-HS	ISPs	1	Al	11 byte(s)
55	newline_char_17 newline character	terminator	1	AsciiString	1 byte(s)
56	discard_thresh_title DISCARDED_ISPS_THRESH=	keyword	1	AsciiString	22 byte(s)
57	discarded_isps_thresh Threshold at which number of ISPs discarded by PF-HS is considered significant	percent	1	Afl	15 byte(s)
58	discard_thresh_units <%>	units	1	AsciiString	3 byte(s)
59	newline_char_18 newline character	terminator	1	AsciiString	1 byte(s)
60	num_rs_title NUM_RS_ISPS=	keyword	1	AsciiString	12 byte(s)
61	num_rs_isps Number of ISPs with Reed Solomon corrections	ISPs	1	Al	11 byte(s)
62	newline_char_19 newline character	terminator	1	AsciiString	1 byte(s)
63	rs_thresh_title RS_THRESH=	keyword	1	AsciiString	10 byte(s)
64	rs_thresh Threshold at which number of ISPs discarded by PF-HS is considered significant	percent	1	Afl	15 byte(s)
65	rs_thresh_units <%>	units	1	AsciiString	3 byte(s)
66	newline_char_20 newline character	terminator	1	AsciiString	1 byte(s)
67	spare_3 Spare	-	1	SpareField	101 byte(s)
68	tx_polar_title TX_RX_POLAR=	keyword	1	AsciiString	12 byte(s)
69	quote_3 quotation mark (""")	ascii	1	AsciiString	1 byte(s)
70	tx_rx_polar Transmitter/receiver polarization (used for ASAR only) for non-ASAR products	ascii	1	AsciiString	5 byte(s)
71	quote_4 quotation mark (""")	ascii	1	AsciiString	1 byte(s)
72	newline_char_22 newline character	terminator	1	AsciiString	1 byte(s)
73	swath_title SWATH=	keyword	1	AsciiString	6 byte(s)
74	quote_5 quotation mark (""")	ascii	1	AsciiString	1 byte(s)
75	swath Swath number (used for ASAR only) for non-ASAR products	ascii	1	AsciiString	3 byte(s)
76	quote_6 quotation mark (""")	ascii	1	AsciiString	1 byte(s)
77	newline_char_23 newline character	terminator	1	AsciiString	1 byte(s)
78	spare_4 Spare	-	1	SpareField	42 byte(s)
79	dsd_spare_5 DSD Spare	-	1	dsd_sp	0 byte(s)

Record Length : 836

DS_NAME : Level 0 SPH

Format Version 114.0

6.6.55 Climatology Variance Data for Land Surface Temperature Retrieval GADS

Table 6.90

Climatology Variance Data for Land Surface Temperature Retrieval GADS

#	Description	Units	Count	Type	Size
Data Record					
0	precipitable_water Precipitable Water The total precipitable water in a column at the latitude and longitude specified and for the month specified. (The3-dimensional array contains one plane for each calendar month.)	0.01mm	720	ss	720*2 byte(s)

Record Length : 1440

DS_NAME : Climatology Variance Data for Land Surface Temperature Retrieval GADS

Format Version 114.0

Table 6.91 Climatology Data for Land Surface Temperature Retrieval

File will contain one record for each parallel of latitude i = 0, 359 and for each month m = 0, 11.

6.6.56 General Parameters for Land Surface Temperature

Retrieval GADS

Table 6.92

General Parameters for Land Surface Temperature Retrieval GADS

#	Description	Units	Count	Type	Size
Data Record					
0	d_water_vapour_factor_for_lst d: Water vapour factor for LST retrieval Constant parameter that scales the precipitable water vapour correction to the a0 retrieval coefficient. Currently the value of 0.4 is used. [XREF to concepts]	-	1	fl	4 byte(s)
1	m_angle_factor_for_lst M: Angle factor for LST retrieval Scale factor governing the dependence of the precipitable water vapour correction on incidence angle. Currently the value of 5 is used. [XREF to concepts]	-	1	ss	2 byte(s)
2	n_class_num_veg_classes N_CLASS: Number of vegetation classes for LST The total number of land vegetation (or biome) types defined in the vegetation class map	-	1	ss	2 byte(s)
3	spare Spare	-	1	SpareField	12 byte(s)

Record Length : 20

DS_NAME : General Parameters for Land Surface Temperature Retrieval GADS

Format Version 114.0

Table 6.93 General Parameters for Land Surface Temperature Retrieval

6.6.57 Land Surface Temperature retrieval coefficients GADS

Table 6.94

Land Surface Temperature retrieval coefficients GADS

#	Description	Units	Count	Type	Size
Data Record					
0	lst_coeff_a0_day_time LST Coefficient A0 (day-time) Constant coefficient (K) for the daytime retrieval	K/100	1	fl	4 byte(s)
1	lst_coeff_a1_day_time LST Coefficient A2 (day-time) Coefficient of 11 micron nadir BT for the daytime retrieval	-	1	fl	4 byte(s)
2	lst_coeff_a2_day_time LST Coefficient A1 (day-time) Coefficient of 12 micron nadir BT for the daytime retrieval	-	1	fl	4 byte(s)
3	lst_coeff_a0_night_time LST Coefficient A0 (night-time) Constant coefficient (K) for the night-time retrieval	K/100	1	fl	4 byte(s)
4	lst_coeff_a1_night_time LST Coefficient A1 (night-time) Coefficient of 11 micron nadir BT for the night-time retrieval	-	1	fl	4 byte(s)
5	lst_coeff_a2_night_time LST Coefficient A2 (night-time) Coefficient of 12 micron nadir BT for the night-time retrieval	-	1	fl	4 byte(s)

Record Length : 24

DS_NAME : Land Surface Temperature retrieval coefficients GADS

Format Version 114.0

Table 6.95 Land Surface Temperature Retrieval Coefficients

File will contain one record for each surface class and surface (vegetation/soil) type.

6.6.58 Topographic Variance data for Land Surface

Temperature Retrieval GADS

Table 6.96

Topographic Variance data for Land Surface Temperature Retrieval GADS

#	Description	Units	Count	Type	Size
Data Record					
0	topographic_variance_flags Topographic variance flags The topographic variance flag is a two-bit integer representing the standard deviation of the land surface in the half-degree by half-degree cell. The flag represents the standard deviation in four bands [as specified], and acts as a simple quality indicator. The larger the flag value, the more rugged the terrain, and the less reliable the LST retrieval.	-	720	ss	720*2 byte(s)

Record Length : 1440

DS_NAME : Topographic Variance data for Land Surface Temperature Retrieval GADS

Format Version 114.0

Table 6.97 Topographic Variance Flag for Land Surface Temperature Retrieval

File will contain one record for each parallel of latitude i = 0, 359.

6.6.59 Surface Vegetation class for Land Surface Temperature Retrieval GADS

Table 6.98

Surface Vegetation class for Land Surface Temperature Retrieval GADS

#	Description	Units	Count	Type	Size
Data Record					
0	vegetation_class_index Vegetation class index Each entry in the table represents the biome type assigned to the corresponding cell of dimension 0.5 in latitude by 0.5 degree in longitude.	-	720	ss	720*2 byte(s)

Record Length : 1440

DS_NAME : Surface Vegetation class for Land Surface Temperature Retrieval GADS

Format Version 114.0

Table 6.99 Surface vegetation class for Land Surface Temperature Retrieval.

File will contain one record for each parallel of latitude i = 0,359.

6.6.60 Vegetation fraction for Land Surface Temperature Retrieval GADS

Table 6.100

Vegetation fraction for Land Surface Temperature Retrieval GADS

#	Description	Units	Count	Type	Size
Data Record					
0	vegetation_fraction Vegetation Fraction Each tabular entry represents the vegetation fraction assigned to the corresponding half-degree by half-degree cell for the specified month. (The3-dimensional array contains one plane for each calendar month.)	0.001	720	ss	720*2 byte(s)

Record Length : 1440

DS_NAME : Vegetation fraction for Land Surface Temperature Retrieval GADS

Format Version 114.0

Table 6.101 Vegetation fraction for Land Surface Temperature Retrieval.

File will contain one record for each parallel of latitude i = 0, 359 and for each month m = 0, ..., 11.

6.6.61 ATS_SST_AX_GADSR

Average SST Retrieval Coefficients GADS

#	Description	Units	Count	Type	Size
Data Record					
0	a0 a[i][j][0]	K/100	1	fl	4 byte(s)
1	a1 a[i][j]1]	-	1	fl	4 byte(s)
2	a2 a[i][j][2]	-	1	fl	4 byte(s)
3	b0 b[i][j][0]	K/100	1	fl	4 byte(s)
4	b1 b[i][j][1]	-	1	fl	4 byte(s)
5	b2 b[i][j][2]	-	1	fl	4 byte(s)
6	b3 b[i][j][3]	-	1	fl	4 byte(s)
7	c0 c[i][j][0]	K/100	1	fl	4 byte(s)
8	c1 c[i][j][1]	-	1	fl	4 byte(s)
9	c2	-	1	fl	4 byte(s)

#	Description	Units	Count	Type	Size
	c[i][j][2]				
10	c3 c[i][j][3]	-	1	fl	4 byte(s)
11	c4 c[i][j][4]	-	1	fl	4 byte(s)
12	d0 d[i][j][0]	K/100	1	fl	4 byte(s)
13	d1 d[i][j][1]	-	1	fl	4 byte(s)
14	d2 d[i][j][2]	-	1	fl	4 byte(s)
15	d3 d[i][j][3]	-	1	fl	4 byte(s)
16	d4 d[i][j][4]	-	1	fl	4 byte(s)
17	d5 d[i][j][5]	-	1	fl	4 byte(s)
18	d6 d[i][j][6]	-	1	fl	4 byte(s)

Record Length : 76

DS_NAME : Average SST Retrieval Coefficients GADS

Format Version 114.0

6.6.62 ATS_TOA_1P_ADSR_pix

Scan and pixel number forward view ADS

#	Description	Units	Count	Type	Size
Data Record					
0	dsr_time Nadir UTC time in MJD format	MJD	1	mjd	12 byte(s)
1	attach_flag Attachment flag (always set to zero for this ADS)	flag	1	BooleanFlag	1 byte(s)
2	spare_1 Spare	-	1	SpareField	3 byte(s)
3	img_scan_y image scan y coordinate	m	1	sl	4 byte(s)
4	instr_scan_num instrument scan number	-	512	us	512*2 byte(s)
5	pix_num pixel number	-	512	us	512*2 byte(s)

Record Length : 2068

DS_NAME : Scan and pixel number forward view ADS

Format Version 114.0

6.6.63 ATS_TOA_1P_MDSR_cl

Cloud flag forward view MDS

#	Description	Units	Count	Type	Size
Data Record					
0	dsr_time Nadir UTC time in MJD format	MJD	1	mjd	12 byte(s)
1	quality_flag Quality Indicator (-1 for blank MDSR, 0 otherwise)	flag	1	BooleanFlag	1 byte(s)
2	spare_1 Spare	-	1	SpareField	3 byte(s)
3	img_scan_y image scan y coordinate	m	1	sl	4 byte(s)
4	cl_land_flags cloud/land flags	flags	512	us	512*2 byte(s)

Record Length : 1044

DS_NAME : Cloud flag forward view MDS

Format Version 114.0

6.6.64 ATS_TOA_1P_ADSR_sa

Forward view solar angles ADS

#	Description	Units	Count	Type	Size
Data Record					
0	dsr_time Nadir UTC time in MJD format	MJD	1	mjd	12 byte(s)
1	attach_flag Attachment Flag (always set to zero for this ADS)	flag	1	BooleanFlag	1 byte(s)
2	spare_1	-	1	SpareField	3 byte(s)

#	Description	Units	Count	Type	Size
	Spare				
3	img_scan_y image scan y coordinate	m	1	sl	4 byte(s)
4	tie_pt_sol_elev tie point solar elevation	mdeg	11	sl	11*4 byte(s)
5	tie_pt_sat_elev_nad tie point satellite elevation nadir	mdeg	11	sl	11*4 byte(s)
6	tie_pt_sol_az tie point solar azimuth	mdeg	11	sl	11*4 byte(s)
7	tie_pt_sat_azi tie point satellite azimuth	mdeg	11	sl	11*4 byte(s)
8	spare_2 Spare	-	1	SpareField	20 byte(s)

Record Length : 216

DS_NAME : Forward view solar angles ADS

Format Version 114.0

6.6.65 ATS_TOA_1P_MDSR_conf

Confidence words forward view MDS

#	Description	Units	Count	Type	Size
Data Record					
0	dsr_time Nadir UTC time in MJD format	MJD	1	mjd	12 byte(s)
1	quality_flag Quality Indicator (-1 for blank MDSR, 0 otherwise)	flag	1	BooleanFlag	1 byte(s)
2	spare_1 Spare	-	1	SpareField	3 byte(s)
3	img_scan_y image scan y coordinate	m	1	sl	4 byte(s)
4	conf_wd_flags Confidence words	flags	512	us	512*2 byte(s)

Record Length : 1044

DS_NAME : Confidence words forward view MDS

Format Version 114.0

Chapter 7

Credits

The AATSR project is funded by the UK Department for Environment, Food and Rural Affairs (DEFRA), the Australian Department of Industry, Science and Resources (DISR), and the UK National Environmental Research Council (NERC).

Written by:

Andrew Birks

Rutherford Appleton Laboratory

Chilton

Didcot

Oxon

OX11 0QX

UK

Telephone: +44 (0)1235 446479

Fax: +44 (0)1235 445848

Email: A.R.Birks@rl.ac.uk

ESA

ESRIN - Product Control Service

Via Galileo Galilei

Casella Postale 64

00044 Frascati (RM)

Italy

Tel: +39 06 94180 000

VEGA Group PLC

2 Falcon Way

Shire Park

Welwyn Garden City

Herts AL7 1TW

United Kingdom

Tel:+44 1707 391 999

Fax: +44 1707 393 909

Earth Observation Science

Space Research Centre

Department of Physics and Astronomy

University of Leicester

University Road

Leicester

LE1 7RH

UK

Telephone: +44 (0) 116 252 3521

Fax: +44 (0) 116 252 5262

With contributions and support from:

Mike Buckley

Astrium Ltd

Anchorage Road

Portsmouth

Hampshire

PO3 5PU

UK

Telephone: +44 (0)2392 705944

Fax: +44 (0)2392 705000

Email: Mike.Buckley@astrium-space.com

Mike Fletcher

Bettercompac Ltd (BSA)

Hooper's Farm

Clevedon Lane

Clapton Wick

North Somerset

BS21 7AG

UK

Telephone/fax: +44 (0)1275 810427

Email: bettercompac@compuserve.com

The Envisat Product Handbook Publishing Infrastructure Project (EPHPI) was developed by Pildo Labs (Pildo Cntg):

Pildo Labs: Fernando Nuñez, Raul Ramos, Daniel Martinez

Pildo Labs (Pildo Consulting S.L.)

Llacuna 162

Barcelona

08018

Spain

Tel: +34 934019782

Fax: +34 934019783

Email: pildo@pildo.com

Email: julie.andrews@pildo.com (no relation)